



A University of Sussex DPhil thesis

Available online via Sussex Research Online:

<http://sro.sussex.ac.uk/>

This thesis is protected by copyright which belongs to the author.

This thesis cannot be reproduced or quoted extensively from without first obtaining permission in writing from the Author

The content must not be changed in any way or sold commercially in any format or medium without the formal permission of the Author

When referring to this work, full bibliographic details including the author, title, awarding institution and date of the thesis must be given

Please visit Sussex Research Online for more information and further details

Morphological and Longshore Sediment Transport processes on Mixed Beaches

Jérôme Curoy

September 2010

Department of Geography,
University of Sussex Falmer,
Brighton, BN1 9QJ, UK

A thesis submitted for the degree of Doctor of Philosophy

Declaration

I hereby declare that this thesis has not been, and will not be, submitted in whole or in part to another University for the award of any other degree. I confirm that this is my own work and the use of all material from other sources has been properly and fully acknowledged.

Signature.....

Jérôme Curoy

*“The sea is calm to-night.
The tide is full, the moon lies fair
Upon the straits; on the French coast the light
Gleams and is gone; the cliffs of England stand;
Glimmering and vast, out in the tranquil bay.
Come to the window, sweet is the night-air!
Only, from the long line of spray
Where the sea meets the moon-blanced land,
Listen! you hear the grating roar
Of pebbles which the waves drawback, and fling,
At their return, up the high strand,
Begin, and cease, and then again begin,
With tremulous cadence slow, and bring
The eternal note of sadness in.”*

Extract of “*Dover Beach*” by Matthew Arnold (1867)

Abstract

Mixed beaches, with sediment sizes ranging over three orders of magnitude, are an increasingly important coastal defence on the heavily populated coasts of SE England and N France. Yet longshore transport rates and volumes, important in understanding beach sustainability, remain understudied for such beaches.

This thesis addresses the knowledge gap via field investigations of beach profile evolution, active layer measurements and tracer pebble scattering patterns on two macrotidal mixed beaches at Cayeux-sur-Mer (France) and Birling Gap (UK), eastern English Channel.

The beach topography data at both sites enabled observation of how reactive the beach profile is to hydrodynamic conditions. Each beach, in different environmental conditions, was found to have a profile that responded extremely quickly to changing hydrodynamics as a result of the combined effects of the High Water Level (HWL) and wave height. The most significant topographical changes are associated primarily with variations in the across-shore position and height of the berm.

The research contributes new baseline data to help refine the currently limited understanding of the relationship between depth of disturbance and wave height, wave period, wave direction and the degree of mixture on mixed beaches.

Consistent patterns of pebble behaviour were identified during each tidal cycle at different locations on the beach profile. The distance travelled varied with location on the beach profile, with pebbles from the upper beach tending to travel further than pebbles placed on lower parts of the beach. Upper beach pebbles generally showed a clear displacement seaward across-shore whereas lower and middle beach pebbles were affected by shorter across-shore displacements. These displacements are explained by variations in the hydrodynamic conditions, swash flows, groundwater flow, beach slope and grain size.

Finally, wave conditions and water level directly influenced the Longshore Sediment Transport (LST) rates. From these results, applying the energy flux approach, a drift coefficient (K) of 0.04 was derived for both sites.

Acknowledgements

This thesis is the accomplishment of a few years of hard work dedicated to the study of gravel beaches and most precisely mixed beaches. While there is only one author on the cover page of the manuscript, this work would never have been completed without the help of many people in different aspects.

I should start to thank my supervisors, Dr. Cherith Moses and Dr. David Robinson, for their patience and support to finalise this work. Cherith gave me the opportunity to start a PhD, she believed in me and for that I cannot thank her enough.

I would like to thank Dr. Uwe Dornbusch for his consistent help during the first two years of my PhD. His consistent guidance, support and advice about this research have made this work possible and enjoyable. Thanks also to Dr. Rendel Williams for his support especially in the early part of my work.

I would also thank all the people that have helped me in the field to collect my data, even at night. So big thanks to: Dr. Ilaria Palestra, Dr. Katie Boon, Dr. Richard Charman, Eleanor Low, Tamsin Watt, Dr. Daniel Buscombe, Julia Basthide, Jean-Charles Curoy, Roland Curoy and Christopher Smith.

I cannot be thankful enough to my friends Fred and Carine, who helped support me during hard times.

Finally, I am eternally thankful to my family and my parents for their support and love. I am still sane thanks to you all.

Table of Contents

Abstract.....	iv
Acknowledgments.....	v
Tables of Contents.....	vi
List of Figures.....	xi
List of Tables.....	xxii
List of Abbreviations and Notations.....	xxvi
Chapter 1. Introduction	1
1.1 Aim of the thesis	1
1.2 Introduction.....	2
1.3 The concept of coastal morphodynamic	4
1.4 Definition of a beach system.....	5
1.5 Concept of Longshore Sediment Transport (LST).....	8
1.6 Modes of sediment transport.....	9
1.7 Classification of gravel beaches and definition of a mixed beach	11
1.8 Definition and location of the different morphological features occurring on a mixed beaches	12
1.8.1 The lower foreshore.....	13
1.8.2 The beach step	14
1.8.3 The beach cusps.....	15
1.8.4 The beach berm	17
1.8.5 Washover lobes	18
1.9 Areas of research on coarse sediment beaches	19
1.10 Recall of the aims of the study.....	22
Chapter 2. Background on the Field Study Areas	25
2.1 Birling Gap	25
2.1.1 Geography and morphology of the study site and its sedimentary cell: From Selsey to Beachy Head.	25
2.1.2 General wind and hydrodynamic conditions of the area.....	29
2.1.3 Recent evolution of Birling Gap	32
2.1.4 Gravel/cobble supplies	35
2.2 The Bas-Champs of Cayeux-sur-Mer.....	37

2.2.1 Geography and morphology of the site and its sedimentary cell: From the Seine Estuary to the Somme Estuary coast.....	37
2.2.2 General wind and hydrodynamic conditions of the area.....	41
2.2.3 Coastal defence management since 1965	45
2.2.4 Recent evolution of the gravel spit of the Bas-Champs.....	48
2.2.5 Gravel/cobble supplies	55
Chapter 3. Sample Design	60
3.1 Introduction.....	60
3.2 Topographic measurements	62
3.2.1 The Differential Global Positional System (DGPS)	62
3.2.2 Design of the topographic surveys.....	63
3.3 Hydrodynamic measurements.....	69
3.3.1 Electromagnetic current meter and pressure sensor S4DW	71
3.3.2 The Midas DWR Wave Recorder.....	73
3.4 Sediment transport.....	75
3.4.1 Tracing experiments-Research on the types of tracers available	75
3.4.2 Tracing experiment-The synthetic pebbles.....	78
3.4.3 Tracing experiment-Fieldwork deployment description.....	82
3.4.4 Active Layer measurement	91
3.5 Sediment variation	95
3.5.1 Background, reflection on the methodologies available.....	95
3.5.2 Methodology chosen.....	96
3.6 Summary.....	97
Chapter 4. Temporal and spatial scales of mixed beach profile changes	100
4.1 Introduction.....	100
4.2 Background.....	101
4.2.1 Classification of the beach profiles.....	101
4.2.2 Spatial and temporal beach profile changes	106
4.3 Morphological changes observed at Cayeux-sur-Mer and Birling Gap	113
4.3.1 Wave conditions at Cayeux-sur-Mer	114
4.3.2 Wave conditions at Birling Gap	114
4.3.3 Tidal to semi-lunar cycle profile changes at Cayeux-sur-Mer.....	122
4.3.4 Tidal to semi-lunar cycle profile changes at Birling Gap	146
4.3.5 Seasonal and Yearly profile changes at Birling Gap	161
4.4 Discussion.....	169
4.4.1 Seasonal elevation changes of the beach profile.....	169
4.4.2 Short time elevation changes on the beach profile.	170
4.4.3 Sediment transfer on the sandy foreshore.....	172

4.4.4 Influence of sediment recycling on beach behaviour	175
4.4.5 Response to storms and extreme storms	177
4.5 Conclusions	180
 Chapter 5. ACTIVE LAYER AND MIXING DEPTH	 183
5.1 Introduction	183
5.2 Background	184
5.2.1 Review of the active layer on sand beaches	184
5.2.2 Review of the active layer on gravel beaches	185
5.3 Measurement of the Active Layer and the Mixing Depth at Cayeux-sur-Mer and Birling Gap	187
5.3.1 Variation of the active layer alongshore	187
5.3.2 Variation of the active layer across-shore	191
5.3.3 Variation of the active layer over time	196
5.3.4 Variation of the mixing depth with the grain size	199
5.3.5 Variation of the mixing depth with the wave height	202
5.3.6 Variation of the mixing depth with the wave direction	207
5.3.7 Variation of the mixing depth with the wave period	210
5.4 Discussion	211
5.4.1 Variation of the active layer across-shore	212
5.4.2 Variation of the mixing depth with the grain size	219
5.4.3 Variation of the active layer with the wave height	220
5.4.4 Variation of the mixing depth with the wave direction	223
5.5 Conclusions	224
 Chapter 6. Longshore Sediment Transport	 226
6.1 Introduction	226
6.2 Background	227
6.2.1 Field-based observations and measurement of sediment transport using tracers.	228
6.2.2 Field-based observations and measurement of sediment transport using topographic surveys	237
6.2.3 Field-based observations and measurement of sediment transport using traps.	238
6.2.4 Laboratory-based longshore sediment transport experiments	240
6.3 Field measurement experiments, Cayeux-sur-Mer, December 2004	242
6.3.1 Wave conditions	243
6.3.2 Tracer recovery and distribution patterns	244
6.3.3 Derivation of the volume transported and the LST rates using tracer pebbles	250

6.3.4 DGPS surveys: digital elevation model and beach elevation changes	251
6.3.5 DGPS surveys: beach volume changes.....	254
6.4 Field measurement experiments, Cayeux-sur-Mer, October/November 2005.....	256
6.4.1 Tracer recovery and distribution patterns	256
6.4.2 Derivation of the volume transported and the LST rates using tracer pebbles	273
6.4.3 DGPS surveys: digital elevation model and beach elevation changes	274
6.4.4 DGPS surveys: beach volume changes.....	280
6.5 Field measurement experiments, Birling Gap, March 2006.....	286
6.5.1 Tracer recovery and distribution patterns	286
6.5.2 Derivation of the volume transported and the LST rates using tracer pebbles	291
6.5.3 DGPS surveys: digital elevation model and beach elevation changes	293
6.5.4 DGPS surveys: beach volume changes.....	296
6.6 Field measurement experiments, Birling Gap, May 2006.....	299
6.6.1 Tracer recovery and distribution patterns	299
6.6.2 Derivation of the volume transported and the LST rates using tracer pebbles	307
6.6.3 DGPS surveys: Beach surface and volume changes.....	309
6.6.4 DGPS surveys: beach volume changes.....	311
6.7 Field measurement experiments, Birling Gap, December 2006	314
6.7.1 Tracer recovery and distribution patterns	314
6.7.2 Derivation of the volume transported and the LST rates using tracer pebbles.....	323
6.7.3 DGPS surveys: digital elevation model and beach elevation changes	323
6.7.4 DGPS surveys: beach volume changes.....	326
6.8 Field measurement experiments, Birling Gap, October 2004 to May 2005: quartzite pebble tracing experiment.	329
6.9 Yearly longshore transport between July 2003 and July 2006.....	333
6.10 Discussion.....	334
6.10.1 Recovery rates and validation of the pebble tracing technique.....	334
6.10.2 Beach sediment dispersion patterns.....	336
6.10.3 Accuracy of the techniques used: a comparison between GPS surveys and tracer pebbles.....	341
6.10.4 Accuracy of the techniques used: a comparison of LST volumes calculated based on active layer measurements and on tracer burial depth	343
6.11 Conclusion.....	344
 Chapter 7. Longshore Sediment Transport: an attempt to derive K.....	 346
7.1 Introduction.....	346

7.2 Background.....	347
7.2.1 LST: the energy flux approach	347
7.2.2 The CERC formula	353
7.3 Towards an estimate of pebble transport efficiency.....	354
7.3.1 Calculation of the K factor from the tracer data	362
7.4 Discussion.....	366
7.4.1 Correlation between longshore wave power and LST rate	366
7.4.2 The coefficient of littoral drift (K).....	368
7.5 Conclusion.....	369
 Chapter 8. Discussion and concluding remarks	 370
8.1 Introduction.....	370
8.2 Meeting the overall aim	370
8.3 Context and relevance of this study to previous research.....	372
8.4 Overview of main findings of this work to the research area	375
8.5 Limitations of this study and recommendations for future work	377
 References	 381
 Appendix I Manufacturing of the synthetic tracer pebbles	 395
Appendix II Grain size characteristics.....	398
Appendix III Sandy beaches typical profile types.....	430
Appendix IV Active Layer measurements	431
Appendix V Pebble tracers' scattering at Cayeux-sur-Mer in December 2004....	438
Appendix VI Pebble tracers' scattering at Cayeux-sur-Mer in October/November 2005	439
Appendix VII Pebble tracers' scattering at Birling Gap in March 2006.....	447

List of Figures

CHAPTER 1

FIGURE 1-1 PRINCIPAL VECTORS OF THE LONGSHORE SEDIMENT TRANSPORT (Q).....	1
FIGURE 1-2 PRIMARY COMPONENTS INVOLVED IN THE COASTAL MORPHODYNAMIC SYSTEM (COWELL AND THOM 1994). Δt : TIME COMPONENT.	4
FIGURE 1-3 SKETCH OF A HIGH ENERGY BEACH SYSTEM INCLUDING THE WAVE TRANSFORMATION AREAS APPROACHING THE SHORELINE AND GENERAL SEDIMENT TRANSPORT (AFTER CARTER, 1994, P.82-93 AND SHORT, 1999, P.4). GENERAL SEDIMENT TRANSPORT IS REPRESENTED BY THE BLACK ARROWS IN PROXIMITY TO THE SEA BED AND THE EQUILIBRIUM BETWEEN THE ONSHORE AND OFFSHORE SEDIMENT TRANSITS IS RELATIVE TO THE LENGTH OF EACH SINGLE ARROW.	6
FIGURE 1-4 WAVE-GENERATED CURRENT PATTERNS OBSERVED NEARSHORE. A) THE INCIDENT WAVE ANGLE IS PERPENDICULAR TO THE SHORE. B) THE INCIDENT WAVE ANGLE IS OBLIQUE TO THE SHORE.	7
FIGURE 1-5 EVIDENCE OF LST IN A GROUYNE FIELD. A) ALONG THE ENGLISH COAST AT PEACEHAVEN (EAST SUSSEX). B) ALONG THE FRENCH COAST AT AULT (NORMANDY). IMAGES COURTESY OF GOOGLE EARTH.	8
FIGURE 1-6 CROSS-SECTION OF A CLASSIC COMPOSITE BEACH SHOWING THE MOST FREQUENTLY OBSERVED MORPHOLOGICAL AND SEDIMENTOLOGICAL FEATURES.....	13
FIGURE 1-7 THE SANDY LOWER FORESHORE AND THE BEACH STEP AT CAYEUX-SUR-MER.	13
FIGURE 1-8 EXAMPLE OF BEACH CUSPS OBSERVED AT BOTH STUDY SITES. A) AT BIRLING GAP, WITH VERY PERPENDICULAR RHYTHMIC HORNS OF SHINGLES AND SANDY EMBAYMENT. B) AT CAYEUX-SUR-MER, WITH PERPENDICULAR RHYTHMIC HORNS MADE OF COARSE PEBBLES AND CUSPS MADE OF GRAVEL.	15
FIGURE 1-9 THE BEACH AT BIRLING GAP. A) DISPLAYING MULTIPLE BERMS. B) THE BERM AT HIGH TIDE.	18

Chapter 2

FIGURE 2-1 LOCATION OF THE UK STUDY SITE: A) ALONG THE CHANNEL. B) WITHIN THE SUB-SEDIMENT CELL BETWEEN SELSEY BILL AND BEACHY HEAD (SOUTH DOWNS COASTAL GROUP, 1996). C) VIEW OF BIRLING GAP.	26
FIGURE 2-2 WIND ROSE AT THE GREENWICH LIGHTSHIP STATION FOR DATA COLLECTED BETWEEN 2001 AND 2006.	29
FIGURE 2-3 TIDAL RANGE (M) AT MEAN SPRING TIDES. SOURCE: LEE AND RAMSTER (1981).	30
FIGURE 2-4 MAXIMUM TIDAL CURRENT SPEED (IN $M.S^{-1}$) AT MEAN SPRING TIDES. SOURCE: SAGER AND SAMMLER (1968).	30
FIGURE 2-5 SIGNIFICANT WAVE HEIGHT RECORDED AT RUSTINGTON BETWEEN 2004 AND 2006.	31
FIGURE 2-6 CHANGE IN GEOMETRY OF A BEACH PROFILE LOCATED 215 M WEST OF THE ACCESS STEPS AT BIRLING GAP. THE 1873 PROFILE IS BASED ON THE LOCATION OF FEATURE LINES ON THE MAP AND ASSOCIATED ELEVATION FROM TIDE DATA. THE 1973 PROFILE IS CALCULATED FROM DIGITAL STEREO AIR PHOTOGRAPHS WITH A GROUND RESOLUTION OF 0.07 M. THE 2005 PROFILE IS EXTRACTED FROM THE LIDAR SURVEY CARRIED OUT BY THE ENVIRONMENT AGENCY.	

CHALK REFERS TO THE CLIFF AND SHORE PLATFORM PART OF THE PROFILE WHILST BEACH REFERS TO THE MOBILE SEDIMENT (DORNBUSCH ET AL., 2008A).....	33
FIGURE 2-7 ILLUSTRATION OF THE COASTLINE EVOLUTION OVER THE LAST 140 YEARS (POSTCARDS COURTESY OF RENDEL WILLIAMS, PHOTOGRAPHS COURTESY OF UWE DORNBUSCH).....	34
FIGURE 2-8 LOCATION OF THE FRENCH STUDY SITE: A) ON THE CHANNEL. B) WITHIN THE SEDIMENT CELL BETWEEN LE HAVRE AND THE SOMME ESTUARY. C) VIEW OF THE GRAVEL BARRIER BETWEEN AULT-ONIVAL AND LE HOURDEL. D) VIEW OF THE SURVEY AREA AT CAYEUX-SUR-MER.....	38
FIGURE 2-9 CROSS-SECTIONAL VIEW OF THE BAS-CHAMPS DEPOSITS (DOLIQUE 1998).....	41
FIGURE 2-10 WIND ROSE AT CAYEUX-SUR-MER FOR DATA COLLECTED BETWEEN 2006 AND 2010. THESE DATA ARE NOT REAL MEASURED VALUES AT THE LOCATION BUT COME FROM A FORECAST MODEL (GLOBAL FORECAST SYSTEM) BASED ON THE NEAREST POINT OF MEASUREMENT.	42
FIGURE 2-11 DISTRIBUTION OF THE WAVE DIRECTIONS BY THEIR SIGNIFICANT WAVE HEIGHT (SOGREAH, 1995A).....	44
FIGURE 2-12 AVERAGE WAVE PERIOD OBSERVED IN THE VICINITY OF DIEPPE ABOVE THE ISOLINE -23.6 M. THESE DATA WERE SIMULATED RETROSPECTIVELY, USING THE SOFTWARE TOMAWAC DEVELOPED BY EDF R&D – LNHE, FROM DATA COLLECTED BETWEEN JANUARY 1979 AND AUGUST 2002 (CETMEF, 2009b).....	45
FIGURE 2-13 COASTAL MANAGEMENT DEVELOPMENTS ALONG THE BAS-CHAMPS. YELLOW COLOURED BOXES AND ARROWS REPRESENT THE MANAGEMENT PLAN USED FROM 1997 TO 2001, WHEREAS THE PURPLE COLOURED ONES REPRESENT THE MANAGEMENT PLAN PRACTICED FROM 2001. NB: THE NUMBER OF GROYNES DRAWN ON THE MAP IS NOT REPRESENTATIVE OF THE ACTUAL NUMBER OF GROYNES IN PLACE, BUT REPRESENTS THE LENGTH OF THE BEACH THAT THEY OCCUPY.	47
FIGURE 2-14 EVOLUTION OF THE BEACH PROFILE BETWEEN 1965 AND 1994 IN PROXIMITY OF THE HÂBLE D’AULT (SOGREAH, 1995; HD-FRENCH HYDROGRAPHYC DATUM).....	51
FIGURE 2-15 EVOLUTION OF THE BAS-CHAMPS AREA SINCE 1939.	52
FIGURE 2-16 AVERAGE FLINT CONTENT OF THE CLIFFS BETWEEN BENOUVILLE AND CRIEL (COSTA, 1997).	56
FIGURE 2-17 CLIFF EROSION CHARACTERISTICS ALONG THE UPPER NORMANDIE IN RELATION TO THE CLIFF TOE STRATIGRAPHY LITHOLOGIC STRUCTURE, PER AREA BETWEEN 1947 AND 1995. (A) SPATIAL LOCATION OF THE AVERAGE CHALK CLIFF RETREAT RATES. (B) AVERAGE REPEAT PERIOD OF CLIFF FALLS. (C) AVERAGE RETREAT PER FALL (COSTA, 1997).	57

CHAPTER 3

FIGURE 3-1 DGPS IN USE.....	63
FIGURE 3-2 LOCATIONS OF A TYPICAL PROFILE PATH SELECTED AT BIRLING GAP. THE CIRCLED BLACK CROSS REPRESENTS THE LOCATION OF THE BASE STATION. THE LOCATION OF THE MIDAS DWR IN THE PROXIMITY OF THE MIXED BEACH IS MARKED BY THE BLUE CROSS. THE BLACK RECTANGLE REPRESENTS THE LOCATION OF THE AREA WHERE THE SYNTHETIC TRACERS WERE DEPLOYED AND THE MEASUREMENTS OF THE ACTIVE LAYER DEPTH OCCURRED (THIS CHAPTER SECTION 3.4.4).....	66
FIGURE 3-3 LOCATIONS OF A TYPICAL PROFILE PATH SELECTED AT CAYEUX-SUR-MER. THE CIRCLED BLACK CROSS REPRESENTS THE LOCATION OF THE BASE STATION. THE LOCATION OF THE S4DW IN THE PROXIMITY OF THE MIXED BEACH IS	

MARKED BY THE BLUE CROSS). THE BLACK RECTANGLE REPRESENTS THE AREA WHERE THE SYNTHETIC TRACERS WERE DEPLOYED AND THE ACTIVE LAYER WAS MEASURED AND THE TRACER PEBBLES WERE DEPLOYED (THIS CHAPTER SECTION 3.4.4).	67
FIGURE 3-4 THE S4DW ELECTROMAGNETIC CURRENT METER AND PRESSURE SENSOR DEPLOYED ON THE SANDY FORESHORE AT CAYEUX-SUR-MER.	71
FIGURE 3-5 THE MIDAS DWR WAVE RECORDER DEPLOYED ON THE CHALK PLATFORM AT BIRLING GAP.	73
FIGURE 3-6 PAINTED PEBBLES. A) EXAMPLE OF SPRAY PAINTED BEACH PEBBLES. B) SPRAY PAINTED PEBBLES AFTER ONLY 5 HOURS IN A TUMBLER.	76
FIGURE 3-7 A NATURAL QUARTZITE TRACER MIXED WITH THE BEACH MATERIAL.	77
FIGURE 3-8 REPRESENTATION OF THE LENGTH OF COPPER NECESSARY TO INSERT IN A SYNTHETIC TRACER AS A FUNCTION OF THE MASS OF THIS SAME SYNTHETIC TRACER.	80
FIGURE 3-9 A SYNTHETIC PEBBLE. MADE OF AN EPOXY RESIN WITH A COPPER CORE INSIDE, ITS SIZE IS: A-AXIS: 60 TO 70 MM, B-AXIS: 35 TO 50 MM, C-AXIS: 35 TO 40 MM. EACH PEBBLE IS COMPLETELY SMOOTHED, WELL ROUNDED AND HAS THE SAME WEIGHT AS A FLINT PEBBLE OF THE SAME SIZE.	80
FIGURE 3-10 DEPLOYMENT OF QUARTZITE PEBBLES AT BIRLING GAP-OCTOBER 2004.	84
FIGURE 3-11 LOCATION OF THE MEASUREMENT POINTS AT CAYEUX-SUR-MER. A) AERIAL PHOTOGRAPH OF THE STUDY SITE, WHERE THE YELLOW RECTANGULAR REPRESENTS THE DGPS SURVEYED AREA AND THE RED RECTANGULAR REPRESENT THE AREA OF DEPLOYMENT OF THE TRACER PEBBLES AND THE MEASUREMENTS OF THE ACTIVE LAYER. B) ZOOM ON THE LOCATION OF THE TRACER INJECTION POINTS (GREEN SQUARES) AND THE PAINTED PEBBLE COLUMNS (RED POINTS)...	86
FIGURE 3-12 LOCATION OF THE MEASUREMENT POINTS AT BIRLING GAP. A) AERIAL PHOTOGRAPH OF THE STUDY SITE, WHERE THE RED RECTANGULAR REPRESENT THE AREA OF DEPLOYMENT OF THE TRACER PEBBLES AND THE MEASUREMENTS OF THE ACTIVE LAYER. B) ZOOM ON THE LOCATION OF THE TRACER INJECTION POINTS (GREEN SQUARES) AND THE PAINTED PEBBLE COLUMNS (RED POINTS).....	87
FIGURE 3-13 A) LAYOUT OF A SYNTHETIC PEBBLES DEPLOYMENT. B) LOCATION OF THE SYNTHETIC PEBBLES DEPLOYMENTS ON A BEACH PROFILE SURVEYED AT BIRLING GAP SURVEYED IN MAY 2005. C) VIEW OF AN <i>IN SITU</i> SYNTHETIC PEBBLES DEPLOYMENT FROM THE SURFACE. THE RED ARROW INDICATES ONE OF THE TRACERS PERFECTLY MIXED WITH THE BEACH MATERIAL. D) INSIDE VIEW OF AN <i>IN SITU</i> SYNTHETIC PEBBLES DEPLOYMENT.	88
FIGURE 3-14 METAL DETECTOR IN USE.	89
FIGURE 3-15 A) METHOD USED TO MEASURE THE ACTIVE LAYER. THE DARK CIRCLES ARE THE PAINTED AND NUMBERED PEBBLES DEPLOYED AT THE FIRST LOW TIDE (TIME, T_0). THE WHITE CIRCLES ARE THE NEW PAINTED AND NUMBERED PEBBLES DEPLOYED AT THE FOLLOWING LOW TIDE (TIME, $T_0 + 1$). B) PLANAR VIEW OF A PAINTED AND NUMBERED PEBBLE COLUMN BUILT UP INTO THE BEACH MATERIAL.	94

CHAPTER 4

FIGURE 4-1 EXAMPLES OF STEP, COMPOSITE AND BAR BEACH PROFILE IDENTIFIED AT LLANRHYSTYD. EACH PROFILE STARTS FROM THE GRAVEL RIDGE CREST. HWS MARKS THE PREDICTED POSITION OF SPRING TIDE HIGH WATER (ORFORD 1986).....	103
---	-----

FIGURE 4-2 BEACH PROFILE DIMENSIONS OF GRAVEL BASED PROFILES AT LLANRHYSTYD (ORFORD, 1978).	103
FIGURE 4-3 BASIC PROFILE TYPES DISTINGUISHED BY CALDWELL AND WILLIAMS (1985).	104
FIGURE 4-4 INSHORE WAVE CONDITIONS AT CAYEUX-SUR-MER FOR THE SURVEY PERIOD, OCTOBER 28 TH TO NOVEMBER 11 TH , 2005. THE MEAN WAVE ANGLE IS REFERRED TO TO THE COAST ORIENTATION (N205°).	116
FIGURE 4-5 OFFSHORE WAVE CONDITIONS COLLECTED AT RUSTINGTON FOR THE SURVEY PERIOD BETWEEN AUGUST 2004 TO JULY 2006. THE MEAN WAVE ANGLE IS REFERRED TO TO THE COAST ORIENTATION (N132°).	117
FIGURE 4-6 INSHORE WAVE CONDITIONS COLLECTED AT BIRLING GAP FOR THE SURVEY PERIOD BETWEEN MARCH 20 TH AND MARCH 24 TH , 2006. THE MEAN WAVE ANGLE IS REFERRED TO TO THE COAST ORIENTATION (N132°).	118
FIGURE 4-7 INSHORE WAVE CONDITIONS COLLECTED AT BIRLING GAP FOR THE SURVEY PERIOD BETWEEN MAY 19 TH AND MAY 24 TH , 2006. THE MEAN WAVE ANGLE IS REFERRED TO TO THE COAST ORIENTATION (N132°).	119
FIGURE 4-8 INSHORE WAVE CONDITIONS COLLECTED AT BIRLING GAP FOR THE SURVEY PERIOD BETWEEN DECEMBER 14 TH AND DECEMBER 19 TH , 2006. THE MEAN WAVE ANGLE IS REFERRED TO TO THE COAST ORIENTATION (N132°).	120
FIGURE 4-9 LOCATION OF THE TWO PROFILE SSURVEYED AT CAYEUX-SUR-MER FROM THE 28 TH OF OCTOBER TO THE 11 TH OF NOVEMBER 2005.....	122
FIGURE 4-10 THE BEACH AT CAYEUX-SUR-MER. A) IN FRONT OF THE RECYCLED AREA (VIEW FROM THE SANDY PLATFORM). B) TOWARDS THE NON DIRECTLY MANAGED ("NATURAL") AREA (VIEW FROM THE SANDY PLATFORM).....	123
FIGURE 4-11 SURFACE PLOT SHOWING THE TEMPORAL VARIATION IN BEACH FACE MORPHOLOGY IN THE RECYCLED AREA BASED ON LOW TIDE SURVEYS AT CAYEUX-SUR-MER FROM OCTOBER 28 TH TO NOVEMBER 11 TH , 2005. A) THE LIGHT AND DARK BLUE REPRESENT RESPECTIVELY ACCRETION OF 10 TO 20 CM AND MORE THAN 20 CM. THE RED COLOUR CHARACTERISES EROSION IN THE SAME COLOUR CODING. B) MAXIMUM AND MINIMUM BEACH PROFILES WITH THE SWEEP ZONE INDICATED BY THE SHADING.....	125
FIGURE 4-12 BEACH PROFILE EVOLUTION IN THE RECYCLED SEDIMENT AREA DURING PHASE 1 OF THE SURVEY PERIOD, OCTOBER 28 TH TO OCTOBER 31 ST , 2005.....	127
FIGURE 4-13 BEACH PROFILE EVOLUTION IN THE RECYCLED SEDIMENT AREA DURING PHASE 2 OF THE SURVEY PERIOD, OCTOBER 31 ST TO NOVEMBER 06 TH , 2005.	128
FIGURE 4-14 BEACH PROFILE EVOLUTION IN THE RECYCLED SEDIMENT AREA DURING PHASE 3 OF THE SURVEY PERIOD, NOVEMBER 06 TH TO NOVEMBER 11 TH , 2005.	129
FIGURE 4-15 BEACH PROFILE EVOLUTION FROM THE LOWER PART OF THE MIXED SEDIMENT BEACH ONTO THE SANDY PLATFORM IN THE RECYCLED AREA DURING THE SURVEY PERIOD, OCTOBER 28 TH TO NOVEMBER 11 TH , 2005.	133
FIGURE 4-16 SURFACE PLOT SHOWING THE TEMPORAL VARIATION IN BEACH FACE MORPHOLOGY IN THE "NATURAL" AREA BASED ON LOW TIDE SURVEYS AT CAYEUX-SUR-MER FROM OCTOBER 28 TH TO NOVEMBER 11 TH , 2005. A) THE LIGHT AND DARK BLUE REPRESENT RESPECTIVELY ACCRETION OF 10 TO 20 CM AND MORE THAN 20 CM. THE RED COLOUR CHARACTERISES EROSION IN THE SAME COLOUR CODING. B) MAXIMUM AND MINIMUM BEACH PROFILES WITH THE SWEEP ZONE INDICATED BY THE SHADING.....	135
FIGURE 4-17 BEACH PROFILE EVOLUTION IN THE "NATURAL" AREA DURING PHASE 1 OF THE SURVEY PERIOD, OCTOBER 28 TH TO NOVEMBER 4 TH 2005..	137
FIGURE 4-18 BEACH PROFILE EVOLUTION IN THE "NATURAL" AREA DURING PHASE 2 OF THE SURVEY PERIOD, NOVEMBER 4 TH TO NOVEMBER 28 TH , 2005..	142

FIGURE 4-19 BEACH PROFILE EVOLUTION FROM THE LOWER PART OF THE MIXED SEDIMENT BEACH ONTO THE SANDY PLATFORM IN THE “NATURAL” AREA DURING THE SURVEY PERIOD, OCTOBER 28 TH TO NOVEMBER 11 TH , 2005.....	144
FIGURE 4-20 LOCATION OF THE BEACH PROFILES, BIRLING GAP.	146
FIGURE 4-21 SURFACE PLOT SHOWING THE TEMPORAL VARIATION IN BEACH FACE MORPHOLOGY BASED ON LOW TIDE SURVEYS ON THE WESTERN PART OF BIRLING GAP FROM MARCH 20 TH TO MARCH 24 TH , 2006. A) THE LIGHT AND DARK BLUE REPRESENT RESPECTIVELY ACCRETION OF 10 TO 20 CM AND MORE THAN 20 CM. THE RED COLOUR CHARACTERISES EROSION IN THE SAME COLOUR CODING. B) MAXIMUM AND MINIMUM BEACH PROFILES WITH THE SWEEP ZONE INDICATED BY THE SHADING.	148
FIGURE 4-22 BEACH PROFILE EVOLUTION OF THE SURVEY PERIOD, MARCH 20 TH TO MARCH 24 TH 2005 AT BIRLING GAP..	149
FIGURE 4-23 SURFACE PLOT SHOWING THE TEMPORAL VARIATION IN BEACH FACE MORPHOLOGY BASED ON LOW TIDE SURVEYS ON THE WESTERN PART OF BIRLING GAP FROM MAY 19 TH TO MAY 23 RD , 2006. A) THE LIGHT AND DARK BLUE REPRESENT RESPECTIVELY ACCRETION OF 10 TO 20CM AND MORE THAN 20CM. THE RED COLOUR CHARACTERISES EROSION IN THE SAME COLOUR CODING. B) MAXIMUM AND MINIMUM BEACH PROFILES WITH THE SWEEP ZONE INDICATED BY THE SHADING.	153
FIGURE 4-24 BEACH BEACH PROFILE EVOLUTION OF THE SURVEY PERIOD, MAY 19 TH TO MAY 23 RD 2005 AT BIRLING GAP.	154
FIGURE 4-25 SURFACE PLOT SHOWING THE TEMPORAL VARIATION IN BEACH FACE MORPHOLOGY BASED ON LOW TIDE SURVEYS ON THE WESTERN PART OF BIRLING GAP FROM DECEMBER 14 TH TO DECEMBER 19 TH , 2006. (A) THE LIGHT AND DARK BLUE REPRESENT RESPECTIVELY ACCRETION OF 10 TO 20CM AND MORE THAN 20CM. THE RED COLOUR CHARACTERISES EROSION IN THE SAME COLOUR CODING (B) MAXIMUM AND MINIMUM BEACH PROFILES WITH THE SWEEP ZONE INDICATED BY THE SHADING.	157
FIGURE 4-26 BEACH PROFILE EVOLUTION DURING PHASE 1 OF THE SURVEY PERIOD, DECEMBER 14 TH TO DECEMBER 19 TH 2005 AT BIRLING GAP.....	158
FIGURE 4-27 BEACH PROFILE EVOLUTION DURING PHASE 2 OF THE SURVEY PERIOD, DECEMBER 14 TH TO DECEMBER 19 TH 2005 AT BIRLING GAP.....	159
FIGURE 4-28 BEACH PROFILE EVOLUTION DURING THE SUMMER 2004 AT BIRLING GAP IN PROXIMITY OF THE ACCESS STEPS.	163
FIGURE 4-29 BEACH PROFILE EVOLUTION DURING THE WINTER 2004/2005 AT BIRLING GAP IN PROXIMITY OF THE ACCESS STEPS.	164
FIGURE 4-30 BEACH PROFILE EVOLUTION DURING THE SUMMER 2005 AT BIRLING GAP IN PROXIMITY OF THE ACCESS STEPS.	165
FIGURE 4-31 BEACH PROFILE EVOLUTION DURING THE WINTER 2005/2006 AT BIRLING GAP IN PROXIMITY OF THE ACCESS STEPS.	166
FIGURE 4-32 BEACH PROFILE EVOLUTION DURING THE SUMMER 2006 AT BIRLING GAP IN PROXIMITY OF THE ACCESS STEP.	167
FIGURE 4-33 PLOT OF THE DIFFERENCE BETWEEN THE MAXIMUM AND THE MINIMUM ELEVATION RECORDED ACROSS THE MIDDLE BEACH PROFILE (AT THE STEPS) OVER THE TWO YEAR SURVEY AT BIRLING GAP.....	168

FIGURE 4-34 PLOT OF THE DIFFERENCE BETWEEN THE MAXIMUM AND THE MINIMUM ELEVATION RECORDED ACROSS THE BEACH PROFILE AT THE STEPS PER SEASON AT BIRLING GAP.	168
FIGURE 4-35 THE BEACH AT CAYEUX-SUR-MER, NOVEMBER 6 TH . A) SEDIMENT SURFACE. B) INTERNAL SEDIMENT DISTRIBUTIONS IN THE RECYCLED AREA.	176
FIGURE 4-36 REPRESENTATION OF THE SURFACE GRAIN SIZE DISTRIBUTION OBSERVED ON BOTH PROFILES SURVEYED AT CAYEUX-SUR-MER ON A TIDAL BASIS. THE PROFILES ARE TWINED FOR EACH LOW TIDE. THE ABOVE GRAIN SIZE DISTRIBUTION LINE REPRESENTS THE PROFILE LOCATED IN THE NATURAL AREA AND THE BELOW THE PROFILE LOCATED IN THE RECYCLED AREA.	177
FIGURE 4-37 EVOLUTION OF THE BEACH VOLUME OVER TIME IN ASSOCIATION TO THE MEAN WAVE APPROACH. THE CIRCLES REPRESENT THE SEDIMENT VOLUME MEASURED FOR EVERY MONTH, THE PLAIN BLACK LINE THE MEAN WAVE APPROACH AND THE DASHED RED BOXES REPRESENT THE SEASONS.	179
FIGURE 4-38 THE BEACH AT BIRLING GAP BEFORE, DURING AND AFTER THE STORMY PERIOD OF DECEMBER 2004/JANUARY 2005. THE RED ARROWS MARK THE SAME LOCATION ON THE PICTURES.	180

CHAPTER 5

FIGURE 5-1 PROFILE MORPHOLOGIES AT THE START AND END OF THE SURVEY PERIOD AT CAYEUX-SUR-MER.	188
FIGURE 5-2 PROFILE MORPHOLOGIES AT THE START AND END OF THE SURVEY PERIOD AT BIRLING GAP. A) IN MARCH 2006. B) IN MAY 2006. C) IN DECEMBER 2006.	189
FIGURE 5-3 PLOT OF THE AVERAGE ACTIVE LAYER THICKNESS OBSERVED AT IDENTICAL CROSS-SHORE LOCATION ON THE VARIOUS PROFILES SURVEYED. THE ASSOCIATED ERROR BARS REPRESENT THE STANDARD DEVIATION BETWEEN THE MEASUREMENTS. A) AT CAYEUX-SUR-MER IN OCTOBER/NOVEMBER 2005. B) AT BIRLING GAP IN MARCH 2006. C) AT BIRLING GAP IN MAY 2006. D) AT BIRLING GAP IN DECEMBER 2006.	190
FIGURE 5-4 EXAMPLES OF PROFILE EVOLUTION AND ACTIVE LAYER MEASURED DURING THE SURVEY PERIOD AT CAYEUX-SUR-MER. THE BLACK ARROWS SHOW THE LOCATION OF THE ACTIVE LAYER MEASUREMENTS. NOTE THAT THE ELEVATION IS REFERRED AS ABOVE HYDROGRAPHIC DATUM (HD, THE FRENCH HYDROGRAPHIC DATUM CORRESPONDS TO THE LOWEST ASTRONOMICAL TIDE LEVEL).	193
FIGURE 5-5 EXAMPLES OF PROFILE EVOLUTION AND ACTIVE LAYER MEASURED DURING THE SURVEY PERIOD AT BIRLING GAP. THE BLACK ARROWS SHOW THE LOCATION OF THE ACTIVE LAYER MEASUREMENTS. NOTE THAT THE ELEVATION IS DISPLAYED AS IN THE BRITISH NATIONAL GRID REFERENCE SYSTEM OSGB36 (ORDNANCE SURVEY GREAT BRITAIN 1936).	194
FIGURE 5-6 ACTIVE LAYER AND TOPOGRAPHIC CHANGES DURING THE 2005 WINTER SURVEY PERIOD AT CAYEUX-SUR-MER FOR ONE PROFILE (TRANSECT 2): A) UPPER, B) UPPER-MIDDLE, C) LOWER-MIDDLE AND D) LOWER BEACH. THE PLAIN BLACK LINE SHOWS THE TOPOGRAPHIC CHANGES RECORDED BY THE D-GPS AND THE DASHED BLACK LINES SHOW THE MARGIN ERROR (+/- 5 CM). PEBBLE COLUMNS USED TO MEASURE ACTIVE LAYER VARIATIONS ARE SHOWN BY THE VERTICAL LINES OF SYMBOLS. FOR EXAMPLE, ON THE UPPER BEACH, THE FIRST COLUMN DEPLOYED (AFTERNOON OCTOBER 28 TH ; WHITE SQUARES) REMAINED INTACT OVER THE FIRST FOUR TIDES. TO KEEP PACE WITH A TOPOGRAPHIC ELEVATION OF 18 CM ON THE FIFTH TIDE, NEW PEBBLES WERE ADDED (AFTERNOON OCTOBER 30 TH ; WHITE TRIANGLES).	

ON THE SIXTH TIDE A FALL IN BEACH ELEVATION OBLITERATED THE EXISTING COLUMN AND IT WAS REPLACED (BLACK XS). EACH SUBSEQUENT ADDITION OF NEW PEBBLES OR COMPLETE NEW COLUMN IS SHOWN BY DIFFERENT SYMBOLS. FOR EXAMPLE, ACCRETION BETWEEN THE AFTERNOON OF NOVEMBER 4 TH AND THE NEXT MORNING MEANT THAT A COMPLETE NEW COLUMN WAS INSTALLED ON THE MORNING OF NOVEMBER 5 TH . VARIATIONS IN PEBBLE COLUMNS DEPLOYED IN THE REMAINDER OF THE BEACH (UPPER-MIDDLE, LOWER-MIDDLE AND LOWER) ARE ILLUSTRATED IN THE SAME WAY.....	197
FIGURE 5-7 ACTIVE LAYER AND TOPOGRAPHIC CHANGES DURING THE SURVEY PERIODS AT BIRLING GAP FOR THE EASTERN PROFILE IN MARCH 2006: A) UPPER, B) UPPER-MIDDLE, C) LOWER-MIDDLE AND D) LOWER BEACH.....	197
FIGURE 5-8 PLOT OF THE MIXING DEPTH AS A FUNCTION OF THE INDEX OF SAMBROOK-SMITH ET AL. (1997). EACH GRAPH REPRESENTS THE DATA COLLECTED AT SPECIFIC LOCATION ON THE BEACH AT CAYEUX-SUR-MER: A) UPPER BEACH, B) MIDDLE, C) LOWER BEACH. EACH POINT IS ANNOTATED WITH THE TIDAL MAXIMUM SIGNIFICANT WAVE HEIGHT ($H_{ST, MAX.}$) OF THE TIDE PRECEDING THE COLUMN SURVEY.....	201
FIGURE 5-9 CORRELATION OF THE AVERAGE DEPTH OF MIXING AND THE TIDAL MAXIMUM SIGNIFICANT WAVE HEIGHT AT THE: A) UPPER, B) MIDDLE, C) LOWER PART OF THE MIXED BEACH AT CAYEUX-SUR-MER. N IS THE TOTAL NUMBER OF MEASUREMENTS WITH AN EXACT VALUE COLLECTED FOR ALL PROFILES. APPROXIMATE VALUES SHOWN IN APPENDIX IV (TABLES IV-1 TO IV-4) ARE NOT USED ON THE GRAPHS. PLEASE NOTE THAT HERE AGAIN IT WAS PREFERRED TO REGROUP THE DATA COLLECTED ON THE UPPER MIDDLE, MIDDLE AND LOWER MIDDLE AT CAYEUX-SUR-MER IN ONE SINGLE MIDDLE SECTION BECAUSE OF THE SMALL NUMBER OF EXACT VALUES COLLECTED IN BOTH THE UPPER MIDDLE AND LOWER MIDDLE SECTIONS OF THE BEACH.	205
FIGURE 5-10 CORRELATION OF THE AVERAGE DEPTH OF MIXING AND THE TIDAL MAXIMUM SIGNIFICANT WAVE HEIGHT AT THE: A) UPPER, B) UPPER MIDDLE, C) LOWER MIDDLE, D) LOWER PART OF THE MIXED BEACH AT BIRLING GAP. N IS THE TOTAL NUMBER OF MEASUREMENTS COLLECTED FOR ALL PROFILES AND USED LATER TO DETERMINE THE TIDAL AVERAGE DEPTH OF MIXING FOR EACH RESPECTIVE ACROSS-SHORE LOCATION. N ONLY CONCERNS MEASUREMENTS WITH AN EXACT VALUE. APPROXIMATE VALUES SHOWN IN APPENDIX IV ON TABLE IV-5 TO IV-10 ARE NOT USED ON THE GRAPHS. .	206
FIGURE 5-11 PLOT OF THE DEPTH OF DISTURBANCE AND THE WAVE DIRECTION AT THE: A) UPPER, B) MIDDLE, C) LOWER PART OF THE MIXED BEACH AT CAYEUX-SUR-MER.	207
FIGURE 5-12 PLOT OF THE DEPTH OF DISTURBANCE AND THE WAVE DIRECTION AT THE: A) UPPER, B) UPPER MIDDLE, C) LOWER MIDDLE, D) LOWER PART OF THE MIXED BEACH AT BIRLING GAP.....	208
FIGURE 5-13 PLOT OF THE ONSHORE WAVE DIRECTION REFERRED TO THE MAGNETIC NORTH AS A FUNCTION OF THE SIGNIFICANT WAVE HEIGHT (H_s) SAMPLED AT CAYEUX-SUR-MER DURING OCTOBER-NOVEMBER 2005.	209
FIGURE 5-14 PLOT OF THE ONSHORE WAVE DIRECTION AS A FUNCTION OF THE SIGNIFICANT WAVE HEIGHT (H_s) SAMPLED AT BIRLING GAP.	209
FIGURE 5-15 CORRELATION BETWEEN DEPTH OF MIXING AND THE PEAK PERIOD, T_p , AT CAYEUX-SUR-MER. N IS TOTAL THE NUMBER OF MEASUREMENTS COLLECTED AND REPRESENTED ON THE GRAPH. N INCLUDES ONLY MEASUREMENTS WITH AN EXACT VALUE. APPROXIMATE VALUES SHOWN IN APPENDIX IV ON TABLES IV-1 TO IV-4 ARE NOT REPRESENTED ON THE GRAPHS.....	210
FIGURE 5-16 CORRELATION BETWEEN DEPTH OF MIXING AND THE PEAK PERIOD, T_p , AT BIRLING GAP. N IS THE TOTAL NUMBER OF MEASUREMENTS COLLECTED AND REPRESENTED ON THE GRAPH. N INCLUDES ONLY MEASUREMENTS WITH AN EXACT	

VALUE. APPROXIMATE VALUES SHOWN IN APPENDIX IV ON TABLES IV-5 TO IV-10 ARE NOT REPRESENTED ON THE GRAPHS.	211
FIGURE 5-17 EXAMPLES OF PROFILE EVOLUTION AND ACTIVE LAYER MEASURED SHOWING THE WAVE BREAKING AREA DURING THE SURVEY PERIOD AT CAYEUX-SUR-MER. THE BLACK ARROWS SHOW THE LOCATION OF THE ACTIVE LAYER MEASUREMENTS.	216
FIGURE 5-18 EXAMPLES OF PROFILE EVOLUTION AND ACTIVE LAYER MEASURED SHOWING THE WAVE BREAKING AREA DURING THE SURVEY PERIOD AT BIRLING GAP. THE BLACK ARROWS SHOW THE LOCATION OF THE ACTIVE LAYER MEASUREMENTS.	217
FIGURE 5-19 FEEDBACK LOOP BETWEEN THE HYDRODYNAMIC CONDITIONS, THE GRAIN SIZE AND THE MIXING DEPTH.	220
 CHAPTER 6	
FIGURE 6-1 WAVE CONDITIONS MEASURED WITH AN S4 ON THE FORESHORE OFF THE TERMINAL GROUYNE AT CAYEUX-SUR-MER. DATA WERE CUT OFF FOR PERIODS WHEN THE S4 WAS NOT COVERED BY MORE THAN 1.5 M OF WATER. THIS CORRESPONDS TO THE LEVEL OF THE BEACH STEP. THE MEAN ANGLE OF WAVE APPROACH TO THE COAST IS RELATIVE TO THE COAST ORIENTATION (APPROXIMATELY N205°). THEREFORE, VALUES ABOVE 90° CORRESPOND TO WAVES COMING FROM NORTHERLY DIRECTIONS WHEREAS VALUES UNDER 90° CORRESPOND TO SOUTHERLY DIRECTIONS.	243
FIGURE 6-2 TRACER PEBBLE DISPERSION RECOVERED ONE TIDE AFTER DEPLOYMENT ON THE MORNING OF DECEMBER 13 TH , 2004. THE BLACK CROSS MARKS THE LOCATION OF THE INJECTION POINT OF THE TRACER PEBBLES ON DECEMBER 12 TH , 2004. EACH BLUE TRIANGLE REPRESENTS A TRACER PEBBLE. THE BIG BLUE DISK SHOWS THE LOCATION OF THE MOUNT OF PEBBLES THAT STAYED STILL OR MOVED VERY LITTLE.	247
FIGURE 6-3 TRACER PEBBLE DISPERSION RECOVERED ONE TIDE AFTER DEPLOYMENT ON THE AFTERNOON OF DECEMBER 13 TH , 2004. THE BLACK CROSS MARKS THE LOCATION OF THE INJECTION POINT OF THE TRACER PEBBLES ON THE MORNING OF DECEMBER 13 TH , 2004. EACH BLUE TRIANGLE REPRESENTS A TRACER PEBBLE.	247
FIGURE 6-4 TRACER PEBBLE DISPERSION RECOVERED TWO TIDES AFTER DEPLOYMENT ON DECEMBER 15 TH , 2004. THE BLACK CROSS MARKS THE LOCATION OF THE INJECTION POINT OF THE TRACER PEBBLES ON DECEMBER 14 TH , 2004. EACH BLUE TRIANGLE REPRESENTS A TRACER PEBBLE.	248
FIGURE 6-5 TRACER PEBBLE DISPERSION RECOVERED TWO TIDES AFTER DEPLOYMENT ON DECEMBER 16 TH , 2004. THE BLACK CROSS MARKS THE LOCATION OF THE INJECTION POINT OF THE TRACER PEBBLES ON DECEMBER 15 TH , 2004. EACH BLUE TRIANGLE REPRESENTS A TRACER PEBBLE.	249
FIGURE 6-6 TRACER PEBBLE DISPERSION RECOVERED TWO TIDES AFTER DEPLOYMENT ON DECEMBER 17 TH , 2004. THE BLACK CROSS MARKS THE LOCATION OF THE INJECTION POINT OF THE TRACER PEBBLES ON DECEMBER 16 TH , 2004.	249
FIGURE 6-7 CHANGES IN BEACH ELEVATION BETWEEN DECEMBER 12 TH AND DECEMBER 17 TH 2004 AT CAYEUX-SUR-MER.	253
FIGURE 6-8 GRID SYSTEM USED TO CALCULATE THE BEACH VOLUME CHANGES FROM THE SURVEY AT CAYEUX-SUR-MER IN DECEMBER 2004.	254
FIGURE 6-9 NET BEACH VOLUME CHANGES PER TIDE MEASURED IN EACH CELL BETWEEN DECEMBER 12 TH AND DECEMBER 17 TH 2004 AT CAYEUX-SUR-MER.	255

FIGURE 6-10 MOVEMENTS OF THE TRACER PEBBLES DEPLOYED ON OCTOBER 28 TH , 2005.	264
FIGURE 6-11 MOVEMENT OF TRACER PEBBLES DEPLOYED ON NOVEMBER 3 RD , 2005.	266
FIGURE 6-12 MOVEMENT OF TRACER PEBBLES DEPLOYED ON OCTOBER 31 ST , 2005.	268
FIGURE 6-13 MOVEMENT OF TRACER PEBBLES DEPLOYED ON NOVEMBER 7 TH , 2005.	270
FIGURE 6-14 MOVEMENT OF TRACER PEBBLES DEPLOYED ON NOVEMBER 8 TH , 2005.	272
FIGURE 6-15 PHOTO OF THE GENTLE CUSPS ON NOVEMBER 8 TH	275
FIGURE 6-16 CHANGES IN BEACH ELEVATION BETWEEN OCTOBER 28 TH AND NOVEMBER 11 TH 2005 AT CAYEUX-SUR-MER.	277
FIGURE 6-17 GRID SYSTEM USED TO DETERMINE THE BEACH VOLUME CHANGE AT CAYEUX-SUR-MER BETWEEN OCTOBER 28 TH TO NOVEMBER 11 TH	280
FIGURE 6-18 NET VOLUME CHANGE ($Q_{L\text{NET}}$) MEASURED FOR EACH CELL BETWEEN TWO CONSECUTIVE SURVEYS AT CAYEUX IN OCTOBER/NOVEMBER 2005. THIS FIGURE IS A COMPILATION OF THE SURVEYS THAT PRESENTED OVERALL ACCRETION ON THE SURVEYED AREA FROM ONE SURVEY TO THE FOLLOWING.	281
FIGURE 6-19 NET VOLUME CHANGE ($Q_{L\text{NET}}$) MEASURED FOR EACH CELL BETWEEN TWO CONSECUTIVE SURVEYS AT CAYEUX IN OCTOBER/NOVEMBER 2005. THIS FIGURE IS A COMPILATION OF THE SURVEYS THAT PRESENTED OVERALL EROSION ON THE SURVEYED AREA FROM ONE SURVEY TO THE FOLLOWING.	282
FIGURE 6-20 NET VOLUME CHANGES MEASURED IN EACH CELL DURING THE TIME PERIOD OF THE SURVEY, BETWEEN OCTOBER 28 TH AND NOVEMBER 11 TH 2005 AT CAYEUX-SUR-MER.	285
FIGURE 6-21 MOVEMENT OF TRACER PEBBLES OBSERVED AFTER ONE TIDE DEPLOYMENT ON MARCH 22 ND , 2006. THE BLACK CROSS MARKS THE LOCATIONS OF THE INJECTION POINTS. EACH TRIANGLE REPRESENTS INDIVIDUAL TRACER PEBBLES RECOVERED AFTER ONE TIDE. THE DISKS MARK THE LOCATION OF THE CENTROIDS. PEBBLES ARE COLOUR CODED: ...	290
FIGURE 6-22 MOVEMENT OF TRACER PEBBLES OBSERVED AFTER ONE TIDE DEPLOYMENT ON MARCH 25 TH , 2006. THE BLACK CROSS MARKS THE LOCATIONS OF THE INJECTION POINTS. EACH TRIANGLE REPRESENTS INDIVIDUAL TRACER PEBBLES RECOVERED AFTER ONE TIDE. THE DISKS MARK THE LOCATION OF THE CENTROIDS. PEBBLES ARE COLOUR CODED: ...	291
FIGURE 6-23 CHANGES IN BEACH ELEVATION BETWEEN MARCH 20 TH AND MARCH 25 TH 2006 AT BIRLING GAP.	295
FIGURE 6-24 GRID SYSTEM USED TO CALCULATE THE BEACH VOLUME CHANGES AT BIRLING GAP IN DECEMBER 2004.	296
FIGURE 6-25 NET VOLUME CHANGE ($Q_{L\text{NET}}$) MEASURED FOR EACH CELL BETWEEN TWO CONSECUTIVE SURVEYS AT BIRLING GAP IN MARCH 2006. THE LEGEND GIVES THE DATE AND TIME OF THE LATER OF THE TWO SURVEYS. AN INCREMENT OF 100 m ³ IS USED BETWEEN THE RESULTS OBTAINED FROM EACH DIGITAL MAP. THE DASHED BLACK LINES REPRESENT EQUILIBRIUM BETWEEN EROSION AND ACCRETION (0 m ³ NET VOLUME CHANGE) FOR THE ASSOCIATED SURVEY LINE.	298
FIGURE 6-26 NET VOLUME CHANGES MEASURED IN EACH CELL DURING THE TIME PERIOD OF THE SURVEY, BETWEEN MARCH 20 TH AND MARCH 25 TH 2006 AT BIRLING GAP.	299
FIGURE 6-27 MOVEMENT OF TRACER PEBBLES DEPLOYED ON MAY 19 TH , 2006.	303
FIGURE 6-28 MOVEMENT OF TRACER PEBBLES DEPLOYED ON MAY 20 TH , 2006.	305
FIGURE 6-29 MOVEMENT OF TRACER PEBBLES DEPLOYED ON MAY 22 ND , 2006.	306
FIGURE 6-30 CHANGES IN BEACH ELEVATION BETWEEN MAY 19 ^H AND MAY 22 ^{SD} 2006 AT BIRLING GAP.	310
FIGURE 6-31 NET VOLUME CHANGE ($Q_{L\text{NET}}$) MEASURED FOR EACH CELL BETWEEN TWO CONSECUTIVE SURVEYS AT BIRLING GAP IN MAY 2006. THE LEGEND GIVES THE DATE AND TIME OF THE LATER OF THE TWO SURVEYS. AN INCREMENT OF	

100 m ³ IS USED BETWEEN THE RESULTS OBTAINED FROM EACH DIGITAL MAP. THE DASHED BLACK LINES REPRESENT EQUILIBRIUM BETWEEN EROSION AND ACCRETION (0 m ³ NET VOLUME CHANGE) FOR THE ASSOCIATED SURVEY LINE.	312
FIGURE 6-32 NET VOLUME CHANGES MEASURED IN EACH CELL DURING THE TIME PERIOD OF THE SURVEY, BETWEEN MAY 19 TH AND MAY 22 ND 2006 AT BIRLING GAP.	313
FIGURE 6-33 MOVEMENT OF TRACER PEBBLES DEPLOYED ON DECEMBER 14 TH , 2006.....	319
FIGURE 6-34 MOVEMENT OF TRACER PEBBLES DEPLOYED ON DECEMBER 16 TH , 2006.....	320
FIGURE 6-35 MOVEMENT OF TRACER PEBBLES DEPLOYED ON DECEMBER 17 TH , 2006.....	321
FIGURE 6-36 MOVEMENT OF TRACER PEBBLES DEPLOYED ON DECEMBER 18 TH , 2006.....	322
FIGURE 6-37 CHANGES IN BEACH ELEVATION BETWEEN DECEMBER 14 TH AND DECEMBER 19 TH 2006 AT BIRLING GAP.	325
FIGURE 6-38 NET VOLUME CHANGE ($Q_{L\text{ NET}}$) MEASURED FOR EACH CELL BETWEEN TWO CONSECUTIVE SURVEYS AT BIRLING GAP IN DECEMBER 2006. THE LEGEND GIVES THE DATE AND TIME OF THE LATER OF THE TWO SURVEYS. AN INCREMENT OF 100 m ³ IS USED BETWEEN THE RESULTS OBTAINED FROM EACH DIGITAL MAP. THE DASHED BLACK LINES REPRESENT EQUILIBRIUM BETWEEN EROSION AND ACCRETION (0 m ³ NET VOLUME CHANGE) FOR THE ASSOCIATED SURVEY LINE.	326
FIGURE 6-39 NET VOLUME CHANGES MEASURED IN EACH CELL DURING THE TIME PERIOD OF THE SURVEY, BETWEEN DECEMBER 14 TH AND DECEMBER 19 TH 2006 AT BIRLING GAP.....	328
FIGURE 6-40 LOCATION OF EACH TRACER RECOVERED OVER THE SURVEY PERIOD FROM OCTOBER 2004 TO MAY 2005...	330
FIGURE 6-41 OFFSHORE WAVE CONDITIONS COLLECTED AT RUSTINGTON FOR THE SURVEY PERIOD BETWEEN OCTOBER 2004 AND MAY 2005.	331
FIGURE 6-42 QUARTZITE PEBBLE TRANSPORT OBSERVED OVER THE SURVEY PERIOD FROM OCTOBER 2004 TO MAY 2005. EACH COLOURED LINE AND DATE REPRESENTS THE TRAJECTORY AND THE TIME OF THE RECOVERY OF ONE TRACER COBBLE.	332

CHAPTER 7

FIGURE 7-1 ESTIMATES OF SHINGLE TRANSPORT EFFICIENCY BASED ON THE SHOREHAM DATA (BRAY ET AL., 1996).	351
FIGURE 7-2 K DERIVED FROM COARSE-GRAINED TRACER AND TRAP DATA (VAN WELLEN ET AL., 2000).	352
FIGURE 7-3 CORRELATIONS BETWEEN THE LONGSHORE ENERGY FLUX (P_L) AND THE NET LONGSHORE SEDIMENT TRANSPORT MEASURED USING TRACER DATA ASSOCIATED WITH THE DEPTH OF DISTURBANCE MEASUREMENTS OR THE DEPTH OF THE DEEPEST TRACERS AT CAYEUX-SUR-MER. ALL THE DATA COLLECTED AT CAYEUX IN DECEMBER 2004 AND OCTOBER/NOVEMBER 2005 IS REPRESENTED HERE.	355
FIGURE 7-4 CORRELATIONS BETWEEN THE LONGSHORE ENERGY FLUX (P_L) AND THE NET LONGSHORE SEDIMENT TRANSPORT MEASURED USING TRACER DATA ASSOCIATED TO THE DEPTH WITH DISTURBANCE MEASUREMENTS OR THE DEPTH OF THE DEEPEST TRACERS AT CAYEUX-SUR-MER. ONLY TRACER PEBBLE RECOVERY RATES SUPERIOR TO 60% ARE REPRESENTED HERE.	356
FIGURE 7-5 CORRELATIONS BETWEEN THE LONGSHORE ENERGY FLUX (P_L) AND THE NET LONGSHORE SEDIMENT TRANSPORT (Q_L) MEASURED USING DGPS TOPOGRAPHIC SURVEY AT CAYEUX-SUR-MER IN OCTOBER/NOVEMBER 2005.	359
FIGURE 7-6 CORRELATIONS BETWEEN THE LONGSHORE ENERGY FLUX (P_{LS}) AND THE NET LONGSHORE SEDIMENT TRANSPORT MEASURED USING TRACER DATA ASSOCIATED WITH THE DEPTH OF DISTURBANCE MEASUREMENTS OR THE DEPTH OF THE	

DEEPEST TRACERS AT BIRLING GAP. ALL THE DATA COLLECTED AT BIRLING GAP IN MARCH, MAY AND DECEMBER 2006 IS REPRESENTED HERE.	360
FIGURE 7-7 CORRELATIONS BETWEEN THE LONGSHORE ENERGY FLUX (P_L) AND THE MEAN NETLONGSHORE SEDIMENT TRANSPORT MEASURED USING TRACER DATA ASSOCIATED WITH THE ACTIVE LAYER MEASUREMENTS OR JUST THE DEPTH OF THE DEEPEST TRACER FOUND ON THE APPROPRIATE DAY AT CAYEUX-SUR-MER. ONLY TRACER PEBBLE RECOVERY RATES SUPERIOR TO 60% ARE REPRESENTED HERE.	361
FIGURE 7-8 CORRELATIONS BETWEEN THE LONGSHORE ENERGY FLUX (P_L) AND THE NET VOLUME CHANGES (Q_s) DETERMINED BY DGPS TOPOGRAPHIC SURVEYS AT BIRLING GAP.	362
FIGURE 7-9 ESTIMATION OF K AT CAYEUX-SUR-MER.	365
FIGURE 7-10 ESTIMATION OF K AT BIRLING GAP.	365
FIGURE 7-11 ESTIMATION OF K USING THE DATA POINT COLLECTED AT BOTH SITES.	366

Appendices

FIGURE I-2 MOULDS	395
FIGURE I-1 SYNTHETIC TRACER PEBBLE.	395
FIGURE II-1 GRAIN SIZE CHARACTERISTICS OBSERVED AT CAYEUX-SUR-MER AND BIRLING GAP DURING THE TIME OF THE EXPERIMENTS.	398
FIGURE V-1 TRACER PEBBLE DISPERSION RECOVERED ONE TIDE AFTER DEPLOYMENT ON THE MORNING OF DECEMBER 14 TH , 2004. THE BLACK CROSS MARKS THE LOCATION OF THE INJECTION POINT OF THE TRACER PEBBLES ON THE AFTERNOON OF DECEMBER 13 TH , 2004. EACH BLUE TRIANGLE REPRESENTS A TRACER PEBBLE.	438
FIGURE V-2 TRACER PEBBLE DISPERSION RECOVERED ONE TIDE AFTER DEPLOYMENT ON THE AFTERNOON OF DECEMBER 14 TH , 2004. THE BLACK CROSS MARKS THE LOCATION OF THE INJECTION POINT OF THE TRACER PEBBLES ON THE MORNING OF DECEMBER 14 TH , 2004. EACH BLUE TRIANGLE REPRESENTS A TRACER PEBBLE.	438
FIGURE VI-1 MOVEMENTS OF THE TRACER PEBBLES DEPLOYED ON OCTOBER 29 TH , 2005.	439
FIGURE VI-2 MOVEMENTS OF THE TRACER PEBBLES DEPLOYED ON OCTOBER 30 TH , 2005.	440
FIGURE VI-3 MOVEMENTS OF THE TRACER PEBBLES DEPLOYED ON NOVEMBER 1 ST , 2005.	441
FIGURE VI-4 MOVEMENTS OF THE TRACER PEBBLES DEPLOYED ON NOVEMBER 2 ND , 2005.	442
FIGURE VI-5 MOVEMENTS OF THE TRACER PEBBLES DEPLOYED ON NOVEMBER 4 TH , 2005.	443
FIGURE VI-6 MOVEMENTS OF THE TRACER PEBBLES DEPLOYED ON NOVEMBER 5 TH , 2005.	444
FIGURE VI-7 MOVEMENTS OF THE TRACER PEBBLES DEPLOYED ON NOVEMBER 6 TH , 2005.	445
FIGURE VI-8 MOVEMENTS OF THE TRACER PEBBLES DEPLOYED ON NOVEMBER 9 TH , 2005.	446
FIGURE VII-1 MOVEMENTS OF THE TRACER PEBBLES DEPLOYED ON MARCH 20 TH , 2006.	447
FIGURE VII-2 MOVEMENTS OF THE TRACER PEBBLES DEPLOYED ON MARCH 23 TH , 2006. SCATTERING OBSERVED AFTER ONE TIDE. (ALL THE TRACERS WERE RECOVERED AFTER ONE TIDE).	448

List of Tables

CHAPTER 1

TABLE 1-1 CLASSIFICATION OF WAVE CONDITIONS USED THROUGHOUT THE THESIS.	24
---	----

CHAPTER 2

TABLE 2-1 FLINT CONTENT FOR FOUR SECTIONS OF THE SUSSEX CHALK CLIFFS (DORNBUSCH ET AL., 2006B).....	35
TABLE 2-2 SYNTHESIS OF THE COASTAL EROSION MEASUREMENTS OR ESTIMATES FROM AULT TO THE AMER SUD (BASED ON COSTA, 1997).	49

CHAPTER 3

TABLE 3-1 CRITERIA OF COMPARISON BETWEEN SYNTHETIC PEBBLES AND ALUMINIUM PEBBLES.	81
---	----

CHAPTER 5

TABLE 5-1 CORRELATION RELATIONSHIP BETWEEN $H_{ST, MAX}$ AND THE DEPTH OF DISTURBANCE AT CAYEUX-SUR-MER.	221
TABLE 5-2 CORRELATION RELATIONSHIP BETWEEN $H_{ST, MAX}$ AND THE DEPTH OF DISTURBANCE (Z_M) AT BIRLING GAP.	222

CHAPTER 6

TABLE 6-1 TRACER PEBBLE RECOVERY RATES AND MEAN DISTANCES TRAVELLED ONE TIDE AFTER DEPLOYMENT AT CAYEUX-SUR-MER, DECEMBER 2004. THE POSITIVE VALUE OF THE ALONGSHORE DISTANCES INDICATES THAT THE CENTROID OF THE PEBBLE SCATTERING IS LOCATED IN A DOWNDRIFT POSITION (I.E. NORTHWARD) FROM ITS INJECTION POINT. A NEGATIVE VALUE MEANS THAT ITS POSITION IS UPDRIFT FROM ITS INJECTION POINT. SIMILARLY, A POSITIVE VALUE OF THE ACROSS-SHORE TRAVELLED DISTANCE INDICATES THAT THE CENTROID IS LOCATED HIGHER UP ON THE BEACH PROFILE THAN ITS INJECTION AND VICE VERSA, A NEGATIVE VALUE INDICATES THAT THE CENTROID IS LOCATED ON LOWER AREAS ON THE BEACH PROFILE THAN ITS INJECTION POINT.	245
TABLE 6-2 CALCULATION OF THE NET LST RATES (Q_{LNET}) USING THE TRACER PEBBLES DISPERSION ON THE MIXED SEDIMENT BEACH AT CAYEUX-SUR-MER BETWEEN DECEMBER 12 TH AND DECEMBER 17 TH , 2004. NOTE THAT THE POSITIVE VALUE INDICATES SEDIMENT TRANSFER IN A DOWNDRIFT DIRECTION FROM THE INJECTION POINT (APPROXIMATELY	

NORTHWARD) WHEREAS NEGATIVE VALUES REFER TO SEDIMENT TRANSFER IN A UPDRIFT DIRECTION (APPROXIMATELY SOUTHWARD).....	251
TABLE 6-3 RECOVERY RATES AND DEPTH OF RECOVERY OF THE TRACERS DURING THE SURVEY PERIOD BETWEEN OCTOBER 28 TH AND NOVEMBER 11 TH . THE FIGURES IN BRACKETS CORRESPOND THE CUMULATIVE NUMBER OF TRACER PEBBLES RECOVERED IN TOTAL.....	258
TABLE 6-4 MEAN DISTANCES TRAVELLED BY THE TRACERS AFTER ONE TIDE DEPLOYMENT AT CAYEUX-SUR-MER IN OCTOBER–NOVEMBER 2005. POSITIVE VALUES OF THE ALONGSHORE DISTANCES INDICATE THAT THE CENTROID OF THE PEBBLE SCATTERING IS LOCATED IN A DOWNDRIFT POSITION FROM ITS INJECTION POINT. NEGATIVE VALUES INDICATE MOVEMENTS IN AN UPDRIFT DIRECTION. SIMILARLY, POSITIVE VALUES OF THE ACROSS-SHORE TRAVELLED DISTANCE INDICATE MOVEMENTS UP THE BEACH IN COMPARISON TO THE LOCATION OF THE INJECTION POINT, AND NEGATIVE VALUES INDICATE MOVEMENTS DOWN THE BEACH.....	261
TABLE 6-5 CALCULATION OF THE LST RATES USING TRACER PEBBLE DISPERSION ON MIXED SEDIMENT BEACH AT CAYEUX-SUR-MER BETWEEN OCTOBER 28 TH AND NOVEMBER 11 TH , 2005.	274
TABLE 6-6 BEACH NET VOLUME CHANGES SURVEYED ON CONSECUTIVE TIDES FOR THE ENTIRE SURVEY AREA AT CAYEUX-SUR-MER IN OCTOBER/NOVEMBER 2005.	283
TABLE 6-7 RECOVERY RATES AND DEPTH OF RECOVERY OF THE TRACERS DURING THE SURVEY PERIOD IN MARCH 2006 AT BIRLING GAP. THE FIGURES IN BRACKETS CORRESPOND TO THE CUMULATIVE NUMBER OF TRACER PEBBLES RECOVERED IN TOTAL.	287
TABLE 6-8 CHARACTERISTICS OF THE SEDIMENT TRANSPORT MEASURED USING THE TRACER PEBBLES AFTER ONE TIDE OF DEPLOYMENT AT BIRLING GAP IN MARCH 2006. NEGATIVE VALUES OF THE ALONGSHORE TRAVELLED DISTANCE INDICATE THAT THE PEBBLES MOVED IN A WESTWARD DIRECTION; POSITIVE VALUES INDICATE ALONGSHORE MOVEMENTS IN AN EASTWARD DIRECTION. NEGATIVE VALUES OF THE ACROSS-SHORE DISTANCE TRAVELLED INDICATE THAT THE PEBBLES MOVED DOWN THE BEACH AND POSITIVE VALUES INDICATE THAT THESE MOVEMENTS ARE UP THE BEACH.	289
TABLE 6-9 CALCULATION OF THE LST RATES USING TRACER PEBBLE DISPERSION ON MIXED SEDIMENT BEACH AT BIRLING GAP IN MARCH 2006. NOTE THAT IT WAS PREFERRED TO KEEP THE CONVENTIONAL SIGN CODE USED EARLIER TO DESCRIBE THE MEAN ALONGSHORE DIRECTIONS OF TRANSPORT WHEN DERIVING THE LST RATES SO THAT THE DIRECTION OF THE TRANSPORT IS STILL SHOWN.	292
TABLE 6-10 RECOVERY RATES AND DEPTH OF RECOVERY OF THE TRACERS EXPERIENCED DURING THE SURVEY PERIOD IN MAY 2006 AT BIRLING GAP. THE FIGURES IN BRACKETS CORRESPOND TO THE CUMULATIVE NUMBER OF TRACER PEBBLES RECOVERED IN TOTAL.....	300
TABLE 6-11 CHARACTERISTICS OF THE SEDIMENT TRANSPORT MEASURED USING THE TRACER PEBBLES AFTER 1 TIDE OF DEPLOYMENT AT BIRLING GAP IN MAY 2006. NEGATIVE VALUES OF THE ALONGSHORE TRAVELLED DISTANCE INDICATE THAT THE PEBBLES MOVED IN A WESTWARD DIRECTION; POSITIVE VALUES INDICATE ALONGSHORE MOVEMENTS IN AN EASTWARD DIRECTION. NEGATIVE VALUES OF THE ACROSS-SHORE TRAVELLED DISTANCE INDICATE THAT THE PEBBLES MOVED DOWN THE BEACH AND POSITIVE VALUES INDICATE THAT THESE MOVEMENTS ARE UP THE BEACH.	302
TABLE 6-12 CALCULATION OF THE LST RATES OBSERVED USING TRACER PEBBLES DISPERSION ON MIXED SEDIMENT BEACH AT BIRLING GAP IN MAY 2006. NOTE THAT IT WAS PREFERRED TO KEEP THE CONVENTIONAL SIGN CODE USED EARLIER TO	

DESCRIBE THE MEAN ALONGSHORE DIRECTIONS OF TRANSPORT WHEN DERIVING THE LST RATES SO THAT THE DIRECTION OF THE TRANSPORT IS STILL SHOWN.	308
TABLE 6-13 RECOVERY RATES AND DEPTH OF RECOVERY OF THE TRACERS DURING THE SURVEY PERIOD IN DECEMBER 2006 AT BIRLING GAP. THE FIGURES IN BRACKETS CORRESPOND TO THE CUMULATIVE NUMBER OF TRACER PEBBLES RECOVERED IN TOTAL.	315
TABLE 6-14 CHARACTERISTICS OF THE SEDIMENT TRANSPORT MEASURED USING THE TRACER PEBBLES AFTER ONE TIDE OF DEPLOYMENT AT BIRLING GAP IN DECEMBER 2006. NEGATIVE VALUES OF THE ALONGSHORE TRAVELLED DISTANCE INDICATE THAT THE PEBBLES MOVED IN A WESTWARD DIRECTION; POSITIVE VALUES INDICATE ALONGSHORE MOVEMENTS IN AN EASTWARD DIRECTION. NEGATIVE VALUES OF THE ACROSS-SHORE TRAVELLED DISTANCE INDICATE THAT THE PEBBLES MOVED DOWN THE BEACH AND POSITIVE VALUES INDICATE THAT THESE MOVEMENTS ARE UP THE BEACH.	318
TABLE 6-15 CALCULATION OF THE LST RATES OBSERVED USING TRACER PEBBLES DISPERSION ON MIXED SEDIMENT BEACH AT BIRLING GAP IN DECEMBER 2006. NOTE THAT IT WAS PREFERRED TO KEEP THE CONVENTIONAL SIGN CODE USED EARLIER TO DESCRIBE THE MEAN ALONGSHORE DIRECTIONS OF TRANSPORT WHEN DERIVING THE LST RATES SO THAT THE DIRECTION OF THE TRANSPORT IS STILL SHOWN.	324
TABLE 6-16 SUMMARY OF THE QUARTZITE COBBLES' DISTRIBUTION ON THE BEACH FROM EITHER SIDE OF THE INJECTION PROFILE OVER THE SURVEY PERIOD FROM OCTOBER 2004 TO MAY 2005.....	330
TABLE 6-17 YEARLY NET VOLUME CHANGES OBSERVED AT BIRLING GAP BETWEEN JULY 2003 AND JULY 2006.....	333

CHAPTER 7

TABLE 7-1 SUMMARY OF THE PARAMETERS NECESSARY TO CALCULATE I_L	363
--	-----

APPENDICES

TABLE IV-1 ACTIVE LAYER DATA MEASURED AT CAYEUX-SUR-MER IN OCTOBER/NOVEMBER 2005 ALONG TRANSECT 1 (FIGURE 3-11), INCLUDING THE MIXING DEPTH (ANNOTATED EROSION IN THE TABLE) AND THE ACCRETION ABOVE THE TOP PAINTED PEBBLE FOUND ON THE COLUMN.	431
TABLE IV-2 ACTIVE LAYER DATA MEASURED AT CAYEUX-SUR-MER IN OCTOBER/NOVEMBER 2005 ALONG TRANSECT 2 (FIGURE 3-11), INCLUDING THE MIXING DEPTH (ANNOTATED EROSION IN THE TABLE) AND THE ACCRETION ABOVE THE TOP PAINTED PEBBLE FOUND ON THE COLUMN.	432
TABLE IV-3 ACTIVE LAYER DATA MEASURED AT CAYEUX-SUR-MER IN OCTOBER/NOVEMBER 2005 ALONG TRANSECT 3 (FIGURE 3-11), INCLUDING THE MIXING DEPTH (ANNOTATED EROSION IN THE TABLE) AND THE ACCRETION ABOVE THE TOP PAINTED PEBBLE FOUND ON THE COLUMN.	433
TABLE IV-4 ACTIVE LAYER DATA MEASURED AT CAYEUX-SUR-MER IN OCTOBER/NOVEMBER 2005 ALONG TRANSECT 4 (FIGURE 3-11), INCLUDING THE MIXING DEPTH (ANNOTATED EROSION IN THE TABLE) AND THE ACCRETION ABOVE THE TOP PAINTED PEBBLE FOUND ON THE COLUMN.	434

TABLE IV-5 ACTIVE LAYER DATA MEASURED AT BIRLING GAP IN MARCH 2006 ALONG THE WESTERN TRANSECT (TRANSECT 1 ON FIGURE 3-12), INCLUDING THE MIXING DEPTH (ANNOTATED EROSION IN THE TABLE) AND THE ACCRETION ABOVE THE TOP PAINTED PEBBLE FOUND ON THE COLUMN.	435
TABLE IV-6 ACTIVE LAYER DATA MEASURED AT BIRLING GAP IN MARCH 2006 ALONG THE EASTERN TRANSECT (TRANSECT 3 ON FIGURE 3-12), INCLUDING THE MIXING DEPTH (ANNOTATED EROSION IN THE TABLE) AND THE ACCRETION ABOVE THE TOP PAINTED PEBBLE FOUND ON THE COLUMN.	435
TABLE IV-7 ACTIVE LAYER DATA MEASURED AT BIRLING GAP IN MAY 2006 ALONG THE EASTERN TRANSECT (TRANSECT 3 ON FIGURE 3-12), INCLUDING THE MIXING DEPTH (ANNOTATED EROSION IN THE TABLE) AND THE ACCRETION ABOVE THE TOP PAINTED PEBBLE FOUND ON THE COLUMN.	436
TABLE IV-8 ACTIVE LAYER DATA MEASURED AT BIRLING GAP IN MAY 2006 ALONG THE WESTERN TRANSECT (TRANSECT 1 ON FIGURE 3-12), INCLUDING THE MIXING DEPTH (ANNOTATED EROSION IN THE TABLE) AND THE ACCRETION ABOVE THE TOP PAINTED PEBBLE FOUND ON THE COLUMN.	436
TABLE IV-9 ACTIVE LAYER DATA MEASURED AT BIRLING GAP IN DECEMBER 2006 ALONG THE WESTERN TRANSECT (TRANSECT 1 ON FIGURE 3-12), INCLUDING THE MIXING DEPTH (ANNOTATED EROSION IN THE TABLE) AND THE ACCRETION ABOVE THE TOP PAINTED PEBBLE FOUND ON THE COLUMN.	437
TABLE IV-10 ACTIVE LAYER DATA MEASURED AT BIRLING GAP IN DECEMBER 2006 ALONG THE EASTERN TRANSECT (TRANSECT 3 ON FIGURE 3-12), INCLUDING THE MIXING DEPTH (ANNOTATED EROSION IN THE TABLE) AND THE ACCRETION ABOVE THE TOP PAINTED PEBBLE FOUND ON THE COLUMN.	437

List of Abbreviations and Notations

DGPS	Differential Global Positioning System	
D ₅₀	Median grain size	(mm)
e	Void ratio	
F _c	Cut off frequency	
g	Gravitational acceleration	(9.81 m ² .s ⁻¹)
GLONASS	Global Orbiting Navigation Satellite System	
GNSS	Global Navigation Satellite System	
GPS	Global Positioning System	
h	High water level elevation	(m)
h _b	Mean water depth at the point of breaking	(m)
H _b	Wave breaking height	(m)
HD	French Hydrographic Datum	(m)
H _s	Significant wave height	(m)
H _{s t. max.}	Maximum significant wave height recorded during one tide	(m)
H _{rms}	Root mean square wave height	(m)
HWL	High Water Level	(m)
I _l	Immersed weight sediment	(N.s ⁻¹)
K	Constant of drift efficiency	
L1	Lambert 1 conic geographic system	
LST	Longshore Sediment Transport	(m ³ .y ⁻¹)
m	Width of the active beach	(m)
NGF	Nivellement général de la France (Average elevation of France)	(m)
OD	Ordinance Datum	
OSGB36	Ordnance Survey Great Britain 1936	
PIT	Passive Integrated Transponder	
P _l	Longshore wave power	(W.m ⁻¹)
Q _l	Generic term for longshore transport rate	(m ³ .y ⁻¹)
Q _{lnet}	Net longshore transport rate	(m ³ .y ⁻¹)
Q _{lgross}	Gross transport rate	(m ³ .y ⁻¹)
Q _{l+}	Dominant transport direction	(m ³ .y ⁻¹)

Q_l	Transport in the opposite direction of the dominant	$(m^3.y^{-1})$
RMS	Root Mean Square	(m)
RTK	Time Kinematic Telemetry	
$\tan \beta$	Beach gradient	
T_z	Zero-upcrossing wave period	(s)
T_p	Wave Peak period	(s)
T_s	Significant wave period	(s)
U_s	Tracer centroid	(m)
Z_m	Mixing depth	(m)
ρ_s	Density of the sediment	$(kg.m^{-3})$
ρ	Density of water	$(kg.m^{-3})$
γ	Breaker index	(0.78)
β^*	Sambrook-Smith index	
ϕ_1 and ϕ_2	modal size	(phi)
F_1 and F_2	Proportion of sediment	
θ	wave angle	(rad)
Q_l	volumetric transport rate	$(m^3.y^{-1})$
P_l	wave energy flux or longshore wave power	$(m^3.y^{-1})$
I_l	Immersed weight transport rate	$(N.s^{-1})$
Γ	conversion factor	

Chapter 1. Introduction

1.1 Aim of the thesis

The aim of this study is to contribute to the understanding of the processes of Longshore Sediment Transport (LST) in open coast, mixed beach environments and to test and improve pre-existing empirical models by collecting and analysing reliable data than can be used to calibrate them.

To meet this aim, this study investigates three major vectors of longshore sediment transport: its width, its thickness and its length (Figure 1-1). Each of these vectors change over time, adapting to the environmental conditions.

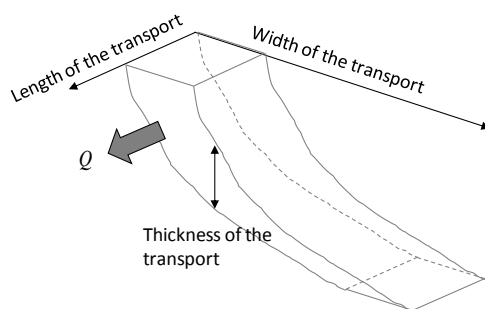


Figure 1-1 Principal vectors of the longshore sediment transport (Q).

The study investigates each of these three vectors individually and at the smallest time scale possible so that their variability, which defines the volumes of sediment transported alongshore, can be related specifically to the hydrodynamic conditions. Therefore, the first objective of this thesis was to collect detailed information on the topographical

changes of the beach profile (the “width” in Figure 1-1). Analysis of the amount of sediment accumulation, or erosion, along the beach profile gives an indication of the nature of the processes of mass transport operating on the beach in both across-shore and alongshore directions.

Next, the thickness of the transport was investigated through the observation and measurement of the active layer (Figure 1-1). Delimiting the depth of disturbance across the beach over time provides a 3D vision of the mobile upper surface of the beach that contributes to sediment transport. Improving knowledge of the depth of disturbance on mixed beaches is a key research requirement for the understanding and accurately quantifying LST.

Finally, the distance of the transport (the “length” in Figure 1-1) was also measured as an indication of the magnitude and direction of sediment migration on the beach. In combination, these three components enable LST rates to be calculated.

Within the objective to collect the most accurate data possible, the time scale of the observations is a key component. The longer the time between consecutive surveys, the harder it is to link the measurements of the three vectors to specific wave conditions and therefore the greater the inaccuracy. For this reason, repeat measurements comprising topographical surveys, active layer thickness, tracer pebble deployments and beach sediment characteristics were made over individual tidal cycles under varying tide heights and prevailing weather conditions.

1.2 Introduction

Two main reasons motivated this research. First, despite the interest in gravel and mixed beaches from the scientific community since the 1930s, quantitative and reliable *in situ* measurements of LST on mixed beaches are few (e.g. Schoonees and Theron, 1993) and knowledge needs to improve greatly to be on a par with sandy beaches. Indeed, although being partially composed of sand, mixed beaches present a broad grain size distribution, from approximately sand sized particles to pebble sized particles. Because

of this mixture, mixed beaches are able to sustain a much steeper beach face and exist under much higher wave energy conditions than sand beaches. They are also normally associated with macrotidal conditions as is the case along the English Channel coasts. This general high energy climate and the fundamental differences in morphology and processes involved on mixed beaches render it impossible to transfer directly the knowledge or the techniques acquired from the study of sandy beaches. This necessitates the redesign of techniques and equipment appropriate for use in the high energy environments experienced on mixed beaches. Because of this, there is a lag in research progress between sandy and mixed beaches.

This knowledge lag on mixed beaches or gravel beaches in general is made very clear by the conclusions reached by Schoonees and Theron (1993) about the reliability of the studies investigating LST. In their inventory of the data sets judged reliable enough to correctly estimate LST rates, only two studies on gravel beaches were considered at that time to be satisfactory: Chadwick (1989) at Shoreham-by-Sea, Sussex, and Nicholls and Wright (1991) at Hengistbury Long Beach, Dorset, and Hurst Castle Spit, Hampshire. Since then, only a few more studies have investigated LST *in situ* on gravel beaches (e.g. Bray, 1996; Bray et al., 1996; Van Wellen, 1999; Van Wellen et al., 2000; Osborne, 2005; Allan et al., 2006; Ciavola and Castiglione, 2009). Thus, at this point in time, the scientific community needs more quantitative and reliable data sets to reach a better understanding of the transport and morphological processes active on mixed beaches (e.g. Schoonees and Theron, 1993; Horn and Walton, 2007).

The second motivation for this study is the necessity of understanding the processes of sediment transport and particle behaviour for improving beach management. The beaches on both coastlines on each side of the Channel generate considerable public interest because of their fauna and flora, use for recreational activities and importance in coast protection. The beach is the last natural defence protecting land against sea flooding and therefore beach sustainability is crucial for protecting land-based human activities and the well being of the economy. The importance of improving knowledge about gravel and mixed beaches can be highlighted by considering the length that such beaches occupy in the UK or in France. In Great Britain, beaches with an important gravel fraction are estimated to occur along approximately 19,000 km of shoreline,

while pure gravel beaches form almost 3500 km of the beaches at mean high water mark (Randall et al., 1990; Sneddon and Randall, 1991). In France, the precise length of coast represented by gravel beaches is not exactly known; however, knowing that 721 km of coast is made of cliffs which are usually bordered by small fringing gravelly beaches and that rocky coasts not backed by cliffs represent 1548 km in total of the French coastline (Conservatoire du Littoral, 2004), a total of 2269 km of coastline is represented by coarse sediment beaches. On both sides of the Channel, coastal authorities have faced important coastline erosion problems that have led to the creation of sea defence management plans, that include for example recharging and recycling of beach material and groyne construction. A better understanding of the processes of sediment transport on mixed beaches will contribute to more efficient beach management and ultimately help to reduce its cost.

The remainder of this Chapter defines the principal features of mixed sediment beaches and the various parameters measured in this study.

1.3 The concept of coastal morphodynamic

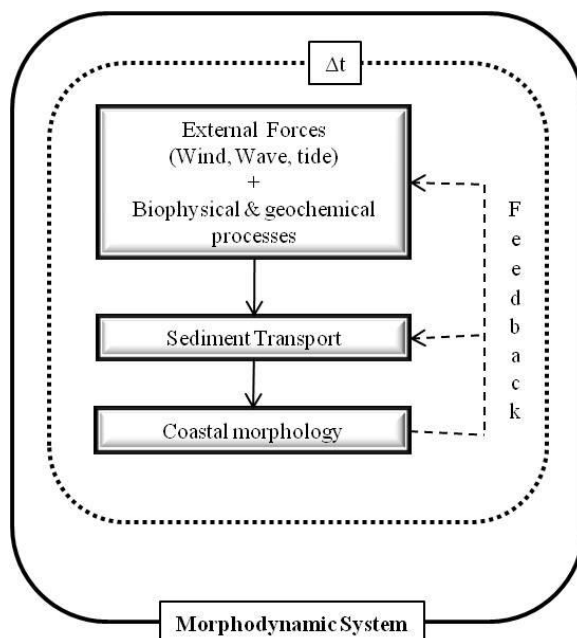


Figure 1-2 Primary components involved in the coastal morphodynamic system (Cowell and Thom 1994). Δt : time component.

Coastal evolution is the product of morphodynamic processes that occur in response to changes in external conditions. A morphodynamic system (Figure 1-2) is represented by the adjustment of a geomorphological feature to external forces. This adjustment consists of a search for equilibrium between the geomorphological object and the forcing processes, resulting in sediment transport over time (Wright and Thom, 1977). The time necessary for the system to be in equilibrium is a function of the sedimentary volume of the feature and

the duration and intensity of the external forces (wind, waves and tides; Kroon, 1994).

The complete system functions as a feedback loop considering that any morphological change over time will influence the boundary conditions for the external forces (Figure 1-2). The feedback can be either negative, i.e. leading towards equilibrium, also called self regulation, or positive, i.e. growing instability and then resulting in new modes of operation, also called self organisation (Cowell and Thom, 1994). “The interaction of these processes provides considerable scope for linkage between physical processes acting over different timescales. For this reason, it is necessary to determine long-term and short-term trends” when studying coastal evolution (Horrillo-Caraballo and Reeve, 2008, p.91).

1.4 Definition of a beach system

A beach is the result of sediment accumulation from the modal wave base to the upper limit of the swash (Short, 1999; Figure 1-3). In deep water, the motion of water under the influence of wind is orbital and waves progress landward without interacting with the seabed and therefore do not involve sediment transport. As the waves progress landward in the nearshore zone, at a depth of approximately half of the wave length, the wave circular orbital motions start to interact with the seabed entraining the sediment to move onshore and offshore in an oscillatory fashion. Progressing landward, because of the friction on the seabed, the wave orbital motions progressively become elliptical. As the waves migrate onshore these elliptical motions become more elongated. At the point of interaction with the seabed the elliptic shape of the wave orbit induces an asymmetric sediment transport with a residual shoreward movement. As the waves continue their movement shoreward, the friction of the wave orbit with the seabed progressively hinders the bottom of the wave motion while the top of the wave retains a higher speed. When the breaker index is approximately 0.78, the velocity difference between the bottom and the top of the wave provokes wave breaking in the surf zone. This surf zone is the area where gravity waves' energy decreases while infragravity waves (longer waves than gravity waves) pursue their course shoreward in the swash zone (cf. Masselink and Hughes, 1998). After the wave breaks, the remaining energy that is mainly dominated by the infragravity waves dissipates into the swash zone. This zone extends from where the wave collapses to the bottom of the water free part of the beach.

MORPHOLOGY	BEACH SYSTEM			INNER CONTINENTAL SHELF
	SUBAERIAL BEACH	SURF ZONE	NEARSHORE ZONE	
Wave process	Swash	Wave breaking	Wave shoaling	

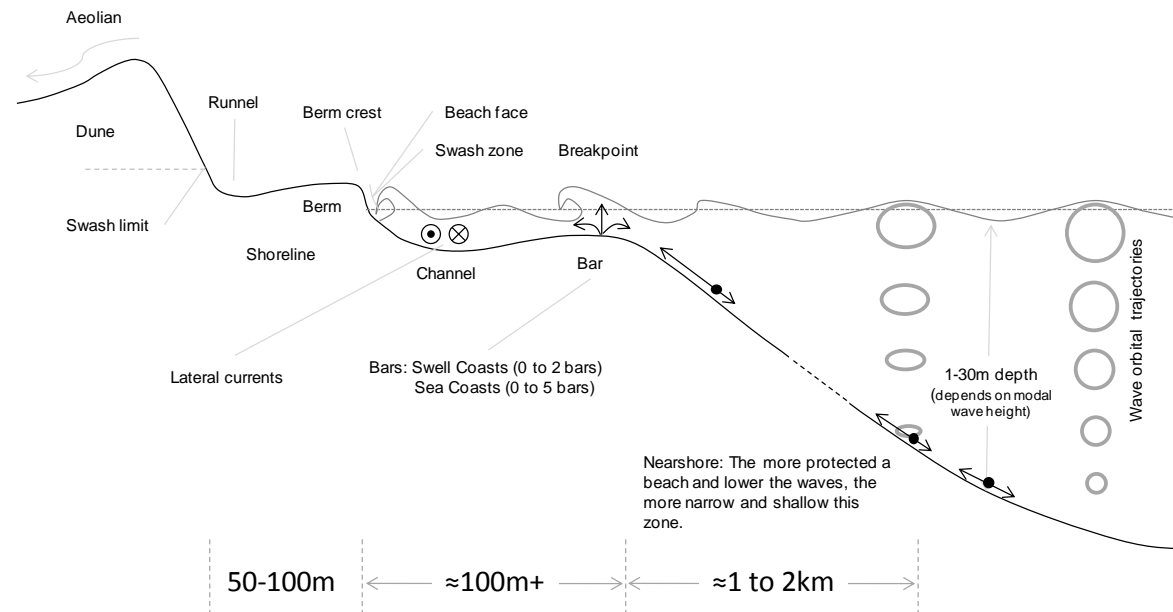


Figure 1-3 Sketch of a high energy beach system including the wave transformation areas approaching the shoreline and general sediment transport (after Carter, 1988, p.82-93 and Short, 1999, p.4). General sediment transport is represented by the black arrows in proximity to the sea bed and the equilibrium between the onshore and offshore sediment transits is relative to the length of each single arrow.

As the wave collapses a thin layer of water, known as the uprush, spreads up the beach face. The energy delivered by the uprush is dissipated by friction on and through infiltration into the beach face. When all of the uprush energy is dissipated, the remaining water runs back to the sea as the backwash. These currents can transport large amounts of beach material and give the beach its shape (e.g. Van Wellen, 1999; Pedrozo-Acuña, 2005). They are a direct consequence of the incoming wave characteristics, including wave height, period and direction, and the beach characteristics, including sediment slope angle and beach face shape. In addition, the uprush and backwash are also affected by the necessity to evacuate the over-flow of water that is delivered to the beach by the incoming waves (Inman et al., 1971).

Note that Figure 1-3 represents only a two dimensional model of the entire beach system showing the wave energy transformation when progressing onshore. There are also lateral, wave-generated, currents along the shore that drive significant sediment transport in the longshore direction.

Wave-generated currents system along and across the shore are also present (Figure 1-4): (a) one where the incident wave angle is perpendicular to slightly angled to the shore and organised in cell circulation systems between rip currents; and (b) another where the incident waves are oblique to the coast at a large angle, generating an uninterrupted flow parallel to the shore until there is a major morphological change in the coastline such as a change in the orientation of the coast, the presence of an estuary, a harbour arm or a headland for example.

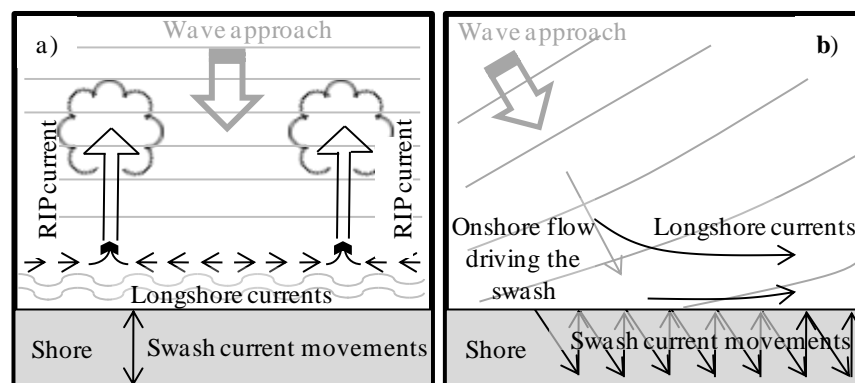


Figure 1-4 Wave-generated current patterns observed nearshore. a) The incident wave angle is perpendicular to the shore. b) The incident wave angle is oblique to the shore (Komar, 1998).

1.5 Concept of Longshore Sediment Transport (LST)

Longshore sediment transport has been widely investigated all over the world (e.g. Wright et al., 1978; Hattori and Suzuki, 1978; US Army Corps of Engineers, 1984; Bailard, 1984; Kamphuis et al., 1986; Morfett, 1988; Chadwick, 1989; Van der Meer, 1990; Kamphuis, 1991; Schoonees and Theron, 1993; Damgaard and Soulsby, 1996; Van Wellen et al., 2000) and is a top priority in coastal management. It partly drives beach erosion by determining the relative stability or gross movement of beach material along the coastline. The effects of LST are easily noticeable in the proximity of groynes or harbour arms. Generally, when LST occurs, the updrift side of such constructions is subject to accumulation of sediment driven by the longshore currents, whereas their downdrift side is characterised by considerable erosion. This is because the loss of sediment directly downdrift of the construction is not balanced by freshly supplied material which is trapped on the updrift side of the construction (Figure 1-5).



Figure 1-5 Evidence of LST in a groyne field. a) Along the English coast at Peacehaven (East Sussex). b) Along the French coast at Ault (Normandy). Images courtesy of Google Earth.

On a day to day basis, waves reach the beach from different directions, varying with the wind; however, on longer time scales, the coast experiences regular seasonal, yearly or even longer wave patterns during which a dominant transport direction is expressed (Q_{L+} , this annotation is assigned with a positive value). Sediment transport can be expressed either as a net longshore transport rate (Q_{Lnet}) or as a gross transport rate (Q_{Lgross}). The net longshore transport rate considers the gain or loss of beach material during an event or a longer period of time. It is expressed mathematically as:

$$Q_{\text{Inet}} = Q_{\text{I+}} + Q_{\text{I-}} \quad (1.1)$$

$Q_{\text{I-}}$ being transport operating in the opposite direction of the dominant transport and therefore assigned a negative value. The gross transport considers the quantities of material transported on the beach face and its mathematical expression is:

$$Q_{\text{Igross}} = Q_{\text{I+}} + |Q_{\text{I-}}| \quad (1.2)$$

Please note that in this thesis, the transport rates considered are always net volumes and their annotation will simply be Q_{I} .

1.6 Modes of sediment transport

The precise mode of transport on gravel beaches remains contentious, especially on mixed beaches where, in contrast with pure gravel beaches, there is a broader range of grain sizes which adds to the complexity of the sediment transport. Once a sediment particle is in motion, its transport can occur in various modes: wash load, suspended load, bed load (Bagnold, 1956) and sheet flow (e.g. Savage, 1984).

The wash load represents the sediment particles that are so small that they never come into contact with the actual surface of the beach. They stay consistently or nearly consistently suspended in the water column (Bagnold, 1956). Since they are so small in comparison to the average grain size distribution on mixed beaches, the volume of sediment transported by wash load can be considered insignificant in comparison to the other modes of transport.

The suspended load occurs when the sediment particle is carried by the currents and turbulence inside the water column and the load has limited contact with the sea bed. On gravel beaches some authors consider that the current velocities necessary to put and keep gravel or pebble size particles in suspension is so high that this mode of transport can be neglected (Walker et al. 1991; Fredsoe and Deigaard, 1992). Despite this, LST formulae generally take into account such transport in their calculations (e.g. Bailard,

1984; Komar and Inman, 1970) whilst suggesting it is negligible. This view is supported by Coates (1994) who observed a large proportion of suspended transport in laboratory experiments, showing how little is actually known about the modes of transport on gravel beaches. Personal observations at the study sites confirm those of Austin and Masselink (2006) on gravel beaches that quasi-suspended transport occurs under plunging wave conditions at the point of wave breaking. At the very precise moment that the wave bore collapses on the beach face, even pebble sized sediment can be moved in suspension at least for a short time. Moreover, because of the high sand content of mixed beaches (15 - 68%; Mason and Coates, 2001), suspended transport is much more likely to be present in greater quantities on such beaches than on pure gravel beaches.

Bed load transport occurs when the sediment particles are transported by a current while interacting with the bed floor. This interaction can involve either intermittent bouncing of particles by saltation motion under a current or continuous traction whereby the sediment particles are rolled or displaced as a single surface layer of the bed floor (Fredsoe and Deigaard, 1992). Bed load transport is reportedly identified as one of the principal modes of transport in the swash on gravel beaches (Horn and Mason, 1994; Van Wellen, 1999; Pedrozo-Acuña, 2005; Pedrozo-Acuña et al., 2006; Austin and Masselink, 2006).

Sheet flow has also been identified as a transport mechanism on gravel beaches (e.g. Austin and Masselink, 2006). Instead of going into full suspension, the sediment particles are transported in layers of slurry sediment, colliding and entrained by the fluid momentum (e.g. Savage, 1984; *in* Buscombe and Masselink, 2006), often washing out bedforms in the process (Van Wellen, 1999). The shield parameter (parameter used to calculate the initiation of motion of sediment in flowing water) associated with this kind of transport is generally ≥ 0.8 (e.g. Wilson 1987, Fredsoe and Deigaard, 1992). However, sheet flow on coarse sediment beaches is still poorly understood (Buscombe and Masselink, 2006).

To summarize, in the nearshore of gravel beaches the modes of sediment transport are still not clearly understood. Bed load and sheet flow are recognised as the two dominant

transport modes, whereas quasi-suspended load occurs only very locally at the point of bore collapse. More specifically on mixed beaches, because of the potentially high content of sand, suspended transport is thought to be greater than on pure gravel beaches (e.g. Van Wellen, 1999).

1.7 Classification of gravel beaches and definition of a mixed beach

With the increase of interest in studies of gravel beaches in a great variety of environments (e.g. barrier, spit) with very variable characteristics, for example beach slope and grain size distribution, Jennings and Shulmeister (2002) attempted to classify such beaches into distinct categories. Based on beaches in New Zealand they distinguished three main types of gravel beaches based on their morphodynamic properties:

- i. *Pure gravel beaches.* These beaches present a steep slope with a gradient of $\tan \beta = 0.1$ to 0.25 and a mean grain size in the gravel range i.e. from -2 to -6 phi (4 to 64 mm). Because of the permeability associated with the large grain size and their steep slope, the uprush infiltrates quickly into the beach face which reduces greatly the backwash potential (Quick and Dysksterhuis, 1994). This asymmetry between the uprush and the backwash forces the sediment to move landward and contributes to sustaining the steepness of the beach face.
- ii. *Mixed sand and gravel beaches.* These beaches are comprised of a homogeneous mixture of sand and gravel whose size distribution ranges from 0.5 to -6 phi (1 to 64 mm). The beach face is characterised by a relatively steep slope angle but one that is lower than for a pure gravel beach, $\tan \beta = 0.04$ to 0.12 .
- iii. *Composite gravel beaches.* These differ from the first two in that they comprise a lower foreshore of sand or a rock platform with a low slope angle, $\tan \beta = 0.03$ to 0.1 . The upper part of the beach is composed of mixed sediment in which gravel sized material is dominant and sustains a steep slope angle $\tan \beta = 0.1$ to 0.15 . Jennings and Shulmeister (2002) suggest that the “mixed beaches” of the UK should be included in this category.

Mason et al. (1997) recognised the latter two categories as being typical of the “mixed beaches” observed in the world but that further investigations were necessary to determine the grain size distribution that was representative of the mixed beaches. Subsequently, Coates and Mason (1998) reported that the sand content of mixed beaches observed around the world ranges from 15 to 68% of the total beach material. The wide range of sediments associated with mixed beaches is linked to sediment sources and supply and the geographic location of the coast. For example, mixed beaches on mid- to high-latitude coastlines (paraglacial coasts) are mostly formed of coarse clastic materials of glacial origin that have been remobilised by non-glacial processes (Forbes and syvitski, 1995; Forbes et al., 1995). The range of sand content mixed with gravel has also been linked to wave exposure (Bluck, 1967). In addition, the observation of seasonal variations in the sand content of the beach material indicates that the grain size distribution of such beaches is influenced by wave climate as well as exposure.

The beaches investigated in this thesis are categorised according to Jennings and Shulmeister’s (2002) classification. The term “composite beach” is used for beach composed of two major units, a lower sandy or rocky platform and an upper mixed sediment gravel unit that will be loosely named a mixed sediment beach. This is not to be confused with the mixed sand and gravel beaches types identified by Jennings and Shulmeister (2002). Finally, the term “gravel beach” is used to categorise any coarse sediment beach.

1.8 Definition and location of the different morphological features occurring on a mixed beaches

All of the morphological features found on pure gravel beaches are also commonly observed on mixed beaches including the step, cusps, high water level ridges (berms) and washover lobes. The significant sand content of mixed beaches makes these features even more visible because of the marked grain size contrasts between the sand and gravel dominated components. The significant sand content also facilitates the

expression of other beach features such as beach “cliffing” at the high water level mark and this is commonly observed on recharged beaches (e.g. Horn and Walton, 2007).

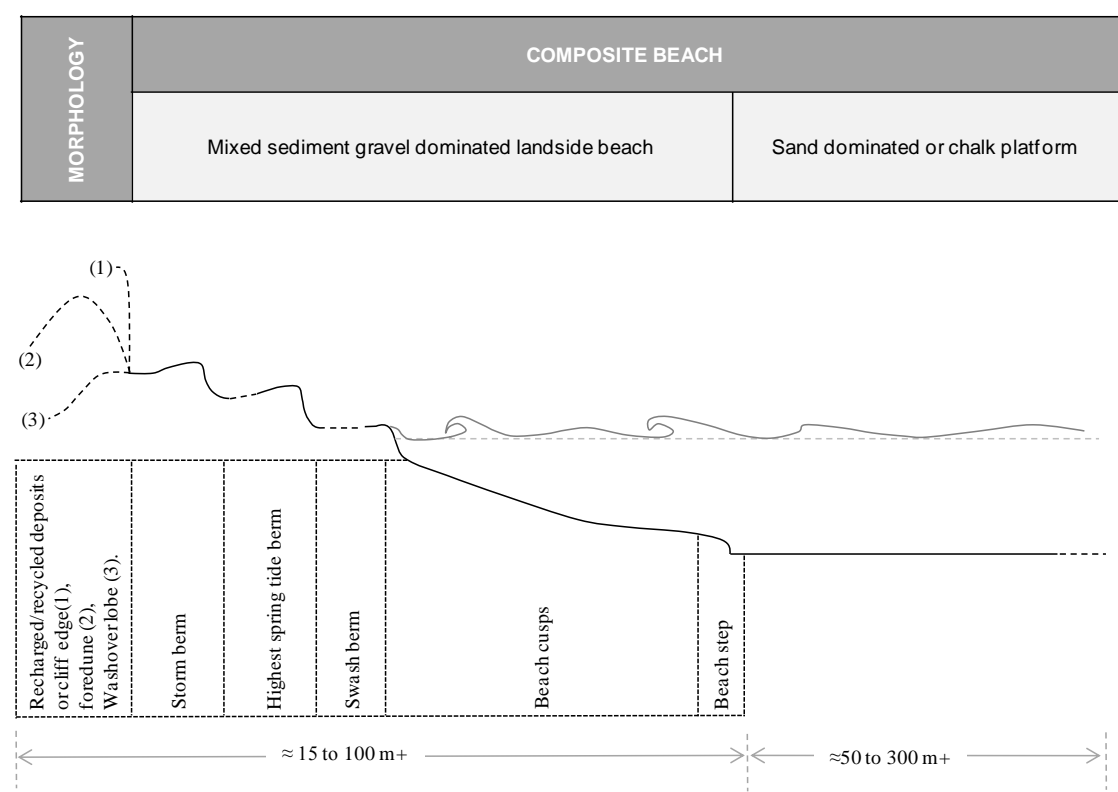


Figure 1-6 Cross-section of a classic composite beach showing the most frequently observed morphological and sedimentological features.

1.8.1 The lower foreshore

On composite beaches, the lower foreshore is composed of a sandy or rocky intertidal platform fringing the lower part of the gravel dominated beach (Figures 1-6 & 1-7). The platform has a low slope angle typical of sandy beaches (0 to 6°; Pontee, 1995) on which waves dissipate through the surf zone by spilling at low tide. The obvious across-shore segregation of particle sizes between the sandy platform and the



Figure 1-7 The sandy lower foreshore and the beach step at Cayeux-sur-Mer.

mixed sediment beach above has been explained by the propensity of sediment to move onshore in

relation to its threshold of motion together with the dominance of the swash (e.g. Inman and Bagnold, 1963; Carr, 1983).

1.8.2 The beach step

The beach step is a small scale morphological feature commonly observed on gravel beaches (Figures 1-6 & 1-7). On pure gravel beaches it corresponds to a clear break of slope near the elevation of mean water level between the nearshore face and the beach face. On mixed beaches it is located at the break of slope between the mixed sediment beach and its lower platform in the intertidal zone. The beach step usually presents a steep seaward face of 20 - 32° (Short, 1984; Larson and Sanamura, 1993). It is generally associated with a grain size distribution that is skewed toward the coarsest sediment present on the beach face (Austin and Buscombe, 2008). On gravel beaches it can exceed one metre in height (Bauer and Allen, 1995). Step initiation and behaviour is linked to the swash zone asymmetry (Matsunaga and Honji, 1980), the tidal stage and backwash vortices (e.g. Bauer and Allen, 1995), the wave conditions (e.g. Ivamy and Kench, 2006; Austin and Masselink, 2006) and the convergence of sediment at the wave breaking (Austin and Buscombe, 2008).

Because of its ability to provoke wave breaking and dissipate wave energy, the role of the beach step that develops on gravel beaches is comparable to the bars that develop on dissipative sand beaches (Buscombe and Masselink, 2006). The beach step has a considerable influence on the hydrodynamics affecting the beach as it forces the waves to break directly above it or in close proximity to it because of the sudden change of depth in the same way that bars do on sand beaches. The combined effects of the beach step and the general steepness of gravel beaches means that the transition from shoaling to breaking waves is prevented or at the very least extremely shortened and as a consequence no wide surf zone is expressed at high tide on such beaches.

1.8.3 The beach cusps

Cusps are quasi-rhythmic, longshore, crescent shaped features running across the beach and formed by the swash flows (Figure 1-8). On gravel beaches, they can be observed: (i) as horns extending from approximately the bottom of the berm to the beach step under accretionary conditions (e.g. Masselink et al., 1997, Figure 1-8); (ii) as crescentic depressions in proximity to the high water level (e.g. Sallenger, 1979; Figure 1-8a) or (iii) as a combination of the two (Carter, 1988; Miller et al., 1989; Sherman et al., 1993; Figure 1-8a). Beach cusps are typically associated with steep reflective beaches and modally low-energy swell conditions with surging breakers (Masselink and Pattiaratchi, 1998).

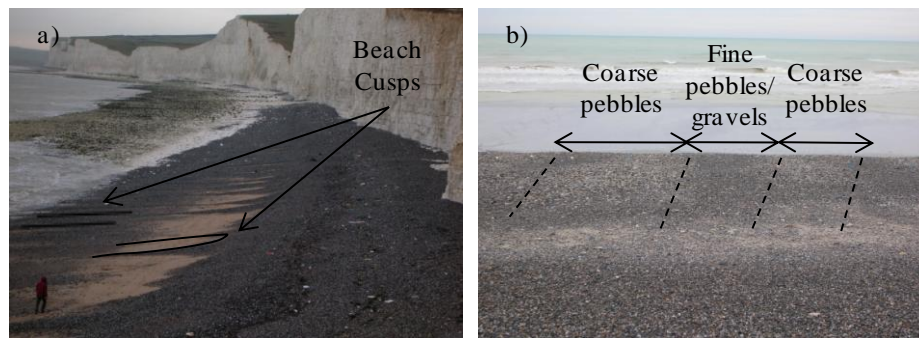


Figure 1-8 Example of beach cusps observed at both study sites. a) At Birling Gap, with very perpendicular rhythmic horns of shingles and sandy embayment. b) At Cayeux-sur-Mer, with perpendicular rhythmic horns made of coarse pebbles and cusps made of gravel.

Gravel beach cusps are different to those observed on sandy beaches. Indeed, on sandy beaches, cusps generally form a more regular morphological pattern, are structurally more stable and are less regularly sorted by size or shape (Buscombe and Masselink, 2006). Because of the large range of grain size distribution observed on mixed beaches, cusp formation generally presents rhythmical sand/fine gravel dominated and coarse gravel/pebble dominated bands. The horns are formed of coarser sediment than the bay located between two horns (Longuet-Higgins and Parkin, 1962; Russel and McIntire, 1965; Komar, 1976; Sallenger, 1979; Komar, 1983; Sherman et al., 1993; Nolan et al., 1999; Buscombe and Masselink, 2006). In association with the size of the sediment particles, the shape of particles also influences the structure of cusps. Sherman et al. (1993) sampled multiple locations on cusps on gravel beaches created under different

wave conditions and found that large angular pebbles were preferentially deposited on the steeper face of the horns, whilst poorly sorted spherical particles of smaller sizes were drawn down into the bay.

The regular spacing, length and elevation of cusps has also been investigated (Gary et al., 1974; Komar, 1983; Mii, 1958; Sallenger, 1979; Werner and Frink, 1993; Holland and Holman, 1996; Nolan et al., 1999; Sunamura, 2004). The distance between horns or bays ranges between 1 and 50 m (Todd Holland, 1998). Nolan et al. (1999) showed how beaches can develop unique spacing and elevation of cusps as a result of dissimilar wave and tidal conditions or sediment distributions. They identified the breaker height as being responsible for cusp elevation whereas the cusp spacing was a function of the variability of the breaker height over the wave length.

There is contention about the formation of beach cusps. One hypothesis relies on the occurrence of edge waves (Bowen and Inman, 1969; Guza and Inman, 1975, Sallenger, 1979; Seymour and Aubrey, 1985), whereas a second considers that cusps are formed through the combined effect of swash circulation and self-organisation patterns (e.g. Werner and Frink, 1993; Masselink et al., 1997, 2004; Coco et al., 1999, 2001, 2003, 2004). Edge waves are gravity waves trapped in the nearshore and the theory relies on the alongshore differential in shoreline fluid motions. During field experiments, Masselink et al. (2004) observed the formation of cusps in the absence of sub-harmonic energy during or just prior to their formation, indicating that the edge wave theory is insufficient on its own to explain how beach cusp formation starts. Earlier, Holland and Holman (1996) made a similar observation in laboratory experiments, therefore reinforcing the second theory.

The self-organization theory relies on the close relationship between swash motions and the feedback from the underlying topography. On gravel beaches for example, existing irregularly spaced perturbations on the featureless shore become more uniform due to the regular succession of incoming swash fronts. Over time, these irregularities will develop strong differences in infiltration which will promote accretion of sediment on the horns and erosion in the bays. This theory is supported by a number of studies; however, as pointed out by Seymour and Aubrey (1985), it does not explain the regular

spacing between the cusps. This suggests that cusp formation has other requirements as well, such as for example the near-correspondence of swash period and incident wave period (Bagnold, 1940; Dean and Maurmeyer, 1980).

1.8.4 The beach berm

The berm is an ephemeral feature located on the upper part of the beach. Its height can range from centimetres to metres (Figure 1-6 & 1-9) and its elevation is determined by the combined effect of the high water level and wave conditions. Berms are distinct features on the beach face comprising a steep seaward face (steeper than the average beach gradient) with a top that is at a lower angle. Indeed, it is not unusual for the beach profile to dip slightly landward after the berm crest. The berm is modelled by the swash (Austin and Masselink, 2006). Its height has been linked to the shoreline elevation and its crest is generally located slightly below the maximum of wave run-up at high tide. When the beach width is long enough, gravel beaches can develop multiple berms. On the upper beach, their location may range from the most recent high tide up to the most recent extreme high water levels such as the highest spring high tide and/or storm surge maxima (e.g. Takada and Sunamura, 1982).

The commonly observed asymmetry in flow velocity and duration between the run-up and the backwash on beaches (Masselink and Hughes, 2003) is even greater on gravel beaches because of their high permeability (Quick, 1991; Quick et al., 1994; Horn, 2006). As a direct consequence, under non-storm conditions on gravel beaches, the run-up is strong enough to push the coarsest particles landward in the upper swash zone while the backwash is not able to pull them down to lower areas because of large scale energy dissipation through infiltration. This phenomenon results in the berm moving landwards in what is commonly called berm “rollover” (e.g. Carter and Orford, 1993; Austin and Masselink, 2006) because particles pushed over the berm crest are protected from draw-down by backwash. During storm conditions, the beach material is literally thrown landwards to form the “storm” berm. Generally, the elevation on the beach profile of such a berm is so high that the material constituting the storm berm is actually lost from the active beach system (Buscombe and Masselink, 2006) until eventually an even bigger storm event happens.

Berms generally build up with coarse grain sediment (e.g. Austin and Masselink, 2006). This is particularly evident on mixed beaches when most of the coarse gravel and pebble fraction of the beach material is literally pushed up the beach face to form the berm, but is not drawn down by the weaker backwash, thus leaving the lower parts of the profile covered predominantly by finer sediment. For this reason, the berm is a very important feature on gravel beaches. Its elevation and volume determines the quantities of sediment available on the active profile for the LST.

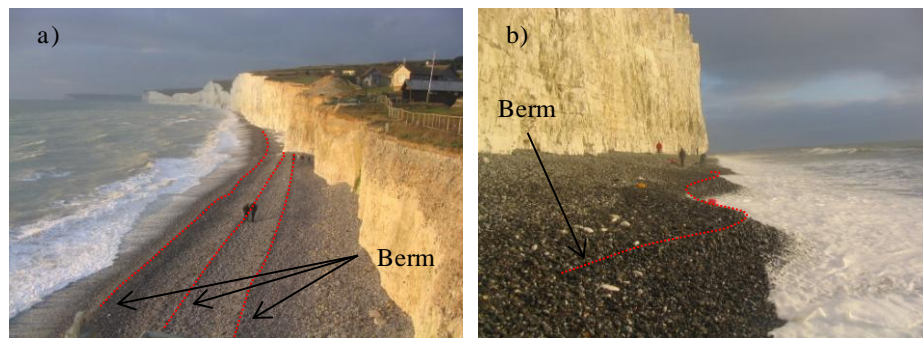


Figure 1-9 The beach at Birling Gap. a) Displaying multiple berms. b) The berm at high tide.

1.8.5 Washover lobes

Located on the landward side of the beach profile, washover lobes are features resulting either from the breaching of a beach or dune ridge under the pressure of a storm surge and wave overtopping, or the reduction of the beach crest height. The common morphology recognised as resulting from such an overwash process is composed of a fan and a “throat” (e.g. Leatherman, 1981). The “throat” is a channel cutting through the beach ridge in which the overwash circulates driving material from the beach face to the back of its ridge crest. The fan is the sediment deposit brought landward by the overwash. In addition to this supply, where fine material exists, the fan is also supplied on a regular basis by eolian transport of sand and other fine sediment (e.g. Schwartz, 1975; Leatherman, 1976). This sediment distribution generally enables rapid vegetation colonisation which is most probably destined to be covered by further deposits of sediment during the next overwash event. It is usual to observe an alternation of pre- and post-storm layers when looking at core samples made into such fans (Kochel and

Dolan, 1986). This suggests that over time, overwash events generally happen in the same places. This idea is supported by observations by Carter and Orford (1980) who highlighted that overwashing is most likely to happen on weakened points or existing depressions on the beach ridge. These are most likely to be the pre-existing “throats” of past breaches. Carter and Orford (1980) and later Forbes et al. (1995) indicate that the frequency and amplitude of the overwash depends on surge levels, breaker heights and types, beach geometry, beach sediment and shore-parallel variation of the beach crest line. Note that washover features were not observed directly in the area surveyed by this study; however they were observed directly north of Cayeux-sur-Mer.

1.9 Areas of research on coarse sediment beaches

As mentioned previously, coarse sediment beaches are widely represented in the UK, especially along the South and South-East shoreline of England and around Ireland; they are also present in the East Channel coast of France. These beaches are generally subject to great volumetric erosion or accretion dynamics and are the natural defence against flooding. Because of this, gravel beaches have been the subject of many research field studies of: their morphology (e.g. Sherman et al., 1993; Quick and Dyksterhuis, 1994; Holmes et al., 1996; Pontee, 1995; Jennings and Shulmeister, 2002; Bradbury and McCabe, 2003; Orford et al., 2003; Pontee et al., 2004; Pedrozo-Acuña, 2005; Austin and Masselink, 2006); their sedimentary characteristics (e.g. Carr, 1969; De Meijer et al., 2002; Watt et al., 2006; Horn and Walton, 2007; Buscombe, 2008); the nearshore hydrodynamics (e.g. Mason, 1997; Ivamy and Kench, 2006); the groundwater fluxes into the beach face (e.g. Mason and Coates, 2001; Blanco et al., 2003; Lee et al., 2007b); their sediment budget (e.g. Dolique, 1998; Dolique and Anthony, 1999; Van Wellen et al., 2000; Dornbusch et al., 2008a); sediment transport (e.g. Bray et al., 1996; Van Wellen, 1999; Voulgaris et al., 1999; Osborne, 2005; Pedrozo-Acuña et al., 2006; Lee et al., 2007a; Curtiss et al., 2009), and their Holocene or long term evolution (e.g. Shulmeister and Kirk, 1993; Orford et al., 1995; Orford and Carter, 1995; Soons et al., 1997; Shulmeister and Kirk, 1997; Orford et al., 2003; Cooper et al., 2004; Kokot et al., 2005).

Most studies have been concerned with beach morphology or the sedimentary characteristics. They usually focus on a particular area of the beach such as the beach step (e.g. Bauer and Allen, 1995; Austin and Buscombe, 2008), the beach berm (e.g. Austin and Masselink, 2006), beach cusps (e.g. Sherman et al., 1993; Nolan et al., 1999; Coco et al., 1999, 2001) or features of overwash (e.g. Carter and Orford, 1980). Because of the importance of the recycling and recharging strategy of management schemes in the UK, the beach profile or the sediment grading response to storm conditions (e.g. Watt et al., 2008) or after a recycling/recharge episode (e.g. Kirk, 1992; Coates et al., 2001; Benedet et al., 2004; Blott and Pye, 2004; She et al., 2006; Horn and Walton, 2007) provide a particular focus for new research.

In contrast, the nearshore conditions on gravel beaches are understudied. This is mainly because of the harsh environmental conditions that occur on coarse sediment beaches and the fragility of the equipment. Most of the studies have tended to focus on the swash. This is for two main reasons: first, it has been identified as the dominant hydrodynamic parameter driving sediment transport on coarse sediment beaches (e.g. Van Wellen, 1999; Pedrozo-Acuña, 2005). Second, the swash zone is easily accessible to deploy and secure equipment to measure current velocities and direction. However, it is important to note that, for reasons of safety and to ensure that data are acquired, *in situ* measurements are generally limited to “calm” hydrodynamic conditions where the wave height is <1m (e.g. Mason, 1997) and there is a lack of data for stormy conditions. Numerical models have been developed to determine and predict the behaviour of nearshore currents on a gravelly beach face but such programs often neglect parameters such as the sediment transport (Lee et al., 2007b). The mean flow and the bed return flow (or undertow) are important currents regarding cross-shore transport on sandy beaches or impermeable slopes (Masselink and Black, 1995; Ting, 2001). However, on gravel beaches, the high permeability, the steep beachface and the quasi-inexistence of a surf-zone reduce considerably the velocities of the undertow (Lara et al., 2002; Pedrozo-Acuña et al., 2006).

LST is the second most investigated subject after morphology and sedimentary characteristics. This is not because it is of lesser interest or importance, but because of problems of satisfactory methodology. Studies to measure LST have progressed in line

with progress in technology. This type of research on gravel beaches has also been impeded because most of the studies undertaken before 1993 were not measuring a sufficient range of parameters to determine an accurate and reliable LST rate as pointed out by Schoonees and Theron (1993). For this reason, Schoonees and Theron (1993) recommended that the following measurements need to be collected simultaneously for such studies to have value: LST rate, wave height, wave period, wave angle, beach slope, and grain size.

Nowadays there are various techniques, of increasing sophistication and accuracy, to measure the LST rates and investigate variations on ever smaller scales. As mentioned previously, some techniques have estimated gross drift from volumes of sediment accumulation on the updrift side of constructions that disrupt the natural drift of the sediment (e.g. Wilson, 1996; Chadwick, 1989; Van Wellen et al., 1997, 1998), Others have examined beach profile changes over periods of time to determine the beach volumes changes (e.g. Dornbusch et al., 2008b), whilst others have used pebble tracers (e.g. Russell, 1960; Crickmore et al., 1972; Wright et al., 1978; Workman et al., 1994; Bray et al., 1996; Van Wellen et al., 1997; Allan et al., 2006).

From the data acquired through these measurements, models have been developed or corrected to predict the longshore drift on gravel beaches. It is important to note that many of the model equations developed are based on the CERC formula (1984) which was originally developed for sandy beaches (e.g. Bailard, 1984; Chadwick, 1989; Morfett, 1988; Van Wellen, 1999; Van Wellen et al. 2000). This highlights how hard it is to develop a model for gravel beaches from scratch that would consider all the parameters driving sediment transport. Mixed beaches are even more difficult to represent than pure gravel or sandy beaches because of the variety of the mixtures possible and the complexity of the grains' interactions.

Beach hydraulic conductivity and groundwater flux studies suffer from the same limitations as the other types of research. Field measurements are difficult because of the harshness of these environments and numerical models encounter issues with replicating all the natural parameters in models (e.g. Lee et al., 2007b). It is difficult to observe two beaches with exactly the same grain size distribution, and given that grain

size largely determines the permeability of the beach, this means that groundwater fluxes will differ from one mixture to another. Mason et al. (1997) highlighted that permeability is greatly reduced once the sand content exceeds approximately 25% of the total mixture. Therefore, it is quite difficult to generalise from observations based on one type of mixed beach given that the sand ratio on a mixed beach can vary from 15 to 68% by volume.

To summarize, despite numerous studies of gravel beaches, and especially on mixed beaches, our knowledge of critical parameters remains limited and this makes accurate modelling of such beaches difficult and imprecise. The fact that each beach or coastal sediment cell is often characterised by a unique sediment mixture further complicates the feasibility of identifying the key factors and their overall role and importance in determining how mixed beaches operate.

1.10 Recall of the aims of the study

This study investigates the LST on two mixed beaches, one on either side of the English Channel, at Cayeux-sur-Mer (France) and at Birling Gap (UK). LST is the second most investigated subject on gravel beaches, but the originality of this study is that it specifically examines mixed beaches whereas most of the studies undertaken to date have focused mostly on pure gravel beaches or mixed sand and gravel beaches (e.g. Osborne, 2005; Ciavola and Gastiglione, 2009) or limited their observation to the mixed sediment part of the beach.

In order to collect valuable and reliable data on sediment transport and further our understanding of the operation and behaviour of mixed beaches, this study looks in particular at:

(i) The topographical changes of the beach profile at both sites;

The analysis of the extent of gravel and sand accumulation or erosion through the beach profile should help to indicate the nature of the mass transport processes, both across-shore and alongshore, operating on the beach. These will also permit the creation of

digital elevation models from which the volumes of sediment transported will be derived.

(ii) The thickness of the layer of beach sediment that is affected by motion;

Knowledge of the depth of disturbance across the beach over time will provide this study with a 3D vision of the top surface layer of the beach thereby permitting observation and measurement of the section of the beach which is actually mobile and contributes to sediment transport.

(iii) The length of the alongshore transport;

This will permit quantification of how far and in what direction the sediment particles migrate along the beach.

The field measurements will be collected on a tidal basis in order to relate them directly to the hydrodynamic conditions impacting on the shore.

It should be noted that nearshore hydrodynamics on a macrotidal beach are very complex to define and sometimes this thesis refers to wave conditions as small, agitated or storm wave conditions. Small, moderate or high energy events are defined according to the specific ranges of H_s above the sensor (Table 1-1).

It is recognized that the energy delivered to the beach and influencing the direction and volumes of sediment transported along the coast is the result of the combination of other parameters not measured such as the wave direction, wave period and length, wave and tidal current and the water level. However, it was decided that the simplest way to categorize wave conditions was simply to use H_s . It should be noted that at both sites, specific H_s are associated with specific wave directions. For example, at both sites, H_s is generally $<1\text{m}$ when the incident waves are from the East sector.

Specific wave height (H_s)	$H_s < 1\text{m}$	$1 < H_s < 1.5\text{m}$	$1.5 < H_s < 2\text{m}$	$H_s > 2\text{m}$
Term used to describe specific H_s	Small/calm conditions	Moderate conditions	Agitated conditions	Stormy conditions

Table 1-1 Classification of wave conditions used throughout the thesis.

To fulfil the aim of this study, two field sites were selected: Birling Gap in East Sussex, UK, and Cayeux-sur-Mer, Upper Normandy, France. The following chapter describes the geological, morphological and evolutionary contexts of both study sites, and introduces the problems encountered in relation to LST in these areas.

Chapter 2. Background on the Field Study Areas

2.1 Birling Gap

2.1.1 Geography and morphology of the study site and its sedimentary cell: From Selsey to Beachy Head.

Birling Gap has a 1.2 km natural mixed sediment beach located on the downdrift end of the 80 km long sub-sedimentary cell 4d between Selsey Bill and Beachy Head (Figure 2-1). Littoral processes along this coastline are extremely dynamic with both erosion and accretion having a strong influence on the present configuration of the coast, along which extensive coastal defences have been built to prevent erosion or flooding. In the west, the coast is low lying and backed for the most part by soft sands and clays of Tertiary age, but in the east the coast is characterised by tall cliffs developed in Chalk which is Cretaceous in age. Along much of the coast, especially in the west, the bedrock geology is overlain by gravel, sand and silt deposits of Quaternary origin. Taking into account the coastal sediment pathways and budgets, the coastal authorities have delimited two major littoral sub-cells within the sub-cell 4d (South Downs Coastal group, 1996; Figure 2-1):

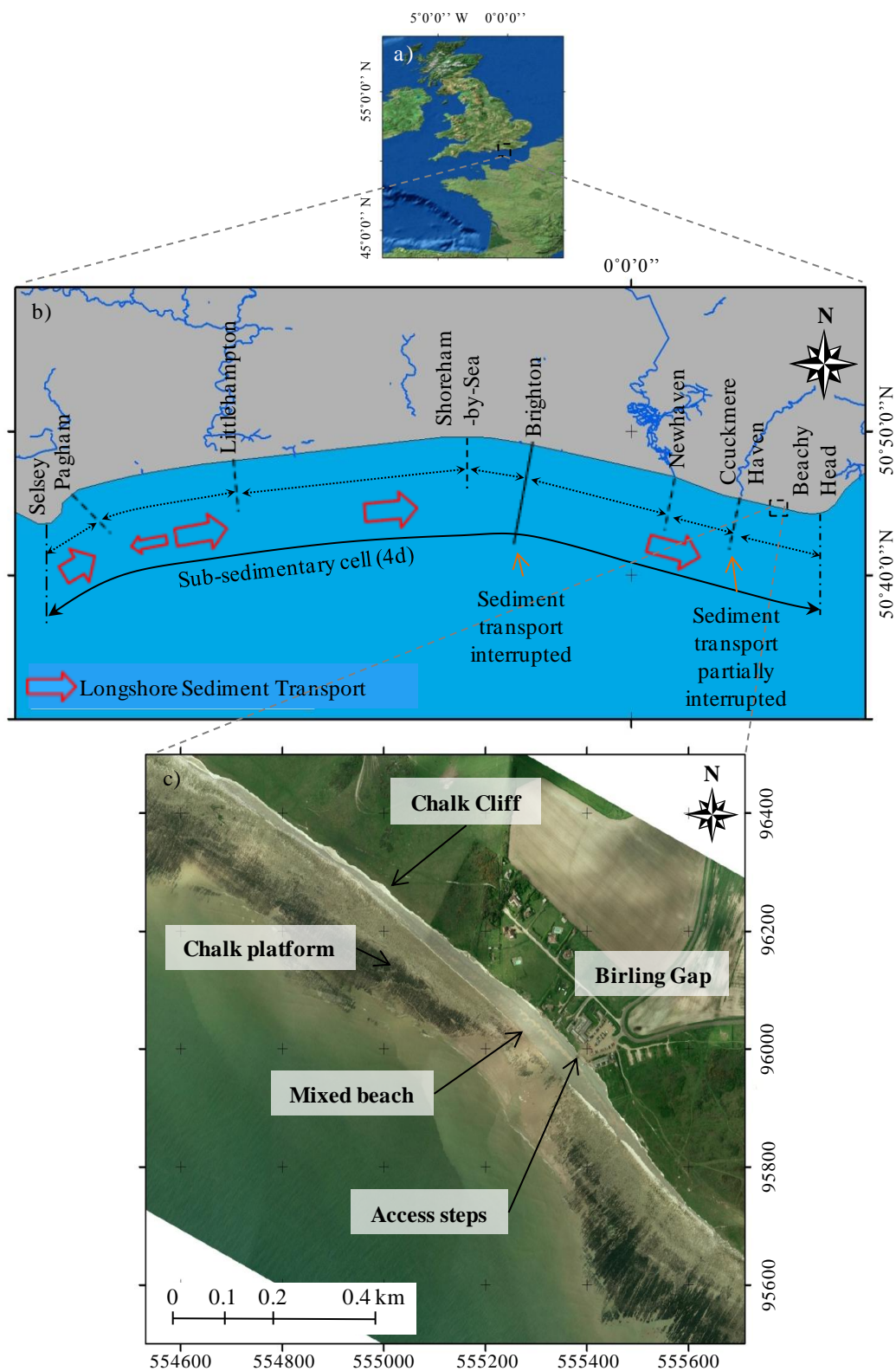


Figure 2-1 Location of the UK study site: a) along the Channel. b) within the sub-sediment cell between Selsey Bill and Beachy Head (South Downs Coastal Group, 1996). c) View of Birling Gap.

1. From Selsey Bill to Brighton Marina: this sub-cell is approximately 52 km long. The littoral zone comprises various types of environment including estuaries, sand dunes, mixed, mixed sand and gravel, and pure gravel beaches. The dominant LST is eastward. This drift is disrupted in places by obstructions, most notably by harbour arms and river mouths at: Pagham, Littlehampton, Shoreham and Brighton Marina, the latter preventing sediment to pass through to further downdrift areas. LST within the cell is nourished by the material eroded on the western side of Selsey Bill, onshore migration of sediment from the Inner Owers Bank and Kirk Arrow Spit, kelp-rafted shingle deposits, river sediment discharges and wave-induced onshore shingle movement (South Downs Coastal group, 1996). The rivers along the coast of the sub-cell 4b currently supply the coast with fine sediment.
2. From Brighton Marina to Beachy Head: this sub-cell is approximately 30 km long. This stretch of coast is less varied comprising throughout a succession of Cretaceous chalk cliffs reaching >100 m in maximum height and fronted by gravel or mixed beaches resting on a chalk shore platform that stretch seaward for approximately 75 to 300 m. The LST is oriented from west to east and, as is the case in the adjacent sub-cell to the west, is partially disrupted by a harbour arm at Newhaven and protective works to maintain the river mouth at Cuckmere Haven. Sediment supply in this cell relies on kelp-rafted sediment, river sediment discharge, wave-induced onshore sediment movement (South Downs Coastal Group, 1996) and cliff erosion (Dornbusch et al., 2006b, 2008a). According to the beach management plan report (South Downs Coastal Group, 1996), this sedimentary sub-cell is much more dependent on a sediment recycling coastal policy along the coast in contrast to the cell between Selsey Bill and Brighton Marina. Beachy Head represents the end of that sub-sedimentary cell because its resistant chalk headland acts as a partial barrier to sediment transport although little contemporary movement occurs.

The entire cell from Selsey to Beachy Head is heavily managed all along by groynes and recycling/recharging management schemes. A review of the soft engineering practices that includes this sediment cell points to the value of nourishing or recycling plans for the sustainability of the Sussex beaches on short time scales but suggests that

the cost of such management clearly compromises its practice on long time scales (Moses and Williams, 2008). The density of the groynes along this coast nowadays makes it difficult to find a stretch of beach that is completely unmanaged. Birling Gap is one of the rare beaches that are not actively managed on the Sussex coastline. Therefore, the beach at Birling Gap is representative of the equilibrium existing between natural longshore drift and natural sediment supply.

Birling Gap is located in the partially independent sediment transport cell between Cuckmere Haven and Beachy Head (Figure 2-1). The beach lies on a shore platform which has a gradient of about 7° in proximity to the beach and approximately 1° near the low water mark (Moore et al., 2001). The beach is backed on its landward side at the extremities by cliffs cut into Seaford Chalk whereas the central part of the beach is backed by frost shattered chalk that lies beneath the floor of a dry valley that exists at the centre of the beach (Nowell, 2007). The beach is orientated WNW-ESE (N110°) and in the central part has a basal sand extension from the base of the cliffs over the upper part of the platform whereas at each end the gravel sits directly on the chalk platform (Figure 2-1). The beach material is primarily composed of flint gravel with a peak grain size distribution of between 30 and 50 mm, and a sand content varying from approximately 0 to 30%. Birling Gap is a relatively isolated beach considering that the closest beach directly updrift is Cuckmere Haven located 4 km away, with only a few deposits of sediment of negligible volume fringing the cliff between these two beaches; and directly downdrift of Birling Gap is Beachy Head, a headland that acts as a barrier to sediment movement.

Only few studies have investigated longshore sediment transport on the East Sussex coast. Jolliffe (1964) investigated the LST using painted pebbles on the beach at Seaford. Unfortunately, in the absence of the wave conditions, no reliable estimate of the yearly transport rates could be determined. As a result of LST, however, the beach management plan between Seaford and Cuckmere Haven aims to hold the line of the shore by recycling material from the east back to the west. This involves the recycling of 75,000 to 100,000 m³/y at Seaford and 7000 m³ y⁻¹ at Cuckmere (between 2004 and 2005) (Williams, 2005). This indicates how important LST is in these areas. The beach at Cuckmere Haven is, in addition, managed with groynes on its western end which slows down the LST in this area.

2.1.2 General wind and hydrodynamic conditions of the area

i. Wind climate.

The long Atlantic fetch drives the general wave climate entering the Channel, however local winds in the Channel itself play an important role in remodelling the local wave climates along the coast. The wind climate (speed and direction) was collected before and during the time of this study between 2001 and 2006 on the Greenwich Lightship (UK Met Office). This station is located at approximately 40 km from the coast to the southeast of Brighton. The prevailing winds throughout these years are from west and south-south west (Figure 2-2) with the strongest winds occurring in winter.

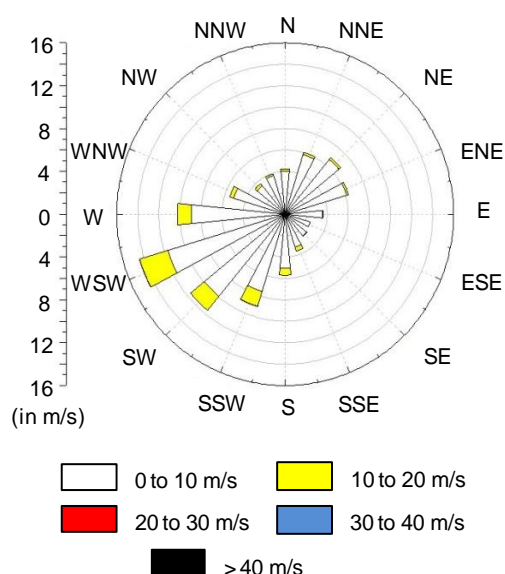


Figure 2-2 Wind rose at the Greenwich lightship station for data collected between 2001 and 2006.

ii. The tide.

In the Channel, the tide comes from the Atlantic and propagates in the Channel from west to east. It is diurnal with a tidal cycle (from one low tide to the following) of approximately 12 hours and 25 minutes. The tidal cycle is asymmetric with the flood being shorter and faster than the ebb (approximately 6 hours against 6 hours and 30 min). The tide at Birling Gap is megatidal with a tidal range at mean spring tides reaching approximately 6 m (Figure 2-3). Tidal currents along the Channel's coasts are too weak to induce longshore pebble movement; however they have a significant influence on sediment transport of the smallest particles such as sand, silt or clay. In the

proximity of Birling Gap, the maximum speed of tidal currents is between 1 and 1.25 m s^{-1} (Figure 2-4).

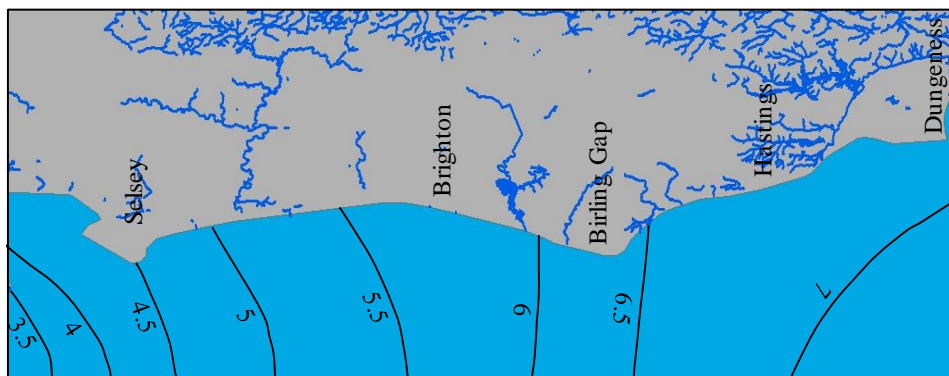


Figure 2-3 Tidal range (m) at mean spring tides. Source: Lee and Ramster (1981).

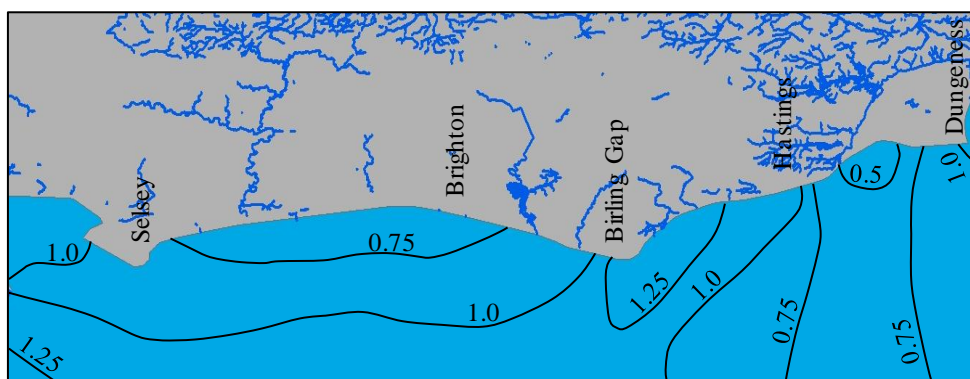


Figure 2-4 Maximum tidal current speed (in m.s^{-1}) at mean spring tides. Source: Sager and Sammler (1968).

iii. Wave climate.

Waves are the dominant parameter responsible for the entrainment of pebble and gravel size particles. Most of the coast is exposed to waves generated by winds coming from the South-West to South. Because of the shape of the Channel, the long North Atlantic fetch drives large waves during periods of strong wind from the west. However, the presence of the Isle of Wright and the concave shape of the shoreline in sub-sediment cell 4d shelter this stretch of coast from waves arriving from the west. The wave characteristics recorded at Rustington (located East of Littlehampton, approximately 7 km offshore, geographic coordinates: $50^{\circ}44.0365'\text{N}$, $00^{\circ}29.6765'\text{W}$) during the time of the data collection of this study between 2004 and 2006 (Figure 2-5) show that the majority of the waves are from a SW direction (approximately 56.1%). The majority,

73.8%, of the waves have a significant height of between 0.1 and 1 m; 21.5 % have a significant wave height between 1 and 2 m; 0.4 % have a wave height between 2 and 3 m, and only 0.05% of the waves have a significant height >3 m. It is clear also that the highest waves are generally observed in the winter between September and April and are from the South to South-West.

The most frequent wave peak periods are between 4 and 7 s, but peak periods >10 s are also quite common (high energy waves). Generally, the high peak periods are associated with Atlantic waves coming from the South-West. In contrast, waves with shorter peak periods are generally the result of local winds (smaller fetch) and therefore deliver less energy onto the shoreline.

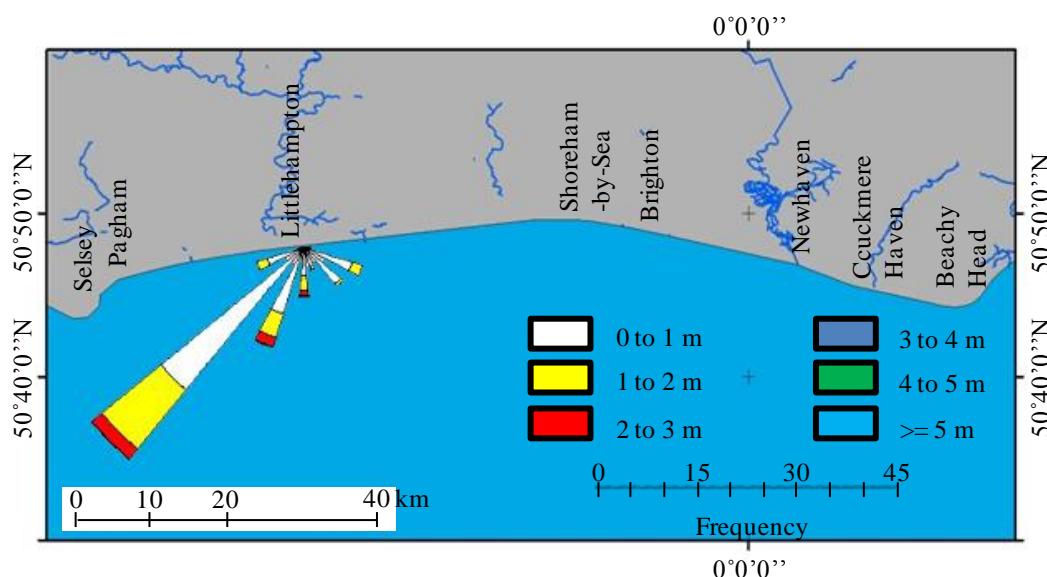


Figure 2-5 Significant wave height recorded at Rustington between 2004 and 2006 (data collected from the Channel Coastal Observatory's website, www.channelcoast.org).

2.1.3 Recent evolution of Birling Gap

Prior to the current study, no regular records of the beach profile evolution at Birling Gap have been made although an historical study has shown cliff retreat of up to 0.7 m y^{-1} and a decrease in the average beach width from 57.3 m to 27.7 m between 1873 and 2001 (Dornbusch et al., 2006b, 2008a). The study used Ordnance Survey Maps at a scale of 1:10,560 from 1873 to 1928, large scale (1:5000) air photographs and one LIDAR survey covering the period from 1973 and 2001, together with regular DGPS surveys from 2003 to 2007 to determine the beach profile morphology, the cliff line, High Water Level (HWL) mark and the average slope sustained by gravel beaches over time. These figures clearly show that the beach at Birling Gap has suffered significant erosion since 1873, suggesting that the supplies of sediment at Birling Gap are not sufficient enough to counterbalance the losses caused by LST.

Between 1873 and 2006 the beach at Birling Gap has been progressively pushed landward simultaneously with the cliff retreat (Figure 2-6). During this period, the elevation of the HWL mark has increased resulting in a shortening of the beach profile and decrease of beach thickness, synonymous with a beach volume decrease. This decrease in beach volume is the result of the combined effect of an increasing HWL over the last 140 years and a reduction in availability of coarse sediment along the stretch of coast between Brighton and Beachy Head (Dornbusch et al., 2008a). In response to a Public Inquiry, Moore et al. (2001) estimated the inputs and outputs of sediment at Birling Gap between 1874 and 2000 and concluded that the beach has a negative sediment budget of about $-386 \text{ m}^3 \text{ y}^{-1}$.

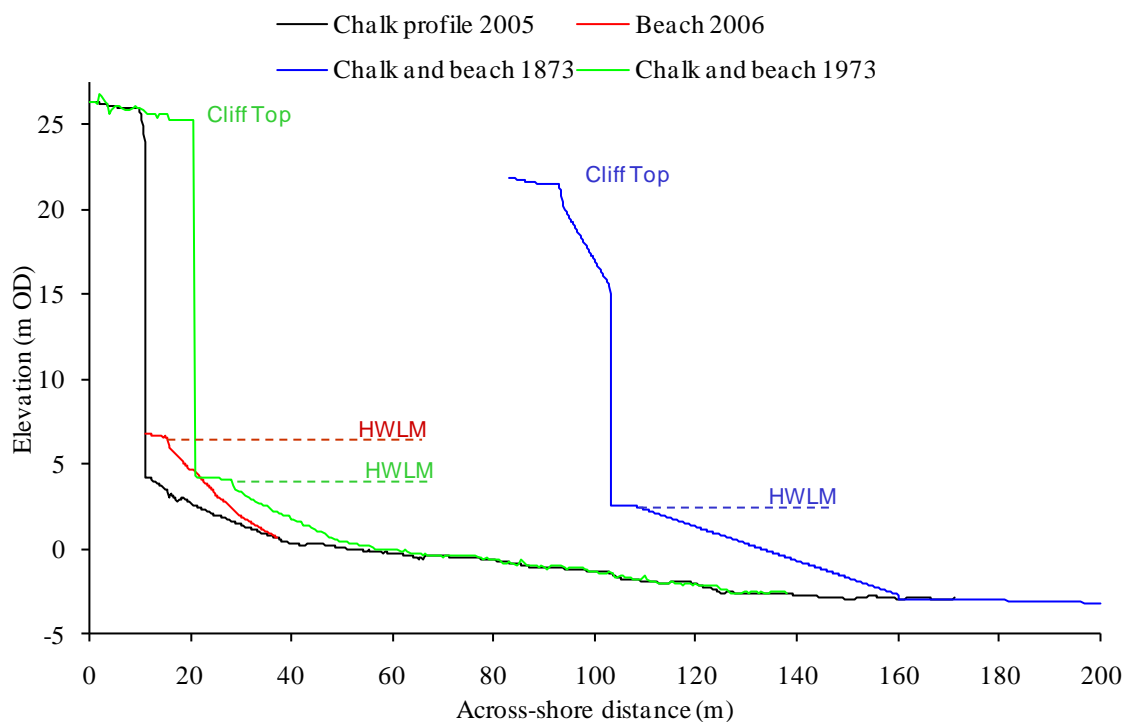


Figure 2-6 Change in geometry of a beach profile located 215 m west of the access steps at Birling Gap. The 1873 profile is based on the location of feature lines on the map and associated elevation from tide data. The 1973 profile is calculated from digital stereo air photographs with a ground resolution of 0.07 m. The 2005 profile is extracted from the LIDAR survey carried out by the Environment Agency. Chalk refers to the cliff and shore platform part of the profile whilst beach refers to the mobile sediment (Dornbusch et al., 2008a).

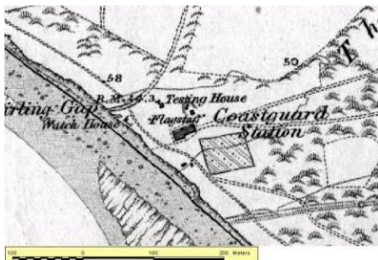
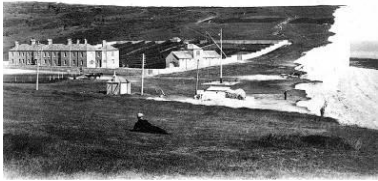




 <p>Ordnance Survey map, 1873 (Scale 1:10560).</p>	 <p>Postcard, 1908.</p>
 <p>Postcard, 1920s</p>	 <p>Postcard, 1970s</p>
 <p>Aerial picture, 2001</p>	 <p>Photograph, 2002</p>
 <p>Photograph, 2008</p>	

Figure 2-7 Illustration of the coastline evolution over the last 140 years (Postcards courtesy of Rendel Williams, Photographs courtesy of Uwe Dornbusch).

2.1.4 Gravel/cobble supplies

The harbour arm at Brighton Marina is assumed to stop the sediment transport coming from the west and therefore the possible sources of sediment currently feeding the sub-sediment cell between Brighton Marina and Beachy Head is thought to rely on kelp-rafted sediment, river sediment discharge, wave-induced onshore sediment movement and cliff erosion (South Downs Coastal Group, 1996). Of these, shingle supply from rivers along that stretch of coast can be discarded as they do not have the competency or the material capacity to deliver coarse particles to the sedimentary system. Shingle supply by kelp-rafting and wave-induced onshore movements is also very limited because of the chalk platform length (reaching up to 300 m long in some parts of the coast). Therefore, the only significant contemporary source of flint sediment for the sedimentary cell comes from the chalk cliffs and platform along the coast between Brighton and Beachy Head.

- Volume of flint produced from cliff erosion between Brighton and Beachy Head

Dornbusch et al. (2006 a, b) determined the cliff retreat and the chalk platform erosion from Brighton to Beachy Head for each 50 m section of coastline for the time period between 1873 and 2001. For each section they determined the cliff height and the flint content to calculate the volume of flint contributed to the beach by cliff retreat. The flint content tends to increase from west to east (Table 2-1).

Coastal Area	Flint Content (%)
Saltdean to Newhaven	1.5 ± 0.5
Seaford Head	3.5 ± 0.5
Cuckmere Haven to Belle Tout	2.5 ± 0.5
Belle Tout to Beachy Head	4.5 ± 0.5

Table 2-1 Flint content for four sections of the Sussex chalk cliffs (Dornbusch et al., 2006b).

Using these measurements, Dornbusch et al. (2006b) calculated that the volume of flint produced by the Sussex cliff falls was equivalent to $4610 \pm 890 \text{ m}^3/\text{y}$. More locally, Moore et al. (2001) estimated that the cliffs at Birling Gap were supplying $315 \text{ m}^3 \text{ y}^{-1}$ of flint between 1874 and 2000.

- Volume of flint produced by the shore platforms between Brighton and Beachy Head

The erosion of the chalk platform can be a second source of flint pebbles to the beaches. Indeed, the chalk platform is comprised of relatively homogeneous layers of chalk separated by well defined bedding planes. Stripping of joint bound blocks from the individual bedding planes often creates predominantly seaward facing micro-cliffs. The joint-bound released boulders are then quickly destroyed by wave action and abrasion which progressively releases the flint contained. Other processes of erosion appear to be of less importance. Dissolution of the chalk platform by sea water is very limited during a tide cycle as the sea water quickly gets saturated in calcium carbonate (Dolique, 1991). Living organisms can also be responsible for chalk platform downwearing (Nestoroff and Melieres, 1967; Andrews and Williams, 2000). For example, Andrews and Williams (2000) measured that the population of limpets can be responsible from 0 to 49 mm of the annual lowering of the chalk platform. On the other hand, other organisms such as algae for example can sometimes play a protecting role acting as a strong cover (Bournerias et al., 1992; Andrews and Williams, 2000). The flint realised by the chalk platform along the East Sussex coast was estimated by Dornbusch et al. (2006b) at $370 \text{ m}^3 \text{ y}^{-1}$.

Based on the measurements of flint delivered by the cliff erosion and the platform backwearing, Dornbusch et al. (2006b) estimated the actual volume of shingle contributing to the beach gross at approximately $7700 \text{ m}^3 \text{ y}^{-1}$ (to determine the volume change from the raw flint produced by the cliffs to the actual volume of flint pebbles contributing to the beach growth a conversion factor of 0.65 was used). This relatively low estimate highlights that the natural sedimentary system is unlikely to sustain itself without human intervention. Indeed, if a beach such as the one at Seaford was not managed, the natural supply would not compensate the estimated $100,000 \text{ m}^3$ of sediment transport experienced on this beach each year.

2.2 The Bas-Champs of Cayeux-sur-Mer

2.2.1 Geography and morphology of the site and its sedimentary cell: From the Seine Estuary to the Somme Estuary coast

Cayeux-sur-Mer is located at the downdrift end of a 146 km long sedimentary cell between the Seine estuary and the Somme estuary in Upper Normandy, northwest of France (Figure 2-8).

The Upper Normandy coast presents a large variety of coastal environments: cliffs, gravel and mixed beaches, sand dunes and estuaries. The coastline can be divided into three different units each having specific geologic and hydro-sedimentary characteristics:

1. From The Havre to Antifer: The coast is approximately 25 km long and is mainly made of Cretaceous chalk cliffs oriented SSW-NNE (approximately N30°) sometimes bordered by coarse sediment beaches. The residual LST is directed southward from the Cap d'Antifer to the Havre.
2. From Antifer to Ault: This coastal area is approximately 105 km and is made of high Cretaceous chalk cliffs (average of 90 m high), but this time oriented SW-NE (approximately N60°). This stretch of coast is concave between Saint-Valérie-en-Caux and Ault with a maximum inflection in the proximity of Dieppe. This unit is dissected by deep valleys across which substantial coarse grained beaches have developed, for example at Fécamp, Veulettes, Saint-Valérie-en-Caux, Pourville, Criel. The length of coastline occupied by these beaches represents in total 25 km (Costa, 1997). The combined effects of the general orientation of the coast in this unit and the dominant wave direction drive a residual LST from Antifer toward Ault. In front of the cliff toe there is an intertidal chalk platform similar to the East Sussex coast. This active coastal cliff line continues further inland in a northeast direction at Ault, where it now forms a fossil cliff because of protection by the Bas-Champs of Cayeux.

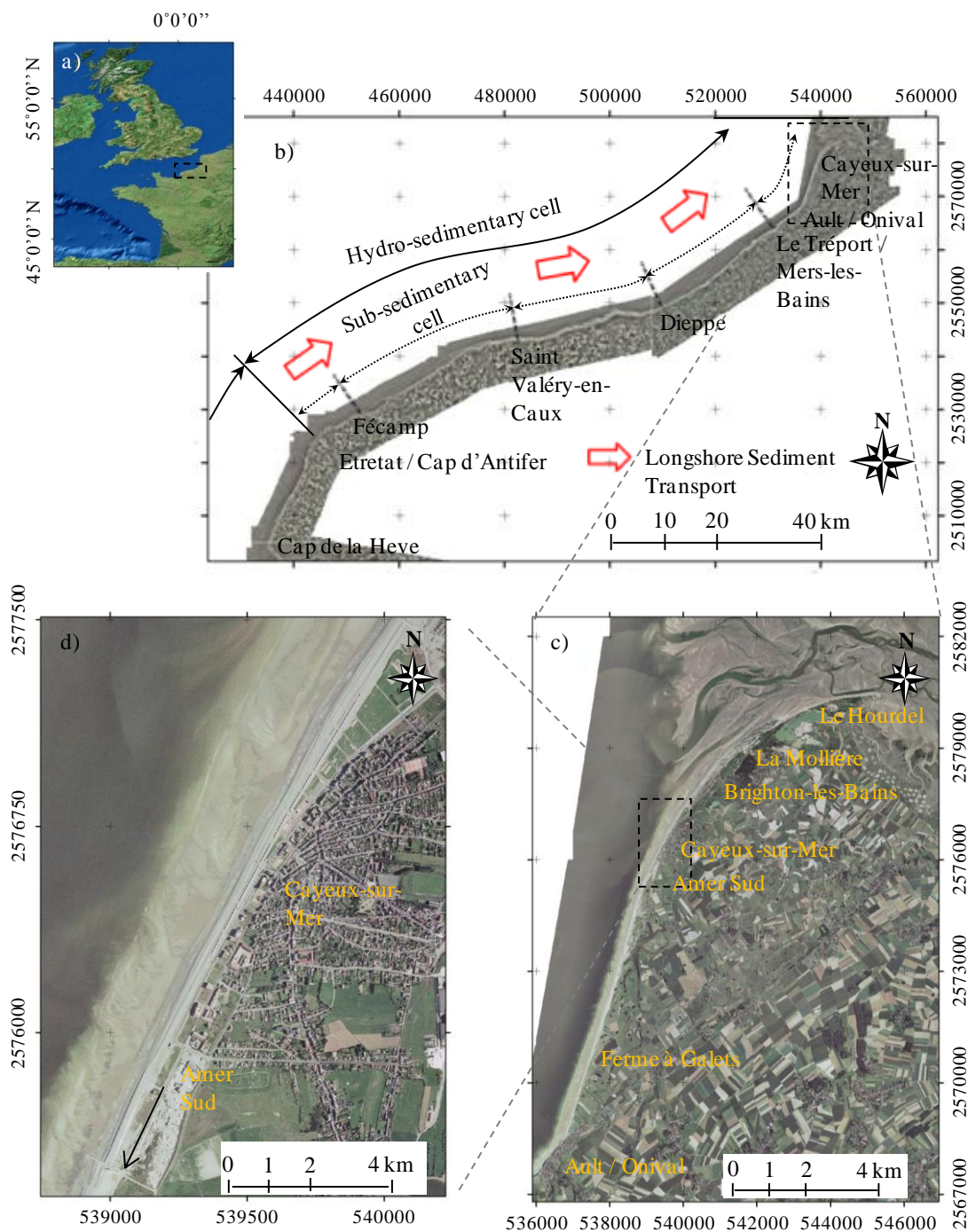


Figure 2-8 Location of the French study site: a) On the Channel. b) Within the sediment cell between Le Havre and the Somme Estuary. c) View of the gravel barrier between Ault-Onival and Le Hourdel. d) View of the survey area at Cayeux-sur-Mer.

3. From Ault to the Somme Estuary: This area corresponds to a 16 km spit oriented N20-30°. The spit has a bimodal particle size distribution with peaks in the medium-sized gravel (10 – 20 mm) and cobble (40 – 50 mm) size ranges and contains approximately 20% sand (Dolique, 1998). Its southern part suffers severely from erosion which, over the last 40 years, has necessitated the intensive installation of groynes and the creation of recycling-recharge management plans. This area is the front line of a colossal triangular shaped accumulation of sand and gravel deposits called the “Bas-Champs” (4200 hectares) which has developed over the last 2500 years (Briquet, 1930) protecting the non-active cliff line. The southern part of the gravel barrier has developed at an angle at 30° to the sea cliffs. The spit here (close to Ault-Onival) presents a steep sea side slope ranging from 8 to 9° and an even steeper slope on its land side. The gravel part of the beach is up to 100 m wide here (Dolique, 1998).

Along the next 7.5 km between Ault and Cayeux-sur-Mer, the coastline is managed by groynes set 90 m apart and sediment recycling/recharge. Before 2001, approximately $30,000 \text{ m}^3 \text{ y}^{-1}$ were recharged on the downdrift end of the spit at Ault-Onival, where the groyne field starts to counterbalance the effect of longshore drift which was estimated to be 30,000 to 40,000 $\text{m}^3 \text{ y}^{-1}$ (Sogreah, 1995b). In 2001, the littoral transport on this stretch of coast was re-estimated down to 15,000 to 20,000 $\text{m}^3 \text{ y}^{-1}$. In accordance with this recalculated LST, the recycled/recharged volumes of beach material were reduced to approximately 19,500 $\text{m}^3 \text{ y}^{-1}$ (Sogreah, 2009).

At Cayeux-sur-Mer, before 2001, approximately 55,000 m^3 of sediment was excavated in the north of Cayeux approximately 3 km beyond the end of the groyned section at the Amer Sud. This sediment plus an additional 20,000 m^3 extracted from a quarry in Le Crotoy was recharged/recycled at the top of the beach along a 450 m stretch just downdrift (north) from the last groyne (Amer Sud). Bulldozers were used to mould it into a steep-faced compact ridge, approximately 4 m high and 10 – 15 m wide which acted like a wall at the back of the beach. Since 2001, this amount of recycled/recharged material was reduced to 42,000 $\text{m}^3 \text{ y}^{-1}$ and extra recharge/recycling was conducted when it is necessary to prevent flooding. This sediment is generally entirely recycled from the

north of Cayeux since 2001 in three to four occasions over the year depending on the necessity to do so (i.e. when the wave climate and the tidal range present a risk of flooding). As the volume of sediment recycled is not sufficient to counter balance the LST in front of Cayeux-sur-Mer, estimated at 70,000 to 80,000 m³ y⁻¹ (Sogreah, 1995b), a deficit of sediment occurs, which is responsible for the threat of flooding experienced recently at Cayeux-sur-Mer. In front of Cayeux-sur-Mer, the ridge is approximately 200 m wide and the sea face slope is less steep, with an angle varying between 6 and 7° (Dolique, 1998).

From Cayeux-sur-Mer to Le Hourdel, multiple fossilised gravel spits can be observed. These are remainders of the past locations of the shoreline and evidence of this area's past evolution. The end of these spits curve landward and are colonised by vegetation. Because of the many fossilised spits accumulated just north of Cayeux the gravel beach reaches up to 600 m in width. At the back of this system of multiple-spits, there are systems of wash over fans and drainage channels. These fans are generally submerged during the highest high tides or overwash events, which feed them with sand and fine sediment. These washover deposits are heavily vegetated.

The Bas-Champs are mainly composed of marine deposits (silt and clay) typical of salt-marshes, polders or overwash features and the surface has matured into fertile soils. These deposits are from the Sub-Boreal and Sub-Atlantic periods i.e. from 5500 years BP to the present (Dolique, 1998). Over the years, the reduction of the natural sediment supplies is particularly noticeable through the landward recession and lowering in elevation of the crest on the basal part of the gravel spit at Ault-Onival, whereas the spit directly north of Cayeux is showing accretion and is progressing northward. The Bas-Champs have an average elevation of +4 to +5 m NGF (average French levelling based on the average water level observe in Marseille and considered as being 0 m elevation) whereas the gravel spit's crest has an average of +9 to +10 m NGF (note that this elevation needs to be sustained by the coastal management planning in the southern part of the spit between Ault and Cayeux). The highest high water levels observed in this area are between +7 to +8 m NGF and therefore the risks of flooding caused by breaching and overwashing of the ridge are great.

Between Cayeux-sur-Mer and Le Hourdel, the back of the gravel spit is bordered by sand dunes most of which are vegetated (Figure 2-9). These sand dunes are on the top of the clay-silt deposits of the Bas-Champs but also on the top of fossilised older spits that have contributed to the growth of the entire system. These sand dunes were created and are nourished by aeolian sand removed from the intertidal sand terrace in front of the Somme Estuary. This sandy platform can be 800 m long in front of Cayeux-sur-Mer and up to 2 km in front of Le Hourdel, giving plenty of time for the sand on the platform to partially dry and be transported by the wind during low tide (Dolique, 1998).

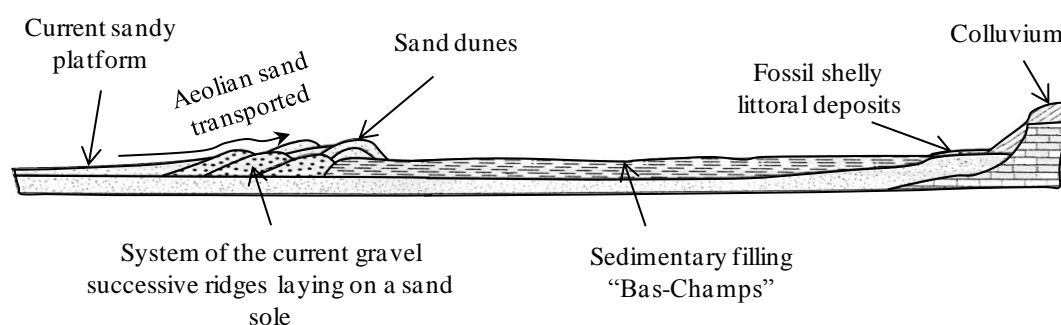


Figure 2-9 Cross-sectional view of the Bas-Champs deposits (Dolique 1998).

2.2.2 General wind and hydrodynamic conditions of the area

In contrast to the UK, access to the meteorological and hydrodynamic data along the Channel is not easy and free in France. In this study onshore wave data were collected for each specific field experiment on the French coast and so the purchase of meteorological and hydrodynamic data was judged unnecessary. For this reason, the description of the weather conditions presented in this section are based on data collected from earlier studies or from models available online from the French authorities (CETMEF, 2009a) which explains the inconsistency of the survey periods for each parameter presented. These data are only used to describe the general conditions along this stretch of coast in order to permit the reader to understand the context in which the spit develops.

i. Wind climate (Figure 2-10)

This particular area of the French coast is subject to frequent strong winds. Analyses of the wind conditions along the Upper Normandy coast were collected in aggregate by

semaphore station from 1951 to 1994 in Dieppe, in La Heve, and also on boats in the Channel from 1960 to 1980. The most frequent wind direction is from South-West to West and less frequently North-East, especially at the end of the spring. The most violent winds are from West between November to March, and North-East from April to June. These winds, operating over the 100 km local fetch in the proximity of the Bas-Champs coastline drive the local wave climate. Costa (1997) estimated that wind wave conditions represent 21% of the annual wave climate.

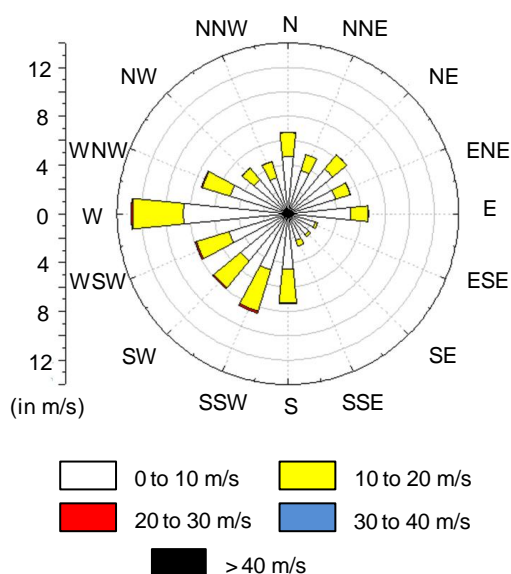


Figure 2-10 Wind rose at Cayeux-sur-Mer for data collected between 2006 and 2010. These data are not real measured values at the location but come from a forecast model (Global Forecast System) based on the nearest point of measurement.

ii. The tide

The tide in the north of France is influenced by the orientation of the coastline such that the tidal range increases from Le Havre to the Somme Estuary. This phenomenon is amplified on the French as compared to the English coast by the rotation momentum of Earth (SHOM, 1997). As a consequence, the tide at Cayeux-sur-Mer is megatidal having a range reaching up to 10.55 m. Haugel and Cherubini (1980) and then Simon (1994) showed that the annual surges are around 60 cm, decadal surges close to 80 cm and centennial surges around 1.10 m.

The tidal current speeds decrease significantly when approaching the coast. At approximately 1.2 km from the coastline, these speeds during the highest spring tides

range from 0.6 m s^{-1} during the flood and 0.35 m s^{-1} during the ebb (Sogreah, 1990) whereas at the very proximity of the gravel ridge, the flood speed is $<0.2 \text{ m s}^{-1}$ during a strong spring tide (LCHF, 1965).

The flood tide is also generally faster than the ebb (5 hours against 7 hours) and therefore the residual tidal current is normally oriented north-eastward, parallel to the coast (Costa, 1997), but this tendency can be reversed by meteorological conditions (Janin and Blanchard, 1992; Janin and Dumas, 1993).

iii. Wave climate (Figure 2-11)

The yearly wave climate along the Upper Normandy and Picardy coasts is dominated by waves coming from the South-West to North-West (approximately 65%). Just over half, 52 %, of these waves have a significant height between 0.1 and 1 m; 25.3 % have a significant height between 1 and 2 m; 12.5 % have a significant wave height between 2 and 3 m, and only 4 % are more than to 3 m.

For every category of significant wave heights measured, waves coming from the west are clearly dominant; however for the smaller significant wave heights (0.1 to 1 m), the distribution between west and north is slightly more balanced. Waves whose significant height is more than 3 m only rarely come from north (Figure 2-11). The most frequent and strongest waves appear in the winter between October and March (Costa, 1997).

The wave periods are generally comprised between 4 and 7 s and are rarely more than 10 s (Figure 2-12).

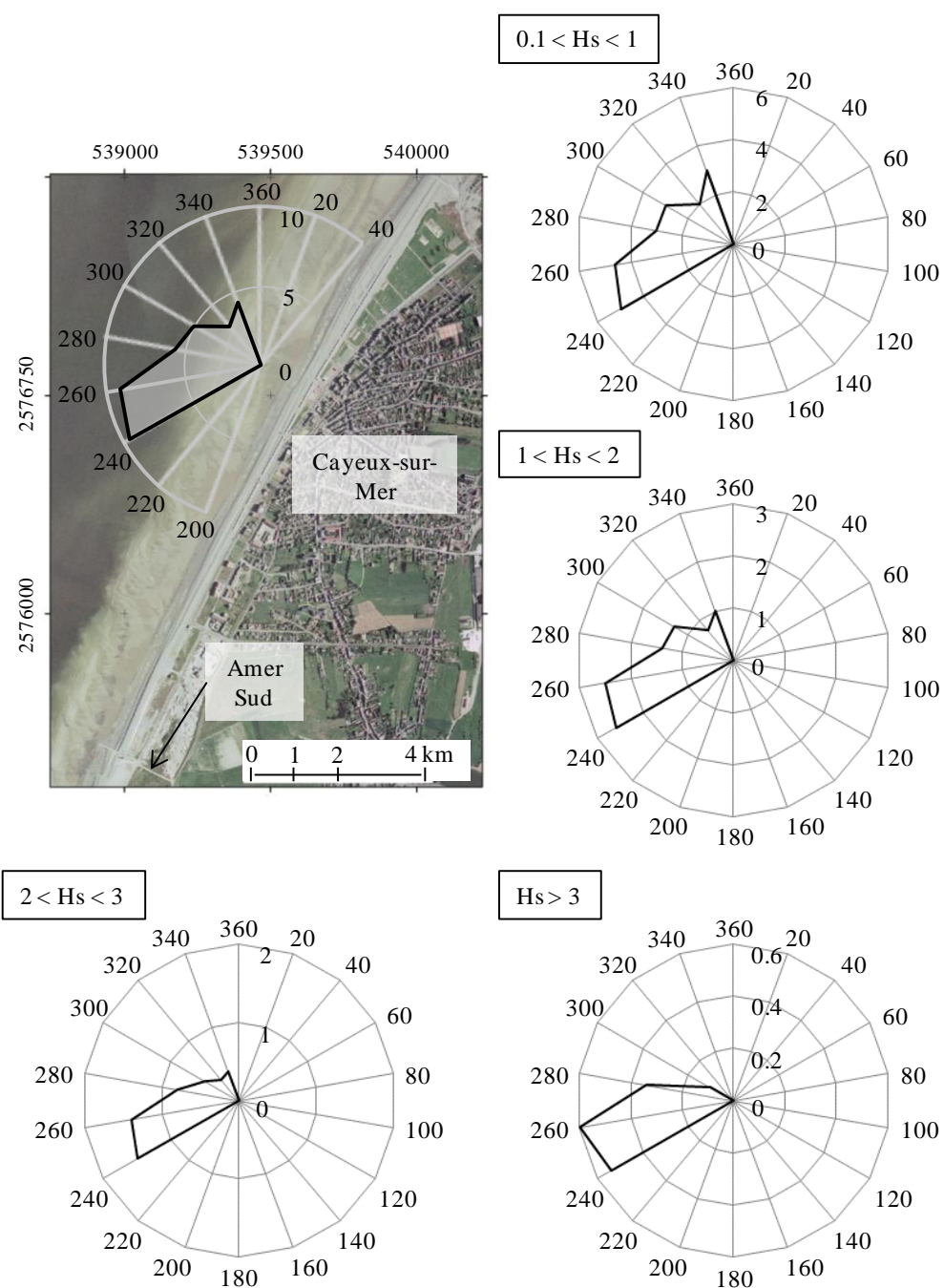


Figure 2-11 Distribution of the wave directions by their significant wave height at Cayeux-sur-Mer (Sogreah, 1995a).

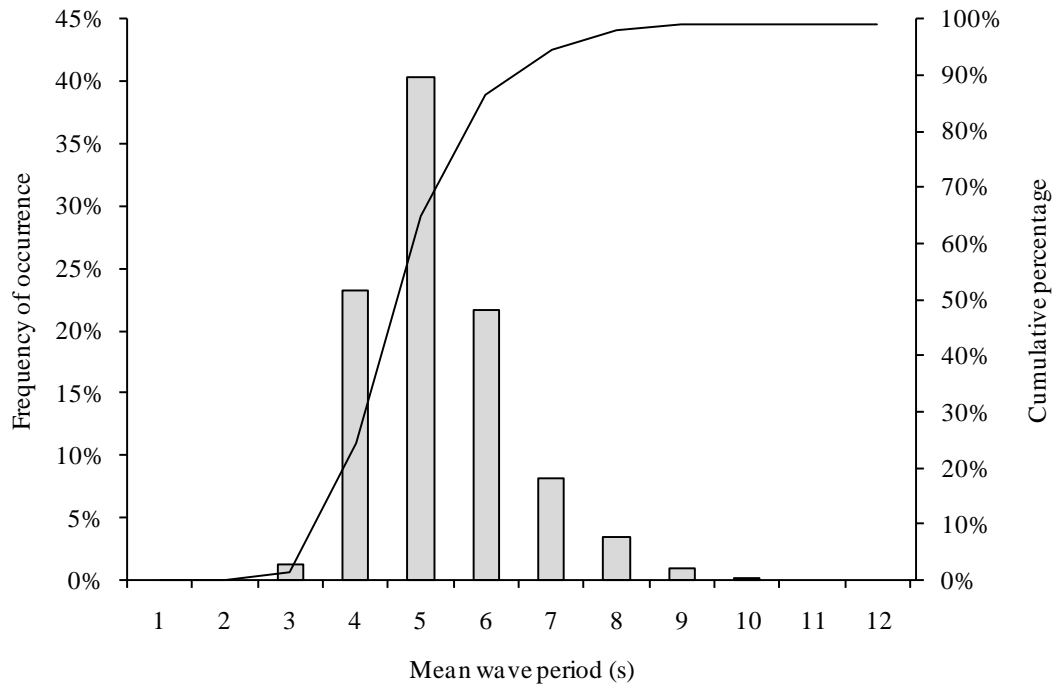


Figure 2-12 Average wave period observed in the vicinity of Dieppe above the isobath -23.6 m. These data were simulated retrospectively, using the software TOMAWAC developed by EDF R&D – LNHE, from data collected between January 1979 and August 2002 (CETMEF, 2009b).

2.2.3 Coastal defence management since 1965

In 1965, because of noticeable erosion of the basal part of the gravel spit in front of Ault-Onival threatening flooding of the Bas-Champs, the authorities set up a coastal defence planning (Figure 2-13). Between 1965 and 1984, the policy was to slow down the natural longshore drift by the construction of fifty groynes. These groynes were each 80 to 90 m long and set 90 m apart. In addition, 160,000 m³ of mixed sediment was recycled from Le Tréport to the most down drift parts of the spit.

Since 1984, for the 20,000 m³ y⁻¹ of cobbles have been extracted from the beach by industry, SILMER who have been required to return an equivalent volume of cobbles to the beach. Twenty percent of this volume was recharged at Ault-Onival while the other 80 % was recharged northward of the last groyne at the time to compensate the LST. SILMER is a traditional industry that has the exclusive right to collect cobbles on the spit. The interest of this industry relies on the purity in silicates that the pebbles on the

beach have. The volumes of pebbles that are recharged by SILMER are of no economical interest for them.

In February 1990, exceptionally stormy weather resulted in significant erosion, beach breaching and flooding of the southern area of the Bas-Champs. To restore and sustain the pre-storm beach volume all along the barrier, the recycling/recharge of 660,000 m³ of gravel was necessary. To supply this volume, 460,000 m³ of gravel were extracted from the down-drift end of the barrier while 200,000 m³ were extracted from quarries. In 1993, five new groynes with the same design and spacing as the elder ones were added 1 km away from the last groyne built up in 1965 in a downdrift direction where the beach breached in 1990 (Figure 2-13). In 2000, twenty five additional groynes were constructed and the original fifty were repaired and improved and a total of 350,000 m³ of sediment (mainly recycled from north of Cayeux) was distributed between the groynes (Figure 2-13). Since 2000, the entire area from Ault to the Amer Sud (south of Cayeux; Figure 2-13) has been managed by groynes and the beach crest sustained at an elevation of +10 m NGF and a width of 20 m. Since then as mentioned earlier (Chapter 2 Section 2.2.1), approximately 42,000 m³ y⁻¹ of sediment are recycled from north of Cayeux to the Amer Sud and approximately 19,500 m³ y⁻¹ are recharged between the groynes between Ault and the Amer Sud.

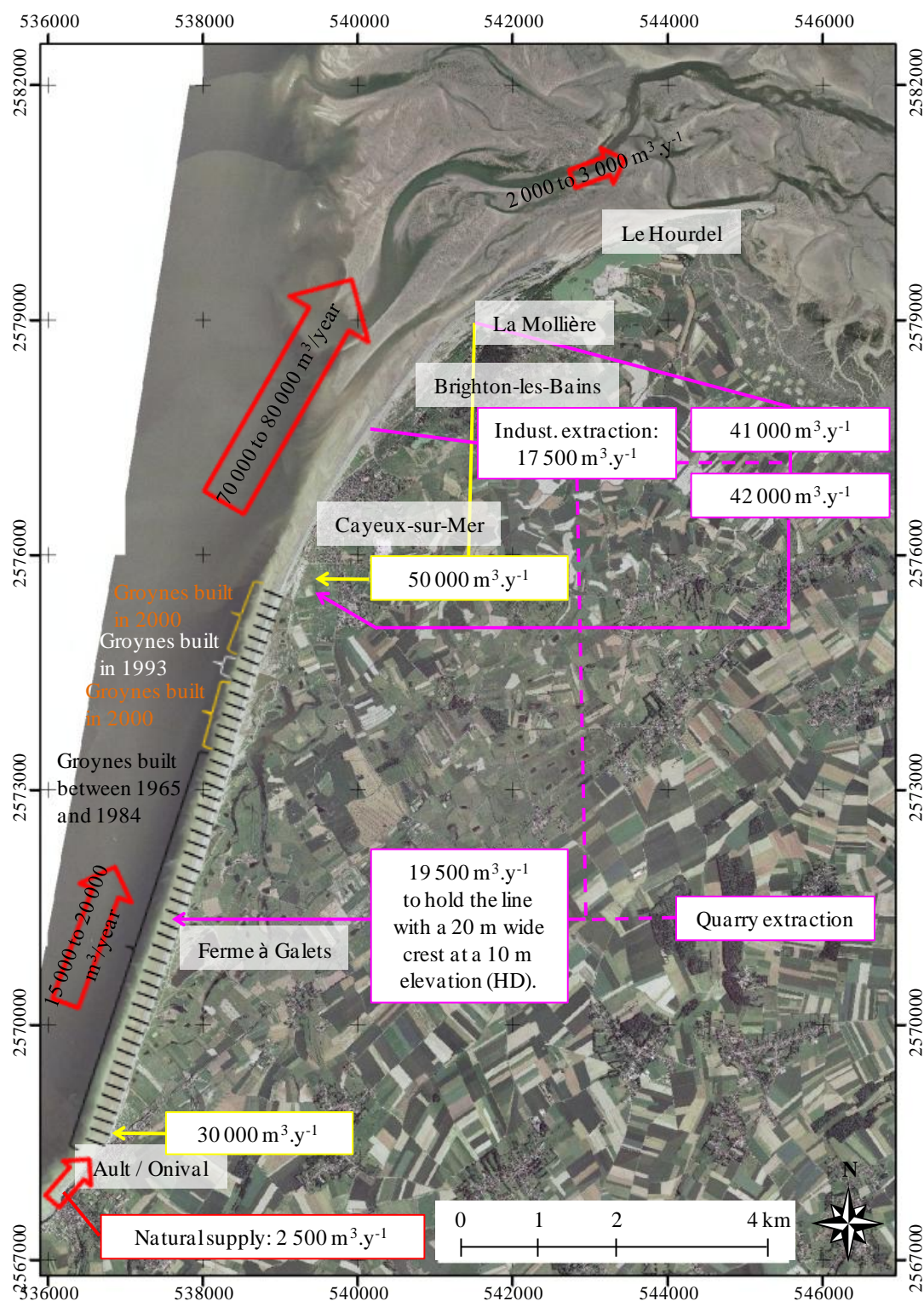


Figure 2-13 Coastal management along the Bas-Champs. Yellow coloured boxes and arrows represent the management plan used from 1997 to 2001, whereas the purple coloured ones represent the management plan practiced from 2001 (based on Sogreah, 2009; Dolique, 1998). NB: The number of groynes drawn on the map is not representative of the actual number of groynes in place, but represents the length of the beach that they occupy.

2.2.4 Recent evolution of the gravel spit of the Bas-Champs

The recent evolution of the spit can be followed using historical maps available from the 18th century; using beach profile surveys done or ordered by local authorities (along a single profile north of the 50th groyne - approximately 4.5 km north of Ault) in 1965, 1990 and 1994; and using from aerial photograph taken from the late 1930s up until now (Table 2-2, Figures 2-14 & 2-15).

Gravel spits can be divided in three zones that exhibit contrasting processes and evolution: a zone of erosion, which is literally “cannibalised” (Orford et al., 1996) to support a second zone where accretion occurs, and between them a “fulcrum” where erosion and accretion are approximately equal. Despite the heavy coastal management that has been in place for more than 50 years now, these three zones can still be identified, although the processes have slowed down.

i. From Ault to Amer Sud

There have been a number of measurements or estimates of beach erosion in the proximity of Ault-Onival and, although the results differ, they all indicate considerable rates of erosion (Table 2-2).

Author	Section of the coastline	Beach retreat rate	Time period
Heraud, 1880	Ault-Onival	-0.7 m y ⁻¹	XVIII century
Bellesort, 1990	Ault-Onival	-0.2 m y ⁻¹	1969 to aprox.1990
Costa and Regnault, 1992	Ault-Onival	-0.35 m y ⁻¹	1969 to aprox.1990
Costa and Regnault, 1992	Onival to Ferme à galets	-0.55 to -0.95 m y ⁻¹	1939 to 1991
Costa, 1997	Ferme à galets to North of Hâble d'Ault	-0.7 to -1.5 m y ⁻¹	1939 to 1991
Dallery, 1955	From Ault to the Hâble d'Ault	-1.3 m y ⁻¹ -1 m y ⁻¹	1884 to 1912 1920 to 1955
Bellesort and Migniot, 1966	From Ault to the Hâble d'Ault	-0.3 m y ⁻¹ -0.5 to -1.5 m y ⁻¹	1884 to 1936 1939 to 1961
Hascoet, 1988	From Ault to the Hâble d'Ault	-1.8 m y ⁻¹	1939 to 1988
Dolique, 1991	From Ault to the Hâble d'Ault	-1.5 m y ⁻¹ -0.2 m y ⁻¹ (in the groynes)	1939 to 1966 1966 to 1991
Costa, 1997	North of Hâble d'Ault to Amer Sud"	-0.5 to -0.2 m y ⁻¹	1939 to 1991
Costa, 1997	North of Hâble d'Ault to Amer Sud	-0.5 to -0.2 m y ⁻¹	1939 to 1991

Table 2-2 Synthesis of the coastal erosion measurements or estimates from Ault to the Amer Sud (based on Costa, 1997).

Based on the changing position of the HWL marks identifiable on aerial photographs taken in 1939, 1961, 2000 and 2008, it has been possible to observe the impact of the managements work that started in 1965 (Figure 2-15). Between Ault and the Hâble

d'Ault, these HWL marks show a clear retreat of the beach since 1939; however, the mark in 2000 is seaward of 1961, this being a direct consequence of the beach management (Figure 2-15). Near Ault-Onival, the erosion can be measured at approximately 41 m between 1939 and 2000, corresponding to an average retreat rate of -0.67 m y^{-1} . However, between 1939 and 1961, before the mass construction of groynes in this area, this retreat had an average erosion rate of -2.3 m y^{-1} (the coastline moved landward by approximately 50 m during that time period, Figure 2-15). Close to the Ferme à galets, between 1939 and 2000, the beach erosion is lower, with a retreat of only 18 m i.e. approximately -0.3 m y^{-1} . However, between 1939 and 1961 the beach had retreated by approximately 41 m i.e. by approximately -1.9 m y^{-1} . The differential between these rates show again the impact of the coastal management works. Between the Ferme à galets and the Hâble d'Ault, the beach displays little erosion with beach retreating up to approximately 10 m between 1939 and 2000 (average rate of approximately -0.16 m y^{-1}). Between 1939 and 1961, the beach retreated by approximately 31 m (-1.4 m y^{-1}). Again, the coastal management work since 1965 permitted to build out the beach to a state close to what the beach was in 1939.

To summarize, these different rates of retreat observed between 1939 and 1961, and between 1939 and 2000 clearly show the impact of the management work onto the beach. The combined effect of both the groyne development and the recycling/recharging policy not only allowed the shoreline to be held in place but also, since the 1960s, has built the beach outwards.

Now, we are going to enter the area of the beach that saw the development of groynes in the latest stage i.e. in 1993 and 2000 (Figure 2-13). For this reason, the beach evolution from here will be different than the updrift area that has just been reviewed. From the Hâble d'Ault going northward, the 1961 HWL mark lies seaward of the one in 2000, indicating that the beach has progressively receded between 1939 until 2000, direct consequence of the lack of hard engineering management here. Between 1939 and 1961, the beach was actually retreating at this location too but not as dramatically as in the updrift areas (from -0.82 to -1.13 m y^{-1}) which is why the coastal management plan stopped at the Hâble d'Ault. Unfortunately, since 1961, the erosion increased at this

place (retreat measured at 50 m between 1961 and 1991) which led to a breach in 1990 during the big flooding event that has marked the history of the Bas-Champs.

Beach profile surveys between 1965 and 1994 were available in this area (Figure 2-14; NB: the only profiles available are those displayed on the figure). The profile evolution clearly displays a 55 m retreat of the beach crest between 1965 and 1990. Notice that the beach crest elevation from 1965 to 1994 increased from +8.8 m to +10 m NGF in accordance with the beach management plan adopted after 1990. For information, during the flooding in 1990 the beach crest elevation lowered to +8.4 m NGF while the sea water level rose to +8 to +9 m NGF (Beauchamps, informal internet report) and ultimately that crest was completely erased in this area during the flooding event (Dolique, 1998).

In the proximity of the Amer Sud, on its updrift side, during the time period between 1939 and 2000, the high water level mark retreated about 45 m. Since 2000, the coastal management plan permitted to hold the line.

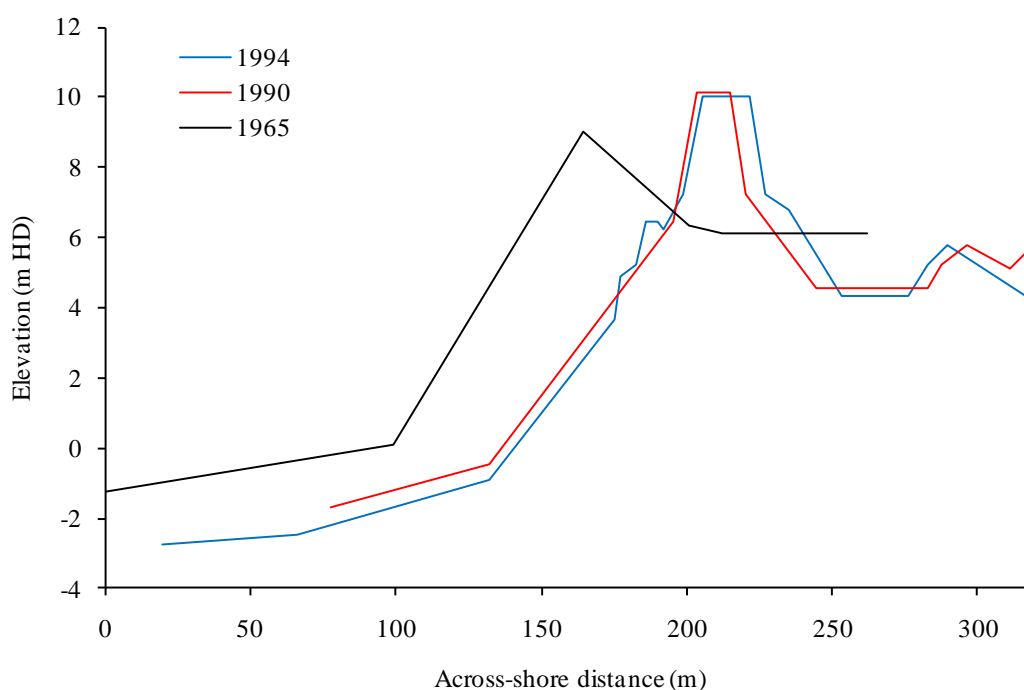


Figure 2-14 Evolution of the beach profile between 1965 and 1994 in proximity of the Hâble d'Ault (Sogreah, 1995b; HD-French Hydrographyc Datum).

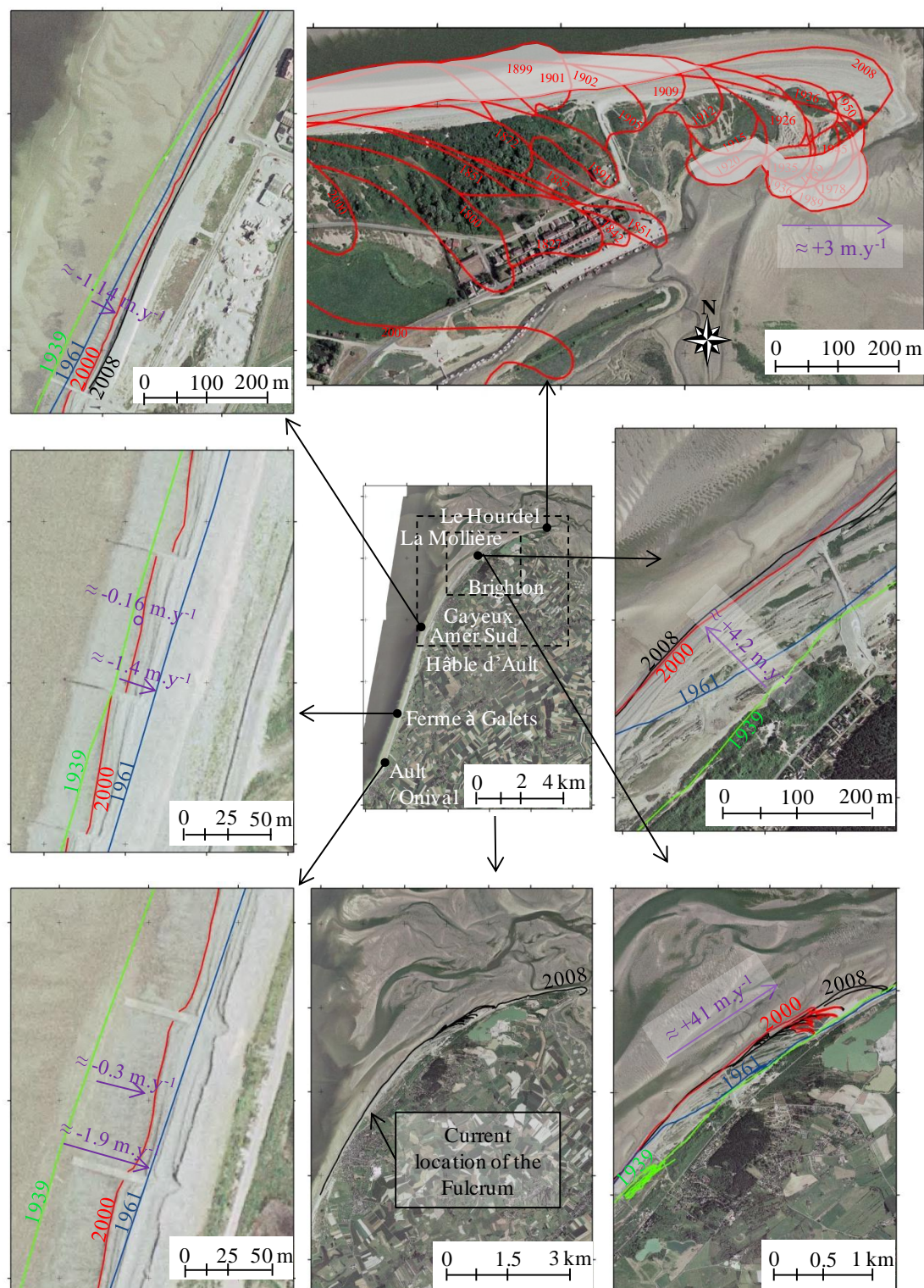


Figure 2-15 Evolution of the Bas-Champs area since 1939.

ii. From the Amer Sud to north of Cayeux-sur-Mer

As previously mentioned, the area just downdrift of Amer Sud is today subject to great erosion and to partially compensate the natural longshore drift, 42,000 m³ of sediment have been recycled here every year since 2001. Between 1939 and 2000 this area eroded by up to 70 m (approximately -1.14 m y⁻¹) but since 2001, the coastline has been stabilised by the recycling management plan. Also, the addition of twenty five extra groynes installed in 2000 had the effect to transpose the point of maximum erosion in a downdrift direction. Today, the Amer Sud represents the emplacement of the terminal groyne on the spit.

In contrast, the area in front of Cayeux-sur-Mer is in relative equilibrium and is where the “fulcrum” is currently located. Various authors have estimated the location of the fulcrum over time. Regrain et al. (1979) estimated its location was 2 km north of Ault in 1925, mid-way between Ault and Cayeux in 1952 and 3 km south of Cayeux in 1979. Dolique (1998) estimated that the fulcrum was in front of Cayeux in 1990. In 2008, the current study estimates that the fulcrum is located in the northern part of the beach at Cayeux (Figure 2-15). From all of these measurements, it can be concluded that the migration of the fulcrum from 1925 to 1990 was approximately 90 to 100 m y⁻¹. This migration has been reduced between 1990 and 2008, to approximately 1 km in the last 18 years (55 m y⁻¹). This slow down in the migration of the fulcrum is almost definitely a consequence of the current coastal defence management and the resulting deficit in sediment experience by the spit.

iii. From north of Cayeux-sur-Mer to Le Hourdel

Between 1994 and 2001, the volume of accretion between slightly north of Cayeux and slightly north of La Mollière was estimated to be up to 313,000 m³ (Sogreah, 2009). Between 1939 and 2008, the current study measured a lateral growth of the beach up to 4.2 m y⁻¹ (Figure 2-15).

Considering the migration of the active spit (in the proximity of La Mollière, just north of Cayeux, Figure 2-15) over time using aerial photographs, a 2.86 km northward growth can be measured between 1939 and 2008. This represents an average accretion rate of >41.5 m y⁻¹. However, this rate is not really representative of the true potential

growth of the spit as human activity has slowed down the natural longshore drift over the last 200 years by reducing the amount of sediment available or by preventing the beach material from circulating freely. The longshore growth of the gravel spit between 1939 and 1961, before the major construction of coastal defences, was nearly 70 m y^{-1} .

In contrast, to the south of Le Hourdel, along a 1.5 km long stretch, the beach shows a lateral retreat of 15 to 20 m between 1971 and 1993 (≈ 3000 to $4000 \text{ m}^3 \text{ y}^{-1}$) (Sogreah, 1995b). Today the material eroded in this area is the main source of coarse sediment feeding the alongshore growth of the extremity of the spit at Le Hourdel which growth was measured at approximately 3 m y^{-1} between 1939 and 2008 based on the aerial photographs.

iv. The sandy foreshore

Comparison of the bathymetry of the sandy platform between 1936 and 1993 shows erosion of the beach between Ault and the Amer Sud. Between Ault and the Ferme à galets, the platform has lowered by approximately 1 m and this increases progressively northwards to reach 2 m at the Amer Sud. In contrast, the sandy platform to the north of Cayeux is accumulating and increasing in elevation (Sogreah, 1995b).

Infilling is a common feature of the natural evolution of estuaries along the Picardy coast and the Somme Estuary is no exception, infilling at the present day. The amount of sand captured by the estuary has been estimated to be around $700,000 \text{ m}^3 \text{ y}^{-1}$ (Sogreah, 1995b). Dolique (1998) suggested that the erosion of the sandy platform south of Cayeux was feeding the accumulation of sand observed north of Cayeux. Part of this sand was also remobilised by the wind to feed the sand dunes that have developed north of Cayeux.

Such bathymetric changes clearly have an impact on the behaviour of the gravel beach. Lowering the platform elevation results in more wave energy delivered to the beach which potentially induces more sediment transport. Reciprocally, increasing the sandy platform elevation, as observed north of Cayeux, tends to reduce the amount of wave energy delivered to the beach. Therefore, the problem of beach erosion suffered in the southern part of gravel spit between Ault and Cayeux is likely to increase with time.

2.2.5 Gravel/cobble supplies

There are only a few possible sources of shingle supply to the sedimentary system located between Antifer and Le Hourdel. The study site sedimentary cell is located in the north-west of the Bassin Parisien. The dominant geology of this sedimentary cell is Upper Cretaceous chalk. Earlier deposits such as the Lower Cretaceous and Jurassic are present only very locally and there are only thin remains of Tertiary deposits of 0.2 to 2 m thick (Costa, 1997). As on the English side of the Channel, the Cretaceous chalk cliffs located between Antifer and Ault-Onival contain considerable volumes of flint that forms the primary natural source of shingle material for nourishing the development of the Bas-Champs area. Flint is generally displayed in the cliffs as homogeneous pluri-kilometric layers (Regrain, 1971) or randomly located nodules. The geological layers have a slight inclination of 8 mm per meter in addition to a down slope tendency orientated NW in association with the Somme's syncline (Prêcheur, 1960). The chalk on the French side of the Channel is denser than that on the English side, contributing to the considerably higher sea cliffs on the French side (Costa, 1997). The intertidal area at the cliff toe comprises a 200 to 400 m wide chalk platform that slopes 0.5 to 1° toward the sea. As on the English coast, the chalk platform is dissected by deep wide runnels corresponding to joints and fault lines or dissolution structures (Costa, 1997).

The rivers along the Upper Normandy coast do not have sufficient capacity or strong enough currents to feed the system with pebble size material. They exclusively carry particles of the sand size or lower. Considerable amounts of coarse sediment material are stored on the floor of the Channel in the proximity of the French coast. These stocks are mostly organised in fossil banks with a sand matrix. These coarse material deposits are barely affected by even the strongest hydrodynamic conditions (Beauchesne and Courtois, 1967; LCHF, 1972).

- Volume of flint produced by the cliffs of Normandy and Picardy

Stéphane Costa has studied the sea cliffs and beaches along the coast of Normandy and Picardy. His observations and measurements, Costa et al. (1996) determined that the

flint content in the chalk varies from 0.9 to 15 % depending on the age of the strata. He also noted that the flint layers are often discontinuous along the coast and determined the percentage of flint at different locations along the cliffs (Figure 2-16).

He showed that the flint content in the cliffs decreases from 6% in the south to 1 % in the north because of the decrease of thickness and the continuity of the flint layer.

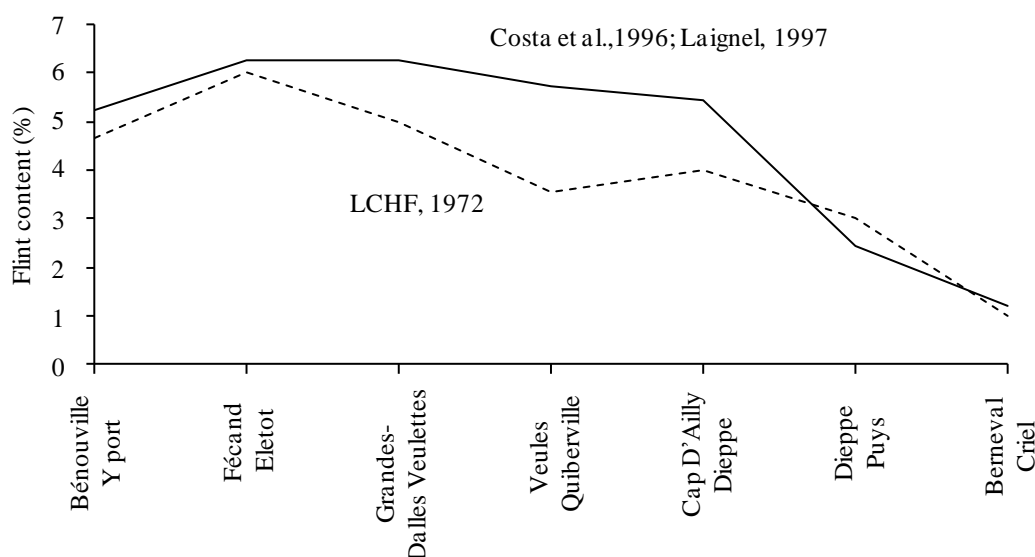
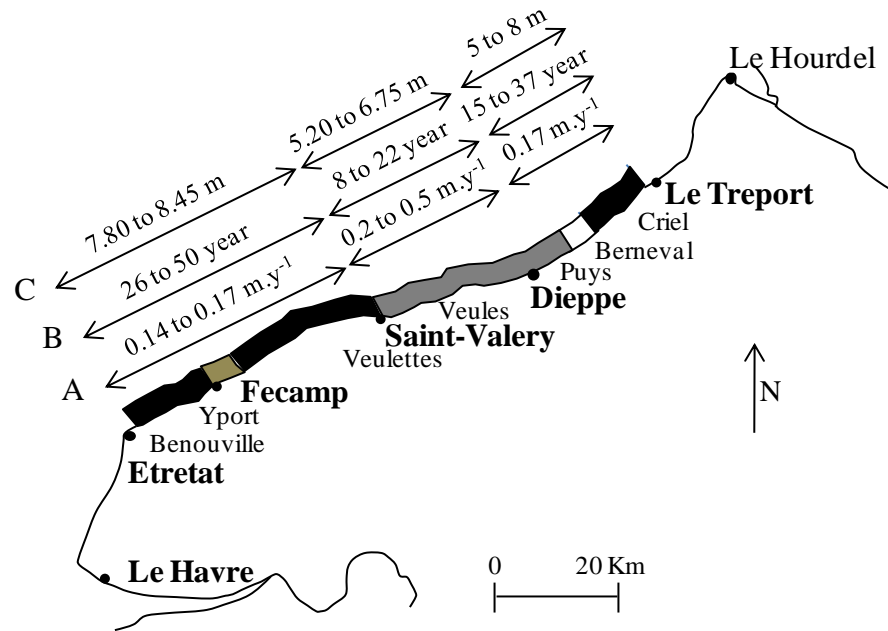
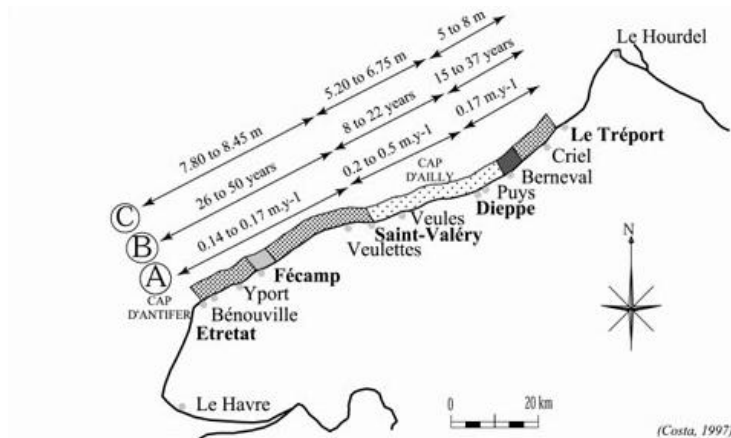
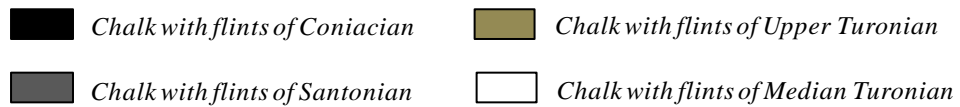


Figure 2-16 Average flint content of the cliffs between Benouville and Criel (Costa, 1997).

For any section of cliff, the cliff retreat rate determines the amount of flint supplied to the beach and thus available for longshore drift. Costa (1997) measured cliff retreat rates from aerial photographs all along the coast of Normandy and Picardy and related them to the geological variations (Figure 2-17). From these measurements Costa and Delahaye (2002) determined that the volume of flint delivered to the sedimentary cell between 1966 and 1995 by the cliff falls between Etretat and Le Tréport is approximately $1,826,687 \text{ m}^3$, which equates to a yearly production of approximately $63,000 \text{ m}^3$ of flint.



Lithologic characteristics of the chalk cliffs (simplified)



Lithologic characteristics of the chalk cliffs (simplified)



Figure 2-17 Cliff erosion characteristics along the Upper Normandie in relation to the cliff toe stratigraphy lithologic structure, per area between 1947 and 1995. (A) Spatial location of the average chalk cliff retreat rates. (B) Average repeat period of cliff falls. (C) Average retreat per fall (Costa, 1997).

- Volume of flint produced by the shore platforms of Normandy and Picardy

In addition, the volume of shingle produce by erosion of the chalk platform erosion has been estimated to be $1000 \text{ m}^3 \text{ y}^{-1}$ (LCHF, 1972). However, only a part of this volume would actually feed the beaches along the Normandy and Picardy coast because some gets stored in the chalk platforms' runnels and some is carried seaward where it may become stuck where there is a high proportion of sand matrix. As a consequence, Costa (1997) estimated the total flint input from the platforms to be $700 \text{ m}^3 \text{ y}^{-1}$.

If the sediment circulation along the Normandy coast was completely free, the LST would be equivalent to approximately 20,000 to 30,000 $\text{m}^3 \text{ y}^{-1}$ (Sogreah, 1995). However, because of the human intervention, the construction of harbour arms and industrial extraction, the volume of shingle available for LST transport in the sedimentary cell is decreasing. Indeed the construction of major harbour arms at Dieppe, Penly and Le Tréport have completely stopped natural transport, and created individual sedimentary sub-cells. In addition, since the beginning of the 20th century, more than 2 million m^3 of shingle have been extracted from the beaches between Antifer and Ault (LCHF, 1972). Currently, the stocks of shingle locked in these sub-cells are estimated at 350,000 m^3 between Dieppe and Le Tréport and 180,000 m^3 between Le Tréport and Ault (Sogreah, 1995). Based on the cliff retreat rate and the flint content, the production of shingle between Le Tréport and Ault feeding the Bas champs area is approximately 2500 to 3000 $\text{m}^3 \text{ y}^{-1}$ (Sogreah, 2009).

Both study sites have proved to be the result of important evolutionary dynamics and they appear to suffer from identical problems, namely the lack of sufficient volumes of natural sediment material to balance the ambient LST and an increasing sea water level. Understanding the processes of LST in the most natural environment possible would certainly help to give better guidance for the management of gravel beaches; however, gravel beaches where sediment transport is not interrupted by groynes or soft management plans are nowadays rare on both sides of the Channel. Fortunately, Cayeux-sur-Mer and Birling Gap can still give this study the opportunity to collect such measurements.

The next chapter describes the complete range of measurements (morphology, tracer pebbles, the active layer and grain size distribution) collected by this study to investigate the LST at both sites.

Chapter 3. Sample Design

3.1 Introduction

This chapter provides a detailed overview of the sample design deployed to measure the three components of the LST identified in Chapter 1 (Figure 1-1) and the associated hydrodynamic conditions. An outline of the instrumentation, the pilot studies, the methodologies used, their accuracy or limitations will be fully reviewed.

To address the overall aim of this thesis, a series of sampling methods have been designed to measure:

- (i) Beach topography;
- (ii) Hydrodynamic forcing (wave and tidal conditions); and,
- (iii) Volumes of sediment transported and directions of movement (using spatial scattering and depth of transport);

on mixed beaches. This involved the design and testing, via pilot experiments where appropriate, of sample designs in order to develop a final sample design for the synchronous collection of these three sets of variables. To fulfil its aim, this research is based on a series of fieldwork phases that have collected data over periods ranging from single tides to a maximum period of two years.

During the longer term field data collection, between August 2004 and July 2006, the beach at Birling Gap was visited on a monthly basis to conduct topographical surveys, or sometimes more frequently if extreme morphological changes had occurred (this chapter Section 3.2). A monthly survey frequency was deemed sufficient to reflect the coastal changes as a function of the wave climate and enable seasonal to yearly sediment transport patterns to be observed.

These monthly surveys were complimented by shorter term data collection experiments during which close to shore wave conditions (onshore in the intertidal zone), topographical surveys, active layer measurements, tracer deployments and sediment sampling were carried out on a tidal basis. These shorter periods of fieldwork were designed to observe the linkages between specific hydrodynamic conditions and the particular response of the beach morphology through sediment transport.

At Birling Gap, these short period surveys varied from three to five consecutive days (from March 20th to March 24th 2006, May 19th to May 22nd 2006 and December 14th to December 19th 2006). The timing of these fieldwork periods was designed to cover a large range of hydrodynamics conditions (the wave height was the parameter mainly considered) so that a large range of beach response scenarios could be observed. During these short fieldwork periods topographic surveys were recorded between each tide. In addition to facilitating detailed study of linkages between hydrodynamic conditions, sediment transport and beach morphology, these high-resolution surveys gave the opportunity to observe detailed variations in the presence and distribution of sand and shingle on the beach. Although this is known to influence beach reactivity very little is known about its dynamics.

Because of the remoteness of the field site in France, monthly surveys were not practical. However, two field measurement periods were organised at Cayeux. The first was a trial experiment which was conducted over five days from the December 12th to December 17th 2004 during which the DGPS surveys design and the tracer pebbles were tested for their practicability *in situ*. This trial survey was then followed by a second data collection period covering a complete neap-spring-neap tide cycle from October 28th to November 11th 2005. During these periods detailed topographic surveys and

close to shore wave conditions were recorded and pebble tracing experiments were carried out. During the later survey period at Cayeux, measurements of the active layer together with sediment sampling completed the data collection.

3.2 Topographic measurements

The research necessitated the development of a specific methodology to collect information on the morphological and volume changes on mixed beaches over both shorter and longer time periods.

3.2.1 The Differential Global Positional System (DGPS)

The Global Positioning System (GPS) jointly developed in the United States by the Department of Defence, the Department of Transportation, and the National Aeronautics and Space Administration had its first satellite launched in 1978 and was fully operational by 1995. The system consists of twenty four satellites arranged in such a way that they revolve around the earth at a height of approximately 11,000 miles in six orbital planes, each with four satellites operational at any given time. Therefore, a user on earth can receive a minimum of seven to twelve satellite signals any time. In practice, this depends on the physical environment. For example, the presence of cliffs can hide some satellite signals in their proximity which can create difficulties in surveying beaches that front high cliffs. Each satellite emits a unique encrypted, singular wavelength and time, signal on two frequency bands, L1 and L2. Therefore a user on earth can determine their position by a simple triangulation between all the signals received. Before 2000, the American Army, for security purposes, jumbled the coverage of the GPS in some areas, Selective Availability-SA, but it is fully available from May 2000. Nowadays, the horizontal resolution of the GPS is ± 10 m but the vertical resolution is poorer. The Russian government put a similar system in place, the Global Orbiting Navigation Satellite System, GLONASS, completed in 1995. Together, these two systems create the Global Navigation Satellite System, GNSS.

In order to improve the accuracy of the GNSS by measuring infinitesimal changes in variables to provide satellite positioning corrections, the Differential Global Positioning System (DGPS) was developed in the late 1990s (Morton et al., 1993). This enables a centimetric vertical and horizontal resolution, and is nowadays commonly used in morphological beach surveys (Stépanian, 2002; Robin, 2007).



Figure 3-1 D GPS in use.

A DGPS is a system designed to improve the accuracy of the GNSS using crossed data between two or more receivers. The receivers observe the same set of satellites, taking similar measurements that produce similar errors when positioned closely together; these errors include: satellite drift; false signals resulting from the true signal bounce off the ground or nearby structures; refraction of the radio waves as they go through the earth's atmosphere; and radio and other interference. One of the receivers has the role of reference, the base station. Being placed at a known

location, it calculates its theoretical position, pre-input by the user, and compares it to the measurements provided by the navigation satellite signals. A correction vector can then be determined and transmitted to the Rover, the mobile part of the DGPS, which then automatically corrects its position. According to TOPCON, the manufacturer of the DGPS used in this research, the accuracy improves from a pluri-metric scale, ± 10 m, to a millimetric scale, ± 5 mm, in the horizontal plane and >1 cm in vertical plane.

DGPS surveys can be achieved through two modes:

- (i) The Real Time Kinematic telemetry, RTK, links between the base station and the rover, or;
- (ii) Post-processing.

The DGPS used in this study was a bi-band TOPCON-DGPS (Figure 3-1).

3.2.2 Design of the topographic surveys

All the topographic surveys were operated with the TOPCON Differential GPS in RTK mode. In theory, the accuracy of the equipment is to within a centimetre, however on

mixed sediment beaches, accuracy is much lower because of the irregular nature of the surface which is often unstable with pebbles protruding from the beach surface. The imbrications of the pebbles from one tide to the next can influence the actual elevation of the beach in places. The effect of pebble imbrications can be appreciated when walking on the beach. On each step upon the beach, the beach material re-organises itself due to the pressure put on it. Usually this re-organisation involves a slight decrease in elevation. It is likely therefore that even without any apparent sediment transport alongshore, the pebbles can be re-organised during a high tide by the hydrodynamics. This re-organisation can lead to a slight change in elevation that would be recorded by the DGPS and then amplified into the digital elevation models from which are directly derived the beach volume changes. For this reason, the accuracy of the survey has to take account of the beach material grain size and surface instability. At both study sites, the dominant grain size in the gravel class is approximately 30 - 50 mm. As a consequence it is wise to consider the vertical accuracy of surveys on these two mixed beaches with the TOPCON DGPS in RTK mode as approximately ± 50 mm (BAR, 2005). The DGPS was set by default to collect the coordinates of longitude, latitude and elevation at 0.3 m intervals. However, for every change in elevation greater than 0.15 m within any 0.3 m space interval, a new point was collected (by RTK) and the interval reset.

The vertical accuracy of the points collected by the DGPS will directly affect the quality and precision of the Digital Elevation Model (DEM) created later in ArcView 3.2. Indeed, the newly created DEM will magnify the elevation error between two consecutive beach profiles. Therefore when analysing the beach elevation change maps and the sediment volume changes derived from DGPS surveys, it is crucial to be aware of DEM limits or imprecision. As an example, if an imprecision of ± 50 mm in elevation is considered for the surface area of the survey at Cayeux, an average beach length of 1.2 km and beach width of 60 m, the volume's margin error would be approximately ± 3600 m³.

With the aim of obtaining a model to fit the actual beach topography as accurately as possible, regular cross-shore profile elevation surveys were recorded 20 to 25 m apart all along the studied beaches. This distance was shortened when the topography of the beach presented any sudden change (Figure 3-2 & 3-3). Please note that the distance

between the profiles increased to approximately 50 m after half way along the survey area at Cayeux because of the straight alignment of the beach after that point.

This specific space interval between each cross-shore profile was deduced from experiments on Saltdean beach (East Sussex) led by the BAR project (BAR, 2005). These experiments aimed to assess the relationship between the number of cross profiles used to create the morphological maps on Arcview 3.2 and the resulting beach volume. The beach at Saltdean was selected because of the simple morphology, i.e. presence of high tide and storm berms, no beach cusps, no pronounced beach step, all beach features perfectly aligned along the shore, between each of the five groynes used as coastal defence, each approximately 50 m apart. The results showed that a regular beach profile interval of 25 m between each profile would only affect the volume accuracy by 0.06% in comparison to the “real” beach volume determined by a topographic survey with a profile interval of approximately 3 m. The Bar interim report (2005) made the point that distance between profiles must take into account the morphology of the beach, and the distance should be reduced if a beach morphological feature appears within the 25 m (this relies on the geomorphological judgement of the surveyor).

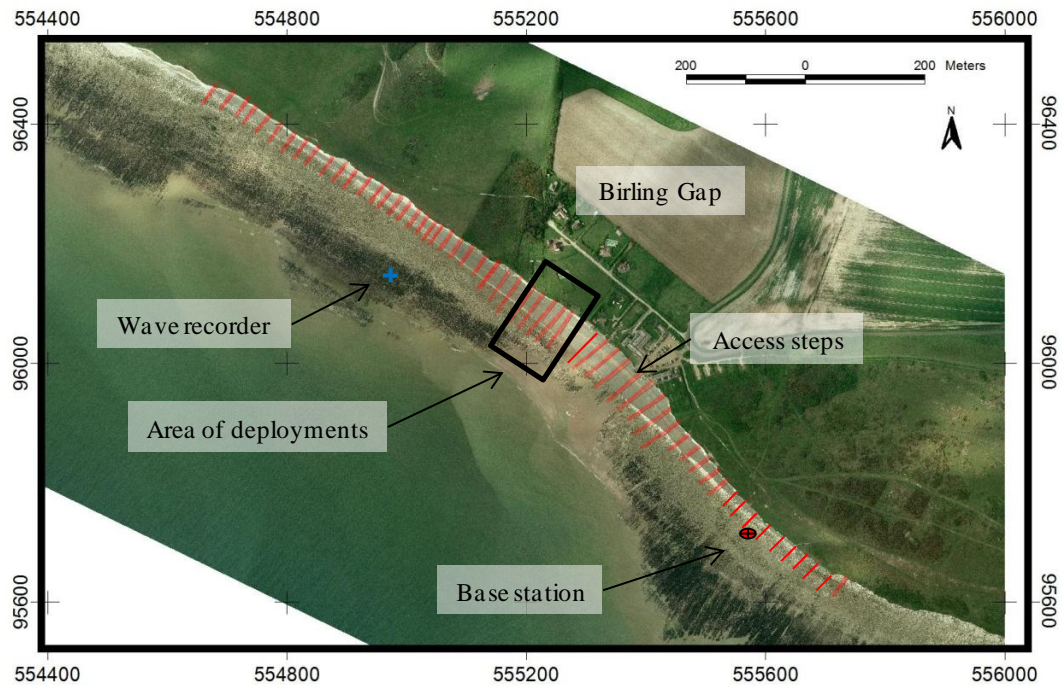


Figure 3-2 Locations of a typical profile path selected at Birling Gap. The circled black cross represents the location of the base station. The location of the wave recorder, Valeport Midas DWR, in the proximity of the mixed beach is marked by the blue cross. The black rectangle represents the location of the area where the synthetic tracers were deployed and the measurements of the active layer depth occurred (this chapter Section 3.4.4).

Although the survey strategy needs to adapt to the beach topography, both study sites, Birling Gap and Cayeux-sur-Mer, presented a simple morphology with perfectly drift-aligned features (berms and beach step). The occurrence and alignment of these barely changed from one survey to another during the detailed field survey periods. As a consequence, the path selected to do the surveys rarely changed and the cross-shore profiles surveyed were consistent from one survey to another. The variation in location was < 5 m.

It is recognised by this study that despite the very narrow variation in location of the beach profiles surveyed and the large amount of elevation points collected along them, by not measuring the elevation of the beach on fixed points an imprecision in the beach elevation is introduced. This imprecision will be interpolated when creating the DEMs and therefore calculating the beach volume changes.

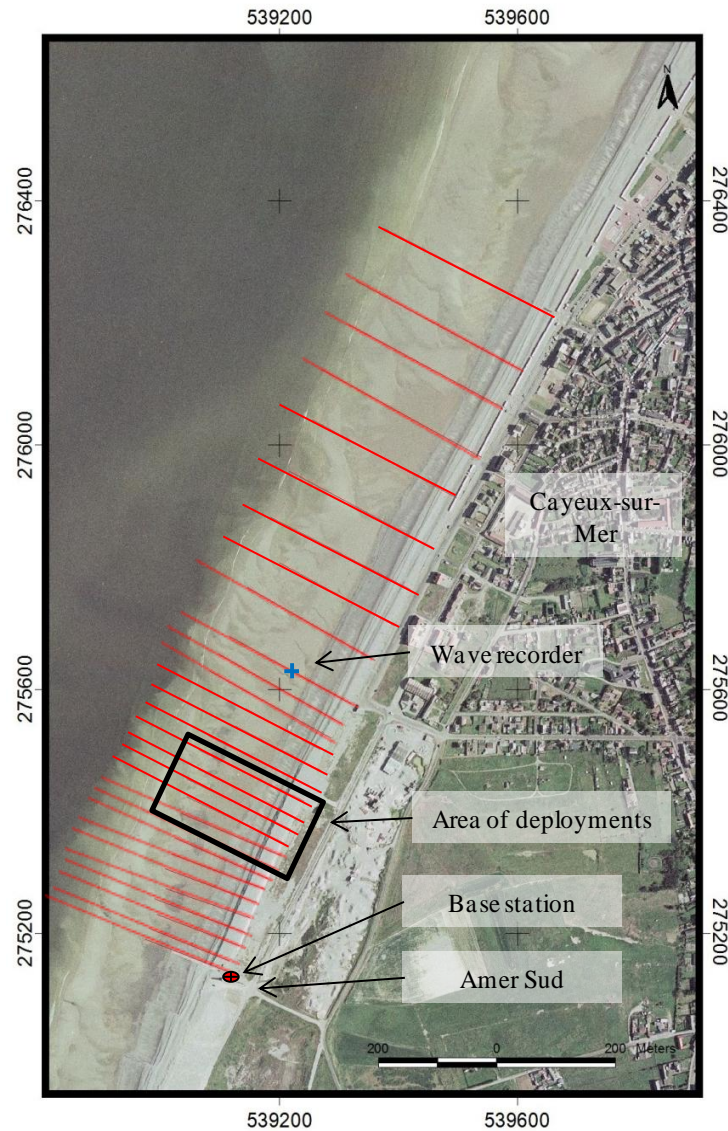


Figure 3-3 Locations of a typical profile path selected at Cayeux-sur-Mer. The circled black cross represents the location of the base station. The location of the S4DW in the proximity of the mixed beach is marked by the blue cross). The black rectangle represents the area where the synthetic tracers were deployed and the active layer was measured and the tracer pebbles were deployed (this chapter Section 3.4.4).

The acquisition of monthly DGPS survey data at Birling Gap was designed to assess long-term changes and to identify the relationships between shingle transport and wave conditions for the calculation of net annual drift rates based on wave climate data. Each monthly survey occurred as close as possible to a spring tide to ensure that the entire beach was water free at low tide; but also on a tide when the beach cusps were not too pronounced as this would potentially cause a topographic imprecision resulting from the interpolation of the digital elevation model on the computer. In January 2005, additional

surveys were carried out after a great storm removed a large amount of beach material leaving the western end of the Birling Gap without a beach for a few days. This beach reformed very quickly afterwards to a lower volume first to regain its original shape only after one or two months. To record this event, it was decided to carry out two surveys during this month (Chapter 4 Figures 4-29 & 4-38).

With the aim of describing and understanding the morphodynamic processes on a mixed beach in a more precise way a series of short time scale surveys were conducted. This series of short time scale surveys started at Cayeux-sur-Mer. During the first trial survey period (December 12th to December 17th 2004), surveys occurred on every low tide for the two first days and only once a day for the three following days over a distance of 400 m directly downdrift of the terminal groyne located at the Amer Sud. Because of the change of the surveyor from one survey to another, some of the surveys extended further to the north (Chapter 6 Figure 6-7) and the location of the surveyed profile was not consistent. For this latter reason the data were excluded from the results in Chapter 4 as it was impossible to observe a consistent profile at the same location on every survey.

During the second survey period at Cayeux-sur-Mer, over a complete neap-spring-neap tide cycle between October 28th and November 11th 2005, a survey was carried out on every low tide (semi-diurnal tides) during the complete semi-lunar cycle. The survey frequency was decreased to a diurnal data collection to improve the level of detail of the beach morphological changes, increase the recovery rates of the tracers deployed at the same time (Chapter 7) and to facilitate linking the data collected to very specific hydrodynamic conditions. This time the beach area surveyed stretched from the terminal groyne located at Amer Sud northward for approximately 1.2 km (Figure 3-3).

At Birling Gap, all the surveys periods in March 2006, May 2006 and December 2006 involved surveying the beach from one end to the other (approximately 1.2 km long) on a semi-diurnal frequency again for the same reasons.

The choice of the survey periods was dictated mainly by the wave conditions, i.e. the best periods to collect data on storm events and swell waves, but also the daylight hours,

i.e. when there was sufficient daylight during the low water conditions to complete all of the data collection (topographic survey, tracer recovery and active layer measurements). At Cayeux-sur-Mer, particular attention had to be paid to avoiding periods of beach management in order to avoid contamination from a source other than the material already in place. Availability of the field assistance was also a factor in deciding on the timing of the fieldwork.

Finally, all the maps were computed using ArcView 3.2 equipped with the extensions Spatial Analyst and 3D Analyst 1.0. First, all points on similar profiles were perfectly re-aligned by ArcView 3.2 to obtain quality maps from the linear interpolation. Second, a preview of the map was created as a “tin” which was then converted into the final output as a “grid”.

Please note that all the topographic data collected at Cayeux-sur-Mer and Birling Gap have been referred to the respective national grid system. Therefore the Lambert conic coordinate system (L1) was used in France and the Ordinance Survey Great Britain 1936 (OSGB36) in UK.

3.3 Hydrodynamic measurements

Because of the different temporal and spatial scales involved in this research, it was decided to collect wave data most appropriate to the actual field data measured in each case. Offshore measurements of the wave conditions provide information about the general hydrodynamic climate in the Channel and are ideal for investigating large geographical areas such as coastal sedimentary cells or sub-cells, over longer time periods. Thus, offshore measurements of the wave conditions are used for correlations with the monthly topographic surveys collected at Birling Gap.

In contrast, measurements of the hydrodynamic parameters as close as possible to the shore provide essential information on localized wave conditions. Therefore, a precise and accurate link in time and space can be drawn between the hydrodynamic processes and the morphodynamic system. For these reasons, it was more suitable to collect

inshore data during the shorter term field experiments in order to facilitate an examination of beach processes on very small spatial and temporal scales.

For this reason, it was not necessary to collect offshore wave data at Cayeux, as only short term measurement periods were conducted. In addition, such data are not freely accessible to the public in France. In contrast, offshore wave data were freely available on the Channel Coastal Observatory website for the Sussex coast (<http://www.channelcoast.org/>, 2010). The wave parameters are recorded at Rustington (West Sussex, UK) using a Datawell Directional WaveRider Mk III buoy. The buoy was deployed on the 09th of July in 2003 from the MV Wessex Explorer approximately 8 km offshore at 9.9 m water depth. The data available, averaged on a 30 minute time period are:

- (i) The buoy geographical coordinates;
- (ii) The significant wave height (H_s in m), which is the average height of the highest one third of waves at a location during a wave measurement period;
- (iii) The maximum wave height (H_{max} in m), being the highest wave recorded during a wave measurement period;
- (iv) The peak wave period (T_p in s), being the wave period at which the highest wave energy is centred;
- (v) The zero-upcrossing wave period (T_z in s), which is defined spectrally and is often referred to as the mean wave period;
- (vi) The mean wave direction (referred to the magnetic North in °).

These data were collected for the two years of the Birling Gap beach DGPS surveys from August 2004 to July 2006.

Based on earlier studies (e.g. Powell, 1990), this study identified that the main hydrodynamic parameters responsible for sediment transport on gravel beaches are:

- (i) The wave height (significant wave height, H_s ; and the maximal significant wave height, $H_{s\ max}$);
- (ii) The wave period (significant wave period, T_s ; and the peak period, T_p);
- (iii) The wave approach to the coast (°); and,
- (iv) The water level.

For this reason, the study ensured that the equipment used to measure the hydrodynamic conditions were able to record these parameters. Two types of wave recorders were used onshore depending on the field site: an electromagnetic current meter equipped with a pressure sensor S4DW and a Midas DWR wave recorder. The S4DW was borrowed from the University of Littoral (Dunkerque) who have authorisation from the French government to deploy such instrument on the shore for field measurements in France.

3.3.1 Electromagnetic current meter and pressure sensor S4DW



This wave recorder was used at Cayeux-sur-Mer during both field studies (Figure 3-4). The S4DW measures the voltage resulting from the motion of the water flow velocities in a spherical magnetic field according to Faraday's law of electromagnetic induction (InterOcean systems inc., 2010).

Figure 3-4 The S4DW electromagnetic current meter and pressure sensor deployed on the sandy foreshore at Cayeux-sur-Mer.

The voltage is linearly proportional to the water flow velocity (Aubrey, 1989). The electromagnetic field is generated by two orthogonal pairs of sensing electrodes placed on the horizontal perimeter of the equipment. The current directions are provided by an internal compass referring to the magnetic North. The S4DW is equipped with a pressure transducer used for measuring the wave height and tidal level. The sensor is an absolute pressure sensor type, i.e. measuring the atmospheric pressure in addition to the water pressure, measuring the pressure fluctuations at high frequency. These fluctuations of pressure are converted into fluctuations of the surface elevation using a linear wave theory spectral transfer function (Thornton and Guza, 1989). These transformations are made using the InterOcean systems inc. software that is supplied with the equipment.

The equipment settings were selected as a compromise between:

- (i) The time period of the experiment;
- (ii) The number of bursts, a burst being a specific amount of data received in one intermittent time period.

- (iii) The time separating two consecutive bursts, and;
- (iv) The memory available and the battery life.

To acquire valuable and quality data on the incoming inshore waves to relate the sediment transport or the other measurements, it was necessary to record the data as near as possible to the shore. During the first survey period in December 2004, the S4DW was located at $\approx 400 - 500$ m south of the terminal groyne at the convenience of the University of Littoral that was leading the experiment. During the following campaign in October/November 2005, the equipment was located much closer to the site of measurements, at ≈ 40 m from the mixed sediment part of the beach attached to a stainless frame 40 cm from the beach surface (Figures 3-3 & 3-4). The recordings were set at a frequency of 2 Hz to sample bursts of 9 minutes every 15 minutes for both survey periods.

1.3.1.1 Analytical treatment of the data

The speed and direction of the tidal currents are read directly from the data extracted from the wave recorder. In contrast, the water level needs to be calibrated by subtracting the atmospheric pressure (this value is called “offset”), and adding the height of the pressure sensor (this value is called the “off bottom”). The offset is given by the equipment itself when it is water free while the off bottom is simply measured with a tape measure when the equipment is deployed. The measurements collected by the S4DW need to be averaged over a minute to remove perturbations linked to the water agitation (Robin, 2007).

The study was interested only in the frequency of the breaking waves and the swash which are in the gravity wave frequency band coverage. When looking at the S4DW records of the hydrodynamic conditions in an intertidal environment, particular attention has to be paid to the wave frequency bands considered because of the presence of “electronic noises”. Indeed, the water level above the pressure sensors is a critical parameter influencing the quality of the data recorded. The cut-off frequency removing electronic noises and delimiting the upper limit of the spectral band usable in the data collected can be determined by the following formula (Levoy, 1994):

$$F_c < \frac{1}{\sqrt{(1.28h)}} \quad (3.3)$$

where F_c is the cut off frequency and h is the high water level elevation (m). When the S4DW was used, the results from Equation 3-3 proved to be higher than the upper limit of the frequency of the breaking waves (i.e. 0.33 H_z). Therefore the upper limit of the wave band considered in this study is 0.33 H_z . The lower limit of the spectral band is delimited by the upper limit of the infra-gravity wave domain which is 0.05 H_z (the infra-gravity wave domain being comprised between 0.005 and 0.05 H_z ; Kroon, 1994; Voulgaris and Simmonds, 1996). To summarise, the spectral analysis was conducted on a frequency range going from 0.05 to 0.33 H_z .

It is important to note that Pierowicz and Boswood (1995) have pointed out that this equipment has to be submerged by a minimum of 80 cm above the sensors to record the best quality data. Therefore, all the data recorded before the water level reached a height of 4.4 m HD (referenced to the French Hydrographic Datum) were discarded. The S4DW, because of its great sensitivity in shallow water, is perfect to collect wave data in the shoaling zone or even the surf zone and is consequently adequate for this study.

3.3.2 The Midas DWR Wave Recorder



Figure 3-5 The MIDAS DWR wave recorder deployed on the chalk platform at Birling Gap.

The second recorder used was a Valeport electromagnetic current meter and pressure sensor of the MIDAS DWR type (Figure 3-5). This wave recorder was used for several short periods of fieldwork at Birling Gap. The Midas DWR is fitted with a two axis electromagnetic current sensor (11 cm discus electromagnetic current sensor) located at the top of the instrument, which measures the voltage resulting from the motion of the water flow velocities just above the wave recorder. The current directions are provided by an internal compass with reference to the magnetic North. The pressure is measured by a strain

gauge of a 50 dbar range. The pressure sensor is absolute and therefore includes the air and water pressure. These fluctuations of pressure are converted into fluctuations of the surface water elevation using a linear wave theory spectral transfer function (Thornton and Guza, 1989). These transformations are carried out in the Midas DWR.

The equipment is fitted with a 64 Mbyte onboard flash memory card. As for the S4DW, the equipment settings were selected as a compromise between:

- (i) The time period of the experiment;
- (ii) The number of bursts, a burst being a specific amount of data received in one intermittent time period.
- (iii) The time separating two consecutive bursts, and;
- (iv) The memory available and the battery life.

With the same objective as with the S4DW i.e. maximizing the quality and the quantity of the data collected close to the shore, the Midas DRW was set up approximately 40 m away from the mixed beach in a stainless steel frame directly laid on the chalk foreshore platform (Figures 3-2 & 3-5). The fieldwork at Birling Gap being more frequent but for briefer periods than at Cayeux-sur-Mer, the wave characteristics recordings were set at a frequency of 4 Hz to sample bursts of 15 minutes every 34 minutes (in March and December 2006) or 10 minutes every 17 minutes (in May 2006). The water level sampling had its own setting too. These were 15 minutes every 16 minutes (in March and December 2006) or 10 minutes every 40 minutes (in May 2006). The timings of the May 2006 fieldwork settings are due to a long time recording period (a month) of wave data collection and the memory limitation of the recorder.

1.3.2.1 Analytical treatment of the data

Data analysis is carried out using the software WaveLog 400. The non-directional data are determined using the frequency analysis and mean pressure. All raw data are passed through a reverse Fourier Transform to back-calculate the surface elevation for every sample in the burst. The directional analysis procedure passes through a Fast Fourier Transform. No correction of the off bottom is necessary as the equipment height is already set up in the Midas DWR programming (30 cm when fixed on the stainless

frame). The offset still has to be corrected as the pressure measured is absolute. Again, the offset is given by the equipment itself when it is water free.

In order to avoid any corrupted data linked to the agitation, only the data recorded when the sensors were submerged by 20 cm or more are considered.

3.4 Sediment transport

Sediment transport on mixed beaches can be measured using different techniques, including:

- (i) Topographic surveys,
- (ii) Sediment traps,
- (iii) Sediment tracers.

Each methodology has advantages and limitations (Chapter 7). To address the aim of this thesis, it was decided to use both topographic surveys (this chapter Section 3.2) and sediment tracers.

3.4.1 Tracing experiments-Research on the types of tracers available

Contrary to sand tracing experiments which have a long established and successful history (Zenkovitch, 1958; Oertel, 1972; Levoy et al., 1998; Balouin et al., 2001; Stépanian, 2002; Vila-Concejo et al., 2004; Tonk and Masselink, 2005), pebble tracing is more problematic. Although measurement of gravel transport by tracers has been used for a long time, the number of studies remains sparse and no detailed experimental protocol for general use has been clearly defined by the scientific community. The sporadic progress and published literature is closely linked to the creation and development of new technology, the efficiency and accuracy of which improves with time (e.g. Richardson, 1902; Kallinske, 1947; Russell, 1960; Caldwell, 1981; Madsen, 1989; Bray et al., 1996; Voulgaris et al., 1999; Allan et al., 2006; Curoy et al., 2007). Despite the lag of knowledge related to the performance of the pebble tracing techniques, the use of tracers on gravel beaches has proved far more reliable for

measurement of longshore drift than have sediment traps (Bray et al., 1996). The range of tracers used and available nowadays can be classified as it follows:

- (i) Indigenous pebbles; such as painted (Jolliffe, 1961, 1964), fluorescent or radioactive pebbles (Kidson and Carr, 1959; Crickmore et al., 1972);
- (ii) Natural exotic tracers; such as quartzite tracers (e.g. BAR, 2005) or other non-indigenous pebbles (e.g. red bricks in Richardson, 1902);
- (iii) Artificial tracers; such as aluminium pebbles (Wright et al., 1978; Nicholls, 1985), radio controlled also called “smart pebbles” (Bray et al., 1996; Lee et al., 2000), PIT cobbles (Allan et al., 2006) or synthetic pebbles (Curoy et al., 2007).

Each of these has advantages and disadvantages.

i. Indigenous pebbles

➤ Painted and fluorescent pebbles

Painted and fluorescent pebbles have the advantage of being easy to produce and the material used is perfectly representative of the beach material. Fluorescent paint has the advantage that it allows night recovery in comparison to normal paint. However, both methods have the significant disadvantage that only pebbles on the beach surface can be easily relocated. Moreover, these tracers have only a short life time, the paint rapidly wearing off the surface of the pebbles (Figure 3-6).

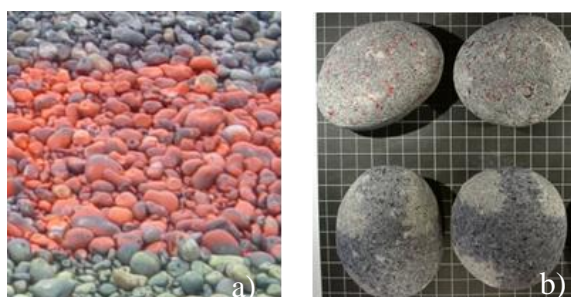


Figure 3-6 Painted pebbles. a) Example of spray painted beach pebbles. b) Spray painted pebbles after only 5 hours in a tumbler.

➤ Radioactive pebbles

Early tracing experiments using the radio activity proved to be successful (e.g. Kidson and Carr, 1959). The flint pebbles were surface-coated with the radioactive isotope barium 140-lanthanum 140 which has a half life of 12 days. The use of this isotope

made it possible to trace pebbles for 6 to 8 weeks. However, nowadays this practice has been banned on public beaches because of health risks.

ii. Natural exotic tracers

Natural pebbles composed of an exotic rock type that can be easily identified can be deployed. In the case of flint, hard crystalline white quartzite is a suitable alternative. Quartzite pebbles closely match the natural flint pebbles in density, and can be bought in a similar shape and size (Figure 3-7). However, as with painted or fluorescent pebbles, this method has the disadvantage that only those on the beach surface can be easily relocated.



Figure 3-7 A natural quartzite tracer mixed with the beach material.

Jolliffe (1961) attempted to solve the issue of “surface recovery” associated with the painted or quartzite tracer methods by excavating beach material after the deployment of fluorescent pebbles at Deal (Kent). Based on these samples, he identified a linear relationship between the number of fluorescent stones underneath the surface and the number of fluorescent stones visible at the surface.

iii. Artificial tracers

➤ Radio signalled pebbles.

Two main types of radio tracers have been used:

1. The first is the “Smart” pebble. Resin manufactured pebbles are equipped with a radio transmitter which sends its location to a local base station, so that the actual displacement of the pebble can be traced. Detection has proved to be problematic in saltwater environments yielding low recovery rates and after several years of research these pebbles are still prototypes. The use of data loggers implanted into the pebbles can avoid the use of a base station.

2. Recently, innovative experiments have been conducted using Passive Integrated Transponder (PIT) tags (Allan et al., 2006). Magnetic tags are attached to the tracer particles and their inside transponder is activated when an antenna passes near them. These tags are detectable and identifiable (unique signal per tracer) to a depth of up to 1 m within the sediment.

➤ Aluminium pebbles

Aluminium tracer pebble techniques yield considerable scope for recovering higher proportions of the injected tracers compared with older techniques. The high recovery rate is essentially linked to the fact that the use of a metal detector allows the recovery of buried pebbles which is not possible with the other simple painted or quartzite tracer methods (excluding the radioactive and radio controlled techniques).

The use of aluminium pebbles provides a precise 3D resolution of the scattering into the beach material. It has been recognised that aluminium pebbles are a successful method to identify coarse sediment particle movements (great range of size and shape of the tracers, 3D recovery, great recovery rate, and tracer usable more than one time); the only disadvantage would be the cost. However, these tools are expensive and therefore prohibit substantial (over one hundred aluminium pebbles) or repetitive deployments.

With this in mind, the BAR Project devised a new cheaper tracer that allowed as easy and quick 3D recovery as the aluminium pebbles or the radio controlled and radioactive pebbles from a mixed sediment material but at a less cost: synthetic pebbles with a copper core.

3.4.2 Tracing experiment-The synthetic pebbles

i. Research and development

Before reaching the final design of the synthetic pebble, a lot of attention and time has been dedicated to their conception. The main points addressed the shape, the size, the density, the resistance to clashes and abrasion.

The majority of the pebbles at Cayeux-sur-Mer and at Birling Gap are well rounded, with a dominant grain size of 30 - 50 mm and composed of flint ($d = 2.68 \text{ g cm}^{-3}$). This rounded shape seems also the most sustainable shape to minimise the pebble attrition over time. Therefore the choice of this shape not only makes the synthetic pebbles representative of the dominant shape of the beach material but also contributes to the capacity of the pebble to resist breakage.

Knowing the dominant grain size for both sites, it was decided to make pebbles with a b-axis of 35 - 50 mm. This size helps to facilitate the visual recovery of the tracer within the beach material; pebble size tracers have a greater chance of being seen than gravel size tracers. Having a consistent size and shape of synthetic pebbles facilitates their mass production and reduces the number of varying parameters for the interpretation of the results.

To make the pebble, a general-purpose epoxy resin was the most adequate option commercially available (Appendix I). The main concern in the choice of this material concerned its resistance to clashes with other natural flint pebbles. The tracer also had to be sensed by a metal detector and so had to be partly made of metal. The performance of metal detectors is good enough to allow a selective detection based on the type of metal (e.g. aluminium, copper, gold, etc). It was preferred to use copper considering that the majority of the flotsam and jetsam are made of aluminium (cans, etc), therefore potentially minimising unsuccessful recovery. Copper has the advantage that it is barely present in the beach material because of its trading cost in recycling centres.

The density of the tracers had to be carefully considered to make sure that they were representative of the natural flint pebbles. Considering that the volume of a synthetic tracer is $\approx 85 \text{ cm}^3$, the density of the epoxy resin is 1.06 g cm^{-3} , the density of copper is 8.92 g cm^{-3} and the density of a natural flint pebble is 2.65 g cm^{-3} , the tracer's density can easily be controlled by varying the length of the copper insert inside the tracer. According to Figure 3-8 displaying the length of the copper inserted into a tracer as a function of the total mass of the same tracer, to produce a tracer pebble of equivalent mass to a natural flint pebble of the same mass i.e. $\approx 225 \text{ g}$, a 33 mm length of copper is required.

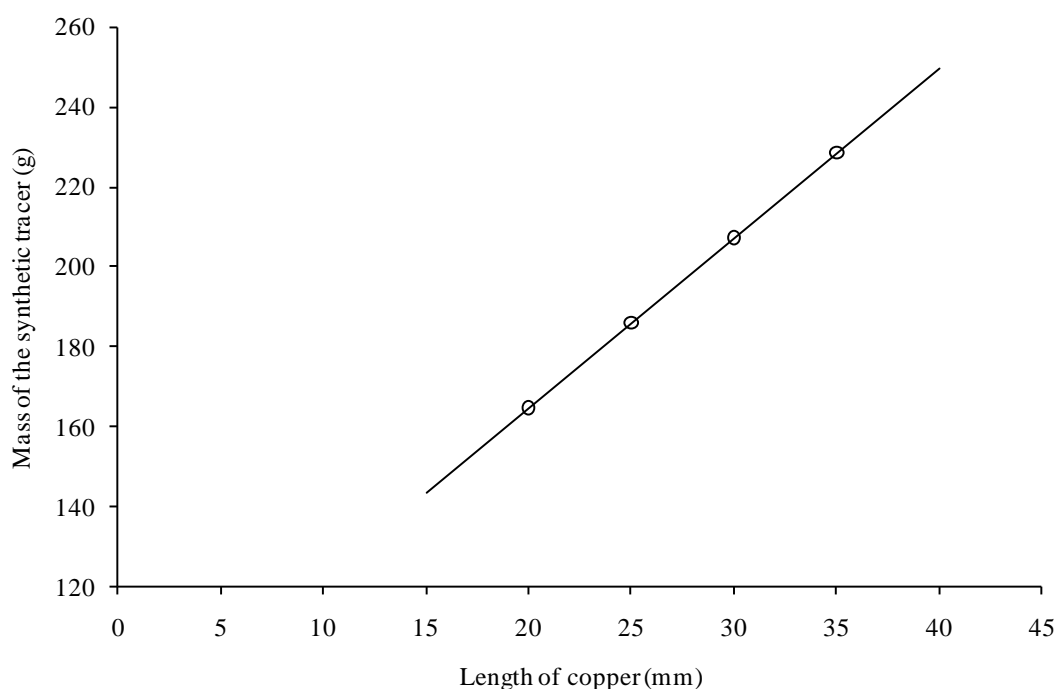


Figure 3-8 Representation of the length of copper necessary to insert in a synthetic tracer as a function of the mass of the synthetic tracer.

The final product is presented on Figure 3-9. Each pebble can be engraved with an identity number making each of them unique.



Figure 3-9 A synthetic pebble. Made of an epoxy resin with a copper core inside, its size is: a-axis: 60 to 70 mm, b-axis: 35 to 50 mm, c-axis: 35 to 40 mm. Each pebble is completely smoothed, well rounded and has the same weight as a flint pebble of the same size.

ii. Performance of the synthetic pebbles

A brief comparison between the synthetic pebbles and the aluminium pebbles highlights the performance of these newly designed tracers (Table 3-1).

Points considered	Synthetic pebbles	Aluminium pebbles
Representativeness of the tracer with the beach material	Can be manufactured at will in size, shape and density. However, the weight balance of the pebble may be difficult.	Can be manufactured at will in size, shape and density (Wright, et al. 1978; Caldwell, 1981).
Detection	The detection is limited only by the metal detector performance (based on experience, 40 cm in a water saturated mixed sediment).	The detection is limited by the metal detector performance. The large amount of aluminium derivate flotsam and jetsam in the beach sediment (e.g. cans) slows down the tracer recovery.
Identification/Marking	Both types of tracers can be made unique by marking them with numbers so that the subsequent movement of individual pebbles can be monitored.	
	Can also be permanently coloured by mixing a colorant into the resin.	If painted, the paint would wear off after few hours in a same way as for painted pebbles.
Cost	The bulk cost is £3 per pebble.	The bulk cost is £4 to £5 per pebble.
Legality/Health and safety	Authorised in public area.	Authorised in public area.

Table 3-1 Criteria of comparison between synthetic pebbles and aluminium pebbles.

In any criteria considered in this comparison, the performance reached by synthetic pebbles are equal to one achieved by the aluminium pebbles.

3.4.3 Tracing experiment-Fieldwork deployment description

In the very early stages of this work the use and performance of tracers were unclear and so both long and short term tracer experiments were conducted. Two kinds of tracers were used: quartzite pebbles and synthetic pebbles. The quartzite pebbles would allow a rapid surface survey of pebble movements over longer time periods (from a month to a year). In contrast, the synthetic pebbles would allow a more detailed 3D short term surveys.

i. Requirements for tracer deployment

When using tracers, many factors must be taken into account in order to have a representative view of what occurs on a mixed sand and gravel beach (considering that their size, shape and density are already representative of the beach material):

1. The water elevation changes: Nicholls and Wright (1991) highlighted that the proportion of longshore wave energy available for shingle movement will fluctuate with the tidal elevation being a maximum at high water. Therefore, the location of the tracer pebble deployment will influence their drift or scattering. This is supported by Van Hijum and Pilarczyk (1982) who, based on gravel entrainment laboratory experiments, clearly illustrated that the motion of a pebble, in addition to other parameters such as the beach shape and slope, is also dependent on the across-shore location of the pebble on the beach face.
2. The wave conditions: the field data from Van Wellen et al. (1998) illustrate the importance of the angle of wave approach to the shoreline for sediment transport.
3. The number of tracers deployed: To date, only a few studies reported the deployment in mass of reliable tracers such as of the aluminium type. Nicholls and Wright (1991) used a total of 759 and 460 aluminium tracers on two gravel beaches at Hurst Castle spit (Dorset, UK) and Hengistbury Long Beach (Hampshire, UK); and later, Curoy et al. (2007) reported the deployment of a total of 510 synthetic tracers on the beach at Cayeux-sur-Mer (Upper Normandy, France). Apart from these studies, the most recent tracer experiments tend to

employ less than a hundred particles. For example, Osborne (2005) deployed three sets of thirty tracers each on a gravel beach in Half Moon Bay (Washington, USA); Allan et al. (2006) used thirty tracers on a mixed beach at Cape Lookout State Park (Oregon, USA); and Bertoni et al. (2010) used slightly less than a hundred pebbles on an artificial pebble beach at Marina Di Pisa (Tuscany, Italy). The use of so small a number of tracers means that even if a 100% recovery rate over one tide is achieved, it represents only a small amount of the total beach volume. It is therefore understandable that the success of this kind of experiment depends on the quantity of tracer used. Moreover, in the situation where large number of tracers are seeded (e.g. \geq three hundred pebble tracers) with low recovery rates (e.g. 33%), the number of pebbles recovered (one hundred pebbles based on the two previous assumptions) would still provide meaningful data about the transport.

4. The depth of deployment of the tracers: it seems reasonable to assume that within the bulk material involved in the drift, particle motion changes with the depth of burial, but no research has been led in that way on gravel or mixed beaches to my knowledge. This will also help to the measurement of the active layer.
5. The time necessary for the tracer to be mixed within the beach material: views on this subject vary from one author to another. A minimum period of two tides is commonly suggested however the mixing is faster under higher waves than under lower waves (Wright, 1982). Bray et al. (1996) mention a mixing time range from two to seven days.

ii. Quartzite pebbles



Figure 3-10 Deployment of quartzite pebbles at Birling Gap-October 2004.

Preliminary tests on measurements of the longshore drift were attempted, using quartzite pebbles, at Birling Gap in October 2004. Given the site's mean south-westerly wave and wind directions, net longshore drift was expected to be to the east. For this reason, three hundred quartzite cobbles were laid out under Went Hill (about 320 m west of the steps, Figures 6-40) in a narrow strip from the head of the beach to the toe (Figure 3-10); cobble locations were recorded using the DGPS. The beach was visited on a monthly basis for six months i.e. until the recovery rate was nil. Recovery was executed on the surface from one end of the beach to the other during low tide.

iii. Synthetic pebbles

➤ First deployments at Cayeux-sur-Mer in December 2004

A total of 170 resin tracer pebbles were deployed on the beach surface in the afternoon of December 12th in a mid-mixed sediment beach position in proximity to the area of deployment in 2005 (Figures 3.3 & 6-6). Searches with a metal detector were carried out in the morning and afternoon of the 13th and 14th and during the morning only of the 15th, 16th and 17th. All recovered pebbles were then re-deposited at the original deployment point.

➤ Other deployments: at Cayeux in October/November 2005; at Birling Gap in March, May and December 2006 (Figures 3-11 & 3-12)

In addition to the points mentioned earlier, the fieldwork design and data collection was aiming to fulfil a few objectives, those being:

1. To acquire good tracer data to enable the calculation of the longshore drift based on pre-existing longshore drift formulae.
2. To study how pebble scattering operates alongshore and across-shore over a large range of wave conditions and water levels.

3. To identify and understand any differential patterns of pebble scattering at different locations across the beach.
4. To contribute to knowledge of the active layer by obtaining data on pebble drift variations associated with their depth of burial.

To address these objectives and the requirements mentioned previously, it was decided to deploy tracers at three different locations at regular interval between the berm and the mixed beach toe. Therefore, the respective behaviour of the sediment particles on the upper, the middle and the lower part of the mixed beach could be observed. At each of these locations, on the first day of the short survey periods at each injection location, up to 125 labelled synthetic pebbles were deployed into a 40 cm deep excavated hole (such depth was proved to be only affected during storm conditions from active layer investigations on a mixed beach at Saltdean, East Sussex). Each point of synthetic pebble deployment was composed of four layers, the three lower layers were 10 cm thick and each was filled with twenty five synthetic pebbles whereas, the fourth top layer although still 10 cm thick, was filled with fifty synthetic pebbles to ensure that a large amount of tracers are remobilised into the sediment transport (Figure 3-13). The total number of synthetic pebble deployed on the following days varied from day to day. Instead of deploying 125 synthetic pebbles every day during short period fieldworks, their total number was limited. This reflected the fact that the use of too many tracers would increase the time required for their recovery and would not allow the search to cover a large area of the beach from toe to top because of the time necessary to excavate them. However, to make sure that enough tracers were deployed to give meaningful data on the tracer movements, a minimum of two top layers of twenty five synthetic pebbles each were injected on every new deployment.

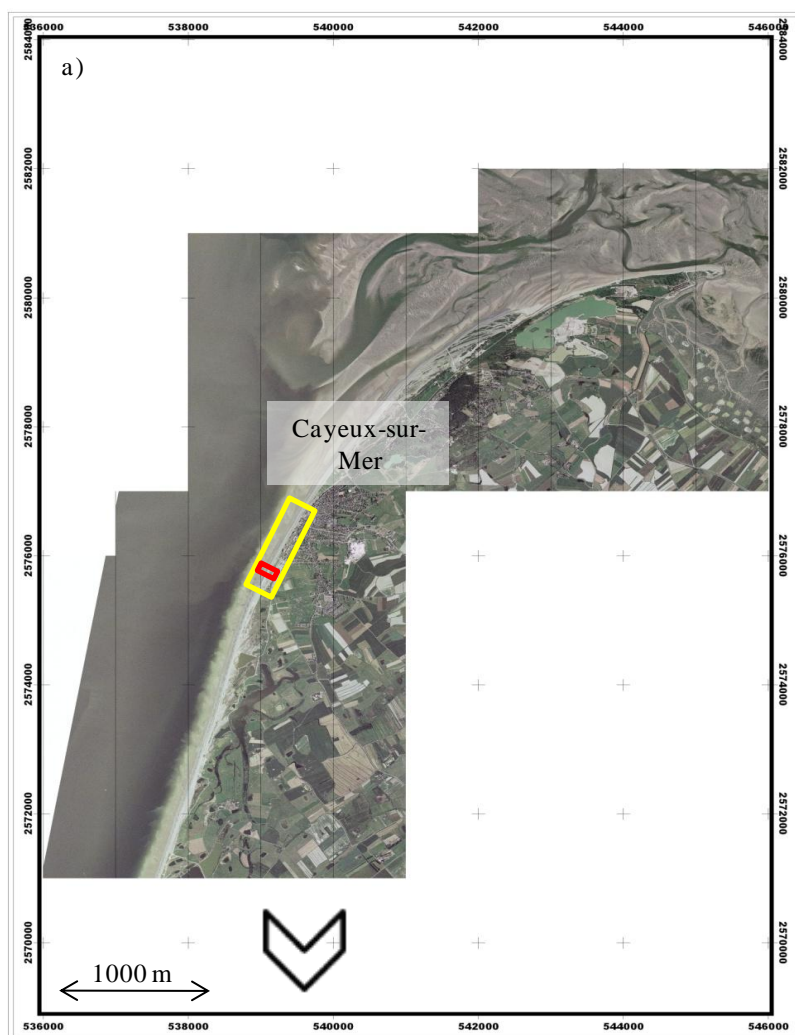
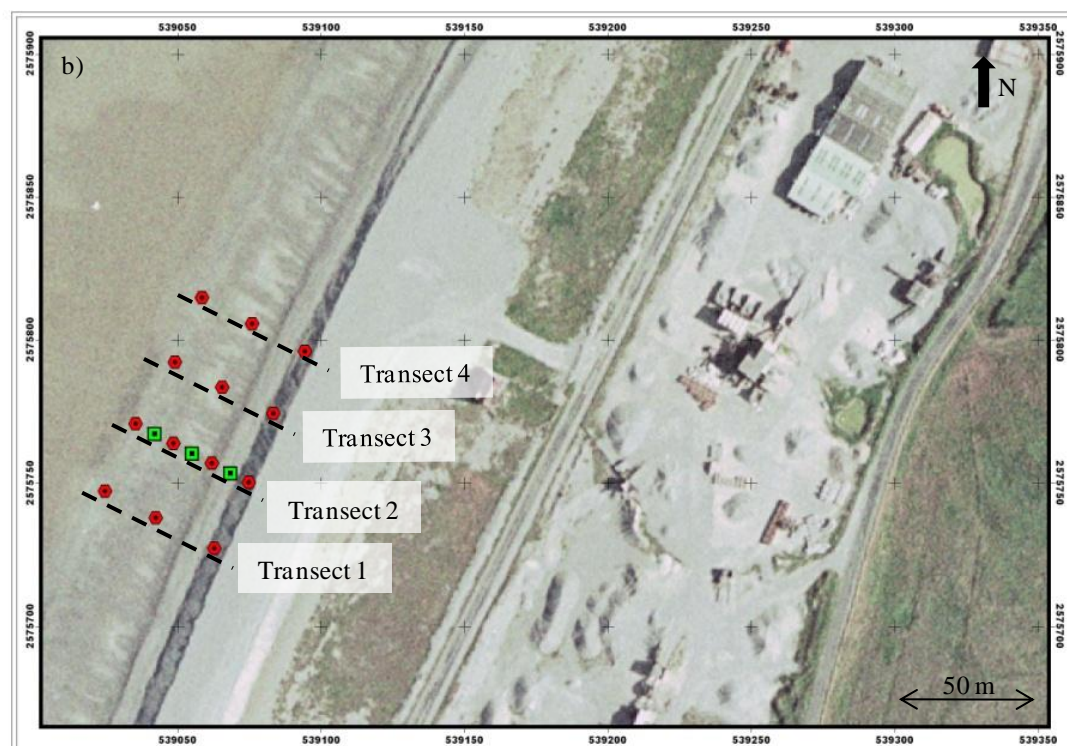


Figure 3-11 Location of the measurement points at Cayeux-sur-Mer. a) Aerial photograph of the study site, where the yellow rectangular represents the DGPS surveyed area and the red rectangular represent the area of deployment of the tracer pebbles and the measurements of the active layer. b) Zoom on the location of the tracer injection points (green squares) and the painted pebble columns (red points).



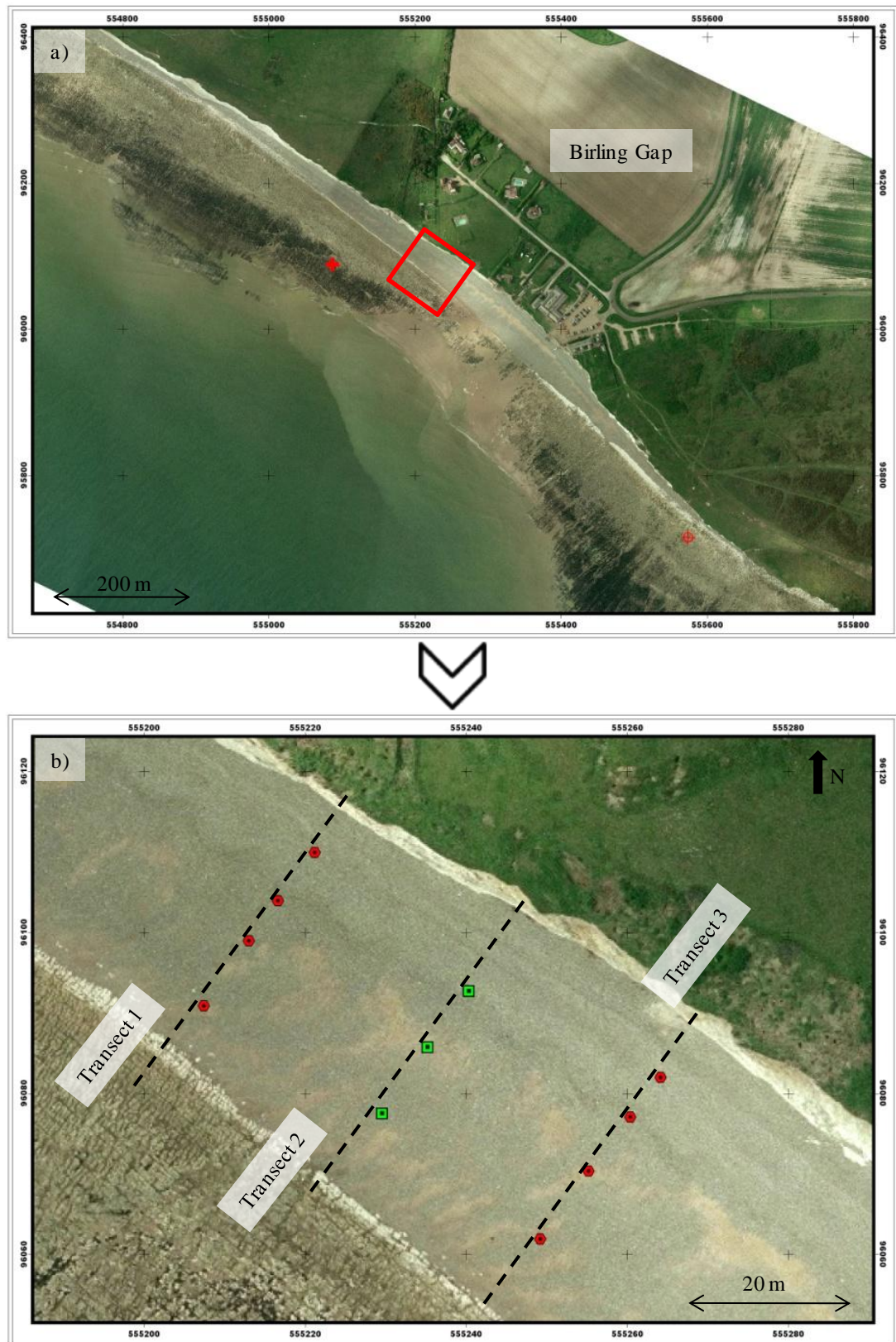


Figure 3-12 Location of the measurement points at Birling Gap. a) Aerial photograph of the study site, where the red rectangular represent the area of deployment of the tracer pebbles and the measurements of the active layer. b) Zoom on the location of the tracer injection points (green squares) and the painted pebble columns (red points).

Each layer was carefully mixed with the indigenous sediment to make sure that the tracer was well integrated into the beach material. Then, each injection point was compacted by stepping onto it to reproduce the original consistency of the beach material. That way, it is assumed that the tracers were perfectly well mixed and completely representative of the beach material even after one tide. These deployments occurred once a day during the night tide to facilitate the recovery during day light.

This method of deploying the synthetic pebbles at three locations on the beach profile and at various depths made it possible to trace differences in pebble movement depending on their initial position on the beach, but also depending of their burial depth.

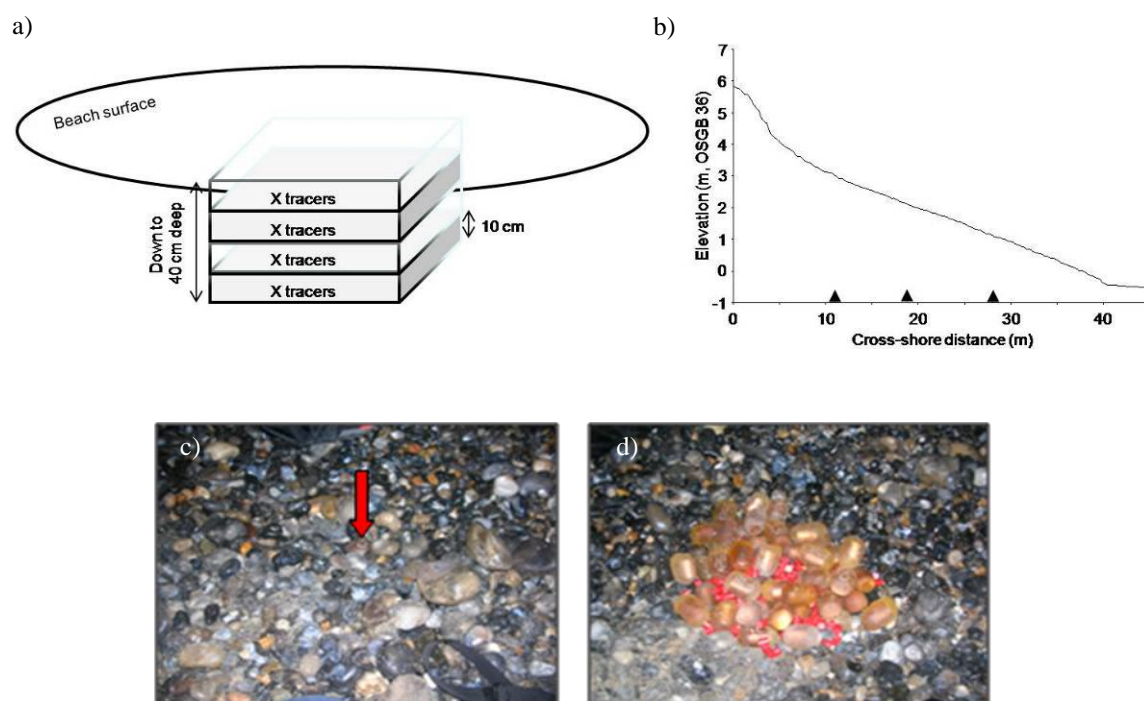


Figure 3-13 a) Layout of a synthetic pebbles deployment. b) Location of the synthetic pebbles deployments on a beach profile surveyed at Birling Gap surveyed in May 2005. Each deployment is represented by a triangle along the x-axis. c) View of an *in situ* synthetic pebbles deployment from the surface. The red arrow indicates one of the tracers perfectly mixed with the beach material. d) Inside view of an *in situ* synthetic pebbles deployment.

It is important to highlight that this methodology is based on the same principle as sand tracing experiments, and therefore some points such as the depth of burial of the tracers and the depth of sediment actually removed during an event are important to take into account. Indeed, for sand tracing experiments, the depth of deployment of the tracers

has to be greater than the active layer thickness in order to measure (i) the depth of sediment removed by the hydrodynamic conditions and (ii) the tracers' dilution within the beach material. The depth of sediment removal is crucial for longshore drift calculations while knowledge of the tracers' dilution allows a precise control of the quantity of tracer scattered into the beach material. Only then can it be judged if the tracing experiment is statistically representative of the actual beach material transported. Despite having carefully considered this point during the tracer injections, sometimes severe erosion or accretion prevented any tracer recovery in their location of injection. For example, significant accretion of beach material above the injection point when the berm is building up (even over one single tide) would make its recovery difficult or impossible because of the sediment instability when excavating material. Significant erosion of the beach face may remove all of the tracers injected. Measuring the active layer at the same time along multiple profiles and at different locations renders the data on the thickness of beach sediment in movement more statistically viable. Knowing that thickness, it can therefore be possible to assume the amount of tracers involved in the transport and deduce their actual dilution ratio in the beach material.

➤ Recovery



Figure 3-14 Metal detector in use.

Pebble detection was carried out once a day during daylight using a metal detector (Figure 3-14). Based on personal experience obtained through intensive use on the beach, the effective detection depth of the equipment to sense a synthetic pebble is about 30 to 40 cm maximum into a mixed sediment of the same type as Cayeux-sur-Mer or Birling Gap. This performance was considered sufficient to enable a full recovery of the tracers remobilised by the sediment transport on the understanding that the active layer would rarely be greater than 30 cm under non-stormy conditions.

Once detected, a precise record of the location and the depth of each synthetic pebble was made using the Differential GPS. At the last stage of the daily experiment procedure, two options were available for the recovered pebbles:

- (i) Either each pebble recovered was collected and “reseeded” in one of the injection points; or,
- (ii) The tracers were not removed, i.e. their location was recorded and they were then replaced exactly where they were found.

The first option (i) has the advantage that it restricts the investigation to a small area but also to allow specific scattering patterns to be related to particular hydrodynamic conditions at specific water levels, meaning that all the variables are reduced to a single event. This method facilitates the study of temporally and spatially small scale events. The second option allows a better mixing of the tracers within the natural sediment, giving the opportunity to highlight individual transportation and showing periods of movement or dormancy of the pebbles. Therefore, a broader view of beach behaviour can potentially be drawn covering greater spatial and temporal scales. The key difference, therefore, between these two options is the spatial and temporal scales that are examined: (i) short term deployment over a relatively small surveyed area facilitating a precise correlation with the hydrodynamic conditions; (ii) longer term deployment over a relatively large surveyed area and also a large spectrum of hydrodynamic conditions that are averaged.

To reach a decision on which methodology was to be used, two practical aspects of the data collection were considered: (i) the time available at low tide, (ii) the time necessary to collect the complete array of data required for a specific aim. The time necessary to collect the data is influenced by the quantity and the resolution of the data collected, the size of the study area and the chances of tracer recovery. Moreover, with the second method, for the data to be meaningful not only do the recovery rates have to be high, but also the same tracers have to be found regularly. This facilitates the identification of tracers’ movement patterns from one tide to another. However, tracer recovery is dependent on the wave conditions and the tracer scattering to ensure that recovery rates are high for the entire period (storm conditions potentially transport the tracers significant distances beyond the survey area). For these reasons, the first option was generally preferred. This methodology confines the tracer recovery to small areas and its execution is simple: detection, excavation, DGPS marking and collection. This methodology also minimises the influence of pebble “dormancy”. Finally one of the most important advantages is related to the time resolution of the method. By reducing

the time between injection and recovery to one high tide, tracer scattering can be directly related to specific hydrodynamic conditions.

To determine the volume of sediment transported, it is necessary to measure the actual depth of sediment that is remobilised by the forcing hydrodynamics over the time period of the tracers' scattering. This layer of sediment, in motion from one tide to another, is known as the active layer.

3.4.4 Active Layer measurement

The thickness and width of the moving sediment layer on beaches is central to calculating longshore transport rates and volumes using tracers. It is generally agreed that this layer is representative of the thickness of material remobilised for nearshore sediment transport (e.g. Sunamura and Kraus, 1985; Sherman et al., 1993, 1994; Ciavola et al., 1997; Ferreira et al., 2000).

- i. Review of techniques described in the literature and reflection on their application for this study

To measure the active layer on gravel beaches, two approaches are generally adopted. One that involves adapting techniques that have originally been designed to study sandy beaches (e.g. Nicholls, 1989; Stapleton et al., 1999; Austin and Masselink, 2006), or one that involves designing a new technique specifically for use on gravel beaches (e.g. Laronne et al., 1994). Most of the techniques used on sand beaches to measure the active layer are not directly transferable to gravel beaches and there are relatively few studies of active layer thickness of gravel beaches. There is, therefore, a knowledge gap between the two beach types regarding the active layer.

Buried columns of aluminium cylinders or tracer material have proved successful to measure the active layer on flint gravel beaches, (e.g. Nicholls, 1989). The columns are easily relocated using a metal detector and the equivalent densities of aluminium and flint mean that the cylinders are representative of the host material except that they are quite differently shaped. The top of the column accords initially with the beach surface and following erosion the missing part corresponds to the maximum depth of removal.

Similar measurements have been made using painted pebbles (Stapleton et al., 1999), although the precise methodology is not explained. These two methods measure the maximum depth of disturbance but provide no information on either the duration of or fluctuations in the disturbance (Stapleton et al., 1999).

According to Van Wellen (1999), tracer pebble deployments can be used in essentially the same way as coloured sand is used on sand beaches (e.g. Levoy et al., 1998; Stépanian, 2002; Tonk and Masselink, 2005). The erosion depth of the column of tracer pebbles for example one tide after deployment gives a direct measurement of the active layer over that tide. This procedure is simple; the tracer pebbles are mixed into the beach material within excavated holes the dimensions of which are known. At the low tide following injection, the depth from the beach surface to the top of the remaining tracers in the injection point reveals the depth of disturbance. The addition of the elevation changes over the same time period allows the full thickness of the active layer to be calculated (Figure 3-15). Van Wellen (1999) recorded the burial depth of the deepest tracers recovered from within the beach sediment and used this depth as being representative of the depth of disturbance. The main advantage of both methods is that two types of measurement, sediment tracing and active layer thickness, can be made simultaneously. Neither, however, permits any insight to be gained into the duration and fluctuation of the disturbance (as per Stapleton et al., 1999).

Another technique devised by Laronne et al. (1994), has the advantage of both measuring the depth of disturbance and also indicating the predominant direction of sediment movement. This technique utilises a steel chain anchored deep within the beach sediment and the depth of removal can be measured using the chain links. Pebble disturbance causes the chain to bend in the general direction of the sediment movement. This method is simple, efficient and quick. However it was designed for rivers and consequently unidirectional sediment flows. On gravel beaches, sediment flow is more chaotic because of the hydrodynamic processes which create multidirectional water flows. Such conditions render the use of this technique on mixed sediment beaches problematic.

A further method, originally developed on sandy beaches, is to insert long metal rods, with loose washers over them, into the beach. The washers are free to fall along the rod down to sediment surface and then their positions are used to measure the depth of activation (Jackson and Nordstrom, 1993; Austin and Masselink, 2006). Whilst these two methods identify topographic changes they do not measure sediment mixing, as is the case when buried columns of tracers are used.

ii. Chosen methodology

The intention was to conduct measurements of the active layer thickness on consecutive low tides at various locations across- and along-shore. For this reason, a methodology that is rapid, representative, simple, reliable, and with the potential be reproduced en mass was necessary. The range of appropriate techniques available to measure the active layer depth on mixed beaches is restricted. The answer to this study's requirements was a combination of the Nicholls (1989) and Stapleton et al. (1999) protocols. The method consists of painted and numbered indigenous pebbles buried vertically as a column into the beach face. The depth and number of each painted pebble is recorded manually during its injection so that when it is recovered later both the mixing depth and the accretion above the columns can be measured (Figure 3-15).

Active layer measurements and DGPS beach topographic surveys were collected along cross-shore profiles. The number of profiles surveyed varied from one study site to another linked in part to the size of the survey area but also to the number of field assistants that were available. Thus, four profiles 25 m apart were surveyed at Cayeux-sur-Mer, whilst two profiles 50 m apart were surveyed at Birling Gap (note: these profiles were located in close proximity to the synthetic tracer pebble deployment locations). Along each profile surveyed, three to four painted pebble columns were inserted at regular distances from the top of the active profile to the beach step. These locations represented the upper, upper-middle, lower-middle and lower beach when four columns were surveyed on the same profile; and the upper, middle and lower beach when three columns were surveyed (Figure 3-11 and 3-12).

Pebbles with b-axes of between 40 - 50 mm (-5.32 - -5.64 phi) were taken from the beach, painted and individually numbered. These were then built into 25 – 35 cm deep

columns in pits excavated into the beach and both the depth and number of each pebble were recorded. The maximum depth was dictated by the stability of the beach sediment. The top of the column was flush with the beach surface (Figure 3-15). The location and elevation of each column was recorded using the DGPS. On every following low tide, the columns were relocated using the DGPS in “stake out” mode. Once relocated, the coordinates and the number of the top pebble were recorded. Where there had been accretion, the top of the column was re-located by digging and new pebbles were inserted from the top of the old column to the new beach surface.

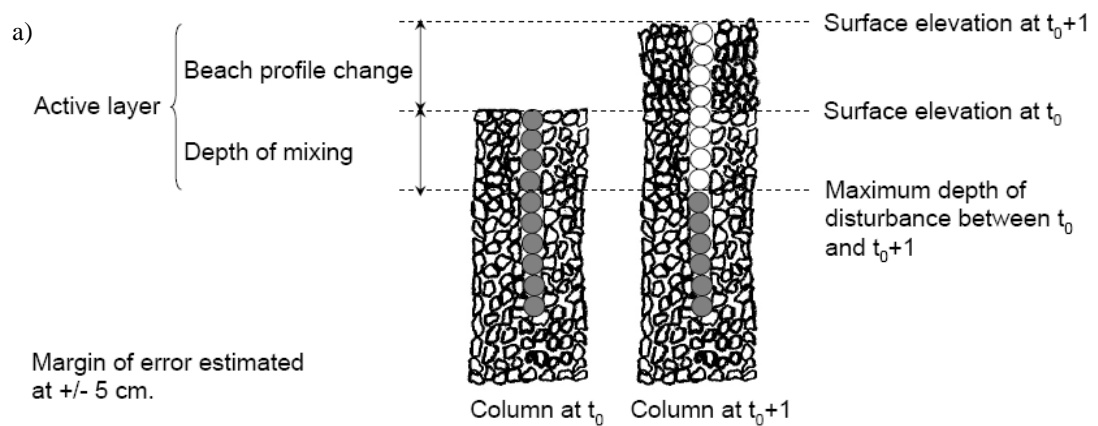


Figure 3-15 a) Method used to measure the active layer. The dark circles are the painted and numbered pebbles deployed at the first low tide (time, t_0). The white circles are the new painted and numbered pebbles deployed at the following low tide (time, $t_0 + 1$). b) Planar view of a painted and numbered pebble column built up into the beach material.

3.5 Sediment variation

The aim was to collect information about the material grain size distribution to characterise the beach material at the time of the various experiments and enable the investigation of linkages between sediment mixing, active layer thickness and synthetic pebble redistribution. An additional aim was to map spatial patterns of surface sediment distributions in response to the forcing hydrodynamics.

3.5.1 Background, reflection on the methodologies available

The surface sediment distribution on a mixed beach varies greatly alongshore and across-shore in accordance with the antecedent forcing hydrodynamics and beach topography (e.g. Horn and Walton, 2007). These grain size re-arrangements affect the permeability of the beach surface and therefore the active layer depth and the volume transported. Consequently, it is necessary to characterize the beach material distribution. Sediment sampling on mixed sediment environments in general remains problematic. The most traditional approach is to carry out bulk sampling (as per Church et al., 1987; Gale and Hoare, 1992, 1994; Dunkerley, 1994; Van Wellen, 1999; Horn, and Walton, 2007). The bulk sampling method requires the determination of the sediment weight that is necessary to be representative of the beach material. Gale and Hoare (1992) recommended collecting more than one hundred sediment particles in each 0.5 phi fraction in order to obtain a reliable sediment sample. Satisfying this requirement on mixed sediment beaches would involve impractical sediment samples because of their great size and weight (> 100 kg). Facing this problem, Van Wellen (1999) assumed that a 70 kg sediment sample was sufficient to characterize the beach material grain size. More recently, the BAR project (2005) argued that it was impractical to collect such large quantity of sediment. With the aim of improving on previous sampling designs, whilst still reflecting the spatial and temporal variability of the surface material on a mixed beach, the BAR project proposed collecting more than a single sample but in smaller sizes (1 to 5 kg). This multiple sampling strategy has the advantage of collecting a large array of grain size distributions on the beach face. As a consequence, such a strategy would be even more representative of the beach material involved in the

sediment transport than those using single large samples. For these reasons, the methodology proposed by the BAR project (2005) was used in this study to characterize the beach grain size distribution.

A particular concern about these sampling strategies was that the samples are only representative of the bulk beach material. It is known that large gravel or mixed beach areas often display alongshore and across-shore surface sediment sorting (c.f. Carter, 1988; Bird, 1996). The occurrence of such sediment means that, in order to characterise the sediment size distribution samples need to be collected over large areas of the beach surface. Watt et al. (2006) and later Dornbusch et al. (2008b) have each observed both shorter and longer term trends in beach surface grain size distributions over large beach areas and recorded grain size distribution patterns.

The frequency of sampling and mapping of beach surface sediment distribution patterns can be adapted to the aims of specific experiments. Tidal surveys of surface sediment distribution may, for example, help to facilitate a greater understanding of beach material response to specific forcing hydrodynamics whilst monthly surveys may express seasonal trends that are more representative of the general hydrodynamic forcing.

3.5.2 Methodology chosen

During the shorter fieldwork periods, the temporal and spatial scales observed using the synthetic pebble scattering and the active layer measurements are confined. At such spatial scales, ≤ 100 m along the beach, it is difficult to observe strong alongshore grain size grading whereas great variations can be observed across the beach. Therefore, grain size distribution data collection and mapping had to capture across-shore grading, where it exists, to deliver valuable information about the material in close proximity to the active layer and synthetic pebble measurements, and also information about the general adaptation patterns of grain size distribution in response to hydrodynamic forcing. To complete the first objective, it was decided to sample sediment at the synthetic pebble injection points. Sediment sampling at these three locations across-shore was adequate to be representative of the beach bulk material, whilst each individual sample was

directly associated with the nearest active layer thickness and the synthetic pebble scattering measurements. As mentioned previously, the sediment samples were collected according to the protocol devised by the BAR (2005); multiple small samples with a weight ranging from 1.1 kg to 12 kg. At Cayeux-sur-Mer, sediment sampling was carried out on a tidal basis whereas at Birling Gap it was only carried out if there was visual evidence of any grain size change from one tide to another. The reason for this different sampling strategy between the two sites was linked to the presence of the recycled material at Cayeux-sur-Mer. This almost continuously supplies the beach with fresh sediment, changing the beach grain size distribution throughout the survey period. In contrast, the grain size distribution at Birling Gap is much less variable over short time scales because there is no equivalent, regular, supply of fresh sediment.

Each sediment sample was collected using a 15 cm diameter corer, up to a depth of 20 cm into the beach. It was deemed unnecessary to dig any deeper into the beach material than this because the main aim was to characterize the grain size distribution of the sediment layer remobilized by the forcing hydrodynamics. Moreover, coring 20 cm of sediment was considered sufficient to collect beach material within the active layer. Later, in the laboratory, grain size analysis of the sediments was carried out by dry-sieving and a shaking time of 10 min per sample. Sieve sizes ranging from -6 to 5 phi were used (size of each sieve: -6, -5.64, -5.12, -4.24, -3.48, -3, -2, -1, 0, 1, 2, 3, 4, 5 phi) and each fraction was weighed. Each sample was mechanically sieved for 10 minutes (Results are in Appendix II).

3.6 Summary

To examine the processes that influence the evolution of a morphodynamic system it is essential to observe the connections between the sedimentary features, the external forces creating these features and the sediment transport resulting from their interaction, over different temporal and spatial scales.

- The beach topography:

The use of a TOPCON Differential GPS in automatic point collection mode allowed the collection of high resolution geomorphological data over large areas in a minimum time. One of the main advantages is that the surveys can be done at any temporal and spatial scale required (e.g. from one tide to weeks, months, decades or more; from one profile to an entire beach). At Birling Gap, topographic surveys were collected over the entire beach from a tidal frequency (during short fieldwork periods only) to a monthly frequency for a two year period. At Cayeux-sur-Mer, topographic surveys were collected on a tidal frequency during two short periods of fieldwork.

- The hydrodynamic conditions:

A large panel of wave recorders able to measure multi-directional currents in both onshore and offshore positions measured the wave conditions at time scales from a single tide to two years. Onshore wave conditions were measured only during short term fieldwork.

- The sediment transport:

Information on sediment transport was gathered using DGPS topographic surveys (see above) and pebble tracing associated with active layer measurements.

Tracer experiments were conducted on a daily basis during the short fieldwork periods. Deployed during the nocturnal low tide, the synthetic pebble recovery occurred during the following daylight tide. Shortening the time between deployment and recovery allows the tracers' scattering to be related to specific forcing hydrodynamics. By repeating these experiments on a large range of wave and tide conditions, an understanding of the morphodynamic system can be reached. Most tracer studies have considered the tracers' dispersion gravity centre (generally used on sand beaches, e.g. Balouin et al., 2001) and the general direction of the transport as representative of the sediment transport. However, recent researches on gravel and mixed beaches, preferred to consider the transposition of each individual tracer to identify the sediment transport patterns as a function of the sediment particles' size and shape (e.g. Osborne, 2005; Allan et al., 2006).

Regular tidal surveys of the active layer thickness at various locations on the beach provided precise measurements of the layer of sediment remobilised by the forcing hydrodynamics. Therefore, both the direction (tracer experiments) and volume (active layer measurements) of sediment transport were precisely observed.

Precise records of the grain size distribution have helped to characterise the beach material variations in association with the forcing hydrodynamics and the beach morphology.

Chapter 4. Temporal and spatial scales of mixed beach profile changes

4.1 Introduction

The aim of this chapter is to understand the beach topographical responses to forcing hydrodynamics and to link these to the synthetic tracers' scattering patterns, discussed in Chapter 6, in order to reveal the processes of sediment transport on mixed beaches.

This chapter discusses the morphological characteristics observed on both mixed beaches studied during this research; from (i) semi-lunar/tidal cycle topographical changes at both field sites to (ii) seasonal and yearly elevation changes for the specific case of Birling Gap (East Sussex). Based on the data collected a clear picture of (iii) the impact of coastal management on the beach profile characteristics and responses is established at Cayeux-sur-Mer (Upper Normandy); and (iv) the collection of beach profiles at various times at both study sites reveal the beach morphological changes in what could be considered three “different” environments: a non managed unconfined mixed beach, a managed mixed beach and a cliff fringing mixed beach.

4.2 Background

A beach profile is the result of long- and cross-shore sediment transport processes in response to the wave and tide climate at a given area (Dean, 1991). This response will be influenced by the pre-configuration of the profile, the beach elevation, the beach width, the grain size distribution of the beach material, the sediment sources and the near-shore geometry (Caldwell and Williams, 1986). Gravel beach active profile types are generally bounded between the gravel seaward edge and the upper limit of the swash reach (Orford, 1986).

The natural shape of a mixed beach profile is generally concave upwards and steepens towards the crest (e.g. Jennings and Shulmeister, 2002; Curoy et al., 2009). As a consequence, these beaches are of the reflective type (e.g. Mason, 1997; Masselink and Hughes, 1998). Their profile generally includes:

- (i) A linear low gradient intertidal platform (1 to 6°) generally composed of sand;
- (ii) A pronounced step at the break of slope generally composed of the coarsest material available to the beach and located between the sandy platform and the mixed sediment beach and;
- (iii) A steep beach face ($\tan \beta = 0.1 - 0.15$);
- (iv) A HWL berm(s), and;
- (v) A maximum of the beach material storage occurs in the sub-aerial part of the profile (Orford, 1978; Hughes and Cowell, 1987; Bradbury and Powell, 1992; Pontee, 1995; Jennings and Shulmeister, 2002; Austin and Masselink, 2006; Austin and Buscombe, 2008).

4.2.1 Classification of the beach profiles

Over the years, many authors have tried to classify beach profiles into groups that are representative of different environments that can be applied to all beaches over the world. Some authors consider the morphology of the beach (e.g. Kirk, 1969) whereas others have focused more on the shape of the beach profile and its characteristic features

(e.g. Sonu and Van Beek, 1971; Orford, 1978; Caldwell and Williams, 1985; Jennings and Shulmeister, 2002).

Kirk (1969) distinguished three main types of mixed sand and shingle beaches in an inventory of the gravel beaches encountered in New Zealand:

- (i) A spit, where the beach is broad, planar or convex upwards;
- (ii) A cliff front, where the profiles are short and steep, and;
- (iii) A river mouth, which is of the similar type as cliff front but is wider with pronounced storm berms.

Despite this first attempt to define distinct types of gravel beach profile as a function of the beach environments, other authors preferred to attempt to create a profile type classification based on the shape and features present on the beach face.

In a similar way as Komar (1976) did for sandy beaches (Appendix III), Orford (1977) identified three basic profiles on a gravel beach in South Wales (Figure 4-1):

- (i) A step profile associated with fair weather (presence and position of berms at the swash limit);
- (ii) A composite profile associated with severe storm conditions, and;
- (iii) A bar profile, intermediate between (i) and (ii) i.e. associated with storm conditions (presence and position of berms at the gravel edge).

Later, Orford (1978) adopted a similar methodology to Sonu and Van Beek (1971) based on the shape of the profile, concave, linear or convex (Appendix III), to identify typical gravel beach profiles. He integrated his earlier identified step/composite/bar profile types on gravel beaches with the three typical profiles (concave, linear and convex) that Sonu and Van Beek (1971) identified on sandy beaches. Based on his observations in South Wales (sixty height beach profiles in total), Orford (1978) judged it reasonable to omit the convex type of profile because of its rarity, generally being observed only during neap tides and very constructive waves that build up the high berm. In his analysis, Orford (1978) also stated that mid-berms (i.e. located in the middle of the beach), as per the definition of the active beach profile type given earlier, are not relevant here. Indeed, the location of the berm is directly a consequence of the

maximum elevation reached by the swash of the tide which corresponds to the upper limit of the active profile per definition. He proposed eight different types of profile observed on gravel beaches as a function of the presence and location of the berm/beach step and the shape of the profile (linear and concave) (Figure 4-2).

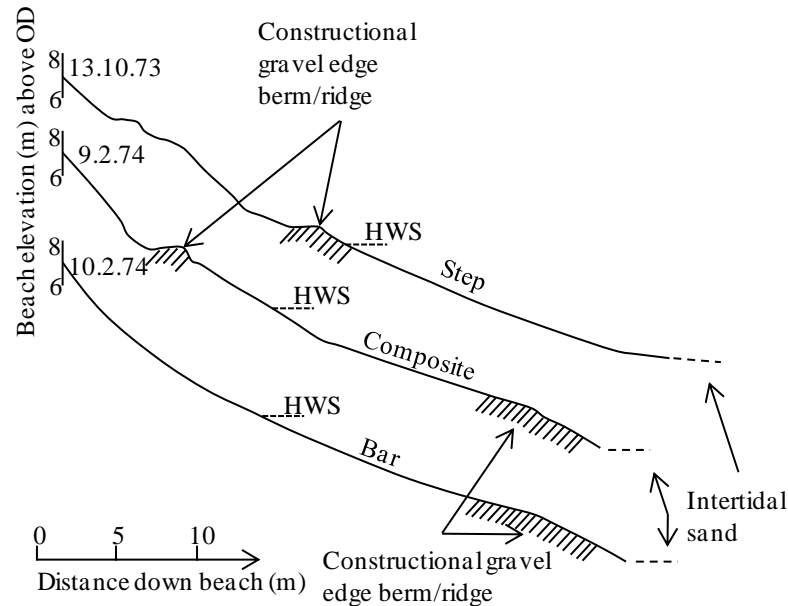


Figure 4-1 Examples of step, composite and bar beach profile identified at Llanrhystyd. Each profile starts from the gravel ridge crest. HWS marks the predicted position of spring tide high water (Orford 1986).

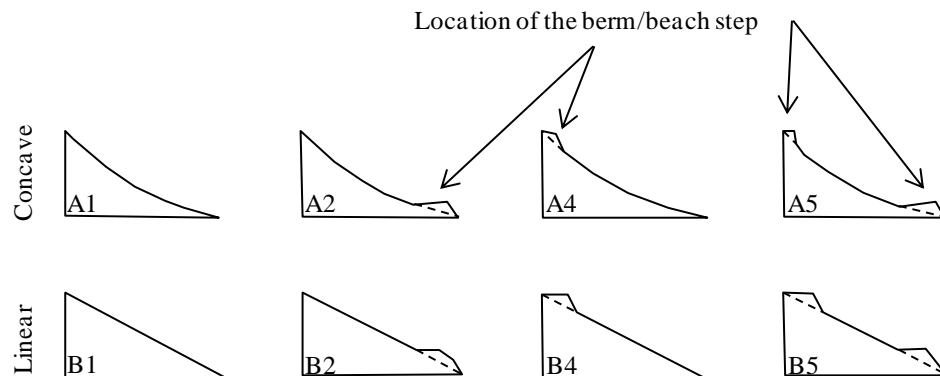


Figure 4-2 Beach profile dimensions of gravel based profiles at Llanrhystyd (Orford, 1978).

Later, Caldwell and Williams (1985) classified coarse clastic beach profiles using a graphical standardization procedure. Out of four hundred and two beach profiles collected on two beaches in South Wales, they were able to identify ten types of Sonu and Van Beek (1971) profiles (Figure 4-3). However, in an attempt to apply this

procedure on his Llanrhystyd profiles, Orford (1986) was not able to identify such clear difference between the types of profile and concluded that more investigation was necessary before obtaining a numerical method to characterise coarse clastic beaches.

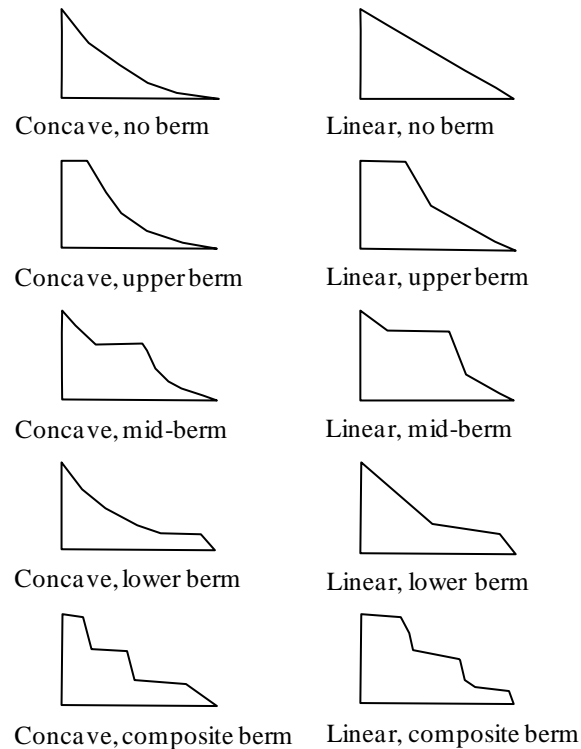


Figure 4-3 Basic profile types distinguished by Caldwell and Williams (1985).

Jennings and Shulmeister (2002) in their classification for gravel beaches clearly identified three types of coarse clastic beach:

- (i) Pure Gravel Beaches;
- (ii) Mixed Sand and Gravel Beaches and;
- (iii) Composite Beaches.

Each category is defined mainly according to profile shape and grain size distribution. In addition to this classification, they identified typical profile shapes most likely to be observed during specific wave conditions. They also stated that the “mixed beaches” of the UK are analogous to composite beaches, which are composed of a two-part profile due to hydraulic sorting. The lower part of the foreshore is sand dominated and has a low gradient ($\tan \beta = 0.03 - 0.1$) whereas the upper foreshore is gravel dominated, with a gradient of $\tan \beta = 0.1 - 0.15$. This has an impact on the hydrodynamic processes on the beach. Spilling waves will form within a dissipative surf zone at low tide and a long-shore bar-trough system may develop on the sandy lower foreshore (Jennings and

Shulmeister, 2002). The upper foreshore is highly reflective and according to Mason and Coates (2001) has a percentage of sand varying between 15 and 68% depending on the beach.

The sand content in a mixed sediment beach has a significant effect on the permeability of the beach face and water table dynamics (Mason et al., 1997) which most likely influences the shape of the beach profile. In their study of a mixed beach in the north of France, Costa et al. (2008) showed that sand transfer operates between the sandy lower foreshore and the gravel dominated upper foreshore. These sand transfers can not only change the permeability of the beach but also influence the shape of the beach if they represent significant volumes. During low wave energy conditions, the sand component generally migrates landward and the sandy platform experiences an increase in elevation. This landward transport facilitates the supply of sand to the mixed sediment beach by wave or wind action. This increase of sand is also supported by the fact that only a thin layer of the mixed sediment beach is remobilised during such wave conditions and therefore the sand that generally percolates deeply within the pebble voids is poorly affected by transport (e.g. Costa et al., 2008; Curoy et al., 2009).

On the contrary, during storm conditions, the sandy lower foreshore shows erosion and the interstitial sand of the mixed sediment beach is preferentially transferred toward the sandy platform (Costa et al., 2008). Costa et al. (2008) stated that a portion of this sand extrudes from the mixed sediment beach to nourish the growth of a small bar on the lower foreshore. This small bar may cause waves to break before they can reach the upper parts of the foreshore so that less energy is delivered onto the mixed sediment beach. The displacement of sediment down the beach makes the beach profile less reflective because the beach step is less pronounced, but may also cause the permeability of the mixed sediment beach to increase. The combination of the two means that more wave energy is dissipated by the beach profile and more rapidly than would otherwise be the case.

Until Costa's study, gravel beach profile models did not extend seaward of the mixed sediment beach. Because of the linkages identified in his study, it seems appropriate to

consider carefully the exchanges existing between the sandy foreshore and its upper foreshore for the beach profile analysis.

4.2.2 Spatial and temporal beach profile changes

“Changes in the form, height and width of beach profiles occur with tidal, daily, seasonal and longer term variations in wave energy. Short term changes are related to the changing pattern of wave energy” (Kirk, 1969, p25).

Geomorphological and sedimentological research on coarse clastic beaches has focused predominantly on medium (seasons) to long term (decades-centuries) timescales (e.g. Carter and Orford, 1984, 1993; McKay and Terich, 1992; Forbes et al., 1995, 1997; Pontee, 1995, Orford et al., 1996, 2002; Shulmeister and Kirk, 1997; Jennings et al., 1998; Pontee et al., 2004), and the stratigraphy of such systems (e.g. Neal et al., 2002; Orford et al., 2003). However, for the creation and good functioning of mid to long term shoreline models, it is crucial to understand shorter term beach dynamics (Mason and Coates, 2001). For this reason, during the last few years, an increasing number of studies have considered short term (hour, day, semi-lunar cycles) beach morphological and sedimentological changes or hydrodynamic processes controlling the sediment transport on coarse clastic beaches (e.g. Sherman, 1991; Mason, 1997; Austin and Masselink, 2006; Watt et al., 2006; Pedrozo-Acuña et al., 2006; Ivamy and Kench, 2006; Austin and Buscombe, 2008; Costa et al., 2008; Horn and Walton, 2007).

Long term beach changes are the result of sediment exchange between the sub-aerial beach and the nearshore zone. These exchanges are determined by the combination of the mean sea level variations and the sediment supply. On the other hand, short term changes of the beach morphology are principally determined by wave climate fluctuations. Between the short and the long term scales, morphodynamic changes such as lunar and seasonal cycles are driven by the combination of wave climate, lunar tidal cycles, wave and current conditions associated to weather conditions (Clarke et al., 1984). Events such as storms may be recorded in the beach morphology and sedimentology. For example, Watt et al. (2006) observed a coarsening of the beach sediment surface in relation to storm events on mixed sediment beaches.

The processes controlling coarse clastic beach, and more specifically mixed beach, morphology and transport of the gravel component are still poorly understood. A quick overview of the principal parameters thought to be driving gravel or mixed beaches profile changes and sediment transport illustrates the complexity of their interaction:

- (i) Wave height: The wave height drives the wave run-up which has been reported in a number of studies as the driving parameter of sediment transport on coarse clastic beaches (e.g. Van Wellen et al., 2000; Pedrozo-Acuña, 2006). The wave run-up is also responsible for the formation and shaping of the berm that is classically observed on gravel beaches at the HWL mark. An increase in wave height also forces an increase in the surf zone width which implies that more wave energy is delivered to the beach (Powell, 1990).

For a given HWL, large wave height conditions induce very high berms on the profile and can occasionally breach the barrier by flattening the crest (Chapter 1 Section 1.8.5) (e.g. Orford and Carter, 1982; Pontee et al., 2004; Austin and Masselink, 2006). The beach step generally migrates seaward when the wave height increases as an attempt to render the beach profile less reflective (e.g. Costa et al., 2008). On mixed beaches, high energy waves can remobilise the interstitial sand between the gravel and cobbles thereby increasing the beach permeability and therefore the ability to the beach face to dissipate wave energy more quickly (e.g. Costa et al., 2008).

- (ii) The wave period: Longer wave period waves deliver more energy to the beach and are therefore responsible for the formation of higher berms (Nicholls and Webber, 1987; Powell, 1990).
- (iii) The duration of the wave action or time of inundation of the beach: Masselink and Short (1993) highlighted the importance of the time of action of the hydrodynamic processes onto the beach face. Powell (1990) observed that the biggest volumetric changes (approximately 80%) on a gravel beach occur in the first 1/6 stage of the total time action of the waves and that the subsequent wave action serves only to hone the final shape of the profile.

The length of time of inundation will directly control the amount of energy delivered by the waves and hence, the volume of sediment transported in the longshore and cross-shore directions.

The length of time of action of the hydrodynamic processes on a composite beaches is even more important as across the beach profile there are two hydrodynamically different entities: (i) a dissipative sandy lower foreshore, where spilling waves will form, with a dissipative surf zone at low tide and where a system of ridges and runnels may develop; and, (ii) a steep reflective coarse clastic upper beach onto which plunging waves break directly (Jennings and Shulmeister, 2002). Such differences are likely to result in different sediment transport processes and volumes between the two entities.

- (iv) Spatial and temporal arrangements of the grain size distribution of the beach material: On mixed beaches, the particular shape of the beach profile (a dissipative sandy lower foreshore and a steep reflective coarse clastic upper beach) and the general sediment distribution has been presented earlier in this chapter (c.f. Jennings and Shulmeister, 2002). The sediment distribution on mixed sediment beaches is even more complex. Observations showed that the grain size distribution and its spatial arrangement changes with time and wave conditions mostly on the across-shore directions. Unfortunately very few field data are available to indicate these temporal and spatial variations on mixed sediment beaches, although there are reports in the literature over seasons or storm events (e.g. Van der Meer, 1988; Bluck, 1967, 1999; Orford et al., 2002; Osborne, 2005; Watt et al., 2006; Horn and Walton, 2007; Costa et al., 2008; Dornbusch et al., 2008b; Curtiss et al., 2009). Despite this lack of data on mixed beaches, it is very likely that the spatial and temporal distribution changes drive the permeability and hence the beach profile answer to wave conditions.

Mason et al. (1997) observed that the permeability changes with the percentage of sand within a mixture of sand and gravel. They showed that the hydraulic conductivity reduces to approximately that of sand when the content of sand in a mixture reaches 25%. They suggested that only 20% of

fine sand would be sufficient to produce this result and that beyond 25% sand, even up to 60%, the hydraulic conductivity would not vary enough to have a significant impact on the beach profile response.

The grain size distribution of the beach material also influences bottom friction which in turn influences the swash characteristics, particularly swash zone width and current speeds, and hence beach profile changes (Pedrozo-Acuña et al., 2006; Horn and Li, 2006).

- (v) The wave direction: According to Van Hijum and Pilarczyk (1982) there is an optimum incident wave angle at which pebble size particles are transported the furthest. For example, the optimum angle is between 50 and 60° to the beach on sandy beaches. It seems reasonable to consider that longshore sediment transport influences the cross-shore rearrangement of the beach sediment by controlling the size, shape and quantity of the material available (e.g. Van Hijum and Pilarczyk, 1982; Van der Meer and Pilarczyk, 1986; Powell, 1990; Pontee, 1995).

On open coasts, specific wave heights are often associated with specific wave directions (Shepard and Lafond, 1940; King and Williams, 1949; Sonu and Van Beek, 1971), and hence according to (i) the beach profile response.

- (vi) The effective depth of beach material: Powell (1990) modelled the influence of the effective beach thickness by incorporating an impermeable membrane parallel to the initial beach slope. By varying the ratio d_B/D_{50} , where d_B is the effective thickness of beach material measured relative to the initial slope and d_{50} is the median diameter of the sediment particles, they showed that for a ratio inferior to approximately 30, the thickness of the beach above the impermeable layer is not sufficient to retain material over the profile and the beach structure breaks down. Horn and Li (2006) identified the hydraulic conductivity, the friction factor, and the ratio of uprush and backwash sediment transport rates as important in the beach profile

response on gravel beaches. Greater thicknesses of beach material will certainly provide a greater potential for beach infiltration, therefore more swash energy will be dissipated by the beach leaving only a little energy available to the backwash. A high value of the ratio uprush/backwash will have a positive impact on the beach profile.

- (vii) The foreshore level: Foreshore elevation will have a direct impact on the beach hydrodynamic processes. Powell (1990) showed that as the level of the foreshore rises, wave breaking occurs further seaward of the beach and so less wave energy is delivered to the beach resulting in the removal of the beach step.
- (viii) The water level: Variations in tidal level play an important role in beach profile changes by causing fluctuations up and down the beach of features such as berms. Kemp (1963) stated that gravel beaches react far more rapidly to tidal level changes than sand beaches. Gravel beach morphologies show cycles in the across-shore spatial arrangement of their features that are linked to tidal cycles (e.g. Osborne, 2005; Austin and Masselink, 2006). These morphological cyclical changes are punctuated by events such as storms (e.g. Van de Meer, 1988; Carter and Orford, 1984, 1993). For example, berm height has been linked to the shoreline elevation and the crest height is associated to recent extreme water levels such as spring tide or storm surges (Takada and Sunamura, 1982; Austin and Masselink, 2006). Van der Meer (1988) looked at the tidal variation and the influence of storm surges on coarse clastic beaches under random waves. He observed that the beach profile reacts extremely quickly to the changing water level, but also that the shape of the beach profile is not as variable as on sandy beaches.
- (ix) The wave steepness: Steep waves erode beaches while low swell waves cause beach accretion (Pontee, 1995). The combined effect of wave steepness and beach slope (itself related to the beach material grain size) drives the type of wave breaking and hence, the type of wave breaking will

have an influence on the sediment transport and hence the beach profile changes (e.g. Kemp, 1963; Orford, 1977; Wright et al., 1979).

- (x) The initial beach profile: Van der Meer (1988), and then supported by Powell (1990), found that the major part of the beach profile change is unaffected by the choice of initial slope. However, they emphasised that the direction and amplitude of the transport and hence the mode of the profile formation varies with slope, supporting the earlier results from Van Hijum and Pilarczyk (1982). The effect of antecedent form on beach profile development depends on the mobility of the beach, and the position of the features (Pontee, 1995). Features in the swash region are most likely to be subjected to the most significant morphological changes on the beach profile as the swash has been identified as the dominant parameter driving the sediment transport on coarse grained beaches (Pedrozo-Acuña et al., 2006).
- (xi) The beach ground dynamics: The beach groundwater system is a highly dynamic, shallow, unconfined aquifer in which flows are driven through saturated and unsaturated sediments by tides, waves and swash or even evaporation/precipitation and exchanges with deeper aquifers (Horn, 2002). Nielsen et al. (2001) and Butt et al. (2001) investigated in detail how infiltration and exfiltration flows influence the sediment entrainment and transport on the beach face of sandy beaches. Water infiltration increases the near bed velocity and hence enhances sediment mobility (Conley and Inman, 1994). Conversely, infiltration also induces downward pressure gradients that impede sediment mobility during the run-up (Hughes et al., 1998; Nielsen, 1997). On the other hand, upward pressure gradients induced by exfiltration on the backwash are not sufficient to enhance fluidisation of the top sediment layer and therefore transport (Butt et al., 2001). Because of the material grain size distribution on gravel beaches, the potential of infiltration/exfiltration on the beach face is a lot greater than on sandy beaches. Because of that, an understanding of the interaction between surface and groundwater flows in the swash zone is necessary to understand

beach profile evolution (Horn, 2002). Lee et al. (2007b) modelled the interaction between the surface and groundwater flows into a gravel beach. Their model showed that vertical fluctuations of the groundwater levels were corresponding respectively to the vertical migrations of the berm on the beach face. They also showed that the wave run-up is reduced by the exfiltration flow from the groundwater. Despite these latest findings, the groundwater flows and their interactions on gravel beaches are still not well understood and even this is even more true on mixed beaches where the hydraulic conductivity is significantly different (e.g. Mason and Coates, 2001).

- (xii) The sediment supply: Long term beach profile changes depend upon the balance between the supply and loss of sediment (Kirk, 1969). Kirk (1969) found that eroding beaches generally present a flatter profile than accreting ones, due to an increase in beach width caused by the landward recession of the beach crest. On the contrary, Pontee (1995) observed on the UK beaches that eroding beaches are steeper than the non-eroding ones because of the landward recession of the low water mark relative to the high water mark. The differences of these two views may certainly be related to what individual researchers consider to be the limits of the beach profile. Orford (1986) pointed out that there is a difference between the beach width and the actual beach profile section that experiences elevation changes. In both cases, Kirk (1969) and Pontee (1995) agree on the fact that the beach profiles are different in beach erosion or accretion conditions, that is to say as a function of sediment supply.
- (xiii) The wind speed and direction: Wind transport is much more important on composite beaches than on pure gravel beaches. Because of an intertidal lower sandy platform, the wind speed and direction can be important for transport of sand particles at low tide. For example, Costa et al. (2008) have reported that where there are extensive sandy foreshores, the wind can transport sand overlays onto the gravelly upper beach. In the current study, direct observations in the field showed that the sand fraction of the mixed

sediment beach on the upper foreshore can dry quickly and be transported by strong winds. This transport cannot be neglected especially if the intertidal zone is as wide as at Cayeux-sur-Mer (800 m directly in front of Cayeux). It is important not to forget that aeolian transport from the sandy platform is at the origin of the dune system north of Cayeux (Chapter 2 Section 2.2).

As mentioned earlier in Chapter 3, measurements of the beach topography were conducted on every low tide of the short period surveys at both field study areas while regular monthly topography surveys between August 2004 and July 2006 were conducted at Birling Gap. The following section of this chapter presents the results collected during the various surveys for each site.

4.3 Morphological changes observed at Cayeux-sur-Mer and Birling Gap

Profile changes for the short period fieldworks were plotted to show accretion/erosion trends (Figures 4-11 to 4-27). The monthly morphological and beach volume changes are represented on Figures 4-28 to 4-34. Because of the number of surveys a day (two), it could be rather confusing if only a date code was used to refer to the profiles. To simplify the reading, an alphanumeric code has been used to represent the dates on each profile. During the survey period at Cayeux-sur-Mer in October/November 2005, each of the two profiles surveyed (Figure 4-9) presented in this section is respectively annotated with the letters “A” (profile in the recycled area) or “B” (profile in the unmanaged area) and the first survey on October 28th is numbered 1 and increases by one for each subsequent survey. Surveys in March 2006, May 2006 and December 2006 conducted along the profile west at Birling Gap (Figure 4-20) were respectively alpha coded, “C”, “D” and “E”.

4.3.1 Wave conditions at Cayeux-sur-Mer

The wave data recorded at Cayeux-sur-Mer during the survey period in October/November 2005 are displayed in Figure 4-4. During this field campaign, from October 28th 2005 to November 11th 2005, the data collected onshore in the intertidal zone show that the water level changed from neap to spring and back to neap tide. The water level reached up to 9.59 m above HD during the spring tide on November 4th 2005 whereas the water level reached up to 7.3 m above HD during the neap tide on November 10th 2005. The wave climate was representative of the year wave height climate (Sogreah, 1995a) with significant wave heights (H_s) ranging from 0.4 m to 2.7 m, punctuated by two storm events on November 1st and 4th 2005. The wave approach was from the West, with a mean angle to the coast of between 37.6 and 89.6° and an average of between 57 and 79°. Almost half (49.7%) of the H_s were less than 1 m, 96.4% less than 2 m, and only 3.6% exceeded 2 m. The majority of the waves at high tide were of the plunging type, breaking directly onto the mixed sediment beach. The wave period varied between 4 and 9 s and two distinct wave periods were clearly identified. Firstly, a group of waves that were the most representative with a period of between 4 and 6 s and secondly, a group with a period of between 6 and 9 s. During the storm events, the significant wave period was actually shortened to a smaller range from 4.7 to 6.6 s. During the tidal cycle, current velocities were the strongest at mid-tide and weakest at high tide. Current direction was mainly northward in accordance with the waves and the expected longshore drift direction. Based on observation, the mixed sediment beach is covered by water for approximately three hours and thirty two minutes during the flood and three hours and thirty six minutes during the ebb, giving a total water inundation duration of seven hours and eight minutes.

4.3.2 Wave conditions at Birling Gap

i. Yearly wave climate (Figure 4-5)

The wave climate observed during the two year survey period at Birling Gap was collected at the Rustington buoy (Chapter 3 Section 3.3). The majority of waves at Birling Gap are of the plunging type because of the steep slope sustained by the beach.

However, during the ebb tide and also when the wave height was low (generally <20 - 30 cm), surging waves were observed.

Because of the highly permeable short and steep beach profile, it is very rare to observe more than one or two wave breaking lines at Birling Gap. The breaking of waves on the beach is generally followed by a very short swash that is quickly dissipated through the permeable beach face. Depending on the water level, the wave breaking line is generally situated directly above or in the very close proximity of the beach step. From August 2004 to July 2006, the H_s reached up to 3.8 m and were distributed as follows: 75.3% were less than 1 m, 96.7% less than 2 m, and 3.3% exceeded 2 m. On an average year distribution, stormy weather occurred on average from September to March/April, and the strongest H_s generally close to December. The average yearly pattern shows that 55.7% of the waves are from the South-West sector and 17.4% are from the South-East. The yearly distribution of the wave peak period (T_p) is similar to the significant wave height yearly distribution pattern, that is to say that the largest periods are observed from September to March and mainly range from 1.7 to 20 s with some peaks at 25 s; whereas from April to August, the wave peak period mainly ranges between 1.7 and 10 s, sometimes peaking close to 15 s.

Based on observation, the gravel part of the beach is covered by water for approximately three hours during the flood and three hours and thirty minutes during the ebb, giving a total water inundation period of six hours and thirty minutes.

ii. Short fieldworks wave climates.

As mentioned in Chapter 3 Section 3.3, the wave climate was recorded onshore in the intertidal zone, directly onto the chalk platform in the close proximity of the beach.

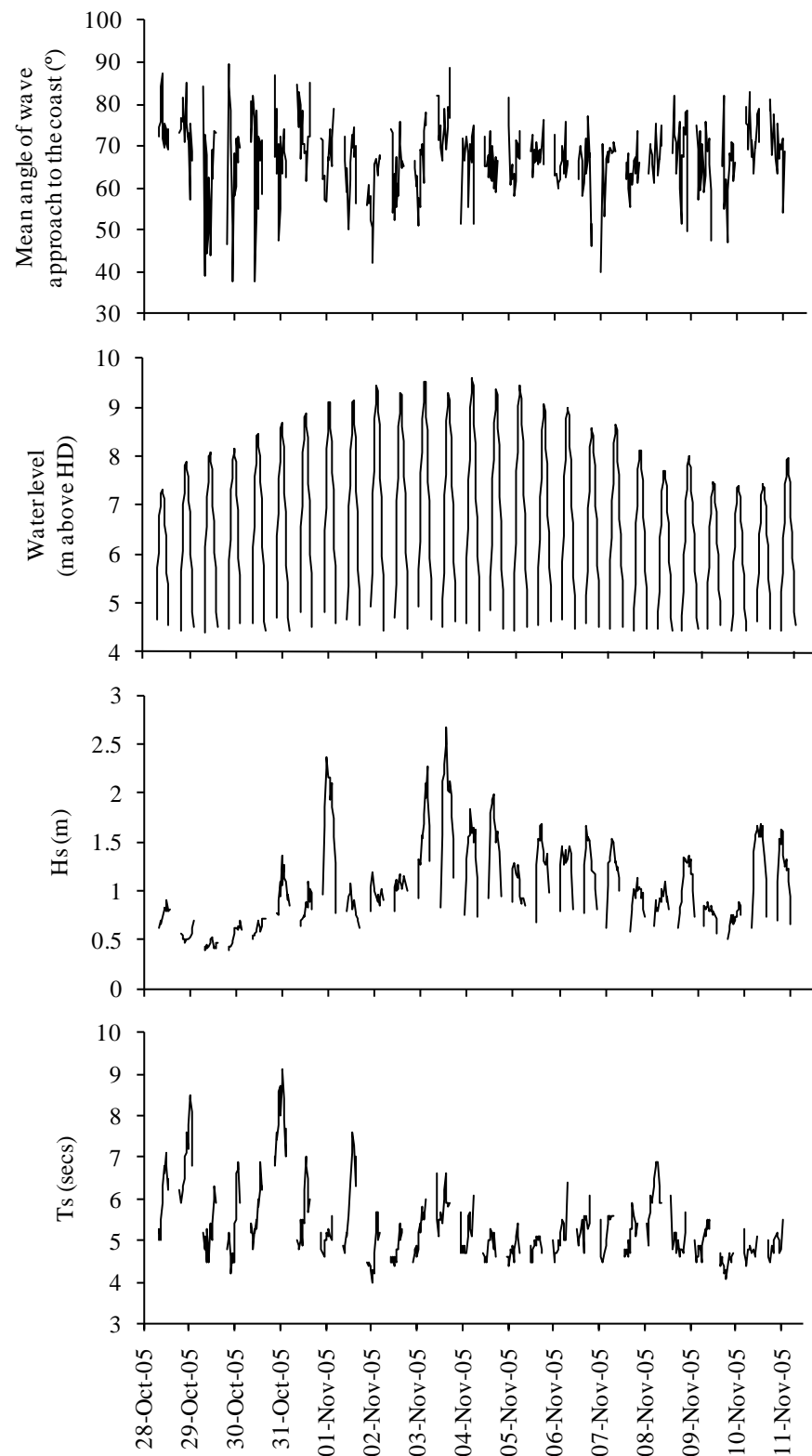


Figure 4-4 Inshore wave conditions at Cayeux-sur-Mer for the survey period, October 28th to November 11th, 2005. The mean wave angle is referred to the coast orientation (N205°).

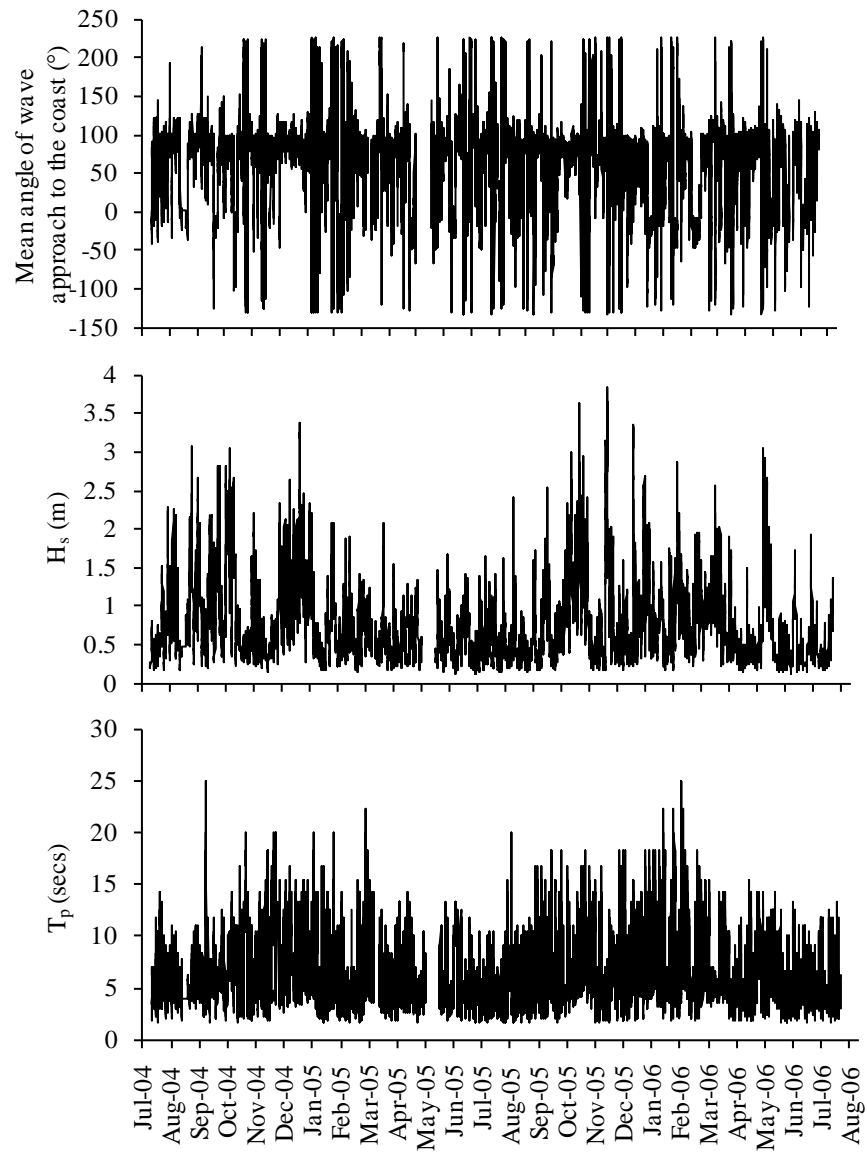


Figure 4-5 Offshore wave conditions collected at Rustington for the survey period between August 2004 to July 2006. The mean wave angle is referred to the coast orientation (N132°).

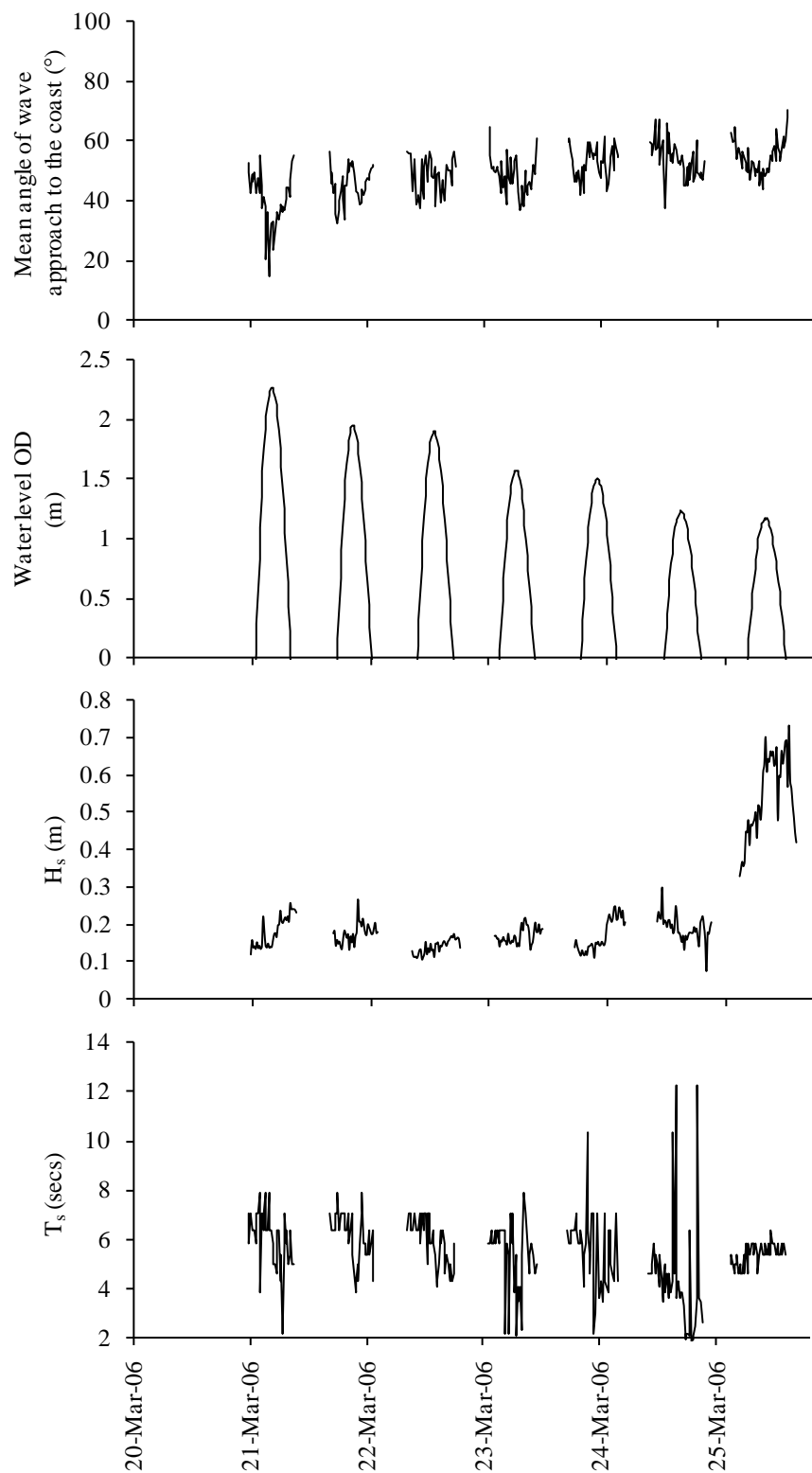


Figure 4-6 Inshore wave conditions collected at Birling Gap for the survey period between March 20th and March 24th, 2006. The mean wave angle is referred to the coast orientation (N132°).

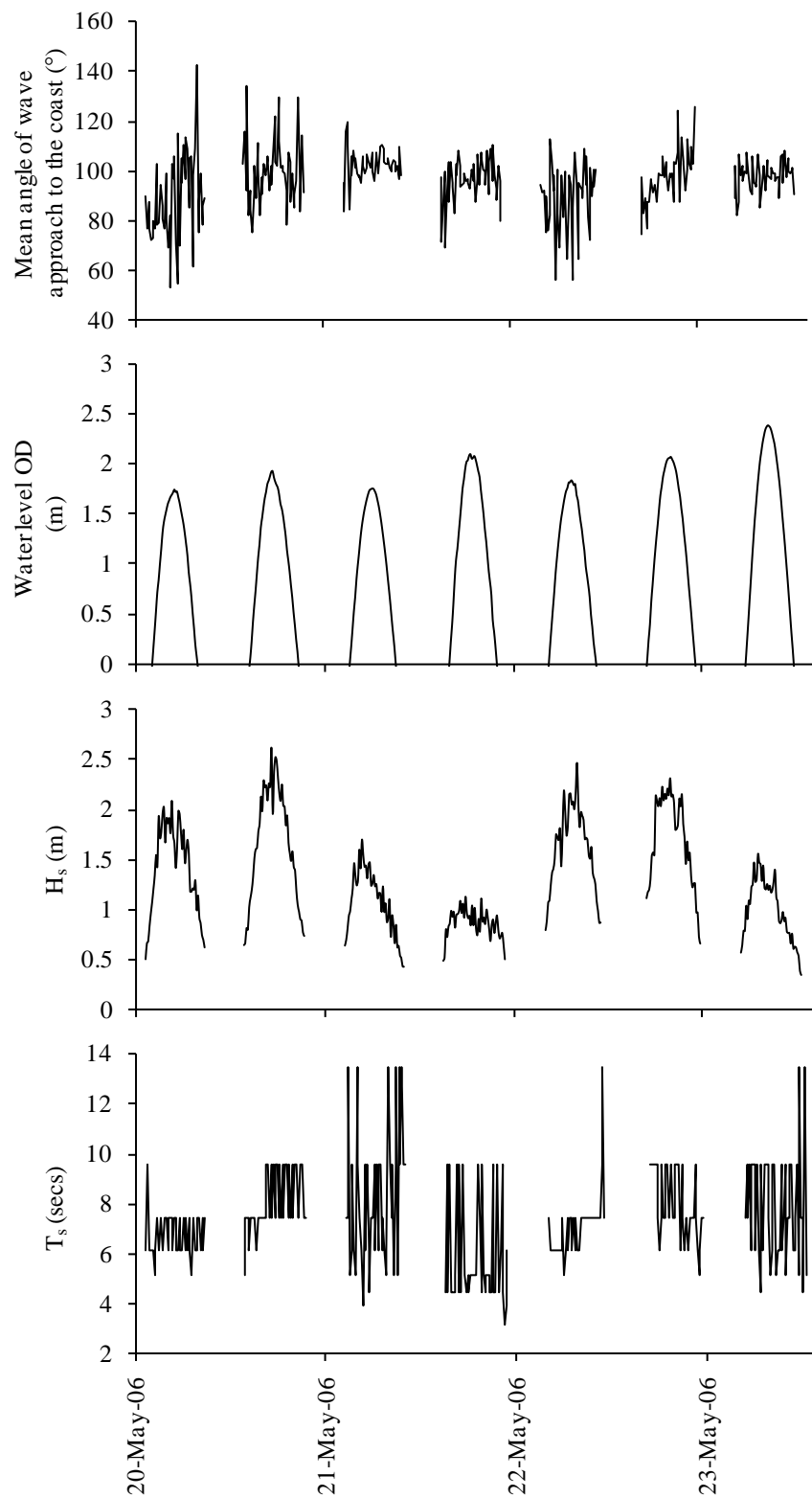


Figure 4-7 Inshore wave conditions collected at Birling Gap for the survey period between May 19th and May 24th, 2006. The mean wave angle is referred to the coast orientation (N132°).

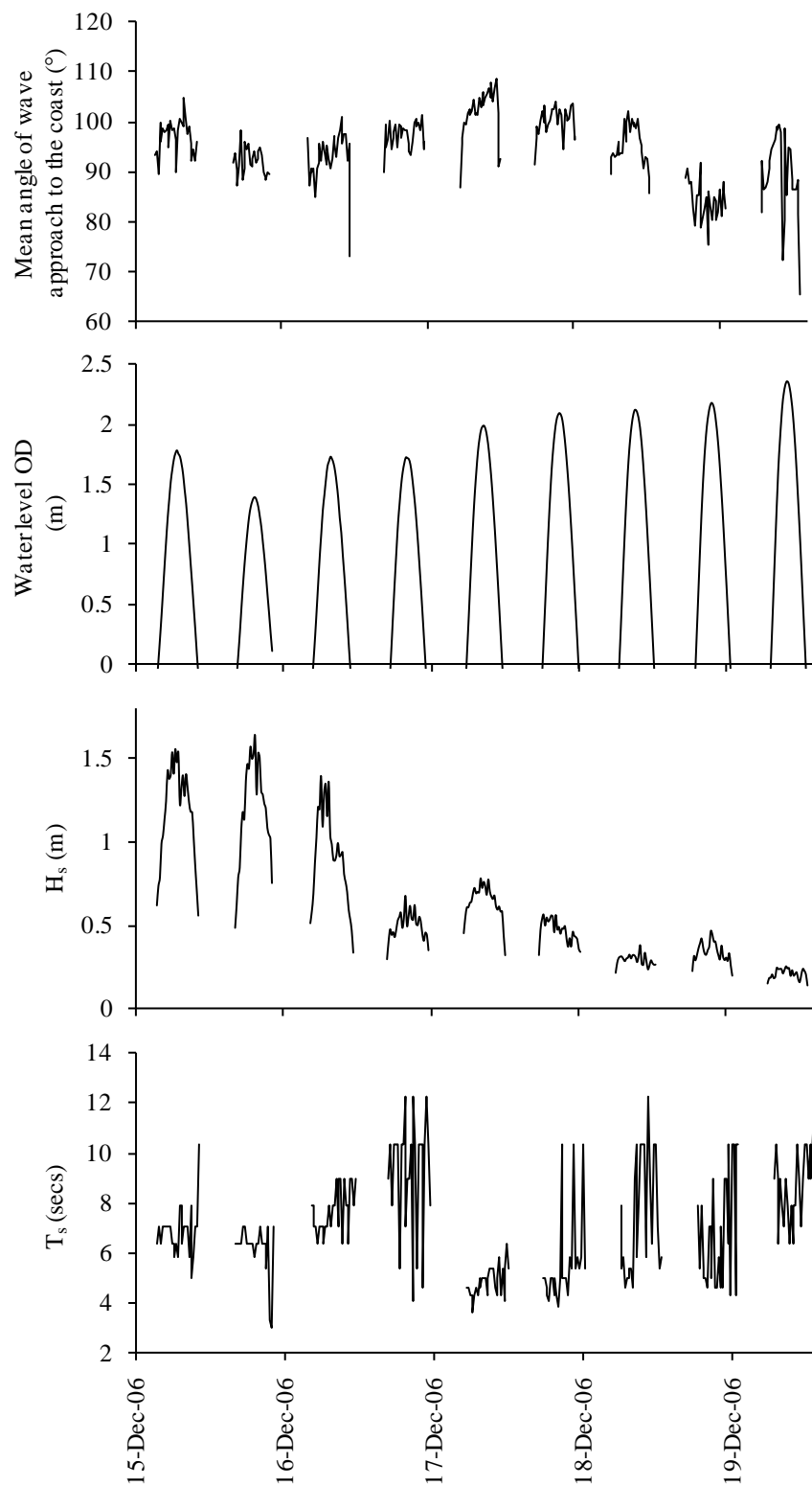


Figure 4-8 Inshore wave conditions collected at Birling Gap for the survey period between December 14th and December 19th, 2006. The mean wave angle is referred to the coast orientation (N132°).

March 2006 (Figure 4-6)

From March 20th to March 25th 2006, the tidal cycle was going from a spring tide toward a neap tide. The high tide water level on the spring tide reached 2.26 m OD while the lowest high tide was 1.04 m OD. During these few days, the wave direction was exclusively from the South, South East (averaging around N180°) i.e. more specifically with mean approach angles to the coast ranging from 14° to 68° (note that these angles are referred to the orientation of the coast orientation, here N132°). The wave conditions were very calm for nearly the entire survey period with significant wave heights of between 0.1 and 0.3 m until March 24th when on the last tide they reached 0.79 m. The significant wave period (T_s) ranged between 2 and 12.2 s.

May 2006 (Figure 4-7)

From May 19th to May 24th 2006, the tidal range was close to a neap tide (neap tide occurred on May 21th 2006). During this period, the high water elevation ranged from 1.64 m to 2.46 m OD. The wave direction was very consistent during the entire survey, being from South-West (N229°) all the time, i.e. an average wave approach nearly perpendicular to the coast. The survey period was marked by very strong South-Westerly winds and a very stormy weather. The significant wave heights observed during this period are the strongest observed during the short survey periods, being generally above 1 m with peaks largely above 2 m (2.6m on the 20th for example). The significant wave period ranged from 3.2 to 13.4 s.

December 2006 (Figure 4-8)

From December 14th to December 19th 2006, the tidal ranged was from a neap tide on December 14th 2006 toward a spring tide. During the survey period, the HWL mark ranged from 1.4 to 2.36 m OD. The wave direction was from West (N283° on average), with an approach mean angle to the coast varying from 72.3 to 106°. On a general note, the wave height decreases with time. The surveyed period can be divided in two when looking at the ranges of significant wave heights collected during this fieldwork. From December 14th to December 16th, the wave conditions were moderate with significant wave heights ranging from 0.9 to 1.6 m at high tide. From December 16th to December 19th, the wave conditions were very calm with significant wave

heights of between 0.6 and 0.8 m at high tide. Significant wave periods varied between 3.3 and 12.2 s during this field experiment.

4.3.3 Tidal to semi-lunar cycle profile changes at Cayeux-sur-Mer.

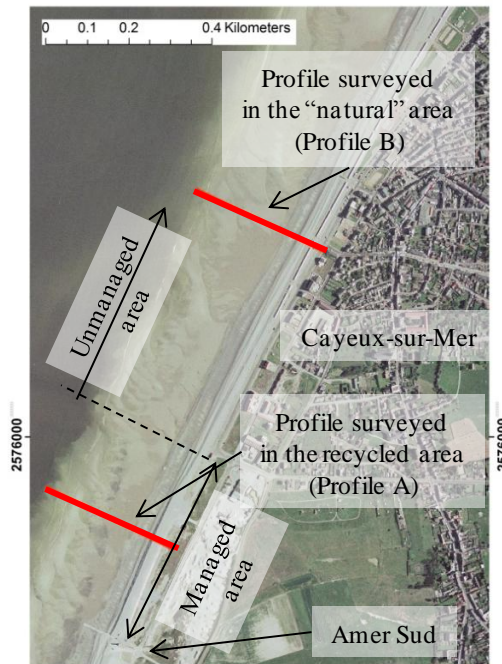


Figure 4-9 Location of the two profiles surveyed at Cayeux-sur-Mer from the 28th of October to the 11th of November 2005.

When looking at the beach profile characteristics at Cayeux-sur-Mer, it is important to make a clear difference between the area which is bordered by recycled material and the area which is not (Figure 4-9). The presence of recycled material acting as an artificial crest against flooding and occasional supply of beach recharge material along the first 400 m of the surveyed beach (Figure 4-10; Chapter 2 Section 2.2) should logically influence the beach profile response to the forcing hydrodynamics in comparison to the downdrift areas that do not benefit from such management. For this reason,

the beach profile evolution has been studied at two locations: one located in front of the recycled area (Profile A) and corresponding to where the tracer pebbles were deployed (Chapter 3 and Figure 4-9); and, another located in front of Cayeux (Profile B), which is not directly managed, approximately 1 km downdrift of the Amer Sud.

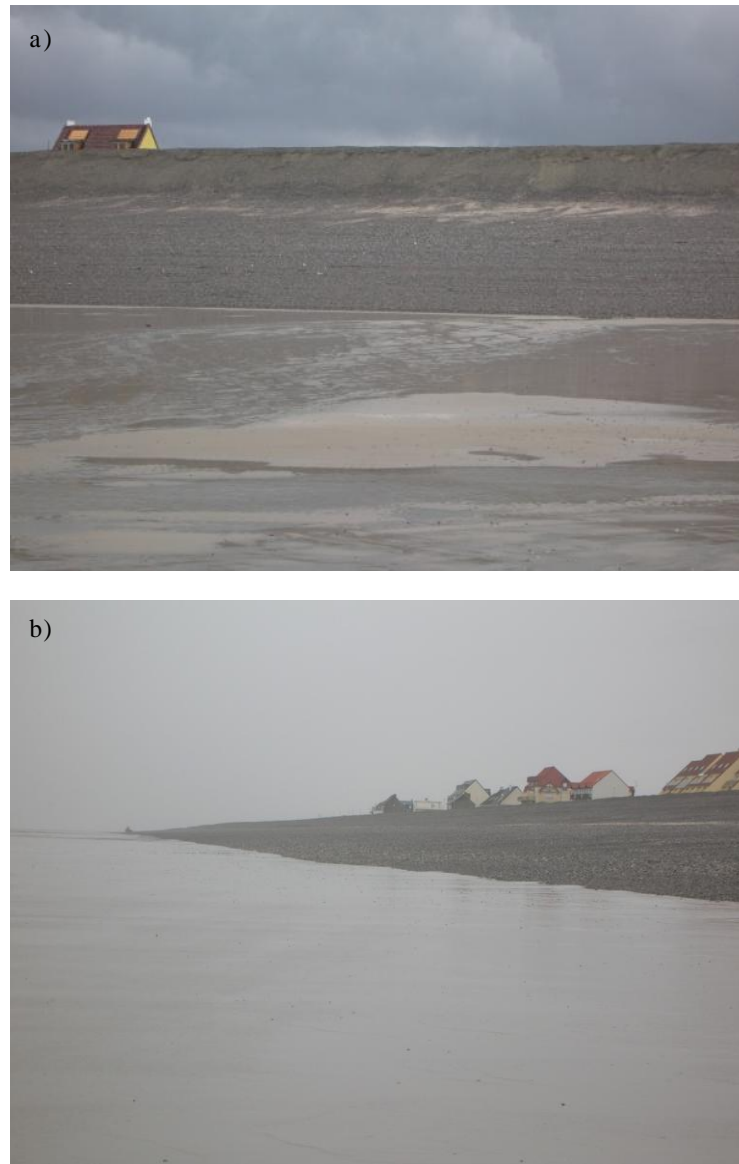


Figure 4-10 The beach at Cayeux-sur-Mer. a) In front of the recycled area (View from the sandy platform). b) Towards the non directly managed (“natural”) area (View from the sandy platform).

i. Short-term evolution of the beach profile in the recycled area (Profile A)

The beach slope at this particular location varied from 7.5° to 9.1° . Figure 4-11 illustrates the topographical changes observed during the survey period. The top of the profile starts approximately 10 m landward of the beach crest, i.e. the top of the seaward face of the recycled sediment wall, and finishes approximately 20 to 25 m seaward of the beach step on the sandy lower foreshore (please note that the surveys extended further across-shore but were cut here to keep a good resolution). The total length of the active profile on the mixed sediment beach in this area was approximately 70 m. The initial profile morphology (profile A1) was characterised by a steep slope (9.1°), a crest, multiple berms and a very pronounced beach step. The most seaward berm observed on the profile corresponds to the most recent high tide level. A second berm in a more landward position corresponds to earlier high tide water levels. Finally, on the most landward part of the beach profile, the recycled wall acts as the beach crest, the position of which corresponds to the maximum shoreline elevation attained either by a storm or the highest spring tides. Over time, these features moved, disappeared or reappeared. This profile evolution can be divided in three different phases relating to berm accretion, retreat, disappearance and re-accretion, or stability.

Phase 1, October 28th to 31st (profile A1 to profile A6): berm retreat (Figures 4-11 & 4-12).

During this period, the beach slope lowered from 9° to 8.8° . The tidal level moved from a neap tide toward a spring tide. The HWL ranged from 2.82 m (referred with the Lambert conic coordinate system, L1) to 3.56 m (L1). The wave conditions were calm, $H_s < 1\text{m}$, and T_s varied between 5 and 9 s. After the neap tide of October 27th, from profile A1 to profile A6, the active berm progressively retreated landward, reaching first the second berm up the beach and finally reaching the toe of the recycled sediment wall by profile A7. From profile A1 to profile A6 the berm had moved 14.4 m backward. This rearward movement up the beach was accompanied by an increase in elevation of the berm measured at 1.68 m. In fact from one tide to another, the backward migration of the berm can be represented by an erosion of the seaward face of the berm and an accretion of a part of this material on its landward side. This characteristic is even more apparent when looking at the transition between the profiles A4, A5, A6.

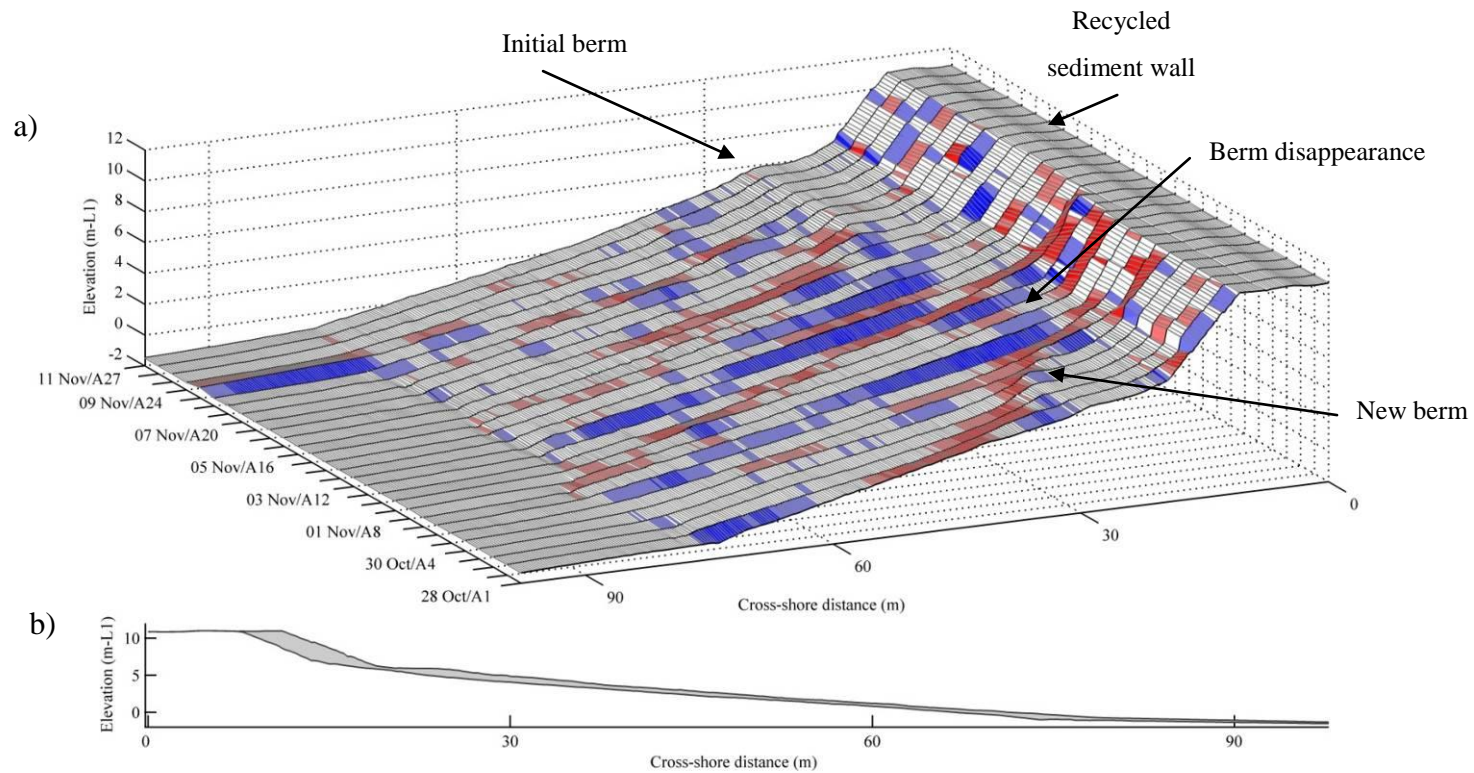


Figure 4-11 Surface plot showing the temporal variation from one tide to the following in beach face morphology in the recycled area along profile A based on low tide surveys at Cayeux-sur-Mer between October 28th and November 11th, 2005. a) The light and dark blue represent respectively accretion of 10 to 20 cm and more than 20 cm. The red colour characterises erosion in the same colour coding. b) Maximum and minimum beach profiles with the sweep zone indicated by the shading.

Between profiles A4 and A5, the only significant part of the beach profile that changes is the berm and it is marked by a retreat of 1.5 m whereas the back of the berm increased in elevation by 20 cm. A similar trend can be observed between profile A5 and profile A6, the berm retreated of 2.9 m but the landward side of the berm increased in elevation by 7 cm.

During this period, the beach toe migrated seaward quite considerably. It migrated rapidly seaward between profiles A1 and A2 by 2.4 m and the break of slope between the mixed sediment beach and the sandy platform became less marked. It migrated quickly seaward again between profiles A3 and A4 by 2.4 m. By the end of this period the beach step had migrated seaward by 4.4 m and accretion directly above the initial location of the beach was measured at 44 cm. On the other hand, the middle of the beach experienced a maximum vertical erosion of 42 cm. It is likely that a part of the material eroded from the middle part of the beach moved onto the beach step, contributing to its smoother profile. The sandy lower foreshore in the first 20 to 25 m from the toe of the beach did not show any noticeable changes in elevation. All these changes made the whole profile less steep and so less reflective.

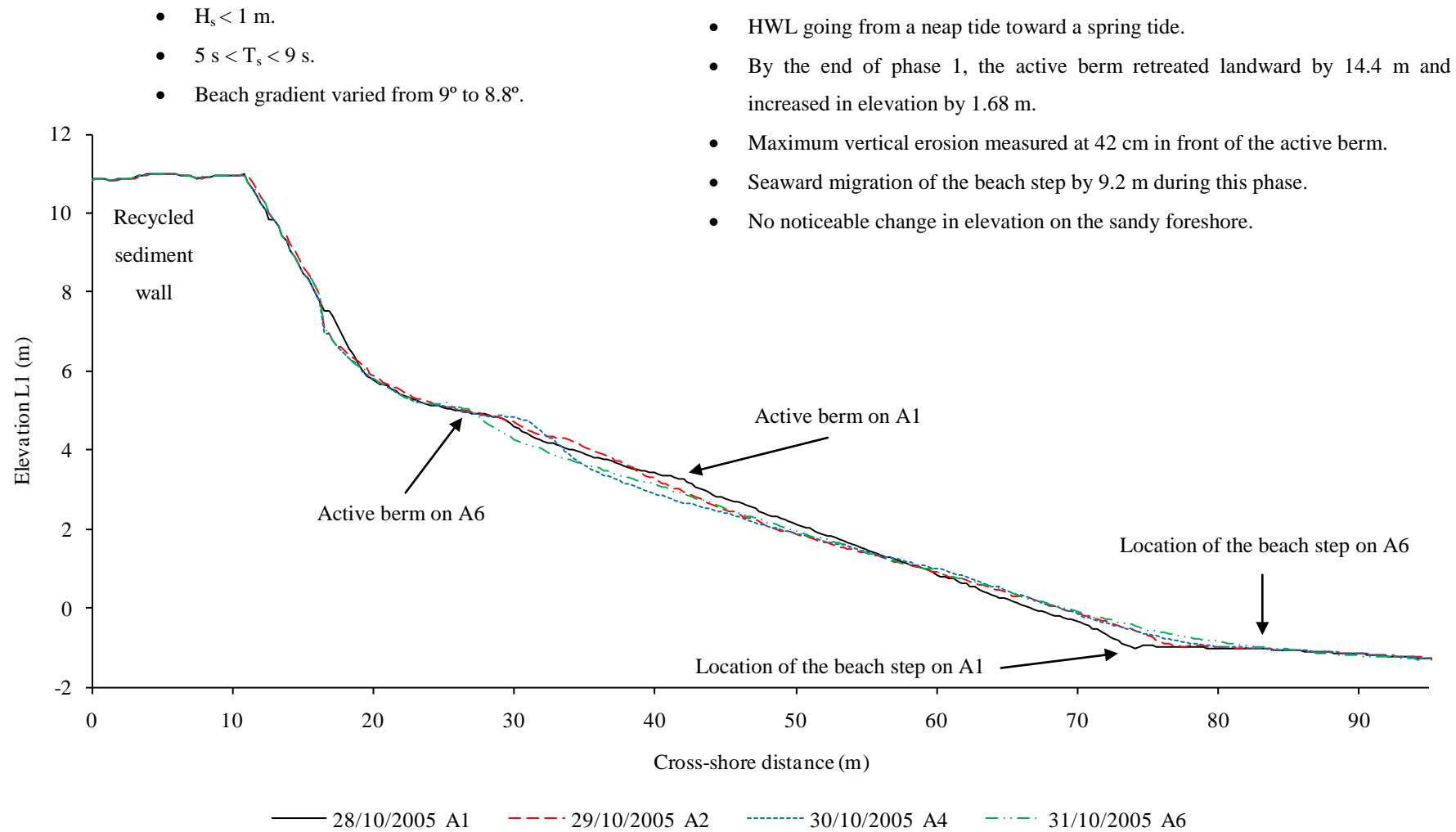


Figure 4-12 Beach profile evolution in the recycled sediment area during phase 1 of the survey period, October 28th to October 31st, 2005.

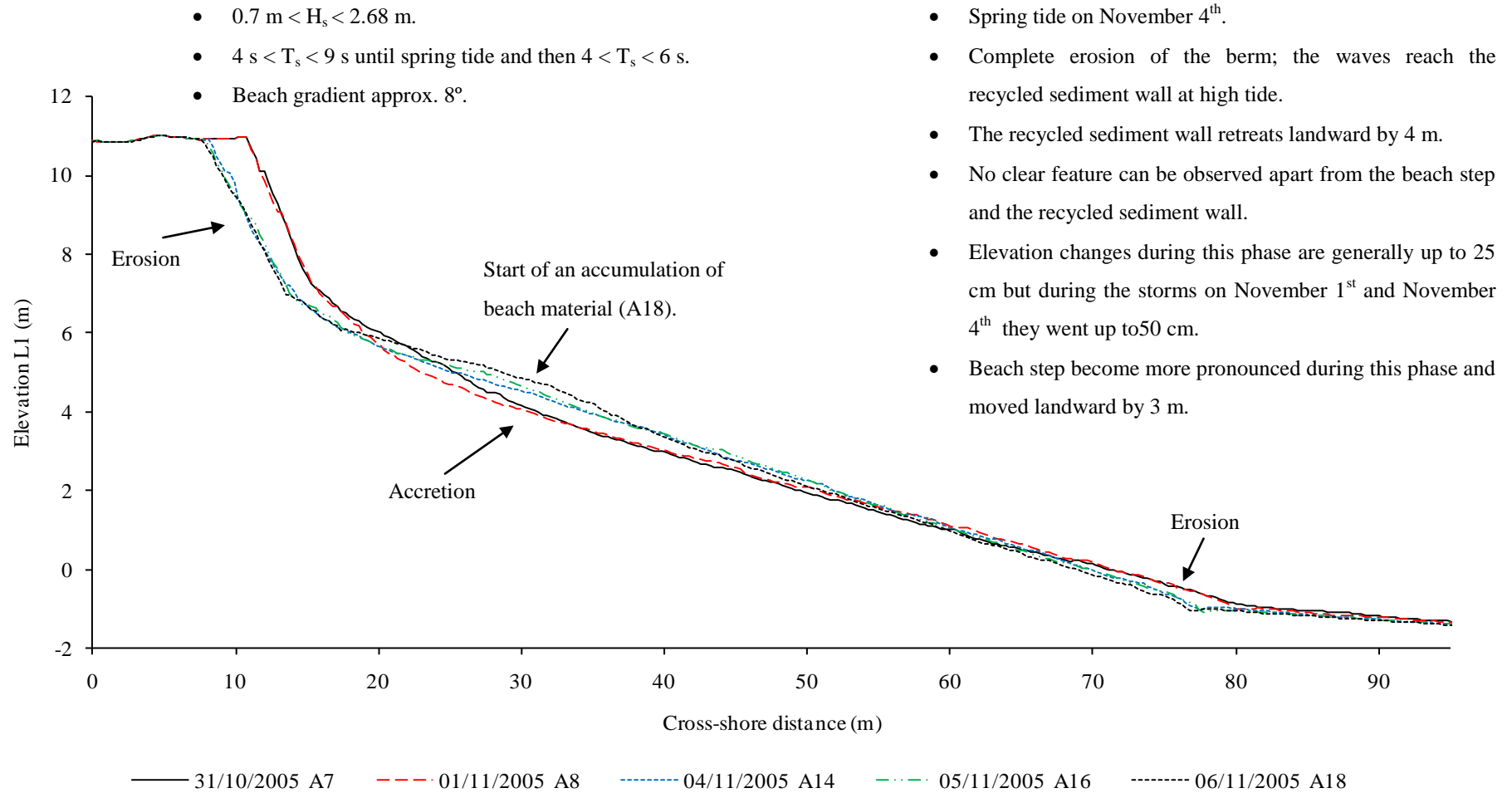


Figure 4-13 Beach profile evolution in the recycled sediment area during phase 2 of the survey period, October 31st to November 06th, 2005.

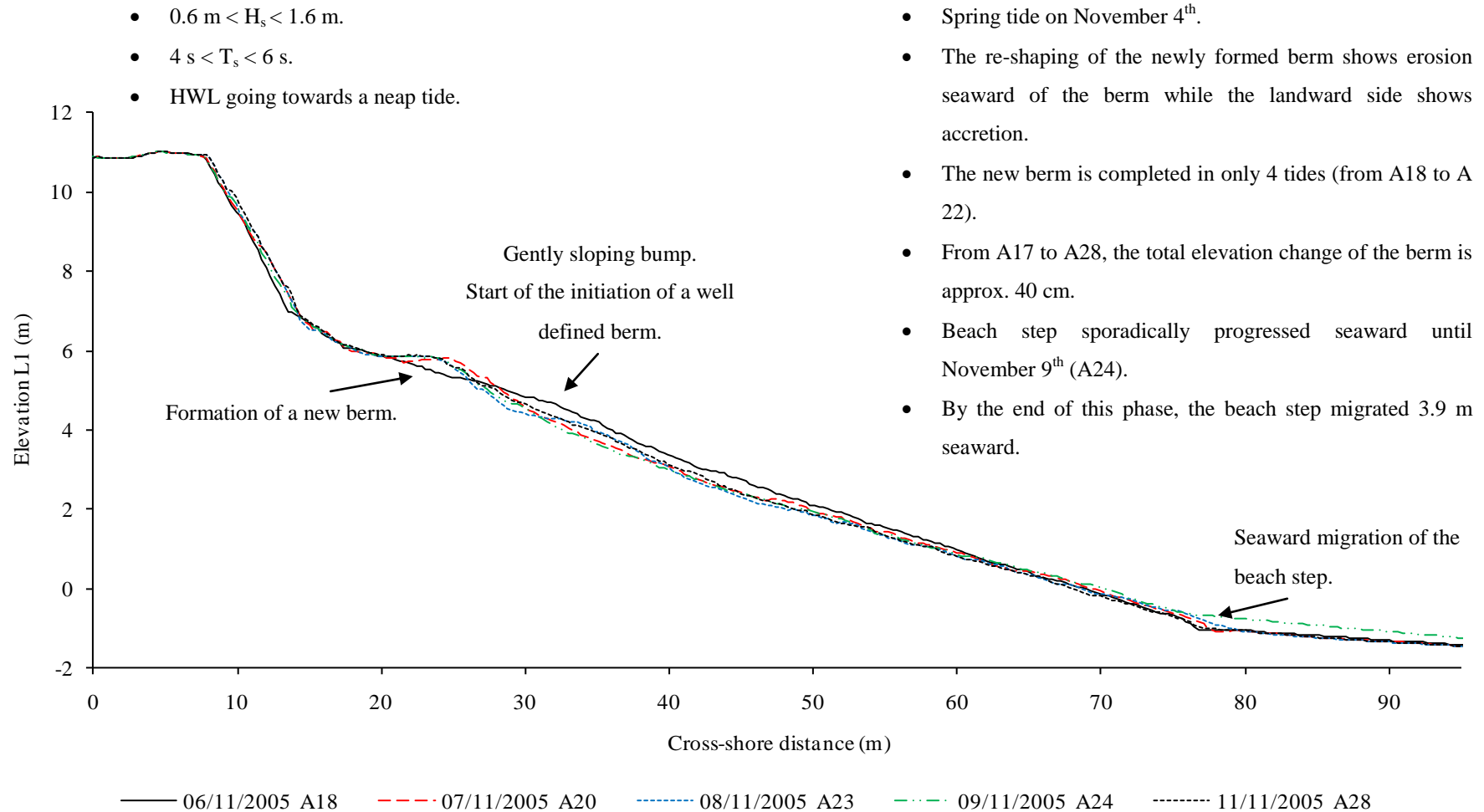


Figure 4-14 Beach profile evolution in the recycled sediment area during phase 3 of the survey period, November 06th to November 11th, 2005.

Phase 2, October 31th – November 5th, profile A7 to profile A16: berm disappearance (Figures 4-11 & 4-13)

The berm was completely eroded, the HWL was high enough to allow the wave to reach the recycled sediment wall and the beach profile became less reflective (8°). The beach profile during that period was completely smoothed with no evident features and its general shape was concave. The elevation changes following each single tide were relatively small except around the time of the two storms of November 1st (profiles A8-A9) and 4th (profiles A14-A15). Elevation changes during this period are within a 50 cm thick layer, they were usually up to 25 cm whereas during the storms they went up to 50 cm. There was some accretion on the beach during this phase but it was due to drawdown of material from the wall of recycled material at the back of the beach, which retreated by 4 m over this period.

The beach step was subject to significant spatial and elevation changes. Before October 31st (profile A7), the step at the limit between the mixed sediment beach and the sandy platform was not very pronounced; however by November 1st (profile A8) it had become much more pronounced and by November 5th (profile A16) had moved landward by 3 m and 30 cm accretion was measured right above the beach step's original location at the start of this phase (profile A7).

Again, the sandy lower foreshore was relatively unaffected by elevation changes. This entire phase spanned several tides before and after the spring tide of November 4th (profile A14). The fact that the storms occurred during the spring tide or close to contributed for a great part to the considerable erosion of the sea wall made of recycled sediment. Wave conditions during this phase varied over a large range of H_s from 0.7 m to 2.68 m. T_s varied between 4 and 9 s until the spring tide and then it slowed to between 4 and 6 s.

Phase 3, November 5th-11th, profile A17 to profile A28: berm accretion and stability (Figures 4-11 & 4-14)

During this phase, a new berm formed and the beach step migrated seaward. As neap tide was approaching, H_s ranged from 0.6 m to 1.6 m, and T_s largely varied between 4 and 7 s. On profile A16 (previous phase), the beach profile presented a 32 cm

accumulation shaped as a gently sloping bump in the upper/middle part of the mixed sediment beach whereas the lower part was characterized by a slight erosion measured at 12 cm maximum. The material constituting this accumulation was in fact the beginnings of a forming berm that started to show up on profile A18 (Figure 4-13). During the following tides, this amount of beach sediment was reshaped to form a new berm located at the HWL. This re-shaping is accompanied by a characteristic erosion seaward of the berm while the landward side of the newly formed berm shows accretion. For example, between profiles A18 and A19, the middle beach is marked by a maximum erosion of up to 30 cm while the landward side of the berm is marked by an accretion of approximately 20 cm. Here, the lower part of the mixed sediment beach was less strongly affected. From November 6th (profile A18), the berm grew rapidly and was completed after only four tides, on November 8th (profile A22). When comparing the elevation of the beach profile between the profiles A17 and A28 where the berm formed, it can be seen that the elevation linked to the berm formation is approximately of 40 cm at its maximum.

The beach step was clearly demarcated on the beach face and sporadically progressed seaward until November 9th (profile A24) when the beach profile experienced significant changes in the lower part of the mixed sediment beach and the sandy platform. Directly above the beach step location on profile A23, the elevation of the sandy foreshore suddenly increased by 30 cm. As a consequence, the break of slope at the beach step migrated 3.9 m landward and was almost 50 cm higher than in its previous location. The profile reverted to its previous form on the following tide. On profile A23, the beach step started to show a smoother face than the rest of the previous profiles. After this the entire beach face showed no further significant topographic changes up to the end of the study period on November 11th.

Comparing the first profile surveyed on October 28th (profile A1) and the last one obtained on November 11th (profile A28), a number of changes can be noted in elevation and in the location of features. First, the sandy lower foreshore elevation increased by 16 cm just in the first 15 m to 20 m in front of the beach step. Second, the beach step remained at the same elevation, although it moved 3.3 m seaward of its initial position. Third, the lower part of the mixed sediment beach experienced a

maximum accretion of 40 cm because of the beach step's seaward migration, whilst the middle part was eroded to a maximum of 44 cm. Fourth, the berm increased in elevation by 1 m and moved inland by 5.4 m. The hydrodynamic conditions during this period caused the beach profile to become more dissipative of wave energy than it was initially, the beach slope going from 9.1° to 8.1° . During the survey period, beach cusps were observed only twice, in the lower-middle part of the beach, on the mornings of November 2nd and November 8th (profile A10 and profiles A22-A23).

The sandy platform in front of the recycled area did not display very clear features such as bars, apart from at the outer edge where a step is uncovered during the very low tide. Figure 4-15 clearly displays that over the entire survey period, the upper sandy platform (from the distance mark 75 to 110 m) experiences a significant and progressive erosion reaching up to approximately 20 cm between October 28th and November 11th. On the other hand, the middle part of the sandy platform (from the distance mark 110 to 130 - 140 m) is very stable, with minimum elevation changes over time. And finally, the lower foreshore is characterised by greater elevation changes of up to 45 - 50 cm which are related to the progressive landward migration of the step. It is important to highlight that this area of the beach was only accessible when the tide was in its lower stages, and that it was not surveyed all the time.

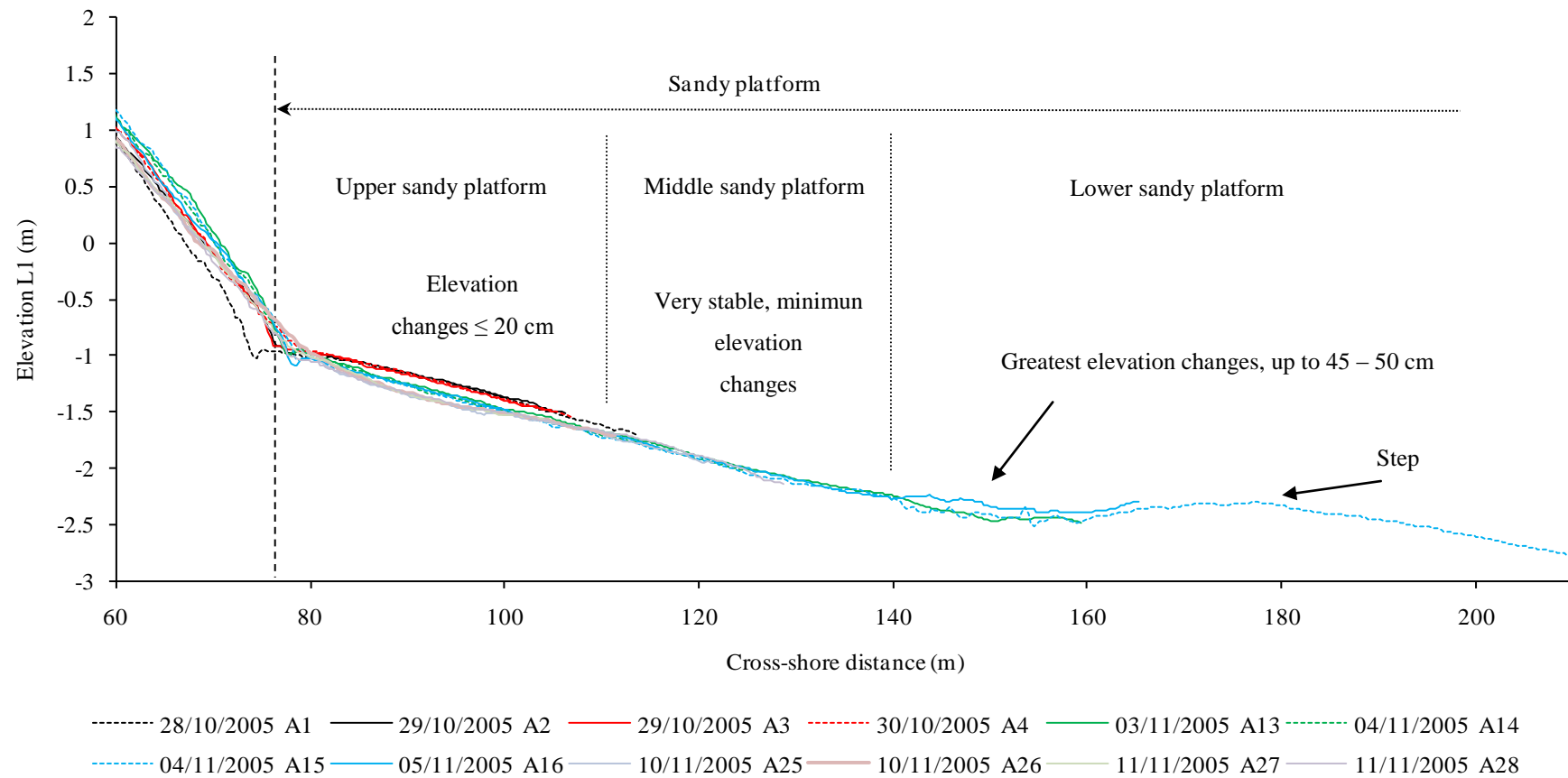


Figure 4-15 Beach profile evolution from the lower part of the mixed sediment beach onto the sandy platform in the recycled area during the survey period, October 28th to November 11th, 2005.

ii. Evolution of the beach profile in the unmanaged (“natural”) area (Profile B; Figures 4-16 to 4-19).

The beach slope at this particular location was very consistent during the survey period, varying around 7.2° by $\pm 0.3^\circ$. Figure 4-16 illustrates the topographical changes observed in the “natural” area during the survey period. The profile length of the mixed sediment beach in this area, i.e. not including the sandy platform, is approximately 90 m long. The starting beach profile (B1) was characterised by a steep reflective slope (7.2°), a large wide crest >10 m, multiple berms (four in total) and a very steep and pronounced beach step. Simple visual observations indicated that the surface sediment distribution in this area was more skewed towards the coarsest sediment particles (gravels and pebbles) in comparison to the recycled area. On this profile, the most recent, and also active berm, is located the most seaward and for the same reasons as on the previous profile (i.e. the HWL fluctuations) corresponds to the most recent high tide level. The most inland berm (or crest) corresponds to the maximum shoreline elevation attained either by a storm or the highest spring tides. The berms between these two extremities are either the result of small storms, or spring tides, or even high tides that occurred after the event that shaped the crest and before the most recent high tide.

Here again, with time, the combined effect of the water level fluctuations and wave conditions, the beach features moved, disappeared or reappeared. The changes in elevation on this profile between profiles B1 and B28 are all within a metre range. The beach step showed great variations in both location and elevation in comparison to the beach step in front of the recycled sediment area. Its location varied over a 10 m wide length of the beach profile while its elevation varied up to 52 cm. During the overall period, the beach profile evolution can be divided in two different phases according to the same characteristics used before; berm accretion, retreat, disappearance and re-accretion, or stability.

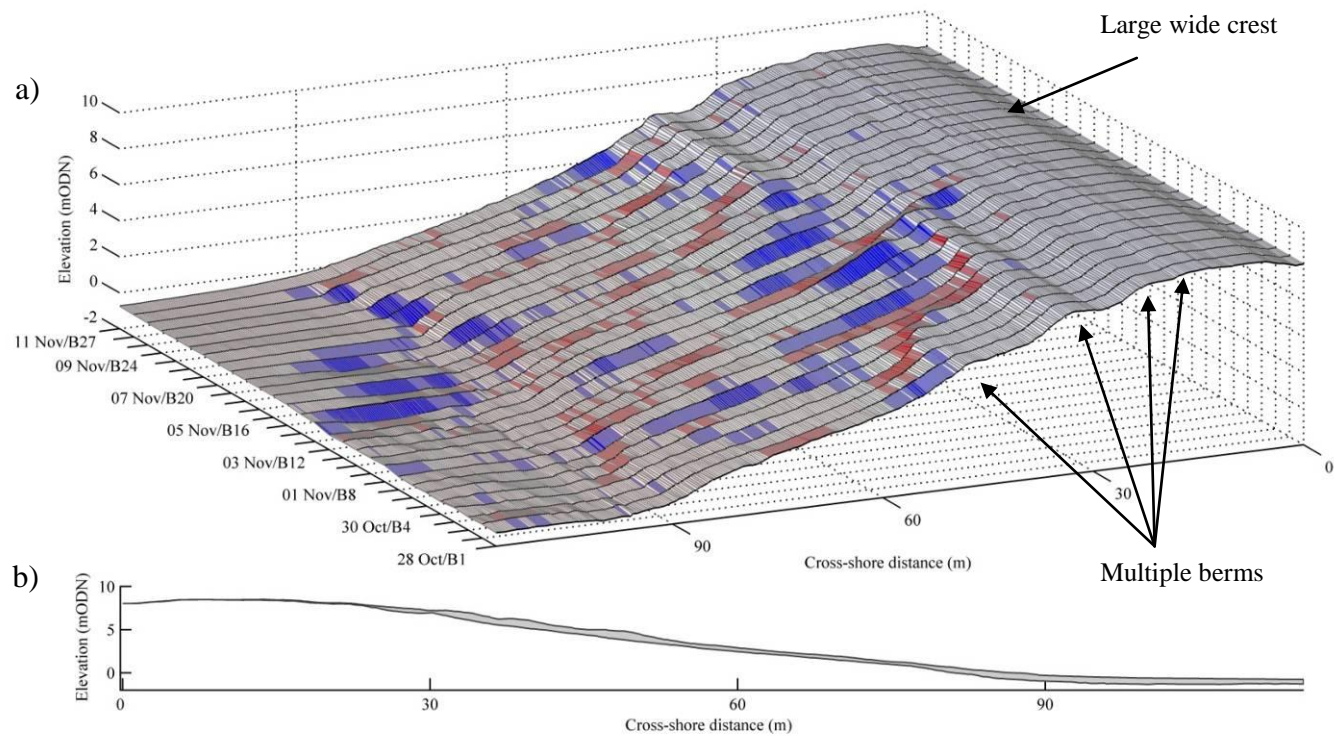


Figure 4-16 Surface plot showing the temporal variation from one tide to the following in beach face morphology in the “natural” area along profile B based on low tide surveys at Cayeux-sur-Mer between October 28th and November 11th, 2005. a) The light and dark blue represent respectively accretion of 10 to 20 cm and more than 20 cm. The red colour characterises erosion in the same colour coding. b) Maximum and minimum beach profiles with the sweep zone indicated by the shading.

Phase 1, October 28th-November 4th, profile B1 to B15: berm retreat (Figures 4-16 & 4-17)

This phase corresponds to the transition from a neap tide (October 28th, profile B1) to a spring tide on November 4th (profile B15). During this phase, the HWL rose from 7.3 m to 9.6 m (L1). The significant wave height ranged from 0.52 to 2.68 m and T_s ranged from 4 to 9.1 s. As mentioned previously, periods of particular wave conditions can be individualized. From November 28th to November 30th (profile B1 to profile B6), H_s was <1 m and T_s ranged from 5.5 to 7.6 s. From November 31st to November 4th (profile B7 to profile B15), H_s was between 1 and 1.24 m but was punctuated by two stormy events, on November 1st and November 4th, (respectively associated to the transition between profiles B8 & B9 and profiles B12-B13-B14-B15). T_s ranged approximately in the same kind of values as previously, from 4 to 9.1 s. However, as mentioned earlier, during the storm events, it can be seen that the significant wave period shortened to a smaller range from 4.7 to 6.6 s.

On November 28th, profile B1 presented a large crest, four clear berms (Figure 4-17) and a very steep beach step that was bordered by a little alongshore runnel at the back of a bar on the sandy platform. During the experiment this runnel had the function of canalizing the excursing water towards the sea at low tide. During the rising tide, this channel was also filled by water before the tide actually covered the sandy bar in front of the mixed sediment beach. While the water level increased from the neap tide toward the spring tide, the most recent berm moved landward. The active berm on profile B1 was completely removed and the 3rd berm and later on the 2nd berm on profile B1 were reactivated.

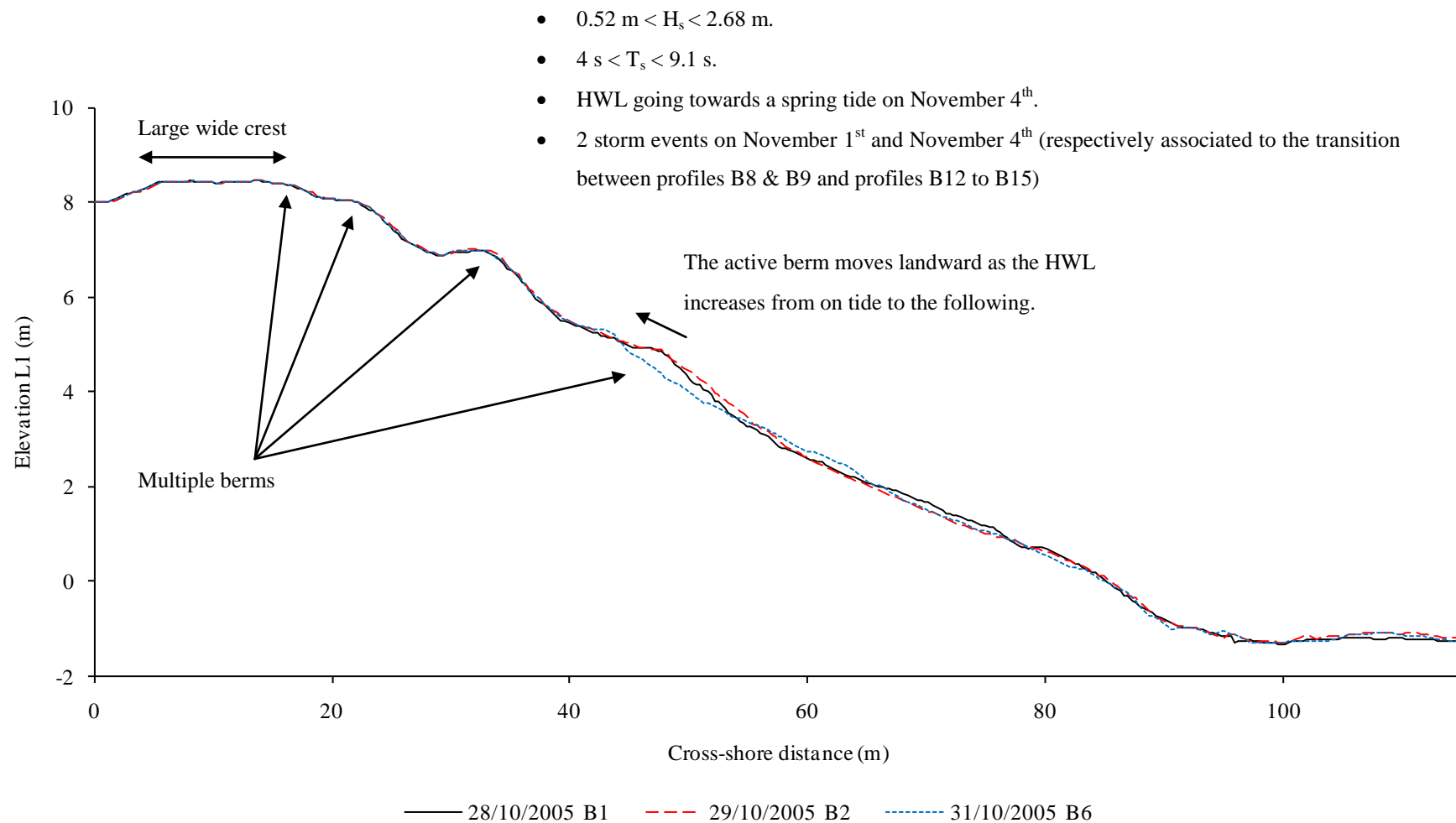


Figure 4-17 Beach profile evolution in the “natural” area during phase 1 of the survey period, October 28th to November 4th 2005. Part 1.

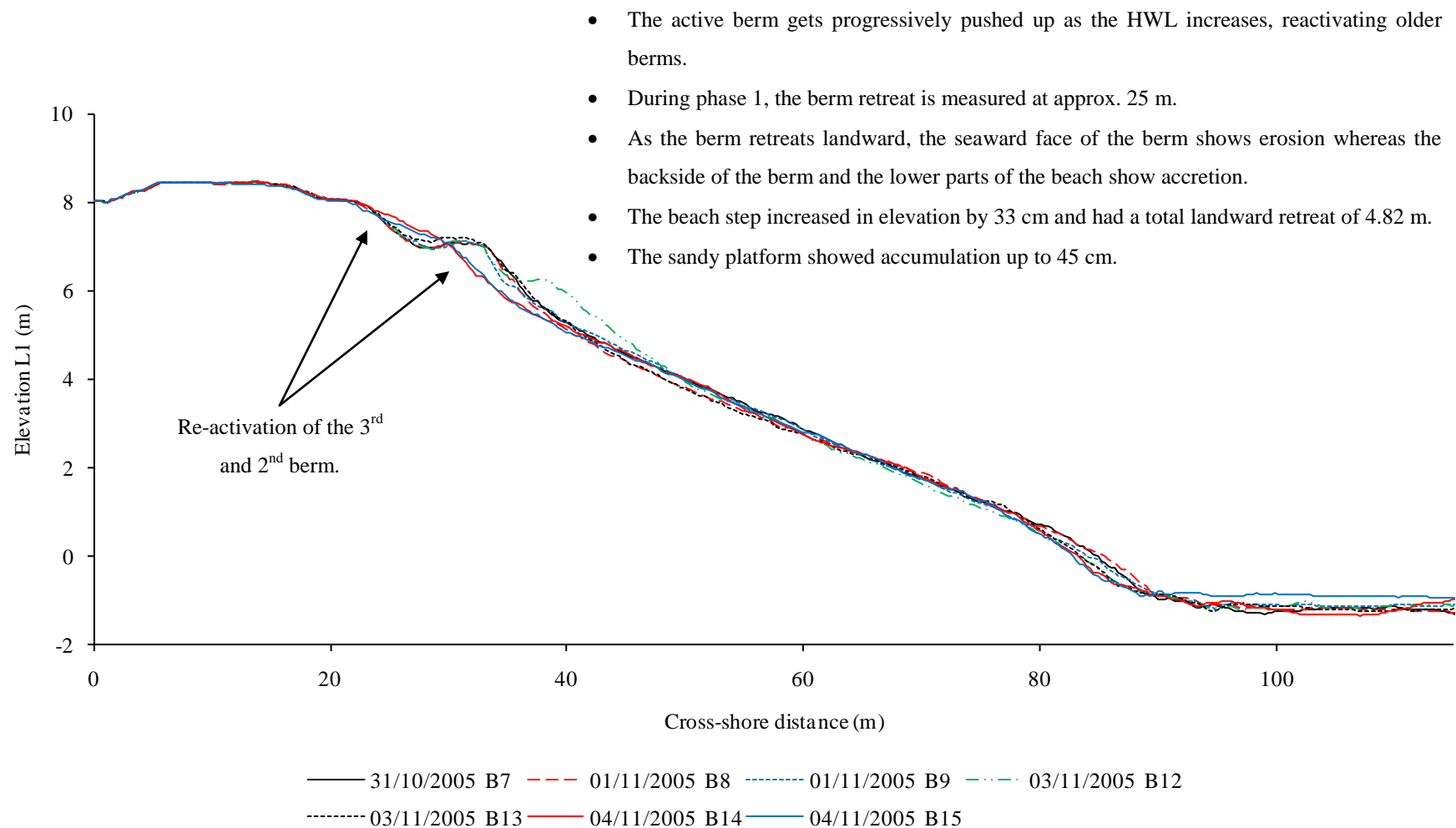


Figure 4-17 Beach profile evolution in the “natural” area during phase 1 of the survey period, October 28th to November 4th, 2005. Part 2.

It is important to highlight that the reactivation of the 2nd berm is only minimal as the 3rd berm did not completely disappear even during the spring tide between profiles B14 and B15. During the overall phase, as the HWL was rising from tide to tide, the active berm retreated approximately by 25 m landward in total while its elevation increased by 3.1 m. This retreat was accompanied by accretion and erosion of the mixed sediment beach face, respectively measured up to 30 cm and 78 cm. Similar to what was observed on the previous profiles, when the berm was retreating in the landward direction, erosion was observed on the seaward face of the berm and accretion was observed at both the backside of the berm (berm rollover) and the lower parts on the beach profile. For example, between profiles B13 and B14, the seaward side of the berm was eroded by up to 0.78 m in some areas whereas the elevation on the landward side of the berm increased by 27 cm at the most and an equivalent increase in elevation was observed on the middle beach directly below the area in erosion. The rest of the mixed sediment beach, excluding the sandy foreshore, showed elevation changes <10 cm.

On the other hand, when the berm did not display any changes in location or elevation, accretion was observed directly seaward of it and erosion was present on lower parts of the beach profile certainly to balance the cross-shore sediment budget. For example, between profiles B1 and B2, the beach shows accretion (change in elevation up to 23 cm) directly onto the toe of the berm whereas equivalent erosion was characterizing lower parts of the mixed sediment beach (again excluding the sandy platform elevation changes).

The beach step during this phase showed great variations in both elevation and location. The elevation of the beach step right at the transition between the sandy platform and the mixed sediment beach steadily increased from -1.16 m (L1) on profile B1 up to -0.83 m (L1) on profile B15. This period of general increase in elevation of the beach step was, however, punctuated by periods of lowering: on October 30th, between profiles B4 and B5; on November 1st - 2nd, between profiles B8 and B10; and on November 2nd - 3rd between profiles B11 and B13.

During this phase, the beach step also displayed a total landward retreat of 4.82 m. This overall retreat was, however, punctuated by phases of landward retreat and seaward

progression. From October 28th to October 31st, between profiles B1 and B7, the beach step showed a progressive landward retreat on every tide. A large retreat of 3.3 m was observed on October 31st between profiles B6 and B7; the rest of the time this retreat was <1 m. From October 31st (profile B7) to November 3rd (profile B13), the beach step showed a progressive seaward migration. This migration was of great magnitude on October 31st (profile B7) and November 01st (profile B9) when it measured in total almost 4 m (respectively 2.08 m and 1.86 m). For the rest of this period, the seaward progression of the beach step was <1 m. From November 3rd (profile B13) to November 4th (profile B15), the beach step started to retreat landward very quickly again. In two tides, the total retreat was approximately 4.14 m (respectively 1.91 m and 2.23 m).

During the entire phase, the sandy platform displayed significant changes too. As mentioned previously, the starting profile of the beach displayed an alongshore runnel bordering the mixed sediment beach. This runnel was bordered on its seaward side by a very large sandy bar. Both of these features were affected by great elevation changes; however the configuration bar/runnel seemed consistent. On November 4th between C14 and C15 a great accumulation of sand directly at the mixed sediment beach toe flattened the profile in this area. This accumulation was measured up to 45 cm.

Phase 2, November 4th-11th, profile B15 to profile B28: berm accretion and stability (Figures 4-16 & 4-18)

This phase corresponds to the transition from a spring tide to the following neap tide. The neap tide occurred on November 10th, however because the survey ended only one day later, November 11th, profiles B27 and B28 have been included within this phase. During this entire phase, the HWL decreased from 9.6 m to 7.4 m (L1). Despite the fact that the highest waves were observed during the first phase, the wave conditions during the second phase were more energetic with H_s ranging from 0.89 to 2 m. T_s ranged from 4.1 to 6.9 s.

During the early morning high tide on November 5th, the beach profile B16 showed a great accumulation of sediment at an elevation corresponding to the HWL mark. This accumulation measured up to 35 cm. It is likely that most of this sediment was eroded from the lower parts on the beach profile, which were simultaneously showing an

erosion of up to 21 cm. With the water level decreasing from one tide to the following, this accumulation of sediment was progressively reshaped. In the first instance, a break of slope was created close to the HWL.

Seaward of this break of slope, the beach face sloped steeply in a straight line towards the lower sandy foreshore. In contrast, the landward side of the break of slope presented a lower angle slope (Figure 4-18). In the later stages, this break of slope became even more pronounced with its seaward face becoming steeper and the landward side becoming either flatter or sloping gently landward (profile B18 to profile B19). From that point on, a clear new berm is identifiable and its elevation is approximately around 6 m (L1). The growth and reshaping of that berm between profiles B16 and B22 was accompanied by erosion tendencies in close proximity to the newly formed berm's toe. In fact, the material eroded on the lower parts of the beach profile had most likely contributed to the sustainability and development of the berm. Such accretion movement can be considerable and represent elevation changes of more than 0.5 m. For example, between profiles B16 and B23, the total growth of the berm represented a total accumulation of 1 m. On November 8th (profile B23), while accretion and erosion movements on the active berm are minimum (<15 cm accretion on its steep face), a new small accretion of sediment occurs at an elevation of approximately 4.4 m (L1), just above the HWL while erosion is affecting most of the lower part of the beach profile. This accumulation corresponds to the initiation of a new berm as described just above. From profile B24 to profile B28 (Figure 4-18), that little accumulation grew to form the new active berm on the profile.

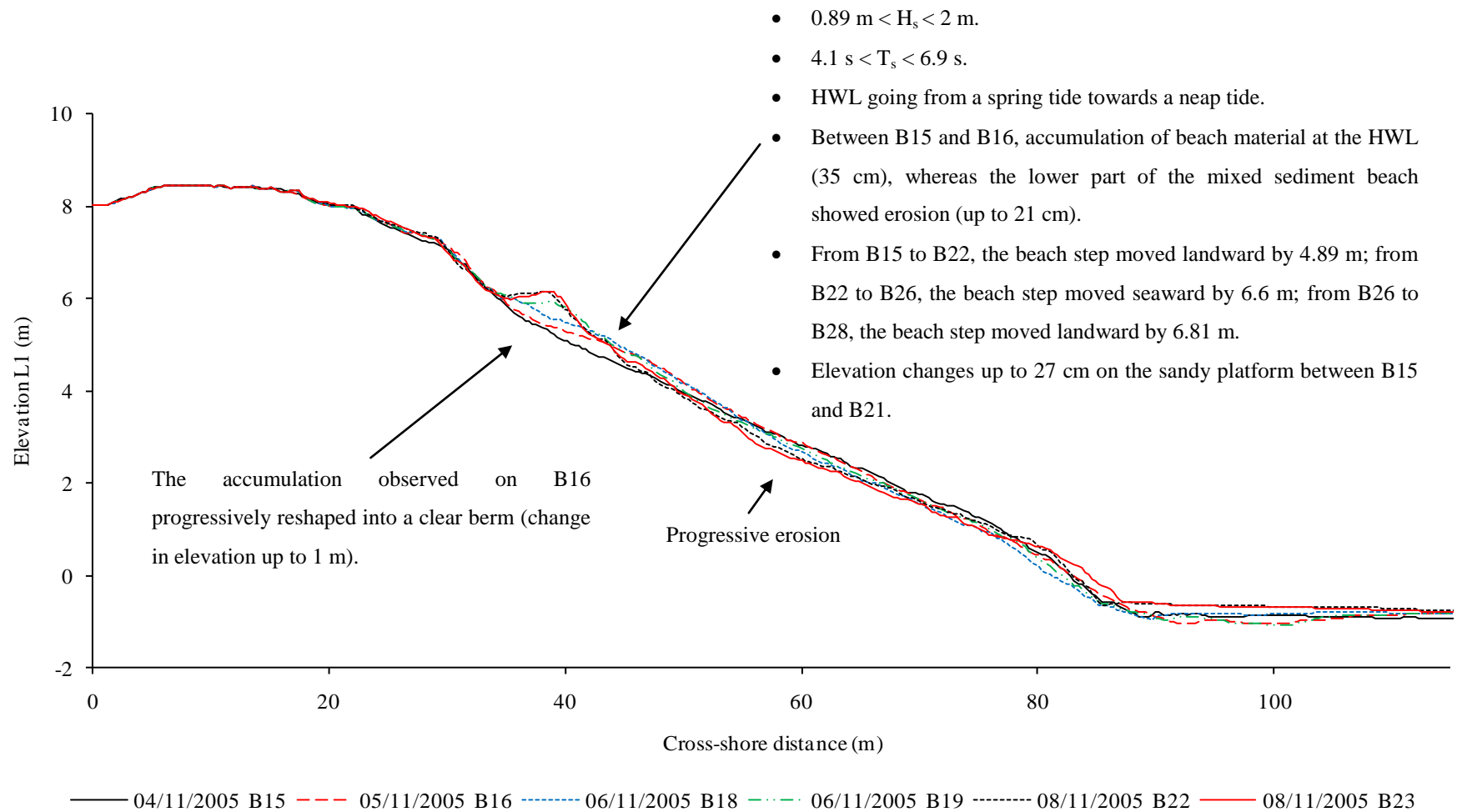


Figure 4-18 Beach profile evolution in the “natural” area during phase 2 of the survey period, November 4th to November 28th, 2005. Part 1.

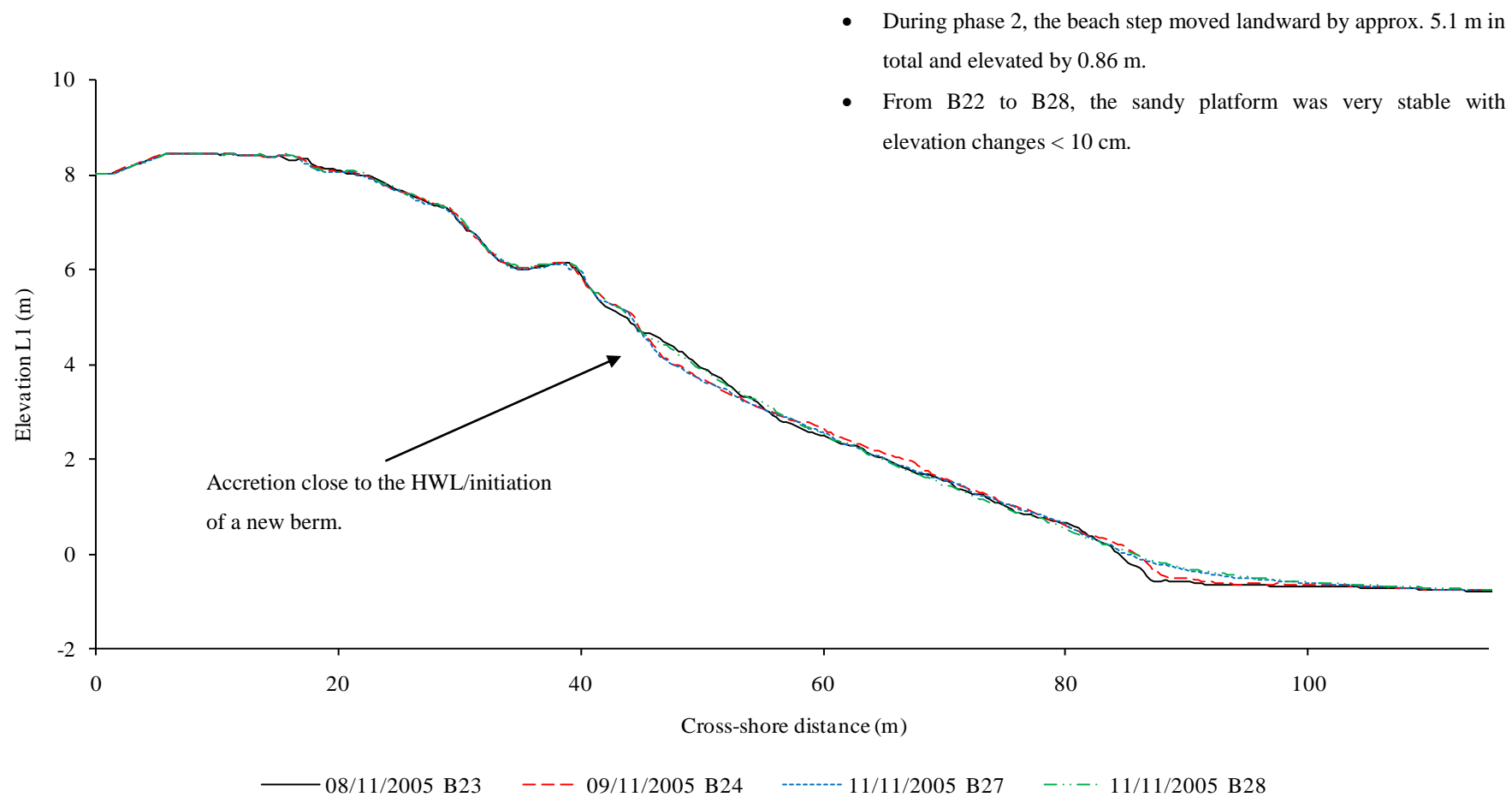


Figure 4-18 Beach profile evolution in the “natural” area during phase 2 of the survey period, November 4th to November 28th, 2005. Part 2.

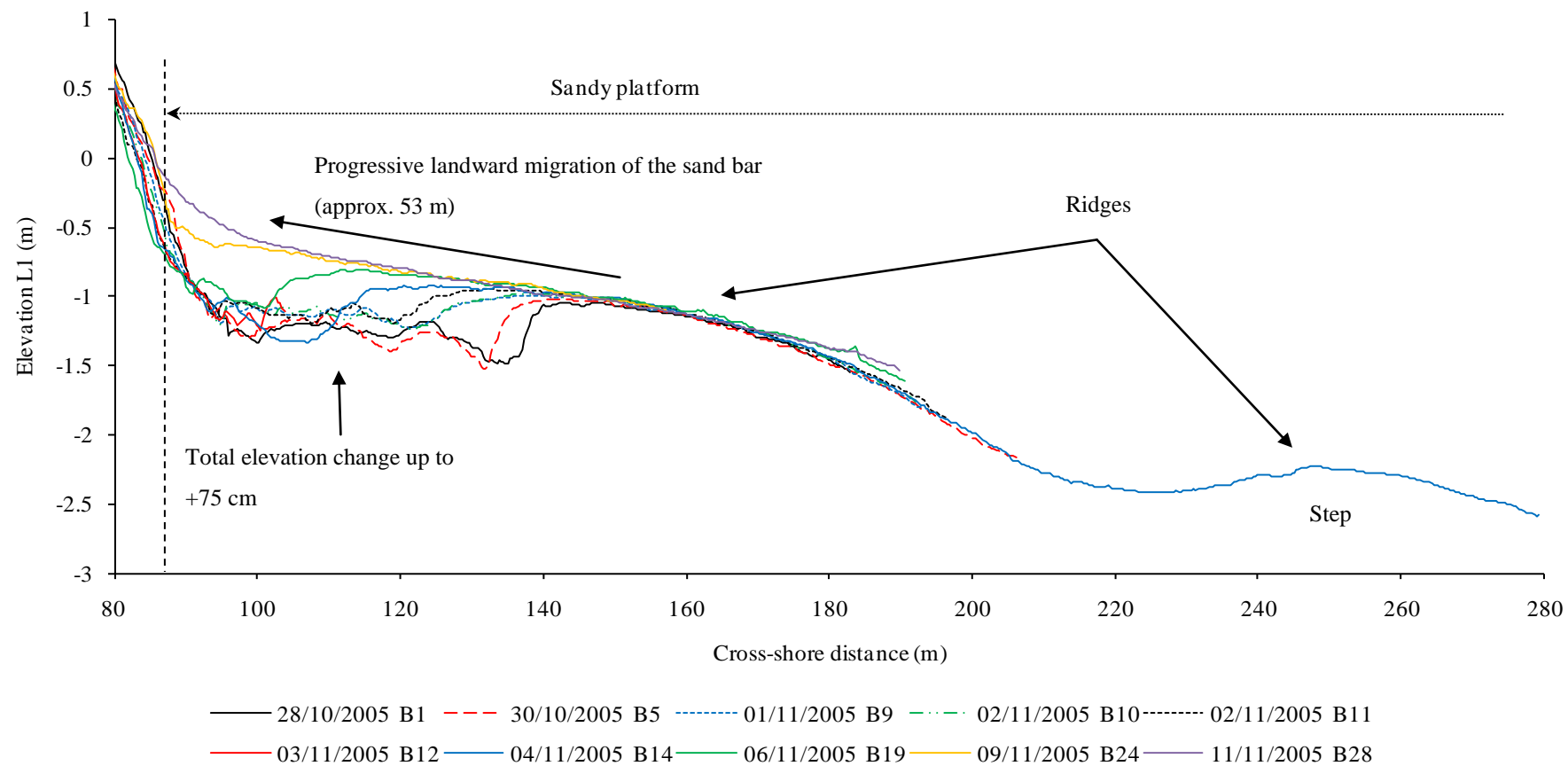


Figure 4-19 Beach profile evolution from the lower part of the mixed sediment beach onto the sandy platform in the “natural” area during the survey period, October 28th to November 11th, 2005.

The beach step during this phase showed great variations in both elevation and location (Figure 4-18). The location of the beach step between November 4th (profile B15) and November 11th (profile B28) moved landward by approximately 5.1 m while its elevation increased by 0.86 m. This overall landward movement of the beach step is punctuated by periods of seaward and landward movements whose amplitude varies with time. From B15 to B22 the beach step moved landward by 4.38 m in total. This landward movement occurred mainly through two main events on November 5th between profiles B16 and B17 (1.31 m) and on November 7th between profiles B20 and B21 (2.9 m). The rest of this period was characterized by movements of <1 m and was disrupted by a very small seaward movement between profiles B17 and B19 which were also <1 m. Between B22 and B26, the beach step progressed seaward by 6.6 m. Apart from the tide on November 9th (between profiles B24 and B25), the beach step locations progressed by 1.89 m. Between profiles B26 and B28, the beach step moved greatly landward while the break of slope associated by definition with this feature on gravel and mixed beaches was becoming less and less clear, adopting a more smooth shape.

During the entire phase, the first metres of sandy platform displayed significant changes too (Figures 4-16 & 4-18). From one tide to the following, the sandy platform showed an alternation of accumulation and erosion events of up to 27 cm changes in elevation. These alternations were very frequent between B15 and B21 whereas between B22 and B28 the sandy platform was very stable and only presented minimal elevation changes (<10 cm).

When looking at the general evolution of the sandy platform in front of the “natural” area (Figure 4-19), the longest beach profile clearly displays two sand ridges: one covering the middle and upper parts of the platform and a second levelled with the lowest low tides observed and probably corresponding to what was called a step earlier for the profile in the recycled zone (profiles A14 & B14 on November 4th respectively on Figures 4-15 & 4-19). The closest sand bar to the mixed sediment beach was visually noticeable on almost every low tide. It had a very low gradient seaward face which was concave shaped, whereas its back (landward side) was characterised by a very steep slope. The regular profile surveys on the sandy platform indicate that the sand bar migrates progressively toward the mixed sediment beach. However, while accretion is observed on the steep side of the bar, atypically its gentle gradient side does not display

any erosion. The total migration of the bar during this study measured approximately 53 m in a landward direction (from the most seaward bar's crest position to the mixed sediment beach step). The runnel that was originally at the back, just in front of the mixed sediment beach, entirely filled resulting in an elevation change up to +75 cm.

4.3.4 Tidal to semi-lunar cycle profile changes at Birling Gap

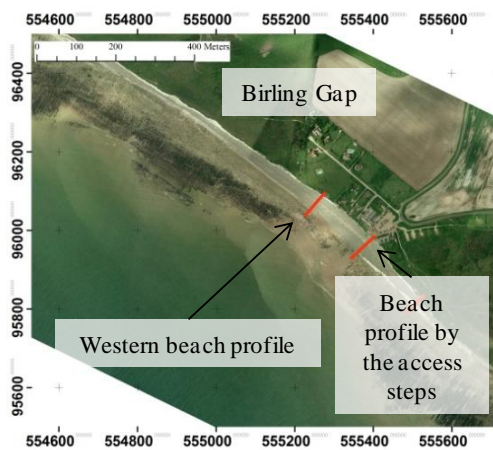


Figure 4-20 Location of the beach profiles, Birling Gap.

Beach profile changes at Birling Gap are produced for the beach profile located where the measurements of the active layer and the tracer injection points are conducted (Figure 4-20; Chapter 3); approximately 150 m west of the access steps.

The beach profile on the western part of Birling Gap is 35 to 45 m long and usually presents berms originating from the most recent high tides (those whose level is low enough to not entirely cover the beach) or sometimes small storms.

1. Beach profile evolution in March 2006 (Figures 4-21, 4-22)

The beach gradient is very reflective during this time of the year varying from 9.5° to 9.7° . The overall shape of the beach profile is concave. Its length was approximately 40 m and its top elevation was 6.5 m OD. The original beach profile (C1) presented a clear berm around the elevation 5 m OD with a flat landward side and a very steep seaward face measured at approximately 20° . The rest of the profile seaward of the berm presented a very consistent lower gradient of 6.8° . The beach step is not pronounced, as it was at Cayeux-sur-Mer, however the coarse material of the beach is associated with a noticeable break of slope between the beach and the chalk platform.

With the exception of one erosion movement measured at 40 cm between profile C1 and profile C2 at the bottom of the berm's toe and probably linked to an instability of the

slope collapse due to the survey team constantly walking over it, the beach during this fieldwork showed very little topographical changes, those being <15 cm. On March 25th, between profiles C7 and C8, H_s nearly doubled compared to the previous days of the survey period. As a direct consequence, it would have been expected to observe bigger topographical changes. However, even during these conditions, the greatest changes observed were only about 10 cm.

The beach step showed very few changes. During the survey period, it progressed slightly seaward by 90 cm. From one tide to the following, the beach step location changes are generally in a 20 cm range, except on March 23rd (between profiles C4 and C5) and on March 25th (between profiles C7 and C8) when the beach moved landward by approximately 40 cm on both days.

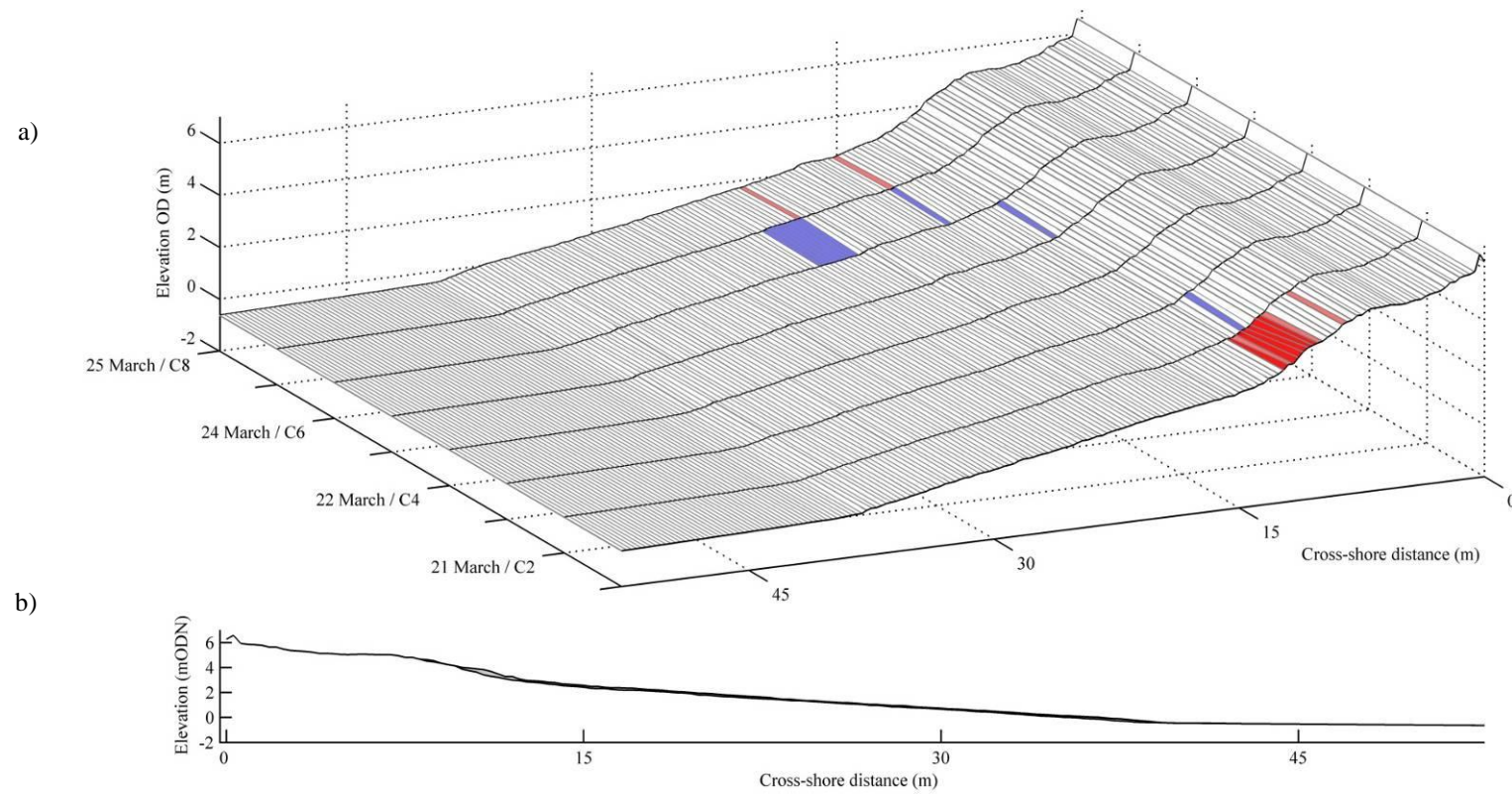


Figure 4-21 Surface plot showing the temporal variation in beach face morphology based on low tide surveys on the western part of Birling Gap from March 20th to March 24th, 2006. a) The light and dark blue represent respectively accretion of 10 to 20 cm and more than 20 cm. The red colour characterises erosion in the same colour coding. b) Maximum and minimum beach profiles with the sweep zone indicated by the shading.

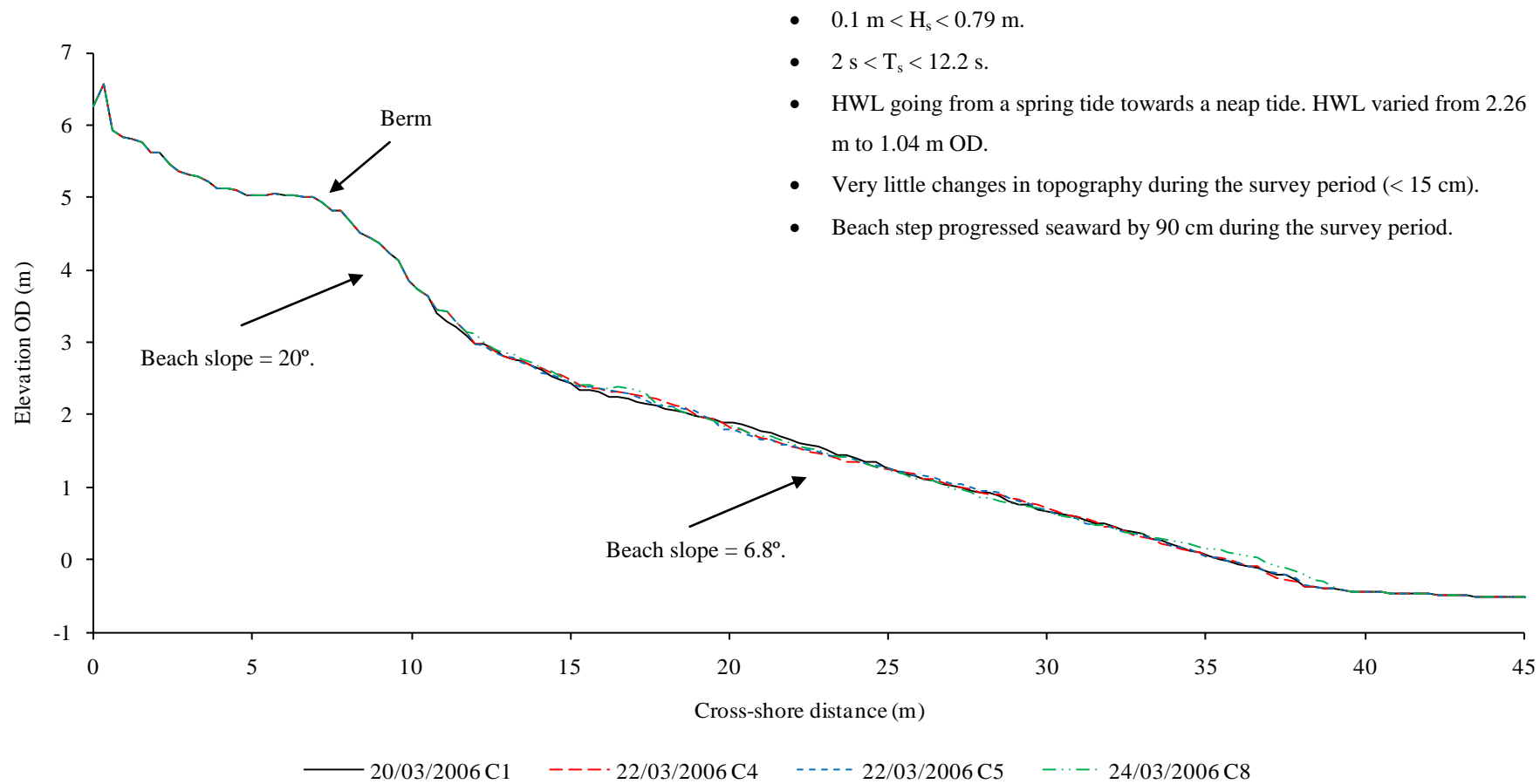


Figure 4-22 Beach profile evolution of the survey period, March 20th to March 24th 2005 at Birling Gap. Part 1.

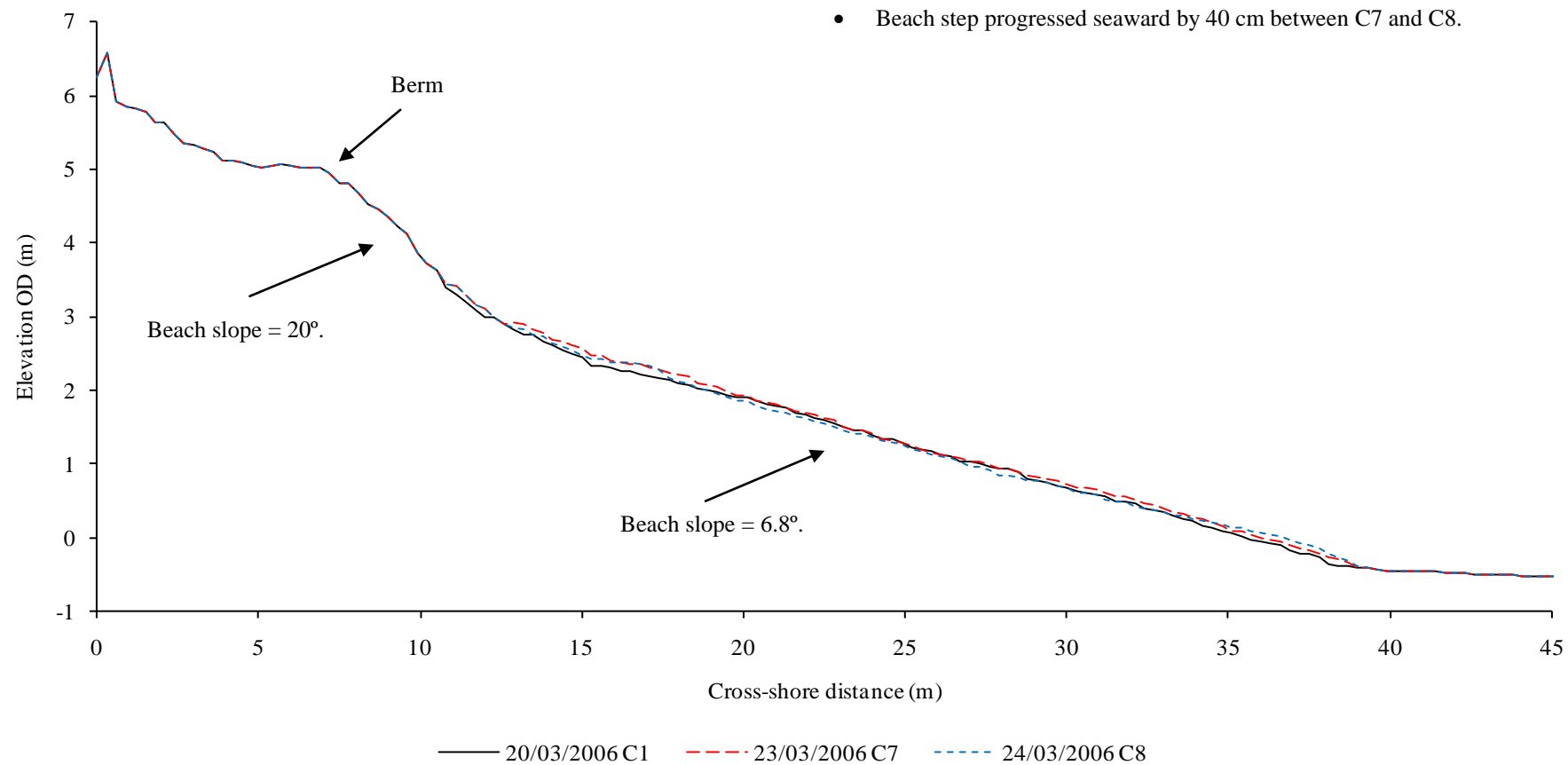


Figure 4-22 Beach profile evolution of the survey period, March 20th to March 24th 2005 at Birling Gap. Part 2.

2. Beach profile evolution in May 2006 (Figures 4-23 & 4-24).

The beach slope angle during this survey period varied from 7.1° to 7.8° , meaning that the beach in May 2006 was less reflective than it was in March 2006. The beach length extended up to 42 m long which is also slightly longer than in March 2006.

The beach material during this period clearly showed a tendency to pile up against the cliff in an attempt to find equilibrium with the forcing hydrodynamics and the HWL. This accumulation was able to sustain a very steep slope close to 20° and its top elevation was close to 5.8 m HD at that time. The rest of the beach until the beach step had a much lower angle of approximately 6° to 6.5° . Contrary to the first survey period in March 2006, the beach step was very pronounced, marking a very clear break of slope between the mixed sediment beach and the chalk platform. The beach step during this period was able to sustain a seaward face with an angle close to 10° over a distance of 1 to 2 m. The thickness of beach material between the crest of the beach step and the chalk platform varied from 16 cm up to 40 cm.

Because of the great H_s observed during that survey period which ranged from 1.13 to 2.61 m and a high and increasing water level, the entire beach profile was reshaped on a tidal basis by the hydrodynamic processes. Between the May 19th (profile D1) and May 23rd (D8), the overall elevation changes of the beach face were great showing general accretion over the first 25 m of the beach profile and general erosion over the last 15 m. These two movements were marked by maxima of elevation changes, measured up to 62 cm and 25 cm respectively. The differences in elevation on a tidal basis were very significant all across the beach too, with topographical changes greater than 10 cm and maxima that could reach 44 cm in accretion and 40 cm in erosion. No clear feature pattern such as berm retreat or build-up can be distinguished over this survey period apart from the tendency that a large volume of the beach material was pushed up against the cliff edge and that the beach steps was very pronounced and varied in location and thickness by great amplitude. The beach step migrated over a total length of 2.5 m while the thickness of the beach step varied from 10 cm up to 40 cm. As a general pattern when the beach step migrated seaward, erosion seemed to be dominant on higher parts of the profile and reciprocally when the beach step migrated landward, accretion

seemed to dominate higher up on the profile. As an example, on May 19th, the profile D1 was presenting a beach step with a very steep seaward face with a slope close to 10° (this angle was very consistent all along the survey period at the exception for profile D8) on approximately 1 m length and the thickness of sediment between its crest and the chalk platform was measured at 23 cm. After a tide, the shape of the profile D2 was quite similar to the one of profile D1. However, the beach step migrated by approximately 1 m landward whereas the rest of the beach profile was marked by a general accretion. The vertical elevation changes resulting from it varied from 12 to 24 cm depending on the location on the profile (Figure 4-24). On the contrary, between D2 and D3, the beach step migrated seaward by 1.30 m and showed accretion up to 26 cm directly above the chalk platform. This accretion movement was associated with an erosion trend of up to 19 cm on higher parts of the beach profile. When looking at the thickness of the beach step above the chalk platform, it appears that the lowest thickness and therefore the lowest break of slopes observed occurred on May 21st and May 23rd (on profile D5 and profile D8). These two profiles are both marked by very high water levels but also the smallest significant wave height observed during this survey.

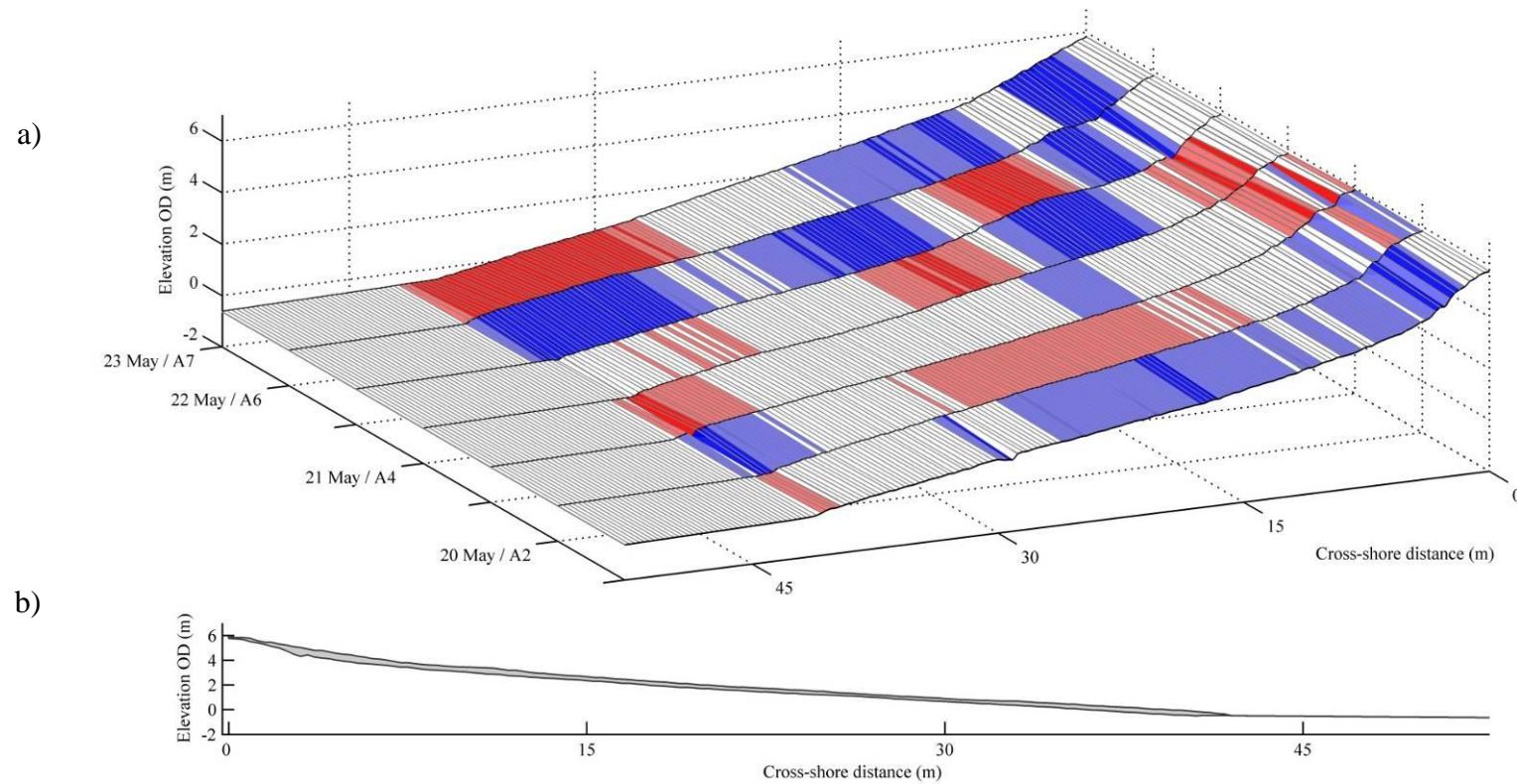


Figure 4-23 Surface plot showing the temporal variation in beach face morphology based on low tide surveys on the western part of Birling Gap from May 19th to May 23rd, 2006. a) The light and dark blue represent respectively accretion of 10 to 20cm and more than 20cm. The red colour characterises erosion in the same colour coding. b) Maximum and minimum beach profiles with the sweep zone indicated by the shading.

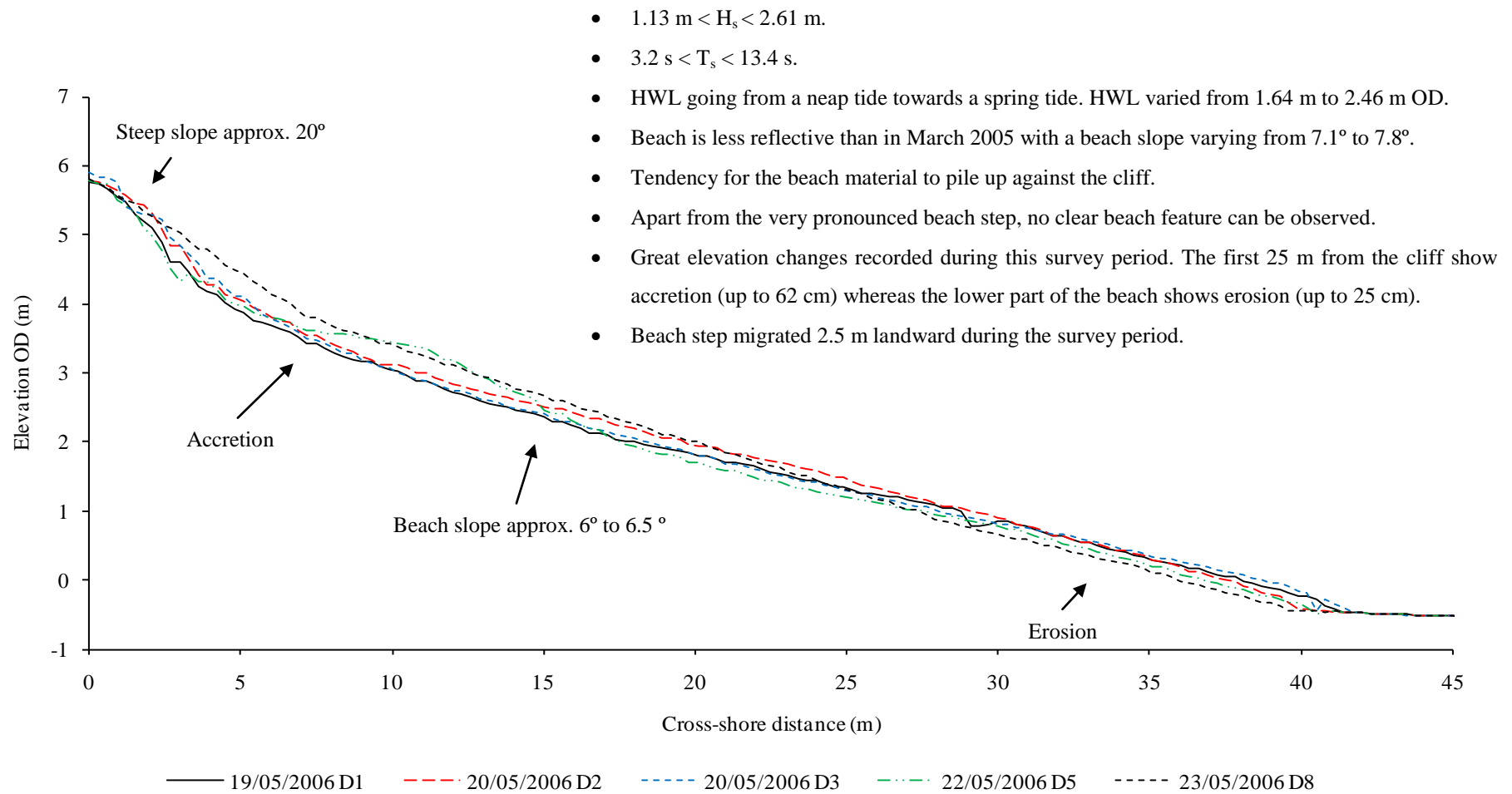


Figure 4-24 Beach profile evolution of the survey period, May 19th to May 23rd 2005 at Birling Gap.

3. Beach profile evolution in December 2006 (Figures 4-25, 4-26 & 4-27).

The beach slope angle during this survey period varied from 8.4° to 9° which makes these gradients intermediary between the beach profiles observed in March and May 2006. The beach profile length extended up to 43 m long which is comparable to the beach profile length observed in April 2006. The top crest of the beach had an elevation of 5.24 m.

The beach profile during this survey period mainly displayed two phases, one corresponding to the erosion of a berm and a second phase corresponding to the progressive build up of a second berm lower down on the beach profile. These two phases also correspond to the two different periods in significant wave heights identified earlier in this chapter (Section 4.3.2).

Phase 1, December 14th-16th, profile E1 to profile E4: berm erosion (Figures 4-25 & 4-26).

This phase corresponds to the start of a semi-lunar cycle going from neap to tide marked with an agitated wave condition. The water level goes from 1.39 m up to 1.73 m OD, H_s is largely more than 1 m being comprised between 1.40 m and 1.64 m and T_s is comprised between 6.2 and 7.7 s. The beach gradient during this period is very close to 8.5° at $\pm 0.1^{\circ}$.

On December 2006, the profile E1 presented a small sharp beach crest fringing the cliff toe most probably resulting from a storm event. Seaward of its crest, the beach profile presented a large number of berms (five berms in total which is very rare), each of them resulting from the water level conditions and the wave conditions following the storm event which shaped the beach crest. The most seaward and clear berm observed on this profile is located around the elevation 3.5 m. On profile E2 this berm shows signs of erosion with a maximum vertical erosion of 21 cm and a slight retreat (less than 1 m). In contrast, the zone located right at the bottom of the berm and in proximity to the HWL is characterised by accretion (maximum accretion measured at 21 cm). The last 20 m of the beach are marked by erosion which maximum reaches 11 cm. On December 16th, profile E3 presents a similar pattern in the organisation of the zone affected by erosion

(≤ 10 cm across the profile) or accretion (maximum vertical change 14 cm), except that the beach berm was not affected by any topographical change. The change in water level from the tide on December 14th (1.79 m OD) December 15th (1.39 m OD) is most likely responsible for the beach berm not being affected by the forcing hydrodynamics. On profile E4, the zone of the beach above the HWL is marked by accretion whose maximum was measured at 43 cm, whereas the rest of the beach profile was affected by erosion which could reach up to 25 cm.

When looking at the beach step, its location did not move over this survey period; however, because of consistent erosion, its break of slope and thickness changed slightly. On profile E1, the beach step had a seaward slope of approximately 10° and its crest was approximately 16 cm above the chalk platform. On profile E2, the beach step crest was slightly eroded by 4 cm but its seaward face sustained a similar angle. On profile E3, the beach step crest eroded by an additional 8 cm, making the break of slope between the mixed sediment beach and the platform a lot smoother (approximately 4°). On profile E4, the beach step only moved landward by 20 cm approximately; however, because of the large erosion affecting the beach profile on the middle and the lower beach, the transition between the mixed sediment beach and the chalk platform became even smoother.

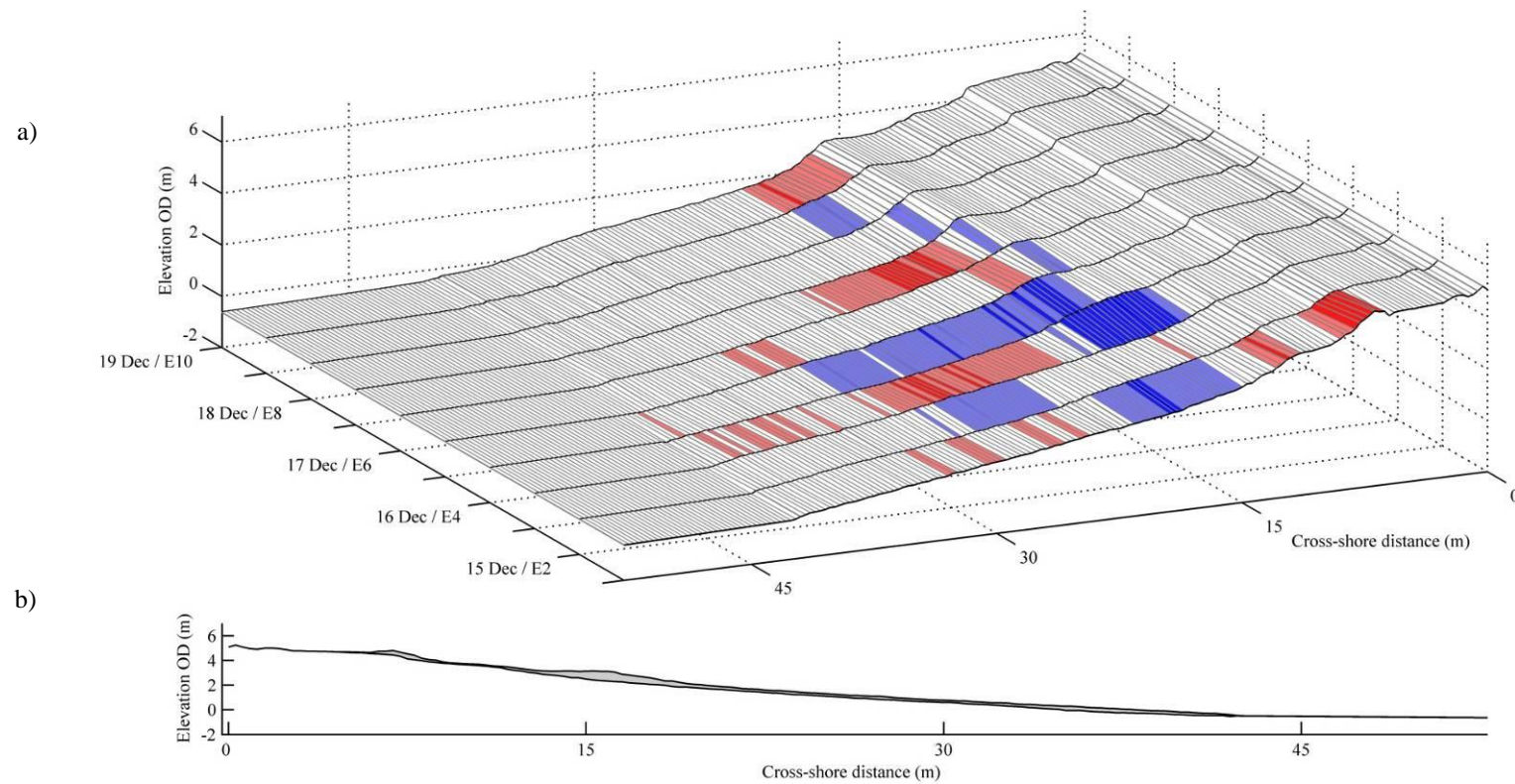


Figure 4-25 Surface plot showing the temporal variation in beach face morphology based on low tide surveys on the western part of Birling Gap from December 14th to December 19th, 2006. (a) The light and dark blue represent respectively accretion of 10 to 20cm and more than 20cm. The red colour characterises erosion in the same colour coding (b) Maximum and minimum beach profiles with the sweep zone indicated by the shading.

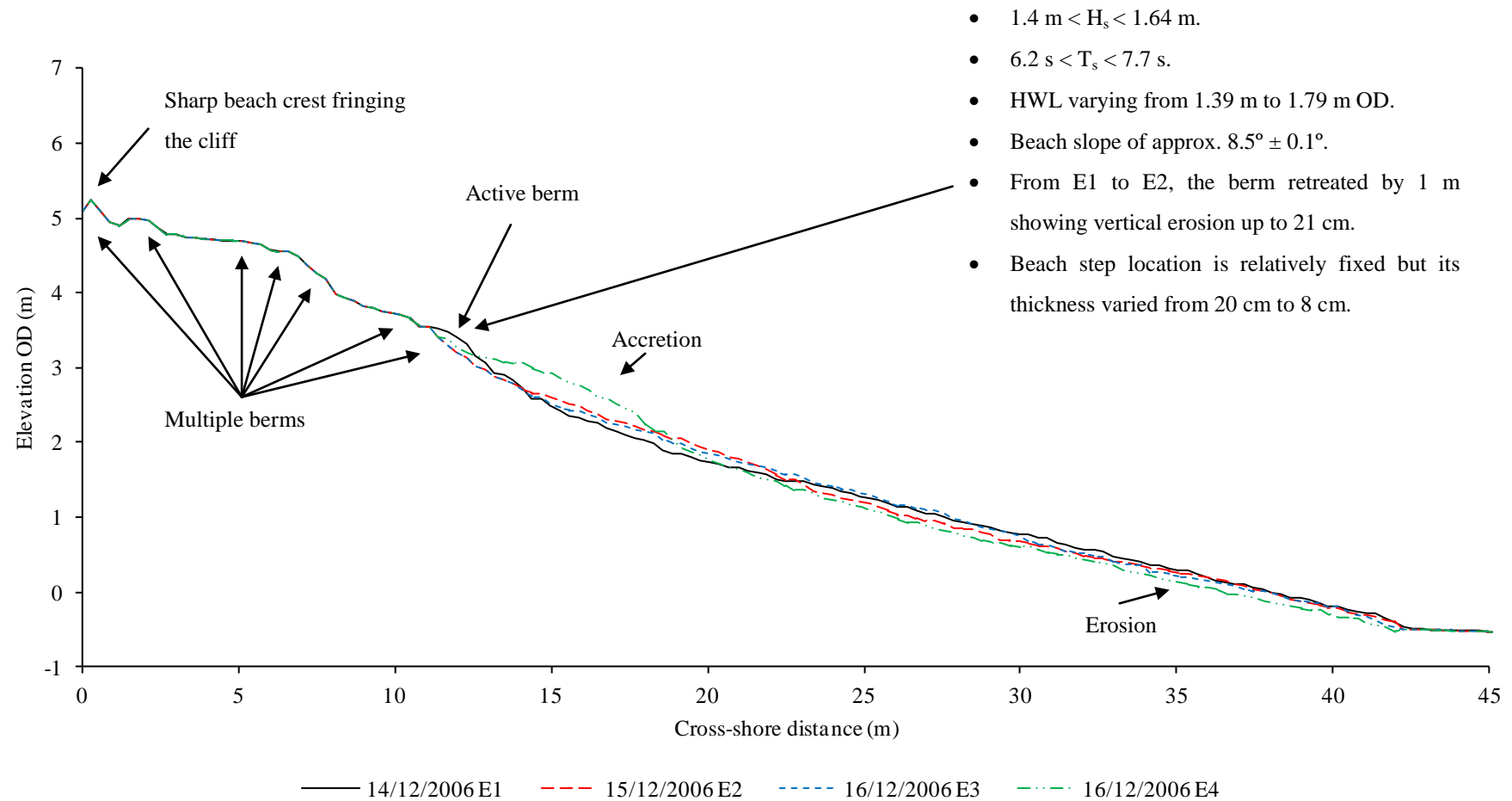


Figure 4-26 Beach profile evolution during phase 1 of the survey period, December 14th to December 19th 2005 at Birling Gap.

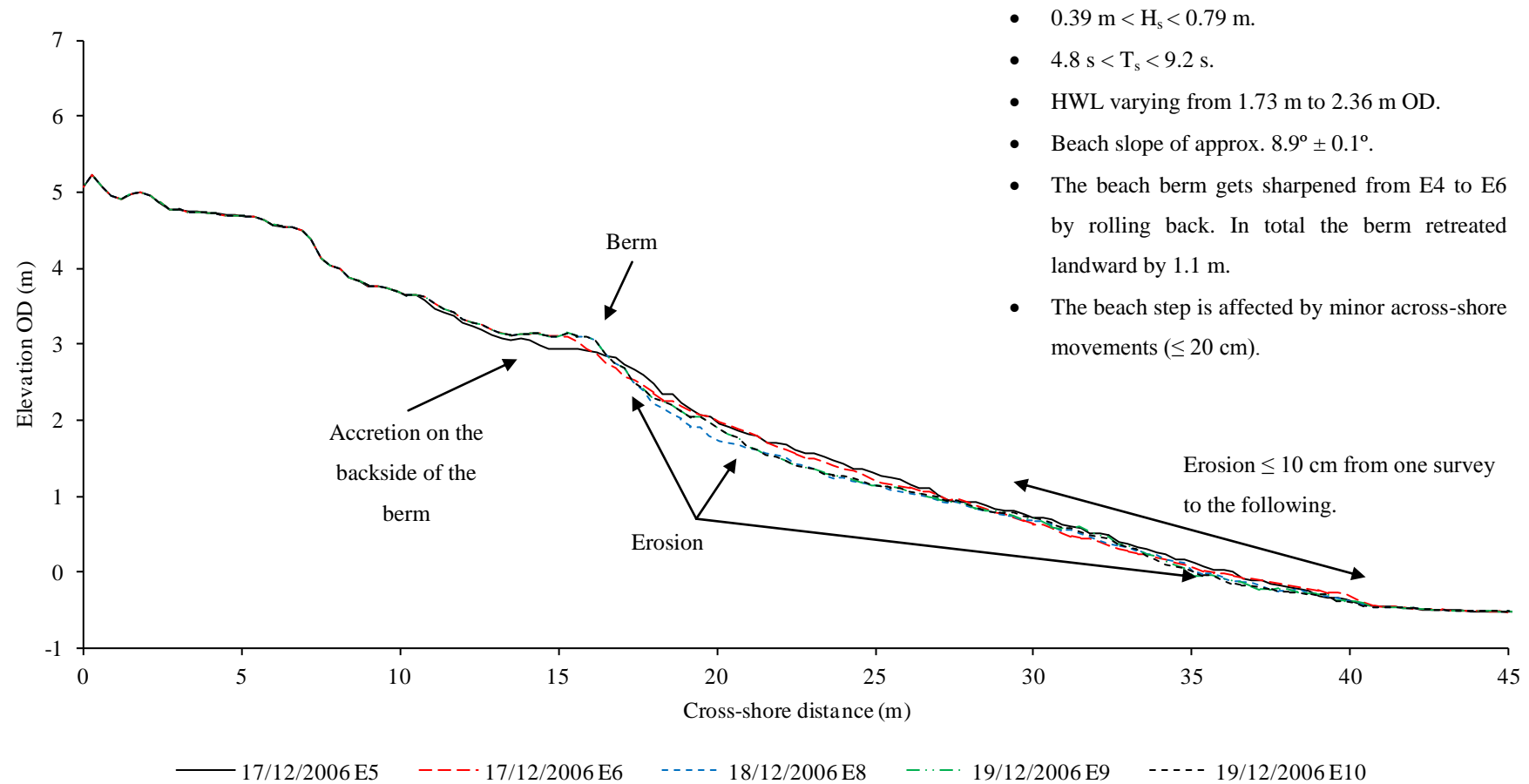


Figure 4-27 Beach profile evolution during phase 2 of the survey period, December 14th to December 19th 2005 at Birling Gap.

Phase 2, December 17th-19th, profile E5 to profile E10: berm accretion and stability (figures 4-25 & 4-27).

This phase corresponds to an increasing water level going from 1.73 m up to 2.36 m OD while the significant wave heights are less than 1m ranging between 0.39 m and 0.79 m. The significant wave period varied between 4.84 and 9.23 s. The beach slope during this period is a little steeper than during phase 1 with an angle close to 8.9° varying by $\pm 0.1^\circ$ over this phase.

The beach profile on E5 showed accretion from the top of the active beach to up to 35 m seaward of the cliffs. The last 7 m of beach were generally affected by erosion which was ≤ 10 cm. It appeared that in addition to the material accumulated above the HWL on profile E4, some more material was added on profile E5. A part of this material was certainly pushed up the beach above the HWL and shaped as a clear berm. On December 17th (profile E6), the berm identified on profile E4 sharpened a bit more. This sharpening is the result of erosion of the seaward face of the berm (16 cm maximum) while directly behind the berm's crest, there is accretion (18 cm maximum). In fact, as the previously observed at Cayeux-sur-Mer, the beach material is rolled back from the steep slope of the berm toward its back side. This morphological change resulted in a landward movement of the berm's crest by 1.1 m and its elevation increased by 24 cm. The rest of the beach profile on E6 also shows mostly erosion (measured up to 14 cm) while the very lower part of the beach profile shows slight accretion (7 cm maximum). While the water level was still increasing, the sharpening of the beach berm increased, presenting a seaward face even steeper than on profile E6 (from 15.1° to 28.5°). This steepening was the result of an accretion movement at the berm's crest (17 cm) while its toe was located at approximately the same height as the HWL (2.1 m HD) was greatly affected by erosion (26 cm for the most deeply affected parts). The rest of the beach profile was affected by changes in elevation ≤ 10 cm. On the following profiles, the beach berm is completely stabilized and is even consolidated by small accretion movements on its seaward face at the HWL on profiles E8 and E9 (respectively 16 cm and 18 cm maximum). The rest of the active beach face is also very consistent by mostly displaying changes in elevation ≤ 10 cm until December 19th.

On December 17th, the beach step on profile E5 retreated landward by 1.6 m. Despite this significant movement, the maximum erosion observed in proximity of the beach

step is up to 10 cm only. Such erosion had the effect to reduce the beach step to a thin layer of sediment above the chalk platform. The usual steep seaside face characterising the beach step is not clearly observable, giving the transition between the beach and the chalk platform a smooth aspect. On profile E6, the beach step regained elevation by 7 cm and was able to re-establish some kind of steep seaward face. On profile E7, erosion affected the beach step in such a way that the beach step crest moved landward by 30 cm approximately. Past December 18th, the beach step was affected by minor across-shore movements (≤ 20 cm) or vertical movements (≤ 6 cm).

4.3.5 Seasonal and Yearly profile changes at Birling Gap (Figures 4-28, 4-29, 4-30, 4-31 & 4-32)

To examine the beach profile evolution on a seasonal or yearly period, it was decided to use the beach profile located in the central part of Birling Gap's beach, close to the access steps (Figure 4-20). This choice was motivated for few reasons:

- First, this area presents the longest beach profile at Birling Gap and therefore has the best potential to express multiple berms corresponding to various hydrodynamic and water level conditions.
- This area is also covered for a longer time than any other part of the beach. For this reason, the beach material gets re-worked for longer time periods and therefore the beach profile is more likely to reach a better equilibrium with the forcing hydrodynamics than anywhere else on the beach.
- This area is also where the biggest and thickest amount of sediment is stocked along the beach. This enables the beach profile to fully adapt morphodynamically to the forcing agents and consequently could reveal seasonal or yearly patterns.
- Finally, the beach profiles on the western and eastern beach are relatively short and easily submerged by water. Long time patterns would have been even more difficult to observe on these profiles.

In order to display all of the profile data acquired on a monthly basis from between August 2004 and July 2006 and identify across-shore morphological patterns, it was

decided to split this two year survey period into groups. Each group was delimited according to the general wave conditions whose yearly patterns were identified in chapter Section 4.3.2. These periods were distributed as follows: from September to March and from April to August, respectively corresponding to winter and summer conditions. Note that this study had at its disposition an early survey made in July 2003 which is displayed in Figure 4-27. Furthermore, one survey is missing in December 2005 because of equipment failure. Finally, two surveys were actually used in January 2005 because of an exceptional storm that greatly affected the beach morphology (Figure 4-28).

Figure 4-33 shows the differences between the maximum and minimum elevation recorded at Birling Gap over the two year monitoring period. When looking at the overall two year survey period, the first 4.5 m at the very top of the beach profile directly in contact with the cliff shows moderate elevation changes with maximum values of between 1 and 1.27 m. These changes in elevation are most likely to be linked to the formation of high level storm or very high spring tide ridges. The maximum changes in elevation observed in the beach profiles occurred over the next 15 m (measured between 1.3 and 1.8 m). This location mainly corresponds to the sweep zone of most of the HWL ridges. The middle of the beach, in the stretch covering a length of approximately 20 to 35 m away from the top of the beach, experiences the lowest changes in elevation (measured from 0.69 to 1.3 m). The lowest part of the beach profile experiences moderate elevation changes (ranging from 1 to 1.23 m).

Monthly changes in beach elevations (Figures 4-28, 4-29, 4-30, 4-31 & 4-32) show significant changes, and the main and greatest changes are related to ridges or beach step accretion or erosion. The maximum accretion observed across the beach profile varies from 0.07 m to 1.08 m and the maximum erosion varies within equivalent amplitudes from 0.09 m to 1.02 m. Generally, the areas of accretion and erosion were behaving at the expense of each other; however, this trend is sometimes hindered because of the longshore transport of sediment.

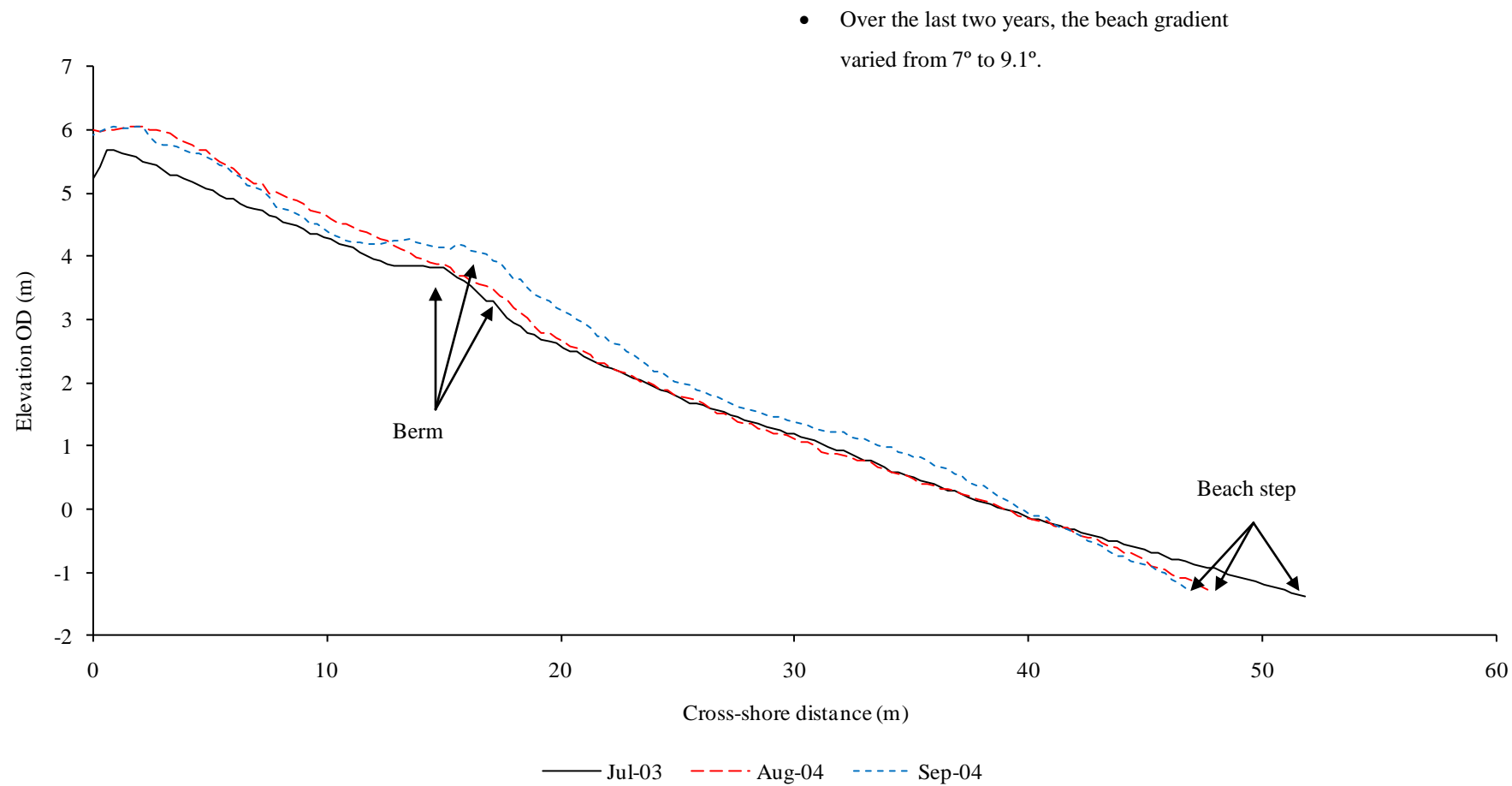


Figure 4-28 Beach profile evolution during the Summer 2004 at Birling Gap in proximity of the access steps.

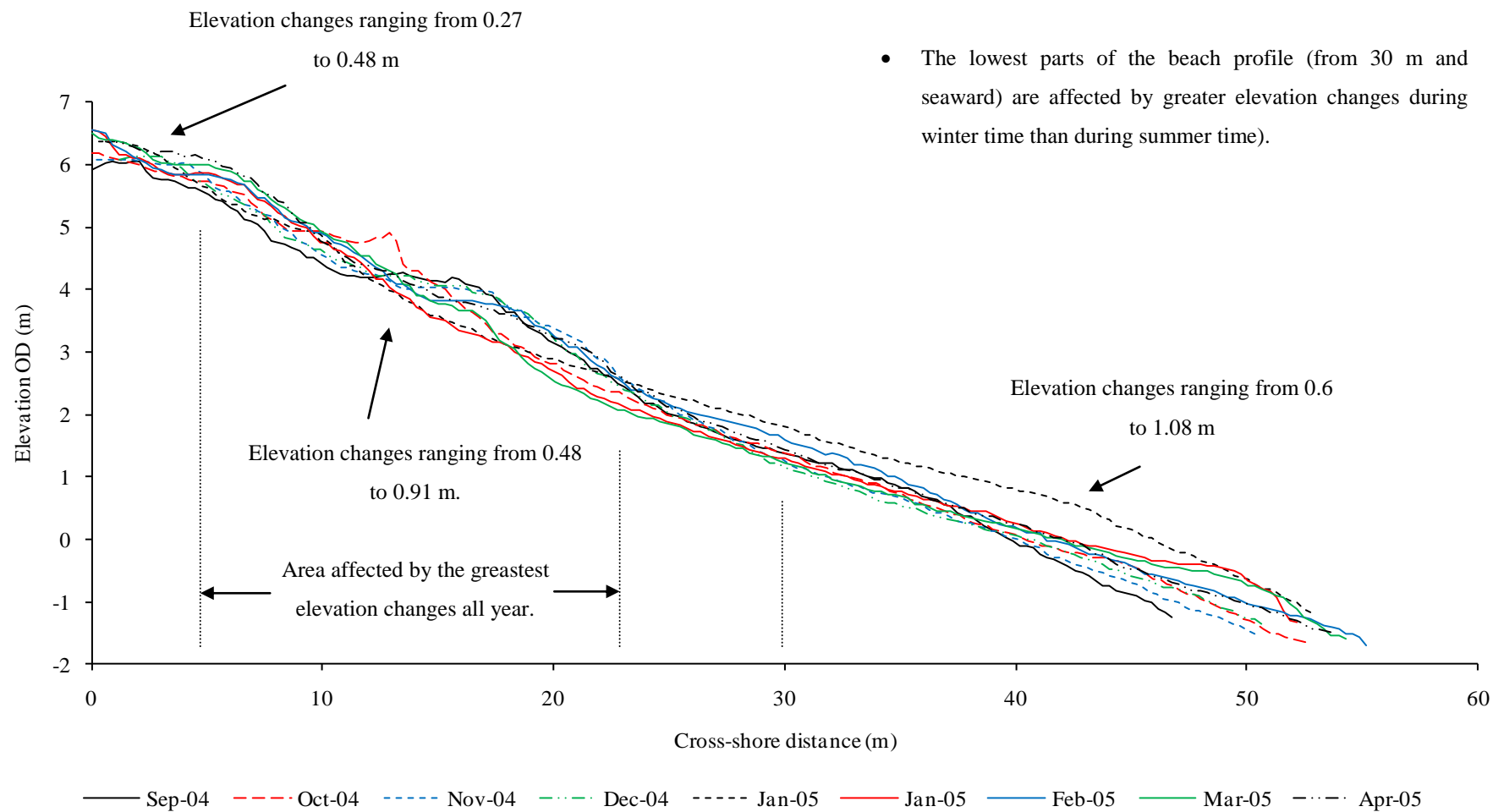


Figure 4-29 Beach profile evolution during the Winter 2004/2005 at Birling Gap in proximity of the access steps.

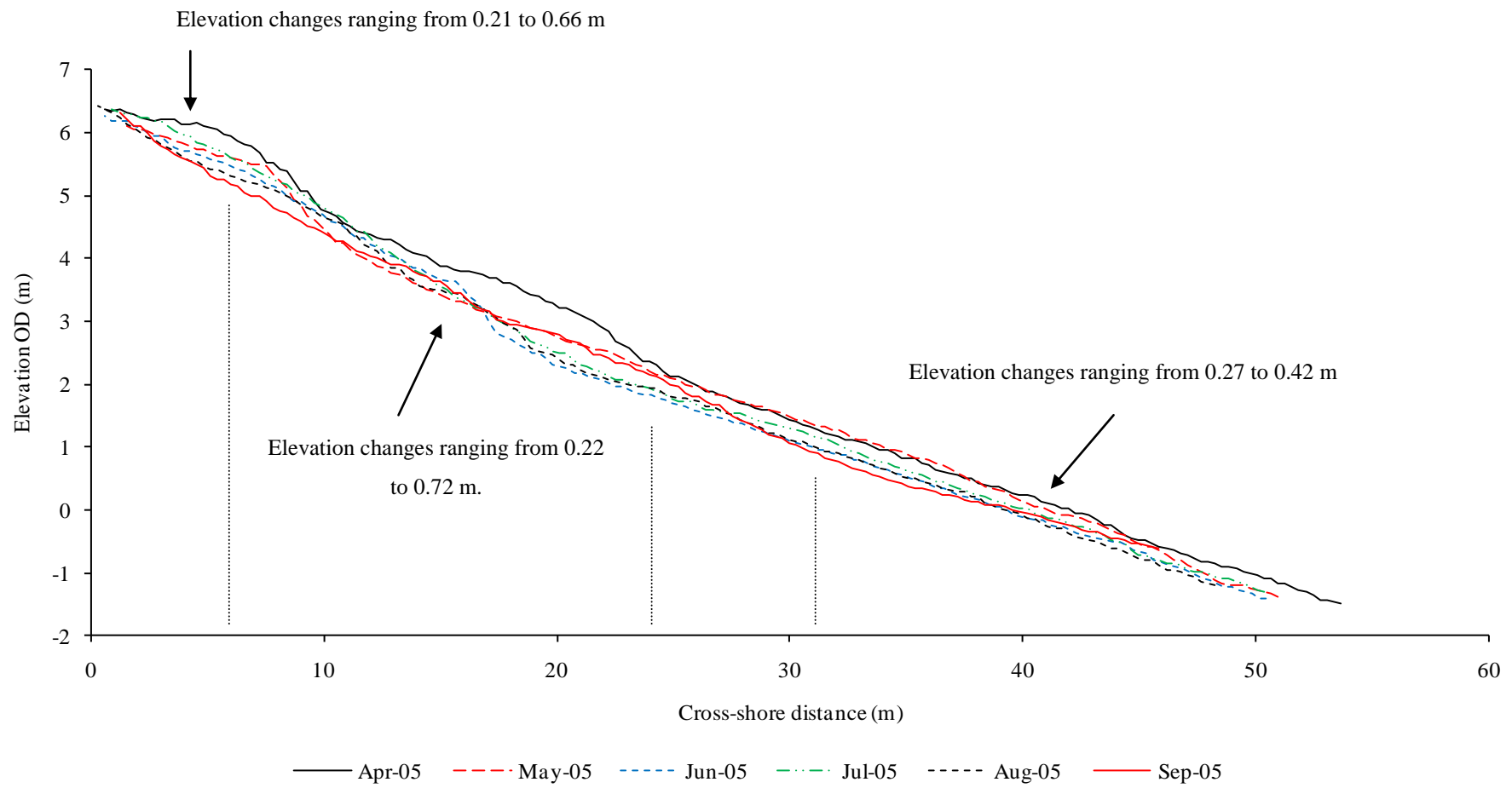


Figure 4-30 Beach profile evolution during the Summer 2005 at Birling Gap in proximity of the access steps.

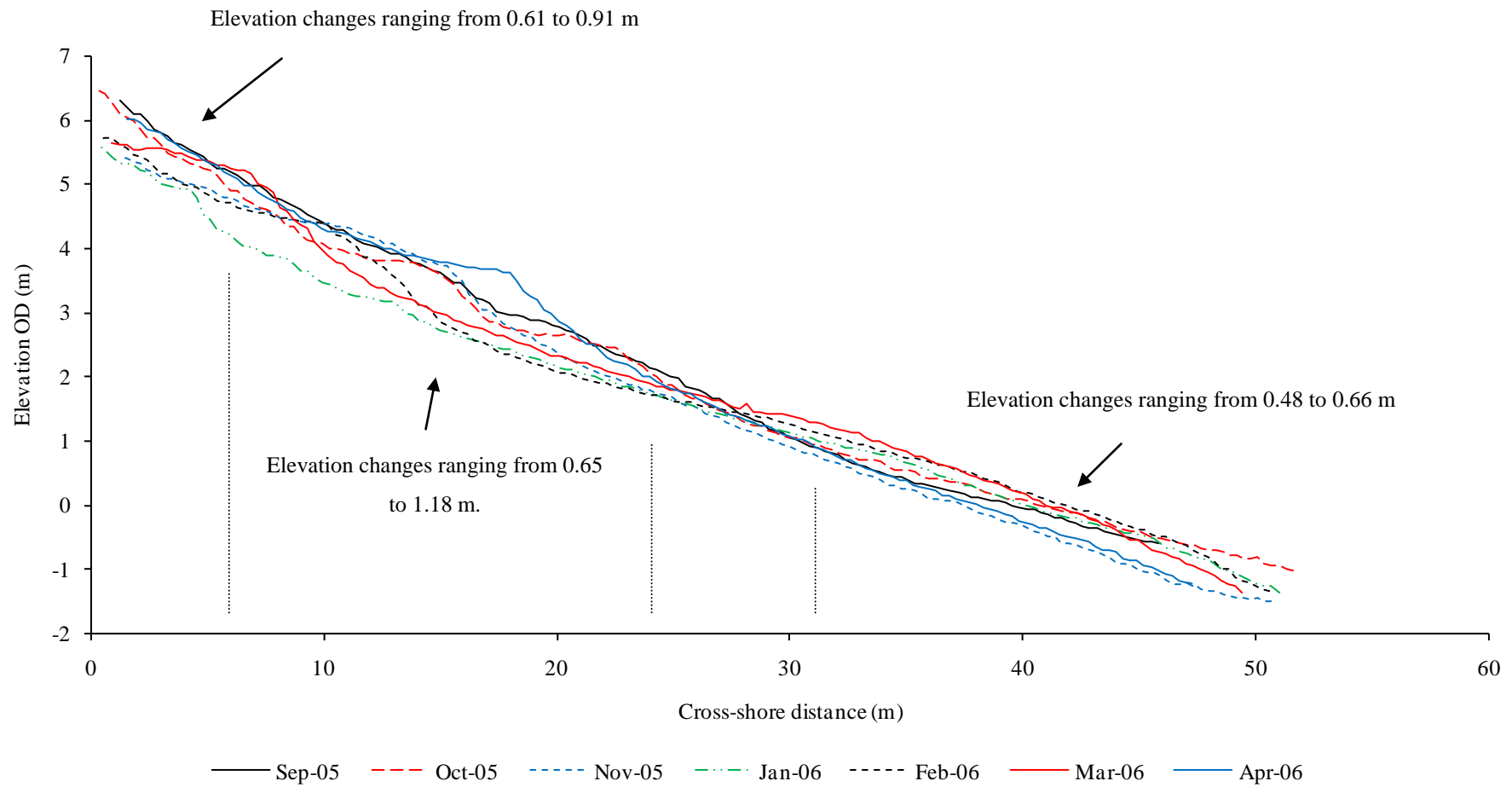


Figure 4-31 Beach profile evolution during the Winter 2005/2006 at Birling Gap in proximity of the access steps.

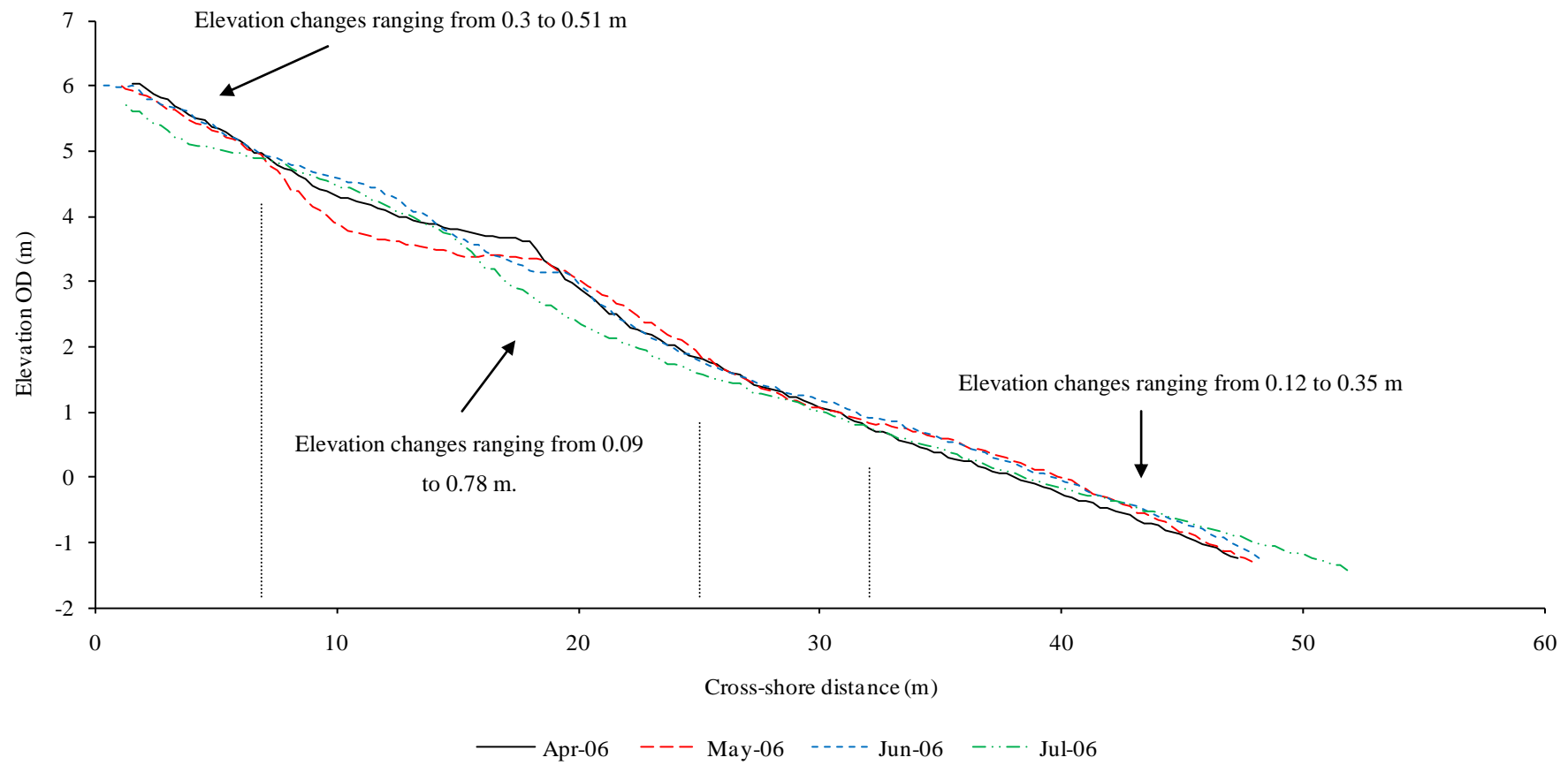


Figure 4-32 Beach profile evolution during the Summer 2006 at Birling Gap in proximity of the access step.

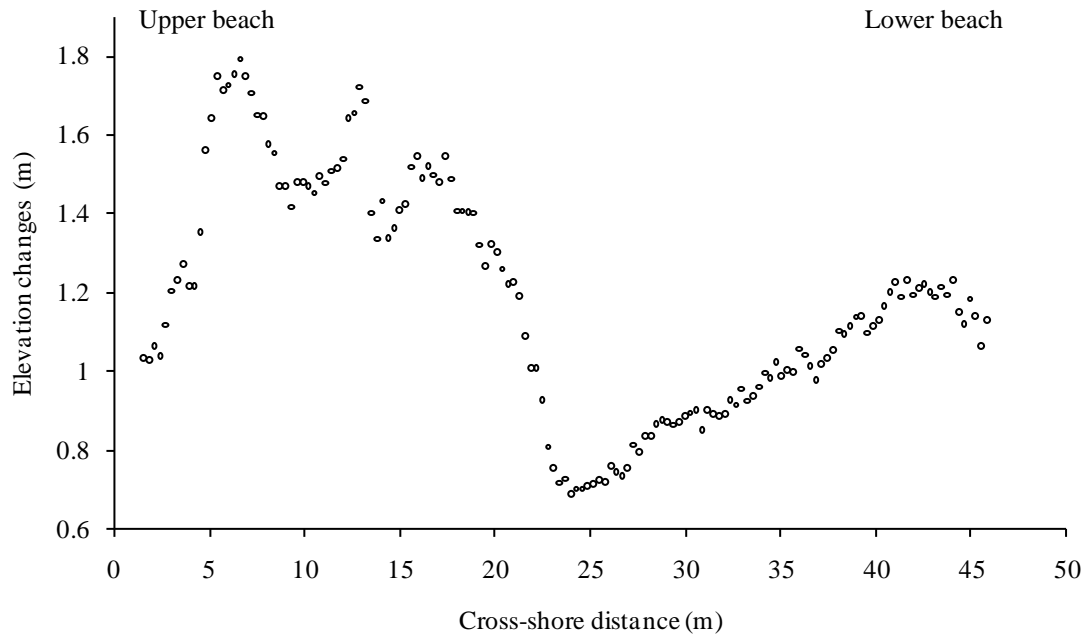


Figure 4-33 Plot of the difference between the maximum and the minimum elevation recorded across the middle beach profile (in front of the access steps) over the two year survey at Birling Gap.

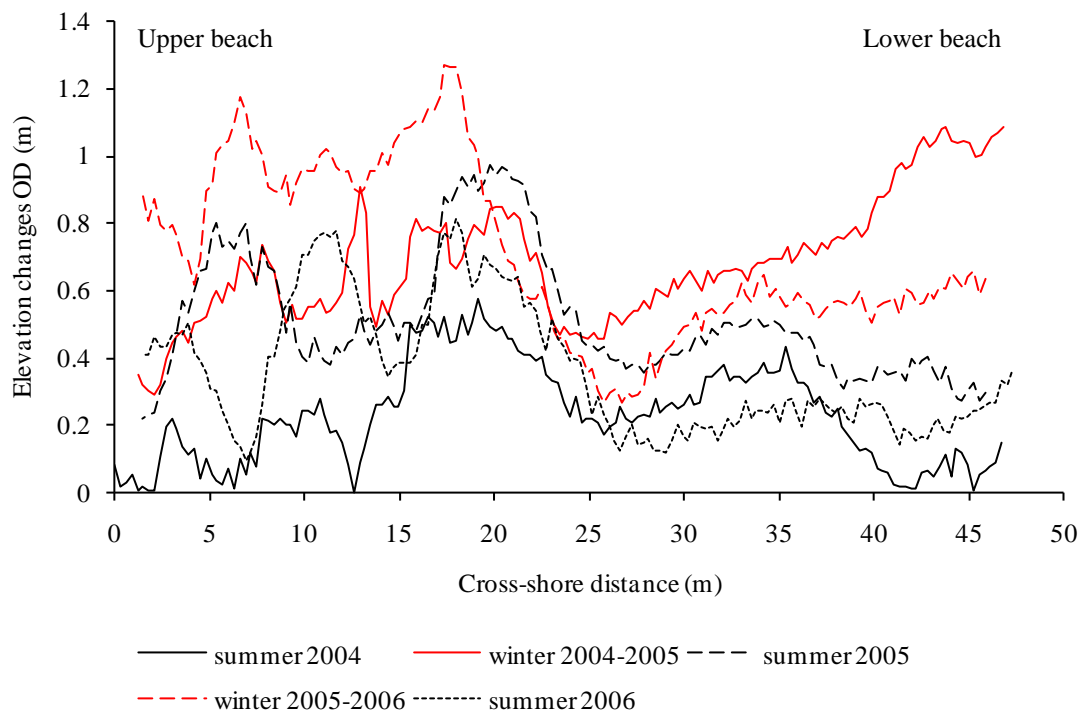


Figure 4-34 Plot of the difference between the maximum and the minimum elevation recorded across the beach profile in front of the access steps per season at Birling Gap.

From Figures 4-28, 4-29, 4-30, 4-31 & 4-32, it is clear that the ranges of elevation change differ from one season to another, in addition to the across-shore variations mentioned earlier.

Based on Figure 4-34 which represents the difference between the maximum and the minimum elevation recorded per season along the beach profile in front of the access steps, it can be seen that the lower parts of the beach profile (from 30 m and over) are more affected by elevation changes during winter time than during summer time. These changes range between 0.12 to 0.35 m during the summer of 2006, 0.27 to 0.42 m during the summer of 2005, 0.48 to 0.66 m during the winter of 2005/2006 and 0.6 to 1.08 m during the winter of 2004/2005.

Within 0 to 5 m of the cliff edge, the highest part of the beach shows that the greatest elevation changes occurred during the winter of 2005/2006 (0.61 to 0.91 m); then the summer of 2005 (0.21 to 0.66 m); followed by the summer of 2006 (0.3 to 0.51 m); and finally, the winter of 2004/2005 (0.27 to 0.48 m). Between 5 and 22 m away from the cliffs, the beach presents the greatest ranges in elevation change. These ranges were the greatest during the summer of 2006 (0.09 to 0.78 m); then the winter of 2005/2006 (0.65 to 1.18 m); followed by the summer of 2005 (0.22 to 0.72 m); and finally, the winter of 2004/2005 (0.48 to 0.91 m). The middle part of the beach between approximately 22 and 30 m from the cliff edge on the across-shore profile presents very similar ranges in elevation change 0.12 and 0.97 m over the year whatever the season. The beach profile gradient during the two year survey period varied from 7 to 9.1° with no particular tendency to follow the seasonality as usually observed on sandy beaches with the alternance of winter and summer beach profiles (Chapter 4 Section 4.2.1).

4.4 Discussion

4.4.1 Seasonal elevation changes of the beach profile.

The generally recognised two-type seasonal beach profiles reported in the literature (e.g. Powell, 1990; Pontee, 1995) are not very well expressed at Birling Gap during the two year survey period. In fact, because the beach fringes cliffs, lays on a rocky platform

and presents a short profile, the beach face does not have the potential to record such long time turn over events. The beach face in the central part of Birling Gap is most likely to record short time events such as spring/neap tide cycles; however on most of the storm or spring tides, the beach face features are entirely erased giving way to new ones. When considering the morphological aspect of that kind of coastal system, it seems fair to say that both tide and waves are the driving parameter shaping the beach morphology. However, there is a slight advantage to the tidal level as it will control which waves reach onto the beach profile, influencing the beach profile reshaping on every tide. Extreme wave conditions can greatly affect the beach profile during very short events such as during the Winter 2004/2005 in January (Figure 4-29), but quickly the tidal level reinstated its dominancy in the beach features development.

The conclusion from the first observation is that no clear summer or winter profile type can be recognised at Birling Gap when regarding the shape and the arrangement of features on the profile. However, when looking more closely at the general elevation changes associated with seasonality, a regular pattern is expressed. The elevation changes between the monthly profiles are greater during the winter than they are during the summer. During the summer, the wave heights are lower than during the winter and therefore the water level fluctuation is the parameter driving the greatest elevation changes on the beach by sweeping and building up berms up and down the profile. During the summer, the other parts of the beach displayed little elevation changes in comparison, direct proof of the importance of the tide on mixed sediment transport. During the winter, high energy waves induced wider and stronger run-ups on the beach face. Therefore, greater remobilisation of beach material was enabled resulting in the built up of higher berms in height and position on the profile for example. Because of these stronger and longer run-ups, the sweep zone of the berm is generally wider during the winter than during the summers.

4.4.2 Short time elevation changes on the beach profile.

During low wave conditions ($H_s < 1$ m), the topographical changes across the upper foreshore (mixed sediment beach) are very dependent on the tidal oscillations during a neap-spring-neap tide cycle. In fact, the oscillations up and down the beach of the berm

are the major topographical changes observed on the profile. The rest of the beach profile is only affected by minor changes as it has been noticed during the short survey made at Birling Gap in March 2006 and December 2006, and at Cayeux in October/November 2005.

At both sites, when the tidal cycle goes from a spring toward a neap tide, the topographical changes on the beach profile are rather limited apart from the build up of berms. Because of the evolution of the tidal levels, a large amount of the beach's coarsest material is quickly stocked up onto the mixed sediment beach. In this configuration, the actual sediment volume of coarse sediment available to the forcing hydrodynamics for LST is reduced as the waves ($H_s < 1$ m) cannot reach and remobilise the material stocked up on the beach while the HWL mark goes down; leaving the intertidal area made of coarse particles anchored into a large sandy or fine gravel matrix. The combined effect of all these parameters (low wave height and consequently small wave run-up, grain size distribution, tidal movement) has the effect to limit the topographical changes in the intertidal area and most probably LST of coarse sediment. In contrast, when the tidal cycle goes from a neap to a spring tide, the topographic changes are greater across the profile. First, a part of the material stocked up on the beach forming the berm(s) is progressively rolled back trying to find equilibrium with the increasing water level, and simultaneously loses progressively sediment to the benefit of the lower parts of the profile. If this sediment is no longer able to roll over backward because of an obstacle such as a coastal defence wall or a cliff edge, or a steeper gradient of the beach, this material is completely eroded (or partly pushed against that obstacle) to be redistributed on lower parts of the beach profile.

During high energy wave conditions (>1 m) at Birling Gap, topographical changes are greater in the berm's sweep zone. However, when looking at the area of the profile in front of the berm, the beach elevation changes from one tide to the following are generally greater than for small waves without for instance being completely drastic (At Birling Gap during the May survey for example or at Cayeux during the two storm events on November 1st and November 3rd-4th). It is obvious from these observations that a lot more transport happens than can be seen through observations of beach elevation changes. This will be considered in more detail in Chapter 5.

The detailed observations of the build up of a HWL ridge permitted the identification of phases of construction. This build up is generally initiated by an accretion of sediment at the HWL whereas erosion is predominantly characterising the lower parts of the profile. With the increasing HWL and the gravel propensity for onshore movement in relation to its threshold of motion and the swash zone action (e.g. Inman and Bagnold 1963; Carr 1983), this accumulation is quickly reshaped into a well shaped ridge characterised by a steep seaward facing slope and a rather flat surface on the landward side of its crest. The growth and development of this feature operates generally through erosion on the seaward face of the berm and lower parts of the beach profile whereas the crest and the back of the berm accrete. The elevation of the crest and the back of the beach are directly levelled with the maximum run-up height of the swash. Depending on the HWL, the upward movement of the berm when the tidal cycle goes toward a spring tide can remobilise the pre-existing berms formed at lower HWL.

4.4.3 Sediment transfer on the sandy foreshore

Exchanges of sediment between the sandy platform and the mixed sediment beach can greatly influence the sediment budget of such a system. These exchanges preferentially concern the sand size sediment particles (e.g. Costa et al., 2008) more than the pebble size sediment particles as it has been shown that gravel and pebble size particles move onshore. This is supported by Curoy et al. (2007) field observations of pebble tracer scatterings on a mixed beach which showed that pebbles hardly migrate onto the sandy platform apart from during extreme weather conditions. Costa et al. (2008) stated that the changes in elevation in the first 15 to 20 m of the sandy platform in front of the mixed sediment beach are indicators of the transfers between these two entities. This study found that just observing the first 10 to 20 m in the recycled area at Cayeux-sur-Mer can be too short to witness these sediment transfers. Indeed, the first few metres of the sandy foreshore at Cayeux in the managed area did not show any significant elevation changes (≤ 10 cm) apart from one single event on November 9th 2005. However, when looking at a longer stretch of beach, the sandy platform evolution suggests that over the survey period the upper and lower sandy platform are actually affected by significant topographical changes (Figure 4-15).

Costa et al. (2008) determined that during neap tide and low energy conditions, the sand transport on the sandy platform is mainly oriented parallel to the coast in accordance to the wave direction with a general propensity to be transported landward. In contrast, high energy wave events are mainly driving the sand size particles across-shore in a seaward direction. They also measured that the volumes of sediment remobilised on the upper sandy foreshore are approximately three times lower than the volumes transported in the lower foreshore (60 to 75 kg/m/tide compared to 200 kg/m/tide during low energy event).

During the overall period of the current study, the beach experienced a wide range of significant wave heights. They ranged from low energy waves ($H_s < 1$ m) to high energy waves (general H_s conditions > 2 m). During the storm conditions, the recycled material on the upper foreshore of the managed area provided a source of fine particles to the beach. This sand addition is most likely the reason why the beach profile in the recycled area presents a sediment surface distribution generally finer than the profile surveyed in the unmanaged area. Because of these wave conditions, the upper sandy platform suffered erosion and sediment was most likely transported alongshore according to the longshore currents and waves direction. According to Costa et al. (2008), it is also most likely that great volumes of sand were transferred from this mixed sediment beach to the sandy platform to form a sandy ridge in front of the mixed sediment beach, to dissipate more efficiently the wave energy. However the general erosion observed on the upper part of the sandy platform in front of the managed area suggests that this transferred material remobilised to downdrift areas.

Elevation changes on the first few metres of the sandy foreshore in front of the unmanaged area are much greater in comparison to the recycled area. These changes have to be related to the growth of a sand bar and the progressive infilling of the runnel directly in front of the mixed sediment beach. An interesting feature of the sand bar development is that atypically, whilst its crest was migrating landward by rapid accretion movements on its steeper face, its low slope face on the seaside was not showing erosion. This raises the question of the origin of the sand used for the growth of the ridge. Two sources of fine sediment are available; one can be transfers from the

mixed sediment beach, and the other from the longshore drift operating on the sandy platform. According to the Costa et al. (2008) model fine sediment transfer between the mixed sediment beach and the sandy platform should happen from the upper foreshore towards lower areas because of the high and moderate wave energy conditions as experienced by the foreshore during the current study. However, it is difficult, just by examining the beach profiles, to exactly define what the sediment volumes are that are associated with these transfers. It seems reasonable to assume that the sediment volumes exchanged between the two domains (sandy platform and mixed sediment beach) are most likely insufficient to explain such drastic elevation changes observed on the sandy foreshore (rates of accretion and erosion on the sandy platform and the mixed sediment beach are discussed later in Chapter 6).

In contrast, the great volumes of sand remobilised over the sandy platform by the drift are most likely to explain the amplitude of these elevation changes. From these observations, the following scenario of evolution can be proposed: Under the forcing hydrodynamics the sand bar, which has its updrift extremity connected to the mixed sediment beach, migrates quickly in both directions, landward and downdrift. The quick infilling of the runnel corresponds in fact to the bar's point of anchor to the mixed sediment beach passing through the location of the surveyed profile. It is most likely that the erosion observed in the upper part of the sandy platform in front of the recycled area is actually feeding the rapid growth of the sand ridge and the general elevation of the sandy platform (see Figures 4-19 & 6-16).

This observation raises questions about the near future of this sand bar and the extent to which such dynamic features feed the mixed sediment beach considering its clear landward migration. It is known from this study that the downdrift areas of Cayeux have even larger intertidal areas and that these areas experience great sand accretions, resulting in the rapid infilling of the Somme Estuary. With such transport dynamics, it is surprising to observe that the sand content of the mixed sediment beach is only on average about 20%. Given that transfers of sand are known to exist between the two domains of the composite beach, this raises the question as to whether there is only a limited amount of sand that a mixed beach can hold under certain conditions. This is a

theme that clearly needs further and more detailed investigation as it will directly influence the permeability of the beach.

4.4.4 Influence of sediment recycling on beach behaviour

The comparison of the two profiles surveyed at Cayeux-sur-Mer allows the assessment of the influence of recycled or recharged material on the beach profile behaviour. During the entire fieldwork period, the recycled sediment sustained a very steep seaward face quite often marked by micro to macro-cliffing. Cliff features are often observed on mixed recycled/recharged beaches and reported (e.g. McFarland et al., 1994; Humphreys et al., 1996). This morphological feature is typically attributed to the high proportion of sand in the grain size distribution, the compaction and the reduced permeability (Whitcombe, 1996; Horn and Walton, 2007). Because of this feature, the beach slope in the recycled area is steeper than in the unmanaged area.

When the top section of the beach profile corresponding to the recycled sediment is not taken into account to determine the beach slope and then compared to the unmanaged section profile, it can be seen that both angles on each profile are very close to each other (differences $<0.7^\circ$). These differences are however greater when the recycled material is reached and eroded by the waves. Indeed, between October 31st and November 5th, when the waves reach the recycled material, the beach slope in the recycled area displays great changes oscillating from 5.9° to 6.8° . During that time, the beach profile slopes between the recycled and the unmanaged areas differ by more than 0.7° (up to 1.2°). The redistribution of the recycled material eroded onto the beach face is most likely the parameter influencing such variations of the beach angle. This statement is supported by the fact that the beach profile in the unmanaged area does not display such variations in the beach gradient over the same time period. A substantial addition of sediment in the upper parts of the beach will clearly steepen the beach profile whereas addition on the lower parts of the beach will lower the angle.

As discussed in Chapter 2, the recycled material is a mixture of sand and shingle directly extracted from the north of Cayeux. This recycled material has the same properties as the general beach distribution, that is to say a bi-modal particle size

distribution with peaks in the medium-sized gravel (10 – 20 mm) and cobble (40 – 50 mm) size range and contains approximately 20% sand (Dolique, 1998; and confirmed orally by the local authorities, 2005).

When looking briefly at the surface sediment distribution on both profiles (Figure 4-35 & 4-36), the beach profile surveyed in the recycled area generally presented finer classes of sediment than on the profile surveyed in front of Cayeux only located approximately 800 m northward (approximately 580 m northward of the recycled area). It seems most likely that the extra sand content of the recycled material is poorly integrated within the gravel. This difficulty to percolate might be related to the fact that the voids between the gravel and pebbles in the recycled area are already overloaded with sand (Figure 4-35) whereas the finer particles in the natural area can percolate more freely and deeply into the beach face; therefore giving the impression of lateral grading.

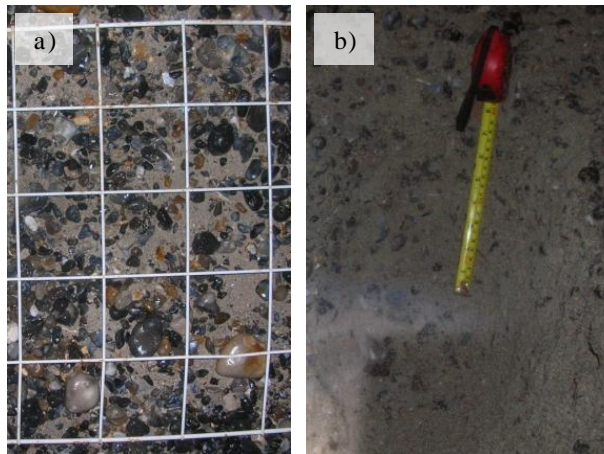


Figure 4-35 The beach at Cayeux-sur-Mer, November 6th. a) Sediment surface. b) Internal sediment distributions in the recycled area.

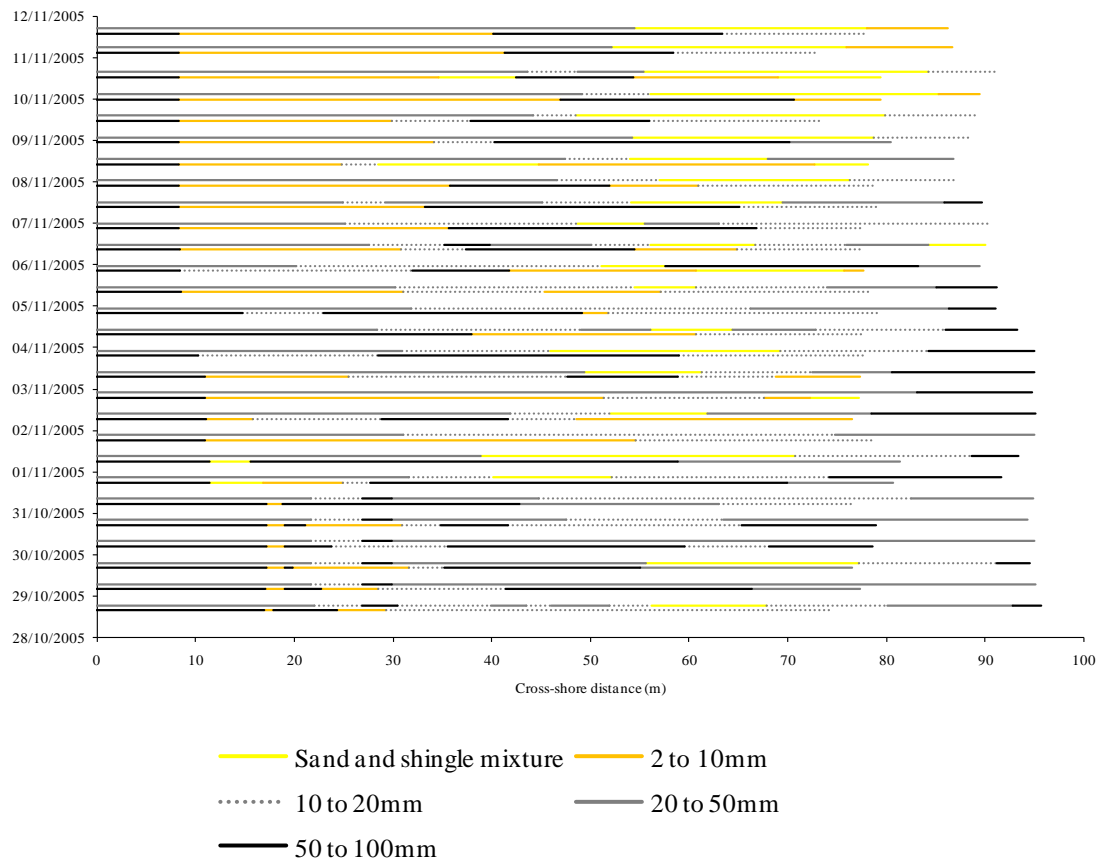


Figure 4-36 Representation of the surface grain size distribution (surface sampling) observed on both profiles surveyed at Cayeux-sur-Mer on a tidal basis. The profiles are twinned for each low tide. The above grain size distribution line represents the profile located in the natural area (Profile B) and the below the profile located in the recycled area (Profile A).

4.4.5 Response to storms and extreme storms

When considering the effect of storms on the beach, it was decided to only look at periods when the significant wave height (H_s) was greater than 2 m during the two years of regular monthly surveys at Birling Gap. This choice had the advantage of fitting the seasonal topographic patterns identified earlier by focusing almost exclusively on winter (Figure 4-5). Despite the observation of a greater variability in the profile elevation changes during the winter (Figures 4-29 & 4-31), the beach profile seems to oscillate around an average profile, meaning that the erosion/accretion movements affecting the beach profile are reversible most of the time. This only proves that the beach profile in the centre of the beach, which is where a maximum of sediment material is stocked, is quite stable even during most of the stormy conditions.

In an attempt to identify the real impact of stormy periods on the beach at Birling Gap, it was decided to use the beach volume changes derived from the beach topographical surveys collected over the two year study period (Figure 4-37). The beach volume at Birling Gap decreased by approximately 70,000 m³ to 100,000 m³ over the two year period of survey. This measurement re-enforces the problem encountered by the East Sussex coast in relation to the lack of sufficient sediment supply to counter balance the longshore drift and sustain naturally the beaches volume.

On a monthly basis between August 2004 and July 2006, the beach volume was affected by oscillating periods of accretion and erosion. These oscillations were important at the start and the end of the winter 2004/2005 but they were compensating each other in general apart from one single event approximately around December 2004-January 2005. This event had a tremendous impact on the beach volumes which never recovered ever after. The beach over the winter 2005/2006 displayed a fairly consistent volume (approximately 19,000 m³). During the summers, the beach volume changes generally showed progressive erosion. This would indicate that summer conditions are more subject to enhance greater net longshore sediment transport at Birling Gap than winter conditions. On the other hand, winter conditions are most likely to cause significant beach topographical and volume changes; however, the changing wave incidences close to the orthogonal to the beach are most likely to compensate each other. Indeed, during the summers, the incident wave direction is generally >90° (referred to the coast orientation N132°, therefore the orthogonal of the coast has a direction of N222° which corresponds to a wave approach of 90°) and their direction is fairly consistent, changing only very occasionally. This means that the longshore transport is mostly directed one way, eastward.

On the contrary, winter conditions are characterized by changing wave directions around the point of orthogonal approach. On average, these changing directions are most likely to compensate each other. This would mean that at Birling Gap wave direction has a greater impact on sediment transport than wave height on the yearly sediment budget.

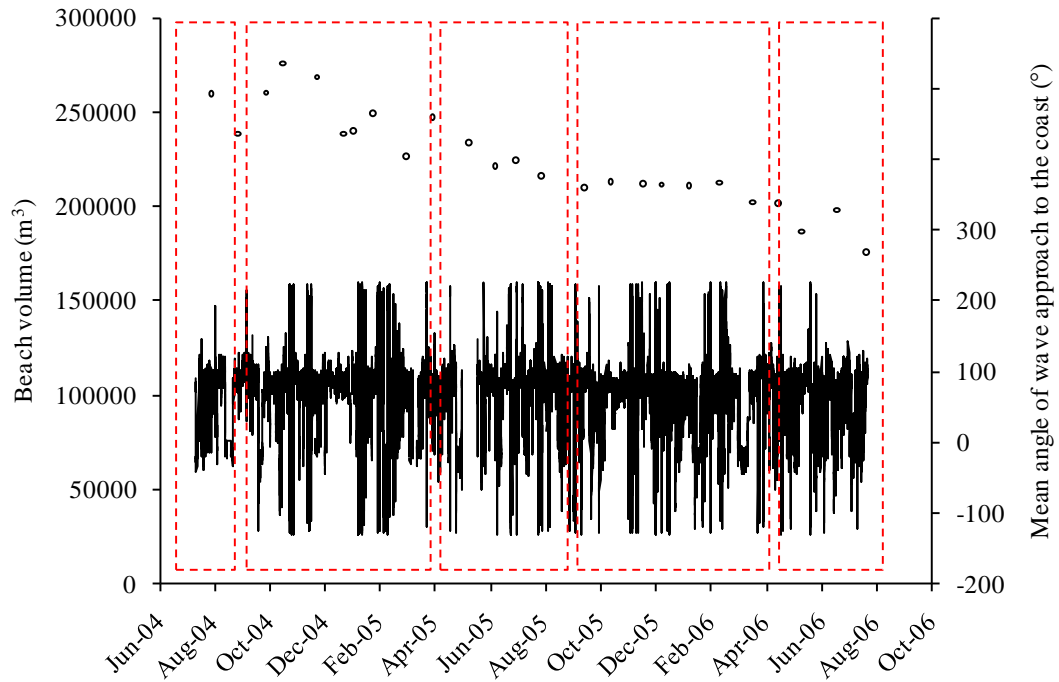


Figure 4-37 Evolution of the beach volume over time in association to the mean wave approach. The circles represent the sediment volume measured for every month, the plain black line the mean wave approach and the dashed red boxes represent the wave climate seasonality (alternance of summer and winter wave conditions).

It was mentioned earlier that the winter 2004/2005 was characterized by beach erosion between December 2004 and February 2005. This event irreversibly affected the beach volumes which never completely recovered from it over the period of survey. During this event, the entire western part of the beach was eroded uncovering the underlying chalk that normally underlies the mixed sediment beach (Figure 4-38). The beach profile surveyed close to the access steps showed that the middle and eastern part of the beach at Birling Gap displayed accretion between December 2004 and January 8th 2005. After only ten days, the same beach profile recovered an elevation comparable to the profile surveyed in December 2004; and in February 2005 the volume of the beach displayed gain of sediment (Figure 4-37). The quick response of the beach profile and volume after such a dramatic event for the beach shows how reactive mixed beaches are to the wave conditions. This quick reactivity plus the fact that it is a relatively closed sediment cell are probably the reasons why such a beach still exists at Birling Gap.



Figure 4-38 The beach at Birling Gap before, during and after the stormy period of December 2004/January 2005. The red arrows mark the same location on the pictures.

It is relevant to point out that the erosion volume measured over the two year survey, 70,000 to 100,000 m³, is concerning. Considering the total volume of the beach (approximately 250,000m³ to 300,000m³), the sustainability of Birling Gap's beach is critical if such loss was consistent. However, old maps and photography bear witness of this beach existence over the years and it still exists today. This means that some sediment supply is most definitely feeding the beach in new material attenuating the natural erosion of that stretch of beach. The most plausible source of sediment would be the updrift beach at Cuckmere Haven which material travels along the cliff plus the cliff falls occurring in the area between these beaches.

4.5 Conclusions

The regular and sporadic collection of beach topography at both sites has facilitated the observation of the extent to which a mixed beach profile responds to hydrodynamic conditions in three different kinds of environment:

- (i) A mixed beach fringing cliff;

- (ii) A managed mixed beach, and;
- (iii) An unmanaged mixed beach.

The fringing beach at Birling Gap generally sustains steeper gradients, has a shorter profile, presents a lot less variability of grain size distribution and has a lot less potential to record morphological features than the barrier at Cayeux-sur-Mer. Despite these differences, each environment proved to have a profile that responded extremely quickly to the changing hydrodynamics. The combined effect of the HWL and the wave height in equal proportion seems to be the driving parameters for the beach profile changes.

Because of the shortness of their profile and the presence of a solid, fixed, feature at their back, fringing beaches have difficulty in showing typical seasonal profiles (e.g. Pontee et al., 1995) or even to record longer time scale patterns. However, seasonality patterns can be deduced from the monthly changes in the beach elevation ranges. Generally, beach face elevation change ranges are greater during the winters.

The berm is the most consistent feature on mixed beaches by its presence. The greatest topographical changes on the beach face of mixed beaches are associated with the variations of both location and height of the berm, which is itself associated with the combined effect of the HWL and the wave height. Apart from the elevation changes linked to the berm and the beach step variations, the rest of the beach face presents very little elevation changes over time. The short time between the surveys allowed examining in detail the processes of formation and development of the HWL ridge over time.

The sediment transport as well as the sediment transfers on the sandy platform cannot be neglected in the sediment budget of the mixed sediment beach as they can have a direct impact the mixed beach profile through hydraulic conductivity (e.g. Mason and Coates, 2001) and wave dissipation (e.g. Costa et al., 2008). However, very little is known yet about the processes of interaction between the sandy platform and the mixed sediment beach.

The presence of recycled/recharged material at the top of the beach has been proven to have a significant impact on the beach profile. First, the beach gradient is steepened by the addition of freshly added material which makes it more reflective. Second, the beach face hydraulic conductivity will be determined by the grain size distribution of this additional source material. By adding sand, the hydraulic conductivity will be reduced on the beach face. Therefore the wave energy will not be dissipated as efficiently as on a pure gravel beach, resulting, theoretically, in more sediment transport.

Finally, in a fringing system such as Birling Gap it was observed that wave direction can have an even greater impact on sediment transport than the wave height itself. As observed by this study, the beach at Birling Gap is more vulnerable to sediment loss during summer conditions, low H_s but consistent wave direction, than during winter conditions, high H_s but changing wave direction. The water level is consequently a critical factor to take into account for the LST as it will drive the length of the active profile especially during calm or moderate conditions.

Now that the morphological evolution of the beach profile has been examined in detail, it is important to look at the actual thickness of sediment that is remobilised during each tidal episode. Such an observation will give an indication of the actual volume of beach material involved in the sediment transport.

Chapter 5. ACTIVE LAYER AND MIXING DEPTH

5.1 Introduction

This chapter describes and quantifies the spatial and temporal variations of the active layer thickness in both alongshore and across-shore directions. Measurements of the mixing depth are correlated with the main parameters of the forcing hydrodynamics, including the wave height, wave period, wave direction and, the grain size distribution so that clear relationships, of the type found on sandy beaches, are investigated (e.g. Ciavola et al., 1997; Bertin et al., 2008). From these relationships, a comparison is drawn between the behaviour of the active layer on both sand and mixed beaches in order to quantitatively examine the differences. Comparisons between the study sites, and with the very few observations on other gravel beaches available in the literature, are also made.

Knowledge of the thickness and width of the moving sediment layer on a beach is essential to the calculation of the longshore drift (Chapter 1 Figure 1-1). Despite its importance, studies investigating the layer of sediment affected by the forcing hydrodynamics on gravel beaches are still rare. This does not represent a lack of interest

from the scientific community but, on the contrary, results from a lack of appropriate techniques for carrying out such measurements in coarse sediment environments or in high energy wave conditions. In contrast, on sandy beaches, the moving layer of sediment has been researched extensively, a range of methodologies have been developed, and correlations between the hydrodynamic conditions and the beach characteristics have been drawn.

5.2 Background

5.2.1 Review of the active layer on sand beaches

Although more research has been carried out on sand beaches, Ferreira et al. (2000) point out how limited knowledge about the active layer on sand beaches still is and emphasise the need to make some progress on our understanding of gravel beaches.

Despite recognition of the necessity to acquire more knowledge on sandy beaches, a few empirical formulae have been produced. These have been derived from field measurements via the application of widely accepted field methodologies such as coloured sand columns, graduated poles (equipped with washers or not) and finally a cut off depth determined by the recovery of 80 % of the tracers in the sample cores. The relationships published in the literature, based on in situ measurements, are generally expressed using the average “depth of mixing” (Z_m) and the breaking wave height (H_b). For sand beaches this relationship varies from:

$$\begin{array}{ll} \text{(Sunamura and Kraus,} & Z_m = 0.027H_b \\ \text{1985)} & \end{array} \quad (5.4)$$

to

$$\begin{array}{ll} \text{(Otvos, 1965;} & Z_m = 0.4H_b \\ \text{Williams, 1971)} & \end{array} \quad (5.5)$$

To explain these differences, a range of parameters in addition to the breaking wave height are considered to influence the mixing depth. These include: the foreshore slope (Williams, 1971; Ciavola et al., 1995; Jackson and Nordstrom, 1993; Ferreira et al., 2000), the beach grain size (King, 1951; Sunamura and Kraus, 1985; Ferreira et al., 2000), the effective shields parameter (Sunamura and Kraus, 1985), the wave direction (Bertin et al., 2008), the wave period (Williams, 1971; Sunamura and Kraus, 1985; Ciavola et al., 1995), the type of breakers (Williams, 1971; Sherman et al., 1994; Caviola et al., 1997), the longshore processes (Sherman et al., 1993, 1994), the beach features such as bedforms migration (Greenwood and Hale, 1980; Sherman et al., 1993) or the presence of beach cusps (Ferreira et al., 1998), the tidal range (Duncan, 1964), and the sampling position across-shore (Komar, 1983).

Aiming to develop an universal empirical expression applicable for both gentle and steep slopes on sandy beaches, Ferreira et al. (2000) derived a correlation that included the foreshore slope and the breaking wave height, both of which are the most commonly recognised as the parameters influencing the mixing depth (Williams, 1971; Jackson and Nordstrom, 1993; Ciavola et al., 1995; Ferreira et al., 2000). The relationship obtained is (Equation 5.6):

$$Z_m = 1.86 H_b \cdot \tan\beta \quad (5.6)$$

where Z_m is the mixing depth, H_b the breaking wave height and $\tan\beta$ the beach gradient. In agreement with other studies (King, 1951; Otvos, 1965; Jackson and Nordstrom, 1993; Ciavola et al., 1997), this empirical formula suggests that the mixing depth is greater on steeper sandy beaches than on gently sloping sand beaches. Across the shore, most authors seem to agree on the spatial variability of the mixing depth on sandy beaches, crediting the greatest mixing depth of sediment to the wave breaking zone (Inman et al., 1980; Kraus, 1985; Otvos, 1965; Williams, 1971; Ferriera et al., 2000).

5.2.2 Review of the active layer on gravel beaches

In comparison to sandy beaches, knowledge on the active layer on gravel beaches, and more specifically on mixed beaches, is scarce. Studies focusing on the active layer on

gravel beaches are rare and inconsistent because of the lack of a clear and consistent methodology and the poor performance of the few techniques available in high energy conditions. Despite this, crucial benchmarks have been set by previous studies.

King (1951) looked at the depth of disturbance on sand beaches and noted that this depth could be expected to be greater on gravel beaches because of the grain size and the permeability of the beach particles (pebbles and cobbles). There appears to be no published record of any studies to verify this assertion for at least the following forty years. The next major step forward in understanding the dynamics of the active layer on gravel and mixed beaches did not occur until Stapleton et al.'s (1999) study. Using tracer columns settled into the beach face at Lancing (West Sussex, UK), Stapleton et al. (1999) measured the depth of disturbance at various locations across-shore and observed that over the tidal influx the greatest depth of disturbance was close to the wave breaking zone. Ivamy and Kench (2006), using rods implanted into the beach face on a mixed sand and gravel beach, observed the greatest depth of disturbance in proximity of the break point step on the beach where the turbulence of the short period wave breaking is the greatest.

In the light of these findings the assumption of a uniform layer of sediment, commonly made in the models and empirical formulae to predict the sediment transport, has to be reconsidered with care. Based on the accumulated knowledge on the mixing depth (or depth of activation or depth of disturbance) on sandy beaches in contrast to that for gravel beaches, it is necessary to investigate the parameters that are driving the mixing depth as the calculation of LST relies on it so that the lag of knowledge is filled and models or empirical formula predict more accurately sediment transport. Using the data collected during this study, the relationship between active layer depth and the following parameters is investigated: wave height, wave period, wave direction and beach grain size distribution.

5.3 Measurement of the Active Layer and the Mixing Depth at Cayeux-sur-Mer and Birling Gap

The methodology and exact location of the measurements of the active layer and beach profiles are described in Chapter 3 Section 3.4.4 and Figures 3-11 & 3-12 & 3-15. Results collected from the painted pebble columns at both sites are displayed in full in Appendix IV. Both the mixing depth from the pre-event surface and the accretion above the remaining painted pebble in the columns are displayed.

At both study sites (Appendix IV, Tables IV-1 to IV-10), it can be seen that the chances of successfully recovering a column after each tide is closely linked to its location across the shore. The columns on the upper beach were recovered more often, giving an almost continuous and accurate set of values for the active layer. In contrast, the columns set into the lower beach were seldom recovered and often had to be replaced. This low recovery on the lower beach measurements occurs for two key reasons. First, the beach step is highly mobile, and second the columns on the lower beach, by necessity because of the shallowness of the beach, do not extend as far into the beach as those on the middle and upper sections. Generally the painted pebble columns were buried as deep as possible but because of a sand dominant matrix and the water springs at Cayeux-sur-Mer, and the chalk platform at Birling Gap, the depth of the lower beach columns was sometimes only about 10 to 15 cm. Despite efforts to bury columns as deep as possible in most cases the depth of burial of the columns was not deep enough to measure the full thickness of the beach material affected by hydrodynamic forcing at this particular location on the beach.

5.3.1 Variation of the active layer alongshore

The survey strategy for the active layer measurements, using multiple survey profiles along the beach, made it possible to identify the alongshore variations that exist between measurements at the same location along the beach (over a 75 m stretch of beach). This survey strategy of the active layer was designed to examine, for mixed beaches, the assumption that existing longshore drift models make about a uniform

across-shore layer of sediment is transported alongshore. In addition, given that exact values of the active layer are sometimes missing for a particular location on each profile, the use of replicate profiles increases the chances of obtaining an exact value of the active layer at each measurement location along a beach profile.

Observations of alongshore topographical changes in the surveyed area can be used as a first indicator of the degree of active layer homogeneity alongshore. If each profile presents the same shape and evolves in the same way, there is a high probability that the sediment transport is homogeneous along the stretch of beach surveyed. Figures 5-1 & 5-2 display the beach profile shapes at the start and end of the survey periods at Cayeux-sur-Mer and Birling Gap. These clearly show how all the beach profiles surveyed are of similar shape at the start of the experiments, and how they evolve similarly by the end of the experiments. From these observations, it is reasonable to assume that if any significant differences have occurred in the active layer thickness between similar across-shore locations on different profiles, topographical variations are unlikely to be the parameter responsible.

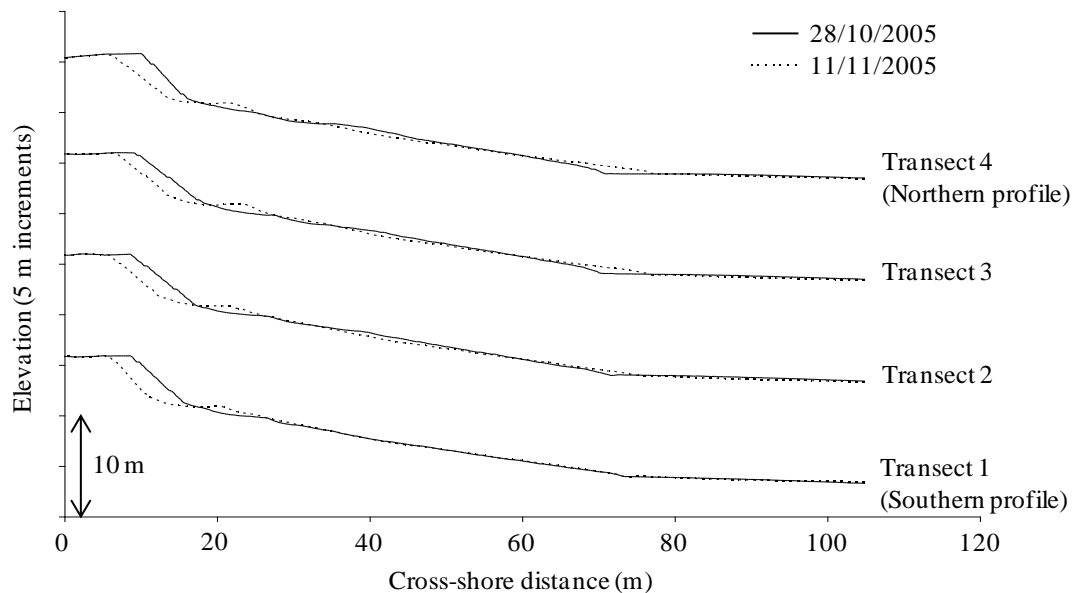


Figure 5-1 Profile morphologies at the start and end of the survey period at Cayeux-sur-Mer.

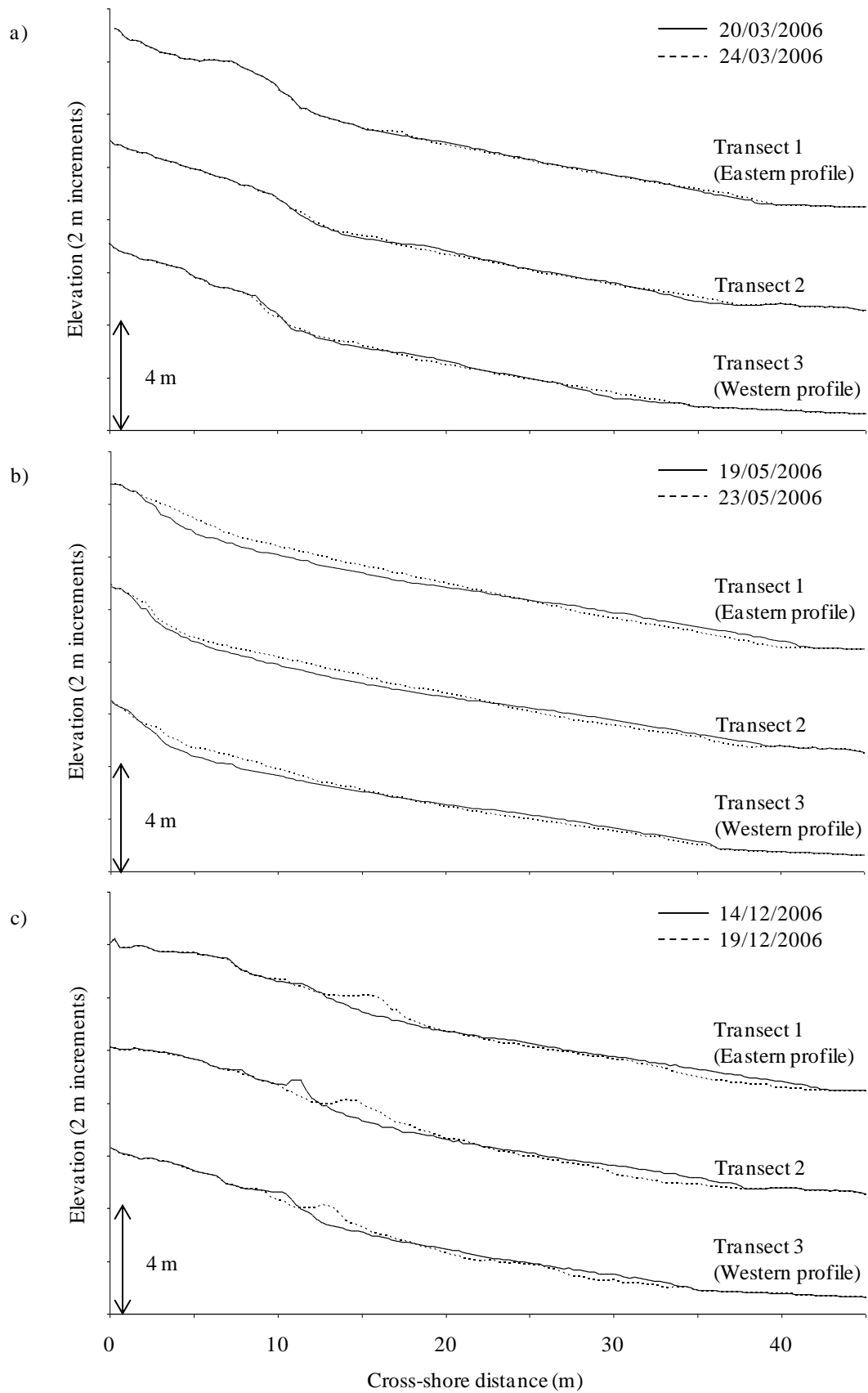


Figure 5-2 Profile morphologies at the start and end of the survey period at Birling Gap. a) In March 2006. b) In May 2006. c) In December 2006.

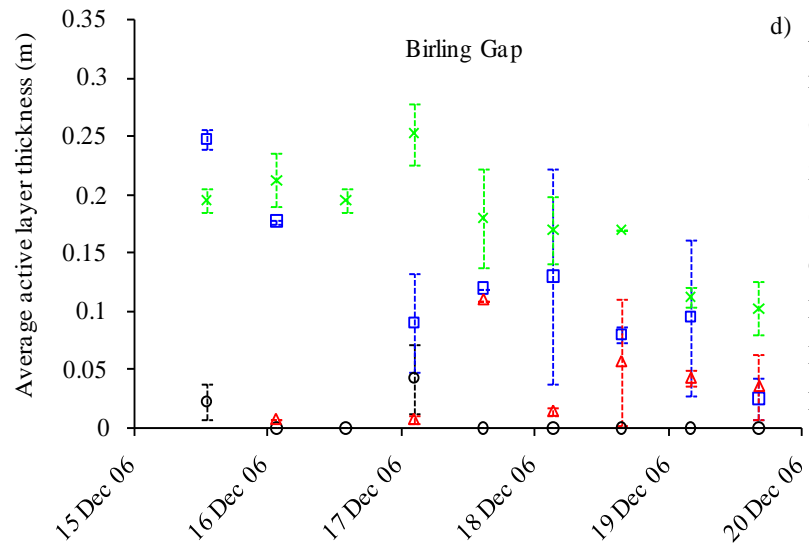
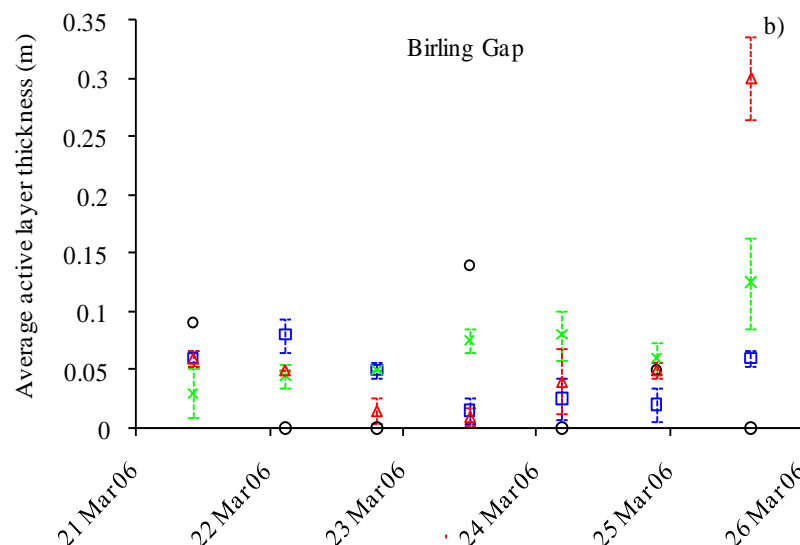
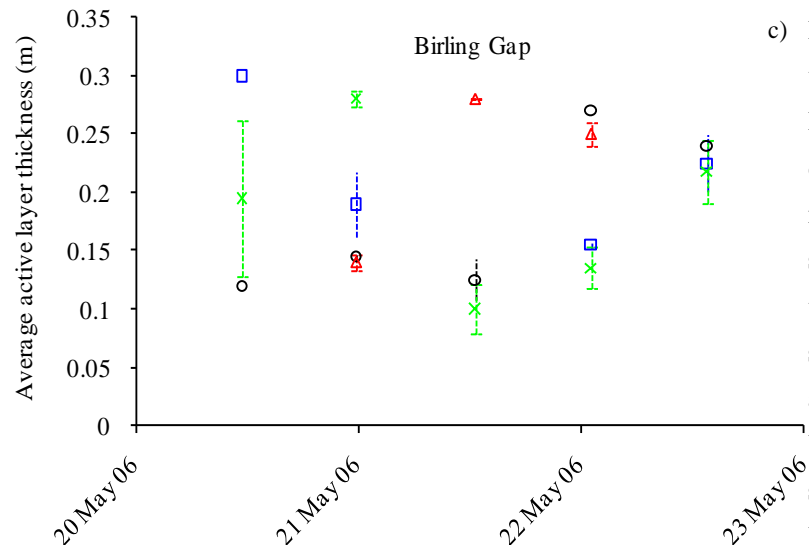
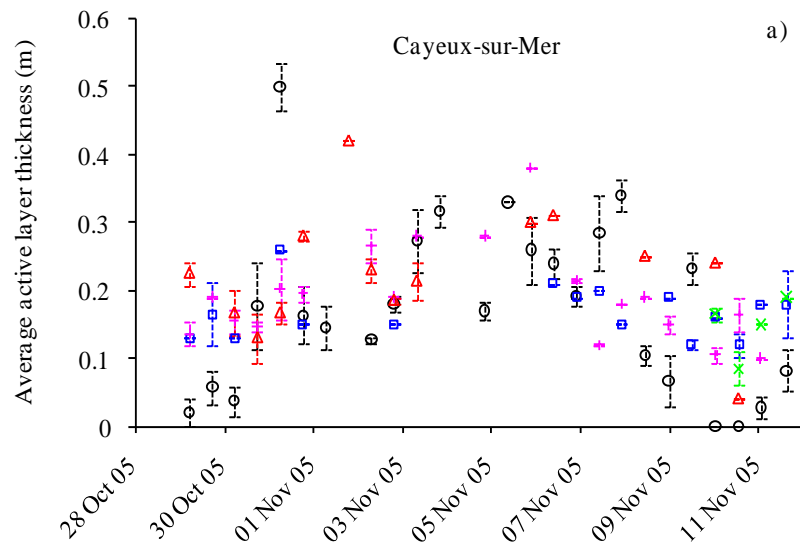


Figure 5-3 Plot of the average active layer thickness observed at identical cross-shore location on the various profiles surveyed. The associated error bars represent the standard deviation between the measurements. a) At Cayeux-sur-Mer in October/November 2005. b) At Birling Gap in March 2006. c) At Birling Gap in May 2006. d) At Birling Gap in December 2006.

○ Upper beach □ Upper middle beach + Middle beach × Lower middle beach △ Lower beach

Figure 5-3 displays the average active layer measured between equivalent across-shore locations on the different beach profile during the same tide. The standard deviation was determined and displayed for each of these values. At both field sites it can be observed that the standard deviation of the active layer thickness between each profile rarely exceeds 10 cm. In fact, it happened only five times for all the data collected during the study periods: at Cayeux-sur-Mer on October 30th and November 7th 2005, both on the upper beach; at Birling Gap on December 17th and 18th 2006 respectively on the lower beach and on the upper middle beach; and, at Birling Gap on May 20th 2006 on the lower middle beach. This indicates very little variation alongshore of the active layer thickness, especially given that the precision of the methodology was estimated to ± 5 cm (Chapter 3 Section 3.4.4). As a result, it can be assumed that as long as no change in the characteristics of the beach (morphology, orientation, elevation and certainly grain size distribution) and the forcing hydrodynamics occurs, the active layer variations alongshore are negligible. Based on this point, the assumption of an alongshore homogeneous layer of sediment involved in the sediment transport that is made in the sediment transport models (Chapter 1 Figure 1-1) can be considered valid on mixed beaches.

5.3.2 Variation of the active layer across-shore

To appropriately illustrate the across-shore variation of the active layer thickness, it was decided to use a combination of the beach topographic profiles before and after the high tide and the resulting measurements of the active layer. Please note that it was decided to use transect 2 at Cayeux and transect 3 at Birling Gap to represent the beach profiles (Chapter 3 Section 3.4.4; Figures 3-11 & 3-12). This combination allows observation of changes in the beach cross-section and sediment transport from tide to tide (Figures 5-4 & 5-5). This approach also reveals whether some areas of the beach face are subjected to more transport than others. Knowing that on gravel beaches some areas are affected by specific hydrodynamic parameters, this also facilitates the identification of the parameter responsible for most of the transport. The first impression when looking at the results (Figures 5-4 & 5-5 and Appendix IV) is that the active layer thickness is closely related to the beach topographical changes.

The movements of morphological features such as the berm on the upper part of the beach or the beach step on the lower part of the beach drive the active layer thickness in their surroundings. For example, an active layer thickness up to 55 cm was measured on the upper beach on December 31st 2005 at Cayeux-sur-Mer corresponding with great berm erosion (Figure 5-4; Appendix IV Table IV-4). From time to time, despite the fact that some exact measurements were missing due to methodological limitations (loss of a column, Chapter 3), the disturbance on the lower part of the mixed beach proved to be as great as that on the upper part of the beach with an active layer thickness being sometimes greater than 45 cm at Cayeux on December 29th (Appendix IV Table IV-4).

In contrast, at both field sites, the middle part of the mixed beach did not display any particular morphological features that migrated up or down the beach face. Cusps and horns that commonly shape gravel beaches were rarely expressed during the survey periods at either site. However, this zone of the beach showed, on average, a thick or thicker active layer than the other part of the beach at both sites especially when topographical changes were minimum at both upper and lower part of the mixed sediment beach (Figure 5-3).

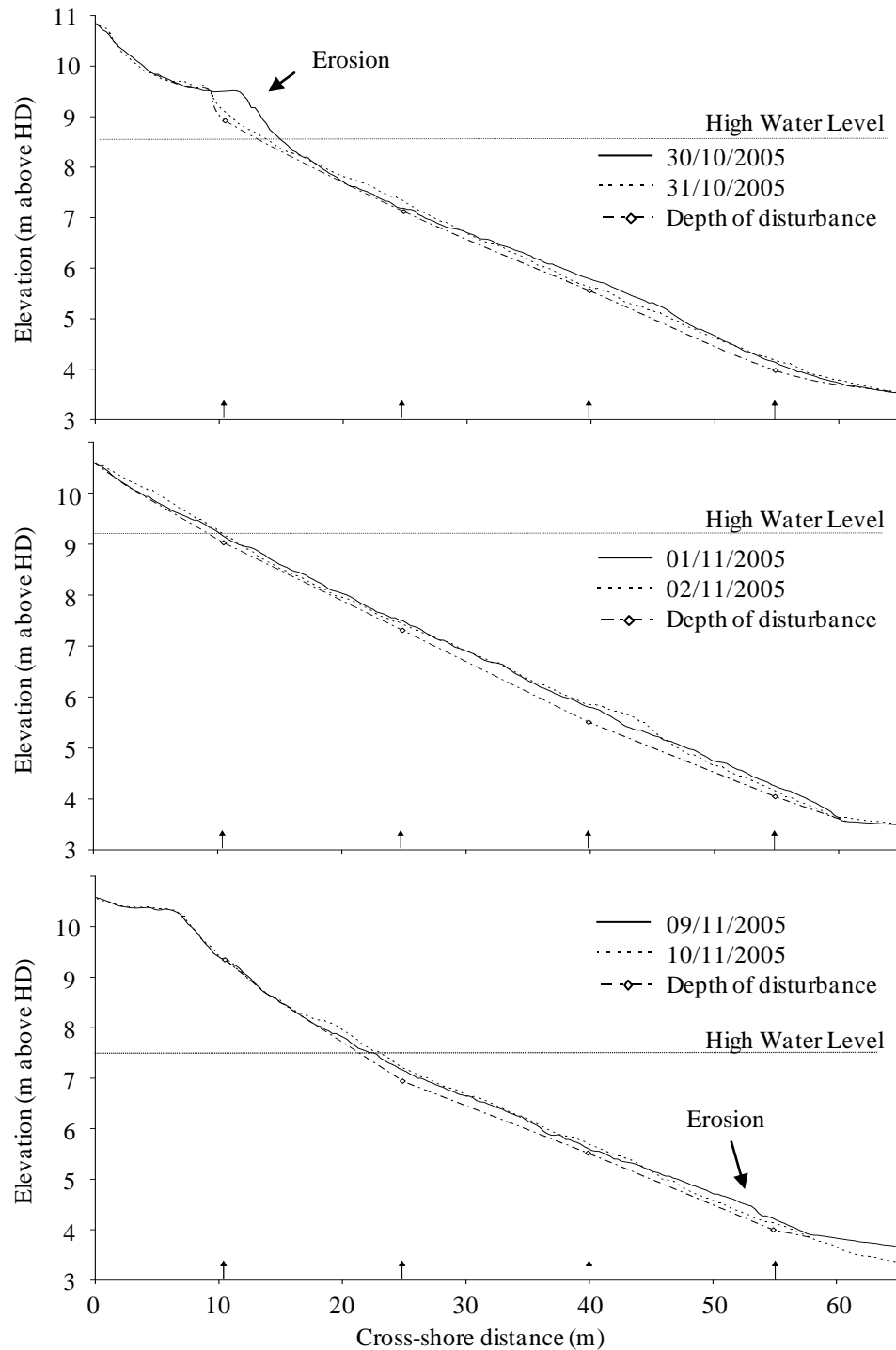


Figure 5-4 Examples of profile evolution (recorded along transect 2) and active layer measured during the survey period at Cayeux-sur-Mer. The black arrows show the location of the active layer measurements. Note that the elevation is referred as above Hydrographic Datum (HD, the French Hydrographic Datum corresponds to the lowest astronomical tide level) and the vertical exaggeration is 3:1.

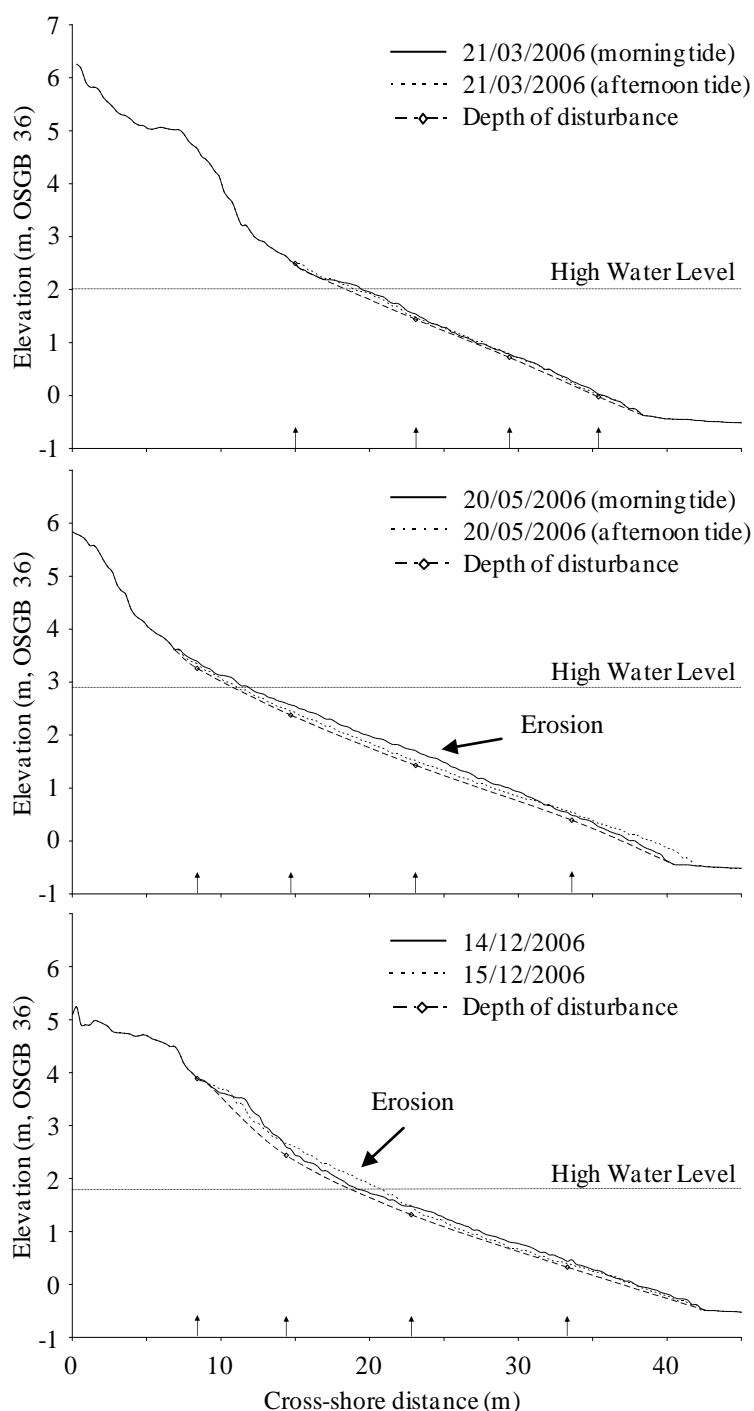


Figure 5-5 Examples of profile evolution (recorded along transect 3) and active layer measured during the survey period at Birling Gap. The black arrows show the location of the active layer measurements. Note that the elevation is displayed as in the British national grid reference system OSGB36 (Ordnance Survey Great Britain 1936) and the vertical exaggeration is 3.8:1. **Part 1.**

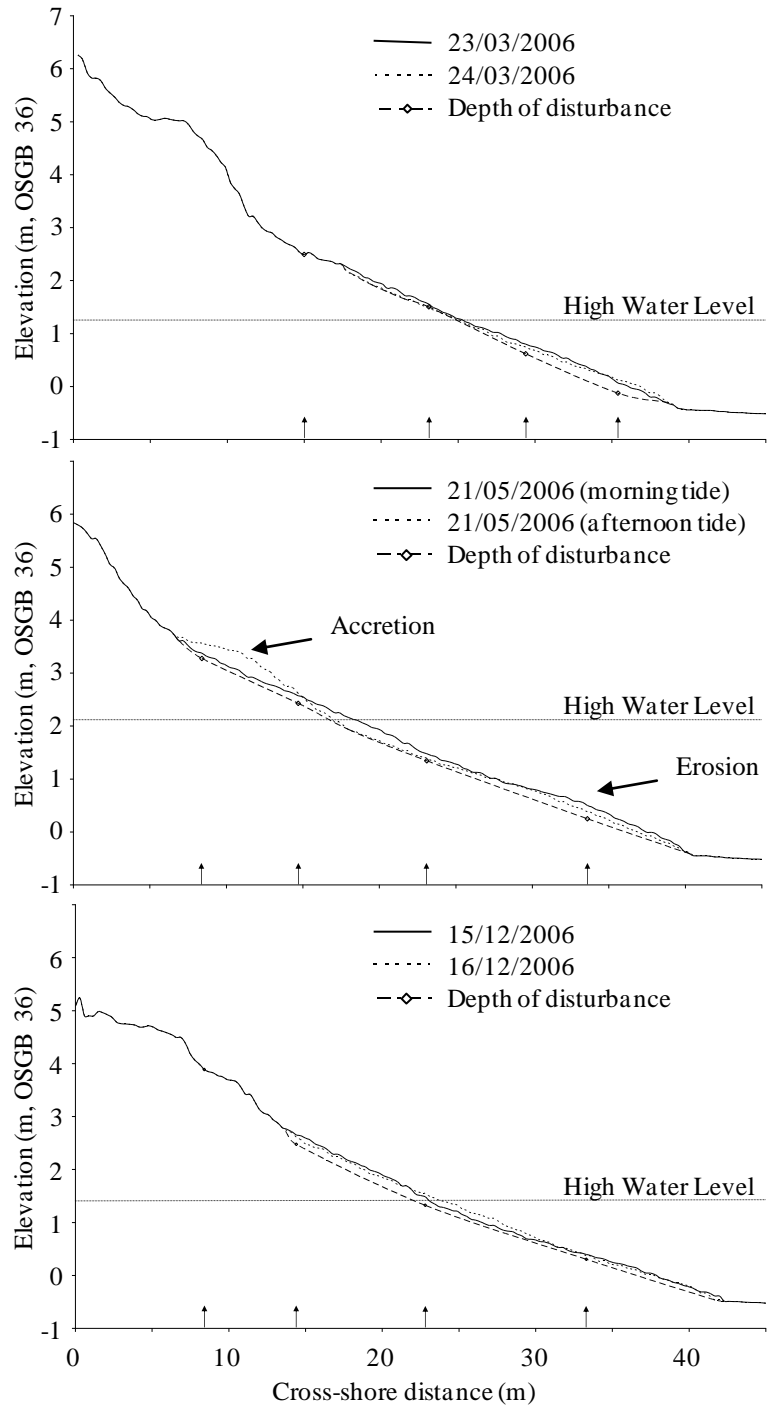


Figure 5-5 Examples of profile evolution (recorded along transect 3) and active layer measured during the survey period at Birling Gap. The black arrows show the location of the active layer measurements. Note that the elevation is displayed as in the British national grid reference system OSGB36 (Ordnance Survey Great Britain 1936) and the vertical exaggeration is 3.8:1. **Part 2.**

5.3.3 Variation of the active layer over time

Figures 5-6 & 5-7 provide a useful insight into the evolution of the painted pebble columns in association with the beach elevation changes on every tide during the short period surveys. Such observations help to better appreciate what thickness of the beach is really “active” and contribute likely reasons to help explain column non-recovery.

These figures show how the topographic changes drive the recovery of the painted pebble columns and therefore the active layer thickness too. This is particularly noticeable when looking at the data collected on the upper part of the beach, which is marked by large accretion or erosion movements mostly caused by the migration of morphological features up and down the beach i.e. the berm in this particular location. As an example of these large mass sediment movements (Figure 5-6), at Cayeux-sur-Mer on the upper beach between the second tide on October 30th and the following tide on the October 31st, the beach elevation decreased sufficiently to remove the painted pebble column set up on the 30th. This event was associated with the landward retreat of the berm. The opposite effect can be seen at Birling Gap (Figure 5-7) between the two tides on the 16th of December where accretion (beach elevation increases of 40 cm on the upper beach measurement site for example) on the upper beach has most likely buried the residual painted column. This accretion is linked to a phase of berm building.

These observations and figures illustrate the performance and limitations of the technique used to measure the active layer, and also permit an insight to the mobile sediment layer into the beach. However, by quantifying the active layer depth, it is possible to quantitatively investigate the parameters that may influence the mixing depth such as for example the grain size, the wave height, the wave direction, the wave period and the beach slope.

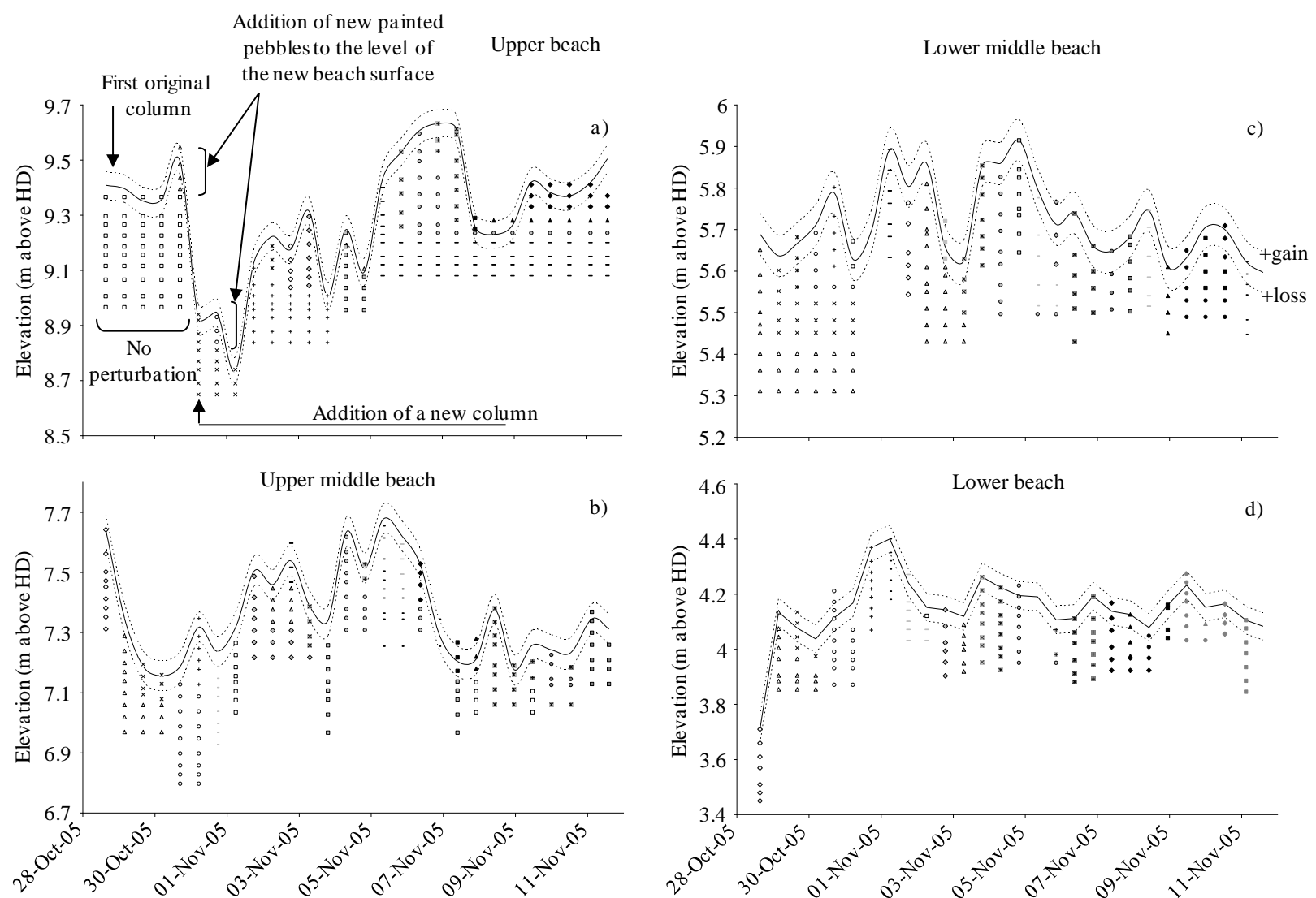


Figure 5-6 Active layer and topographic changes during the 2005 winter survey period at Cayeux-sur-Mer for one profile (transect 2): a) upper, b) upper-middle, c) lower-middle and d) lower beach. The plain black line shows the topographic changes recorded by the D-GPS and the dashed black lines show the margin error (± 5 cm). Pebble columns used to measure active layer variations are shown by the vertical lines of symbols. For example, on the upper beach, the first column deployed (afternoon October 28th; white squares) remained intact over the first four tides. To keep pace with a topographic elevation of 18 cm on the fifth tide, new pebbles were added (afternoon October 30th; white triangles). On the sixth tide a fall in beach elevation obliterated the existing column and it was replaced (black Xs). Each subsequent addition of new pebbles or complete new column is shown by different symbols. For example, accretion between the afternoon of November 4th and the next morning meant that a complete new column was installed on the morning of November 5th. Variations in pebble columns deployed in the remainder of the beach (upper-middle, lower-middle and lower) are illustrated in the same way.

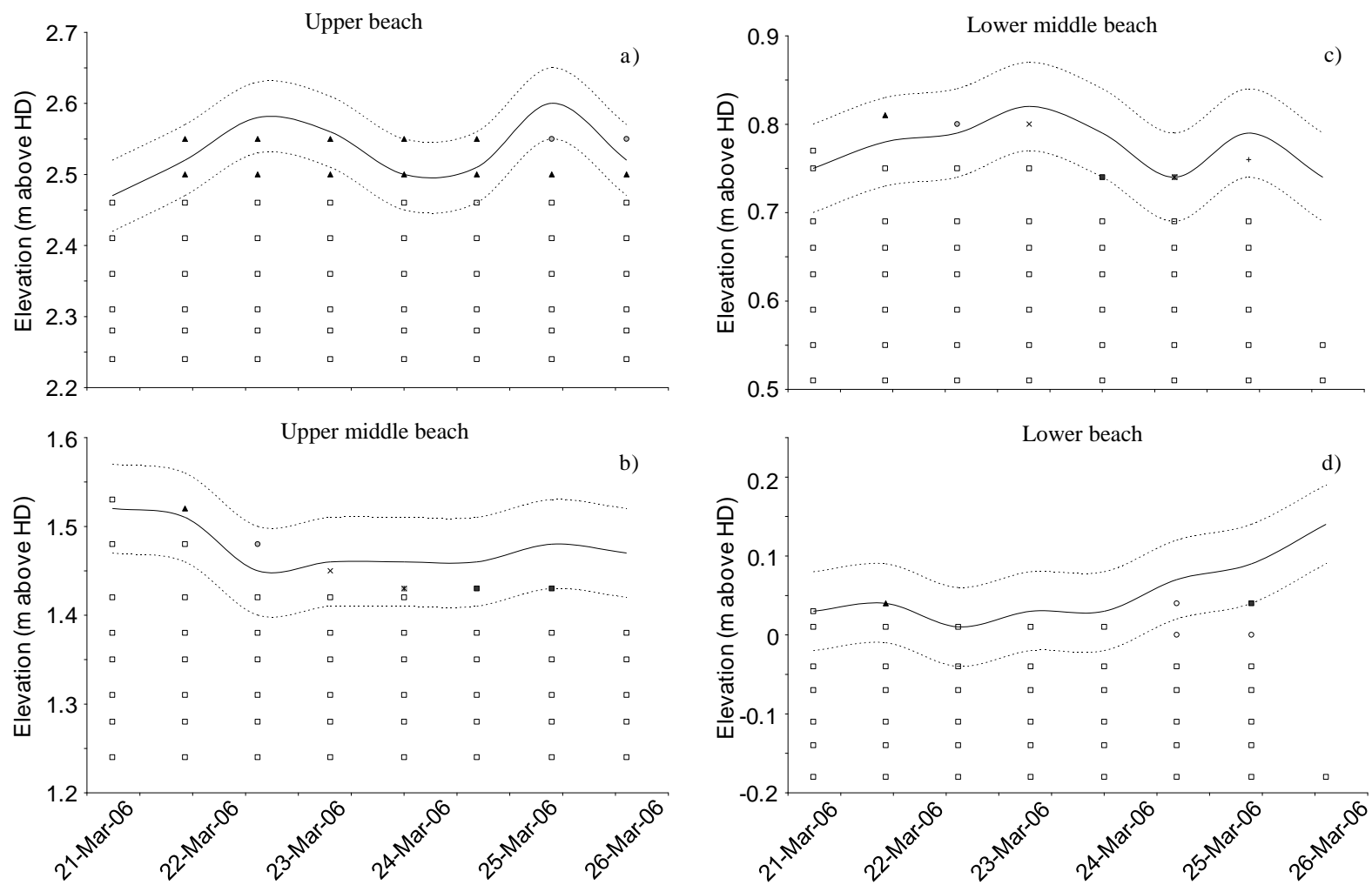


Figure 5-7 Active layer and topographic changes during the survey periods at Birling Gap for the eastern profile in March 2006: a) upper, b) upper-middle, c) lower-middle and d) lower beach. Part 1.

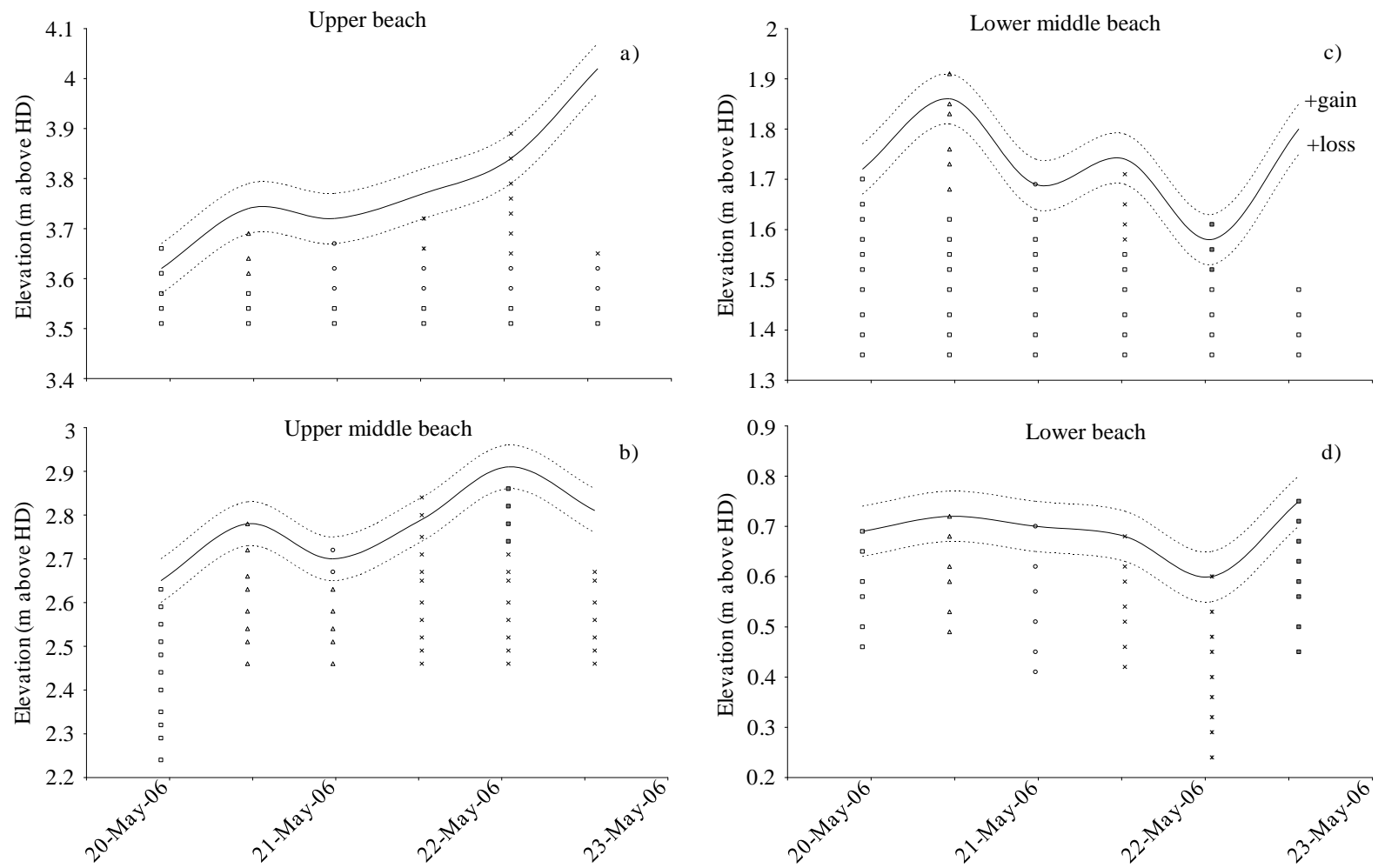


Figure 5-7 Active layer and topographic changes during the survey periods at Birling Gap for the eastern profile in May 2006: a) upper, b) upper-middle, c) lower-middle and d) lower beach. **Part 2.**

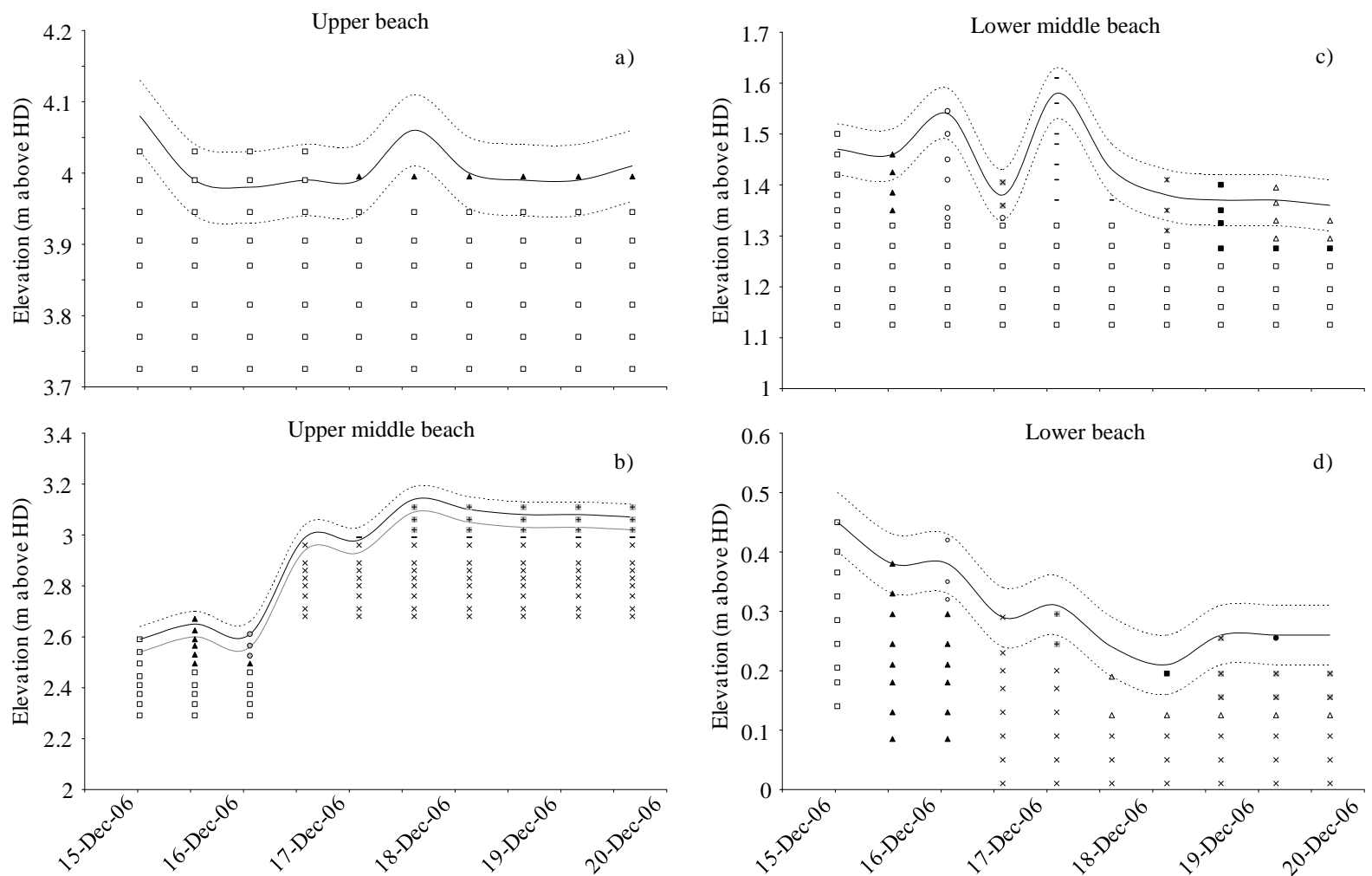


Figure 5-7 Active layer and topographic changes during the survey periods at Birling Gap for the eastern profile December 2006: a) upper, b) upper-middle, c) lower-middle and d) lower beach. **Part 3.**

5.3.4 Variation of the mixing depth with the grain size

Sediment sampling has been undertaken on a tidal basis during the survey period at Cayeux-sur-Mer. The sampling frequency was directed by the great changes that were visible in the beach surface grain size distribution over relatively short time periods and the occasional fresh sediment supply from the recycled material placed on the upper part of the beach (Chapter 3 Section 3.5.2). Because the beach material distribution is less variable at Birling Gap, sediment sampling was undertaken only when a noticeable sediment surface change was recognised (Chapter 3 Section 3.5.2). Experience showed that at Birling Gap, even when sediment samples were taken on various days or months (March, May, December 2006), the sediment distribution did not show much of a difference (Appendix II). Therefore, the influence of grain size changes on the depth of mixing could not be appreciated from the results collected at Birling Gap. In contrast, the sediment mixture variations observed at Cayeux-sur-Mer is large enough to investigate such an influence on the mixing depth.

The samples have been sieved (Chapter 3 Section 3.5.1) and factors of degree of bi-modality have been calculated according to Sambrook-Smith et al.'s (1997) formula (Equation 5-7). The advantage of using such an index is that its value is representative for specific sediments with supposedly similar hydrodynamic behaviours. Thus, this index was deemed appropriate to characterise the various beach sediment mixtures into groups of sediment which respond similarly to the forcing hydrodynamics.

$$B^* = |\phi_2 - \phi_1| \frac{F_2}{F_1} \quad (5.7)$$

Where ϕ_1 and ϕ_2 are the modal sizes in phi units and F_1 and F_2 the proportion of sediment contained in each mode, and subscript 1 refers to the primary mode and subscript 2 to the secondary mode.

The index is based on the modal sizes in the sand and the gravel components and the proportions of sediment contained in each mode. It is unit-less and the transition between uni-modality and bi-modality ranges from 1.5 to 2. Sediment mixtures having

an index < 1.5 will be considered as uni-modal while those having an index > 2 are bi-modal; between 1.5 and 2 the character of the sediment mixture is not well defined. In Figure 5-8, the Sambrook-Smith et al. (1997) index of each sediment sample collected at Cayeux-sur-Mer has been plotted against the depth of mixing observed during the various field campaigns.

Note that it was preferred to include the few data collected on the upper-middle and lower-middle measurement points to the ones measured on the middle measurement points on transects 1, 3 and 4 at Cayeux-sur-Mer (Chapter 3 Figure 3-11). This decision was motivated by the very low number of data on the upper middle and lower middle measurement points. Spatially, all these measurement points are fairly close to each other, and contrary to Birling Gap, the upper-middle and lower-middle part of the beach at Cayeux were not noticeably affected by elevation changes in relation to the migration of beach features (Figure 5-4). It was therefore assumed that their respective mixing depths would be very similar.

As seen on Figure 5-8, values of the Sambrook-Smith index seem to be repeated consistently during the time of the experiment at Cayeux in October/November 2005. This suggests that even though there are frequent changes in surface sediment at Cayeux, there are in fact only a confined number of sediment mixtures. These “groups” with close values of B^* can be divided according these values: from 0 to 1, from 1 to 1.5, from 1.5 to 2, from 2 to 3 and from 3 and above.

Each of the data points used in Figure 5-8 are labelled with the tidal maximum significant wave height ($H_{s\ t. \max.}$) measured simultaneously with the sediment mixture and the mixing depth. It appears that within each group identified and at the three locations of measurement on the beach, the mixing depth increases on average (excluding the odd values) with an increase of the tidal maximum significant wave height ($H_{s\ t. \max.}$). This would suggest that for a similar mixture the mixing depth increases with the wave height.

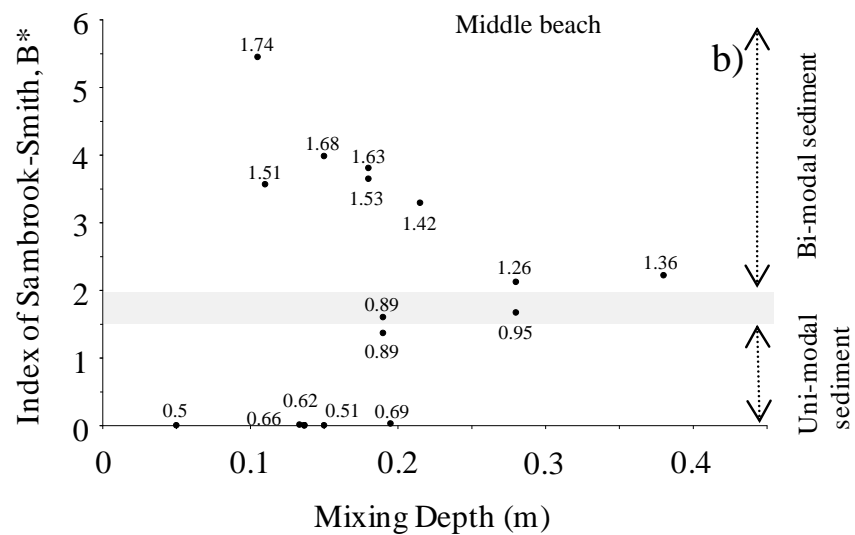
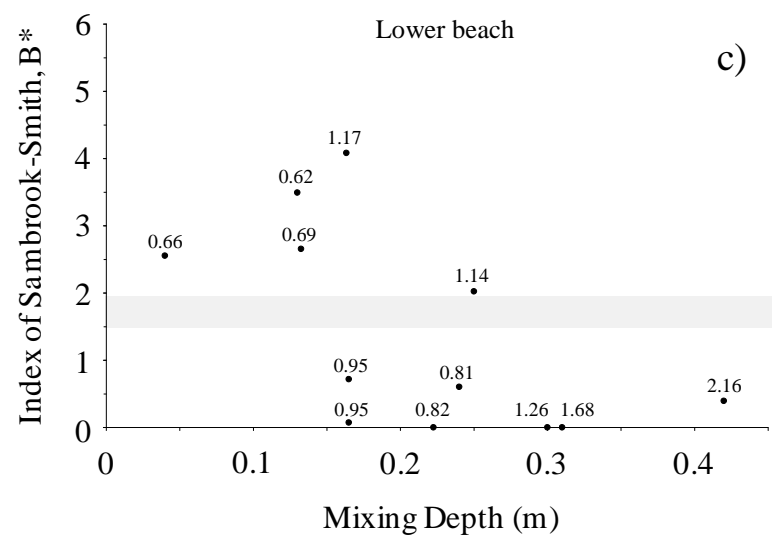
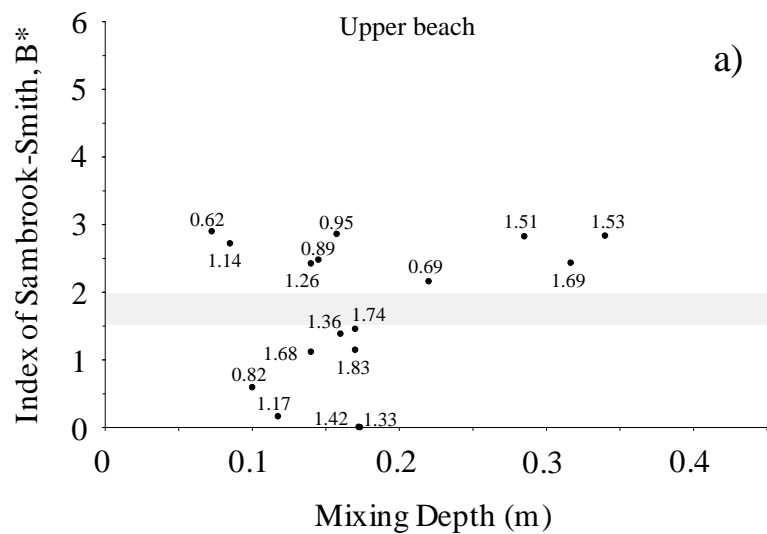


Figure 5-8 Plot of the mixing depth as a function of the index of Sambrook-Smith et al. (1997). Each graph represents the data collected at specific location on the beach at Cayeux-sur-Mer: a) upper beach, b) middle, c) lower beach. Each point is annotated with the tidal maximum significant wave height ($H_{st, \max}$) of the tide preceding the column survey.

It also appears that on the middle beach measurement, for an equivalent mixing depth, the $H_{s\ t.\ max.}$ increases with the index β^* . Indeed, higher wave heights are necessary to remove bi-modal sediment than uni-modal sediment (Figure 5-8) suggesting therefore that the grain size distribution of the beach material has a greater influence than the wave height. For example, to remove 0.28 m of a sediment mixture with an index of 2.32 (bi-modal transport behaviour), a $H_{s\ t.\ max.}$ of 1.83 m is necessary whereas to disturb an equivalent depth of a sediment mixture with an index of 0.002 (uni-modal transport behaviour) requires an $H_{s\ t.\ max.}$ of only 1.17 m (Figure 5-8).

Such an observation is slightly more obscure on the upper and lower measurement points; it is important to keep in mind that both of the measurement locations are affected by great elevation change over the tides which might blur the tendency observed in the middle of the beach. However, these results suggest that the sediment mixture has a great impact on the mixing depth by controlling the effect of the wave height.

5.3.5 Variation of the mixing depth with the wave height

To date, only three published papers have investigated the variation of the mixing depth with the wave height on gravel beaches (e.g. Austin and Masselink, 2006; Curoy et al. 2009; Saini et al., 2009), and apart from the publications from the present research, none have investigated a mixed beach (the two others being respectively on a pure gravel beach and on a mixed sand and gravel beach, c.f. Jennings and Shulmeister, 2002) or produced any explicit correlation.

Because of the high reflective profile associated with the mixed beaches studied in this work ($\tan\beta \approx 0.12$ to 0.17) and the impossibility to compare this study's results to similar environments, it was decided to examine steep sandy beaches in particular ($\tan\beta \approx 0.11$ in Ciavola et al., 1997). This was primarily because there are published data available and the reported beach gradients are the closest to those measured at Cayeux and Birling Gap.

The linear correlation between significant wave height at breaking (H_b), and average sand-mixing depth (Z_m) for steep beaches with a mean grain size ranging from 0.26 to 0.38 mm (1.94 to 1.39 phi) is (Ciavola et al., 1997; Equation 5-8):

$$Z_m = 0.27H_b \quad (5.8)$$

This relationship seemed especially relevant because of its application to steep beach gradients and it was considered of interest to examine the differences that might be observed for a completely different range of grain size mixtures.

There are, however, a few crucial differences between Ciavola et al.'s study (1997) and this work that need to be discussed. First, the wave parameter measured in this study is the significant wave height (H_s) in proximity to the gravel/pebble part of the beach (Chapter 3 Section 3.3.1) whereas Ciavola et al. (1997) used the significant wave height at breaking (H_b). The advantage of measuring H_s is that the data is accurately recorded by equipment whereas the measurement of H_b involves visual reading during the rising tide. It was judged to be too impractical to measure the wave height in this way because of the hard work that was already involved in recording all of the other measurements at every low tide. In order to simplify the analysis, the maximum significant wave height recorded during each high tide ($H_{s \text{ t. max.}}$) was used. The relevance of using this value is further supported by the fact that the maximal significant wave heights are observed close to the high tide stage. This corresponds to the period when the mixed sediment part of the beach is fully affected by the hydrodynamic forcing. The values of $H_{s \text{ t. max.}}$ recorded during all of the short survey periods of this study at both sites ranged from 0.18 m to 2.68 m, whereas in Ciavola et al. (1997)'s work, H_b ranged between 0.34 m and 0.80 m. Therefore, the wave range considered by Ciavola et al. (1997) is much lower than that collected in this study. The beach gradients also differ slightly, with a $\tan\beta \approx 0.11$ on Ciavola's beaches whereas on this study's beaches gradients $\tan\beta$, for all the data collected, was between 0.12 and 0.17. Despite these differences, comparing the empirical formulae obtained by both studies should give an idea of the order of magnitude of any differences in the reactivity of the mixing depth in a sandy environment compared with a mixed sediment environment with a pebble grain size dominance.

It is also important to note that both of the studies cited earlier (Austin and Masselink, 2006; Saini et al., 2009) investigating the “depth of activation” on gravel beaches conducted their observations during very calm wave conditions ($<1\text{m}$). It is important that future studies add to this baseline database by collecting data during high energy events in order to develop models that would be more representative of high LST events and therefore be of great value to coastal managers.

It is important to highlight that all the data collected on the upper beach at both field sites were filtered to discard all zero values i.e. no erosion or accretion. This occurred on days when the water level was not high enough for the swash or the waves to reach and disturb the sediment on the upper beach. Including these values in the results would lead to an error as they are not part of the active profile at the time.

At both sites (Figures 5-9 & 5-10), it can be observed that the depth of disturbance increases with the wave height. However, the relationships do not appear to be strictly linear all the time. At Cayeux-sur-Mer, clear individual groups on the middle parts of the beach can be identified. These groups seem to be delimited into specific wave height ranges. For example (Figure 5-9), the data collected from all the columns in the middle zone of the beach can be reduced to two main groups, one were $H_{s\ t.\ max.}$ ranges from 0 to 1.3 m and another from 1.3 to 1.83 m. In the results from Birling Gap (Figure 5-10), no such clear groups can be identified in the middle beach measurements.

Linear regressions are drawn for each location across-shore at both sites (Figure 5-9 & 5-10). The results of these correlations are discussed in Section 5.4.3.

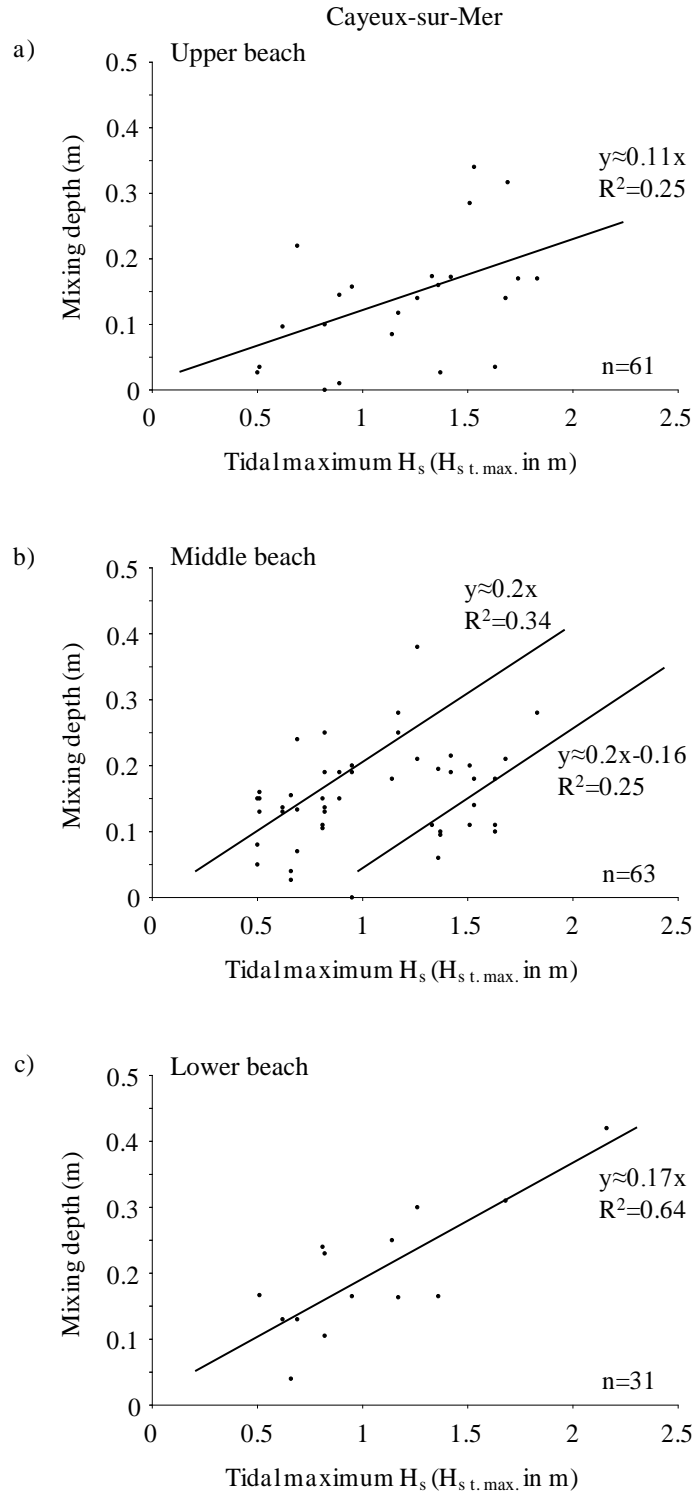
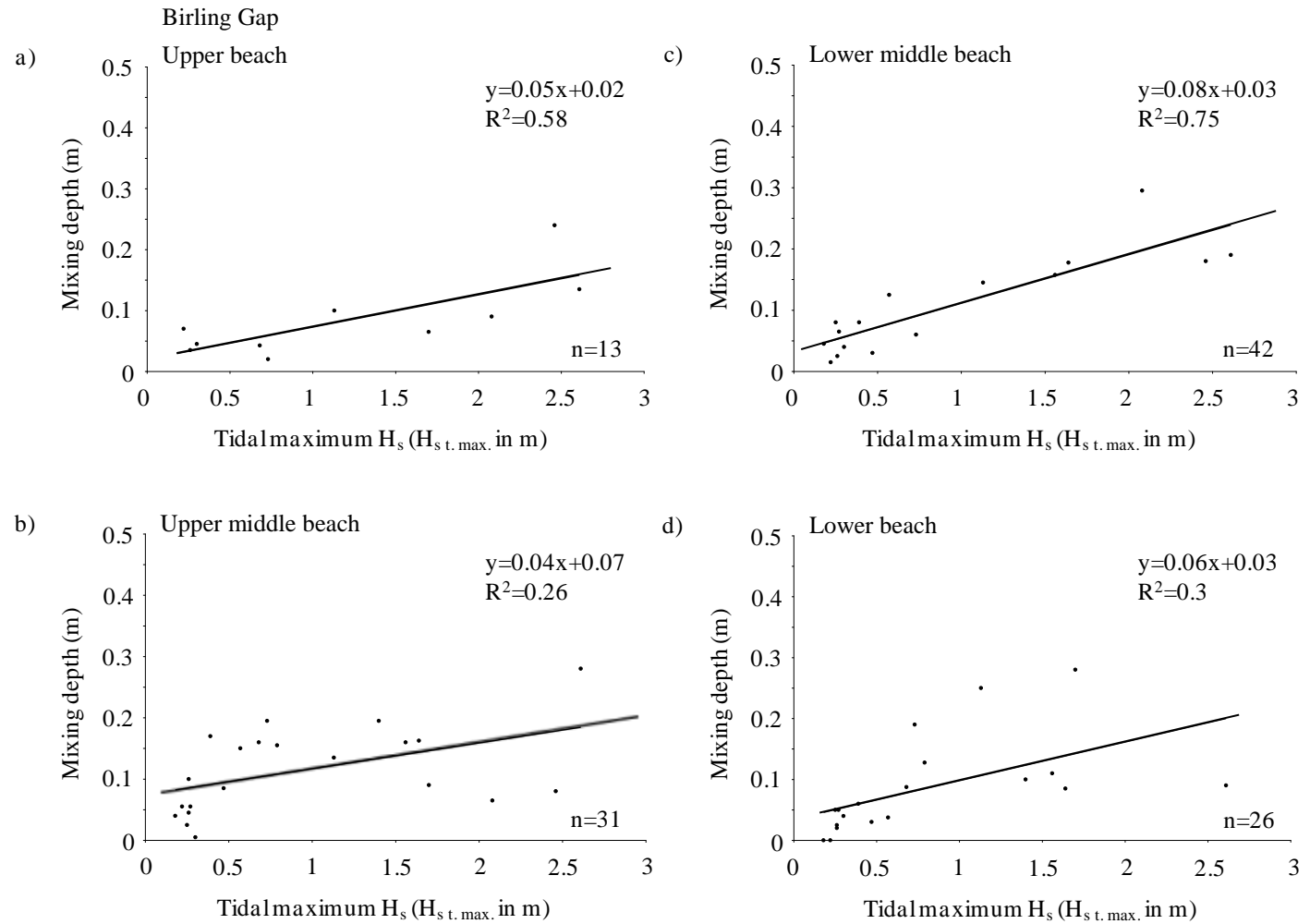


Figure 5-9 Correlation of the average depth of mixing and the tidal maximum significant wave height at the: a) upper, b) middle, c) lower part of the mixed beach at Cayeux-sur-Mer. n is the total number of measurements with an exact value collected for all profiles. Approximate values shown in Appendix IV (Tables IV-1 to IV-4) are not used on the graphs. Please note that here again it was preferred to regroup the data collected on the upper middle, middle and lower middle at Cayeux-sur-Mer in one single middle section because of the small number of exact values collected in both the upper middle and lower middle sections of the beach.

Figure 5-10 Correlation of the average depth of mixing and the tidal maximum significant wave height at the: a) upper, b) upper middle, c) lower middle, d) lower part of the mixed beach at Birling Gap. n is the total number of measurements collected for all profiles and used later to determine the tidal average depth of mixing for each respective across-shore location. n only concerns measurements with an exact value. Approximate values shown in Appendix IV on Table IV-5 to IV-10 are not used on the graphs.



5.3.6 Variation of the mixing depth with the wave direction

Correlations between the depth of disturbance and the wave direction are presented for both sites in Figures 5-11 & 5-12.

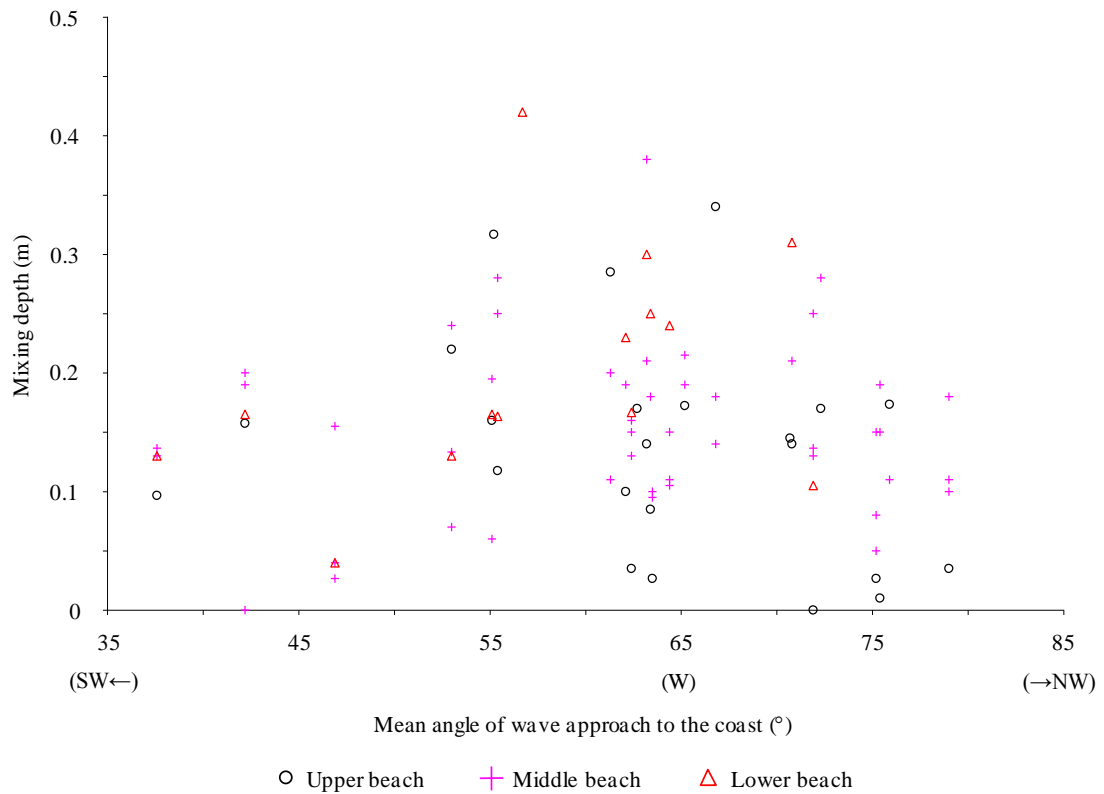


Figure 5-11 Plot of the depth of disturbance and the wave direction at the: a) upper, b) middle, c) lower part of the mixed beach at Cayeux-sur-Mer.

Based on the data collected at Cayeux-sur-Mer during the October/November 2005 survey period, no clear linear relationship can be observed between the wave direction and the mixing depth. The main reason for this is because of the consistency of the wave coming from one direction during the experiment (Figure 5-13; Chapter 4 Figure 4-4). The wave approach was from the South-West at an angle to the beach that varied from 37.6° to 89.6° , with the greatest frequency between 57° and 79° . In contrast, at Birling Gap a large spectrum of wave directions occurred during the various sampling periods, with the mean angle of wave approach varied from 22° to 152° , approaching from South-East to the South-West.

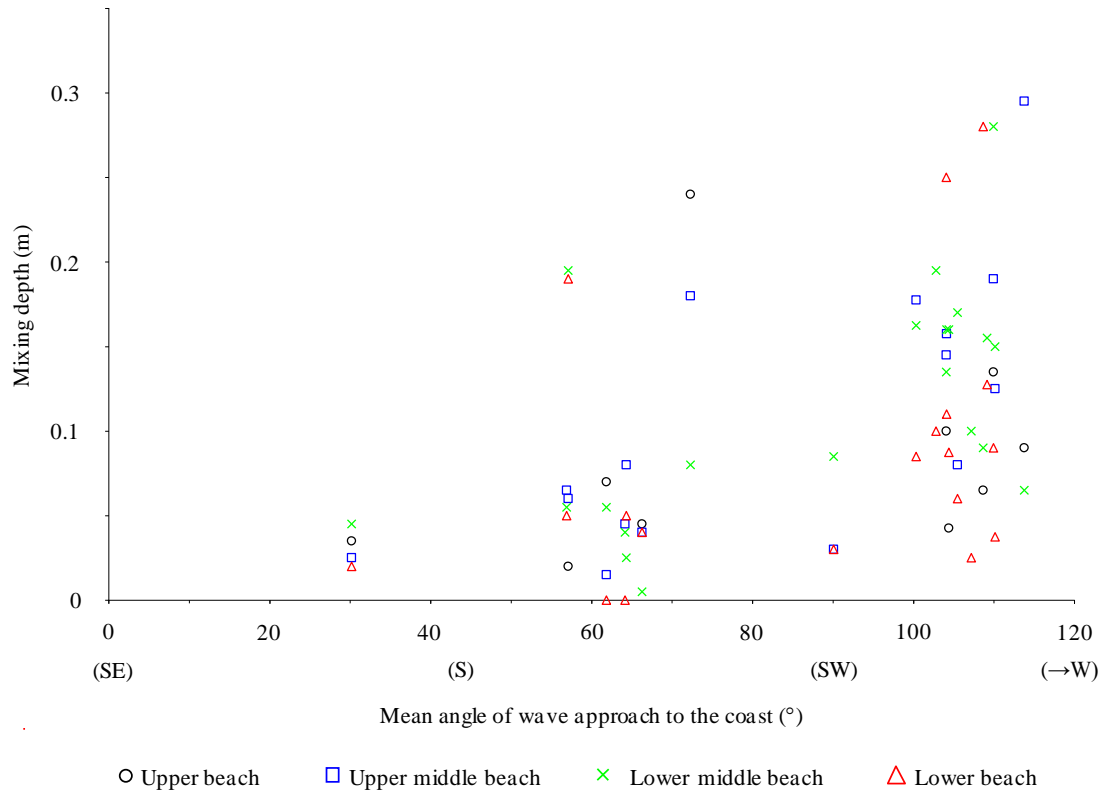


Figure 5-12 Aggregated plot of the depth of disturbance and the wave direction at the: a) upper, b) upper middle, c) lower middle, d) lower part of the mixed beach at Birling Gap.

Considering the distribution of the significant wave height as a function of the wave direction at Birling Gap (Figure 5-14), it can be seen that the highest significant wave heights observed are associated with specific wave directions. During the short period surveys, the highest waves (> 1.5 m) tend to come from a western direction whereas the smallest (< 0.5 m) are from South or South-East. Figure 5-12, shows that the mixing depth tends to increase with the wave angle on the middle (upper middle and lower middle) and lower parts of the beach. Thus, in the proximity of the middle beach a maximum depth of disturbance of 4.5 cm (mean angle of wave approach to the coast of 30°) is observed for waves coming from a South South-Easterly direction while a maximum depth of disturbance of 29.5 cm (mean angle of wave approach to the coast of 114°) is observed for waves coming from a West Wouth-Westerly direction.

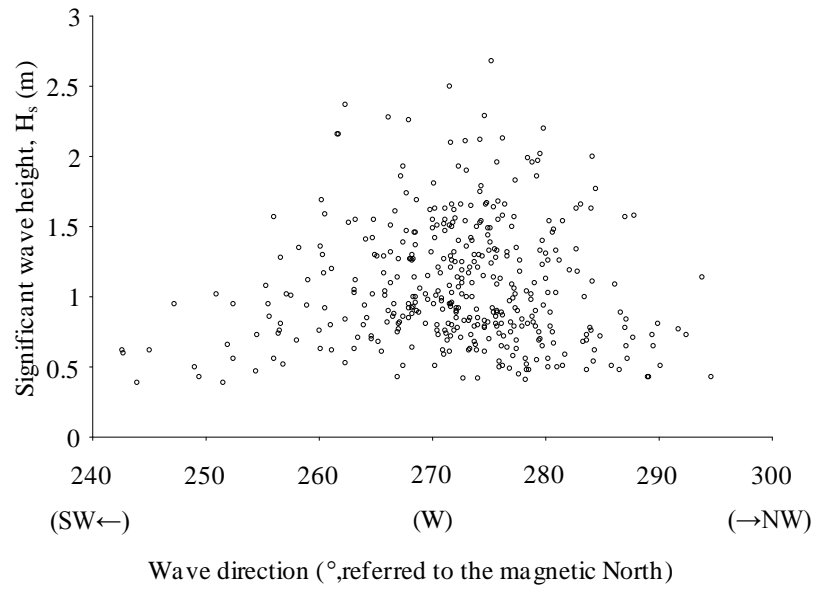


Figure 5-13 Aggregated plot of the onshore wave direction referred to the magnetic North as a function of the significant wave height (H_s) sampled at Cayeux-sur-Mer during October-November 2005.

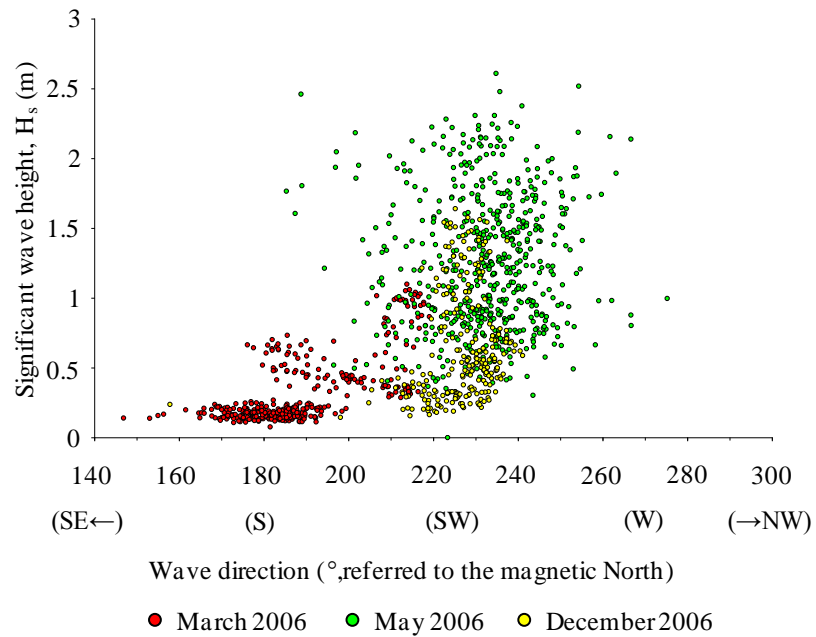


Figure 5-14 Aggregated plot of the onshore wave direction as a function of the significant wave height (H_s) sampled at Birling Gap.

5.3.7 Variation of the mixing depth with the wave period

Plots of the mixing depth and the peak period, T_p , for both sites are shown on Figure 5-15 & 5-16. Based on the observation made at Cayeux-sur-Mer and at Birling Gap, no clear relationship is apparent between the mixing depth and the peak period for either of the sites or in any location across-shore on the beach.

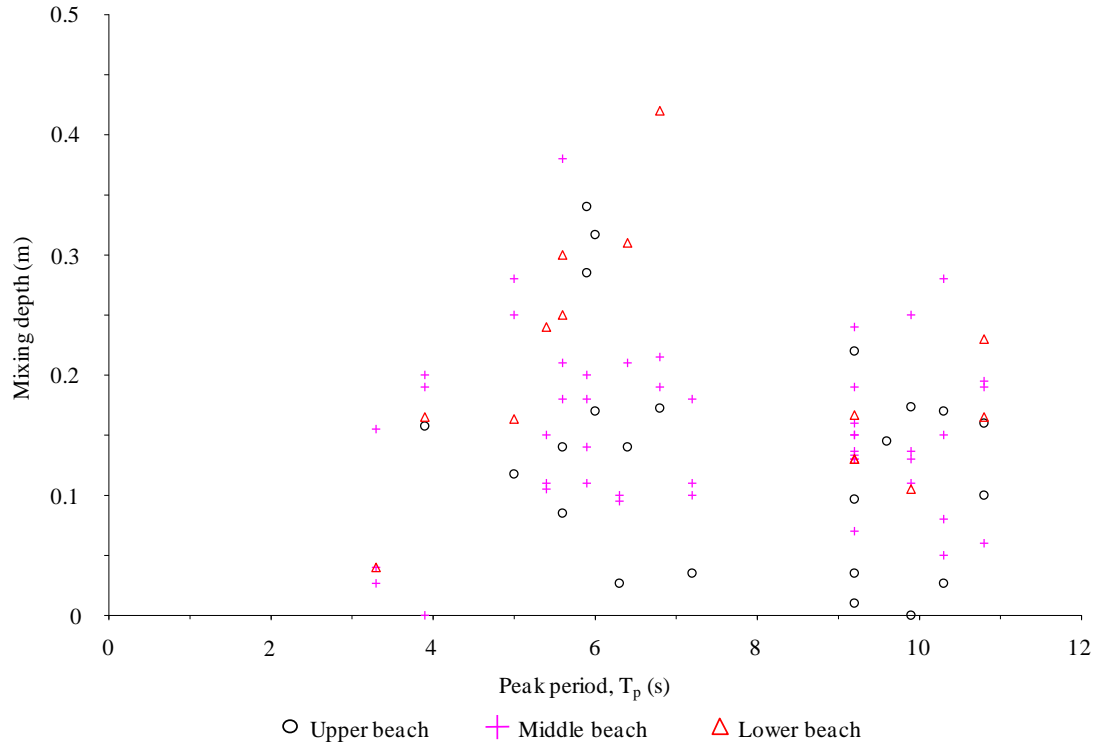


Figure 5-15 Correlation between depth of mixing and the peak period, T_p , at Cayeux-sur-Mer. n is total the number of measurements collected and represented on the graph. n includes only measurements with an exact value. Approximate values shown in Appendix IV on Tables IV-1 to IV-4 are not represented on the graphs.

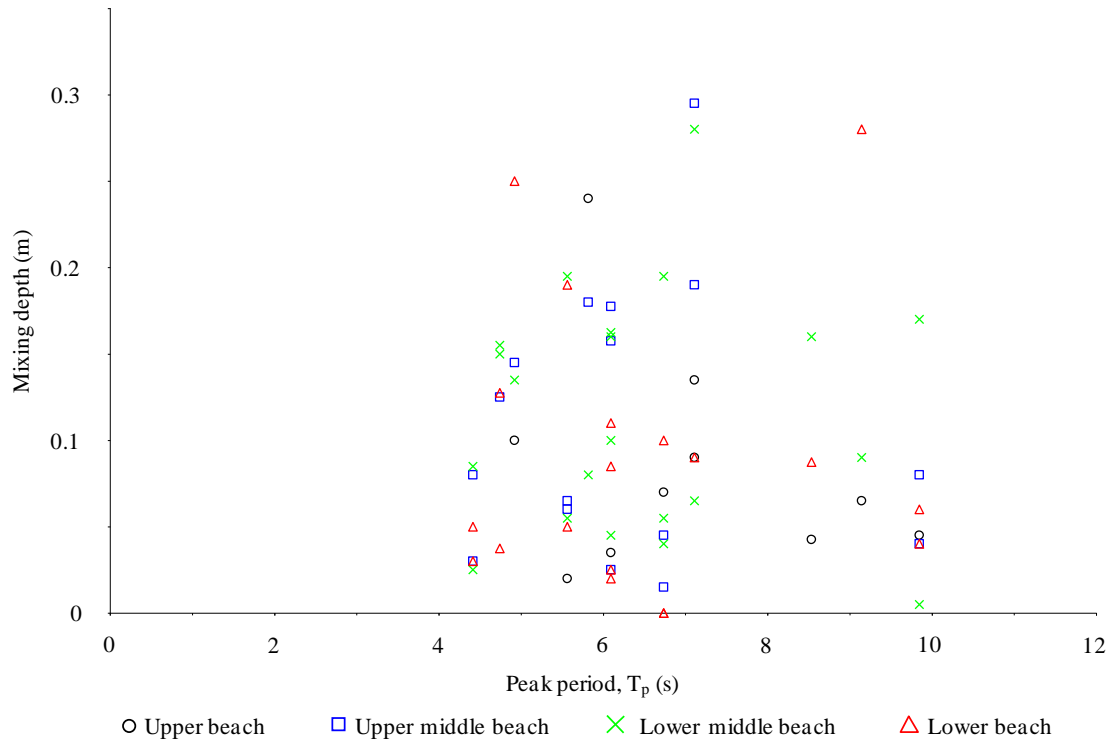


Figure 5-16 Correlation between depth of mixing and the peak period, T_p , at Birling Gap. n is the total number of measurements collected and represented on the graph. n includes only measurements with an exact value. Approximate values shown in Appendix IV on Tables IV-5 to IV-10 are not represented on the graphs.

5.4 Discussion

As shown (Chapter 5 Section 5.3.1), there is little variation in the active layer alongshore. Thus, as long as variables such as the hydrodynamic conditions, homogeneous distribution of the wave energy alongshore or the beach properties (e.g. grain size, slope, orientation, and elevation) do not change alongshore, the active layer will be homogeneous. This implies that the assumption of a uniform active layer made in longshore transport models is valid for mixed beaches.

In contrast, the cross-shore sections of the beach face at both sites clearly display a non-uniform active layer thickness. Specific areas on the beach face are characterized by specific hydrodynamic conditions or morphological features i.e. berm, beach cusps, beach step. The upper part of the beach is largely dominated by a dynamic swash zone and is characterized by a berm migrating up and down in accordance with the

hydrodynamic forcing and the water level. In contrast, the middle and lower parts of the beach are under the influence of the breaking waves for longer and are marked by the presence of beach cusps (which were rare during the field experiments of this study) and the migrations of the beach step. As a result of these differences, it is reasonable to consider each part of the beach as a specific hydrodynamic unit.

During the short period surveys at Cayeux and Birling Gap, the beach gradient on both beaches was found to vary by no more than 1.5° (Chapter 4 Section 4.3). Therefore, it is most likely that the beach slope during the surveyed periods had very little effect on the variations of the mixing depth. In addition, it was shown in the results that no clear relationship is visible between the mixing depth and the peak period (T_p) at either of the sites all across-shore locations considered (Figures 5-15 & 5-16).

5.4.1 Variation of the active layer across-shore

The beach face morphology on mixed beaches reacts extremely rapidly to the forcing hydrodynamics. Recent research has shown that the swash is the dominant parameter driving sediment motion and beach morphological changes on gravel beaches (Van Wellen et al., 2000; Pedrozo-Acuña et al., 2006). The swash surge is essentially driven by a number of parameters, including the wave height, wave direction, water level, beach slope, beach permeability and water saturation of the sediment. The combination of both the wave height (directly responsible for the swash) and the water level is responsible for the upwards and downwards migration of the berm on gravel beaches (Austin and Masselink, 2006). The extreme spatial and volumetric variabilities of the berm in response to the forcing hydrodynamics are the most probable reasons for the sudden erosion or accretion movements indicated by the pebble columns' data. These movements are most probably also responsible for the loss of columns in the upper beach. Figures 5-6, 5-5, 5-6 & 5-7 clearly show that topographic changes are largely responsible for the occurrence of a thick active layer on the upper part of the beach. This observation confirms that, in the same way as on sandy beaches, the migration of topographic features on mixed beaches greatly influences the active layer thickness.

The beach step can be extremely mobile too, migrating landward and seaward in accordance with the rising and falling tide (Bauer and Allen, 1995; Austin and Masselink, 2006). These across-shore fluctuations during tidal inundations are the most likely cause of complete removal of the painted pebble columns which resulted in low recovery rates during the short period surveys. This highlights the fact that for most of the time the present study underestimates the full thickness of the active layer in proximity to the beach step immediately above the sandy or chalky foreshore. Indeed, the presence of the chalk platform at Birling Gap limits the potential to observe greater depths of sediment disturbance.

Similarly, at Cayeux-sur-Mer, despite the fact that the columns were set as deep as possible (10 to 15 cm maximum) into the sand dominated matrix lying beneath the gravel dominant beach, the depth of these columns was still too small to consistently include the full depth of the active layer. This observation suggests that this part of the beach, the sandy matrix on which the mixed sediment mixture lies, is probably affected by the forcing hydrodynamics during the high tide. This implies that, during a high tide, a considerable amount of sand size sediment (even at depth) is redistributed from the lower mixed beach toward other areas on the beach, either the upper parts of the mixed beach or the sandy platform in the case of Cayeux-sur-Mer or the chalk foreshore in the case of Birling Gap. The beach step cross-shore fluctuations during a tidal cycle are again a perfect example of how the migration of beach features greatly influences the thickness of the active layer.

The thinness of the beach and the presence of the underlying chalk platform at Birling Gap limit the depth and volume of beach material available for transport. However, it is interesting to point out that from one field survey period to another at Birling Gap, remains of painted pebble columns were recovered at the upper-middle and lower middle points of measurements on the eastern profile between March and May 2006. The wave climate between these two fieldwork periods varied from calm to agitated and storm conditions during the second fieldwork. This shows that the threshold related to the platform is a limit to the active layer measurement only during extreme hydrodynamic conditions and can be considered to have no effect on the active layer during “non storm” conditions.

It is important to draw particular attention to the depth reached by specific forcing hydrodynamics. At Cayeux-sur-Mer, for example, the active layer measurements and profile surveys show that, in the early stages of the neap tide, the berm retreats and the run up pushes sediment landward from the steep berm face (e.g. October 30th, afternoon tide; Figure 5-6a). During this study period, the upper beach is exclusively swash dominated (no storm, therefore no influence of breaking waves) and it can be seen that the beach material was disturbed to a depth of 20 cm. This shows how the swash can deeply affect a mixed sediment beach material.

It is less easy to clearly identify the effect of specific hydrodynamic forcing at Birling Gap. The wideness (30 to 40 m average) and steepness of the mixed beach in the area surveyed force the wave to break and the swash to occur suddenly within a very confined zone. The swash occurs at the very top of the beach, modelling the berm. Because the berm is comprised of coarse pebbles at Birling Gap, the swash infiltrates very quickly into the beach and therefore its spread onto the beach face is very short. This is why it is very difficult to isolate the influence of the swash when looking at most of the results.

Earlier in this chapter (Section 5.3.2), it was identified that some areas of the beach face are subjected to greater remobilization than others. The main observation was that the columns located in the middle of the beach were often subjected to more erosion than in areas on the beach where no great topographic change occurs (Figure 5-3).

Stapleton et al. (1999) observed a similar tendency and identified that most disturbance occurs in the zone of wave breaking. Therefore, with the aim of verifying such a relationship, the wave breaking zone needed to be delimited. The wave breaking zone is usually calculated using the McCowan wave breaking index (Equation 5-9):

$$H_b = \gamma h_b \quad (5.9)$$

where H_b is the breaker height, h_b is the mean water depth at the point of breaking and γ is the breaker index (Masselink and Hughes, 2003). Again, the breaker height, H_b , was not measured during this study but the significant wave height was measured in very

close proximity to the mixed sand-and-gravel beach. Field observations indicated that wave breaking occurred directly when the wave interacts with the mixed sand and gravel beach. Therefore for the purposes of this study, the tidal maximum significant wave height ($H_{s \text{ t. max.}}$) was substituted for the breaker height (H_b) in the McCowan formula in order to calculate the maximum elevation at which breaking waves occur. A commonly used first order approximation for the breaker index of 0.78 was used and the results are displayed in Figures 5-17 & 5-18.

Figures 5-17 & 5-18 clearly show that if no significant topographical change occurs the deepest active layer corresponds to the zone of wave breaking, therefore supporting Stapleton's findings (Stapleton et al., 1999) on a similar environment. In this wave breaking zone, even the coarsest sediment is put into suspension for a short period of time during wave collapse (providing that enough energy is delivered by the breaking waves) whereas, in the swash zone, it is exclusively transported as a bed load sheet. This implies that the use of topographical surveys alone may underestimate the real volumes of sediment involved in longshore and cross-shore transport.

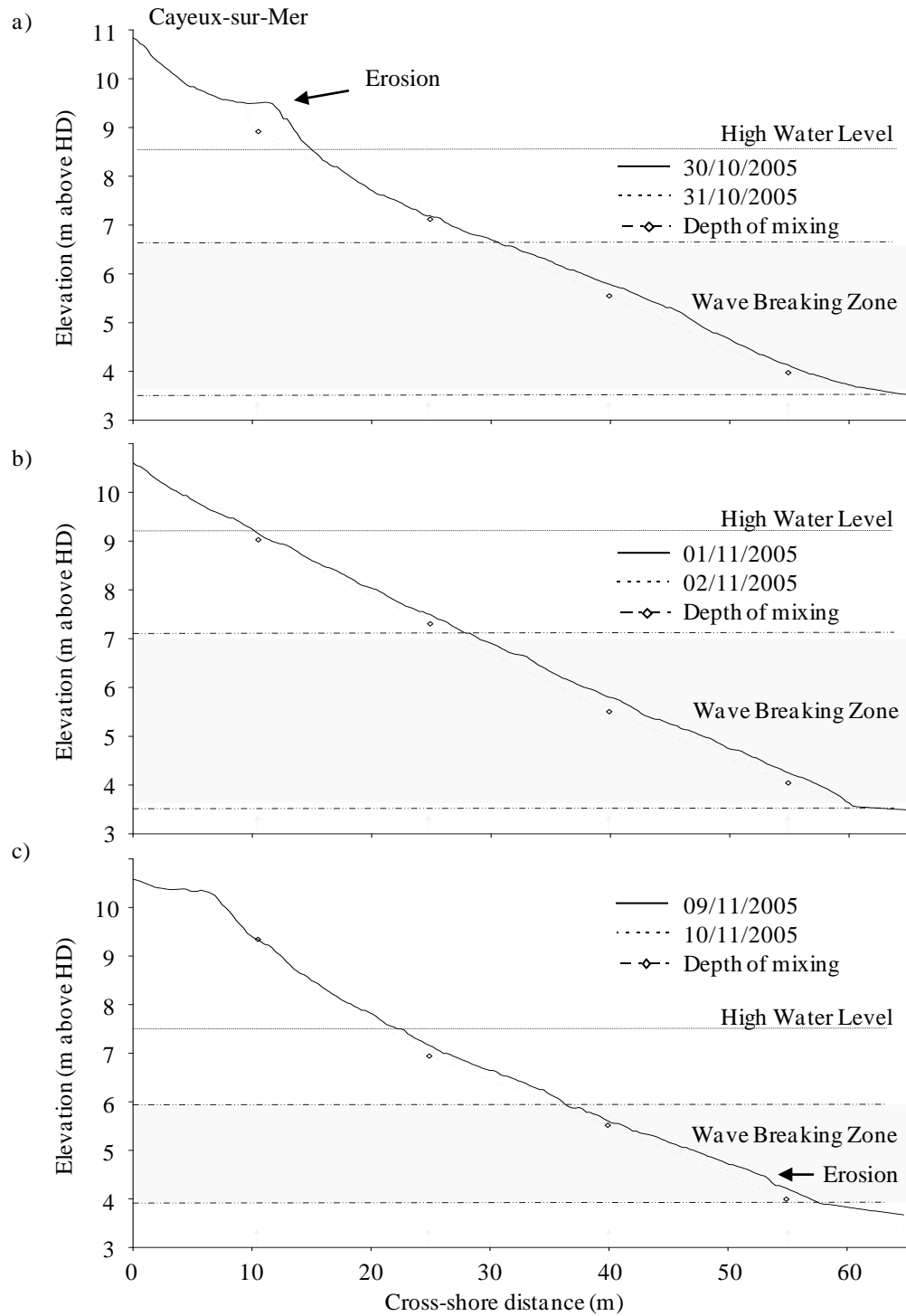


Figure 5-17 Examples of profile evolution and active layer measured showing the wave breaking area during the survey period at Cayeux-sur-Mer. The black arrows show the location of the active layer measurements.

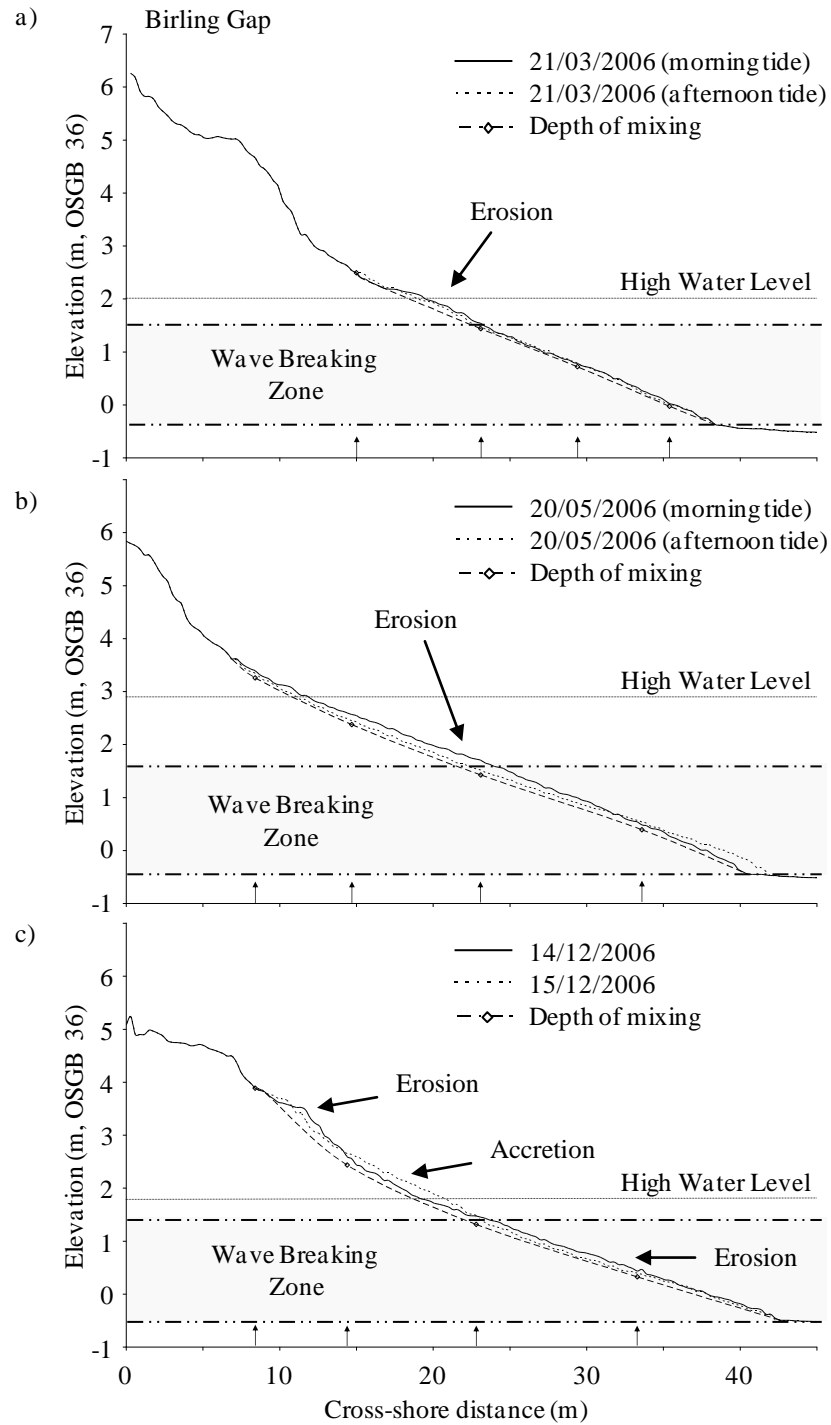


Figure 5-18 Examples of profile evolution and active layer measured showing the wave breaking area during the survey period at Birling Gap. The black arrows show the location of the active layer measurements. Part 1.

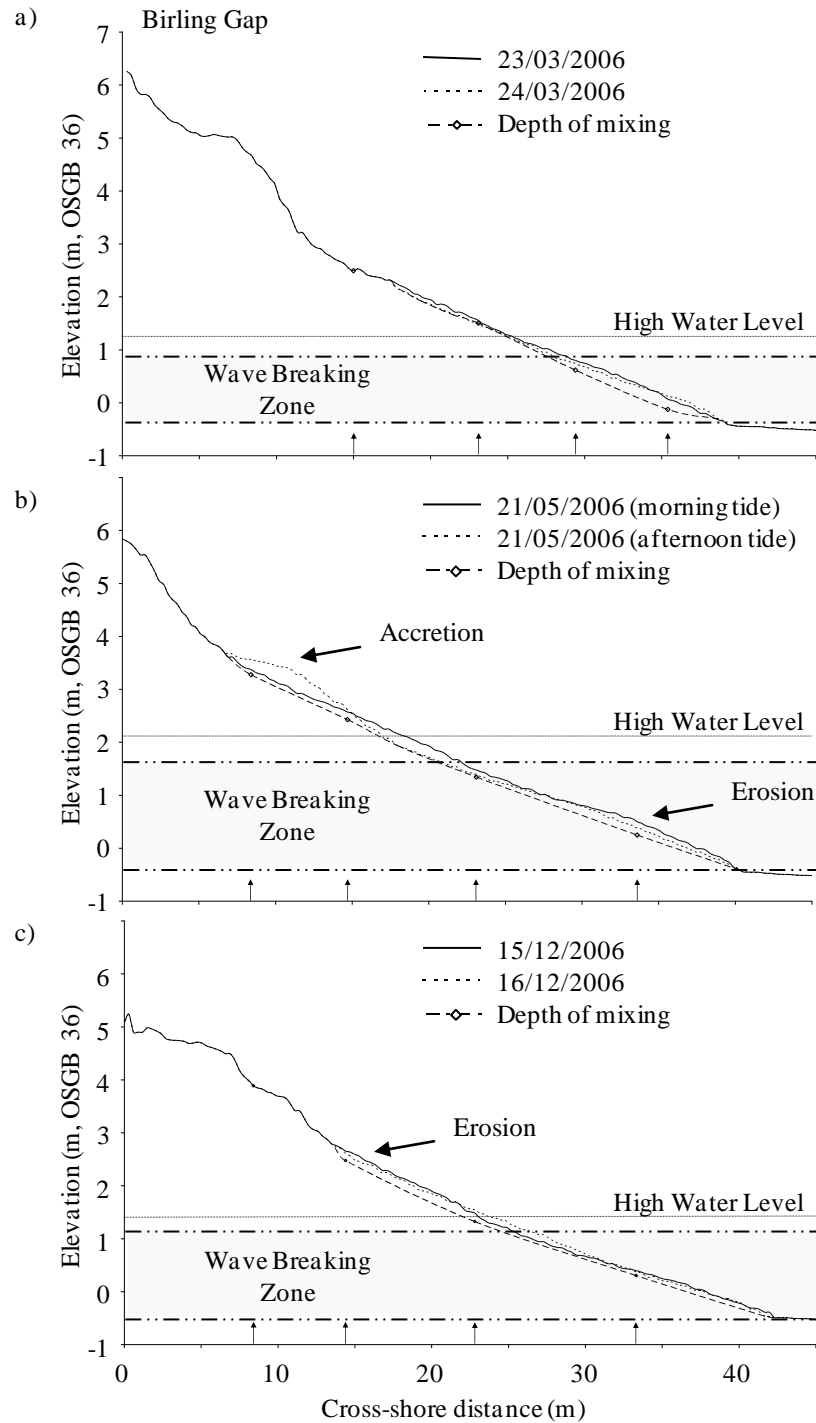


Figure 5-18 Examples of profile evolution and active layer measured showing the wave breaking area during the survey period at Birling Gap. The black arrows show the location of the active layer measurements. **Part 2.**

5.4.2 Variation of the mixing depth with the grain size

Calculation of the indexes of Sambrook-Smith et al. (1997) classifies sediment mixtures in groups that respond similarly to the hydrodynamic forcing. On Figure 5-8, it was observed that groups exist with close values of index and that within these groups, generally the $H_{s\ t\ max.}$ increased with the mixing depth, suggesting that the mixing depth increases with the wave height, confirming the results observed earlier about the relationship between the mixing depth and the wave height. On the other hand, it was also observed on the middle beach measurements that for equivalent mixing depth, that $H_{s\ t\ max.}$ increased with an increase of the Sambrook-Smith index β^* suggesting that the sediment mixture has an influence on the mixing depth by controlling the effect of the waves height.

The grain size distribution of the beach material is known to exert a significant control on the beach permeability (e.g. Mason and Coates, 2001) and therefore the energy dissipation of the incoming waves. Mason (1997) showed that the hydraulic conductivity of a sand gravel mixture is markedly reduced once the sand content exceeds 25%. According to the Sambrook-Smith index, the greater its value the greater is the sand content in the mixture. Therefore, the increase of sand in the sediment mixture has the direct effect of reducing the hydraulic permeability. By reducing the permeability the water infiltration/exfiltration fluxes are reduced and therefore the beach material is less easily re-mobilised or entrained by the hydrodynamic processes. On the contrary, for small indexes of Sambrook-Smith, the content of sand in the mixture is low and the hydraulic permeability is high. The infiltration/exfiltration fluxes tend to ease the remobilisation of the coarse particles (e.g. Butt et al., 2001) and therefore sediment can be mixed at depth more easily by smaller waves than is the case for a strongly bi-modal sediment mixture.

Given that the grain size distribution along and across a mixed beach is a direct consequence of the forcing hydrodynamics (Watt et al., 2006), it is therefore suggested a feedback loop exists between grain size distribution, wave height and mixing depth. On the one hand, wave height drives grain size distribution and their combined effect depends upon the mixing depth. On the other hand, the internal structure of mixed

beaches is made of layers within which grain size distribution varies in equilibrium with the hydrodynamics forcing occurring at the time of deposition (Dornbusch et al., 2005). The sand content is normally greater in the underlying layer than in the surface layer. This is because the smaller grains fall into the voids created by the bigger grains in a process that is driven by the sea water infiltrating the beach. Therefore, variations of the mixing depth partially influence the type of material available to be redistributed at the surface. Changes in the grain size distribution will then influence the sea water infiltration for the following tide and consequently have an impact on the following mixing depth, which completes the feedback loop suggested earlier (Figure 5-19).

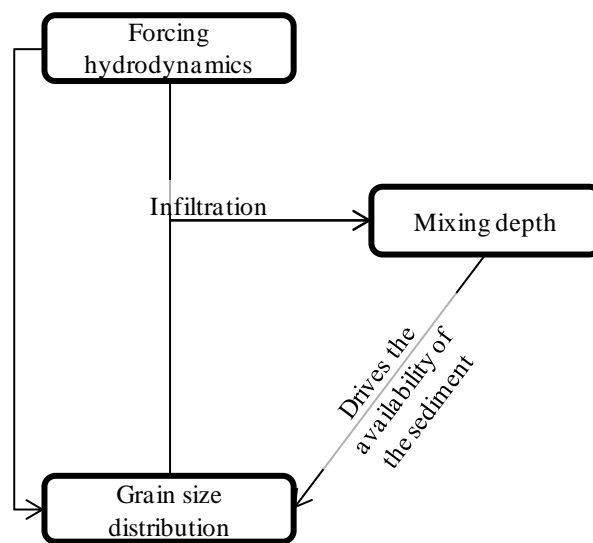


Figure 5-19 Feedback loop between the hydrodynamic conditions, the grain size and the mixing depth.

5.4.3 Variation of the active layer with the wave height

Clear groups of points can be distinguished for the results collected in the middle parts of the beach at Cayeux-sur-Mer (Figure 5-9). For both groups, the linear tendencies obtained have the same coefficient (0.2) for their relationship between wave height and the depth of sediment disturbed. This means that for both groups their mixing depth increases by the same order of magnitude when $H_{s\ t. \max.}$ increases, but one group is delayed compared to the other. The explanation could be linked to a variation in wave breaking location with incident wave height. Bigger waves break earlier on the beach face compared to smaller ones. The steepness and morphology of the beach in

association with the great amount of energy and water delivered by the biggest wave would induce a second, or more, lines of wave breaking, the energy and wave breaking height of which will be of lesser importance. Therefore, when the highest waves break early on the beach (i.e. on the most seaward areas), a resulting second or eventually third wave breaking line with less energy (smaller waves) is formed breaking further up the beach. The second waves affect the depth of disturbance in the same way that waves of equivalent height would do on their first breaking stage. This theory should be applicable to the upper part of the beach and it appears that three groups can be loosely identified: $0.5 < H_{s\ t.\ max} < 1$; $1 < H_{s\ t.\ max} < 1.5$, $H_{s\ t.\ max} > 1.5$ (Figure 5-9). However, the coefficient of determination (R^2) for each group individually is extremely low ($<<1$). This cancels out any notion of a relationship between the mixing depth and the wave height on the upper beach. This area is also greatly influenced by water level fluctuations and beach morphological changes, which most probably alters the relationship obtained for the upper beach. For this reason, it was decided not to consider all the data from the upper part of the beach at Cayeux-sur-Mer as a single set.

Table 5-1 shows the relationship equations based on the data for the upper the middle and the lower beach at Cayeux-sur-Mer.

Part of the mixed beach	Linear correlation	Correlation coefficient	Total number of measurements used (Equation number)
Upper	$Z_m \approx 0.11H_{s\ t.\ max.}$	0.25	61 (5.10)
Middle	$Z_m \approx 0.2H_{s\ t.\ max.}$	0,25 0,34	63 (5.11)
Lower	$Z_m \approx 0.17H_{s\ t.\ max.}$	0.64	31 (5.12)

Table 5-1 Correlation relationship between $H_{s\ t.\ max.}$ and the depth of disturbance at Cayeux-sur-Mer.

Regarding the data collected at Birling Gap, logarithmic trends on the upper middle, lower middle and lower beach data present better correlations than linear trends:

- Upper beach: $Z_m \approx 0.044 \ln (H_{s\ t.\ max.}) + 0.09$, $R^2=0.41$ (5.13)

- Upper middle beach: $Z_m \approx 0.072 \ln (H_{s\ t.\ max.}) + 0.14$, $R^2=0.75$ (5.14)

- Lower middle beach: $Z_m \approx 0.046 \ln (H_{s\ t.\ max.}) + 0.13$, $R^2=0.34$ (5.15)

- Lower beach: $Z_m \approx 0.064 \ln (H_{s\ t.\ max.}) + 0.12$, $R^2=0.45$ (5.16)

The use of logarithmic curves suggests the existence of a threshold value of the H_s that needs to be reached before any pebble movement is observed. It seems obvious that before pebble size particles are removed a threshold energy is necessary to be reached whereas for sand size particle this threshold is assumed to be zero. This hypothesis is most likely correct. However, it has been preferred to keep the relationship to linear trends in order to ease comparisons between the field sites of this study and other studies (e.g. Ciavola et al., 1997; Table 5-2).

Part of the mixed beach	Linear correlation	Correlation coefficient	Total number of measurements used (Equation number)
Upper	$Z_m \approx 0.05H_{s\ t.\ max.} + 0.02$	0.58	13 (5.17)
Upper middle	$Z_m \approx 0.08H_{s\ t.\ max.} + 0.03$	0.75	31 (5.18)
Lower middle	$Z_m \approx 0.04H_{s\ t.\ max.} + 0.07$	0.26	42 (5.19)
Lower	$Z_m \approx 0.06H_{s\ t.\ max.} + 0.03$	0.3	26 (5.20)

Table 5-2 Correlation relationship between $H_{s\ t.\ max.}$ and the depth of disturbance (Z_m) at Birling Gap.

The correlations obtained at Birling Gap and at Cayeux-sur-Mer are clearly different (Tables 5-1 and 5-2). In general, the mixing depth is greater at Cayeux than at Birling Gap. For example, when looking at the mixing depth measured at the mid-beach, the mixing depth at Cayeux is 60 to 80% higher than at Birling Gap. Despite the obvious geographical variation of both beaches, a few other reasons can cause these differences. The beach at Birling Gap is narrower than the one at Cayeux-sur-Mer (35 to 45 m and 50 to 60 m wide respectively) but they both sustain very steep slopes (respectively approximately 10 and 8°). Because of its steeper gradient, the beach at Birling Gap is more reflective than the one at Cayeux-sur-Mer. The beach sediment at Birling Gap is also a lot less variable and exposes overall less sand size sediment at its surface than the beach at Cayeux-sur-Mer even though based on all the sediment samples collected at both sites (Appendix II) both beaches have comparable amount of sand (from 0 to 40% based on individual sampling areas). For this reason, infiltration and exfiltration of sea water are very quick and consequently the beach at Birling Gap is more disposed to quickly dissipate wave energy than the beach at Cayeux-sur-Mer. As previously shown,

the beach sediment variation also influences the depth of disturbance. These reasons may help to explain the differences observed in the relationship determined.

A general comparison between the correlations presented by this study and the correlation obtained on steep sandy beaches (Ciavola et al., 1997) clearly shows that the depth of disturbance on steep sandy beaches is greater than on mixed beaches. However, for comparison between Caviola's predictions and the linear trends obtained in this study at both sites, it is probably best to consider only the relationship determined for the middle sections of the beaches. This is because this zone of the beaches is characterised by the absence of migrating beach features. Therefore, topographical changes will not be of a great influence with the active layer. However, looking solely at this zone, the linear trends show that the depth of disturbance in the middle section of Cayeux-sur-Mer's beach is 26% less than expected for a steep sandy beach whereas at Birling Gap this depth is 70 to 85% lower.

5.4.4 Variation of the mixing depth with the wave direction

Figure 5-11 clearly displays no relationship between the wave direction and the mixing depth on the mixed beach at Cayeux-sur-Mer, which is no surprise given the consistent angle of wave approach during the survey period. In contrast, at Birling Gap a tendency for the mixing depth to increase with the wave angle of approach can be seen on the lower and middle beach, but not for the upper beach. It was explained previously that the upper part of a mixed beach is greatly influenced by the fluctuations of the HWL and therefore such influence might explain why no clear relationship is apparent between the mixing depth and the wave direction on the highest parts of the beach profile. When representing significant wave heights as a function of wave direction for the Birling Gap data, it can be seen that they both increase as wave direction increases (Figure 5-14). Thus, waves coming from a East South-Easterly direction are generally smaller (<50 cm) than waves coming from a West South-Westerly direction (reaching up to 2.61 m) while waves coming from the South have intermediary heights (from 0.16 to 1.64 m). At the same time, the mixing depth on the middle and lower parts of the mixed beach increases with the wave height. Consequently, it can be seen how wave direction influences, indirectly, the mixing depth at this particular site. This is most likely a result of the confined morphology of the Channel and semi-circular shape of the

sediment cell from Selsey to Beachy Head, along with the presence of the chalk platform which makes the beach area surveyed variably exposed to or protected from incoming waves from different directions (also the respective strength of winds due to prevailing the movement of cyclones).

5.5 Conclusions

Each part of the beach face (upper, upper middle, middle, lower middle and lower beach) has been considered individually. Even if they are obviously interdependent it was necessary to isolate the different parts of the beach because of the extent to which they are influenced by the migration of beach features. The main conclusions are:

The active layer on mixed beaches is homogeneous alongshore as long as the hydrodynamic conditions and the beach properties (i.e. grain size, slope, orientation, elevation, and beach morphology) do not change.

From the observations of the parameters influencing the mixing depth on mixed beaches, this study can conclude that:

1. No clear relationship was noted between the depth of disturbance and the peak period (T_p).
2. The grain size distribution influences the mixing depth by regulating the forcing hydrodynamics through infiltration. However, the mixing depth influences also the grain size distribution by releasing or capturing beach material sediment. There exists a feedback loop system.
3. The active layer thickness is greatly affected by the migration of beach features. The build up or breakdown of the berm creates great elevation changes on mixed beaches, elevation changes that are taken into account in the active layer definition.

4. The swash has the potential to move sediment to significant depths and its influence is not to be underestimated when considering the mixing depth.
5. When the migration of beach features is not occurring, the deepest mixing depths are located in the wave breaking zone. The wave breaking zone is an extremely dynamic area in which even coarse particles can be put into suspension for a short moment.
6. The upper part of the mixed beach is greatly influenced by the HWL fluctuations and beach morphological changes, which alter the relationships obtained for the upper beach (compared to those measured in the middle beach).
7. The wave direction proved to be an indirect influence on the mixing depth as a consequence of the geomorphology of the coast.
8. Linear relationships were determined between the maximum significant wave height and the depth of disturbance. The correlations determined from the measurements located at the middle sections of the beach are 26% lower at Cayeux-sur-Mer and 70 to 85% lower at Birling Gap when compared with Ciavola et al.'s (1997) empirical formula for steep sand beaches.

The following chapter will now investigate the final component necessary to measure Longshore Sediment Transport: “its length” (Chapter 1 Section 1.1 & Figure 1.1).

Chapter 6. Longshore Sediment Transport

6.1 Introduction

The aim of this chapter is to identify and quantify the processes of longshore sediment transport and sediment motion on a mixed sediment beach.

In earlier chapters, particular attention has been paid to the beach profile evolution and the active layer thickness on mixed beaches at both study sites. This chapter focuses on the longshore and cross-shore sediment transport patterns and LST rates on these beaches. For each fieldwork survey organised during this research, two methods (tracer and topographical surveys) have been used to measure LST rates. This chapter presents:

- (a) a description of the recovery rates for each deployment,
- (b) a detailed description of the most recurrent dispersion patterns in relation to the very specific hydrodynamic conditions and the general evolution on the beach profile.
- (c) the calculation of LST from these patterns and the average alongshore distance travelled. These calculations are done using two methods, (i) using the depth of disturbance, the component of the active layer measured in Chapter 5. This is supposedly the most accurate (e.g. Nicholls and Wright, 1991; Van Wellen et al., 2000) but also the most understudied on gravel beaches (e.g. Stapleton et al., 1999; Curoy et al., 2009); and, (ii) using the depth of burial of the deepest

tracers. This latter is the most commonly used method but also the most criticized over its key assumption of there being a uniform moving layer across the beach (e.g. Nicholls and Wright, 1991; Van Wellen et al., 2000).

- (d) the creation of digital elevation models from the topographic surveys enabled the calculation of beach volume changes on a tidal basis.
- (e) a discussion and comparison, from the results, of the performance and limits of the techniques used for the field measurements and the data collected.
- (f) an explanation of the most recurrent dispersion patterns on the basis of existing knowledge of the ground water flows, HWL fluctuations and hydrodynamics processes operating on gravel beaches.

6.2 Background

Longshore sediment transport is certainly the phenomena most investigated all over the world in studies regarding the coastline evolution. A lot of predictive formulae or models have been specifically designed for the calculation of longshore sediment transport. However, most of the number of documented studies, data acquired in laboratory, field experiments and analytical/numerical models are dedicated to sandy beaches and very few consider gravel beaches directly. This delay in the progress of research is essentially due to the limitations of the equipment and techniques presently available, and because of the dynamics of the environment and the complexity of the grain size distribution.

On gravel beaches the sediment dynamics are clearly much more complex than those on sand beaches. For this reason, simplifying assumptions are made and consequently measurements of LST are a lot more approximate.

Because of the complex processes operating on gravel beaches, a large number of parameters need to be collected simultaneously. Schoonees and Theron (1993) collected field data from studies on longshore sediment transport for 273 points from all over the world (sandy and gravel beaches). After evaluation of the number of measured parameters during these studies, they classified them by order of reliability. The parameters that Schoonees and Theron (1993) took into account were the wave

conditions (wave height, wave period and wave angle), the longshore sediment transport rate and the method to measure it (tracers or sediment trap), the beach gradient and grain size. In their review, a lot of studies were judged unreliable because of their lack of concurrent wave measurements. They recommended that to estimate the random error involved in the data and to demonstrate the consistency of the measurements to be used for models calibration, multiple measurements of sediment transport rates need to be made simultaneously. A certain degree of awareness of the limits associated with the methods used to measure LST rates is necessary when calibrating models. These limits are discussed later in this chapter.

Over the years the techniques to measure LST have improved significantly. These techniques can be grouped in three main categories. The most commonly used techniques are (i) tracers (e.g. Jolliffe, 1961; Hattori and Suzuki, 1978; Wright et al., 1978; Caldwell, 1981; Workman et al., 1994; Bray et al., 1996; Van Wellen et al., 1997, 1998); then, maybe as popular as the tracer, (ii) sediment traps (e.g. Chadwick 1989; Austin and Masselink, 2006; Dawe, 2006) and finally (iii) DGPS topographic surveys (e.g. Morton et al., 1993; Van Wellen et al., 1998). The following section will focus on earlier studies using these techniques and some of their results. Note that this is not a full inventory of all the published studies or field experiments on gravel or mixed beaches, but it focuses the research considered most relevant to the aims of this study.

6.2.1 Field-based observations and measurement of sediment transport using tracers

In order to study pebble behaviour *in situ* and to quantify longshore transport on shingle and mixed beaches, many tracer techniques can be used: fluorescent painted pebbles (e.g. Jolliffe, 1961), aluminium pebbles (e.g. Van Wellen et al., 1998), electronic pebbles (e.g. Workman et al., 1994), non-indigenous pebbles (e.g. Hattori and Suzuki 1978), radioactive pebbles (e.g. Kidson and Carr, 1959). Chapter 3 provides a detailed review of the most classical tracer pebbles and their advantages and limitations.

The use of tracers can provide an estimate of transport rates over time periods from hours to months. Tracers are commonly placed in the swash or surf zone where they can

be tracked on the beach. The dispersion pattern and the distance travelled by the tracers provide information about the sediment transport rates over a determined period of time. The general advantage of tracers is that it is a non-invasive technique and has been used successfully (i.e. high recovery rates) in high-energy conditions (e.g. Curoy et al., 2007). However, as pointed out by Van Wellen et al. in 2000, one of the major limitations related to the use of tracer pebbles in the current state of the scientific research is that the actual depth of disturbance for the calculation of transport rates is still only estimated, and therefore the depth of disturbance on mixed beaches or gravel beaches in general requires further investigation in order to quantify and develop accurate models of LST.

Many previous research studies have used tracers to study how pebbles behave. Jolliffe (1961) carried out LST experiments on different shingle beaches using fluorescent tracers and a method called: “The Dilution Method”. The Dilution method was developed in the laboratory in order to estimate the concentration of tracer pebbles in the beach sediment based on the recovery of pebbles on the beach surface. Based on his samples, he identified a linear relationship between the number of fluorescent tracers underneath the surface and the number visible at the surface. However, one of the major failures from the dilution method is that it is based on the assumption that the concentration of the tracer material is constant within the active layer. Recent experiments such as Osborne (2005) or Curoy et al. (2007) investigating the tracer pebbles dispersion at depth indicate that such an assumption is wrong.

Later, Jolliffe (1964) conducted further experiments using fluorescent tracers at Seaford (East Sussex, East Sussex) and collected some evidence showing that larger pebbles travel faster. This observation was later confirmed Bird (1989; 1996) on Chesil beach (Dorset), and explained by Carter (1988) through phenomena of impedance, acceptance and rejection of pebbles within a sediment mixture. Sear et al. (2001) using electronic pebbles on the mixed sediment beach of Shoreham-by-Sea observed this same phenomenon. Such observation highlights how important it is for the tracers to be representative of the beach material to derive reliable LST rates.

One of the biggest tracing experiments ever made in situ was the one conducted by Hattori and Suzuki (1978) in Suruga Bay (Japan). They deployed a total of 7000 non-

indigenous tracers (made of dacite) on a microtidal sand and gravel beach and simultaneously recorded the offshore wave data. Because of the tracers type, only surface recovery was possible and consequently the recovery rates were low (2 to 3% for each survey). However, because of the amount of tracers deployed, such study cannot be ignored. To date the amount of tracer pebbles recovered during this experiment (350 tracers in total) is amongst the highest ever measured. Generally, as pointed out by Van Wellen (1999), “passive” tracer experiments are based on a maximum of 100 to 150 clasts. With an expected recovery of $\geq 60\%$ associated with “passive” tracers (Allan et al., 2006) this only represents sixty to ninety pebbles. Hattori and Suzuki’s (1978) study is even more interesting as it recorded sediment transport for various wave conditions. Indeed, based on their data, they identified mean tracer movement of 2 m day^{-1} in “typical” wave conditions, $50 \text{ to } 60 \text{ m day}^{-1}$ during “storm” conditions and 1 km day^{-1} during “typhoon” conditions. This study is most certainly very valuable for the research on gravel beaches; Komar (1988) even integrated these data into the CERC equation to derivate a littoral drift efficiency constant (K) of 0.1 (dimensionless constant) for gravel beaches. However such coefficient should be taken with care as the calibration uses only results from a surface recovery; the limits of such experiment is clearly self explained by considering that 97 to 98% of the tracers deployed were mixed and lost into the beach material with no idea of their position. Indeed, these pebbles could have travelled a lot further than those recovered or on the contrary they could have been dormant in the deepest layers of the beach face and travelled very little. Because of such limits with the methods, these data are not sufficiently reliable to produce reliable LST rates on gravel beaches.

Wright et al. (1978) used aluminium tracers in large quantities on Hengistbury Long Beach (Hampshire). They conducted two main experiments in May 1977 when they deployed seventy five aluminium pebbles and in February/March 1978 when they deployed 460 aluminium pebbles. The tracer pebble used had a D_{50} of 40 mm which was close to the mean beach grain size measured at approximately 32 mm. The results were very encouraging as over respectively sixteen and twenty days, the recovery rates were above 63 %.

Nicholls and Wright (1991) completed this work by using two different grain sizes on a beach located only 14 km west of Wright et al.’s study site (1978). In March 1982, they

seeded 759 aluminium tracers at (Hengistbury Long Beach (Hampshire) and Hurst Castle Spit (Dorset) and traced their movements during fifty days. The grain size selected for the tracers (eleven types in total, D_{50} of 27 to 49 mm) were representative of the peaks observed in the grain size distribution of the coarse fraction of the beach material (D_{50} of 32mm). After fifty days of deployment respectively, the cumulative recovery rate was 62%. Based on Komar and Inman's work (1970), they developed a method to calculate the drift rate (Q_l). Based on three parameters: the velocity of movement of the tracer centroid (U_s), the width of the active beach (m) and the thickness of the moving sediment layer (n) (mixing depth or depth of the deepest pebble recovered), the equation is:

$$Q_l = U_s \cdot m \cdot n \quad (6.21)$$

Note that the depth of disturbance can be taken into account as the depth of the boundary between the moving and the non-moving tracers (Voulgaris et al., 1999). To measure that depth with tracer pebbles, Van Wellen (1999) used the depth above which 95% of the moving tracers were recovered. One of the principal assumptions made by this analytical model is that there is no-loss offshore of sediment in the system. This was supported by Nicholls and Wright (1991).

From the data acquired in both study sites (Hurst Castle Spit, Dorset), Nicholls and Wright (1991) attempted to estimate a value for K that represents the drift efficiency on gravel beaches based on the CERC formula (Komar and Inman, 1970; U.S. Army corps of Engineers, 1984). Their result showed that K for pebbles with c-axis of between 15 and 30 mm has a value of 0.02 (with respect to H_s , see Chapter 7 for more information). Both of these studies were completed with wave conditions, sediment size, beach gradient and depth and width of movement measurements allowing them to pass the requirements of Schooneess and Theron (1993) as mentioned earlier which indicates that they measured reliable LST rates supporting the reliability of their estimate of the K value.

Bray (1996) conducted a large scale aluminium tracer experiment simultaneously on two beaches: a pure gravel beach at St Gabriel's (Dorset) and a mixed sand and gravel beach at Charmouth (Dorset). The tracer recovery was undertaken in forty searches

distributed over one year. Over this period a large spectrum of wave energy conditions were observed and consideration given to variables that included the tracer size, shape and position on the beach. The main outcomes from the tracers' movements indicate that pebbles on the upper beach are the most rapid and it also appears that the biggest pebbles travel the fastest.

With improving technology Workman et al. (1994), followed by Bray et al. (1996) and then Sear et al. (2001) have used electronic pebbles and aluminium pebbles to trace sediment transport at Shoreham-by-Sea (West Sussex). The deployment was distributed in three across-shore locations. The high recovery rates (>80%) experienced during the eleven days long survey period by the electronic pebbles and the high energy conditions recorded at the time proved how successful they can be. In comparison, recovery rates for the aluminium pebbles are lower but with recovery rates down to 47% during the exact same conditions. In low and intermediate energies, both types of tracers proved to have recovery rates superior to 90%. In an attempt to judge and compare the performances of both of the tracers, Bray et al. (1996) calculated the volumes of sediment transport associated with both tracers' dispersion. The LST rates calculated ranged from 9 (low energy conditions) to 3280 m³ tide⁻¹ (high energy conditions) using the electronic tracers, and 13 (low energy conditions) to 1952 m³ tide⁻¹ (high energy conditions) using the aluminium pebbles. The faster and deeper search capacities of the electronic pebbles are most certainly the factor increasing the recovery rates especially after high energy wave events. As a consequence they deliver better representation of the actual LST rates occurring. Bray (1996) highlighted that the location of a tracer's injection point has a greater influence on its transport than its actual shape. This was later confirmed by the results obtained by Lee et al. (2000) and Sear et al. (2001).

Van Wellen et al. (1998, 2000) also worked on the beach at Shoreham-by-Sea. Using various types of tracers (painted or indigenous pebbles, aluminium tracers, and electronic tracers, all covering a large range of grain sizes) and topographical surveys, they compared the LST derived from their results to those predicted by LST analytical models. They indicated that the transport rates derived from the tracers generally over-estimated the expected LST. It was suggested that the error could be coming from the calculations technique for obtaining sediment transport rates from the tracer data.

Indeed, the temporal and spatial variability in the depth of sediment disturbance and the width of the active profile need to be accurately measured to calculate a precise LST rate.

Along the same lines as Bray et al. (1996), much of the earliest work using aluminium or electronic tracers had been designed around the specific aim to calibrate LST formulae. However, more recent studies have begun to examine sediment transport patterns and processes operating on gravel beaches by looking more specifically at individual particles. The aim to quantify accurately the LST to calibrate or create predictive models remains the driving force yet current research tends to focus more on the influence of size and shape of the particles.

Osborne (2005) recorded the movement of the gravel and cobble size particles to measure LST on a mixed sand, gravel and cobble beach at Half Moon Bay Harbor (Washington, USA). The originality of his tracer technique was to tag sediment particles sampled *in situ* (his sampling method was according to Wolman, 1954) with a “small but powerful” magnet glued to the sediment particle by an epoxy resin. Osborne (2005) deployed three sets of thirty tracer particles each during the time period from December 2003 to February 2004. Despite the low number of tracers used in the study, the overall recovery rate was very high; approximately 93% and some interesting points were observed. First, larger and smaller particle tended to move alongshore rather than across-shore. Second, the smaller particles were affected by greater across-shore movements than the larger ones. He also confirmed that in general the bigger particle travel further distances than the smaller ones, confirming Bray’s observation (1996). However, Osborne (2005) indicated that this tendency is observed up to a critical size or mass beyond which the particle travel distance decreases with an increase in size. In the studies that have observed this trend, the differential in transport capacity has been related to the ratio of the particle surface area in contact to the competency of the fluid forces (e.g. Bray, 1996; Lee et al., 2000; Sear et al. 2001 and Osborne 2005). To summarize, bigger particles are more likely to offer larger surface areas of contact to the fluid forces than the smaller particles which are most likely buried or protected within the voids between the coarser materials. Through his experiment, Osborne (2005) also observed across-shore grading with the larger and more disc-shaped particles showing a

propensity to accumulate higher on the beach profile in the swash zone, whereas the smaller and spherical particles rolled down the slope. This phenomenon reinforces the sediment grading processes of acceptance, rejection or impedance (Carr, 1969) and highlights, once again, the necessity to deploy tracers of the same characteristics as those of the beach material to derive reliable LST rates.

Allan et al. (2006) investigated the transport of coarse sediment particles on a mixed sand and gravel beach on the Oregon (USA) coast with a newly developed type of tracer using a Passive Integrated Transponder (PIT). Such a system proved to be very successful in terms of recovery, 90% after eight months' deployment. The great benefit of such a system lies in the fact that the detection system activates the integrated transponder of the tracer up to a depth of 1 m when walking in its proximity. When the transponder activates, the receiver records the location, the depth and the ID of the tracer. This method allows a quick search and therefore the coverage of large areas on the beach is possible. An additional advantage is that the recovery does not need any digging and therefore the beach material is not disturbed for the good continuation of the experiment. Allan et al. (2006) deployed a total of four hundred PIT tracers that were released in two different periods, one in March 2004 and another in January 2005. During each deployment period, injection occurred on the lower and the upper section of the mixed sediment beach. Unlike the previous studies, Allan observed that the movements of his tracers were faster on the mid- and lower beach indicating that this seemed to be where the bulk of the tracers congregate. Here again, the coarser particles seemed to travel faster than the smaller ones. Allan et al. (2006) also noticed that the shape of the sediment particle is of no real significance to its distance travelled, supporting earlier observations from Bray (1996), Lee et al. (2000), and Sear et al. (2001).

After such a review of a few of the tracer pebble experiments conducted over the years, it is important to keep in mind the limits of these techniques. Bodge and Kraus (1991) investigated the reliability of the tracers and stated that LST rates derived from tracers could be in error by a factor of 4 due to limitations in recovery rates. Nicholls and Wright (1991), later supported by Van Wellen et al. (1998) rigorously insisted on the

necessity to measure precisely both the depth of disturbance and the width of the beach in order to derive reliable LST rates.

In order to determine the correct amount of tracer pebbles necessary to be deployed to have a representative study of the actual LST, Lee et al. (2007a) developed a statistical method specifically designed for gravel and pebble tracers studies. The urge from the scientific community for such a tool is becoming more and more important, as pebble tracer studies keep growing but no clear experiment protocol of deployment is yet in place. Such a statistical method would help to harmonise the type of data collected around the world on gravel beaches by enabling the control of either the accuracy of a tracing experiment in the literature, or determine the number of tracers required to achieve an accurate result prior to an experiment. Such filtering control would also increase the precision of the current LST models in use.

This statistical method still requires further refinements. Indeed, despite claiming that the shape of the sediment particles is of no influence on their model, it seems curious to only consider the size of the pebble for its representativeness. Indeed, two pebbles can have the same size but their shape can be different and therefore the hydraulic behaviour will be different too. It is common, for example, to observe grading by shape on gravel beaches (Bluck, 1967, Orford, 1975). It seems necessary therefore that this tool requires further investigation before it is used recurrently to judge and classify tracer studies qualities.

Information delivered by tracers' dispersion is commonly used to calibrate or develop longshore transport models, however such a technique presents few limitations based on the assumptions that the tracer behaves in the same manner as the natural beach material and that the tracer's motion can be adequately monitored (Kraus, 1987; White, 1998; Komar, 1998). On gravel beaches in general, additional difficulties are encountered. The large spectrum of the particles' grain sizes and shapes plus the great volumes of material transported can raise some doubts about the degree of representativeness of such techniques. Therefore, to be representative of the LST on gravel beaches, tracing experiments should be looking at multiple grain sizes and shapes present in the indigenous beach material (e.g. Osborne, 2005) and be deployed in great quantities to

make sure that the dispersion of the tracers is representative of the general LST (e.g. Hattori and Suzuki, 1978). Unfortunately, in the context of present day technological progress, both of these requirements are generally working against each other. For example, painted, fluorescent or “exotic” tracers can be produced and deployed in large quantities; however, such tracing techniques afford only a surface recovery, lowering greatly the recovery rates. On the other hand, techniques such as aluminium or electronic tracers allow the production of tracers with the same sizes and shapes as the indigenous beach material and reach good recovery rates even at depth. However, such techniques are more costly and most often their deployment is restricted in number (e.g. Van Wellen, 1999) because of the time consuming recovery procedure. Moreover, the ability to tag particles or even find them easily in the matrix of the beach material is often limited to a certain size. For example, the PIT system used by Allan et al. (2006) can tag particles down to 16 mm. Such small aluminium tracers would not only be very hard to detect with a metal detector, but also very hard to identify within the mixture of the beach material (this observation is based on personal experience using aluminium tracer of approximately 1 cm b-axis and 0.5 cm a-axis).

The main uncertainty when using tracers is related to the tracers not found. Indeed, these tracers can either be buried deep into the beach material or have travelled out of the survey area. Such imprecision biases the transport rates measured in the study area (Chadwick, 1990; Kamphuis, 1992). Therefore, it is necessary to define precisely the spatial (x, y and z direction) limits of the surveyed area. An easy way to minimise the loss of tracers is to conduct the surveys preferentially during low wave energy conditions. The introduction of electronic tracers that can be detected up to 1 m depth and the rather quick search of this technique clearly improved the results (e.g. as mentioned earlier, Allan et al. experienced a 90% recovery rate after eight month deployment). It is important to mention that detection problems can also influence the results just by missing the detection signal made by the equipment.

Finally, the across-shore location of a tracer also influences its movements on the beach (e.g. Allan et al., 2006). Therefore, when using tracer pebbles it is recommended to deploy them widely across the beach.

6.2.2 Field-based observations and measurement of sediment transport using topographic surveys

Topographic survey is the most commonly used technique to observe numerically the beach morphological changes over time. In the proximity of coastal structures that are able to stop the longshore drift, such as major harbour arms, repeat surveys may be used to monitor the beach volume changes over time giving an indication of the LST (e.g. Morton et al., 1993; Van Wellen et al., 1998, Van Wellen, 1999; BAR, 2008). This technique is also called the impoundment technique, and its performance are largely recognised for the study of sandy beaches, however only a few studies (e.g. Bodge and Kraus, 1991; Van Wellen et al., 1998) have considered its performance on gravel beaches even though it is widely used by coastal managers along the UK coast.

According to Van Wellen (1999), the use of topographic surveys to measure LST rates has limitations. In order to minimise these limitations and deliver reliable information on LST rates, the surveyed area must be of a large extent in both directions, across-shore and alongshore. Both of the field sites used in this study were generally widely uncovered by water at low tide permitting the surveyed area far onto the sandy platform in an across-shore direction at Cayeux-sur-Mer (Chapter 4) and at Birling Gap onto the solid chalk platform.

Because of the presence of a coastal structure interrupting the LST, the coast on either side re-orientates itself. As shown in Chapter 1 Figure 1-5, the updrift side of a groyne or harbour arm will present an accretive concave shaped beach whereas on its down drift side will show an erosive convex shaped beach. For this reason it is important to extend to a maximum alongshore length of the survey area on either side to reach an average value for the sediment transport that is representative of the actual LST rates (Van Wellen et al., 1998). Van Wellen et al. (1998) pointed out that the 1cm vertical error reached by a DGPS, which this study used, is adequate to deliver reliable results for beach volume changes.

Bodge and Kraus (1991) suggested that impoundment techniques are inaccurate with error margins going from 10 to 100% in regards to the measurement of LST. This error

is caused by spurious trapping of sediment that is unrelated to the actual longshore transport.

Finally, one the last sources of imprecision of the method can be related to the amount of points collected during the topographical survey. Generally, the more points collected the better resolution can be reached. The BAR project (BAR Interim report 2005) showed that good quality results in modelling the beach topography were reached for a distance interval between the profiles of approximately 25 m (Chapter 3 Section 3.2).

The interpolation of the digital elevation model is also a source of approximation from the software based on the type of interpolation. Contrary to sandy beaches which digital elevation models are quite often interpolated using a kriging method (Cressie, 1990), this study opted for a linear method approach. Such an approach was strongly motivated because of the physical form of gravel beaches to get perfectly swash aligned in a quick time. The BAR project (BAR, 2005) led a battery of tests to judge of the performances of either of the two interpolation methods and concluded that the linear method produces more reliable digital elevation models than the kriging method.

6.2.3 Field-based observations and measurement of sediment transport using traps

There are two main types of sediment trapping strategies. Firstly, the use of a number of small rectangular traps deployed across-shore. Each trap, consisting of a steel cage, is mounted on the beach surface and anchored with a rod into the beach or onto an existing structure. The open mouth of the trap is generally oriented to face the expected drift in order to capture the incoming sediment. The traps are generally emptied and weighed on every tide (e.g. Chadwick 1990, Bray et al. 1996, Morfett, 1989). The second strategy involved measuring the sediment transported by single waves into the run-up and the backwash onto the beach face. The principle is actually the same; a cage is put on the beach face but this time for only a very short time, just enough to sample the sediment transported in the run-up or the backwash. Mobile traps are very popular on gravel beaches to measure instant LST rate (e.g. Kraus, 1987; Van Wellen et al., 1997; Austin and Masselink, 2006; Ivamy and Kench, 2006).

The mobile sediment traps have greater advantages to most of the sediment tracers as the sediment transport can be linked to very specific wave and current conditions at a specific point in time and space (Kraus, 1987). Such results are very useful to the calibration of existing analytical models. The first type of sediment trap method (settled on the beach) has proven to deliver valuable information when a number of sediment traps are deployed simultaneously across-shore so that the measurement of the distribution of the transport rates across the beach is rendered possible (Chadwick, 1990). The specific modes of transport of the particles on gravel beaches, i.e. bedload, sheet flow and quasi-suspended load at the point of wave bore collapse (Austin and Masselink, 2006) render the use of sediment traps very successful in capturing reliable sediment samples of the mass in movement.

However, on gravel beaches the competency of the sediment traps to deliver reliable information on sediment transport is mainly limited to low wave energy conditions. For example, Chadwick (1989) in his study at Shoreham-by-Sea was able to derive short term transport rates from traps located at mid-tide level of 4 to 32 m³ day⁻¹ though his observations were limited to waves with H_{rms} between 0.23 to 0.48 m. Chadwick (1989) indicated that in high energy conditions, the total capacity of the traps can be quickly filled up and therefore no reliable sediment transport can be determined.

Mobile traps are also limited during high energy conditions because on the practicability of such heavy load. Indeed, the strong swash resulting from high waves makes it difficult to go in and out the water to collect sediment with the traps. The power of the drag combined with the weight of the cage and the sediment sample, makes the pulling out from the water very difficult.

Another problem encountered with sediment traps concerns their stability on the beach face. The partial removal, complete removal or just change in orientation of a trap would affect the reliability of the volume of sediment sampled and therefore falsify the calculation of the LST rate (Van Wellen et al., 2000). It can also be argued that the frame and the anchoring of the sediment traps alter the water and sediment flows and therefore influence the quality of the sediment sample. For example scouring is often observed around sediment traps (e.g. Chadwick, 1989). Obstruction or interference from

flotsam and jetsam can also affect the volumes of sediment trapped by the cages. Finally, but not least, the mesh size of the cage is a critical limitation that has to be taken into account. A small mesh would capture a wide range of grain sizes; however, it would fill quicker than a bigger mesh and therefore risks being filled over a tide are much greater, especially on gravel beaches. On the other hand, using a big mesh would let the smallest particles slip away from the trap and therefore valuable information on the LST is discarded. Such limitations have to be taken into account when imputing such data in a model.

In order to verify the reliability of the techniques for measuring LST, Bray et al. (1996) compared the results obtained by sediment traps to those obtained from tracers. The main observation was that the estimated volumes of sediment transported using traps were significantly lower than those measured using tracers. For this reason, Bray et al. (1996) concluded that sediment traps on gravel beaches are unreliable in conditions other than low energy wave conditions.

Note that because of the heavy labour required to conduct fieldwork at low tide for the search of the tracer pebbles, the active layer measurements and the DGPS surveys, plus considering the conclusions of Bray et al. (1996) about the quality of the results based on the use of traps, it was decided not to use sediment traps at all for this research.

6.2.4 Laboratory-based longshore sediment transport experiments

Laboratory studies examining the processes governing longshore sediment transport on gravel beaches were for a long time disregarded because of the scale problems and the difficulties in reproducing the exact characteristics of a natural gravel beach. Instead, researchers focused on aspects that are more easily replicated such as the evolution of the beach profiles, beach permeability and porosity, the ground water and the infiltration/exfiltration fluxes, the swash transport potential, etc (e.g. Powell 1990; She et al. 2007; Nielsen et al., 2001; Trim et al., 2002; Lorang, 2002; Blanco et al., 2003, Pedrozo Acuña, 2005; Lee et al., 2007b). By investigating such parameters, the studies deliver valuable information on the parameters driving sediment transport on gravel beaches and more specifically for this study, mixed beaches.

Van Hijum and Pilarczyk (1982) conducted one of the first laboratory studies that specifically examined LST on gravel beaches. Through their experimentations, they tried to identify the effects of various factors influencing pebble behaviour such as its initial across-shore location, the grain size and shape of the pebble, the wave angle and the beach slope. They concluded that the transport of material takes place essentially as a single moving layer, and not as the independent responses of individual sediment fractions, because the larger pebbles impede the movement of the smaller ones (e.g. Carter, 1988). Van Hijum and Pilarczyk (1982) also proved through their laboratory experiments that when the incident wave angle to the beach increases, the across-shore component of the motion becomes smaller and the alongshore component larger. From all these important implications on the longshore transport processes Van Hijum and Pilarczyk (1982) developed an analytical equation known as the Delft equation.

Later, Kamphuis (1991) using partly Van Hijum and Pilarczyk's results (1982) and laboratory experiments, developed an expression to predict sediment transport measured for a wide grain size range. Their results showed that sediment transport was proportional to wave energy, supporting the application of the wave energy approach to gravel beaches, which is explained further in Chapter 7.

In the laboratory, Coates (1994) examined longshore transport using crushed anthracite to model gravel size particles and traps all around the basin that would catch the particles as they would try to leave the water tank as a direct consequence of LST. One of the most interesting points is that, he observed that there was a large proportion of suspended load transport (cited in Van Wellen, 2000). On the contrary, Austin and Masselink's (2006) in situ observations led them to claim that transport occurs as bed load and as sheet flow through the swash motion, with some quasi-suspended load at the point of bore collapse. This discrepancy between the results is a perfect example of how sometimes modelling experiments in the laboratory can vary from what is observed in nature (Brampton and Motoka, 1987). Maybe some of the particles of dacite were actually crushed and too small to represent adequately gravel size particles as in nature. Horn and Mason (1994) and then Pedrozo Acuña's (2005) research in the laboratory are

in agreement with Austin and Masselink's (2006) observations, clearly pointing out Coates (1994) misrepresentation in his modelled experiment.

Lee et al. (2007b) investigated, in laboratory conditions, the effect of groundwater and the flow pattern in the surf and swash zones on the deformation of the beach profile. The scientific community has largely recognised that the swash is the factor driving longshore sediment transport on gravel beaches and therefore being able to model the effect of the flows onto the beach profile evolution is a further step forward a better understanding on sediment transport.

6.3 Field measurement experiments, Cayeux-sur-Mer, December 2004

It was stated in Chapter 3 that two field campaigns were organised to collect data on the beach at Cayeux; one in December 2004 and a second in October/November 2005. Due to the significant differences in the experimental protocols used in each survey period (inconsistency in the location of the beach profiles, no strict measurement of the active layer in the survey of 2004), some of the data from December 2004 were incompatible with those from October/November 2005 as well as those from Birling Gap in 2006. This resulted in the omission of the morphological changes and active layer measurements observed at Cayeux in 2004 from the results in the previous chapters. However, in the current chapter, despite these changes of methodology, the beach volume changes and the tracer pebbles scattering are still delivering qualitative and pertinent data useable to derive LST rates.

6.3.1 Wave conditions

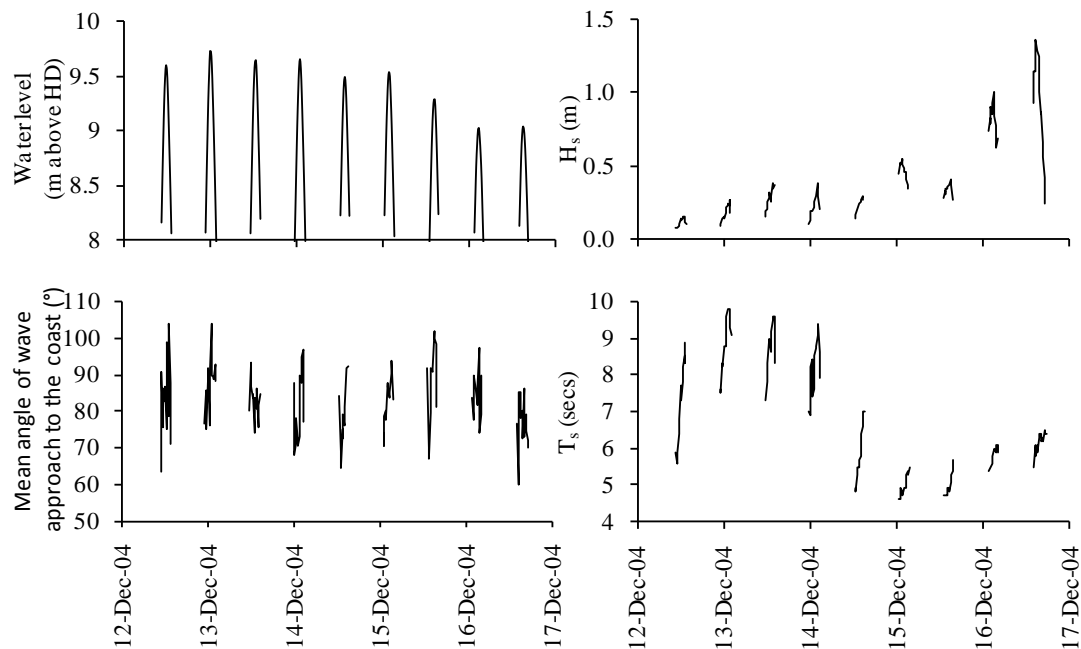


Figure 6-1 Wave conditions measured with an S4 on the foreshore off the terminal groyne at Cayeux-sur-Mer. Data were cut off for periods when the S4 was not covered by more than 1.5 m of water. This corresponds to the level of the beach step. The mean angle of wave approach to the coast is relative to the coast orientation (approximately N205°). Therefore, values above 90° correspond to waves coming from northerly directions whereas values under 90° correspond to southerly directions.

The wave data recorded at Cayeux-sur-Mer from December 12th to December 17th are presented in Figure 6-1. The survey period started one tide before spring tide (HWL measured at 9.72 m HD on the 13th) and finished when the HWL was going towards a neap tide (measured at 9.02 m HD on the 17th). Apart from the last tide, the mean angle of wave approach to the coast was very close to orthogonal with angle of approach varying during the overall period from 65 to 104°. On the first two tides, the wave approach was oscillating between North-Westerly's and South-Westerly's, with waves coming from a southern direction during the flood and waves coming from a northern direction during the ebb. On the following tides until December 16th, the waves were predominantly from the South-West. During the high tide on the morning of the 16th, waves were again approaching the coast close to its orthogonal. Afterwards from December 16th, mean wave approach was coming increasingly from South-West. The significant wave height increased with time. H_s was comprised between 0.1 and 0.3 m

on the first 3 days (from December 12th to December 15th), close to 0.5 m on the fourth day (December 15th) and finally reached up to 1 and 1.3 m respectively on the last two tides on December 17th. T_s can be split into two groups during the survey period. The first group, corresponding to the first two days, shows wave periods varying from 6 to 10 s between December 12th and 14th and the second group corresponding to the rest of the survey period shows wave periods from approximately 4 to 6 s. During the tidal cycle, current velocities were the strongest at mid-tide and weakest at high tide. Current direction was mainly northward in accordance with the waves and the expected longshore drift direction.

6.3.2 Tracer recovery and distribution patterns

As described in Chapter 3, the field data collection on December 2004 at Cayeux-sur-Mer was essentially organised to be a trial to establish an experimental protocol for the oncoming field campaigns at Cayeux, but also at Birling Gap. The main difference in methodology here in comparison to the latest field measurements of this study is that the deployment of the tracer pebbles occurred in only one location, in the middle of the beach, instead of three deployment points distributed at regular intervals along the beach profile (upper, mid- and lower mixed sediment beach) as described in the methodology for the other field measurement campaigns. The recovery of the tracers occurred one tide after deployment from December 12th to December 14th whereas for the deployments on December 15th and December 16th, two tides were passed before their search. This decision was forced by the time of the tides and the sunlight available on these days.

Date of deployment (max depth of deployment)	Location of the injection on the mixed sediment beach	Recovery rates (Total of pebble recovered)	Mean distance travelled (m)	Mean direction travelled (referred to the North in °)	Mean alongshore distance travelled after one tide (m)	Mean across-shore distance travelled after one tide (m)	Depth of recovery/ number of pebbles
12/12/04 afternoon (surface)	Mid-beach	100% (170)	≈1	114	0	1	Surface/170
13/12/04 morning (surface)	Mid-beach	82% (139)	4.7	297.8	0.2	-4.7	Surface/91 0- 10cm/44 10- 20cm/3 20-30cm/1
13/12/04 afternoon (surface)	Mid-beach	63% (108)	2.1	264.4	-1.1	-1.8	Surface/32 0-10cm/58 10-20cm/13 20- 30cm/5
14/12/04 morning (surface)	Mid-beach	76% (129)	2.9	331.0	1.7	-2.4	Surface/67 0-10cm/59 10-20cm/3
14/12/04 afternoon (surface)	Mid-beach	94% (160)	5.1	320.5	2.2	-4.6	Surface/110 0-10cm/48 10-20cm/2
15/12/04 (surface)	Mid-beach	68% (115)	33.0	14.2	32.5	-6.2	Surface/84 0-10cm/26 10-20cm/3 20-30cm/2
16/12/04 (surface)	Mid-beach	15% (25)	86.7	17.7	82.7	-11.1	Surface/6 0-10cm/10 10-20cm/4 20-30cm/5

Table 6-1 Tracer pebble recovery rates and mean distances travelled one tide after deployment at Cayeux-sur-Mer, December 2004. The positive value of the alongshore distances indicates that the centroid of the pebble scattering is located in a downdrift position (i.e. northward) from its injection point. A negative value means that its position is updrift from its injection point. Similarly, a positive value of the across-shore travelled distance indicates that the centroid is located higher up on the beach profile than its injection and vice versa, a negative value indicates that the centroid is located on lower areas on the beach profile than its injection point.

Please note that as in the table, the convention in the text is that positive values of the alongshore distances indicates that the centroid of the pebble scattering is located in a downdrift position (i.e. northward) from its injection point. A negative value means that its position is updrift from its injection point. Similarly, a positive value of the across-shore travelled distance indicates that the centroid is located higher up on the beach profile than its injection and vice versa, a negative value indicates that the centroid is located on lower areas on the beach profile than its injection point.

Recovery rates during this field survey were very high, being >60% for almost all the deployments except for the pebbles deployed on December 16th when it went down to 15% (Table 6-1). After the initial deployment of tracer pebbles on the evening of December 12th, the beach was visited on the following tide i.e. on the morning of December 13th. On that visit, it could be seen that a few tracer pebbles had dispersed within a 3 m radius around the injection point whilst most did not move much (Figure 6-2). The average movement over this period was measured at $\approx +1$ m up the beach. All the tracers recovered on that particular tide were detected by sight (no need to use the metal detector). The 100% recovery rate associated with this “visual detection” shows how little the tracer pebbles were buried during the ambient wave conditions of December 12th/13th.

The following recovery surveys from December 13th to December 15th showed slightly more dispersion of the tracers from their injection point. This dispersion was mainly across-shore down the beach with the centroid of the tracers’ scattering moving between -1.8 and -4.7 m across-shore from the injection point. The longshore dispersion increased with time; however the dispersion cloud was still within a 10 m radius from the injection point. The absolute value of the mean alongshore travelled distance varied from +0.2 m on the afternoon of December 13th to 2.2 m on December 15th (Figure 6-3, 6-4; Table 6-1).

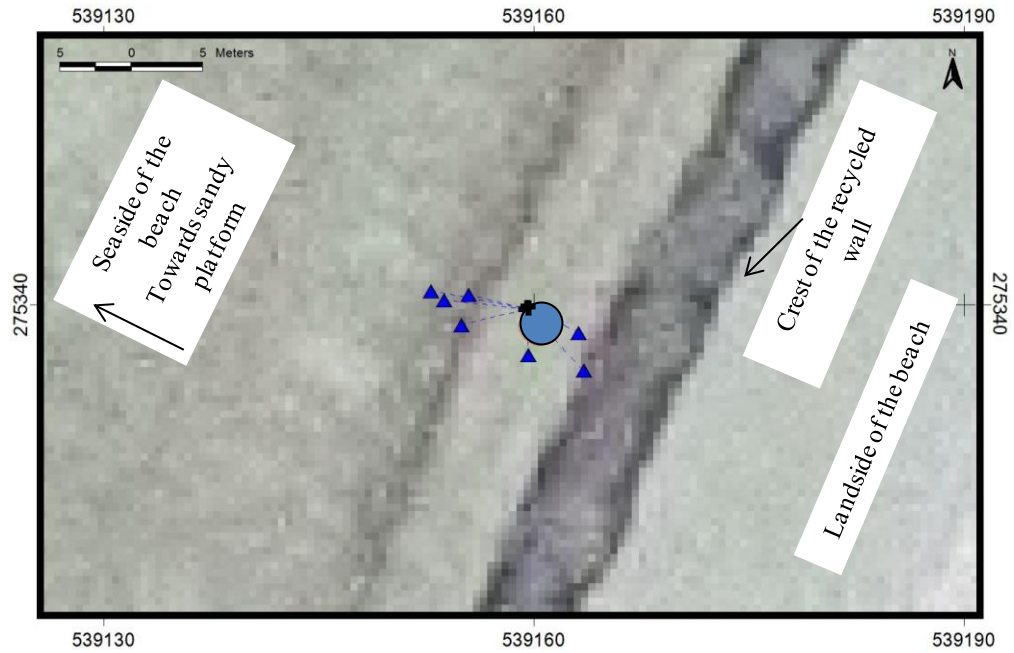


Figure 6-2 Tracer pebble dispersion recovered one tide after deployment on the morning of December 13th, 2004. The black cross marks the location of the injection point of the tracer pebbles on December 12th, 2004. Each blue triangle represents a tracer pebble. The big blue disk shows the location of the mount of pebbles that stayed still or moved very little. See Figure 3-11 for general location.

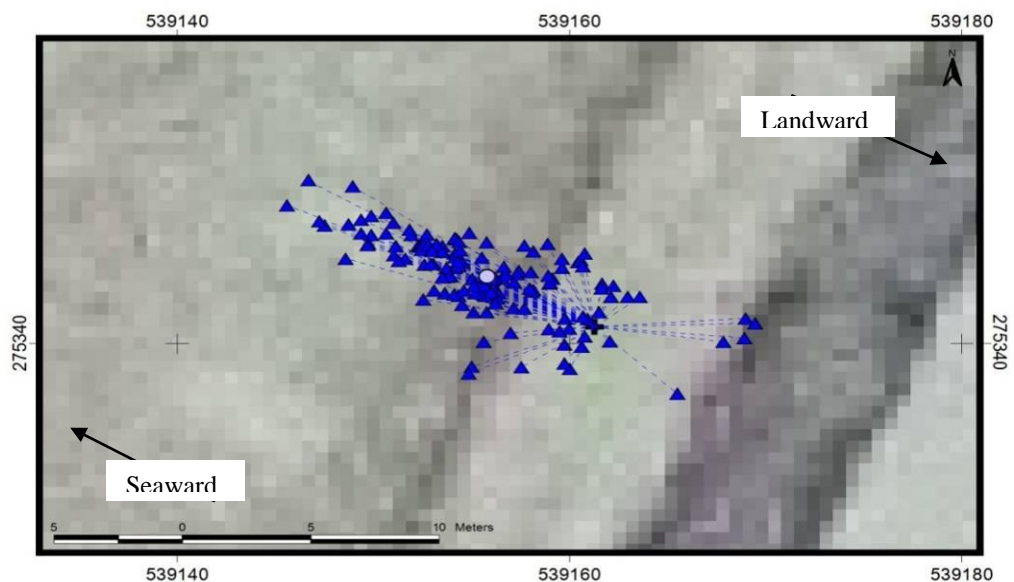


Figure 6-3 Tracer pebble dispersion recovered one tide after deployment on the afternoon of December 13th, 2004. The black cross marks the location of the injection point of the tracer pebbles on the morning of December 13th, 2004. Each blue triangle represents a tracer pebble.

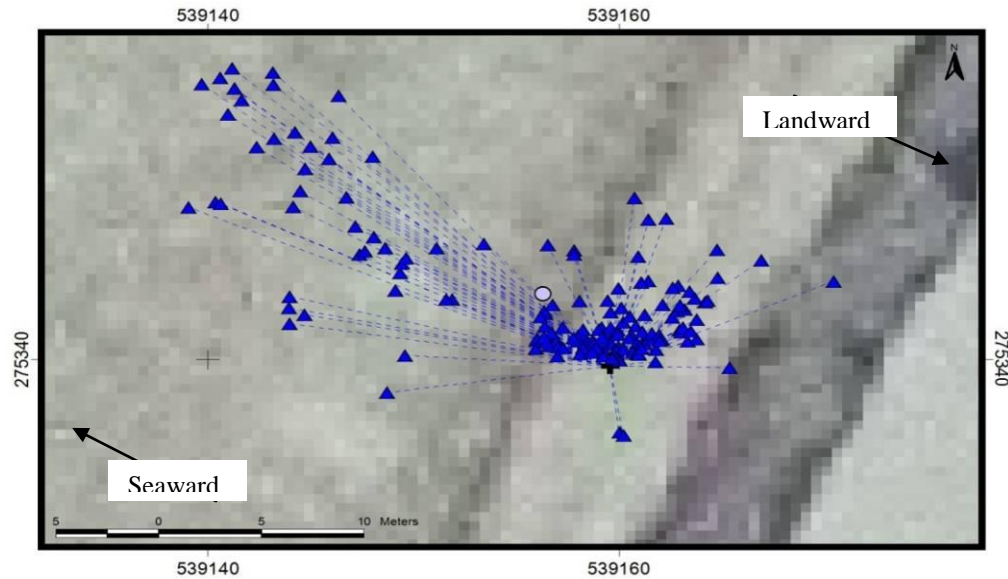


Figure 6-4 Tracer pebble dispersion recovered two tides after deployment on December 15th, 2004. The black cross marks the location of the injection point of the tracer pebbles on December 14th, 2004. Each blue triangle represents a tracer pebble.

On December 16th and 17th (Figure 6-5, 6-6; Table 6-1), the mean longshore distances travelled by the tracers were greater; the mean alongshore distances shown by the tracers' dispersions are measured up to 32.5 and 82.7 m respectively. The across-shore distances present an increase too, being respectively measured at -6.2 and -11.1 m, and showing a tendency to migrate down the beach. Despite this dispersion, the recovery rate on December 16th was 68% and a large amount of tracer pebbles were found at the surface (73%) or in the first 10 cm (22.6%) of the beach face. The furthest tracer pebble found on that day was 75 m away from the injection point. On December 17th (deployment proceeded on December 16th), the even greater dispersion of the tracer pebbles had the impact to reduce the recovery rate to only 15%. The furthest tracer pebble found was 165 m away from the injection point. The poor tracer recovery at the surface or the first 10 cm suggests that the tracers were considerably mixed and deeply buried within the beach material, and most certainly left the area covered by the survey. This is a clear example of the limitations of the techniques using tracers detectable with a metal detector to derive LST rates. These limitations being the size of the area that can be surveyed in the time available during low tide, but also the depth to which the metal detector can sense the tracers.

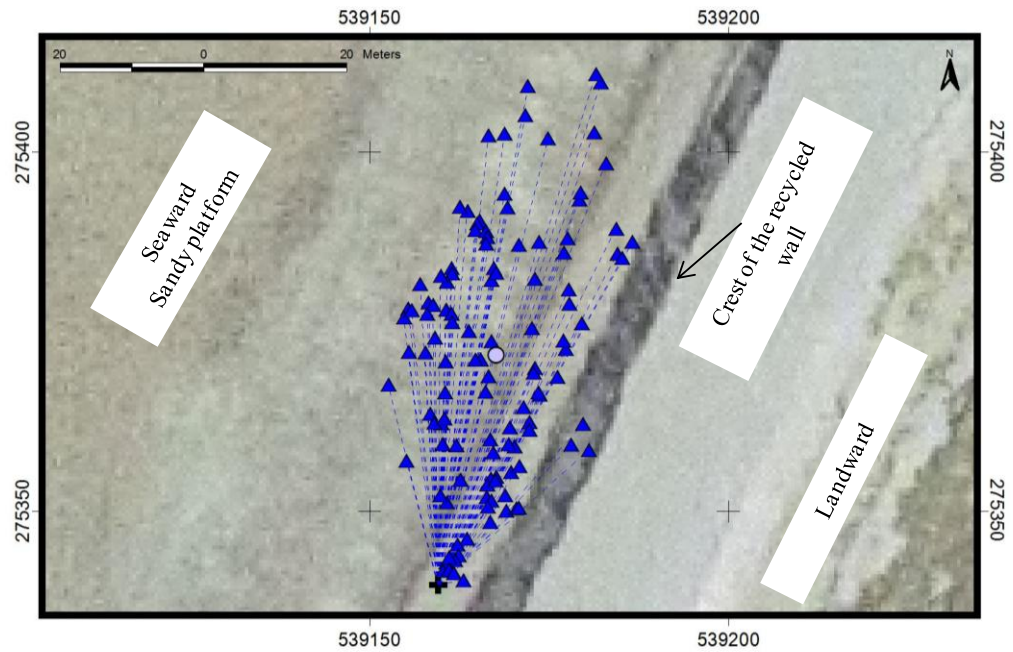


Figure 6-5 Tracer pebble dispersion recovered two tides after deployment on December 16th, 2004. The black cross marks the location of the injection point of the tracer pebbles on December 15th, 2004. Each blue triangle represents a tracer pebble.

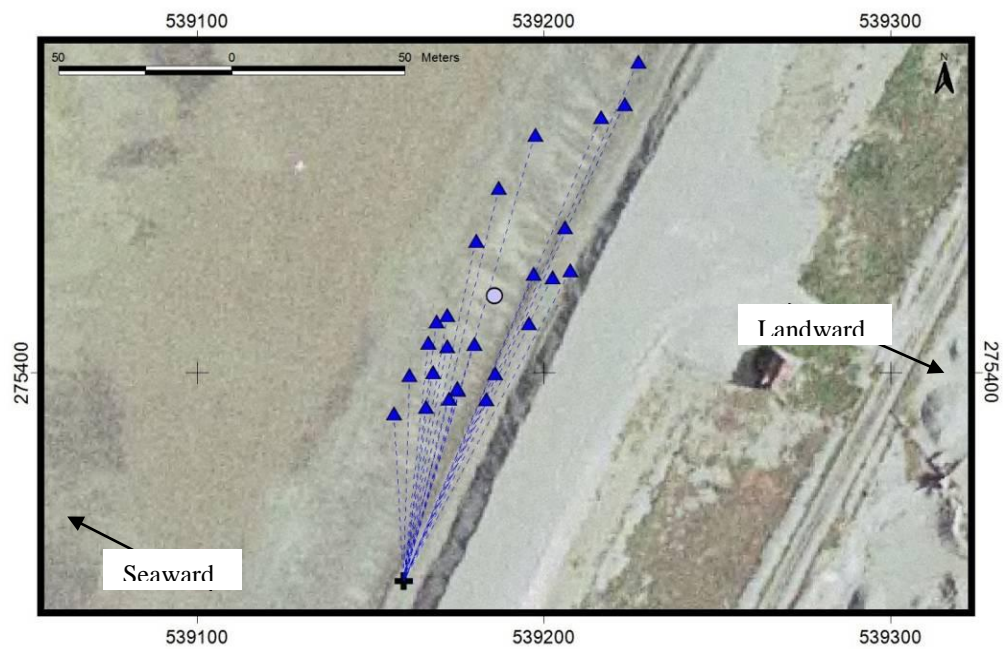


Figure 6-6 Tracer pebble dispersion recovered two tides after deployment on December 17th, 2004. The black cross marks the location of the injection point of the tracer pebbles on December 16th, 2004.

6.3.3 Derivation of the volume transported and the LST rates using tracer pebbles

By taking into account the mean alongshore distances travelled by the tracers on each deployment, knowing the average length of the active beach profile and assuming that the depth of disturbance is equivalent to the depth of the deepest tracer pebbles found (no measurement of the active layer were proceeded during this survey period), this study was able to derive LST rates (Q_l) for each tide or day (Table 6-2). Note that in contrast to Van Wellen (1999) who used the depth above which 95% of the moving tracers were recovered, it was decided by this study to consider the depth of the deepest pebbles found. This choice was motivated by: (i) no guidance has ever been given regarding such technique on gravel beaches; (ii) the detection at depth by the metal detector is limited to a threshold depth (based on experience, approximately 30 to 40 cm) and it is more than likely that many pebbles not recovered during the experiments are partly because they are too deep to be detected. Therefore, by using the depth of the deepest pebbles, this study estimates that a representative estimate of the mixing depth is reached.

Not only did the distance travelled by the tracers increase during the survey period but the depth of recovery did too (Table 6-1). On December 12th, this depth was only 5 cm (all pebbles found at the surface) whereas the deepest pebble found on December 16th and 17th (deployments of December 15th and 16th) was at depths up to 30 cm for pebbles that travelled the furthest. This corresponds to the combined effect of both the significant wave height increasing constantly over the time of the experiment, from less than 10 cm up to 1.3 m, an increasing mixing depth according to the relationships identified in Chapter 5, and a mean angle of wave approach that changed from being nearly orthogonal to the coast to being clearly from the south-west with an angle to the coast of approximately 77°, pushing the sediment in a northward direction. As a consequence, the greatest LST rates during the survey period are calculated for the two latter days with respectively 253.5 m³.tide⁻¹ and 787.7 m³.tide⁻¹ (Table 6-2). The earliest days of measurement were only subject to minor LST rates which were $\ll 30$ m³.tide⁻¹ on the mixed sediment beach. At the end of the survey period, the beach in front of the recycled area experienced a net volume loss of 2112.8 m³ according to the tracer data.

Date of deployment	Mean alongshore distance travelled after one tide (m)	Depth of the deepest tracer pebbles recovered (m)	Average length of the beach (m)	Q_{net} (m ³ tide ⁻¹)
12/12/04 afternoon	0	0.05	39	0
13/12/04 morning	0.2	0.25	40	2
13/12/04 afternoon	-1.1	0.2	45	-9.9
14/12/04 morning	1.7	0.2	48	16.3
14/12/04 afternoon	2.2	0.2	50	22
15/12/04	32.5	0.3	52	253.5 (507 for two tides)
16/12/04	82.7	0.3	63.5	787.7 (1575.4 for two tides)
Net volume loss for the entire survey period (m ³)				2112.8

Table 6-2 Calculation of the net LST rates (Q_{net}) using the tracer pebbles dispersion on the mixed sediment beach at Cayeux-sur-Mer between December 12th and December 17th, 2004. Note that the positive value indicates sediment transfer in a downdrift direction from the injection point (approximately northward) whereas negative values refer to sediment transfer in a updrift direction (approximately southward).

6.3.4 DGPS surveys: digital elevation model and beach elevation changes

The DGPS topographical surveys collected over the study period were used to create digital elevation maps from which the difference in altitude allows the calculation of the volume changes between two periods. The changes in elevation are represented on the digital maps on Figure 6-7.

When interpolating the elevation changes from one survey to the following during the survey period of December 2004, it can be seen that on some occasions (for example on the elevation map between December 12th PM to 13th AM or between December 13th AM and PM on Figure 6-7, the elevation change contours are parallel to the across-shore profile lines surveyed. These errors in interpolation from the software are linked to the irregular wide spacing between the profiles, the gentle cusps observed during the survey period and the linear interpolation method used to create the digital elevation models. This explanation is supported by the observation of equivalent but opposing

accretion and erosion movements in the southern part of the survey area. Despite these slight errors, it can be seen that most of the elevation changes occurred between December 16th PM and December 17th PM. Between these two days, erosion movements greater than -1.8 m and accretion movements greater than 1.2 m can be observed. In contrast, the changes in elevation between the surveys from December 12th to December 16th were mainly dominated by minor elevation changes (± 20 cm) on the mixed sediment part of the beach.

Because of the inaccuracies of the digital elevation models and the small beach elevation changes shown between December 12th and December 16th, it was decided to only consider the elevation changes observed during the overall survey period. The elevation changes map covering the period from December 12th to December 17th, displays severe erosion of the recycled material on the upper part of the beach (Figure 6-7). This erosion corresponds to a recession of the recycled sediment wall measured from 4 to 6 m in the southern part of the survey area, whereas in the northern part of the survey area, it corresponds to the recession of the berm. The material eroded from the upper parts of the mixed sediment beach clearly was to the benefit of the lower parts on the profile as the mixed sediment beach presents accumulation up to 0.85 m on its middle and lower parts.

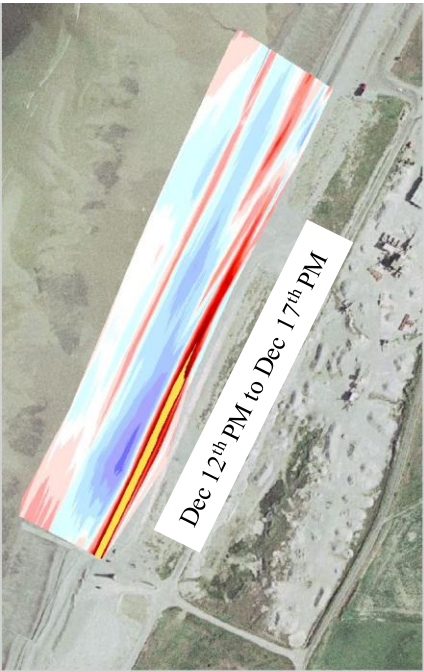
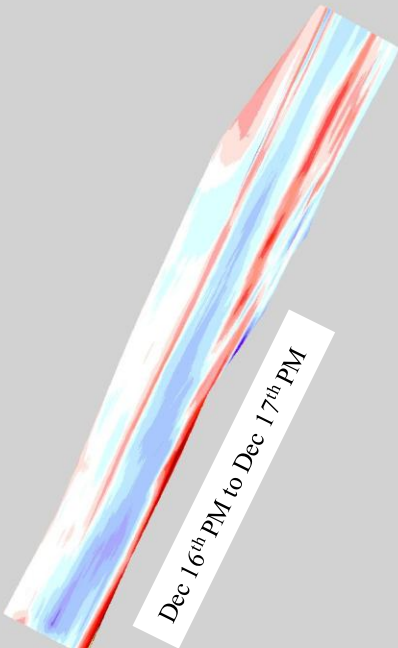
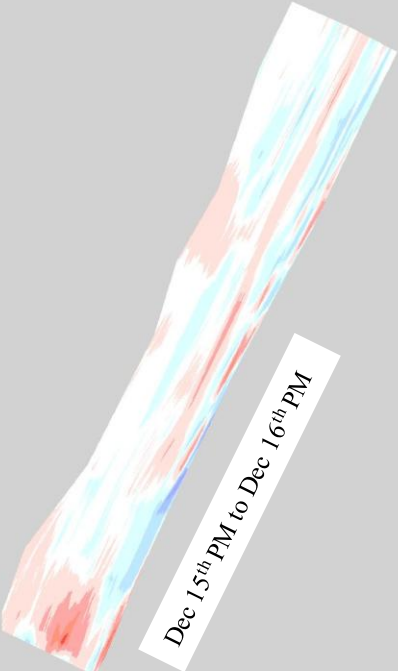
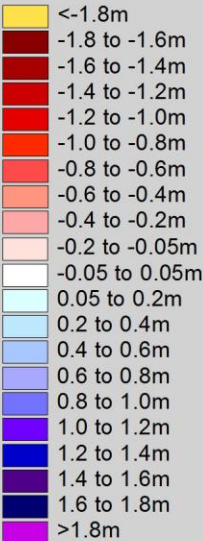
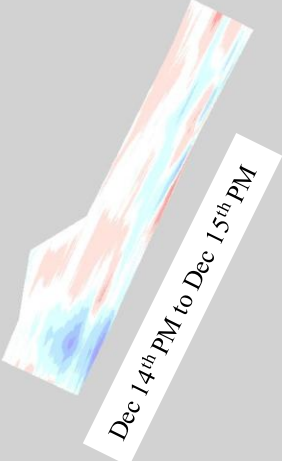
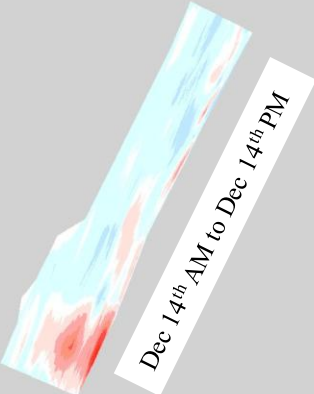
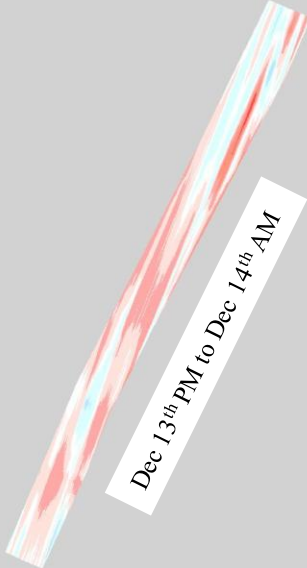
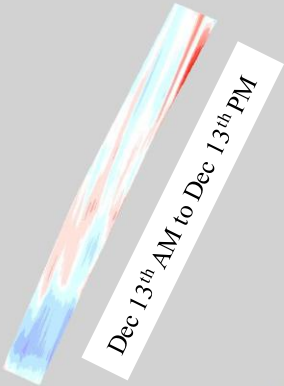
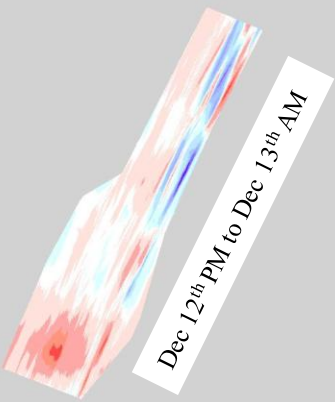


Figure 6-7 Changes in beach elevation between December 12th and December 17th 2004 at Cayeux-sur-Mer.



6.3.5 DGPS surveys: beach volume changes



Figure 6-8 Grid system used to calculate the beach volume changes from the survey at Cayeux-sur-Mer in December 2004.

To calculate the beach volume changes a grid system was adopted (Figure 6-8). This grid system was designed in such a way that the beach was sectioned into 100 m wide cells (in an alongshore direction) while in an across-shore direction, the beach was divided into two parts, one covering the mixed sediment beach and the second one covering the sandy foreshore. The alongshore width of the cells was derived on the basis of the longest distance between two profiles so that the volumes changes in each cell is at least interpolated from two profiles. The limit between the mixed sediment beach and the sandy foreshore was delimited by the maximum extent of the mixed sediment beach during the survey period. The advantage of dividing the beach into alongshore sections is that areas of sediment departure or arrival can be identified alongshore through time.

Whilst some of the eroded material was deposited on the lower beach and upper foreshore as shown by the digital elevation changes map (Figure 6-7), the net volume change during the overall survey period is dominated by erosion on the mixed sediment beach. The total erosion from cell 1 to cell 4 was measured up to 2121.9 m³. Only the cell located in the most downdrift area of the surveyed area displayed accretion but by a mere 60 m³, 2.7% of the volume eroded just updrift. The net volume loss over the time period for the surveyed area between December 12th and December 17th (nine tides in total) was measured as being 2063.4 m³ (Figure 6-9).

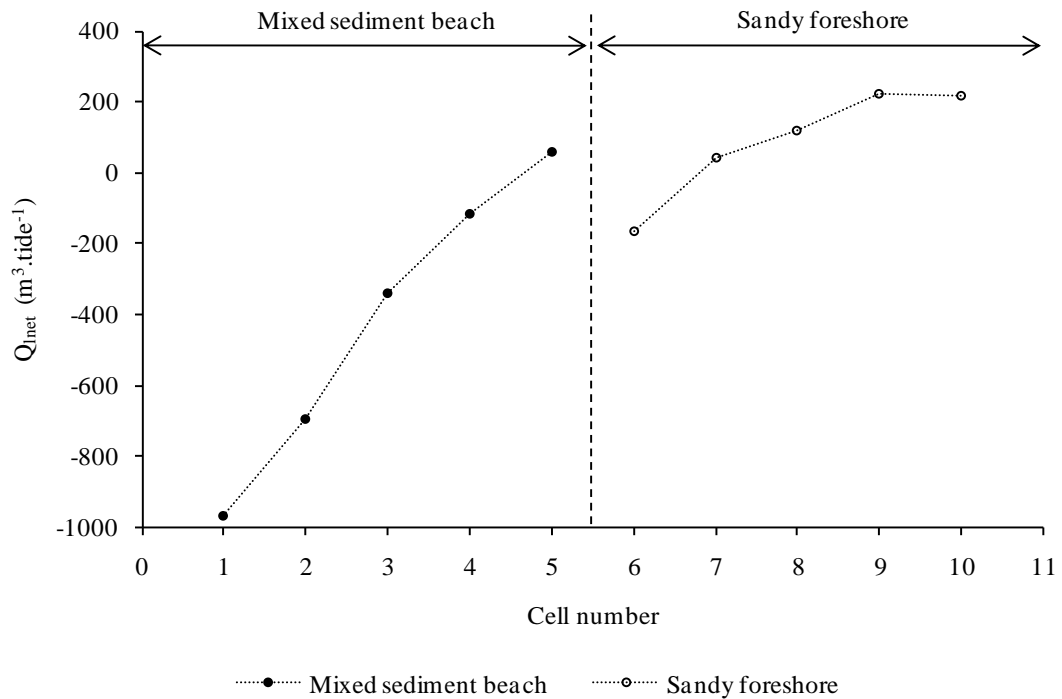


Figure 6-9 Net beach volume changes per tide measured in each cell between December 12th and December 17th 2004 at Cayeux-sur-Mer.

It is interesting to point out here that both techniques used to measure the LST at Cayeux came out with fairly equivalent estimates: 2112.8 m³ of material transported updrift was derived from the tracers' dispersion method while the DGPS surveys showed a total erosion of 2063.4 m³. However, considering the low recovery rate of the tracers on the last day of experiment (15%), it is very doubtful that the LST rate measured by the tracers injected on December 16th was accurate. It is most likely that the actual LST rate on that day was underestimated. Despite the imprecision linked to this low recovery rate, the similarity between the results derived from the tracers' scattering and the DGPS surveys were very encouraging regarding the reliability of both techniques.

In only the nine tides corresponding to the survey period, the volumes of sediment transported were equivalent to 2.6 to 2.9% of the yearly LST rate estimated by the local coastal defence managers (i.e. 70,000 to 80,000 m³ y⁻¹). If the figure derived from this short, nine-tide, survey period is extrapolated it yields an annual transport rate of 161,743.7 m³ y⁻¹ which is more than the double the LST rate estimated by the coastal defence managers.

Please note that from here, the wave conditions were already presented in Chapter 4 and consequently they will not be repeated in the following sections. However, relevant information about the wave conditions will be recalled when necessary from the description and interpretation of the tracer patterns or volume changes.

6.4 Field measurement experiments, Cayeux-sur-Mer, October/November 2005

6.4.1 Tracer recovery and distribution patterns

The beach is divided into across-shore zones (upper, mid- and lower beach) for a better understanding of the processes. Each zone is characterised by different processes influencing the morphological changes (Chapter 4) and the depth of disturbance (Chapter 5) for example. Within the objectives and aims of this study, plus the limitations imparted to the use of tracers (Chapter 3), where possible the results of the pebble recovery rate are presented for the individual injection points (i.e. upper, mid- and lower mixed sediment beach) as well as together for the beach as a whole. Recovery rates of the tracers are also shown after one tide, three tides and finally at the end of the observation period (Table 6-3).

By the end of this survey period, recovery rates were very variable, going from a low 10% on October 30th to a high 90% on October 31st. The lowest recovery rates are actually observed on the first three days of the survey period. It is believed that this three day period corresponds to the time necessary for the surveyors to feel comfortable with the methodology (i.e. an efficient way to scan a large area of the beach with the metal detector within the time allowed by the tide) and the equipment (it is necessary to practice proficiently with the metal detector to be able to appreciate the nuances of the sound effects produced by the detection). Once the surveyors were familiarized with the survey routine and the equipment workability, the recovery rates were close to or above 60%.

On the first day of the survey, October 28th, the tracer pebbles were deployed at three locations (upper, mid- and lower parts of the mixed sediment beach) in which four layer columns of tracer pebbles were injected. Each layer was 10 cm thick and filled with twenty five tracer pebbles each (Chapter 3, note that the amount of tracer varied from one day to another depending on the recovery rates of the previous search and the amount of tracers available). When the beach was visited one tide after deployment, on October 29th, the tracers located on the upper part of the mixed sediment beach did not display any movement even though they were reached by the top extent of the swash zone. For this reason, it was decided to leave them in place for the rest of the experiment. On the middle injection point, only the top layer was disturbed which led to the decision not to introduce anymore tracer on this area too. On the contrary, because no tracer was recovered in the lowest injection point, it was decided to re-introduce one hundred tracers distributed in four layers of 10 cm. On October 30th, 100 tracer pebbles were re-introduced in the upper and middle sections of the beach to compensate the tracer injection on October 29th.

From the field observations on these first three days and the familiarisation with the recovery routine, it was decided on December 31st to simultaneously deploy of tracers in the three across-shore locations again, but this time at lower depths (Table 6-3) because it was noticed that only the top layers of the columns previously injected were remobilised. From now on the recovery routine of deployment and recovery was well handled which resulted in high recovery rates thereafter. Because of the very large number of tracer pebbles already introduced into the beach material, it was decided to reduce the amount of newly deployed tracers on the following days (from November 1st to November 6th) to favour the recovery of the tracers injected at earlier times. Unfortunately, this was not very successful and recovery rates remained low at the end of the study period for the injections on October 28th, 29th and 30th. From November 1st to November 6th, pebbles tracers were only injected into the middle section of the mixed sediment beach.

Date of deployment (max depth of deployment)	Location of the injection on the mixed sediment beach	Recovery rates (Total of pebble recovered)						Depth of recovery/ number of pebbles
		After one tide	Total after one tide	After three tides	Total after three tides	At the end of the experiment	Overall	
28/10/05 (40cm)	Upper beach	No movement	4.7%	20% (20)	26.7%	38% (38)	49%	Surface/39 0 to 10cm/54 10 to 20cm/48 20 to 30cm/6
	Middle beach	10% (10)		36% (36)		79% (79)		
	Lower beach	4% (4)/Rest did not move		21% (21)		30% (30)		
29/10/05 (40cm)	Lower beach	16% (16)	NA	18% (18)	NA	35% (35)	NA	Surface/10 0 to 10cm/16 10 to 20cm/6 20 to 30cm/3
30/10/05 (40cm)	Upper beach	10% (10)	7%	12% (12)	8%	13% (13)	10%	Surface5/ 0 to 10cm/13 10 to 20cm/2
	Middle beach	4% (4)		4% (4)		7% (7)		
31/10/05 (20cm)	Upper beach	47% (37)	38.8%	59% (47)	61.5%	86% (68)	90%	Surface/45 0 to 10cm/104 10 to 20cm/34 20 to 30cm/5
	Middle beach	39% (31)		65% (52)		95% (76)		
	Lower beach	26% (13)		58% (29)		88% (44)		

Table 6-3 Recovery rates and depth of recovery of the tracers during the survey period between October 28th and November 11th. The figures in brackets correspond the cumulative number of tracer pebbles recovered in total. Part 1.

Date of deployment (max depth of deployment)	Location of the injection on the mixed sediment beach	Recovery rates (Total of pebble recovered)						Depth of recovery/ number of pebbles
		After one tide	Total after one tide	After three tides	Total after three tides	At the end of the experiment	Overall	
01/11/05 (20cm)	Middle beach	23% (17)	NA	36.5% (27)	NA	59.5% (44)	NA	Surface/12 0 to 10cm/24 10 to 20cm/7 20 to 30cm/1
02/11/05 (30cm)	Middle beach	55.1% (54)	NA	57.1% (56)	NA	72.5% (71)	NA	Surface/34 0 to 10cm/26 10 to 20cm/11
03/11/05 (40cm)	Middle beach	15.5% (15)	NA	34% (33)	NA	70.1% (68)	NA	Surface/40 0 to 10cm/24 10 to 20cm/4
04/11/05 (40cm)	Middle beach	27.4% (31)	NA	53.1% (60)	NA	68.1% (77)	NA	Surface/49 0 to 10cm/28
05/11/05 (20cm)	Middle beach	45.5% (30)	NA	53% (35)	NA	74.2% (49)	NA	Surface/21 0 to 10cm/27 10 to 20cm/1

Table 6-3 Recovery rates and depth of recovery of the tracers during the survey period between October 28th and November 11th. The figures in brackets correspond the cumulative number of tracer pebbles recovered in total. Part 2.

Date of deployment (max depth of deployment)	Location of the injection on the mixed sediment beach	Recovery rates (Total of pebble recovered)						Depth of recovery/ number of pebbles
		After one tide	Total after one tide	After three tides	Total after three tides	At the end of the experiments	Overall	
06/11/05 (30cm)	Middle beach	37.5% (36)	NA	53.1% (51)	NA	71.9% (69)	NA	Surface/23 0 to 10cm/45 10 to 20cm/1
07/11/05 (20cm)	Upper beach	44% (22)	50%	56% (28)	72%	60% (30)	80%	Surface/58 0 to 10cm/56 10 to 20cm/6
	Middle beach	64% (32)		84% (42)		92% (46)		
	Lower beach	42% (21)		76% (38)		88% (44)		
08/11/05 (20cm)	Upper beach	78% (39)	65.3%	84% (42)	74.7%	88% (44)	79.3%	Surface/47 0 to 10cm/69 10 to 20cm/3
	Middle beach	70% (35)		78% (39)		82% (41)		
	Lower beach	48% (24)		62% (31)		68% (34)		
09/11/05 (10cm)	Middle beach	66% (33)	NA	70% (35)	NA	NA	70% (35)	Surface/28 0 to 10cm/7

Table 6-3 Recovery rates and depth of recovery of the tracers during the survey period between October 28th and November 11th. The figures in brackets correspond the cumulative number of tracer pebbles recovered in total. Part 3.

Date of deployment	Location of the injection on the mixed sediment beach	Mean distance travelled after one tide (m)	Overall mean distance travelled by the overall amount of tracers after one tide (m)	Mean direction travelled (referred to magnetic North in °)	Overall mean direction travelled by the overall amount of tracers (referred to magnetic North in °)	Mean alongshore distance travelled after one tide	Overall mean alongshore distance travelled after one tide	Mean across-shore distance travelled by the overall amount of tracers after one tide	Overall mean across-shore distance travelled by the overall amount of tracers after one tide
28/10/05	Upper beach	NA							
	Middle beach	15.4	15.2	302.1	301.5	1.9	1.7	-15.2	-15.1
	Lower beach	0.6		288.1		~0		-0.6	
29/10/05	Lower beach	6.3	NA	65.0	NA	4.8	NA	4.1	NA
30/10/05	Middle beach	11.9	7.6	355.5	51.4°	10.4	6.8	-5.9	3.4
	Lower beach	5.8		299.9		0.5		-5.7	
31/10/05	Upper beach	28.8	13.6	321.1	337.5°	12.6	9.2	-25.8	-10.1
	Middle beach	11.6		329.8		6.6		-9.5	
	Lower beach	7.7		61.5		6.2		4.6	
01/11/05	Middle beach	40.4	NA	23.6	NA	40.4	NA	-1	NA
02/11/05	Middle beach	40.1	NA	29.8	NA	40	NA	3.4	NA
03/11/05	Middle beach	47.2	NA	15.7	NA	46.6	NA	-7.6	NA
04/11/05	Middle beach	28.5	NA	8.3	NA	27.3	NA	-8.2	NA

Table 6-4 Mean distances travelled by the tracers after one tide deployment at Cayeux-sur-Mer in October–November 2005. Positive values of the alongshore distances indicate that the centroid of the pebble scattering is located in a downdrift position from its injection point. Negative values indicate movements in an updrift direction. Similarly, positive values of the across-shore travelled distance indicate movements up the beach in comparison to the location of the injection point, and negative values indicate movements down the beach. Part 1.

Date of deployment	Location of the injection on the mixed sediment beach	Mean distance travelled after one tide (m)	Overall mean distance travelled by the overall amount of tracers after one tide (m)	Mean direction travelled (referred to magnetic North in °)	Overall mean direction travelled by the overall amount of tracers (referred to magnetic North in °)	Mean alongshore distance travelled after one tide	Overall mean alongshore distance travelled after one tide	Mean across-shore distance travelled by the overall amount of tracers after one tide	Overall mean across-shore distance travelled by the overall amount of tracers after one tide
05/11/05	Middle beach	25.5	NA	19.8	NA	25.4	NA	-2.3	NA
06/11/05	Middle beach	45.1	NA	16.8	NA	44.6	NA	-6.4	NA
07/11/05	Upper beach	33.6	23.6	2.9	23.8	30.4	23.6	-14.3	-0.5
	Middle beach	21.7		22.0		21.6		-1.1	
	Lower beach	21.3		57.4		18.0		11.4	
08/11/05	Upper beach	35.0	22.4	357.8	12.1	31.1	21.8	-16.0	-5.0
	Middle beach	14.0		357.2		12.3		-6.5	
	Lower beach	23.4		34.3		23.1		3.8	
09/11/05	Middle beach	23.6	NA	23.8	NA	11.1	NA	-0.3	NA

Table 6-4 Mean distances travelled by the tracers after one tide deployment at Cayeux-sur-Mer in October–November 2005. Positive values of the alongshore distances indicate that the centroid of the pebble scattering is located in a downdrift position from its injection point. Negative values indicate movements in an updrift direction. Similarly, positive values of the across-shore travelled distance indicate movements up the beach in comparison to the location of the injection point, and negative values indicate movements down the beach. Part 2.

With the aim to get a basic understanding of the pebbles movements in the beach topographical changes, and because the stocks of tracer pebbles were sufficient to do so, it was decided to re-introduce tracers in the upper, middle and lower parts of the mixed sediment beach on December 7th and 8th. On December 9th an additional fifty tracer pebbles were introduced in the middle injection point. The last days of the survey period were dedicated to the recovery of the tracer pebbles injected during the previous days in order to increase the recovery rates.

From October 28th to November 11th 2005, the sustained South-Westerly waves and currents (Chapter 4 Section 4.3.1) entrained the tracer pebbles which scattered to the North of their injection point on every measurement. During the period of the experiment no tracers were found to have moved in an updrift direction. After only one tide, the longest travelled tracer pebble was recovered 144.52 m from its injection point (deployed on December 6th, middle injection point). At the end of the experiment, the longest-travelled tracer pebble was 391.4 m from its injection point after only twelve tides (deployed on December 4th, middle injection). The shortest-travelled tracer pebbles after one tide was only 0.61 m from its injection point (deployed on December 30th, middle injection) whilst after twenty five tides the shortest-travelled pebble was 34.4 m from its injection point (deployed on December 28th, middle injection).

The position of the centroids were determined for each individual injection point, but also for the three injection points combined in order to derive the average longshore transport rates (Tables 6-4). It was decided also to focus attention on the scatterings expressed after only one tide so that the scattering and the transport rate can be related to a specific wave climate.

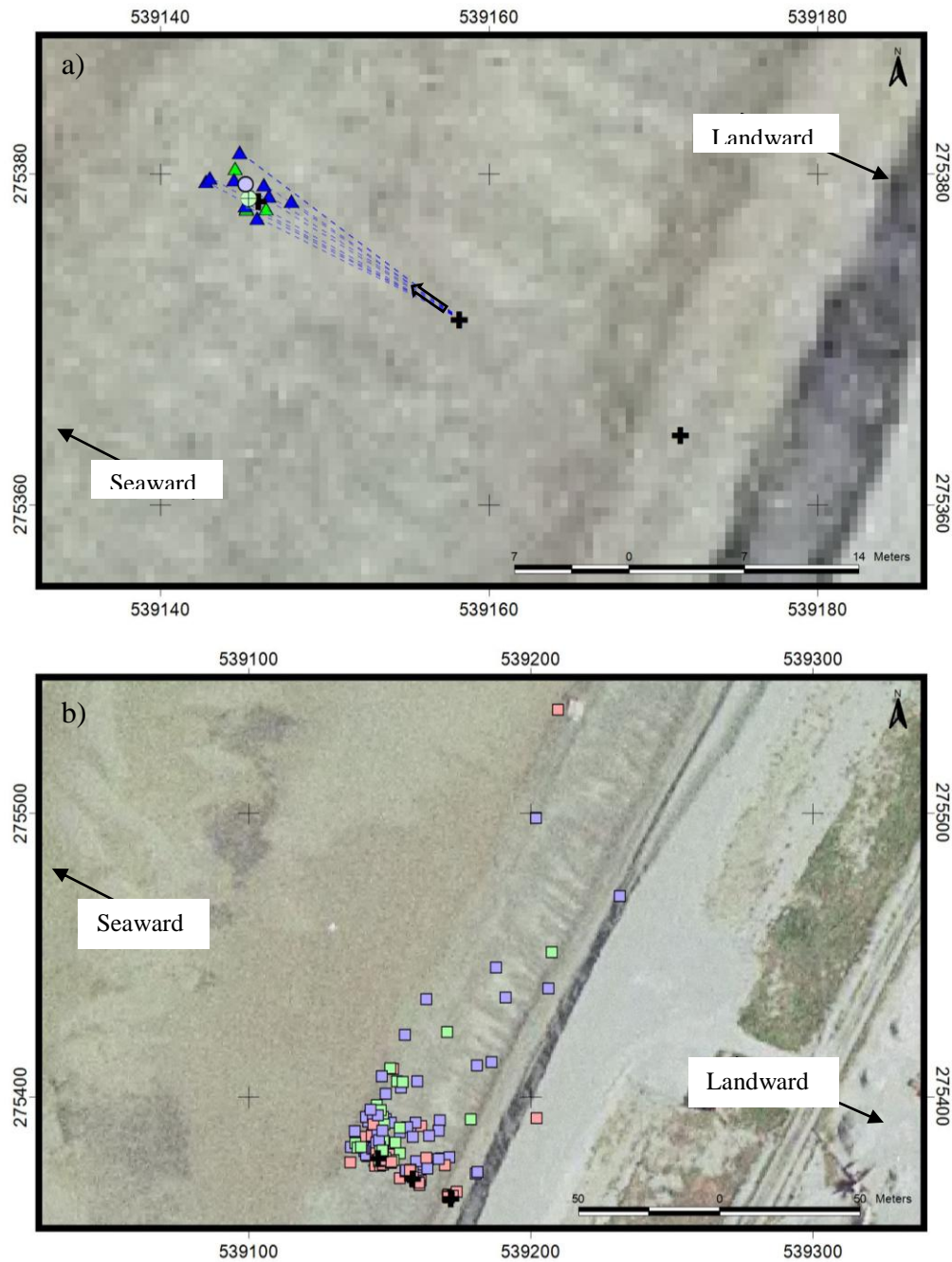


Figure 6-10 Movements of the tracer pebbles deployed on October 28th, 2005.

a) Scattering observed after one tide. Arrows indicate the mean orientation of the pebbles movement.

b) Scattering observed over the whole survey period.

The black cross marks the injection point locations. Each triangle represents individual tracer pebbles recovered after one tide while the squares represent individual tracer pebbles recovered after more than one tide. The disks mark the location of the centroids. Pebbles are colour coded: red = upper injection point, blue = middle injection point, green = lower injection point.

During the survey period, the smallest mean movements from the tracers were recorded on October 28th (Figure 6-10), with an across-shore movement of -0.6 m down the beach whereas its alongshore component was zero. During the corresponding high tide, the wave approach angle to the coast ranged from 69 to 87°, averaging 74.9°; the significant wave height ranged from 0.63 to 0.9 m, averaging 0.77 m; the significant wave period ranged from 5 to 7.1 s and averaged 6.1 s (Chapter 4 Figure 4-4). In contrast, the greatest mean distance was observed on November 3rd (Figure 6-11), with an alongshore travelled distance of 46.6 m and an across-shore distance of -7.6 m down the beach. On that tide, the wave conditions were the most energetic recorded during the survey period. The significant wave height (H_s) ranged from 0.84 to 2.68 m, averaging 1.9 m; the wave approach angle to the coast varied from 51 to 78°, averaging 65.3°; and, the wave period varied from 5.1 s to 6.6 s, averaging 5.8 s.

The simultaneous observation of the tracers' scattering for the three across-shore locations makes it possible to examine the influence of the initial position of a pebble on the beach on its migration. The observation of such differential was possible on four deployments, those of October 28th, October 31st, November 7th and November 8th. Apart from the deployment on October 28th which displayed essentially across-shore movements, -15.1 m against 1.7 m of alongshore movement, the movement patterns shown by tracers on October 31st, November 7th and November 8th show the sustained downdrift migrations characterising almost the entire survey period (Figure 6-10, 6-12, 6-13 & 6-14; Appendix VI). Mean alongshore movements during these four days were respectively measured at 0, 9.2, 23.6 and 21.8 m (Table 6-4).

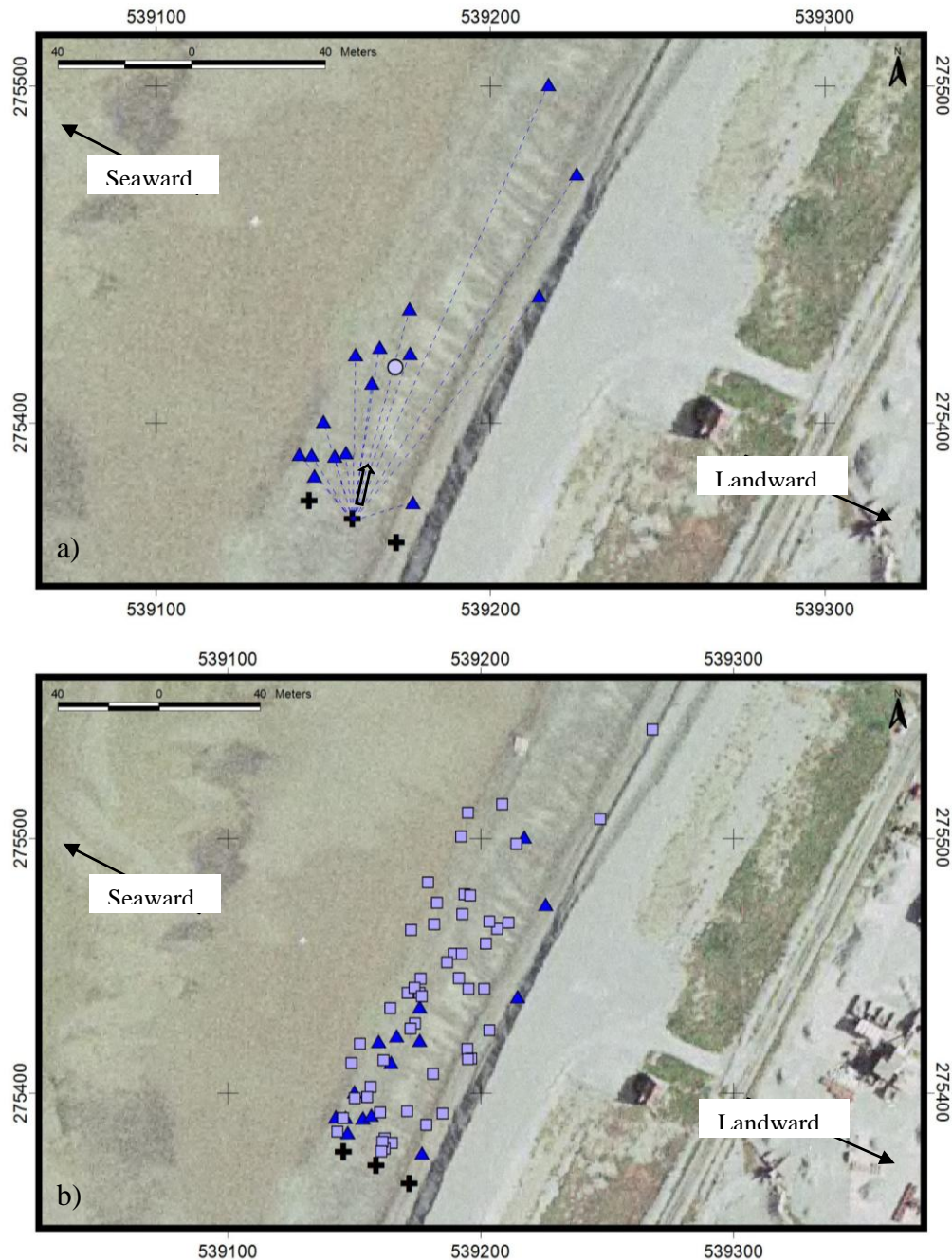


Figure 6-11 Movement of tracer pebbles deployed on November 3rd, 2005.

a) Scattering observed after one tide. Arrows indicate the mean orientation of the pebbles movement.

b) Scattering observed over the whole survey period.

The black cross marks the locations of the injection points. Each triangle represents individual tracer pebbles recovered after one tide while the squares represent individual tracer pebbles recovered after more than one tide. The disks mark the location of the centroids. Pebbles are colour coded:

red = upper injection point, blue = middle injection point, green = lower injection point.

On the first tracer pebble deployments on October 28th, as mentioned earlier, no movement was recorded on the upper injection point on the mixed sediment beach and very few tracers had moved from the middle beach injection point. The mean distance travelled by the overall tracers deployed on that day was 15.2 m, mostly in an across-shore direction down the beach (across-shore component measured at -15.1 m). When considering individual injection points, most of the movements were recorded for pebbles from the middle injection point, which travelled across-shore -15.2 m down the beach while the pebbles from the lower injection only travelled -0.6 m. By the end of the experiment, the pebbles injected on October 28th had travelled up to 176.3 m away from their injection point (twenty five tides after deployment, upper injection point).

Over the high tide after the deployment on October 31st, the wave approach angle to the coast ranged from 47.4 to 86.7°, averaging 67.5°; the significant wave height ranged from 0.76 to 1.36 m, averaging 0.99 m; the significant wave period ranged from 6.8 to 9.1 s and averaged 7.9 s (Chapter 4 Section 4.3.1). The centroid's location obtained from the scattering of the tracer pebbles recovered for each deployment location, showed that the mean distance travelled after one tide by the tracers deployed at the top of the beach was 28.8 m (Figure 6-12). Tracers deployed in the middle and lower beach travelled only 11.6 m and 7.7 m respectively. This initial observation indicates that pebbles located at higher elevations on the beach have the potential to travel further than those at lower elevations. However, when taking into account the bearing of the centroid trajectory from its deployment point, the tracers from the middle and lower deployment points travelled almost equal alongshore distances (respectively 6.6 and 6.2 m) while the upper deployment tracer still travelled the furthest (12.6 m). When looking at the across-shore component of the pebbles' motion, the results indicated that tracers injected in the upper beach had travelled -25.8 m downwards across the beach. Those injected into the middle beach recorded mean movements of -9.5 m downwards across the beach too. Tracer pebbles that were injected into the lower beach unexpectedly recorded mean movements up the beach by 4.6 m.

By the end of the experiment, pebbles injected on October 31st travelled up to 311.88 m away from their injection point (twenty one tides after deployment, lower injection point, Figure 6-12).

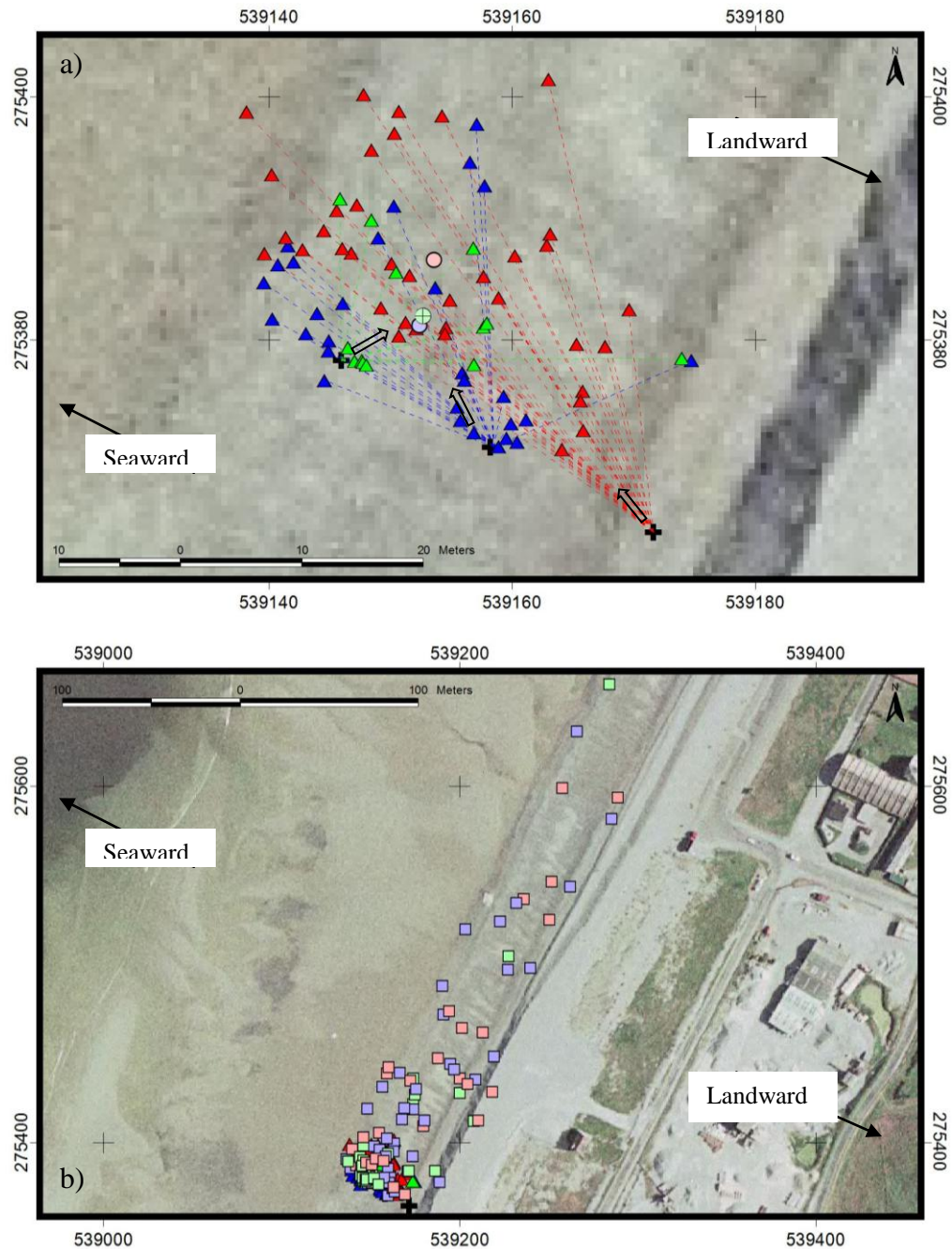


Figure 6-12 Movement of tracer pebbles deployed on October 31st, 2005.

a) Scattering observed after one tide. Arrows indicate the mean orientation of the pebble movement.

b) Scattering observed over the whole survey period.

The black cross marks the locations of the injection points. Each triangle represents individual tracer pebbles recovered after one tide while the squares represent individual tracer pebbles recovered after more than one tide. The disks mark the location of the centroids. Pebbles are colour coded:

red = upper injection point, blue = middle injection point, green = lower injection point.

In summary, on October 31st, tracer pebbles injected on the upper part of the mixed sediment travelled longer distances than the other tracers from their respective injection points. Pebbles from the middle and lower injection points on the mixed sediment beach typically travelled on average less than half the alongshore distances recorded by those deployed on the upper injection point. The mean across-shore distances travelled by the pebbles deployed on the upper part of the mixed sediment beach proved to be the greatest too, followed by the tracers injected on the middle injection point. In addition, pebbles injected on the upper and middle parts of the mixed sediment beach display across-shore movement oriented down the beach whereas those injected on the lower part of the mixed sediment beach scattered up the beach.

After the injection on November 7th, the furthest-travelled pebble recovered was 101.6 m away from its injection point on the 11th of November 2005 (seven tides after deployment, Figure 6-13). After one tide, tracers were scattered distances of between 1.34 and 68.9 m from their injection points. The location and orientation of centroids after one tide on the upper, middle and lower mixed sediment beach were, respectively: 33.6 m with an angle to the North of 2.9°, 21.7 m with an angle of 22° and 21.3 m with an angle of 57.4° (Table 6-4). Here again, the same patterns of tracer dispersion are observed. The pebbles deployed in the upper injection point travelled the furthest alongshore and across-shore distances. The pebbles deployed on the upper and middle part of the mixed sediment beach showed across-shore movement down the beach while the pebbles injection on the lower point travelled up the beach.

The difference between the mean angle of scatter of tracers deployed on October 31st and November 7th showed that pebbles were affected by less cross-shore transport and more longshore movements on November 7th. During the high tide between November 7th and November 8th, H_s varied from 0.59 to 1.14 m, averaging 0.92 m; T_s varied from 4.6 s to 5.9 s, averaging 5.1 s; the wave direction varied from 55.5 to 73.7° averaging 64.2°.

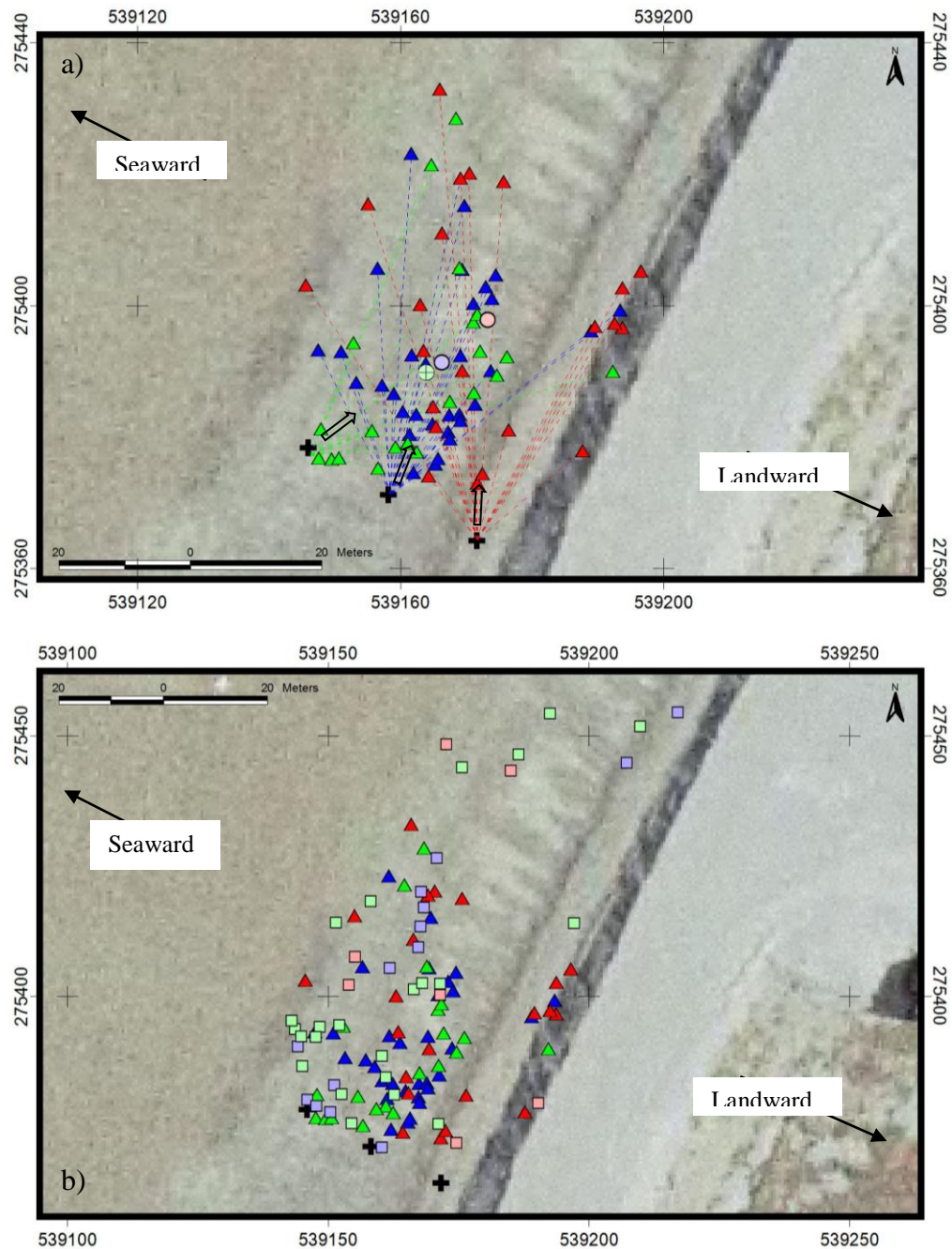


Figure 6-13 Movement of tracer pebbles deployed on November 7th, 2005.

a) Scattering observed after one tide. Arrows indicate the mean orientation of the pebble movement.

b) Scattering observed over the whole survey period.

The black cross marks the locations of the injection points. Each triangle represents individual tracer pebbles recovered after one tide while the squares represent individual tracer pebbles recovered after more than one tide. The disks mark the location of the centroids. Pebbles are colour coded:

red = upper injection point, blue = middle injection point, green = lower injection point.

On the deployment of November 8th, the furthest-travelled tracer pebble after one tide was 75.5 m from its injection point and the furthest pebble found until the end of the experiment was 101.6 m away, for a total of seven tides deployment (Figure 6-14). The centroid locations for the upper, the middle and the lower injections tracers scattering after one tide travelled respectively: a mean distance of 35 m with a mean angle to the North of 357.8°, 14 m with a mean angle to the north of 357.2° and 23.4 m with an angle of 34.3° (Table 6-4).

In summary, the results on November 8th displayed similar tendencies in tracer dispersion as on October 31st and November 7th; tracers from the upper and the middle beach moved downwards across the beach whereas pebbles from the lower part of the mixed sediment beach tended to migrate up the beach. Moreover, pebbles from the upper parts of the beach tended to travel longer distances than those on the rest of the mixed sediment beach. However, the tracers injected into the middle of the beach travelled a significantly shorter distance than it would have been expected considering the previous examples. On that date, the wave approach was between 49.5 and 82° (averaging 69°), the wave height ranged between 0.62 to 1.36 m (averaging 1.1 m) and the significant wave period varied between 4.6 and 6.1 s (averaging 5.0 s).

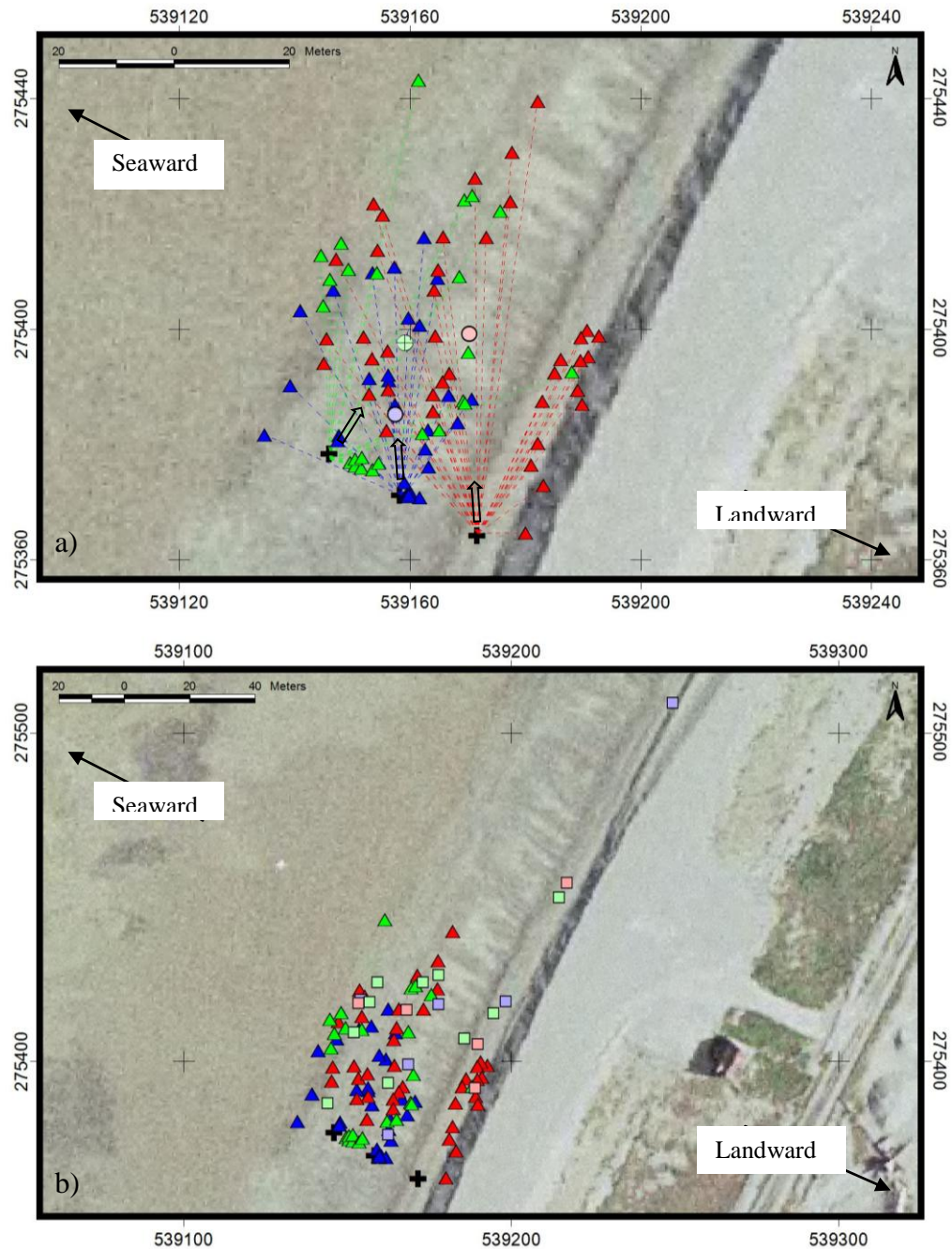


Figure 6-14 Movement of tracer pebbles deployed on November 8th, 2005.

a) Scattering observed after one tide. Arrows indicate the mean orientation of the pebbles movement.

b) Scattering observed over the whole survey period.

The black cross marks the locations of the injection points. Each triangle represents individual tracer pebbles recovered after one tide while the squares represent individual tracer pebbles recovered after more than one tide. The disks mark the location of the centroids. Pebbles are colour coded:

red = upper injection point, blue = middle injection point, green = lower injection point.

The results of the experiment have revealed patterns of tracer pebble movement that are dependent on the across-shore location of the injection point. Tracers deployed on the upper beach travelled the furthest distances. They were also subject to the most significant cross-shore movement in a seaward direction in comparison to those deployed in the middle and lower parts of the mixed sediment beach. Tracers deployed in the middle and lower beach travelled equivalent distances but their mean movements were in different directions. Indeed, pebbles deployed in the middle of the beach showed a tendency to migrate seaward; although the main component of their movement was alongshore rather than across-shore. In contrast, pebbles deployed on the lower beach displayed a tendency to migrate landwards, keeping however that dominant alongshore migration component.

In addition, tracers deployed at different times during the experiment travelled different distances. Those on the 28th of October did not move significantly apart from in an across-shore direction. Then, when movements alongshore were observed, those deployed on the 31st of October travelled, on average, a shorter distance than those injected on the 7th and the 8th of November 2005. They also recorded a stronger cross-shore movement component than those deployed on the two later dates.

6.4.2 Derivation of the volume transported and the LST rates using tracer pebbles

LST rates were calculated, using two approaches, for every deployment day using the data collected during this study case (Table 6-4). The first approach calculated LST by multiplying (i) the average alongshore distance travelled by the tracers by (ii) the area of sediment remobilised on a cross-shore section of the beach, which was determined using the active layer measurements presented and discussed in Chapter 5. The second approach calculated LST rate by multiplying (i) the average longshore distance travelled by the tracers, (ii) the depth of deepest tracers recovered for that specific deployment and (iii) the length of the beach profile (according to Equation 6.21). Comparative results are presented in Table 6-5. If only the difference in transport rate, in $\text{m}^3 \cdot \text{tide}^{-1}$, between the two approaches is considered, differences seem small in some cases.

However, when this difference is expressed as a percentage of the transport rate calculated using the second approach, the differences vary from 6.7 to 134.2%. During the transition from a neap tide to a spring tide, the LST rates based on the second approach are generally greater than those calculated using the first approach. On the contrary, when the tidal level goes from the spring tide to the neap tide, the LST rates calculated using the second approach are lower than those calculated using the first approach (Table 6-5).

Date of deployment	Mean alongshore distance travelled after one tide (m)	Area of the beach material removed (m ²)	Maximum depth of tracer pebbles recovered (m)	Average length of the beach (m)	LST rate / depth of disturbance (m ³ tide ⁻¹)	LST rate / depth of tracers (m ³ tide ⁻¹)	Difference between the LST rates	Percentage of difference between the LST rates (%)
28/10/05	1.7	9.4	0.23	47.7	15.9	18.7	2.7	14.5
29/10/05	4.8	5.8	0.25	47.7	27.8	57.2	29.4	51.4
30/10/05	6.8	6.0	0.22	56.7	40.5	84.8	44.4	52.3
31/10/05	9.2	13.0	0.17	70.4	119.3	110.1	-9.2	8.4
01/11/05	40.4	NA	0.22	64.4	NA	572.4	NA	NA
02/11/05	40	11.5	0.18	68.5	460.4	493.2	32.8	6.7
03/11/05	46.6	NA	0.2	69.7	NA	649.6	NA	NA
04/11/05	27.3	NA	0.15	64.8	NA	265.4	NA	NA
05/11/05	25.4	14.0	0.1	59.6	354.6	151.4	-203.2	134.2
06/11/05	44.6	11.6	0.1	54.5	517.8	243.1	-274.7	113.0
07/11/05	23.6	11.6	0.2	54.5	274.7	257.2	-17.5	6.8
08/11/05	21.8	NA	0.15	53.9	NA	176.3	NA	NA
09/11/05	11.1	2.5	0.05	40.6	28.3	22.5	-5.8	25.6

Table 6-5 Calculation of the LST rates using tracer pebble dispersion on mixed sediment beach at Cayeux-sur-Mer between October 28th and November 11th, 2005.

6.4.3 DGPS surveys: digital elevation model and beach elevation changes

In a similar way as for the survey in December 2004 at Cayeux-sur-Mer, elevation changes maps were created from one tide to the following for the overall survey period (Figure 6-16). It is less obvious than before, however it can be seen that the contour line the maps are parallel to the across-shore profiles surveyed on some occasions. This is most noticeable in the southern part of the survey area, close to the terminal groyne. For

example the elevation changes map calculated between November 1st PM and November 2nd AM (Figure 6-16) displays such error. Similar to December 2004, the linear interpolation method used to create the digital elevation maps is at the origin of such misrepresentation of the actual beach elevation. However, the short distance between each profile permits to minimise these errors of interpolation to get the best result possible.

Fortunately, gentle cusping occurred only once during this survey period on November 8th (Figure 6-15) and the addition of alongshore transects on the area covered with these gentle cusps allowed a good representation of these forms on the digital elevation model. This helped to further minimise the imprecision of the model.



Figure 6-15 Photo of the gentle cusps on November 8th.

From the digital elevation maps (Figures 6-16), it can be seen that during the complete survey period from October 28th to November 11th, the greatest erosion movements measured up to -3.8 m. This movement corresponds to the remobilisation of some of the material from the recycled

sediment wall on the upper beach under wave attack. The greatest accretion proved to be in

the lower part of the mixed sediment beach directly in contact with the terminal groyne and measured up to +1.2 m. It is believed that this accretion is due to the wave refraction around the groyne that stocks up the coarsest particles directly in contact with it. This hypothesis is supported by the convex shape of the beach that results directly from the wave refraction around the terminal groyne.

The general pattern of distribution of the erosion and the accretion shows that the middle of the mixed sediment beach was affected by erosion reaching up to -1.6 m in the terminal groyne area, whereas the lower part of the mixed sediment beach and the upper part of the mixed beach (excluding the recycled sediment wall area) present accretion, measured respectively at +1.2 and +0.9 m. This accretion measured on the upper part of the beach corresponds to the build up of a berm.

The detailed tidal elevation changes along two surveyed profiles for this survey period are presented in Chapter 4. The average beach elevation changes on a tidal basis were within a range from -0.6 to +0.6 m, excluding the elevation changes observed on the recycled sediment wall that reached up to 2.6 m on November 4th. In general, erosion and accretion movements were organised along alongshore stripes on the mixed sediment beach. These stripes seem to exist at the benefit or expense of each other. During the phase going from the neap to the spring tide (October 28th to November 4th), the upper beach shows recession of the beach berm. The recession is expressed on the maps by the migration upward on the beach of an erosion stripe backed up by a very thin accretion stripe slightly higher on the profile. The area directly below on the profile generally presents accretion. Conversely, during the transition from spring to neap tide, accretion is expressed in the upper parts of the beach profile whilst erosion is observed on lower parts of the profile. Two days, November 4th and November 8th, are very peculiar during the survey period. In contrast to the rest of the elevation changes maps, these two days reveal general erosion over the entire surveyed area. The observation of the profiles surveyed earlier in Chapter 4 does not support such overall erosion on the beach for both of these days. It is therefore proposed that the DGPS surveys and consequently the interpolation of the digital elevation models create errors as expected and identified earlier in the sample design (Chapter 3 Section 3.2.2) had a significant impact on the beach elevation changes maps (these errors are discussed further in depth in this chapter Section 6.4.4).

Over the survey period, the elevation changes on the sandy platform ranged between -0.4 and +0.2 m.

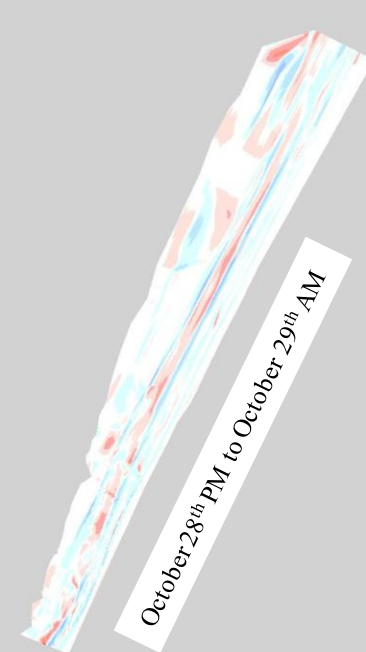
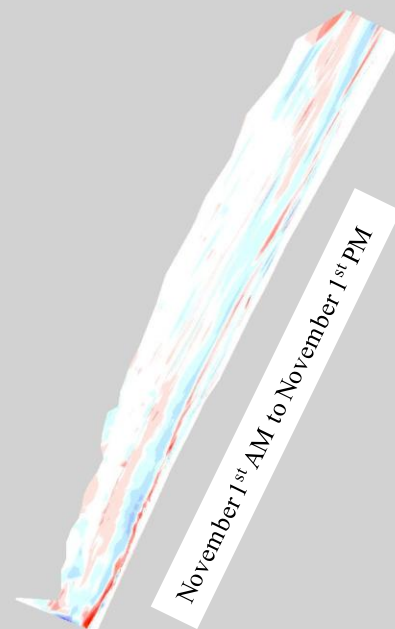
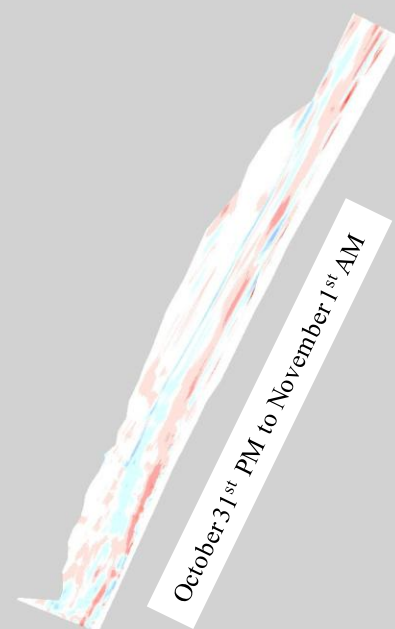
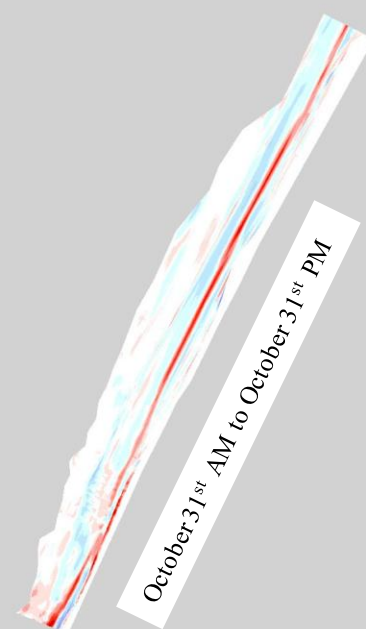
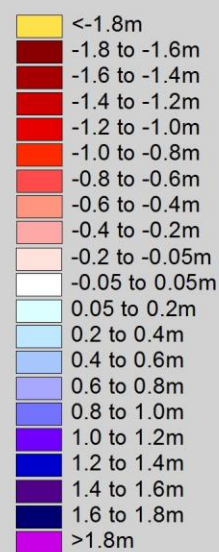


Figure 6-16 Changes in beach elevation between October 28th and November 11th 2005 at Cayeux-sur-Mer, Part 1.



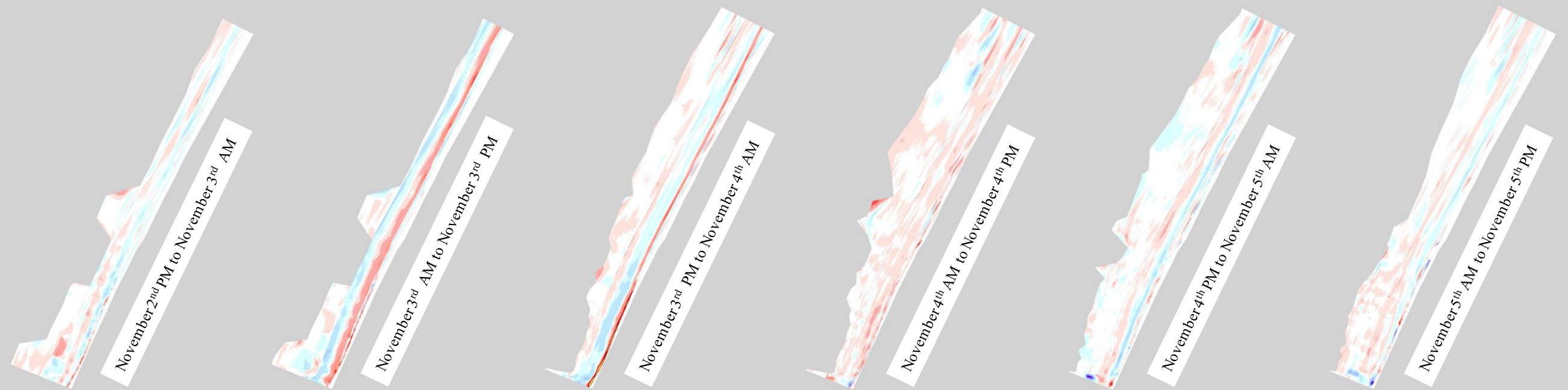
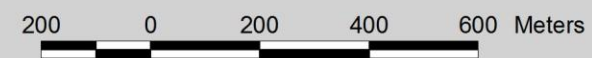
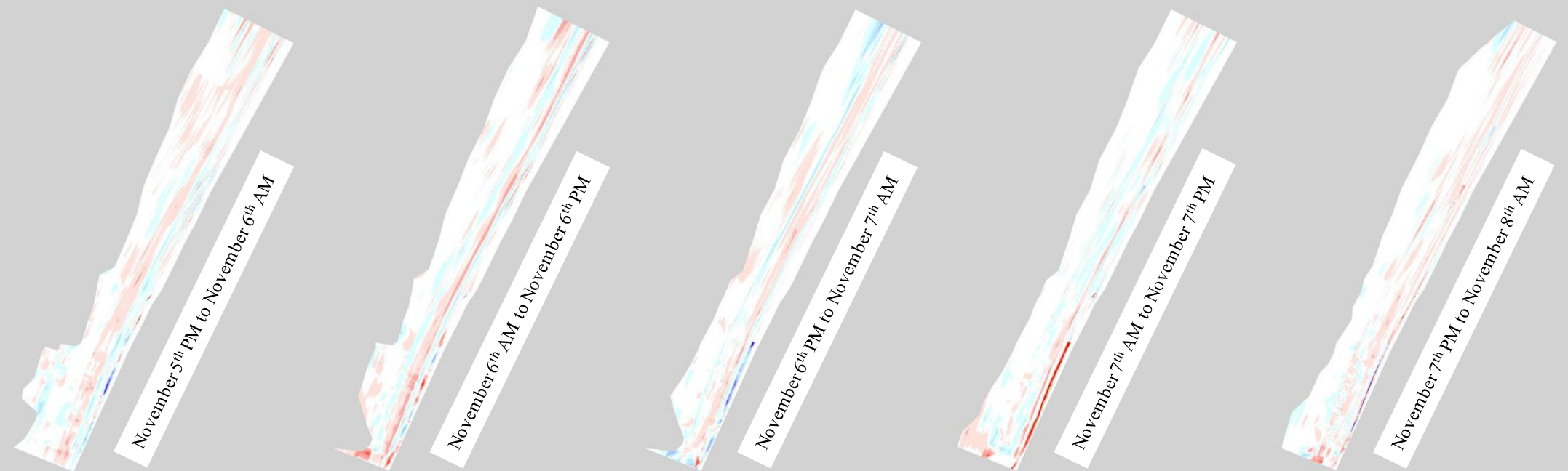
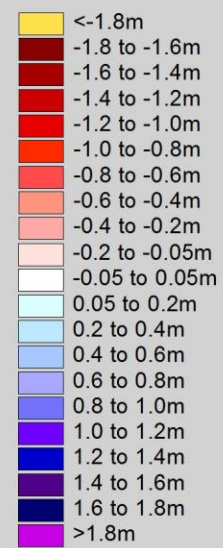
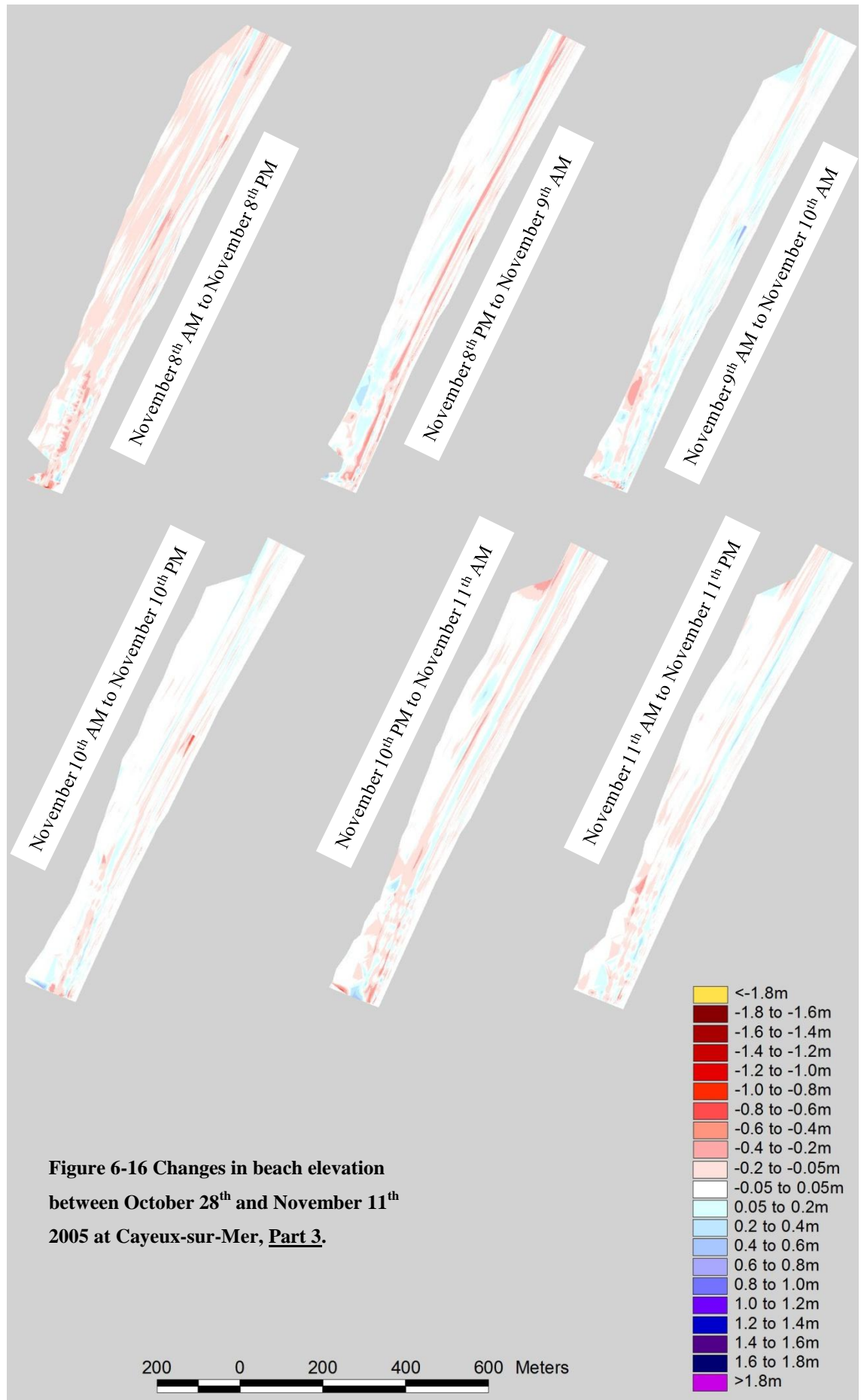


Figure 6-16 Changes in beach elevation between October 28th and November 11th 2005 at Cayeux-sur-Mer, Part 2.





6.4.4 DGPS surveys: beach volume changes



Figure 6-17 Grid system used to determine the beach volume change at Cayeux-sur-Mer between October 28th to November 11th.

To calculate the beach volume changes a grid system, similar to that used in the previous year's survey (December 2004), was adopted (Figure 6-17). As before, the width of the cells was driven by the longest distance between the profiles. The distance between two consecutive profiles increased at the end of the surveyed area to approximately 50 m. With the aim of keeping good precision for the volume difference calculations, it was decided to keep the cells 100 m wide ensuring again that at least two profiles per cell would be used for the interpolation. Here again, volume changes on the sandy platform and the mixed sediment beach were separated to be able to derivate LST rates for the mixed sediment beach only. Again, the limit between the sandy platform and the mixed

sediment beach was delimited according to the maximum extent of the mixed sediment beach. The original idea behind this grid system was to be able to observe the volume of sediment transfer from one cell to another over time in a northward direction while the southern part of the survey area is literally "cannibalised" under the wave attack, given that the sediment supply here is close to zero because of the presence of the terminal groyne.

Such a grid system should theoretically supply a very good visual support to the interpretation of the beach volume alongshore transfers in a semi-closed beach system. However, this system does not seem to work on the mixed beach at Cayeux. Figure 6-18 & 6-19 represent the volume changes recorded from one tide to the next for each individual cell during the survey period. To simplify the reading of the figures, the results are divided into two groups. This first group, Figure 6-18, displays the volume changes that showed overall accretion on the mixed sediment beach in the survey area. The second group, Figure 6-19, presents the volumes changes per cell for the surveys that showed overall erosion on the mixed sediment beach. The results were split into

two groups for two reasons. First, it is easier to read the figures and second, accretion on the overall surveyed area was not expected to be observed, suggesting that an error is introduced when interpolating the digital elevation maps. Indeed, overall accretion in the survey area is most likely to be mistaken as theoretically, the terminal groyne directly updrift should stop or limit greatly any sediment supply.

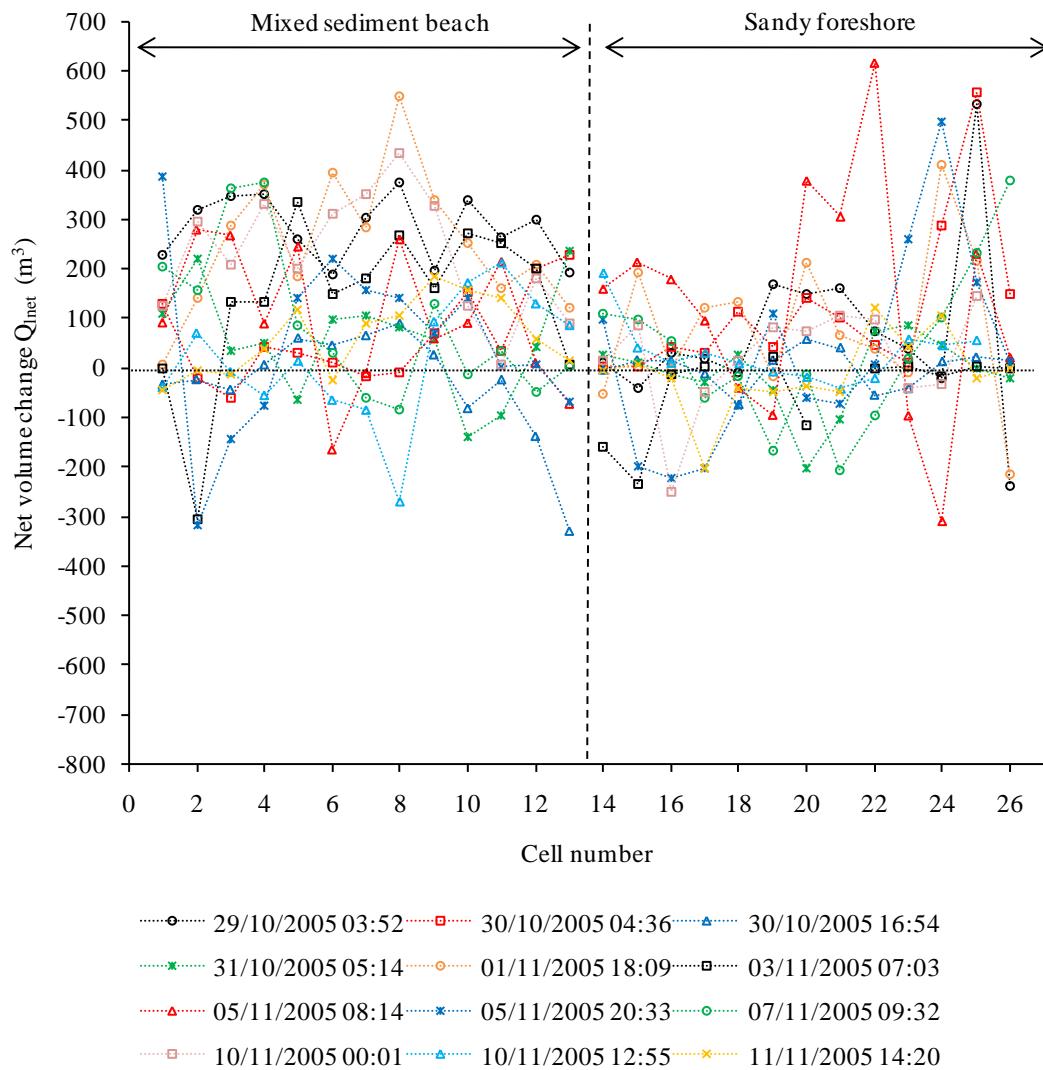


Figure 6-18 Net volume change (Q_{net}) measured for each cell between two consecutive surveys at Cayeux in October/November 2005. This figure is a compilation of the surveys that presented overall accretion on the surveyed area from one survey to the following.

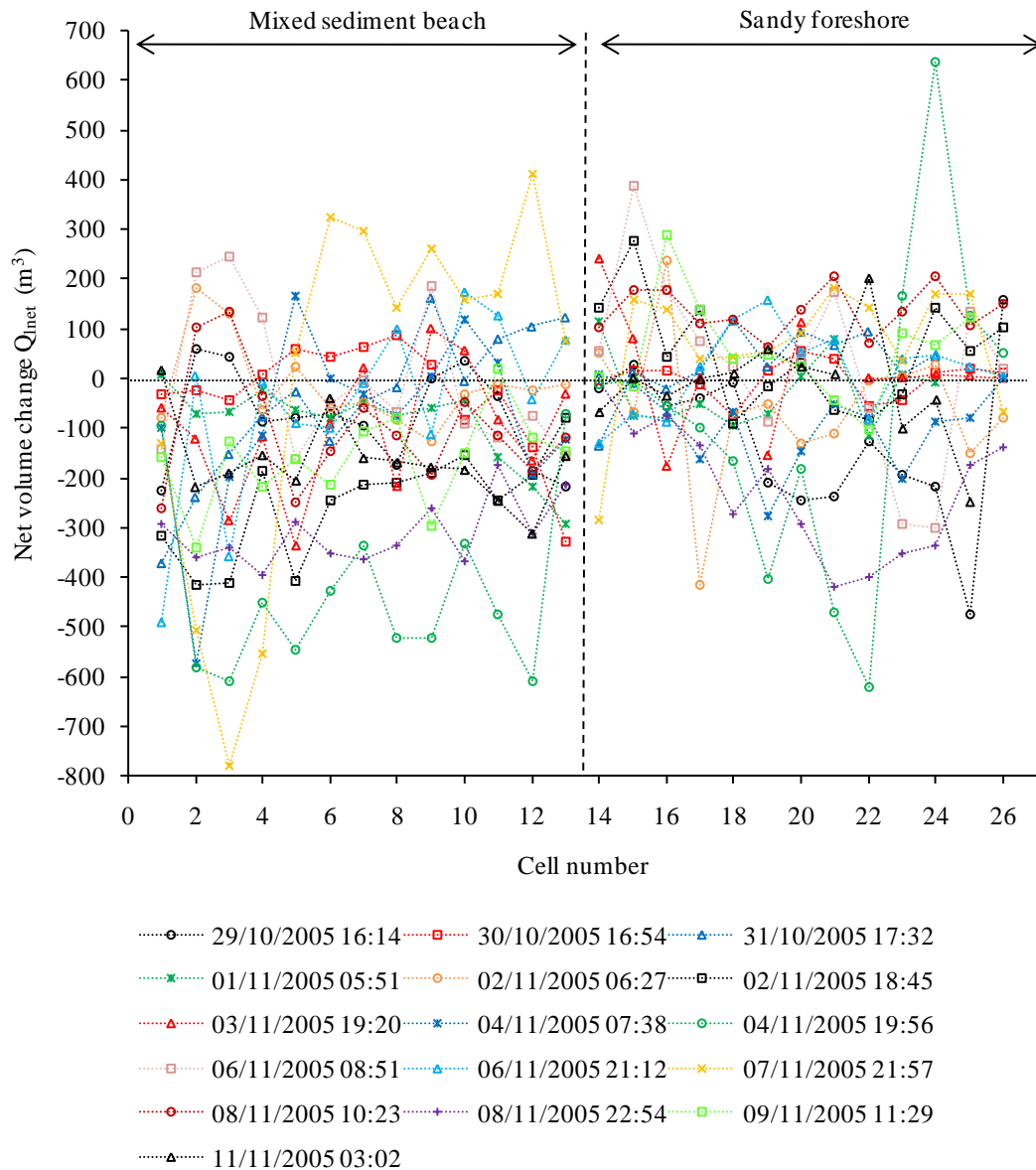


Figure 6-19 Net volume change (Q_{net}) measured for each cell between two consecutive surveys at Cayeux in October/November 2005. This figure is a compilation of the surveys that presented overall erosion on the surveyed area from one survey to the following.

A clear example of the error in the volume calculation here can be observed between the survey on the afternoon of October 28th and the morning of October 29th (Figure 6-16 and Table 6-6). During the high tide between these two dates, it is first rather confusing to observe a net accretion of 3667.3 m^3 on the overall survey area when considering that the wave conditions were calm ($H_s < 0.5m$) and from the South-West. Indeed, accretion in the survey area would have been understood if the waves were coming from the North, creating a LST oriented southward. However, as already mentioned, the beach system is semi-closed and no sediment entry or only a very little is possible from the

South. This confusion is emphasized when looking at the information delivered by the tracer pebbles scattering (Table 6-4 and Figure 6-10) that showed very little alongshore movement (+1.7 m) and in a Northward direction (LST rates $<20 \text{ m}^3 \text{ tide}^{-1}$). Therefore, it is clear that an error is to be linked to the derivation of the beach volumes from the DGPS surveys.

	Net volume change on the mixed sediment beach (m^3)
29/10/2005 03:52	3667.3
29/10/2005 16:14	-1029.93
30/10/2005 04:36	797.27
30/10/2005 16:54	-381.22
31/10/2005 05:14	734.93
31/10/2005 17:32	-579.51
01/11/2005 05:51	-1189.2
01/11/2005 18:09	3310.65
02/11/2005 06:27	-205.81
02/11/2005 18:45	-3265.33
03/11/2005 07:03	1785.28
03/11/2005 19:20	-1344.16
04/11/2005 07:38	-1083.44
04/11/2005 19:56	-5583.72
05/11/2005 08:14	1370.7
05/11/2005 20:33	660.26
06/11/2005 08:51	-93.09
06/11/2005 21:12	-729.26
07/11/2005 09:32	1182.79
07/11/2005 21:57	-80.83
08/11/2005 10:23	-1284.26
08/11/2005 22:54	-4059.44
09/11/2005 11:29	-2093.58
10/11/2005 00:01	2993.38
10/11/2005 12:55	257.46
11/11/2005 03:02	-2185.97
11/11/2005 14:20	818.21

Table 6-6 Beach net volume changes surveyed on consecutive tides for the entire survey area at Cayeux-sur-Mer in October/November 2005.

The most probable source of error in the derivation of the volume changes is to be linked to the combined effect of the beach material grain size, pebble imbrications and the location where the measure point is taken with the DGPS as identified earlier in Chapter 3 (Section 3.2.2). As said earlier in the sampling design, the volume's margin

error for a survey area as large as the one at Cayeux-sur-Mer would be approximately of $\pm 3600 \text{ m}^3$. Such a margin error would actually cover most of the volumes changes observed from one tide to the following during the whole survey period (Table 6-6). This would suggest that a DGPS technique is not appropriate to measure small volume changes on mixed beaches.

Results for the overall volume change at Cayeux-sur-Mer between October 28th and November 11th per cell are presented on Figure 6-20. As expected, this time erosion characterised most of the surveyed area on the mixed sediment beach for a total volume change of -4420.1 m^3 whereas accretion was observed on the sandy platform for a total volume of $+2206.8 \text{ m}^3$. In more detail, the first 660 m on the mixed sediment beach from the terminal groyne displayed a total erosion measured at -5457.4 m^3 , the following 500 m showed a $+2415.3 \text{ m}^3$ accretion and the last 200 m of the survey, in front of the town centre, displayed erosion measured up to -1378 m^3 . The growth observed on the 500 m section of beach is related to the sediment transfer from an updrift to a downdrift area.

When considering the sandy platform (Figure 6-20), accretion and erosion areas can also be identified. In detail, from the terminal groyne to the downdrift areas the first 260 m display a 602 m^3 accretion, the following 300 m display erosion measured up to -1116.5 m^3 ; the next 200 m (cells 20 & 21) show only slight changes ($+78.7 \text{ m}^3$); cells 22 & 23 displayed erosion measured at -625.9 m^3 ; and finally, the very end of the survey area shows great accretion measured at $+3268.4 \text{ m}^3$. Again, it is most likely that the general erosion observed on the first 1 km contributed in part to the accretion movement observed at the very end of the survey area.

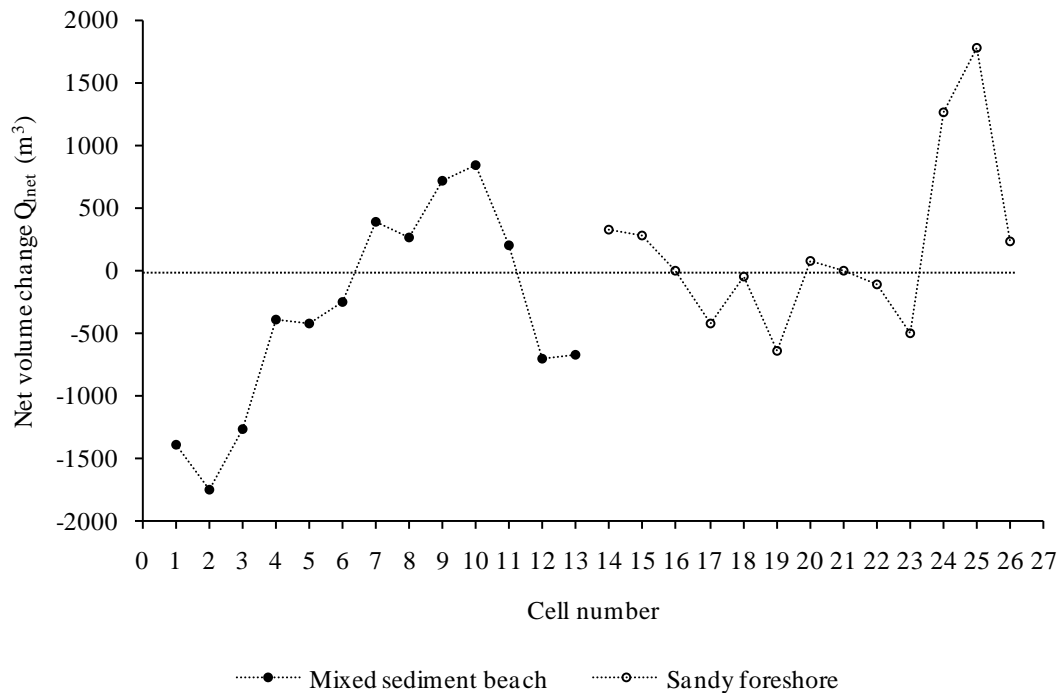


Figure 6-20 Net volume changes measured in each cell during the time period of the survey, between October 28th and November 11th 2005 at Cayeux-sur-Mer.

Based on this observation, the volumes remobilised during this survey period represent 5.5 to 6.3% of the yearly LST expected by the coastal defence authorities at Cayeux-sur-Mer. When extrapolating the volumes observed during this period to a yearly volume ratio, the predictions of transport would be approximately $92,822.1 \text{ m}^3 \text{ y}^{-1}$. This estimation is fairly close to the yearly sediment budget estimated by the local coastal defence managers ($70,000$ to $80,000 \text{ m}^3 \text{ y}^{-1}$). Considering that the wave climate observed at Cayeux during this survey period was representative of the yearly wave height climate and that only waves from South-West were observed, it is understandable that the LST rate deduced from this survey period would overestimate the actual yearly sediment rate. Indeed, the northward transport rate is sometimes counterbalanced by updrift movements when waves are coming from a North or North-East directions. The inclusion of such wave directions into the yearly sediment transport rate determined by this study ($92,822.1 \text{ m}^3 \text{ y}^{-1}$) would most likely counterbalance this result to a rate closer to the one expected. This would suggest that the use of DGPS surveys over long time survey periods or for periods marked by large volumes of longshore sediment transport is adequate to measure LST.

6.5 Field measurement experiments, Birling Gap, March 2006

6.5.1 Tracer recovery and distribution patterns

In March 2006 (Table 6-7), after one tide deployment, the lowest recovery rates per day of deployment were far above the expected recovery rates for “passive” tracers according to Allan et al. (2006) with rates going from 68.7 to 100% after one tide. Recovery rates only dropped down from a nearly perfect recovery on the last day of deployment, linked to a slight change in the wave direction on March 25th. As described in Chapter 4, the tidal cycle was going from a spring tide toward a neap tide, the wave approach to the coast was from the South-East with a mean angle to the coast ranging from 14° to 68°, the H_s were very low between 0.1 and 0.3 m until March 24th when they reached up to 0.79 m; and the T_s ranged between 2 and 12.2 s (Chapter 4 Section 4.3.2).

On the first day of the experiment, March 20th, tracer pebbles were deployed according to the methodology outlined in Chapter 3 at a depth of up to 30 - 40 cm. Unfortunately, the hydrodynamic conditions were not sufficient enough to entrain the majority of the tracers far enough from their injection point to be noticeable (Table 6-8; Appendix VII). Indeed, only a few pebbles from the lower injection point were remobilised (five in total out of one hundred). As a consequence, it was decided to deploy tracers only in the first 10 cm of the beach face on the following days of deployment. This decision was later supported by the fact that the tracers were recovered either at the surface or in the first 10 cm of the beach face during March 2006.

Date of deployment (max depth of deployment)	Location of the injection	Recovery rates (Total of pebble recovered)						Depth of recovery/ number of pebbles
		After one tide	Total after one tide	After three tide	Total after three tides	At the end of the experiments	Overall total	
20/03/2006 afternoon (30cm)	Upper beach	100 pebbles retrieved from each injection	NA					
	Middle beach							
	Lower beach	100% (5)/ 95 pebbles retrieved from injection	NA	100% (5)	NA	100% (5)	NA	Surface/5
22/03/2006 morning (10cm)	Upper beach	96% (48)	98.7%	96% (48)	98.7%	96% (48)	98.7%	Surface/116 0 to 10cm/32
	Middle beach	100% (50)		100% (50)		100% (50)		
	Lower beach	100% (50)		100% (50)		100% (50)		
23/03/2006 afternoon (10cm)	Upper beach	50 pebbles Retrieved from injection	NA					
	Middle beach	100% (50)						
	Lower beach	100% (50)	100%	100% (50)	100%	100% (50)	100%	Surface/73 0 to 10cm/27
25/03/2006 morning (10cm)	Upper beach	90% (45)	68.7%	90% (45)	68.7%	90% (45)	68.7%	Surface/39 0 to 10cm/64
	Middle beach	68% (34)		68% (34)		68% (34)		
	Lower beach	48% (24)		48% (24)		48% (24)		

Table 6-7 Recovery rates and depth of recovery of the tracers during the survey period in March 2006 at Birling Gap. The figures in brackets correspond to the cumulative number of tracer pebbles recovered in total.

The general pattern of the tracer pebble scattering over the March 2006 field campaign, was that the majority of pebbles tended to migrate in a westerly direction which is in accordance with the general wave direction observed. The furthest tracer pebble recovered travelled in a westerly direction up to 79.6 m from its injection point in only one tide on the deployment of March 25th. The furthest tracer that travelled in an eastern direction was less than 1 m away from the injection area (alongshore distance), all

measurements considered. The position of the tracers' centroid for each injection point after one tide were calculated and displayed in Table 6-8 and Figures 6-21 & 6-22; and Appendix VII). As can be seen the mean alongshore movement of the tracers measured for each day of deployment increases with time, being of -1.2 m on the deployment of March 20th, -2.5 m on the deployment of March 22nd, -3.7 m on the deployment of March 23rd and -20 m on the deployment of March 25th.

When considering injection points individually, in a similar way as at Cayeux-sur-Mer, on March 22nd (Figure 6-21), the tracers pebbles deployed in the upper injection point travelled the furthest alongshore distance (-3.5 m) while the pebbles injected in the middle and lower parts of the mixed sediment beach travelled equivalent distances, -1.9 and -2.1 m respectively. The pebbles located on the upper and middle beach travelled down the beach (-4.5 and -4.2 m respectively), contrary to the results obtained at Cayeux, the pebbles injected on the lower part of the mixed sediment beach were also affected by downward movements on the beach. This tendency for the tracers deployed on the lower injection point to move down the beach is recurrent during the whole survey period apart from on March 20th. However, on March 20th (Appendix VII Figure VII-1), the dispersion of the tracers was very poor and no pattern of distribution was discernible. On March 23rd (Appendix VII Figure VII-2), it can be seen that again the alongshore distances travelled by the pebbles deployed on the middle and lower injection points travelled equivalent distances. On March 25th (Figure 6-22), the dispersion of the tracers was more significant than for the previous deployments. The mean alongshore distance travelled was measured at -20 m which was slightly more than six times the distance travelled by the tracers on the previous days. Such transport is to be related to the significant increase in wave height on March 24th when H_s increased up to 0.79 m in contrast to 0.3 m for the earlier deployments. Atypically to all the preceding results, including those from Cayeux, the furthest alongshore distances are travelled by the tracers deployed on the lower part of the mixed sediment beach (-41.3 m), then the middle part (-18 m), and finally the upper part (-10.1 m).

Date of deployment	Location of the injection on the mixed sediment beach	Mean distance travelled After one tide (m)	Overall mean distance travelled After one tide	Mean angle of the transport measured after one tide (referred to the magnetic North, in °)	Overall mean angle of the transport measured after one tide (referred to the magnetic North, in °)	Mean alongshore distance travelled after one tide (m)	Overall mean alongshore distance travelled after one tide (m)	Mean across-shore distance travelled after one tide (m)	Overall mean across-shore distance travelled after one tide (m)
20/03/2006	Upper beach	NA							
	Middle beach								
	Lower beach	1.4	NA	333.6	NA	-1.2	NA	0.7	NA
22/03/2006	Upper beach	5.7	4.9	253.1	245.7	-3.5	-2.5	-4.5	-4.2
	Middle beach	4.6		238.9		-1.9		-4.2	
	Lower beach	4.1		246.0		-2.1		-3.5	
23/03/2006	Upper beach	NA							
	Middle beach								
	Lower beach	5.6	252.3	-3.4	-4.4				
25/03/2006	Upper beach	10.2	20.1	310.4	309.1	-10.1	-20.0	-0.9	-1.4
	Middle beach	18.0		304.8		-18.0		-0.1	
	Lower beach	41.5		311.1		-41.3		-4.4	

Table 6-8 Characteristics of the sediment transport measured using the tracer pebbles after one tide of deployment at Birling Gap in March 2006. Negative values of the alongshore travelled distance indicate that the pebbles moved in a westward direction; positive values indicate alongshore movements in an eastward direction. Negative values of the across-shore distance travelled indicate that the pebbles moved down the beach and positive values indicate that these movements are up the beach.

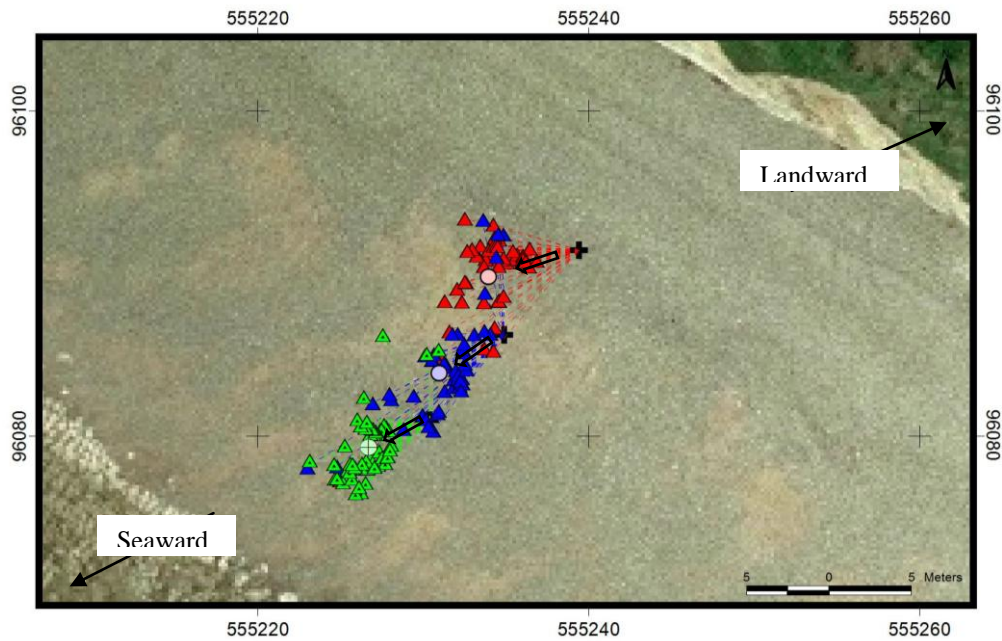


Figure 6-21 Movement of tracer pebbles observed after one tide deployment on March 22nd, 2006. The black cross marks the locations of the injection points. Each triangle represents individual tracer pebbles recovered after one tide. The disks mark the location of the centroids. Pebbles are colour coded: red = upper injection point, blue = middle injection point, green = lower injection point. Arrows indicate the mean orientation of the pebbles movement.

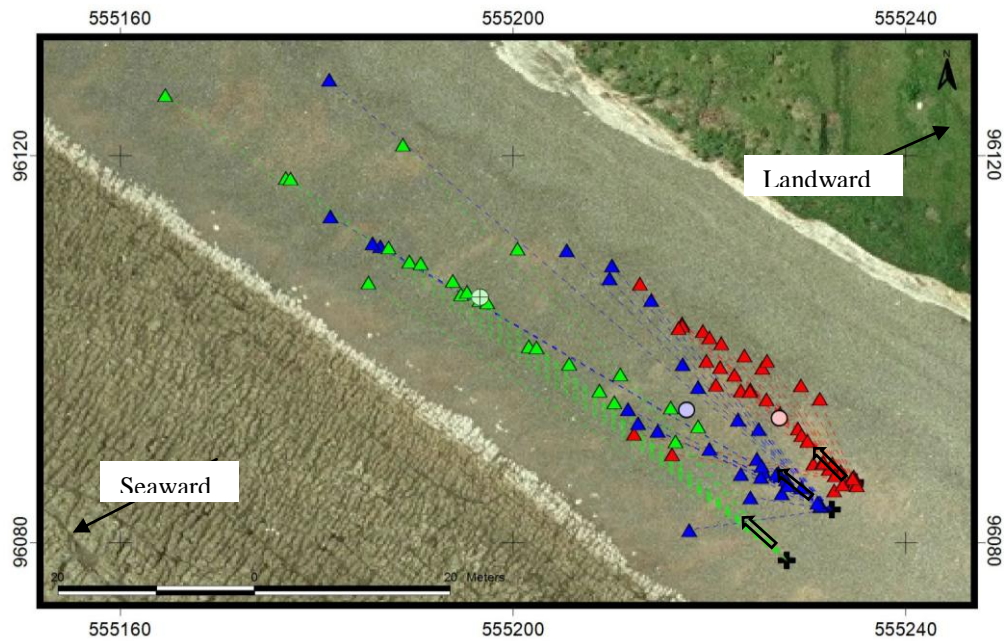


Figure 6-22 Movement of tracer pebbles observed after one tide deployment on March 25th, 2006. The Black cross marks the locations of the injection points. Each triangle represents individual tracer pebbles recovered after one tide. The disks mark the location of the centroids. Pebbles are colour coded: red = upper injection point, blue = middle injection point, green = lower injection point. Arrows indicate the mean orientation of the pebbles movement.

6.5.2 Derivation of the volume transported and the LST rates using tracer pebbles

As for Cayeux, LST rates were derived from two methods: (i) the use of only the tracer data, and (ii) use of the depth of disturbance and the tracer data (Table 6-9). Again when just looking at the values of the difference between the two LST rates derived, these can seem negligible considering that they are less than 4 m³. However, when these differences are expressed as a percentage of the LST rate derived from the use of the tracers' data only, it appears that in general, the volume derived from the tracer overestimate the “real” beach volume remobilised. These differences in percentage can range from 6.8 to 60.7%.

Date of deployment	Mean alongshore distance travelled after one tide (m)	Area of the beach material removed (m ²)	Maximum depth of tracer pebbles recovered (m)	Average length of the beach (m)	LST rate derived from the use of the depth of disturbance (m ³ tide ⁻¹)	LST rate derived from the depth of the deepest tracers (m ³ tide ⁻¹)	Difference between the LST rates (m ³ tide ⁻¹)	Percentage of difference between the LST rates (%)
20/03/2006	-0.7	0.92	0.1	23.4	-0.644	-1.64	-1	60.7
22/03/2006	-2.5	1.22	0.1	15.3	-3.05	-3.82	-0.8	20.3
23/03/2006	-3.7	1.07	0.1	15.9	-3.959	-5.88	-1.9	32.7
25/03/2006	-20.0	2.53	0.1	23.7	-50.6	-47.4	3.2	6.8

Table 6-9 Calculation of the LST rates using tracer pebble dispersion on mixed sediment beach at Birling Gap in March 2006. Note that it was preferred to keep the conventional sign code used earlier to describe the mean alongshore directions of transport when deriving the LST rates so that the direction of the transport is still shown.

6.5.3 DGPS surveys: digital elevation model and beach elevation changes

On Figure 6-23 it can be seen that the beach elevation changes were mostly > 0.05 m from one tide to the following. The greatest elevation changes are within 0.3 m, with a few extreme values measured at ± 1.2 m in local places. These extreme changes are generally very close to the cliff edge or in the eastern end of the beach. The extreme changes in elevation in proximity to the cliff edge are most likely to be linked to the survey methodology. Indeed, by having a lateral error of ± 1 to 2 m on the location of each profile surveyed, some of the profiles extended onto the chalk on the very bottom of the cliffs and some others were not. Because of the characteristics of the interpolation, this slight error was introduced into the digital elevation changes maps forming these extreme elevation changes.

On the eastern end of the beach there are a few caves at the bottom of the chalk cliffs. These cavities generally trap a large amount of sediment and visual observations over the two year of research in this site showed that the volume of sediment trapped by these cavities was extremely variable. However, this does not explain why such elevation variation is observed in their proximity on short time scales.

This area is also characterised by very local and frequent cliff falls. The raw chalk block deposits quite often partially filled up these caves which made it difficult to keep a fixed location for the profile line. This may create an error when interpolating the elevation changes as discussed just earlier. Moreover, the sudden but consistent supply in chalk and its wash-over could have contributed to the elevation changes measured. For these reasons and in order to minimize the error margin, it was decided to exclude the far eastern elevation changes of the beach from the calculation of the beach volume changes.

The two last beach elevation change maps made between March 24th and 25th and the two low tides on March 25th display the greatest changes of all. Between the tide on the 24th and the 25th, the beach displays predominantly accretion mostly comprised between 0.05 and 0.2 m. On the contrary, the elevation changes between the two tides on the 25th, most of the beach displays erosion with most of the changes comprised between -0.05 and -0.2 m.

When looking at the elevation changes over the entire survey period, from March 20th to March 25th, the whole beach is mainly affected by slight erosion <0.2 m with a very few local spots showing erosion >0.2 m (Figure 6-23). Two thin strips of accretion <0.2 m can be seen in the middle and at the bottom of the beach towards the western end of the surveyed area. The thin accretion strip observed in the middle of the beach most certainly corresponds to the position of a new berm built up until March 25th in comparison to March 20th.

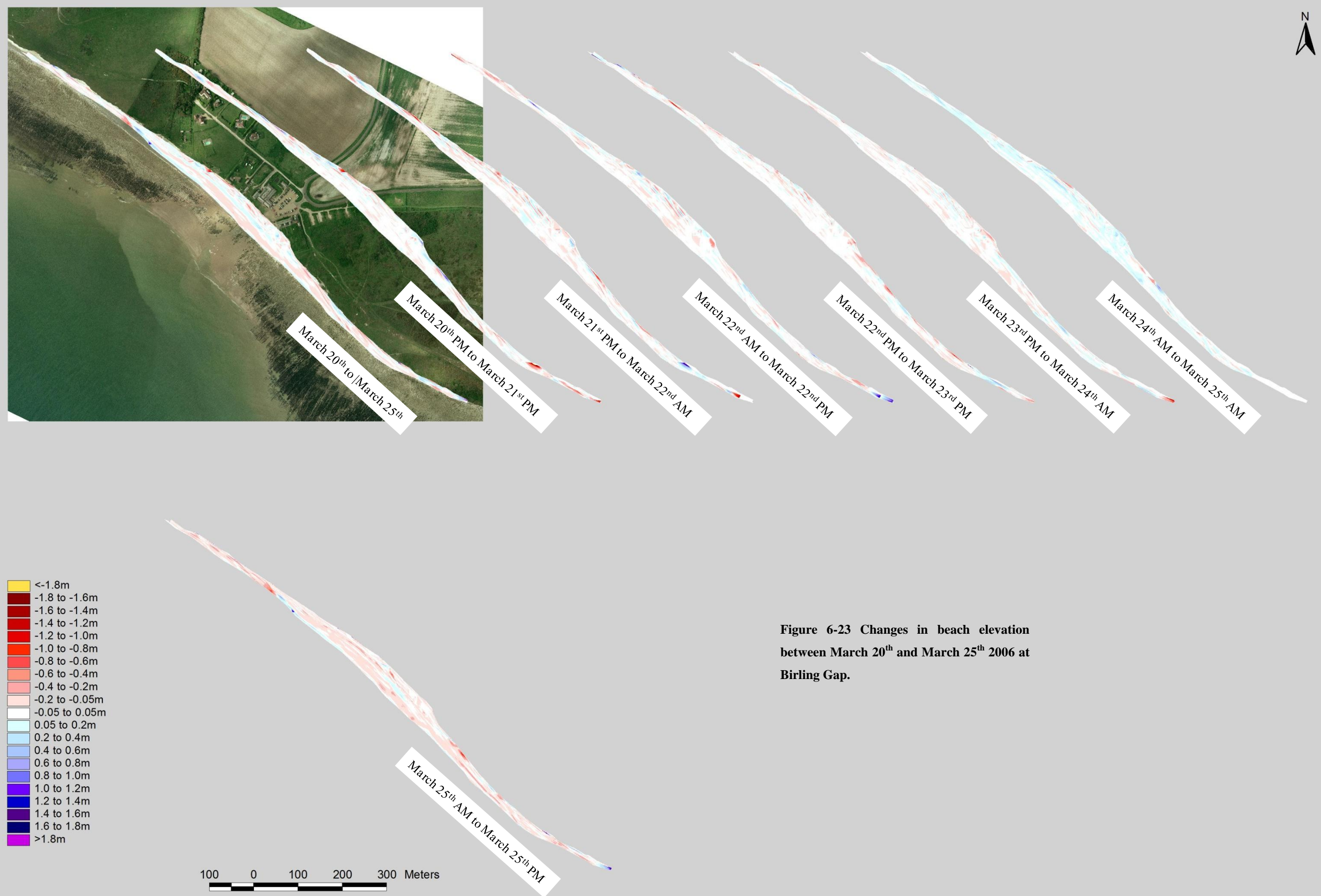


Figure 6-23 Changes in beach elevation between March 20th and March 25th 2006 at Birling Gap.

6.5.4 DGPS surveys: beach volume changes

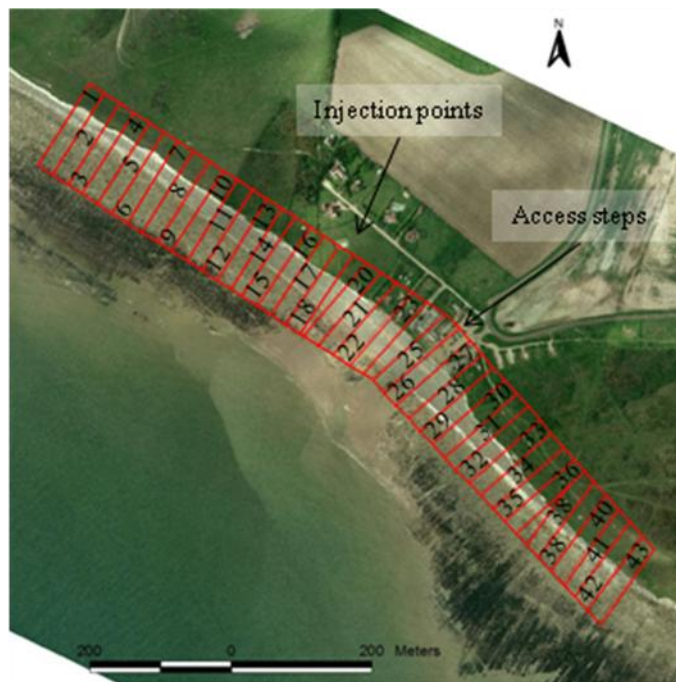


Figure 6-24 Grid system used to calculate the beach volume changes at Birling Gap in December 2004.

As for Cayeux-sur-Mer, the beach at Birling Gap was divided into cells to determine the volume changes along the beach (Figure 6-24). Again, the width of these cells was determined by the average distance between two consecutive beach profiles to ensure the relevance of the volume changes within each cell. The average distance

between two profiles at Birling gap was approximately 20 m. For

this reason 25 m wide cells were used to derive the beach volume changes along the shore. Using this method, areas marked by overall accretion or erosion can be highlighted on the beach, and volume transfers from one area to another can be deduced using the wave conditions and the tracers' movements.

Figure 6-25 represents the volumes changes observed between two consecutive topographical surveys. Each respective dashed grid line represents the equilibrium stage between erosion and accretion i.e. volume change equal to zero. Therefore when a point is above the corresponding dashed line, the cell experiences accretion, and when a point is below the line, the cell experiences erosion. For a better reading, it was possible here (contrary to Cayeux earlier) to use increments of 100 m^3 between each tide for which the volumes changes were calculated.

The use of this graph allows a better view of the areas that experience gain or loss of sediment along the beach for each cell and permits a clearer understanding of the volume transfers along the beach. Until March 25th, the volume changes for each cell

were low all along the beach, mainly oscillating between -50 and +50 m³ in each cell. For this reason, it is rather difficult to identify any sediment transport.

The overall beach volumes changes from March 20th to March 24th were measured at: March 21st, +153m³; March 22nd morning, -151 m³; March 22nd afternoon, -55 m³; March 23rd, -205 m³; and, March 24th, +42 m³. In contrast, the last two elevation change maps made for March 24th AM to March 25th AM and March 25th AM to March 25th PM show significant volume changes measured respectively at +1553 m³ and -1466 m³.

Between March 24th AM and March 25th AM, the whole beach experienced accretion, but the greatest accretions are located in the area between approximately the location of the injection points and approximately 100 m eastward of the access steps (approximately cell 30). In contrast, between March 25th AM and March 25th PM, nearly the whole beach experienced erosion, with the greatest erosion mainly located from the injection points to approximately 200 m eastward of the access steps (approximately cell 34).

Because of the error associated with the DGPS surveys and the interpolation of digital elevation maps (± 5 cm, BAR, 2005), the fairly low volumes involved in the sediment transport and the poor control on the entries and exits of sediment in the beach system, it was judged rather difficult to directly link LST rates to those observed with the DGPS on Figure 6-25. Therefore instead of directly comparing the results, it was preferred to judge them individually when plotted against the longshore wave power (P_l). This will be done in Chapter 7.

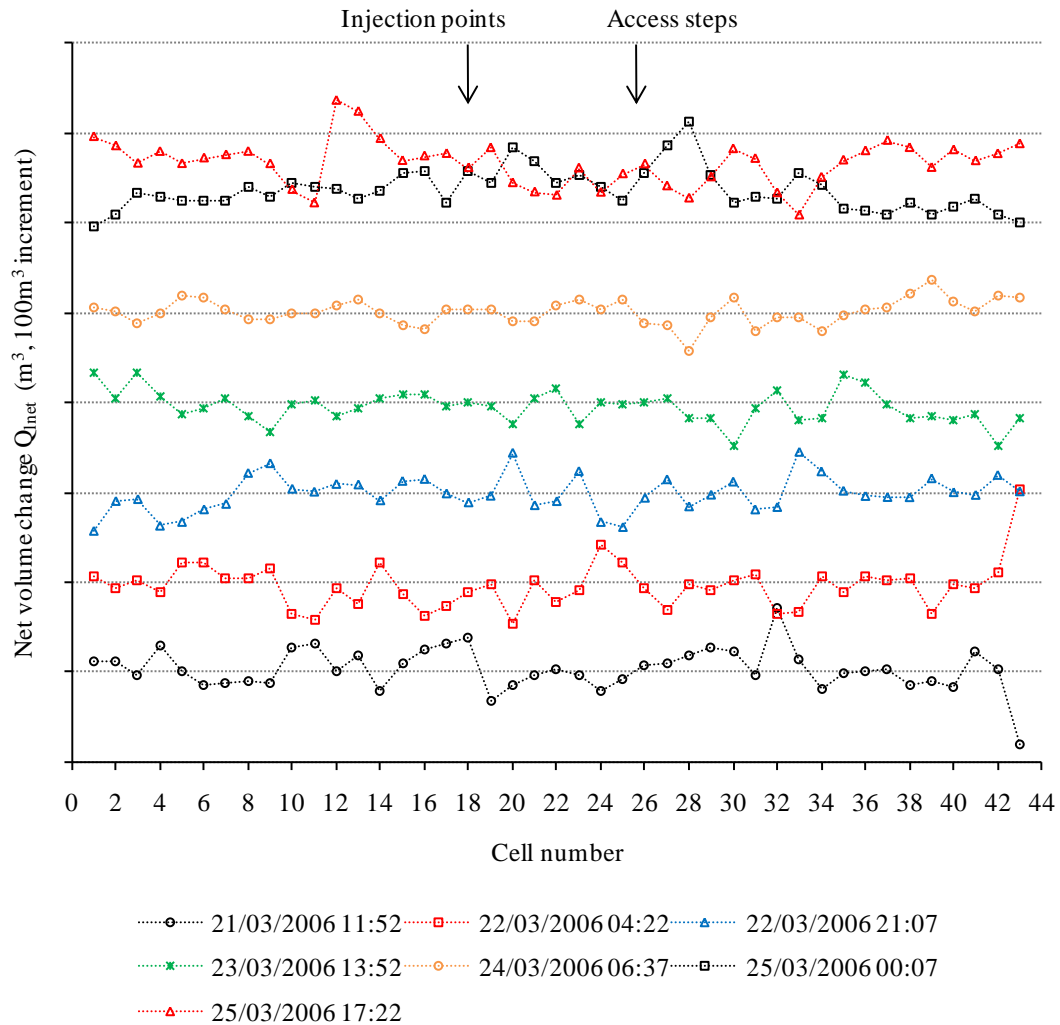


Figure 6-25 Net volume change (Q_{net}) measured for each cell between two consecutive surveys at Birling Gap in March 2006. The legend gives the date and time of the later of the two surveys. An increment of 100 m^3 is used between the results obtained from each digital map. The dashed black lines represent equilibrium between erosion and accretion (0 m^3 net volume change) for the associated survey line.

Results for the overall volume change at Birling Gap between March 20th and March 25th per cell are presented on Figure 6-26. As can be seen, erosion and accretion oscillate along the beach within a range of -60 to $+80 \text{ m}^3$ per cell. It appears however that the area from approximately the location of the injection points to the eastern end of the beach is mainly affected by erosion (Q_{net} measured at -296.7 m^3 between cell 19 and cell 43). In contrast, a 175 m long beach area directly updrift of injection points (cell 18) displays accretion measured at $+253 \text{ m}^3$. Considering the wave direction during the survey period (from the South-East) and the sediment transport directions measured using the tracer pebbles, it is likely that the volume of sediment eroded on the eastern

end of the beach moved towards the western end of the beach. Therefore, it is most probable that the accretion movement observed just updrift of the tracer pebbles' injection points is partly due to the westward transfer of these volumes.

The total volume change during the survey period from March 20th to March 25th presented a net loss of -130 m³.

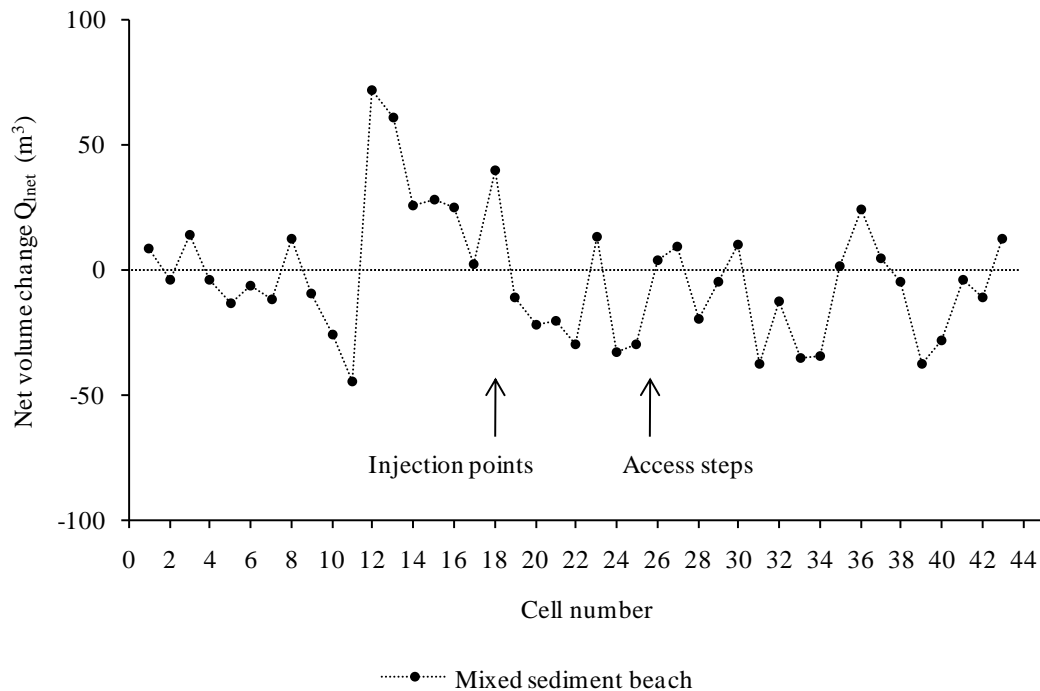


Figure 6-26 Net volume changes measured in each cell during the time period of the survey, between March 20th and March 25th 2006 at Birling Gap.

6.6 Field measurement experiments, Birling Gap, May 2006

6.6.1 Tracer recovery and distribution patterns

In May 2006, the maximum H_s observed went generally from moderate to stormy conditions (>1 m) and consequently, the recovery rates after only one tide is considerably lower than in March, between 39 and 49.3% (Table 6-10). However, the recovery rates increased greatly with time, reaching 72 to 95% by the end of this survey period. In general, the recovery rates proved to be greater on the lower beach after one tide; however, they were more evenly distributed between injection points by the end of the experiment.

The tidal conditions were close to a neap tide (neap tide occurred on May 21th 2006) and the wave direction was consistent with waves coming from the South-West with an angle to the coast oscillating around its orthogonal, mean angle of wave approach to the coast varying from 52 to 142°. H_s ranged from above 1 m with peaks above 2 m (2.6 m on the 20th). T_s ranged from 3 to 9 s (Chapter 4 Section 4.3.2).

Date of deployment (max depth of deployment)	Location of the injection	Recovery rates (Total of pebble recovered)						Depth of recovery/ number of pebbles
		After one tide	Total after one tide	After three tides	Total after three tides	At the end of the experiments	Overall total	
19/05/2006 (30cm)	Upper beach	20% (10) retrieved 50	39%	70% (35)	75.5%	96% (48)	95%	Surface/57 0 to 10cm/19 10 to 20cm/2
	Middle beach	30% (15) retrieved 50		72% (36)		98% (49)		
	Lower beach	53% (53)		80% (80)		93% (93)		
20/05/2006 (10cm)	Upper beach	56% (14)	49.3%	56% (14)	56%	60% (15)	72%	Surface/27 0 to 10cm/10
	Middle beach	36% (9)		56% (14)		76% (19)		
	Lower beach	56% (14)		56% (14)		80% (20)		
22/05/2006 (10cm)	Upper beach	23% (7)	40%	66.6% (20)	74.7%	66.6% (20)	74.7%	Surface/26 0 to 10cm/10
	Middle beach	46.6% (14)		83.3% (25)		83.3% (25)		
	Lower beach	50% (15)		73.3% (22)		73.3% (22)		

Table 6-10 Recovery rates and depth of recovery of the tracers experienced during the survey period in May 2006 at Birling Gap. The figures in brackets correspond to the cumulative number of tracer pebbles recovered in total.

When considering the distance travelled by the tracer pebbles on each deployment, it can be seen that on May 19th the furthest pebbles travelled a maximum distance of 50.8 m and this was achieved after only one tide (Figure 6-27). On the deployment of May 20th, the furthest pebble was found 12.3 m away from its injection point after one tide deployment and by the end of the survey period the furthest pebbles found was 45.3 m (Figure 6-28). On the last deployment day, May 22nd, the furthest travelled distance was measured up to 62.8 m for the whole survey period (Figure 6-29). This

distance was travelled in only one tide too. The values presented in Table 6-12 show that the LST on May 19th and 22st were oriented westward with respective average alongshore distances measured at -17.2 and -28.1 m from their injection points, whereas the transport on March 20th had an average alongshore transport oriented eastward and measured at only 4 m.

The two patterns of distribution observed earlier are again expressed during this survey period. As a reminder, the first one showed that the tracers deployed at the top of the beach travel on average longest distances and were affected by greater across-shore movements than the tracers deployed on lower parts of the beach. This pattern is expressed on the deployments of May 19th and 22st with the upper pebbles travelling average longshore distances respectively of -31.6 and -31.9 m, whereas the alongshore distance travelled by the tracers from the middle injection point are respectively -23.2 and -29.4 m, and the alongshore distances travelled by the lower injection pebbles are respectively -12.9 and -25.5 m (Table 6-11).

The second pattern shows that the longest distances travelled by the tracers deployed on the lower part of the mixed sediment beach; and the lowest are travelled by the pebbles deployed on the upper injection point. On May 20th, the tracers injected on the lower part of the mixed sediment beach travelled on average an alongshore distance of 6.7 m, those deployed on the middle beach travelled on average 4.4 m and finally the upper injection tracers travelled only by 0.7 m. On that same deployment, the pebbles were affected by a general across-shore movement up the beach (respectively from the upper to the lower injection point being 3.9 m, 6.7 m and 8.5 m). In fact, the greatest across-shore movements were observed for the lower injection point pebbles and it decreases with increasing elevation up the beach face.

Date of deployment	Location of the injection on the mixed sediment beach	Mean distance travelled After one tide (m)	Overall mean distance travelled After one tide	Mean angle of the transport measured after one tide (referred to the magnetic North, in °)	Overall mean angle of the transport measured after one tide (referred to the magnetic North, in °)	Mean alongshore distance travelled after one tide (m)	Overall mean alongshore distance travelled after one tide (m)	Mean across-shore distance travelled after one tide (m)	Overall mean across-shore distance travelled after one tide (m)
19/05/2006	Upper beach	32.6	17.6	290.4	292.2	-31.6	-17.2	-8.2	-3.9
	Middle beach	23.8		292.4		-23.2		-5.2	
	Lower beach	14.1		328.5		-12.9		5.6	
20/05/2006	Upper beach	4.0	7.1	44.9	69.4	0.7	4.0	3.9	5.8
	Middle beach	8.0		68.4		4.4		6.7	
	Lower beach	10.8		73.5		6.7		8.5	
22/05/2006	Upper beach	36.1	28.9	277.3	291.2	-31.9	-28.1	-16.8	-6.9
	Middle beach	30.1		292.7		-29.4		-6.4	
	Lower beach	25.7		311.8		-25.5		3.1	

Table 6-11 Characteristics of the sediment transport measured using the tracer pebbles after 1 tide of deployment at Birling Gap in May 2006. Negative values of the alongshore travelled distance indicate that the pebbles moved in a westward direction; positive values indicate alongshore movements in an eastward direction. Negative values of the across-shore travelled distance indicate that the pebbles moved down the beach and positive values indicate that these movements are up the beach.

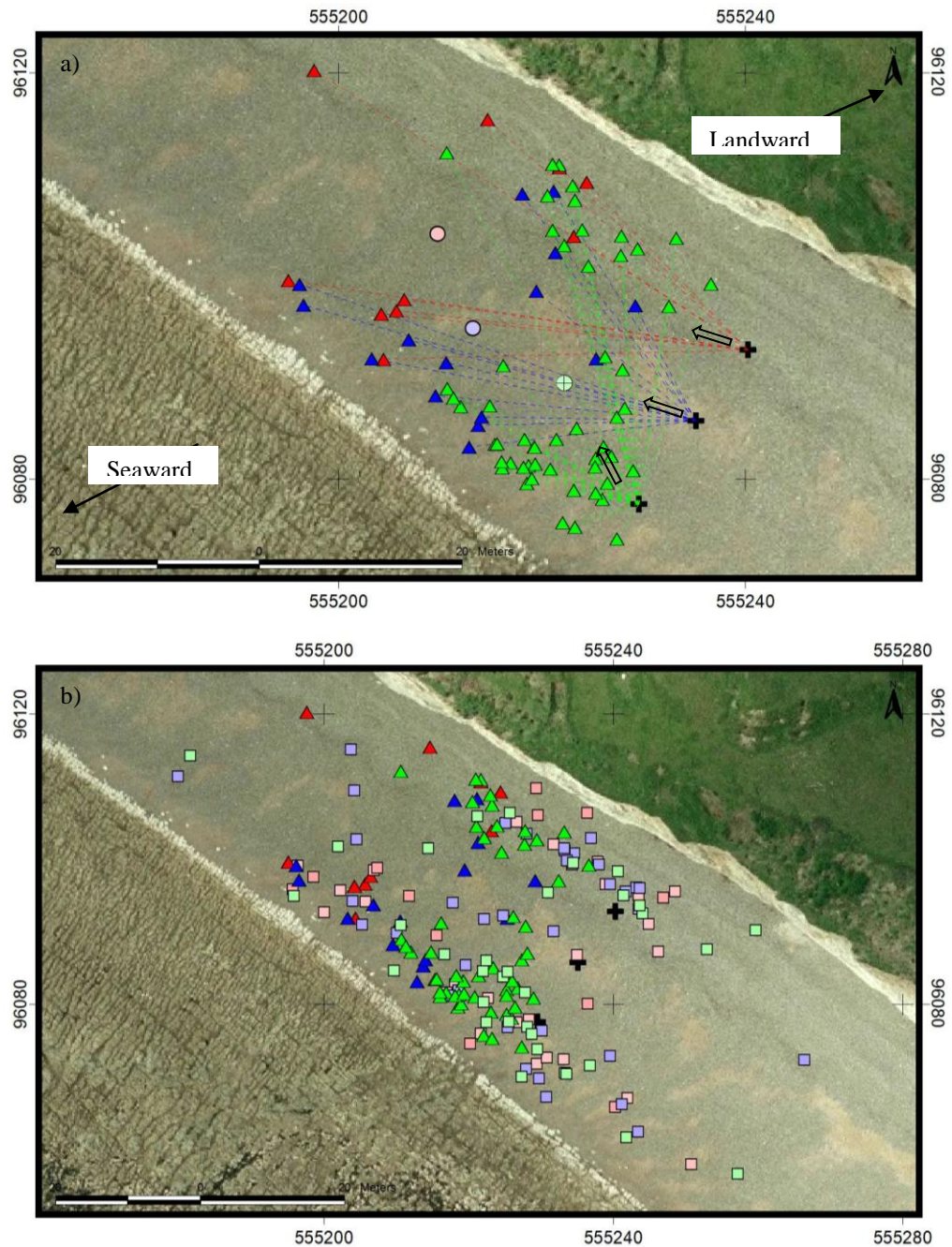


Figure 6-27 Movement of tracer pebbles deployed on May 19th, 2006.

a) Scattering observed after one tide. Arrows indicate the mean orientation of the pebbles movement.

b) Scattering observed over the whole survey period.

The Black cross marks the locations of the injection points. Each triangle represents individual tracer pebbles recovered after one tide while the squares represent individual tracer pebbles recovered after more than one tide. The disks mark the location of the centroids. Pebbles are colour coded: red = upper injection point, blue = middle injection point, green = lower injection point.

The general distribution of all the pebbles deployed on May 19th and recovered by the end of the survey period clearly shows accumulations of pebbles on both the upper and lower parts of the beach (Figure 6-31). On the following deployment, May 20th, the general distribution of the tracer pebbles showed a similar pattern (Figure 6-32). In contrast, the distribution of the pebbles deployed on May 22nd does not display such obvious distribution (Figure 6-33). Indeed, pebbles recovered after more than one tide seem to be equally scattered across-shore. Because of the low recovery rate, it is rather difficult to explain such a pattern. However, it is very likely that a great amount of pebbles deployed on the 22nd were dragged up the beach to build up the berm and were buried too deep to be detected by the metal detector, giving the impression that the pebbles are spread out equally across the beach. This would also explain the low recovery rate.

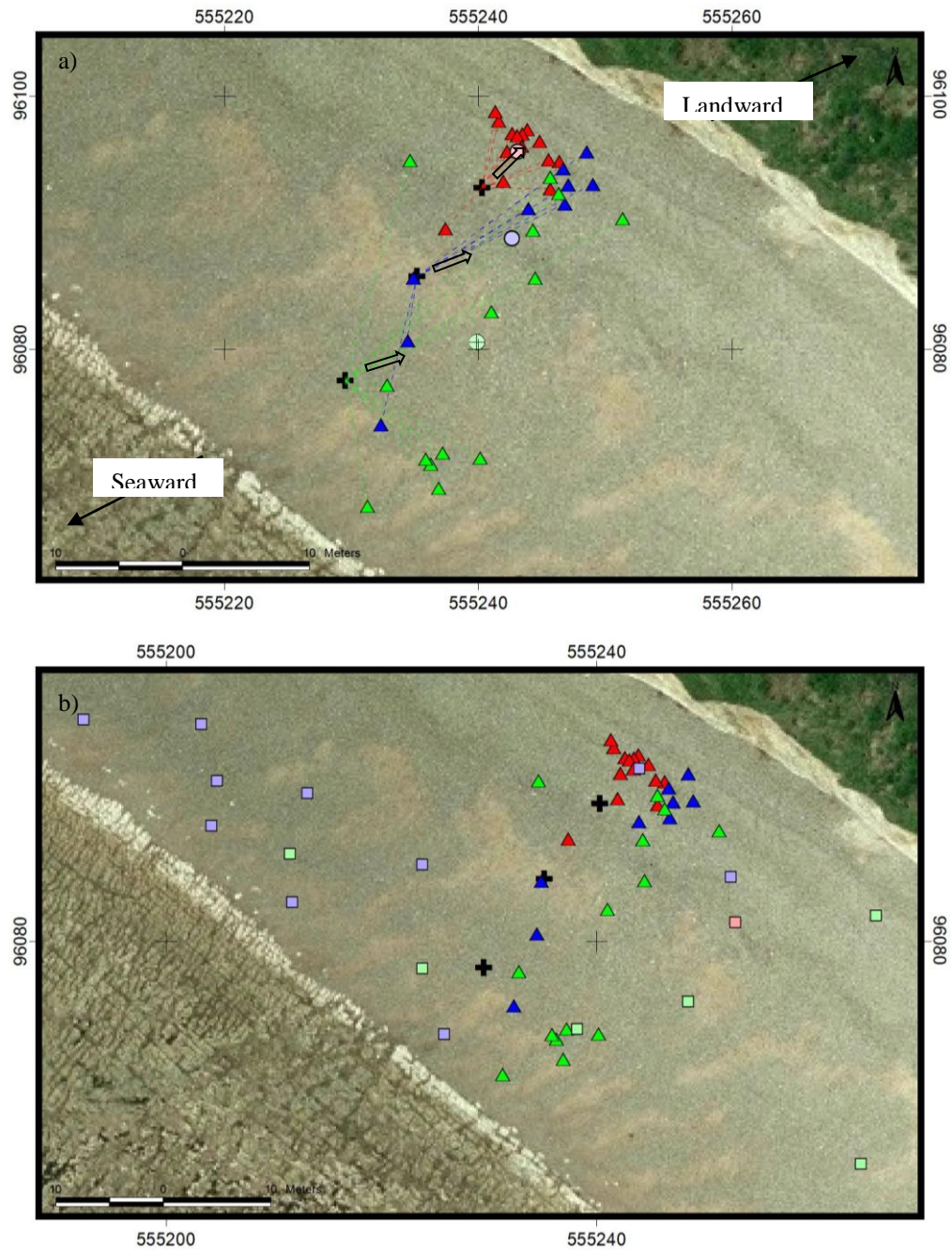


Figure 6-28 Movement of tracer pebbles deployed on May 20th, 2006.

a) Scattering observed after one tide. Arrows indicate the mean orientation of the pebbles movement.

b) Scattering observed over the whole survey period.

The Black cross marks the locations of the injection points. Each triangle represents individual tracer pebbles recovered after one tide while the squares represent individual tracer pebbles recovered after more than one tide. The disks mark the location of the centroids. Pebbles are colour coded: red = upper injection point, blue = middle injection point, green = lower injection point.

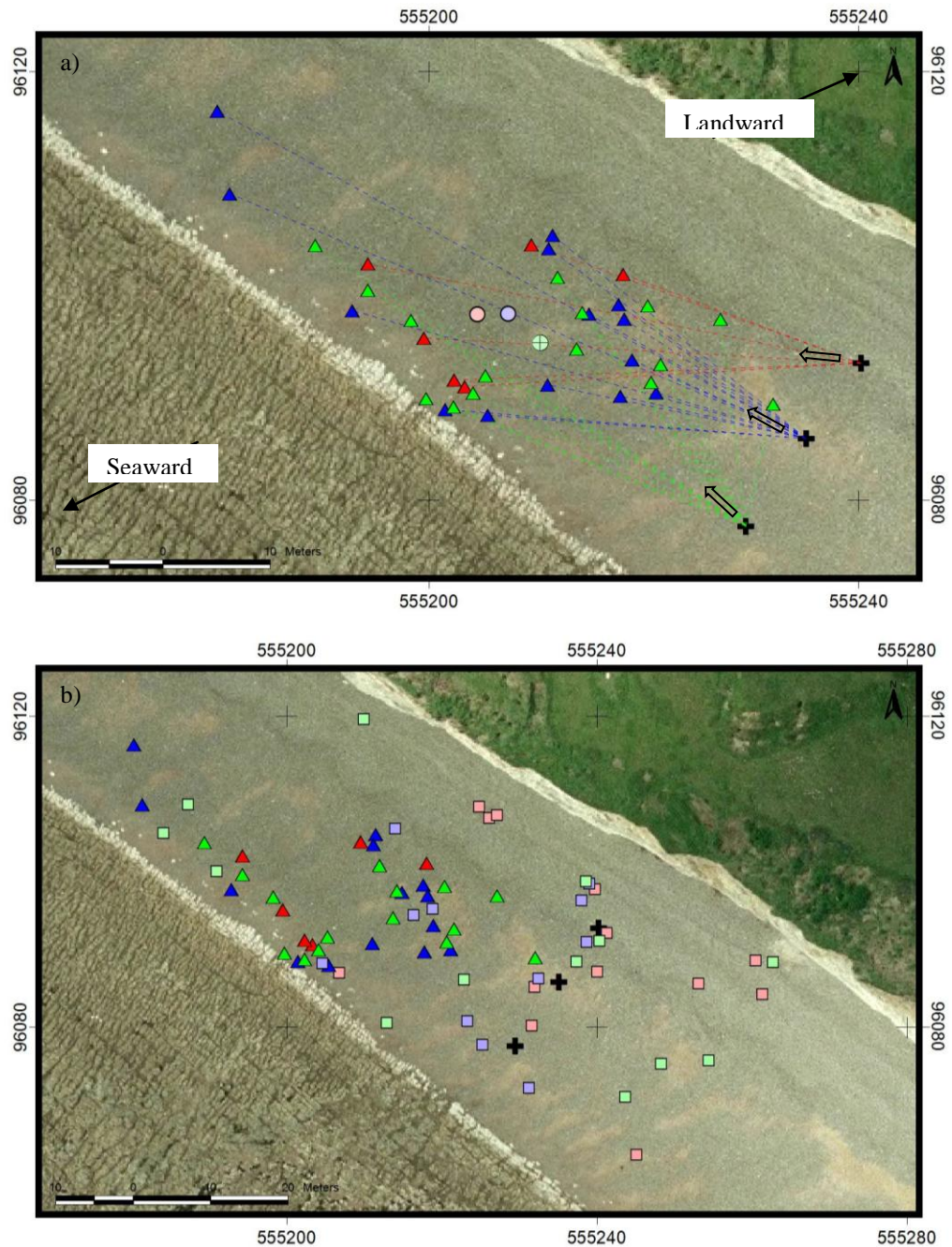


Figure 6-29 Movement of tracer pebbles deployed on May 22nd, 2006.

a) Scattering observed after one tide. Arrows indicate the mean orientation of the pebbles movement.

b) Scattering observed over the whole survey period.

The Black cross marks the locations of the injection points. Each triangle represents individual tracer pebbles recovered after one tide while the squares represent individual tracer pebbles recovered after more than one tide. The disks mark the location of the centroids. Pebbles are colour coded: red = upper injection point, blue = middle injection point, green = lower injection point.

6.6.2 Derivation of the volume transported and the LST rates using tracer pebbles

When looking at the LST rates determined using the same techniques as earlier described (measurements of the depth of disturbance or inclusion of the deepest tracer recovered in complement to the length of the profile), it can be seen that the percentage of difference between each technique is less than 25%, meaning that both results are actually very close (Table 6-12).

Both methods indicate that the LST rate was very low on May 20th (between 15.7 and 17.4 m³ tide⁻¹) in comparison to the two other days of measurements on May 19th and 22st which are 6 to 8.6 times greater, measured respectively between -104.2 and -136.2 m³ tide⁻¹ and between -108.8 and -120.6 m³ tide⁻¹. It is important to point out that the average transport on the 20th is oriented east while on the two others days of deployment, the transport was in a westerly direction.

Date of deployment	Mean alongshore distance travelled after one tide (m)	Area of the beach material removed (m ²)	Maximum depth of tracer pebbles recovered (m)	Average length of the beach (m)	LST rate derived from the use of the depth of disturbance (m ³ tide ⁻¹)	LST rate derived from the depth of the deepest tracers (m ³ tide ⁻¹)	Difference between the LST rates (m ³ tide ⁻¹)	Percentage of difference between the LST rates (%)
19/05/2006	-17.2	6.06	0.20	39.6	-104.23	-136.224	-31.992	23.5
20/05/2006	4.0	4.34	0.10	39.3	17.36	15.72	-1.64	10.4
22/05/2006	-28.1	4.29	0.10	38.7	-120.55	-108.75	11.80	10.9

Table 6-12 Calculation of the LST rates observed using tracer pebbles dispersion on mixed sediment beach at Birling Gap in May 2006. Note that it was preferred to keep the conventional sign code used earlier to describe the mean alongshore directions of transport when deriving the LST rates so that the direction of the transport is still shown.

6.6.3 DGPS surveys: Beach surface and volume changes

Elevation changes maps were calculated between each tide and also for the overall survey period. Note that during this survey period, the inaccuracy associated with the topographical survey collected in the morning of May 22nd was too great to be considered negligible and it was excluded from the results shown on Figure 6-30.

On a tidal basis, the elevation changes are generally between -0.4 and +0.8 m during the survey period until May 21st. They are greater between May 21st and May 22nd being measured between -0.8 and +1.6 m but this survey covers two tides instead of one for the rest of the elevation changes maps. Note that this extreme accretion value (+1.6 m) corresponds to the location of one of the cavities in the chalk cliff discussed earlier as being source of misrepresentation on the digital model.

When looking at the general pattern of distribution between the areas showing erosion or accretion, at the start of the experiment, between May 19th and May 20th, the top of the beach on the western side of the beach was showing accretion whereas the rest of the beach displayed mostly erosion. In contrast, the topographical changes between the two low tides on May 20th showed that accretion characterised the lower part of the beach whereas the top of the beach displayed erosion. Between May 20th and May 21st, a similar pattern as for May 19th to May 20th of distribution between erosion and accretion movements can be observed. From May 21st to May 22nd, accretion generally marked the upper and lower parts of the beach whereas the middle parts displayed erosion. The maximum erosion was measured up to -0.8 m just opposite the access steps. As mentioned earlier in this thesis (Chapter 4 Section 4.3.5), this area is submerged by water for longer period of time on every tide and experiences also the most wave energy as the wave breaking is nearly constant here (personal observation).

The overall elevation changes during this study period show that on average the top of the beach on the western half of Birling Gap displayed accretion whereas the other parts of the beach mostly showed erosion.

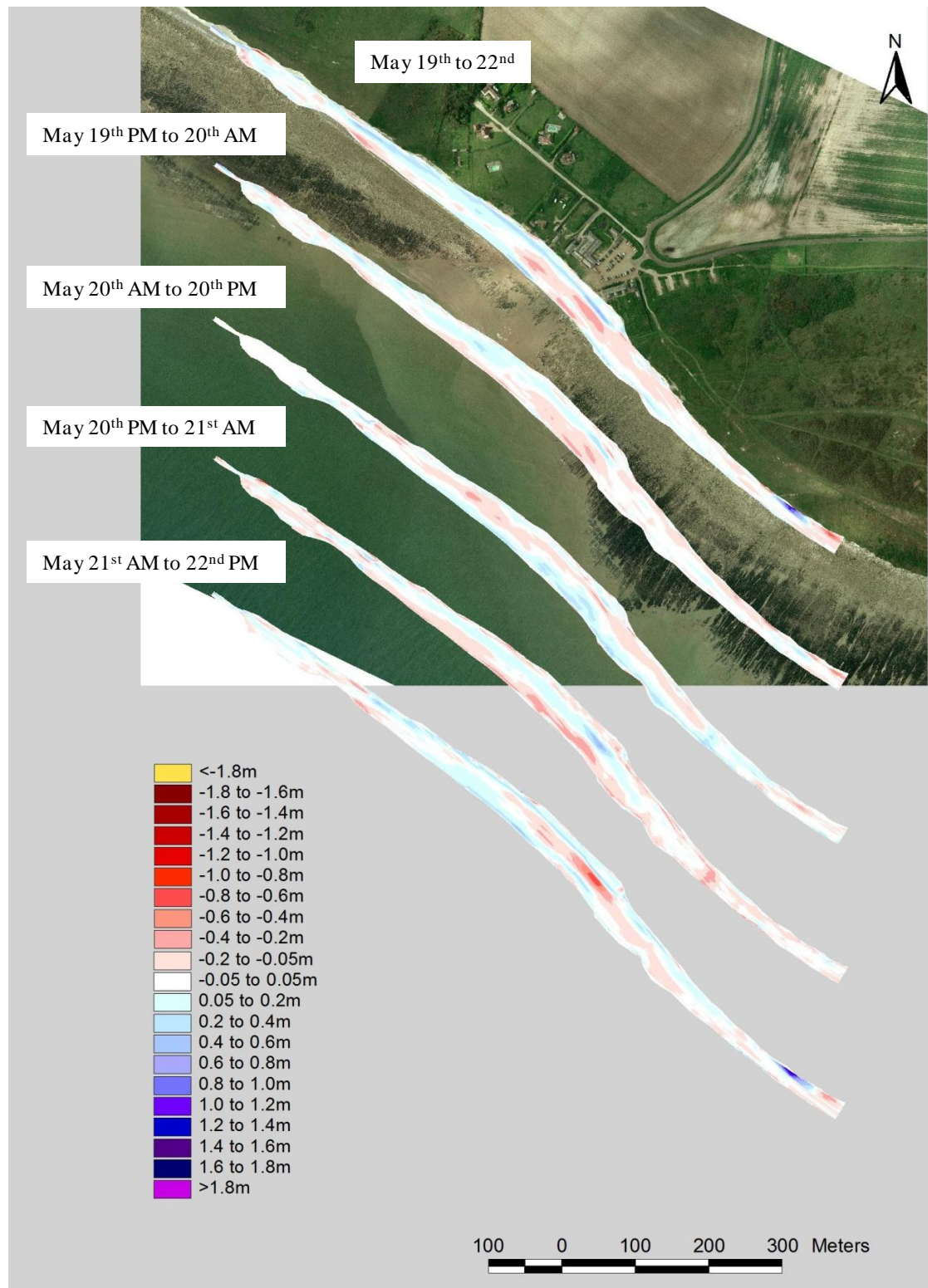


Figure 6-30 Changes in beach elevation between May 19th and May 22nd 2006 at Birling Gap.

The beach presented changes in elevation on average between -0.3 and +0.65 m with peaks in erosion and accretion at -0.7 and +1.4 m respectively in the far eastern end of the survey area where the cavities in the chalk cliffs are found.

6.6.4 DGPS surveys: beach volume changes

Beach volume changes were derived from the digital elevation changes maps. Figure 6-31 displays the net volume change measured per cell between two consecutive surveys between May 19th and May 22nd. It can be seen that on average during the survey period, the maximum volume changes are located in an area starting approximately 170 m (cell 11) west of the injection point and finishing approximately 125 m (cell 31) east from the access steps.

When considering the beach volumes changes from one tide to the following, on May 20th (morning tide), the western part of the beach revealed accretion of +454.6 m³, whereas the eastern part display erosion of -360.1 m³; the transition between these two areas being approximately 75m west of the access steps. Considering the wave conditions ($H_{s\ max}=2.1$ m and waves coming from the South-East) and tracer pebbles' scattering, it seems very likely that the volumes eroded on the eastern part contributed to the growth of the beach observed on the western part.

Between the two tides on May 20th, the western part of the beach identified just earlier sees very little changes of volumes being very close to zero. On the other hand, the eastern part of the beach experienced accretion of up to +770.1 m³. During this survey period the waves were coming from the South-West (approximately N233° with $H_{s\ max}=2.61$ m) meaning that sediment transport should be from the western end to the eastern end of the beach. Therefore, some sediment from further west than the surveyed area was transported to the beach probably compensating any loss of sediment on the western end that fed the growth of the eastern side of the beach; or possibly even contributing to the growth of the eastern part of the beach.

Between May 20th and May 21st, the beach volumes show consistent but low erosion in each cell with a total erosion of -706.1 m³. It is most likely here that sediment was driven towards the area further downdrift, beyond the surveyed area and this deficit in sediment is to be linked to sediment sources that were insufficient to compensate the

LST. During the high tide corresponding to these two surveys, the waves were coming from South-West and the $H_{st, max}$ was measured at 1.7 m.

The volume changes between May 21st and May 22nd reveal more variations. It is necessary not to forget that these changes cover two high tides during which the waves were coming from South-West, nearly perpendicular to the coast and the $H_{st, max}$ was between 1.1 and 2.5 m. On average the beach experienced accretion here, the net volume change over that day measured at +1065.6 m³. Erosion is limited on this survey, the main erosion being observed close to the access steps over an approximately 100 m long section of beach (-178.1m³) (Figure 6-31). The other beach sections represent in total only -79.6 m³ erosion.

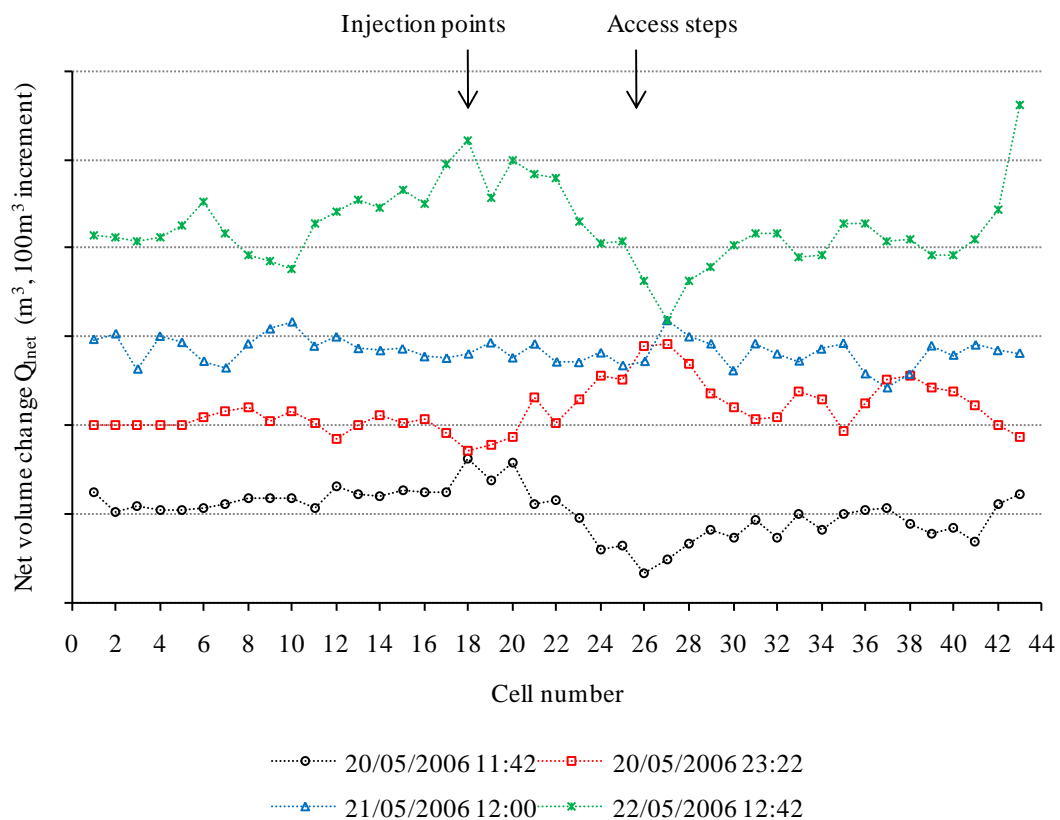


Figure 6-31 Net volume change ($Q_{l, net}$) measured for each cell between two consecutive surveys at Birling Gap in May 2006. The legend gives the date and time of the later of the two surveys. An increment of 100 m³ is used between the results obtained from each digital map. The dashed black lines represent equilibrium between erosion and accretion (0 m³ net volume change) for the associated survey line.

The volume data derived from the DGPS surveys in May 2006 constitute the perfect example of what was aimed for in the earlier results by dividing the survey area into

cells to analyse the sediment alongshore transfers. It was very unfortunate that up until now the precision of the survey was such that no clear pattern could be identified.

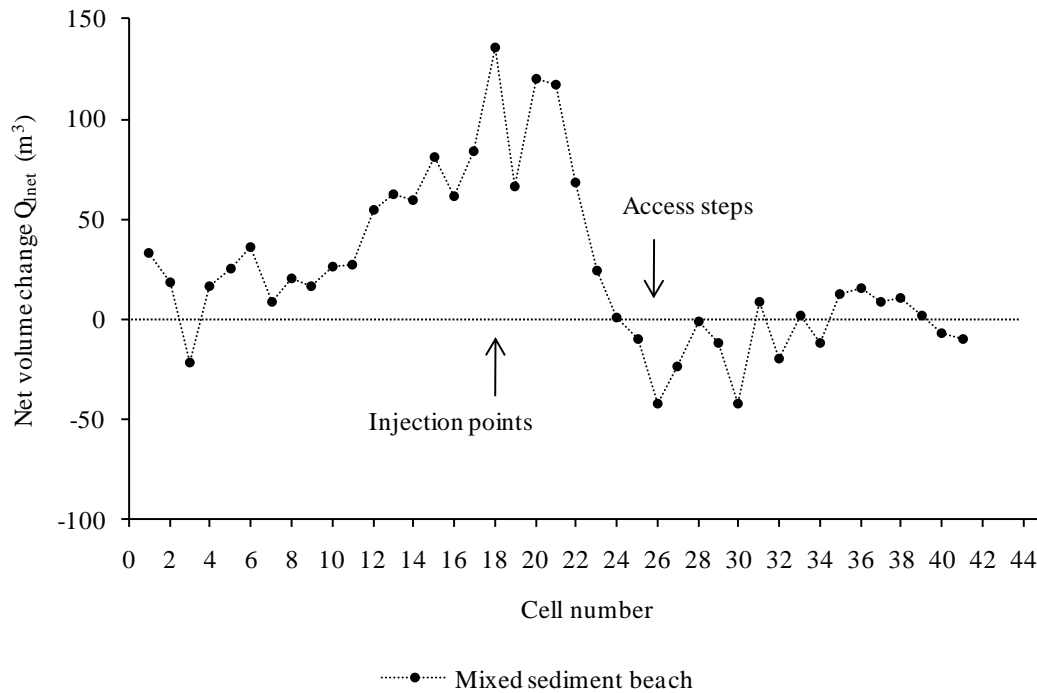


Figure 6-32 Net volume changes measured in each cell during the time period of the survey, between May 19th and May 22nd 2006 at Birling Gap.

Results for the overall volume changes per cell at Birling Gap between May 19th and May 22nd are presented on Figure 6-32. Accretion is clearly characterising the area from the western end of the beach to the access steps with a net volume change of +1146 m^3 . In contrast the surveyed area from the access steps to the most downdrift directions are characterised on average by slight erosion with a volume change of -117.3 m^3 . The overall sediment budget during this period was +1028.8 m^3 .

6.7 Field measurement experiments, Birling Gap, December 2006

6.7.1 Tracer recovery and distribution patterns

During this survey period, as mentioned just earlier, the wave condition went from moderate to calm. Waves were on average coming from the South-West (approximately N232°) with an mean angle of approach to the coast varying from 52 to 142°. The Significant wave periods varied between 3 and 7.4 s during this field experiment and the tidal level varied from a neap tide on December 14th 2006 toward a spring tide (Chapter 4 Section 4.3.2).

When considering the recovery rates on each day of deployment (Table 6-13), it can be seen that very low recovery rates were experienced after one tide on December 16th (27%) and were also low at the end of the short field experiment (58.4%). The recovery rates for the other days of deployments were largely above this expected recovery rate even after only one tide deployment.

A large number of tracer pebbles deployed were recovered at their injection point on the following tide (Table 6-13). This indicates that the forcing hydrodynamics delivered just enough energy to affect a thin surface layer of the beach face during this survey period. The upper part of the mixed beach was only affected by clear transport on the deployment of December 14th when the combined effect of both wave height and water level were sufficient to entrain into motion sediment particles of the pebble size. Despite an increasing water level from December 15th and onwards, the forcing hydrodynamics were not able to remobilise the tracer pebbles located on the upper mixed beach, especially when H_s fell below 1m. The lower parts of the beach profile were the most affected by transport as less tracer pebbles were extracted after one tide from the lowest deployment points.

Date of deployment (max depth of deployment)	Location of the injection	Recovery rates (Total of pebble recovered)					Overall total	Depth of recovery/ number of pebbles
		After one tide	Total after one tide	After three tides	Total after three tides	At the end of the experiments		
14/12/2006 (30cm)	Upper beach	71.9% (59) retrieved 18	78.4 %	74.4 % (61)	82.7 %	76.8% (63)	86.2%	Surface/121 0-10cm/58 10-20cm/3
	Middle beach	88% (44) retrieved 50		90% 45		92% (46)		
	Lower beach	79% (79)		86% (86)		91% (91)		
16/12/2006 (20cm)	Upper beach	NA/retrieved 50	27%	NA	52.8 %	NA	58.4%	Surface/9 0-10cm/9 10-20cm/5 20-30cm/1
	Middle beach	23.1% (9) retrieved 11		38.5 % (15)		43.6% (17)		
	Lower beach	30% (15)		64% (32)		70% (35)		
17/12/2006 (20cm)	Upper beach	NA/retrieved 75	65.4 %	NA	72.7 %	NA	74.5%	Surface/12 0-10cm/24
	Middle beach	100% (5) retrieved 70		100% (5)		100% (5)		
	Lower beach	62% (31) retrieved 25		70% (35)		72% (36)		
18/12/2006 (20cm)	Upper beach	NA/retrieved 75	90.3 %	NA	94.4 %	NA	94.4%	Surface/35 0-10cm/24 10-20cm/6
	Middle beach	72.7% (16) retrieved 53		86.4 % (19)		86.4% (19)		
	Lower beach	98% (49) retrieved 25		98% (49)		98% (49)		

Table 6-13 Recovery rates and depth of recovery of the tracers during the survey period in December 2006 at Birling Gap. The figures in brackets correspond to the cumulative number of tracer pebbles recovered in total.

During this survey period, the furthest distance travelled by a tracer pebble injected on December 14th was 23.6 m after only one tide. This was also the furthest distance travelled by the end of the survey period for the pebbles injected on that date. The

average alongshore distance travelled after one tide by the pebbles deployed on that day was 6.5 m in an eastward direction (Table 6-14 & Figure 6-33).

On the deployment of December 16th, the furthest pebble found after one tide travelled a total distance of 20.3 m. Here again, this distance is also the furthest distance travelled by a tracer for the whole survey period that was injected on December 16th. Despite this relatively important distance for the furthest pebble recovered, the average movements of the pebbles after one tide is very low with an alongshore and an across-shore transposition of only -0.9 m and 4 m respectively (Table 6-14 & Figure 6-34). The average transport during this tide was therefore slightly westward and upward on the beach face.

On the deployment of December 17th, the furthest distance travelled by a tracer pebble after one tide was 11.2 m away from its injection point. The furthest distance travelled by the pebble deployed on that day for the entire survey period was up to 15.3 m. Here again, when looking at the average distance travelled by the tracers after one tide, it can be observed that the alongshore movements are very small and oriented West, measured at 0.8 m, while their across-shore component is again greater, being measured up to -6.4 m from the middle injection point (Table 6-14 & Figure 6-35).

Again, the tracers' movement on December 18th are very limited in space. The maximum distance travelled by a pebble after one tide was 6.3 m from its injection point. Again this was also the furthest distance observed for the pebbles deployed on that day for the whole survey period. The average longshore distance travelled is very low again, 0 m, and the across-shore travelled distance is approximately -5.8 m down the beach from the middle injection point (Table 6-14 & Figure 6-36).

During this survey period, the three deployments were affected by movements simultaneously only on the deployment of the 14th (Table 6-14 & Figure 6-33). The comparison of the average distance travelled by the respective tracers of each injection displays again a pattern observed in all the experiments proceeded before. The pebble located at the top of the beach travel the furthest alongshore distances, 9.3m against 7.9 m for those deployed in the middle of the beach, and are affected by movements across-shore down the beach (-4 m). On the contrary, pebbles located on the lower part

of the mixed sediment beach travel the less and are affected by movement up the beach face, in this case up to 5 m.

On the following days, only the surface of the two lowest injection points was removed by the hydrodynamics and as it was suggested by the average distances travelled by the pebbles just before (Table 6-14), after one tide the tracers deployed at individual injection points were affected by greater across-shore than alongshore movements except for the December 17th on the middle injection point (2.3 m alongshore and 0.8 m across-shore).

One of the most interesting features is that on the deployments of December 16th and 18th, the lower and middle injection point tracers' scattering show average alongshore dispersion in opposite directions. Indeed, on December 16th the tracers deployed on the middle of the mixed sediment beach show an average alongshore movement in a western direction of up to -3.8 m whereas the pebbles from the lower injection show an average movement eastward of 0.7 m. On December 18th, the middle injection tracers dispersed in an eastern direction by 0.8m whereas those from the lower injection moved in a western direction by -0.4 m.

Date of deployment	Location of the injection on the mixed sediment beach	Mean distance travelled After one tide (m)	Overall mean distance travelled After one tide (m)	Mean angle of the transport measured after one tide (referred to the magnetic North, in °)	Overall mean angle of the transport measured after one tide (referred to the magnetic North, in °)	Mean alongshore distance travelled after one tide (m)	Overall mean alongshore distance travelled after one tide (m)	Mean across-shore distance travelled after one tide (m)	Overall mean across-shore distance travelled after one tide (m)
14/12/2006	Upper beach	10.1	6.5	148.5	124.7	9.3	6.5	-4.0	0.0
	Middle beach	8.4		104.4		7.9		3.0	
	Lower beach	6.1		70.2		3.5		5.0	
16/12/2006	Upper beach		4.1		22.2		-0.9		4.0
	Middle beach	5.4		350.6		-3.8		3.9	
	Lower beach	14.1		37.9		0.7		14.1	
17/12/2006	Upper beach		6.4		208.3		0.8		-6.4
	Middle beach	2.4		106.2		2.3		0.8	
	Lower beach	2.5		44.5		0.4		2.4	
18/12/2006	Upper beach		5.8		215.0		0.0		-5.8
	Middle beach	1.4		182.3		0.8		-1.2	
	Lower beach	2.8		27.7		-0.4		2.7	

Table 6-14 Characteristics of the sediment transport measured using the tracer pebbles after one tide of deployment at Birling Gap in December 2006. Negative values of the alongshore travelled distance indicate that the pebbles moved in a westward direction; positive values indicate alongshore movements in an eastward direction. Negative values of the across-shore travelled distance indicate that the pebbles moved down the beach and positive values indicate that these movements are up the beach.

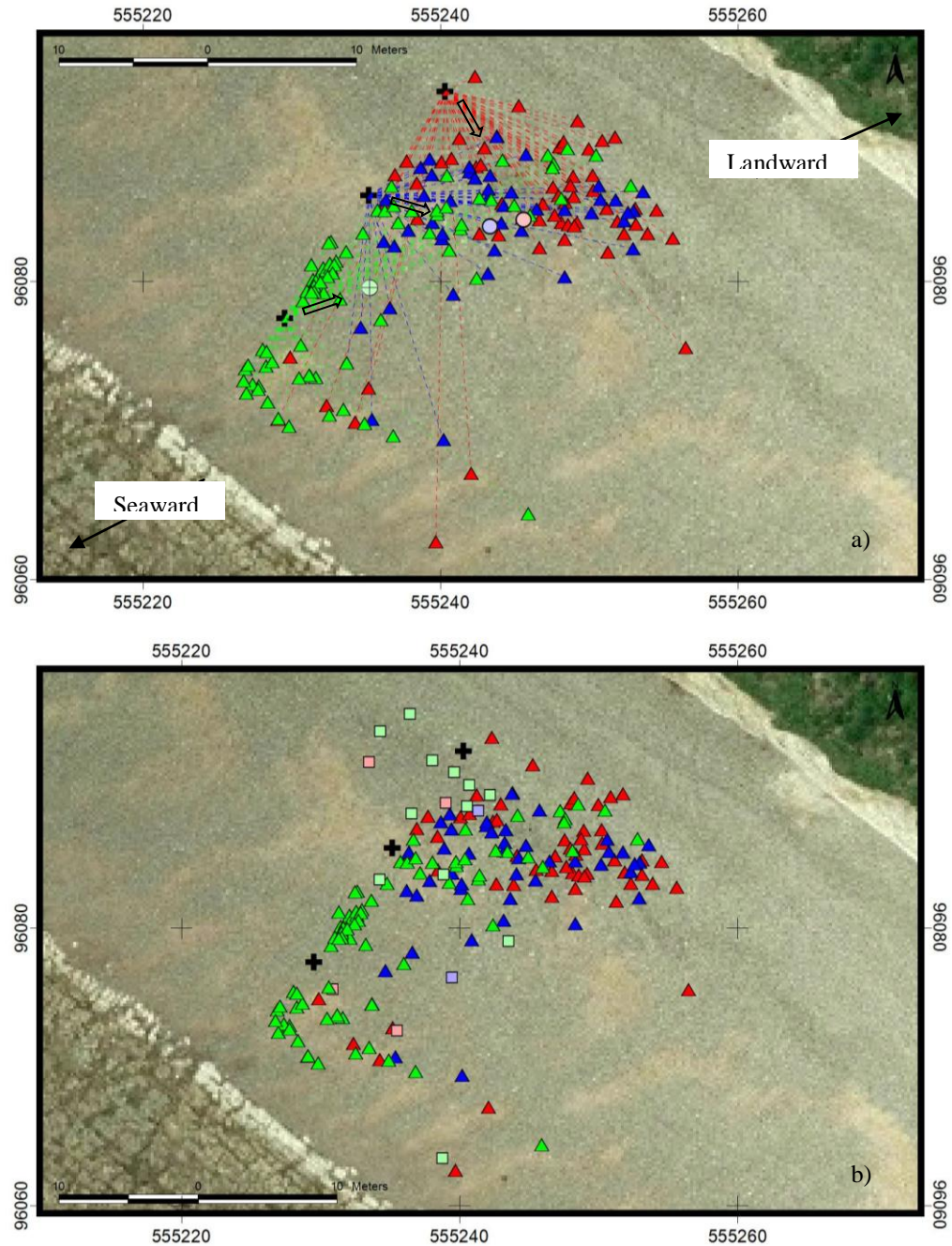


Figure 6-33 Movement of tracer pebbles deployed on December 14th, 2006.

a) Scattering observed after one tide. Arrows indicate the mean orientation of the pebbles movement.

b) Scattering observed over the whole survey period.

The Black cross marks the locations of the injection points. Each triangle represents individual tracer pebbles recovered after one tide while the squares represent individual tracer pebbles recovered after more than one tide. The disks mark the location of the centroids. Pebbles are colour coded: red = upper injection point, blue = middle injection point, green = lower injection point.

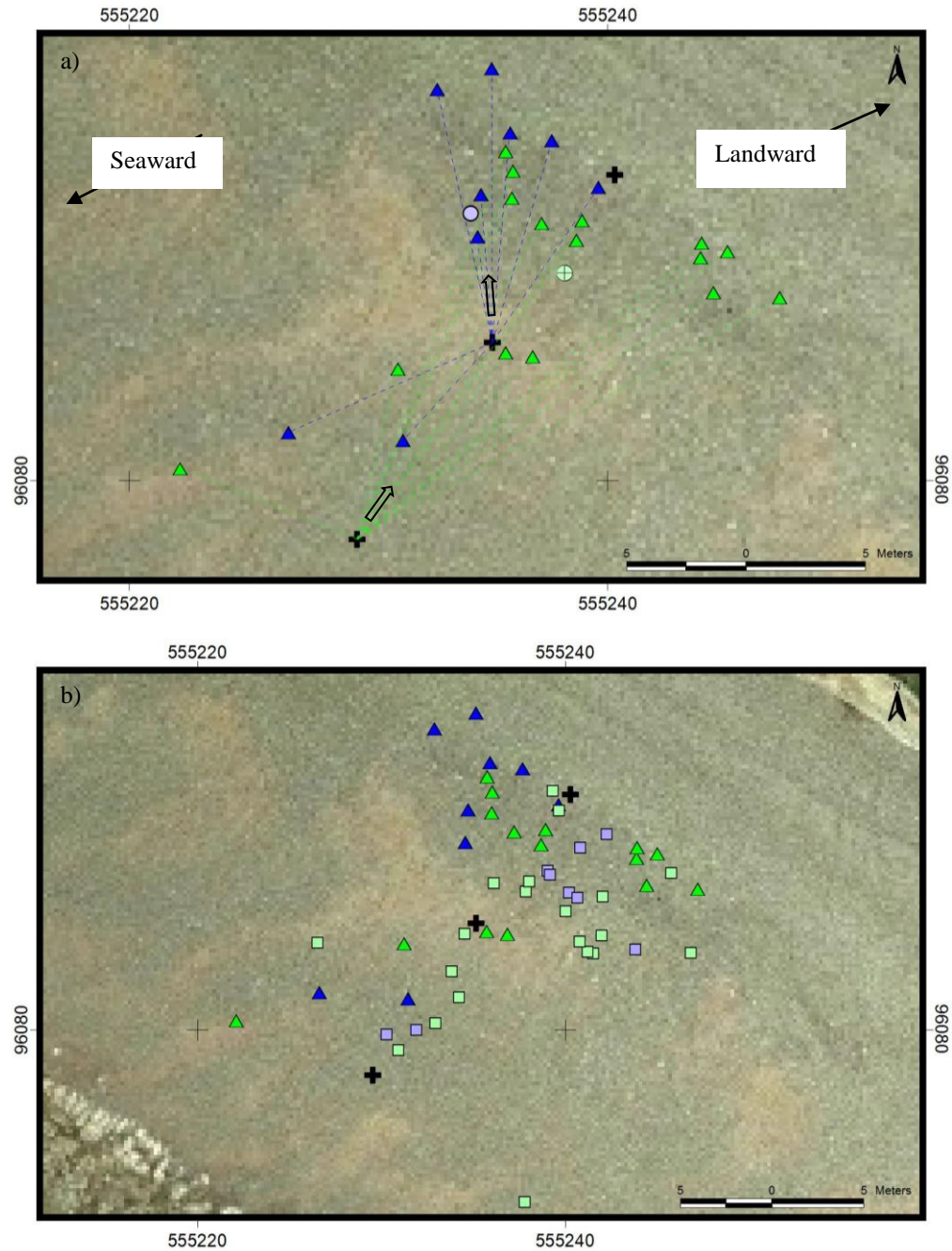


Figure 6-34 Movement of tracer pebbles deployed on December 16th, 2006.

a) Scattering observed after one tide. Arrows indicate the mean orientation of the pebbles movement.

b) Scattering observed over the whole survey period.

The Black cross marks the locations of the injection points. Each triangle represents individual tracer pebbles recovered after one tide while the squares represent individual tracer pebbles recovered after more than one tide. The disks mark the location of the centroids. Pebbles are colour coded: red = upper injection point, blue = middle injection point, green = lower injection point.

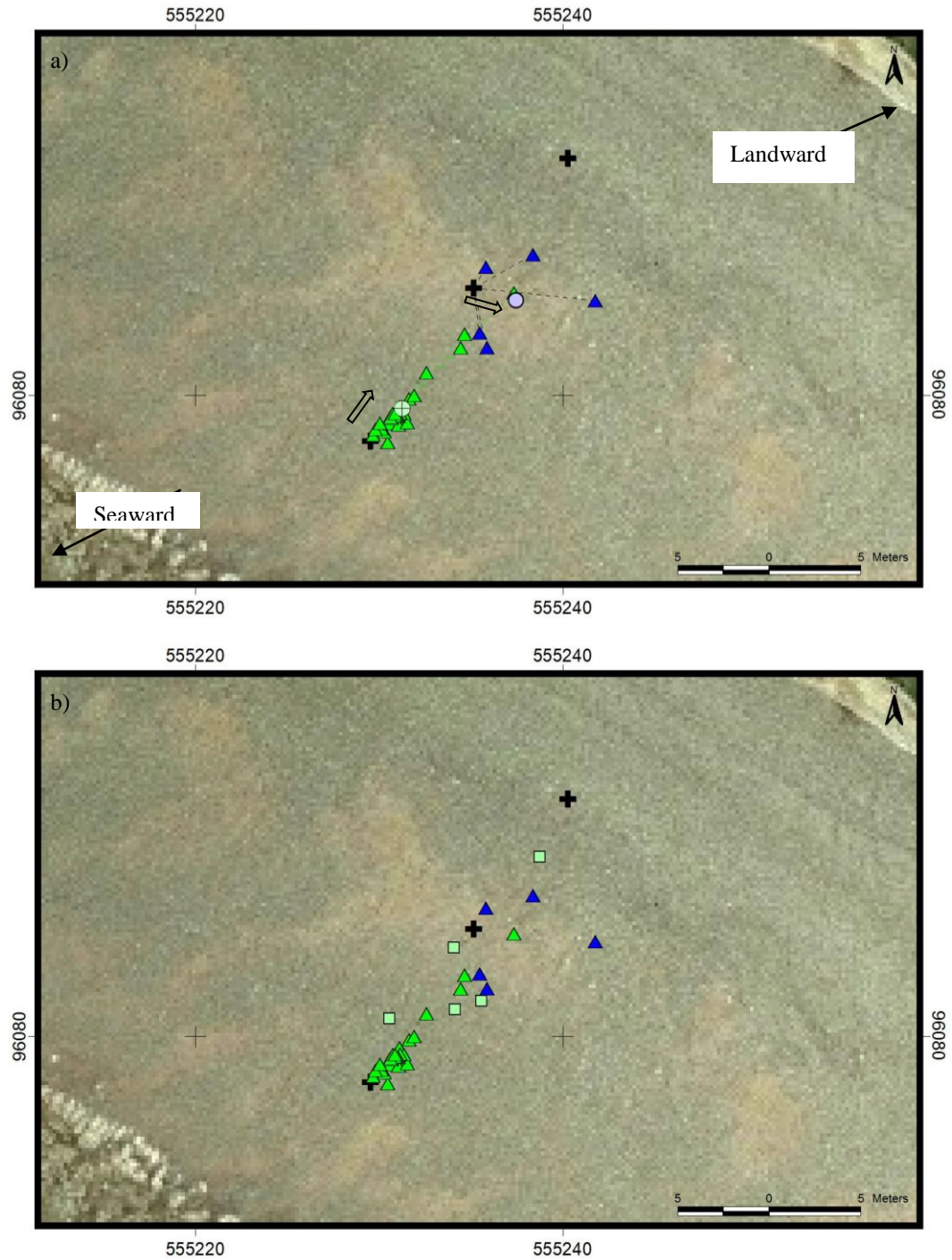


Figure 6-35 Movement of tracer pebbles deployed on December 17th, 2006.

a) Scattering observed after one tide. Arrows indicate the mean orientation of the pebbles movement.

b) Scattering observed over the whole survey period.

The Black cross marks the locations of the injection points. Each triangle represents individual tracer pebbles recovered after one tide while the squares represent individual tracer pebbles recovered after more than one tide. The disks mark the location of the centroids. Pebbles are colour coded: red = upper injection point, blue = middle injection point, green = lower injection point.

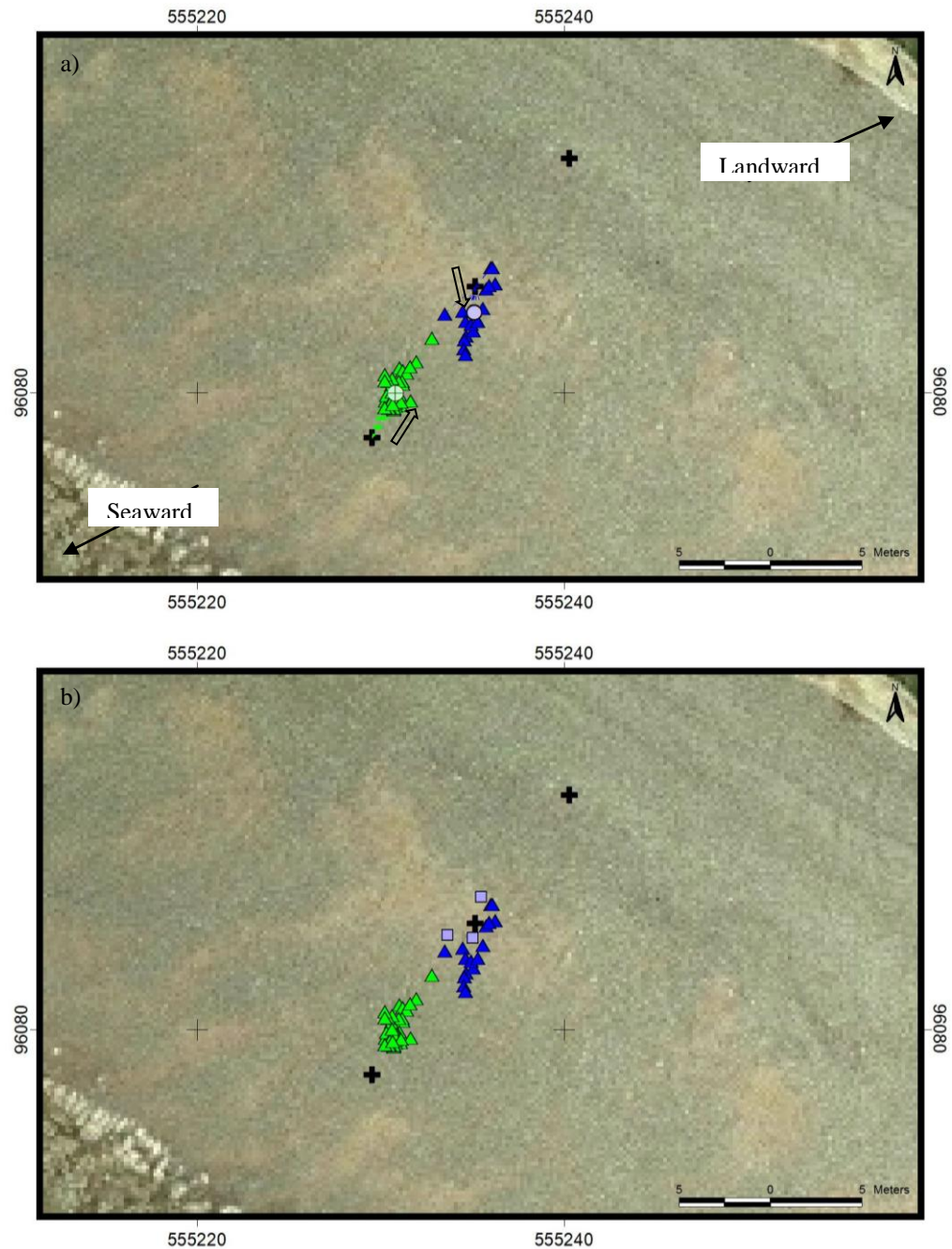


Figure 6-36 Movement of tracer pebbles deployed on December 18th, 2006.

a) Scattering observed after one tide. Arrows indicate the mean orientation of the pebbles movement.

b) Scattering observed over the whole survey period.

The Black cross marks the locations of the injection points. Each triangle represents individual tracer pebbles recovered after one tide while the squares represent individual tracer pebbles recovered after more than one tide. The disks mark the location of the centroids. Pebbles are colour coded: red = upper injection point, blue = middle injection point, green = lower injection point.

6.7.2 Derivation of the volume transported and the LST rates using tracer pebbles

In a similar way as before for the previous survey periods, rates of LST were determined using the measurements of the depth of disturbance or the depth of the deepest tracer pebble found (Table 6-15). On a general note, the volumes derived by the tracer are overestimating those derived from the depth of disturbance data. These differences can reach up to 60.2%. Note that no LST rate was recorded on December 18th because of the zero alongshore distance travelled by the tracer pebbles.

6.7.3 DGPS surveys: digital elevation model and beach elevation changes

Elevation changes on a tidal basis during this survey period varied on average from -0.4 to +0.4 m with localised peaks of up to -0.9 and +0.9 m (Figure 6-37). The three first elevation maps seem to describe more changes than those of the following days; however there is no clear pattern of evolution in contrast to the previous survey periods. This is most likely to be related to the wave conditions that changed from agitated to calm.

The observation of the elevation changes over the whole survey period, i.e. between December 14th and December 19th, displays erosion on the lower parts of the beach whereas accretion marks the upper parts of the beach along a thin stripe. This stripe most likely corresponds to the HWL berm that built up during the transition from a neap towards a spring tide. The elevation changes during the whole survey period showed variation on average within erosion movements of -0.6 m and accretion movements of 0.8 m with very localised peaks measured at -0.8 and 1.15 m respectively.

Date of deployment	Alongshore distance travelled after one tide	Area of the beach material removed	LST rate (m ³ tide ⁻¹) Based on active layer measurements	Maximum depth of tracer pebbles recovered	Average length of the beach	LST rate (m ³ tide ⁻¹)	Difference between the LST rates (m ³ tide ⁻¹)	Percentage of difference between the LST rates (%)
14/12/06	6.5	5.1	33.0	0.20	34.2	44.5	11.5	25.9
16/12/06	-0.9	3.3	-3.0	0.25	33.6	-7.6	-4.6	60.2
17/12/06	0.8	2.4	1.9	0.10	26.4	2.1	0.2	9.1
18/12/06	0.0	2.2	0	0.15	17.7	0	0	0

Table 6-15 Calculation of the LST rates observed using tracer pebbles dispersion on mixed sediment beach at Birling Gap in December 2006. Note that it was preferred to keep the conventional sign code used earlier to describe the mean alongshore directions of transport when deriving the LST rates so that the direction of the transport is still shown.



Dec 14th to Dec 19th

Dec 14th PM to Dec 15th PM

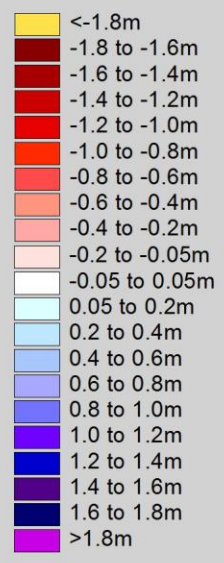
Dec 15th PM to Dec 16th AM

Dec 16th AM to Dec 16th PM

Dec 16th PM to Dec 17th AM

Dec 17th AM to Dec 17th PM

Dec 17th PM to Dec 18th AM



Dec 18th AM to Dec 18th PM

Dec 18th PM to Dec 19th AM

Dec 19th AM to Dec 19th PM

Figure 6-37 Changes in beach elevation between December 14th and December 19th 2006 at Birling Gap.

6.7.4 DGPS surveys: beach volume changes

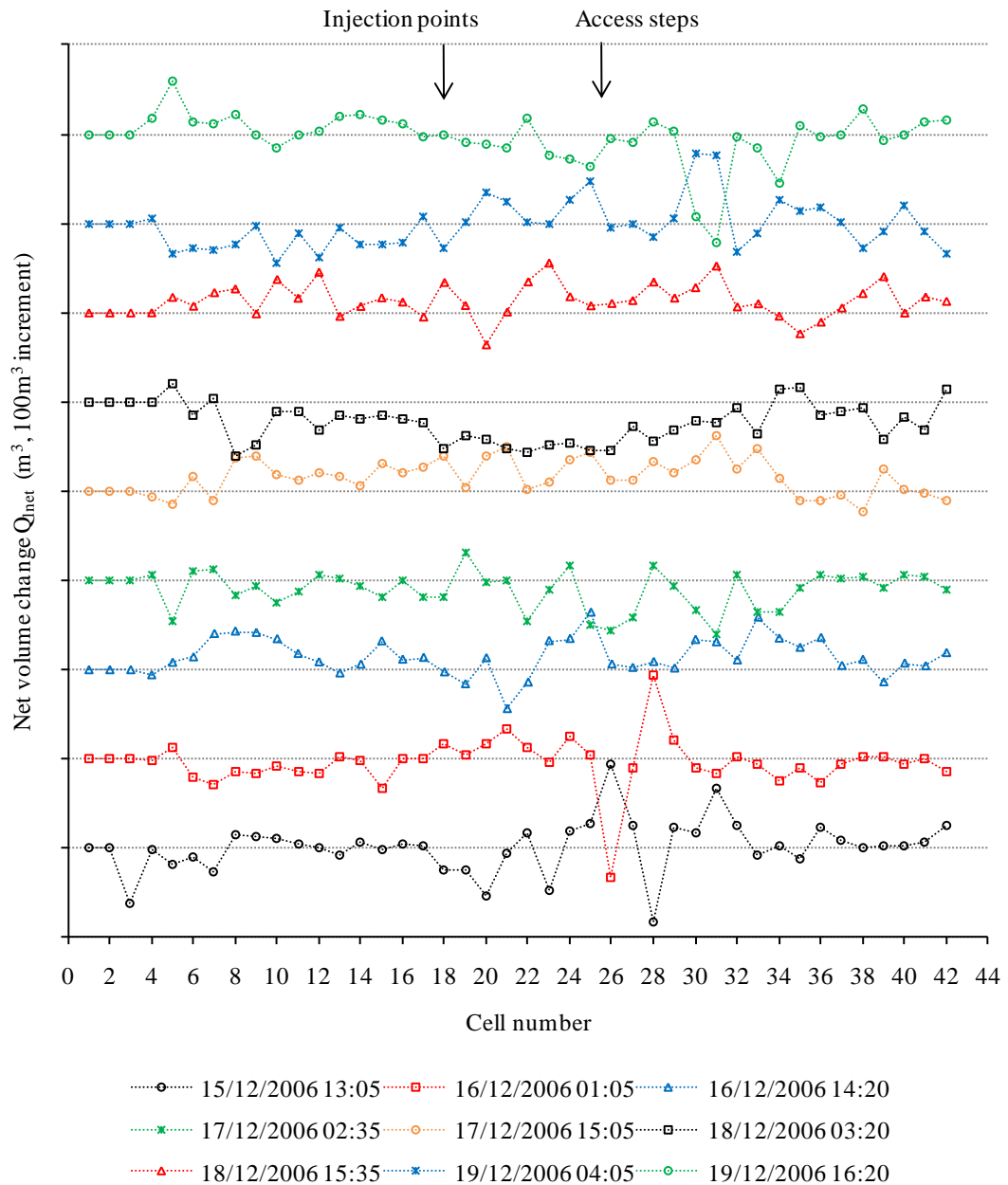


Figure 6-38 Net volume change ($Q_{l\ net}$) measured for each cell between two consecutive surveys at Birling Gap in December 2006. The legend gives the date and time of the later of the two surveys. An increment of $100\ m^3$ is used between the results obtained from each digital map. The dashed black lines represent equilibrium between erosion and accretion ($0\ m^3$ net volume change) for the associated survey line.

Figure 6-38 presents the beach net volume changes per cell between two consecutive surveys. Between the survey on December 14th and December 15th, it can be seen that

the majority of the volumes changes happened between the location of the tracer injection points and 200 m downdrift of the access steps (approximately cell 33). This area is affected by approximately equal accretion and erosion movements that counterbalance each other. Considering the average sediment transport observed using the tracer pebbles dispersion, it can be deduced that the erosion observed in cells 18 to 23 (-134.7 m^3 in total, note that cell 22 shows a slight accretion) contributes to the accretion observed directly downdrift on cells 24 to 27 ($+167.8 \text{ m}^3$). Similarly the erosion observed on cell 28 (-83.3 m^3) contributes partly to the accretion observed on cells 29 to 32 ($+134.1 \text{ m}^3$). The total volume change of the beach for this epoch showed a small accretion of $+95.4 \text{ m}^3$.

On the following survey, on the morning of December 16th, the general erosion observed from cell 6 to 16 (-145.3 m^3) most certainly is at the origin of the accretion just downdrift measured at $+116.83 \text{ m}^3$. It is the same for the two peaks of erosion and accretion observed between cell 25 and 30 which were respectively measured at -142.5 and $+116.3 \text{ m}^3$. The total volume changes on this survey is measured at -153.1 m^3 most of which is covered by the general erosion located from cell 30 to further downdrift areas (erosion measured at -109.2 m^3).

On the afternoon of December 16th, most of the beach displays a volume increase of $+608.2 \text{ m}^3$. On the contrary, the survey on the morning of December 17th displays general erosion of -433.4 m^3 . This alternation between tidal surveys presenting general addition or loss of beach material carries on until December 18th evening. The respective beach volume changes for each survey were as follow: December 17th afternoon, 658.9 m^3 ; December 18th morning, -851.2 m^3 ; and, December 18th evening, $+478.7 \text{ m}^3$. These greater oscillating volume changes are rather suspicious because the wave conditions went from agitated to calm during this period and therefore less transport was expected. Moreover, the tracer pebbles experiment proved that the beach material was more affected by across-shore movements than alongshore. This period of the survey was affected by the presence of gentle cusping forms. These features will have influenced the beach volume changes calculated. The two last surveys on December 19th showed overall erosion of -148.4 m^3 and -72.3 m^3 .

Beach volume changes over the whole survey period between December 14th and December 19th per cell are presented on Figure 6-39. Erosion and accretion oscillate

along the beach within a range going from -130 to $+103 \text{ m}^3$ depending on the cell. It appears that the area located from the injection points to approximately 175-200 m eastward of the access steps is affected by the greatest volume changes in comparison to the rest of the beach. From the location of the injection points down to cell 23, the erosion was up to -180.7 m^3 whereas the accretion measured just downdrift of this area was $+159.3 \text{ m}^3$. The second erosion movement observed in cells 26 and 27 represent a total volume of -163.5 m^3 whereas the accretion movement just downdrift again represents a sediment volume of $+220.5 \text{ m}^3$. Considering the direction and amplitude of the sediment transport observed using the tracer pebbles, it is most likely that the sediment eroded from the cells 18 to 23 fed the supply of cells 24 and 25, most possibly fed partly further downdrift areas (cells 26 and 27 for example). In a similar way, cells 26 and 27 fed the supply of cells 28 to 33. The overall beach volume change during the survey period was measured at $+182.9 \text{ m}^3$.

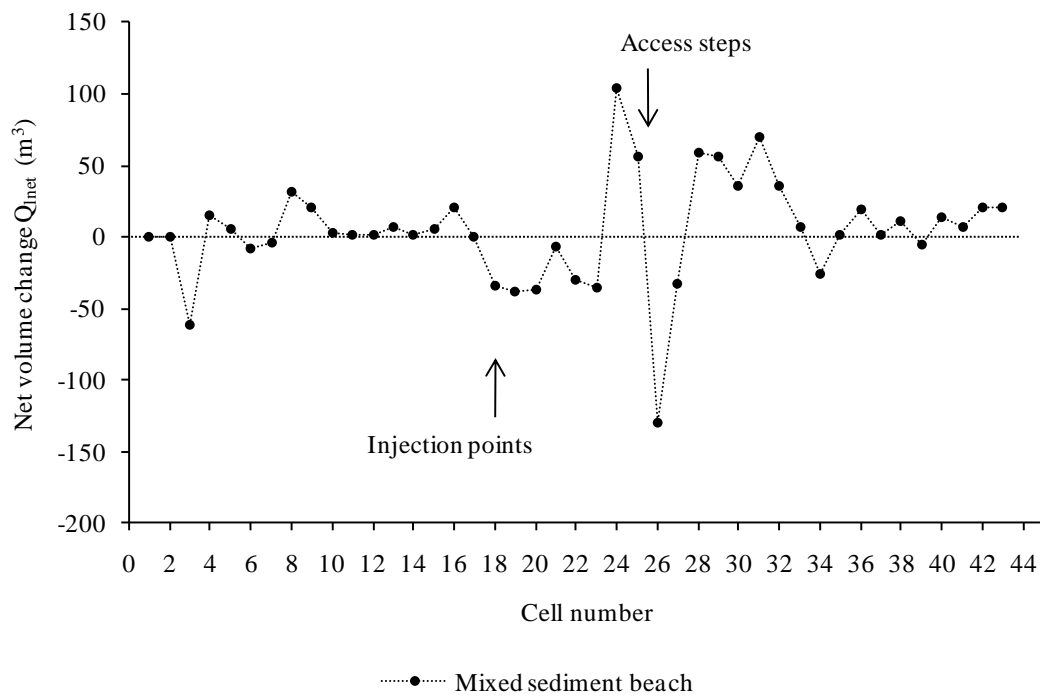


Figure 6-39 Net volume changes measured in each cell during the time period of the survey, between December 14th and December 19th 2006 at Birling Gap.

6.8 Field measurement experiments, Birling Gap, October 2004 to May 2005: quartzite pebble tracing experiment.

As explained in Chapter 3, the first experiment to measure the LST over long time periods used quartzite cobbles. The results are presented on Figure 6-40.

This experiment was the first attempt of this study to measure LST and at the time the wave conditions were measured offshore by the buoy located at Rustington (Figure 6-41; Chapter 3 Section 3.3).

The recovery rate for the tracing experiment varied from 2.3 to 9.6% depending on the time of the survey. Because of these very low recovery rates of the cobbles and the fact that recovery was only made at the surface of the beach, the results of the experiments had to be carefully considered.

The first results (October 2004) recorded a westward drift reaching up to 101.7 m from the deployment area and only one tracer was recovered on an eastern direction to the deployment area. Considering the general direction of the LST on the East Sussex coast, this first observation was a little surprising. A brief examination of the wave conditions collected between the date of deployment and the first visit on the beach showed that from October 7th to October 12th, waves were coming from the South and South-East with wave heights ranging from 0.34 to 1.85 m and wave peak periods comprised between 2 and 8.1 s (Figure 6-41). In contrast, from October 12th to October 16th, waves were coming from the South-West with higher significant wave heights ranging from 0.46 to 2.85 m. The wave peak periods were between 2.8 and 12.5 s (Figure 6-41). Therefore, given that almost all of the tracers recovered were east of their deployment area, it appears that the South-easterly waves, despite being less energetic than the South-westerly waves, had a bigger impact on the sediment transport at Birling Gap. This observation can be directly related to previous observations made about the monthly beach volume changes observed during the two year survey period in Chapter 4 Section 4.4.5. It was observed that during the summer the beach was affected by greater loss of sediment than during the winter conditions.

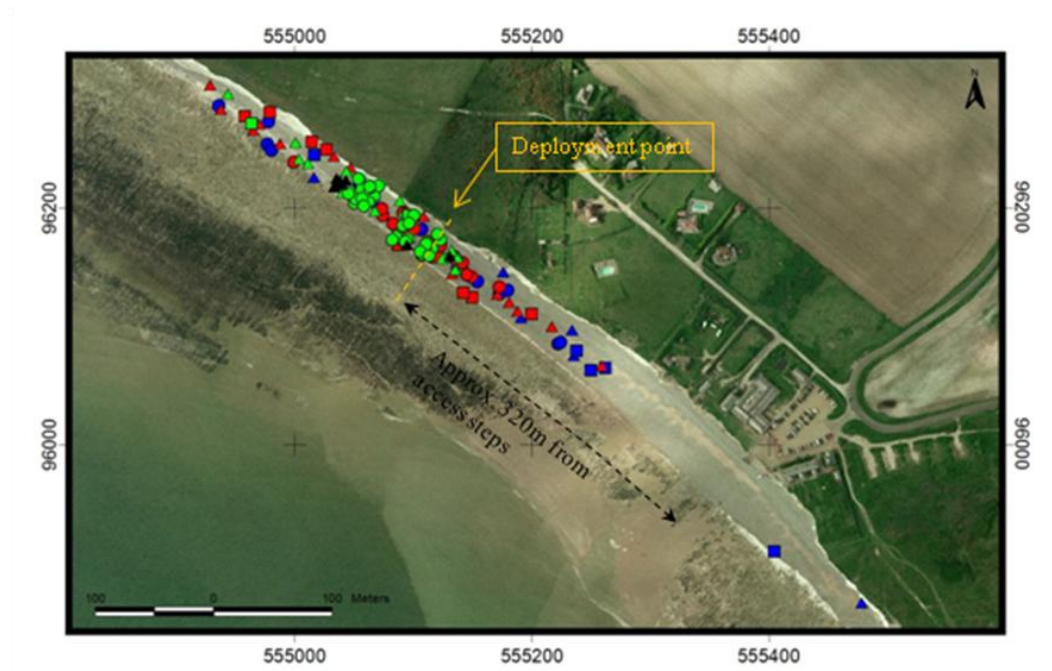


Figure 6-40 Location of each tracer recovered over the survey period from October 2004 to May 2005.

	Date of visit to the beach	Furthest distance reached by a cobble recovered on the western side of its injection point (number of pebbles found on the western side)	Furthest distance reached by a cobble recovered on the eastern side of its injection point (number of pebbles found on the eastern side)	Recovery rate (number of cobbles)
	07/10/2004			100% (300)
▲	16/10/2004	101.7m (6)	14.7m (1)	2.3% (7)
●	20/10/2004	83.8m (26)	2.1m (3)	9.6% (29)
■	22/11/2004	187.1m (4)	(0)	1.3% (4)
▲	30/11/2004	147.1m (8)	27.1m (7)	5% (15)
●	06/12/2004	55.3m (7)	64.2m (7)	4.6% (14)
■	09/01/2005	195.3m (7)	100m (5)	4.3% (13)
▲	17/02/2005	233.7m (10)	173.2m (9)	6.3% (19)
●	23/03/2005	219.1m (7)	131.8m (5)	4% (12)
■	22/04/2005	131m (2)	382.8m (4)	2% (6)
▲	20/05/2005	117.7m (1)	468.7m (6)	2.3% (7)

Table 6-16: Summary of the quartzite cobbles' distribution on the beach from either side of the injection profile over the survey period from October 2004 to May 2005.

During the summer, the occurrence of south-easterly waves is very scarce, whereas during the winter it is more frequent. Therefore, it is most likely that the occurrence of south-easterly waves during the winter greatly influences the sediment budget, counterbalancing all the sediment transport going in an eastward direction under the action of the south-westerly waves and keeping the beach volume relatively consistent. On the other hand, the scarcity of south-easterly waves during the summer means that the eastward drift of sediment is not counterbalanced (or less counterbalanced), inducing greater loss of beach material during the summer.

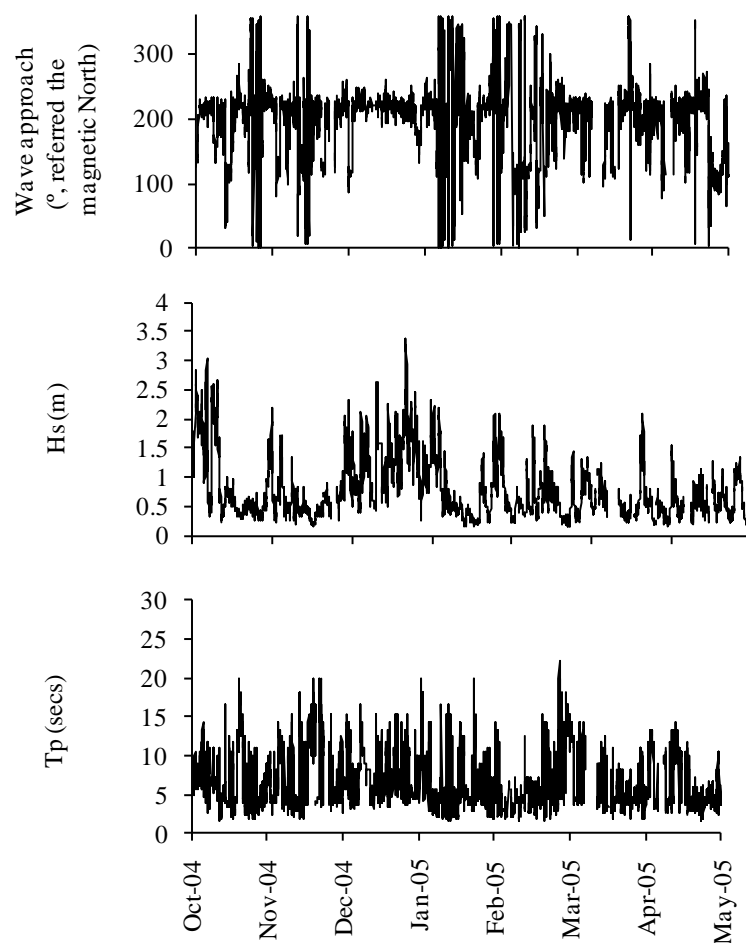


Figure 6-41 Offshore wave conditions collected at Rustington for the survey period between October 2004 and May 2005.

Further surveys conducted after October 2004 until May 2005 showed, on average, an increasing eastward drift with the greatest travelled distance recorded at 468.7 m in an eastwards direction on May 20th 2005. The number of tracers found on the east side of the deployment area increases with time too, whereas the number of tracers found west

side is relatively consistent apart from the one on October 20th when the recovery was “exceptional” (26 tracer pebbles). During the overall period, the wave height varied from 0.17 to 3.3 m and the wave peak periods ranged from 1.8 to 22.2 s. South-westerly waves were dominant whereas south-easterly waves were only sporadic for very short periods of time going from a tide up to a maximum of six days. In addition, the south-easterly waves were in great majority amongst the lowest wave heights observed during this period (in majority <1 m). Such wave conditions had very little impact on sediment transport explaining why the residual transport observed with the quartzite pebbles showed eastward movements. The south-westerly waves experienced during this period showed H_s mostly above 1.5 and up to 3.3 m.

Such technique seems perfectly reliable to observe long term sediment transport and is easily related to the environmental wave conditions; however, because of the low recovery rates experienced with such tracers, this data is not reliable enough to be used for the quantifications of an accurate LST rate.

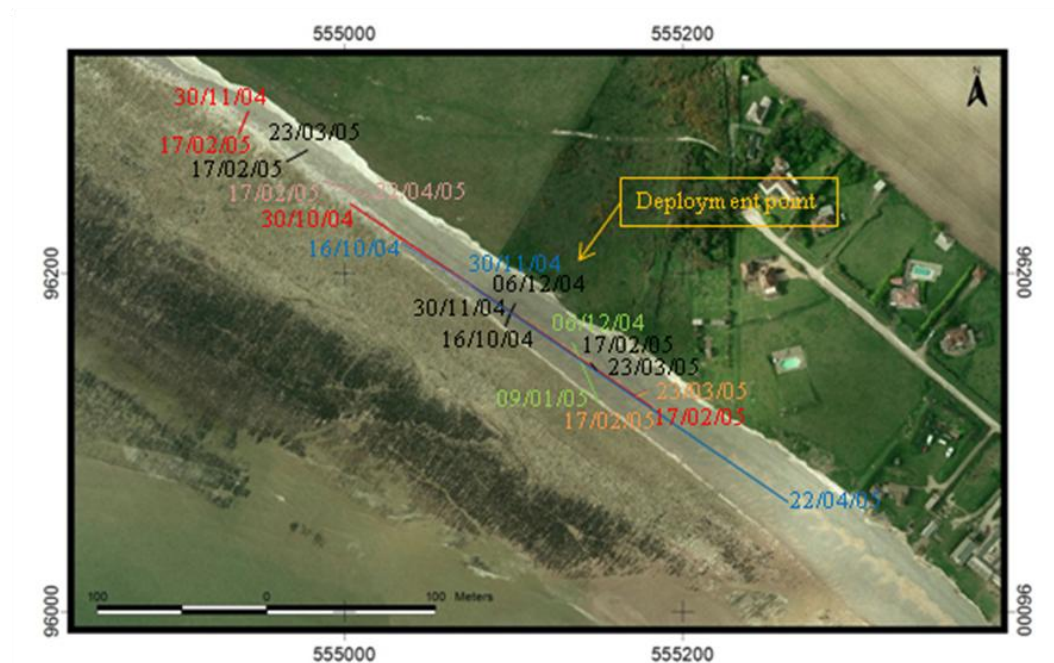


Figure 6-42 Quartzite pebble transport observed over the survey period from October 2004 to May 2005. Each coloured line and date represents the trajectory and the time of the recovery of one tracer cobble.

In October, the pebbles were marked once recovered in order to identify them again later during the experiment if recovered. A few pebbles were found twice or even three

times during the overall survey period. Figure 6-42 shows the trajectories of these pebbles. It can be seen that the longest cobble movement traced was 235.3 m, travelling from October 16th 2004 to April 22nd 2005. Generally, pebbles affected by great longshore movements were recovered after long period of time (four to six month) whereas pebbles affected mainly by an across-shore transposition were recovered within a month or two from their last recovery. Although the number of marked pebbles recovered was low, one of the common characteristics to all the movements observed is that all the pebbles re-found, affected by great longshore transport or not, showed movements in a western direction. These movements can be directly linked to the dominant south-westerly wave conditions observed during the survey period.

6.9 Yearly longshore transport between July 2003 and July 2006

The net beach volume changes were plotted earlier on the same graphic as the wave direction in Chapter 4 Section 4.4.5 Figure 4-37. Over the two year survey and including an earlier survey made in July 2003, it was possible to quantify the yearly beach volumes changes (Table 6-17). As pointed out earlier in Chapter 4, the beach at Birling gap shows an increasing erosion between July 2003 and July 2006. It appears that beach volume loss essentially happens during summer time whereas the beach volume stays relatively consistent during winter time.

	Net volume change ($\text{m}^3 \cdot \text{y}^{-1}$)
July 2003 to July 2004	7470
August 2004 to July 2005	-35329.8
August 2005 to July 2006	-48547.5

Table 6-17 Yearly net volume changes observed at Birling Gap between July 2003 and July 2006.

6.10 Discussion

6.10.1 Recovery rates and validation of the pebble tracing technique

One of the first points to discuss here is about the performance and the validation of the tracing and detection techniques. The use of a metal detector allowed the detection of tracers at depths of up to 30 to 40 cm. The high recovery rates at both sites during the experiments confirm that such a depth of detection facilitated by this technique allows successful relocation of tracer pebbles even during stormy or agitated conditions.

Despite no longshore movement occurring for a few days during the various short period field surveys (December 2004 at Cayeux-sur-Mer for example), the results for these days are extremely valuable information to judge the performances of the synthetic tracer pebbles specially designed for this study. Indeed, the tracer pebbles first used during December 2004 at Cayeux demonstrated, through the various depth of recovery up to 30 cm, that despite a subsurface deployment only one tide was necessary for the pebbles to mix at depth with indigenous beach material even during calm wave conditions. This observation supports Wright's (1982) suggestion about the quick integration of tracers in the beach material and indicated that two tides were sufficient to allow good mixing of the tracers within the beach material. Based on the results from this study, only one tide appeared to be enough. In addition to that, the distribution of depths at which tracers were found clearly shows that even under low energy wave conditions the beach material is still removed at depth. For example at Cayeux-sur-Mer when the H_s was less than 0.5 m, the mixing of the shingle occurs to a depth of 30 cm into the matrix supported subsurface layer after only one tide on December 13th 2004 PM. Bray et al. (1996) mentioned a mixing time ranging from 2 to 7 days for the tracers to be well mixed within the beach material. In order to mediate between the aim of this study and Bray's observation (1996), the deployments of the tracer pebbles during the short time surveys were done at depth and with great care to mix the tracers into a large matrix of beach material.

During the survey period October-November 2005 at Cayeux-sur-Mer, the recovery rates on the lower injection points were the lowest observed in comparison with the

other injection points on the same days. One possible explanation for the low recovery rate of pebbles injected into the lower part of the beach was movement of pebbles from the beach onto the adjacent sandy foreshore. This hypothesis is weakened given the following points:

- Nicholls and Wright (1991) stating that exchanges in pebbles between the onshore and the offshore zone are limited;
- The natural propensity of the pebbles to move onshore; and, finally,
- The numerous unsuccessful attempts of this study to detect tracers on the sandy platform or on the chalk platform even during relatively agitated periods.

Nevertheless, the shingle beach toe is an area of important topographic change induced by the change of slope and the combined effect of wave breakage and swash during each tidal cycle. As a result, the most likely explanation for the low recovery rates of pebbles placed on the lower beach is their burial within the indigenous beach material to depths below the detection limits of the metal detector.

Burial of the tracers to depths below the detection limit is probably the explanation also for the “abnormally” low recovery rate for those injected into the top of the beach on November 7th 2005. On this occasion burial most probably resulted from the change in water level between the spring and neap tides of the tidal cycle. At the time the tracers were injected, wave and tide conditions were transporting the coarser beach material up-beach to create a berm which probably trapped and buried many of the tracers below detection depths.

An overview of the recovery rates experienced at Birling Gap in March, May and December 2006 shows that they are generally a lot greater than at Cayeux after one tide. This is most likely linked to the width of the beach. Because of the very narrow beach profile at Birling Gap it was much easier and quicker than at Cayeux to conduct a complete scan of the beach on a reasonable alongshore distance to detect a maximum number of tracer pebbles. The investigation on the active layer and especially the depth of disturbance showed that the thickness of sediment moved by the hydrodynamics is lower at Birling Gap than at Cayeux, which also contributed to the higher recovery rates as the tracer pebbles were buried at lower depths than at Cayeux (Chapter 5). The presence of the solid chalk platform can also cap the burial depth of the tracers too. Indeed, as discussed in chapter 5, the presence of the underlying chalk platform can

limit the depth of disturbance. This observation is obvious on the lower part of the mixed sediment beach where only a thin layer beach material covers the platform rendering the detection very easy.

During the field experiments at Birling Gap, tracer pebbles were very often dug out from the injection points after one tide. These tracer pebbles not being remobilised by the hydrodynamic processes helped to determine the tracers' dilution into the beach material as well as to double check the depth at which the beach material was disturbed in addition to the coloured pebble columns.

The use of the quartzite pebbles at Birling Gap proved to be reliable to express the general trends of the LST. Indeed, the surface distribution patterns observed by those tracers proved to answer adequately to the changing hydrodynamics during the survey period. Moreover, a residual eastward sediment transport direction has been recorded by these pebbles (Figure 6-42) which is in accordance with the expected residual LST along the East Sussex coast. The large range of grain size, shape of the quartzite pebbles and their close density to the one of flint makes certainly them reliable to track sediment transport. However, the surface recovery method makes a more limited contribution to the understanding of sediment movement patterns. This is largely because observation of the scattering of the tracers into the beach, as well as across the surface, is not possible. The distance travelled by these tracers cannot be used to derive a reliable LST rates. The first reason is to be related to the low recovery rates; secondly, again that no indication of the tracers' dispersion deep into the beach can be deduced; and thirdly, it was very rare to find more than once the same pebble despite a seven month long survey period. Less than ten pebbles were found more than once during the all survey period. For these reasons, it is necessary to be really careful when using models that have been calibrated using exotic or painted pebbles.

6.10.2 Beach sediment dispersion patterns

(i) Cayeux-sur-Mer, October/November 2005

The tracers injected on the upper beach demonstrate a clear tendency to move seawards across-shore and move further than those injected in the mid and lower beach (Figures 6-12, 6-13 & 6-14). It is well known that on a steep coarse grained beach, the width of the swash zone may be significantly greater than that of the surf zone. It has been shown

in models and experiments (e.g. Van Wellen, 1999; Pedrozo Acuña, 2005; Austin and Masselink, 2006), that most of the morphological changes on a steep beach profile occur in the swash zone. The difference in distance travelled is a function of the greater time swash is active and is the reason why pebbles from the upper beach move furthest. Regarding the strong seaward cross-shore tendency, Van Hijum and Pilarczyk (1982) showed that the distance covered is a function of time spent in the swash. However, this does not explain why the tracers injected at the lower beach migrate landward while pebbles from the top of the beach migrate seaward.

Nielsen (1997) identified ground water dynamics in the swash zone as one of the processes that might be important for predicting net sediment transport in this area. Ground water flows are a determining factor of variations in the morphology of beaches with a high permeability (Elfrink and Baldock, 2002). These flows are even more significant when the tidal range is larger, which creates high hydraulic gradients between the water table and the water level (Turner, 1995). Because of their specific locations across the beach, the three injection points were in completely different ground water environments. The injection point on the upper beach was above the water table throughout the tidal cycle. The injection point in the middle of the beach was also above the water table at low tide but when the tide rises it was quickly saturated by water. At the bottom of the beach considerable quantities of water drained out of the sediment even at low tide.

Observation of the tracers as the tide rose over the lower site, showed that they were immediately mobilised and quickly dispersed, apparently due to seaward migration. This may result from swash flows interacting with the groundwater flow. The consequence of downward directed pressure gradients increases the effective weight of the sediment, stabilises the bed and decreases the potential of sediment to be transported during the uprush. In contrast, during the backwash the upward directed pressure gradient increases sediment transport reducing the effect of the weight of sediment. The net effect of this process is movement towards the offshore direction (Hughes et al., 1997; Nielsen, 1997). However, the majority of the tracers from the lower beach eventually move up the beach. This may be explained by the fact that after a short period of time, with the rising tide, the water level and the water table are at an equal

height. This impedes the ground water flow, resulting in the uprush becoming dominant and beach material being moved up the beach. This uprush only affects a thin surface layer of sediment. As the water level continues to rise, the steepness of the beach face causes the waves to break directly onto the beach. As a result much energy is delivered to the beach face in a very short period of time which results in entrainment, mixing and movement of a greater depth of material. During this period the tracers at the surface of the sediment are likely to become well mixed with the beach sediment and buried at depth, where the backwash during the falling tide cannot remobilise them. The net result is for the pebbles to migrate landward. This is in addition to the main tendency for them to move down-drift, alongshore.

The middle of the beach is above the water table level and as a result all the wave energy released in the uprush will transport the surface sediment landward. At the same time, infiltration into the beach face will strongly reduce the energy of the backwash. This tendency changes when the water table and the water level reach the same elevation. At that point, the sediment will be saturated by water, and seaward currents will be strong enough to remobilise the beach material during the high tide (at least that of a comparable size to the tracers used). In addition, the backwash during the falling tide drags surface material down across the beach. During the three days corresponding of the tracers' deployment in the three locations on the beach profile, wave breakage at high tide occurred between the shingle beach toe and just below the point where the middle tracers were injected. Under the breaking waves, some tracers were buried deep enough not to be removed by the decreasing tide and the associated swash.

It has been identified that on November 7th and 8th, the movement of the tracers' cloud centroid of mass was at a smaller angle than that of the 31st of October, whilst the mean distance travelled was greater than on the 31st (Figures 6-12, 6-13 & 6-14). On November 7th and 8th, berm accretion occurred, coinciding with the changeover of tidal level from a spring tide to a neap tide. As a consequence, coarse material on the upper beach was pushed landward to build up the berm. In contrast, on October 31st, the berm suffered erosion because the tidal range moved toward a spring tide and the coarse upper beach material was spread out across the beach as described by the surface elevation changes maps (Figure 6-16). It is mainly pebbles from the upper beach area

that contribute to the berm construction. The distance travelled by the tracers is mainly due to the energy delivered by the wave onto the shore face. Considering the wave conditions and the water level (Chapter 4 Section 4.3.1), there was little difference in H_s (being respectively in chronological order 1.36 m, 1.14 m and 1.36 m ($H_{s\ t. \max}$ values)), water level (8.47 m, 8.66 m and 7.71 m) and wave approach to the orthogonal of the coast (22.7° , 27.4° and 22.4° from the south-west) during the periods shown. However, there was a significant difference in the significant wave period (7.9s, 5.1s and 5s). Because of that, waves on the 7th and the 8th are steeper than those on the 30th which probably explains why the distances travelled are greater on November 7th and the 8th of than on October 31st 2005.

(ii) Birling Gap, March, May and December 2006

Because of the high recovery rates experienced after only one tide the results at Birling Gap give a high level of confidence regarding the pattern of transport the tracer pebbles display (Tables 6-7, 6-10 & 6-13). As observed at Cayeux-sur-Mer, on March 22nd, May 19th, 22nd and December 14th, the tracers injected on the upper beach demonstrate a clear tendency to move seawards across-shore and move further than those injected in the mid and lower beach (Figures 6-21, 6-27, 6-29 & 6-33). This has to be related again for the same reasons as at Cayeux to the swash and its time of action.

On the other hand, on two occasions, on March 25th and May 20th (Figures 6-22 & 6-28), a new pattern emerged whereby the lowest injection point's tracers travelled the furthest distances while pebbles from other injection points across the beach travel lower distances. In fact, the distance travelled decreases with the increase in elevation on the beach face. This pattern is explained by the water level conditions. Indeed, both of these days were characterised by very low high water level, being 1.17 and 1.76 m respectively. Because of these low HWL wave breaking occurred in the very first few metres of the beach or just before the mixed sediment beach on the chalk platform because of its shallowness especially considering that the wave height associated with these event days were 0.7 and 1.7 m respectively. The energy of the wave breaking is dissipated very quickly by the mixed sediment beach mainly through infiltration. The combined effect of both the very quick infiltration and the position of the high water level mark meant that most of the wave energy was used and dissipated in the very first

few metres of the mixed sediment beach which corresponded to the location of the lowest injection points. This energy was decreasing as the beach elevation increased so that the very last end of the swash was slightly moving the tracer pebbles displayed on the upper part of the beach.

The across-shore movements associated with the tracers removed from each injection point are also very similar to those observed at Cayeux-sur-Mer. It appeared however that during the experiments on March 2006, even the tracers from the lower injection points showed downward movements across the beach. The low significant wave heights during this period most likely enabled the sandy fraction of the beach material to percolate to the deepest layers of the beach creating a thin layer of sand above the chalk platform. This rendered the beach even more permeable and the infiltration is quick.

At Birling Gap, it appears that the tracers from each injection points display more freedom in their cross-shore movements than at Cayeux, spreading along the entire beach profile. For example, when a berm developed on March 25th and December 14th 2006, it appears that pebbles from each injection point contributed to the built up. These contributions are greater from the upper injection point pebbles and decreased with elevation on the beach profile. However, contributions from the other injection points increase with time as shown on Figures 6-22 & 6-33.

The combined effect of the short length of the beach profile at Birling Gap and the long time of swash action during the inundation is the most likely explanation for the very rapid tracer migration from the upper to the lowest parts of the mixed sediment beach and vice versa. Despite these significant across-shore exchanges of sediment between the different areas of the active beach, the depth of disturbance and the active layer at Birling Gap were lower than those observed at Cayeux. This indicates that the LST on a beach such at Birling Gap only affects a very thin surface layer of sediment which gets reworked constantly by the wave conditions and that very occasionally during stormy events does the deepest layer of the beach material get remobilised and transported. This point accords to an observation made by this study in Chapter 5 when traces of previous active layer columns from March 2006 were recovered in place during May 2006. This

suggests that saltation, traction-bedload and sheetflow are the modes of transport dominating the nearshore on mixed beaches such as Birling Gap.

6.10.3 Accuracy of the techniques used: a comparison between GPS surveys and tracer pebbles

(i) Cayeux-sur-Mer

The preliminary work at Cayeux-sur-Mer in 2004 has shown promising results to determine the longshore transport rates from both DGPS topographic surveys and tracer pebbles. Indeed, the volumes of sediment transport determined by the respective methods of measurement lead to equivalent results, -2121.9 m^3 and -2112.8 m^3 of sediment loss respectively. These results first confirmed that the choice in site of the study area was right. Previous authors (e.g. Van Wellen et al. 1997) stated that topographic surveys work well to the study of LST in a closed or semi-close sedimentary system. The volumes measured for the overall period by the tracer pebbles are slightly lower than those of the topographic surveys. This difference can be linked to the very low recovery rate on December 17th 2004 (15%). On that particular tide, the wave conditions were energetic enough to either bury the tracers at a depth beyond the detection limit or transport them away from the surveyed area. The distribution of the recovered pebbles on December 17th (closest pebble found from the injection was 48 m away from its injection point) suggests that a large number of pebbles travelled out of the survey zone. This would explain the underestimation of the beach volume transported in comparison to the topographic survey method. This observation highlights one of the limitations when using tracers concerning the position of the centroid. The mean distance travelled (centroid) used to determine the beach volume changes can easily be influenced by adding or subtracting pebbles from the cloud distribution and therefore falsifying the results. The key factor when using such a technique is therefore the recovery rate. The higher the recovery rate the more accurate the centroid's position will be and therefore the more accurate the volumes of sediment transport will be. Note that error margin for the length of the active profile was very low as it was occasionally measured *in situ* and can also be easily measured from the beach profile surveys.

The following survey period at Cayeux-sur-Mer in October-November 2005 proved to be less satisfactory as both methods (DGPS surveys and tracer pebbles) were sometimes giving contradictory beach volume changes for identical wave conditions (Tables 6-5 & 6-6). Under the assumption that no sediment was supplied to the beach from the updrift side of the terminal groyne and considering the consistent south-westerly wave direction, and finally that the tracer data was clearly indicating a transport in a northward direction with no tracer even been found updrift of its injection, erosion should have been consistent from one tide to the following during the survey period.

Taking into account that the vertical accuracy of the DGPS is 1 cm according to manufacturer and that the specially designed survey technique (Chapter 3; BAR, 2005) produces reliable and accurate digital elevation models, another explanation needs to be considered. In the search of an explanation, the combined effect of pebble imbrications and the inexact location of consecutive beach elevation measurements seem to be a reasonable explanation for these slight changes. Because of the sand matrix and the general grain size and shape of the sediment on mixed beaches, the pebbles can sustain different imbrications; it is not unusual to observe protuberant pebbles on a mixed beach. Therefore, the combination of (i) the randomness imparted to where the measurement was taken; (ii), the inherent error associated to the interpolation between each beach profile surveyed; and (iii), the actual low beach volumes changes observed from one tide to another is most likely the reason why such discrepancy between the techniques of LST measurements exists. The validity of beach topographical surveys to produce reliable beach volume changes on mixed beaches is not questioned here; however, it is important to understand what the limits are when using a technique to measure LST on mixed beaches. The observations from this study confirm the early results of the BAR project (2005) conferring an error margin of ± 5 cm to the DGPS technique.

To prevent such an error from being significant in comparison to the actual beach volume change, the time between two consecutive surveys should be increased on the premise that sufficient sediment transport occurs between the two visits for a change to be recorded. This is supported in part by the results obtained at Cayeux during both of the field data collection campaigns. Both of the overall volume changes clearly

demonstrate that the southern part of the survey areas was literally “cannibalised” under the hydrodynamic conditions. Van Wellen et al. (1998) insisted also on the importance that the length of the survey area needs to be sufficient to take into account the beach re-orientation when dealing with closed or semi-closed environment. Therefore, the key factors for accurate volume changes using a DGPS on mixed beaches are the combination of length of the survey area and the timing between the surveys.

(ii) Birling Gap

Topographical surveys at Birling Gap suffered for the same imprecision as at Cayeux-sur-Mer. However, they were accurate enough to appreciate the sediment transfers from one area to another, the direction of the transfers being deduced from the wave conditions and the tracer experiments. In a similar way as for Cayeux-sur-Mer, pebble imbrications and the location of the elevation measurement point on the beach is even more likely to influence the topographical survey as slightly coarser grain sizes were generally observed at Birling Gap.

6.10.4 Accuracy of the techniques used: a comparison of LST volumes

calculated based on active layer measurements and on tracer burial depth

While the width of beach undergoing transport is relatively easy to determine to an accuracy of a few metres, delimiting the depth of disturbance has remained rather more problematical until now.

Nicholls and Wright (1991) and then Van Wellen et al. (2000) expressed the necessity to investigate the depth of disturbance on gravel beaches when using tracer pebble techniques because of the risks of overestimating the actual LST. As it appears, their assumption was mostly well founded. The method based on the deepest pebbles depth generally overestimates the transport volumes derived from the depth of disturbance on the profiles (measured up to 60.7%, Table 6-9). Only a few measurements showed underestimation of these volumes. The underestimations occurred generally during period of berm build up (up to 134.2%, Table 6-5). From this observation, it can be assumed that the coarsest material is remobilised from the mid- and lower beach to contribute to the build up of the berm (Chapter 4, e.g. Buscombe and Masselink, 2006) leaving a finer matrix of sand or fine gravel into which the few tracers left cannot

penetrate because of the phenomenon of acceptance and rejection (e.g. Carr, 1969; Bird, 1996). On the other hand, the detection of the pebble tracers in the berm was very difficult because of the greater depths of tracer burial and the equipment detection limits. For this reason only the shallowest tracer pebbles in the berm were recovered. The combination of both of these reasons might certainly be at the origin of the underestimations observed during the transitions from neap tides to spring tides. This assumption is also supported by the surface grain distributions collected along the beach profile surveyed (Chapter 4 Figure 4-36) that show an increasing coverage of sand or fine gravel on the mid- and lower parts of the beach profile in the recharged area. The explanation for overestimation from the method based on the use of the tracers only is very straight forward too. The assumption of a uniform rectangular moving layer will overestimate the real LST.

6.11 Conclusion

Observations of hydrodynamic conditions inshore, morphological changes and sediment motion from one low tide to the following have been made on two mixed sand and shingle beaches at Cayeux-sur-Mer and Birling Gap, in France and UK, respectively on each side of the English Channel. The results highlight constant patterns of movement for a specific grain size over time and for specific wave conditions. The grain size selected for the tracers is representative of the dominant grain size in the coarsest fraction of the beach material at both sites. Good recovery rates allow a high level of confidence in the results. The new findings provide a better insight to particle behaviour on mixed sand and shingle beaches, drawing on existing knowledge of hydrodynamic conditions, swash flows, groundwater flow, beach slope and grain size.

Material from the upper part of the beach tends to migrate seaward and further down-drift than that from the other parts of the beach. It is suggested that this is linked to a continuous swash action from the high tide to the low tide. Pebbles from the lower beach tend to migrate up towards the back of the beach, although alongshore transportation is dominant. It is suggested that these movements are explained by the combined effect of the groundwater flow, the swash flows and the action of breaking

waves. Pebbles from the middle of the beach display a preference to move seaward which may also be explained by the interaction between the groundwater flow, swash flows and the action of the breaking waves. Alongshore drift is again significantly greater than cross-shore movement.

The experiments show that pebble behaviour on a mixed sediment beach is extremely sensitive to position on the beach profile and to changes in the water level and wave conditions associated with tidal conditions.

The results demonstrate the limitations associated with the measurement techniques that are classically used to measure LST on beaches in general. The use of DGPS surveys and digital elevation models prove to have limitations that need to be understood and carefully considered when investigating coarse grained beaches such as mixed or gravel beaches. To measure accurate and realistic results of LST on mixed beaches it is necessary to survey large areas alongshore and across-shore in a semi-confined or closed area as indicated by Van Wellen et al. (1998); but also the time between the surveys needs to be sufficient enough for the area to be marked by significant changes in beach volume so that the error margin represents only a small amount of the total volume change.

In a similar way, the combined use of tracers and measurements of the depth of disturbance across-shore have shown that the assumption of a uniform moving layer made by Equation 6-21 generally used by researchers can greatly (up to 60.7%) overestimate the actual volume involved in the transport.

Formulae and models for longshore drift largely fail to take this differential transport on such beaches into account and this could be one of the main reasons for their inaccuracy. The next chapter considers this in more detail by attempting to calibrate a model based on the data discussed in this chapter according to the energy flux approach.

Chapter 7. Longshore Sediment Transport: an attempt to derive K

7.1 Introduction

The aim of this chapter is to derive a reliable value of the drift efficiency coefficient K which is used in the CERC formula based on the energy flux approach (c.f. Komar and Inman, 1970). This value will contribute to the small data sets already obtained from a variety of gravel and mixed beaches around the world.

This chapter:

- (a) discusses the energy flux approach, the CERC formula and the drift efficiency coefficient K .
- (b) examines the performance of techniques used to measure LST and the relationship between LST and longshore wave power. The net volumes of sediment transport measured (Q_l) from the data collected at both study sites will be plotted against the longshore wave power (P_l) to examine if the assumption of proportionality made by the energy flux approach applies to mixed beaches.
- (c) attempts to derive a calibrated K value for each study site according to the relationship between P_l and the immersed weight transport rate (I_l) (e.g. Komar, 1988; Chadwick, 1989; Bray, 1997; Nicholls and Wright, 1991; Van Wellen et al., 2000).

Please note that the values of K and P_l presented by this thesis are given with respect to H_s and not H_{rms} . The conversion factor is almost exactly two, with the RMS value being the greatest (Nicholls and Wright, 1991). For example, the K value suggested for sand when using H_{rms} is 0.77 whereas when using H_s this coefficient goes down to 0.39.

7.2 Background

7.2.1 LST: the energy flux approach

Longshore transport formulae can be divided into three groups depending on the concepts and theory they are based on (Van Wellen et al., 2000): (i) the energy flux approach (e.g. Komar and Inman, 1970; Nicholls and Wright, 1991; Van Wellen et al., 2000), based on the principle that the immersed weight of sediment transported alongshore (I_l) is proportional to the longshore wave power (P_l), this study will focus on this later; (ii) the stream power approach (Bagnold, 1963; Bailard, 1984; Morfett, 1988), based on the principle that a part of the stream power is used for the sediment transport as bed and suspended load; and finally (iii) the force-balance approach relating the sediment transport to the bed shear stress (Damgaard and Soulsby, 1996).

This study focuses on the energy flux approach as, in part because of its relative simplicity, it is one of the most commonly used theories for the study of longshore sediment transport (the CERC formula for example).

(i) Relation between LST rates and P_l

The alongshore wave power corresponds to the amount of energy delivered by waves to the beach and is calculated using Equation 7-22 (US Army Corps of Engineers, 2002).

$$P_l = EC_g \sin\theta \cos\theta \quad (7.22)$$

where E is the wave energy, C_g is the wave group speed, and θ the wave angle.

$$E = \frac{1}{8} \rho g H^2 \quad (7.23)$$

$$C_g = \sqrt{g d_b} = \left(\frac{g H}{k} \right)^{1/2} \quad (7.24)$$

Where g is the acceleration due to gravity, ρ is the mass density of water, H the wave height and k is the breaker index.

It is generally agreed that the LST rate is proportional to P_l . This assumption on coarse sediment was supported by studies such as those of Kamphuis (1991) and Wang et al. (1998) which examined the relationship between the total LST measured using various techniques (e.g. sediment tracers, sediment traps, topographical surveys) and each parameter used in the calculation of the alongshore energy flux (wave energy flux EC_g and wave angle θ). On the other hand, based on field measurements of LST rates using GPS surveys and tracing experiments simultaneously, Van Wellen (1999) obtained “poor” correlations (respectively at 0.52 and 0.71) when plotting Q_l and P_l against each other. The poor correlations highlighted a lack of reliability of the techniques of measurement and Van Wellen concluded that the vertical precision of the GPS used was not good enough to produce a reliable volume of sediment transported. He also concluded that the lack of precision with the LST rate derived from the tracers was a result of the use of the depth of the tracers to determine the depth of disturbance. The current study has already highlighted in Chapter 6 how DGPS surveys can produce poor accuracy LST rates; and also how significantly different LST rates produced by the use of tracers only or by the use of the depth of disturbance in the calculations..

Van Wellen’s work (Van Wellen et al., 1998; Van Wellen, 1999) suggested that on gravel beaches the correlation between the alongshore wave power and the LST rates is only proportional after a threshold of energy is passed; this threshold corresponds to the energy necessary to start the entrainment of pebble size particles.

(ii) Longshore sediment transport formulae and the K coefficient

To calculate LST, a large number of formulae are available. Van Wellen et al. (2000) has identified and assessed a total of fourteen empirical formulae (Bailard, 1984, Kamphuis et al., 1986, 1991; Morfett, 1988; Chadwick, 1989; Van der Meer, 1990;

Schoonees and Theron, 1993; Damgaard and Soulsby, 1996; Van Wellen et al., 2000) in terms of their ability to predict the annual longshore sediment transport at Shoreham-by-Sea. Twelve of these formulae were collected from various sources although a few of them were actually developed by the same people who sometimes developed a variation of their original formula to include a new parameter such as the type of shape of the coast, the type of sediment, or even the type of field data collected. The results of Van Wellen's assessment showed that the best fitting answers to his field measurements were obtained by formulae that were actually calibrated by data previously acquired on his study site (Shoreham-by-Sea) or the neighbouring beaches. The rest of the formulae were generally over-estimating the yearly volume changes by a factor of more than 2. This highlights the fact that longshore sediment transport formulae developed for gravel beaches are site specific which subsequently express how unique each gravel beach is, for example, its grain size distribution, its beach gradient, and its morphology. This creates very real problems for the creation of empirical models that are applicable world-wide.

The LST formulae that follow the energy flux approach on gravel beaches are generally derived from the CERC formula that was originally designed for sandy beaches (Komar and Inman, 1970). The transference of this formula from sandy beaches to gravel beaches is done by calibrating the dimensionless constant K (drift efficiency coefficient; Equation 7.22; e.g. Brampton and Motyka, 1987; Bray et al., 1996; Chadwick, 1989; Nicholls and Wright, 1991; Van Wellen et al., 2000). However, attempts by various studies to calibrate K show that its value varies from one gravel beach to another and, so far, no universal value has been derived to be generally applicable on gravel beaches due to their unique character.

To give an idea of the range of values of K derived by previous studies, a non exhaustive list of the values encountered in the literature has been addressed. Komar (1988), based on Hattori and Suzuki's (1978) "exotic" tracers experiment ($D_{50}=20\text{mm}$) in Suruga Bay (Japan), estimated a K value for gravel beaches of 0.1 (using H_{rms}). Very little confidence is given to this value as it was derived from sediment surface recovery only and the study used anthracite tracers that were slightly coarser than the indigenous sediment. Nicholls and Wright (1991), based on tracer experiments covering a large

range of grain sizes, agreed at a value of 0.02 (using H_s) at the beaches of Hengistbury, Long Beach and Hurst Castle Spit (Hampshire). Chadwick (1989) used sediment traps to determine a K value varying from 0.02 to 0.06 (using H_{rms}) at Shoreham by Sea. However, because of the problems associated with the use of sediment traps, these values were derived from low energy wave conditions. Bray et al. (1996), on the same beach but using electronic and aluminium tracers on a large spectrum of wave energies, calculated K values of between 0.003 and 0.03 (using H_{rms}). Later, Bray et al. (1996) presented a new set of values for K this time covering a wide range of wave energies (from what he considered “low to high”) (Figure 7-1). Using less than one hundred tracers in total but experiencing high recovery rates (from 60 to 100%), he observed K values ranging from 0.02 to 0.36. Using the energy flux approach and field data from different sources (Chadwick’s (1989) sediments traps data at Shoreham-by-Sea, Bray et al.’s (1996) electronic and aluminium tracer data at Shoreham-by-Sea and Nicholls and Wright’s (1991) aluminium tracer data at Hengistbury Long Beach and Hurst Castle Spit), Van Wellen et al. (2000) tried to derive a reliable K value that would be useable for gravel beaches in general. Unfortunately, very poor confidence is given to this value as its correlation was judged “poor” by the author himself ($R^2=0.62$). Moreover, the K value he derived ($K=0.22$) seems very high in comparison to the K estimates made by each study individually (Figure 7-2).

The variability of the drift efficient coefficient (K) from one study to another clearly identifies the necessity to understand and identify the limits of the sampling methods before considering them as absolute and inputting/calibrating K into LST models. It is necessary to indicate precisely what the beach characteristics are, what techniques are used to measure the LST, and specify what the hydrodynamic parameters measured are before calibrating models with field data. As pointed out at the beginning of this chapter, the use of different wave condition parameters alone (H_s or H_{rms} , for example) can lead to significant changes in the values of K. Complete transparency regarding the data collection and parameters measured are necessary to make sure of the validity of the K values derived.

Nicholls and Wright (1991), observing that larger pebbles move the fastest on Hurst Castle Spit, stated that K increases with the grain size which was later supported by Van Wellen et al. (2000). However, determining a reliable and accurate value of K for gravel beaches is still to be achieved.

Generally, derivations of a K value based on field data collected on gravel beaches only involve a small amount of data points derived from low wave energies (e.g. Chadwick, 1989; Nicholls and Wright, 1991). Figure 7-1 & 7-2 are perfect examples of the amount of data used to derive K . As pointed out just earlier, it can be seen on both figures that the distribution of the data point across the alongshore wave power spectrum is poorly distributed. This observation will later support the relevance of the data collection and analysis of this thesis. As Komar (1988) indicated, knowledge about the K value will improve with increase of experimental data collection such as that contributed by this study.

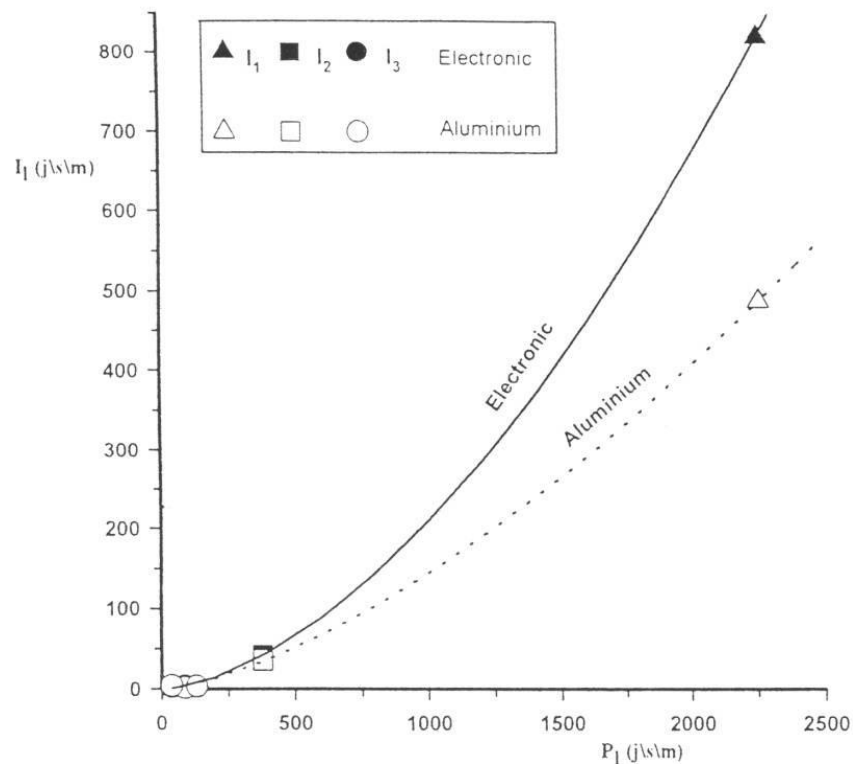
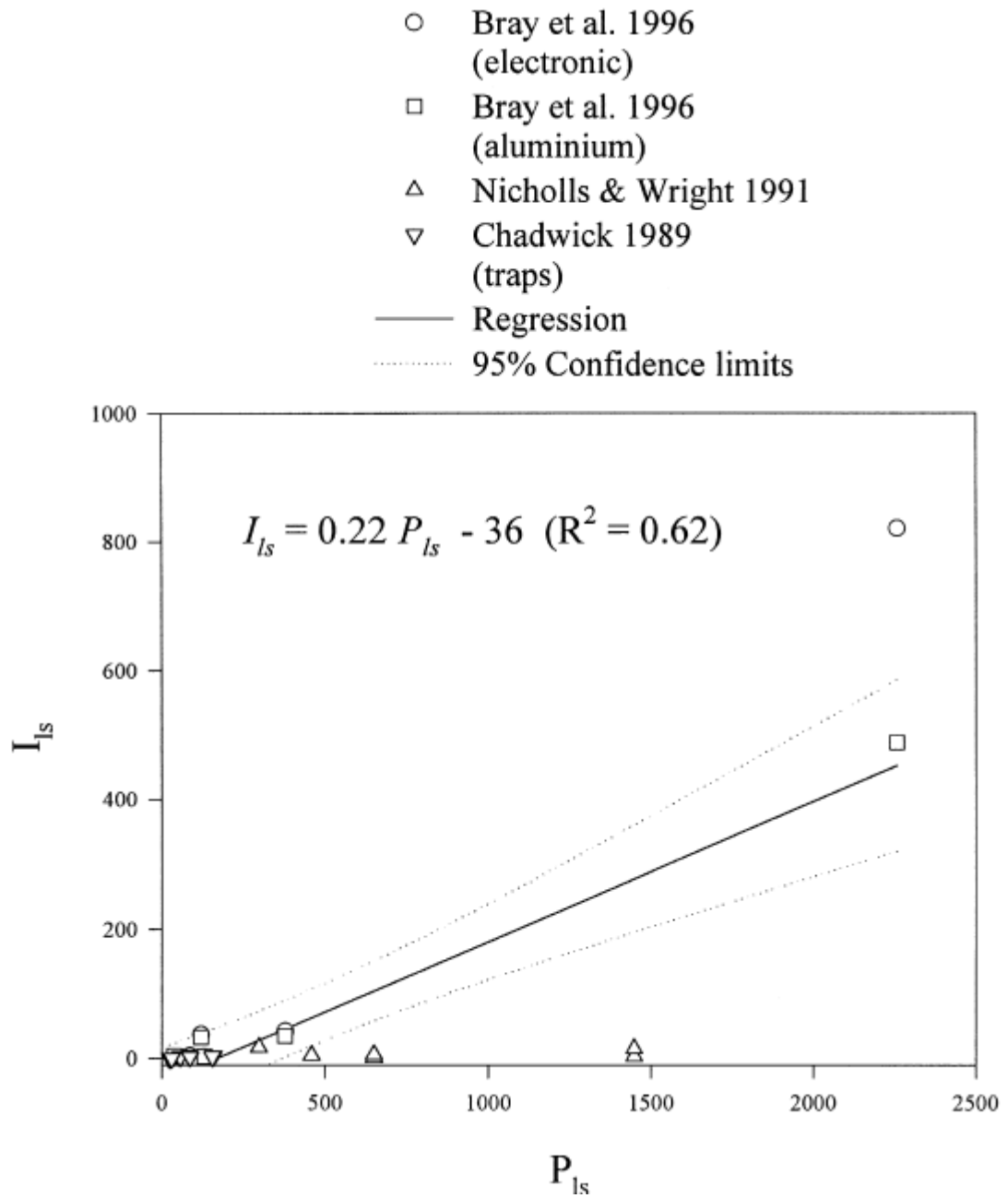


Figure 7-1 Estimates of shingle transport efficiency based on the Shoreham data (Bray et al., 1996).



7.2.2 The CERC formula

The CERC formula (Komar and Inman, 1970) presented in the Shore Protection Manual (US Army Corps of Engineers, 1984) relies on the proportionality existing between the immersed weight transport rate (I_l) and the wave energy flux (P_l) and is empirically expressed as:

$$I_l = K P_l \quad (7.25)$$

K being a constant (this chapter Section 7.2.1).

Another way to calculate I_l would be by using the volumetric transport rate (Q_l) according to the following equation (*in* Van Wellen et al., 2000):

$$I_l = \Gamma Q_l \quad (7.26)$$

Γ is a conversion factor that can be expressed as:

$$\Gamma = \frac{(\rho_s - \rho)g}{1 + e} \quad (7.27)$$

where, ρ_s is the density of the sediment, ρ is the density of water, e is the void ratio, g is the gravitational acceleration.

One of the most evident limits when looking at the CERC formula is that there is no direct input for parameters such as beach slope, grain size distribution, shape of the pebbles or mode of transport. Considering that this formula was originally developed on sandy beaches, and that the characteristics of sandy beaches (e.g. grain size, shape, beach gradient) are fundamentally different from those of gravel beaches, doubts about the performance of such a formula arise. Qualitatively, it would mean that the model is not able to differentiate between steep and low slope beaches or even between sandy and gravel beaches, or flat and round particles, which have been proven to have an influence on the distances and directions of transport (e.g. Van Hijum and Pilarczyk, 1982; Bluck, 1967; Orford, 1975; Carter, 1988). Komar (1988) defended the reliability

of the CERC formula explaining that such variations in beach characteristics are taken into account through the value of K .

Despite its limitations, the performances of the CERC formula is widely supported (e.g. Kamphuis, 1986; Kamphuis, 1991; Wang et al., 1998) and used for the derivation of LST on sandy and gravel beaches. Various authors developed formulae from derivation of the CERC formula (e.g. Chadwick, 1989; Bailard, 1984; Morfett, 1988). Models aiming at the prediction of LST on gravel beaches used by coastal managers are also developed from the CERC formula; for example BEACHPLAN developed by HR Wallingford (<http://www.hrwallingford.co.uk/>) uses a formulation of total longshore transport rate based on the CERC formula.

7.3 Towards an estimate of pebble transport efficiency

In the current study, the derivation of P_l was done using Equations 7-22, 7-23 and 7-24. Based on the energy flux approach, the net beach volume change or LST rates (Q_l) and the longshore energy flux (P_l) increase proportionally with each other. Considering this, both of the LST rates measured for each site (i.e. using the tracers and including or excluding the depth of disturbance and the net volume changes measured using topographical surveys) were plotted in order to assess the applicability of this approach to the data collected in this study. However, because of the poor quality of the beach volume changes interpolated from the DGPS surveys (Chapter 6) these are plotted separately.

(i) Cayeux-sur-Mer

Having shown, in Chapter 6, that the use of the depth of disturbance sometimes greatly overestimated the LST rates compared to those derived from the depth of the deepest pebbles, it may have been logical to use only the most accurate data to determine the most accurate relationship between the net beach volume transported (Q_l) and the longshore wave power (P_l). However, in some cases, accurate evaluations of the depth of disturbance along the beach profile were not possible because of a missing measurement due to the loss of a painted pebble column. As a result, Q_l was derived

using the depth of tracer burial data in order to ensure that a correlation was possible. Tracer burial depths are commonly used in the estimation of the depth of disturbance (Nicholls and Wright, 1991; Van Wellen, 1999). The use of both of the results permits an examination of how the error margin of measurements of the depth of disturbance affects the correlation between the volumes of sediment transported and the longshore wave power.

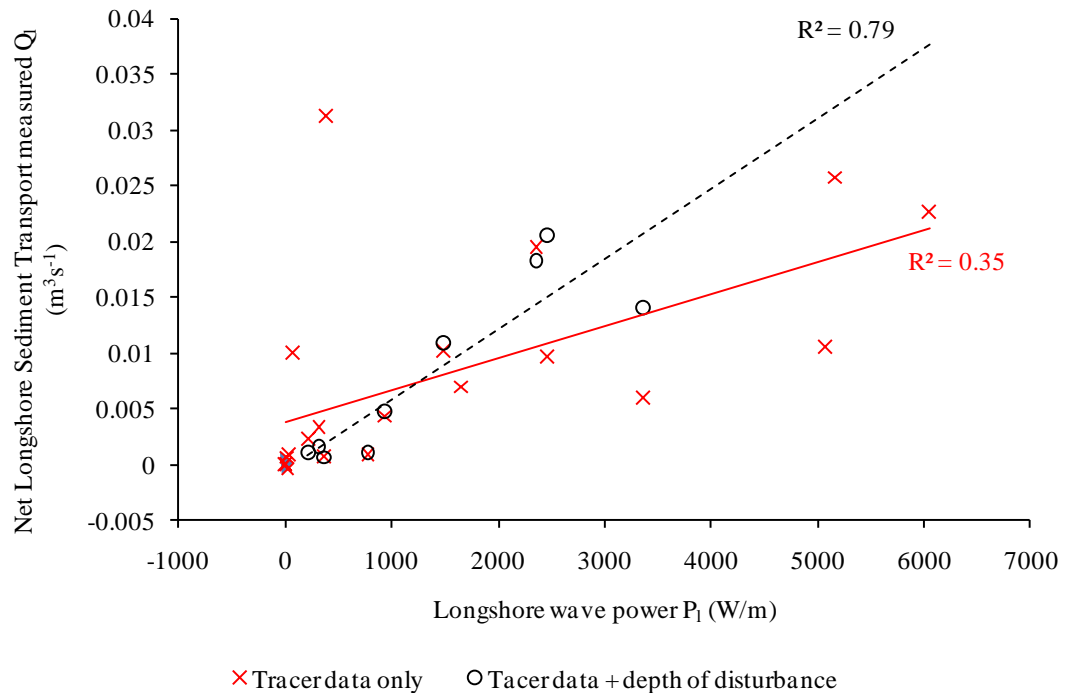


Figure 7-3 Correlations between the longshore energy flux (P_l) and the net longshore sediment transport measured using tracer data associated with the depth of disturbance measurements or the depth of the deepest tracers at Cayeux-sur-Mer. All the data collected at Cayeux in December 2004 and October/November 2005 is represented here.

The correlations obtained for each set of measurements show some discrepancy (Figure 7-3). The correlation between P_l and Q_l using only the tracer data has a low coefficient of 0.35, whereas that using the depth of disturbance data has a correlation coefficient of 0.79. By not being the perfect correlation the energy flux approach assumes (the correlations not crossing the x and y axes at 0), it can be deduced that errors or limitations are associated with the data collected. However, considering the respective correlation coefficients it can be seen that LST rates calculated using the depth of

disturbance are more accurate than the LST rates based on the use of the tracers only at Cayeux-sur-Mer.

Some of the data points used on Figure 7-3 are actually derived from tracers with a low recovery rate and therefore the validity of these measurements can be contested. To improve the accuracy and derive the most reliable LST rates to derive an accurate value of K for later use, the data were filtered using the percentage of recovery of the tracers. The minimum recovery percentage considered was 60% which corresponds to the expected recovery rate of “passive” tracers (Allan et al., 2006) and is also the minimum recovery rate normally used in the literature to derive values of K (e.g. Nicholls and Wright, 1991). Therefore, every data point that had a recovery rate lower than 60% was rejected from the model. Figure 7-4 shows the results of this filtering.

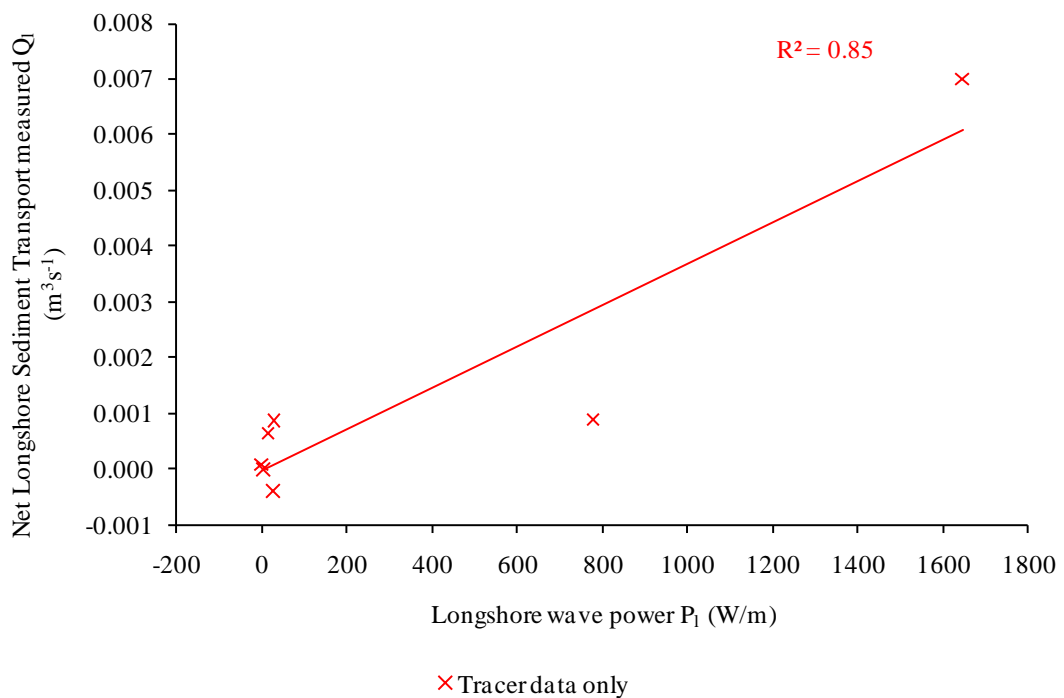


Figure 7-4 Correlations between the longshore energy flux (P_l) and the net longshore sediment transport measured using tracer data associated with depth of disturbance measurements or the depth of the deepest tracers at Cayeux-sur-Mer. Only tracer pebble recovery rates superior to 60% are represented here.

Unfortunately, the data filtering eliminated all the measurements of LST rates derived from the depth of disturbance (Figure 7-4). However, a few LST rates derived from the

depth of burial of the tracers were still available so a correlation was attempted. This correlation has a coefficient of 0.85 which is considered very significant. Thus, the coefficient of the correlation increases significantly after filtering the data in relation to their percentage of recovery. This suggests that the precision of a tracer method increases with the recovery rate, emphasizing the necessity to create practical statistical tools that allow researchers to know how many pebbles need to be deployed for a reliable representation of the volume of sediment being transported (e.g. Lee et al., 2007a).

Observing Figure 7-4, it can be argued that the filtering method has disadvantages. (1) First, it reduces the number of points used to derive a correlation, which weakens its statistical validity. (2) Next, the scatter of the points in this study is poorly distributed with isolated points in the highest energy flux values (P_1). Such isolated points most certainly influence the result of the correlation.

The scatter of the data points is to be directly related to the wave energy delivered to the beach during the field measurements. Low net longshore sediment transport is most likely to be associated to low wave energy events. During the field experiments, low net longshore sediment transport was generally characterised by a small scatter and a shallow burial depth of the tracers in the proximity of their injection points. As a direct consequence, recovery was quick and very successful with rates largely above 60%. This would explain why many of the data points with low wave energy are kept after the filtering. In contrast, the highest net longshore sediment transports are generally associated with high wave energy events. High net longshore sediment transport entrains the tracers and scatters them further distances alongshore and at greater depth of burial within the beach material. Recovery following these events did not achieve the expected recovery rate of artificial tracers. This would explain the small amount of data point with high value of P_1 available to derive a correlation after the filtering.

Considering these points, uncertainties in the validity of the correlations cannot be denied; however each of the data points is the result of very accurate measurements. The longshore wave power (P_1) is very accurate considering that it is based on the wave conditions on one tidal cycle only (Equation 7.22). Then, because of the filtering of the LST rates measured, the error margin of Q_1 is minimised too. The only parameters that could influence the results would be the depth of burial of the tracers in comparison to

the real depth of disturbance. Unfortunately, because most of the data used on Figure 7-4 were collected in December 2004, no direct measurement of the depth of disturbance was available. However, in comparison to other previous studies that only used the depth of the tracers to derive Q_i , this study by having the same assumptions presents at the same kind of margin error as them (e.g. Bray et al. 1996, Van Wellen et al., 2000; Sear et al., 2001).

In conclusion, filtering the results with a 60% recovery threshold seemed to be the most appropriate method to make sure of the validity of each point to derive a correlation; however because of the very few points left to derive the correlation uncertainties about validity of the correlation itself exist.

The same type of correlation between the longshore wave power (P_l) and the volumes of sediment transported (Q_l) was done using data from the topographical DGPS surveys (Figure 7-5). The correlation coefficient (R^2) of zero suggests that no linear relationship exist between Q_l and P_l , therefore the use of DGPS surveys and digital elevation models are not suitable for the calculation of precise and reliable sediment transport volume between two consecutive low tides on mixed beaches. This confirms the observations made in Chapter 6.

In Chapter 6, it was suggested that the combined effect of the imbrications and rearrangements of the pebbles after each tide, plus the imprecision of the exact measurement of a location's elevation and the interpolation of the digital elevation models can alter the precision of the actual volume changes between two consecutive low tides. The proposed solution was to increase the time between the topographical surveys so that greater volumes of sediment are transported and the error margin associated with the DGPS survey would represent only a small fraction of the total volume change observed.

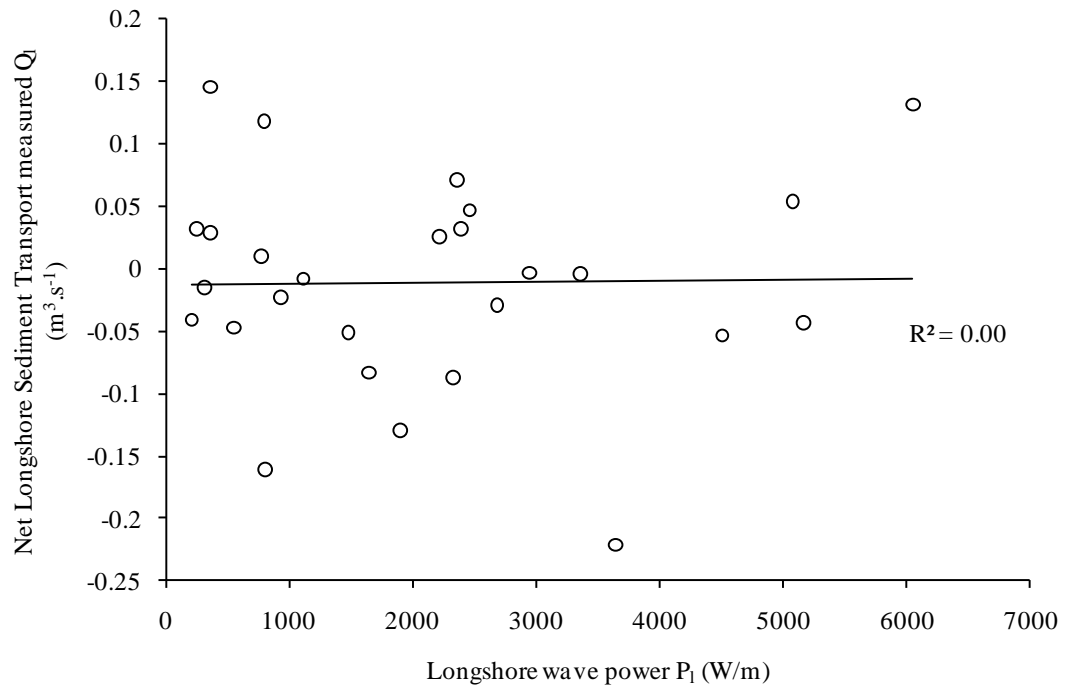


Figure 7-5 Correlations between the longshore energy flux (P_l) and the net longshore sediment transport (Q_l) measured using DGPS topographic survey at Cayeux-sur-Mer in October/November 2005.

(ii) Birling Gap

Initial observation of the correlations between P_1 and Q_1 was attempted using all the data collected at Birling Gap (Figure 7-6). This correlation was then refined to include only the data points characterised by tracer recovery rates over 60% (Figure 7-7).

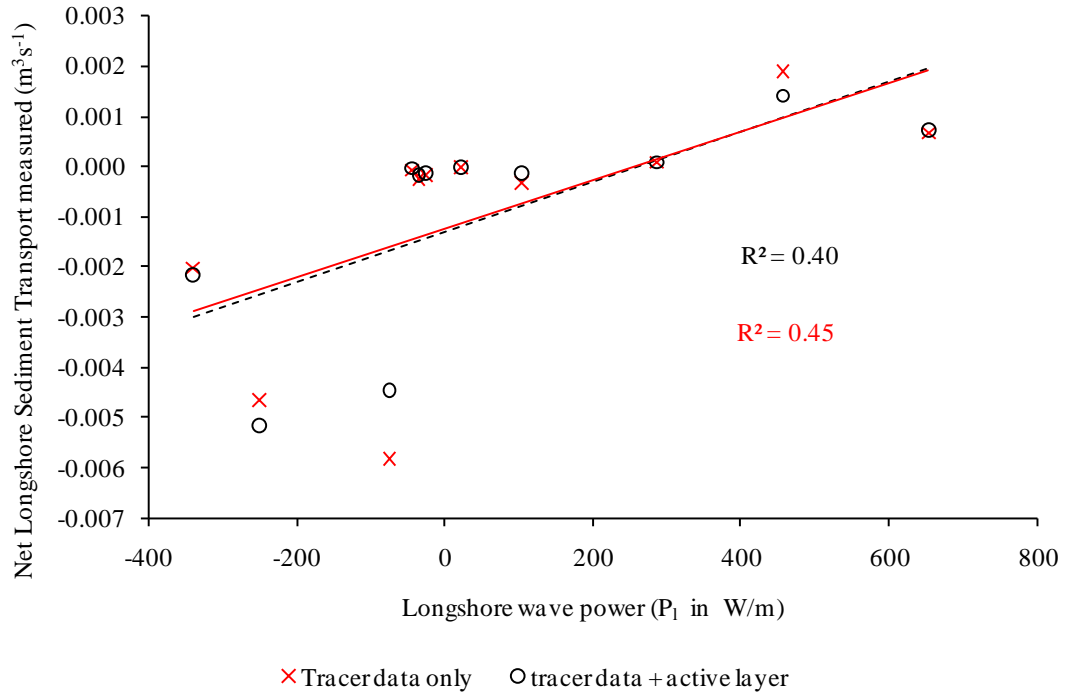


Figure 7-6 Correlations between the longshore energy flux (P_{1s}) and the net longshore sediment transport measured using tracer data associated with the depth of disturbance measurements or the depth of the deepest tracers at Birling Gap. All the data collected at Birling Gap in March, May and December 2006 is represented here.

Firstly, when observing the data distribution on Figure 7-6, it can be seen that the regression lines drawn for both techniques based on the tracers measuring the LST rates are very close to each other, and that they both have low correlation coefficients; 0.40 for the method using the depth of disturbance and 0.45 for the method based on the depth of the tracers. It is interesting that these correlations are so similar considering that Chapter 6 (Tables 6-9, 6-12 & 6-15) showed that the volumes produced by each technique could differ by up to 60.7%. Because of the relatively small volumes transported at Birling Gap, when converting the volumes from $\text{m}^3\text{.tide}^{-1}$ to $\text{m}^3\text{.s}^{-1}$ these differences represented even smaller differences in volume transport, which largely explains why the data points are very close between each technique (Figure 7-6).

When the data were filtered to include only tracer data with a recovery rate $\geq 60\%$, the correlations went up by a factor of nearly two, with $R^2 \geq 0.82$, and described a fairly consistent linear relationship between the longshore wave power and the volume of sediment transported alongshore, therefore suggesting the good performance of the tracers to represent the LST (Figure 7-7). In comparison to Cayeux, it should be noted that the correlation is based on a much better range of wave power values.

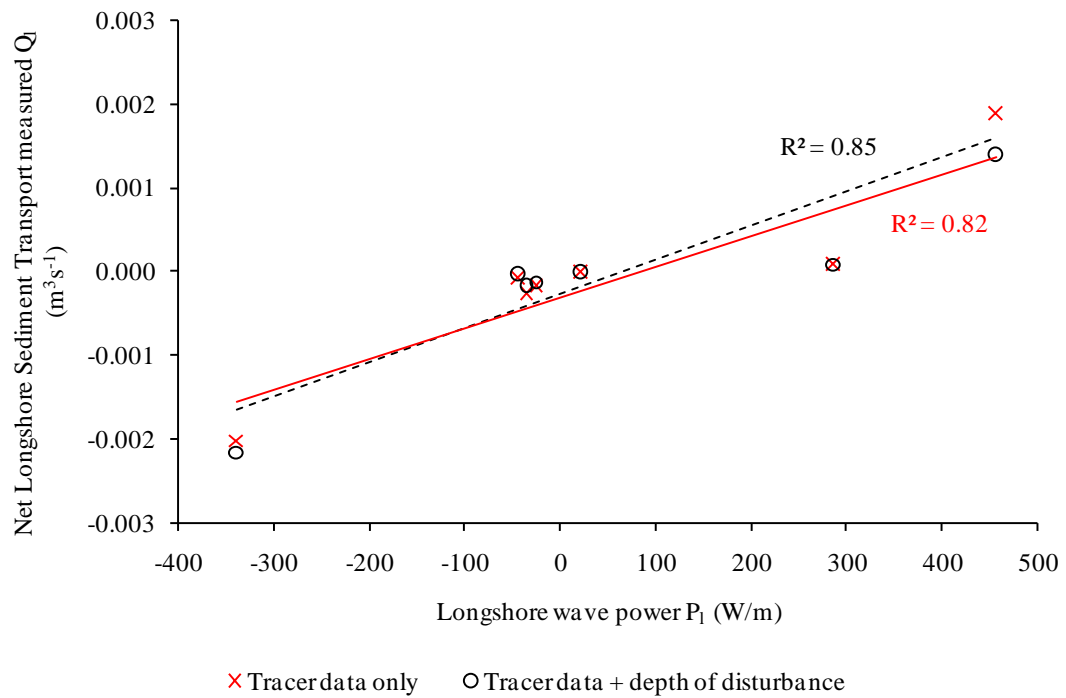


Figure 7-7 Correlations between the longshore energy flux (P_1) and the mean netlongshore sediment transport measured using tracer data associated with the active layer measurements or just the depth of the deepest tracer found on the appropriate day at Cayeux-sur-Mer. Only tracer pebble recovery rates superior to 60% are represented here.

The correlation between the beach net longshore sediment transport (Q_l) measured using DGPS surveys and the alongshore wave power (P_1) was also tested (Figure 7-8). The results show again a very poor correlation with a $R^2 = 0.22$, suggesting once again the poor accuracy of the DGPS data to measure LST rates.

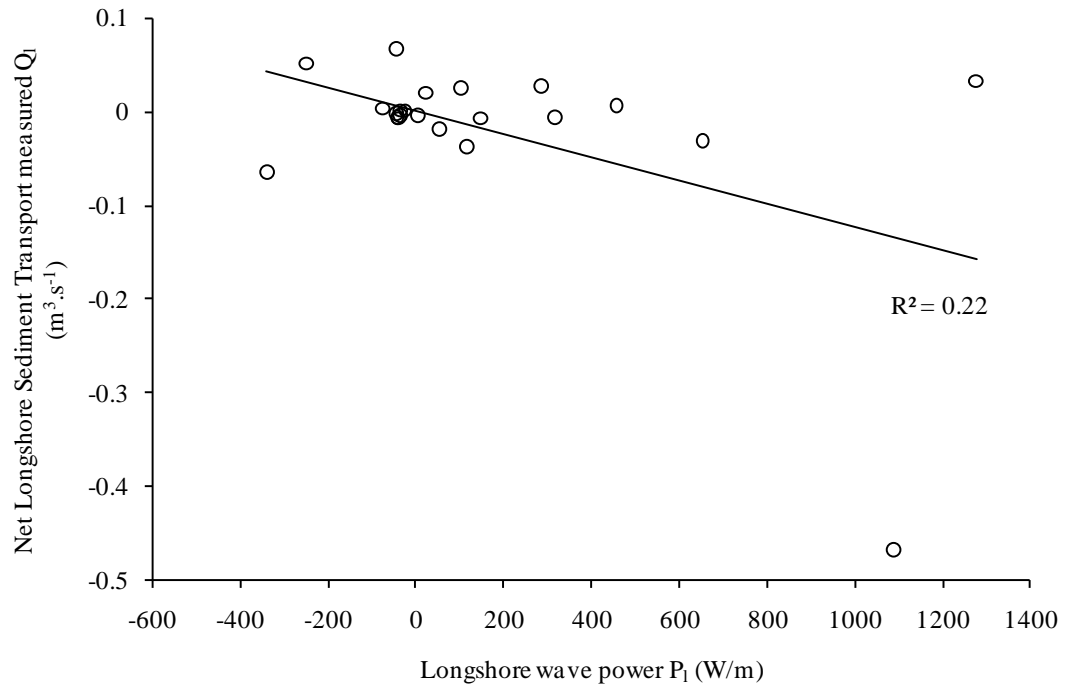


Figure 7-8 Correlations between the longshore energy flux (P_l) and the net volume changes (Q_l) determined by DGPS topographic surveys at Birling Gap.

7.3.1 Calculation of the K factor from the tracer data (Equations 7-25, 7-26 & 7-27)

At both study sites, when recovery rate is above 60% the LST rates show a trend to increase linearly with increasing longshore wave power, supporting the good performance of the tracers to measure LST. Therefore, it was decided to use this data to derive a value of K for each field site by plotting the longshore wave power (P_l) against the immersed longshore transport (I_l) (according to Equation 7-25). The coefficient of the regression line on such plot indicates the value of K.

P_l is easily derived from the wave conditions according to Equation 7-22, whereas I_l is derived from Equation 7-26. The values of the parameters necessary to calculate Γ (Equation 7-27) are listed in Table 7-1 whereas Q_l was calculated and used in earlier results (values are available in Chapter 6 and Figures 7-4 & 7-7).

Parameter	Value
ρ_s	2650 kg m ⁻³
ρ	1030 kg m ⁻³
e (Cayeux)	0.47
e (Birling Gap)	0.47
g	9.81 m ² s ⁻¹

Table 7-1 Summary of the parameters necessary to calculate I_p .

Before presenting the results, it is important to highlight once more that the CERC formula does not directly take into account parameters such as the beach slope or the grain size in its formulation (Komar, 1988). However, it is obvious that before movement, a pebble will require an energy threshold to be reached whereas for sand this threshold can be neglected which is why I_p is considered proportional to P_p . Because of the existence of such a threshold, it was decided not to force the regression line to intersect both axes at 0.

The results show that K has a value of 0.04 at both sites, using either only tracer data or using the measurements on the depth of disturbance (Figures 7-9 & 7-10). The coefficients of correlation are however very different from one site to another. At Cayeux, $R^2=0.85$ which is considered a strong correlation coefficient, giving confidence to the value of K. By contrast, at Birling Gap both correlations, derived from the tracer data only and from the depth of disturbance had R^2 's respectively 0.68 and 0.58, which are considered relatively weak.

Again, considering the scattering of the data points plotted for Cayeux or even Birling Gap, some doubts about the actual reliability of the correlations used to derive K may be raised. Indeed, the data are mostly distributed on the extremes which influence the correlation coefficients. However, for the same reason as earlier corresponding to the filtering of data used for the correlations, it cannot be denied that the K values obtained at each site are reliable based on the data collected. Moreover, studies in the literature generally derived values of K based on very low energetic conditions (wave height $\ll 1$ m, e.g. Chadwick, 1989; Wright et al., 2000), therefore the opportunity to use values corresponding to highly energetic wave conditions such as the extreme values

observed at both sites is of great interest. Finally, as shown in the introduction of this chapter (Section 7.2.1), the early studies of Bray et al. (1996) and Van Wellen et al. (2000) derived values of K with the same assumptions (Figure 7-1 & 7-2).

It is interesting that the regression line at Cayeux actually intersects the x and y axes at 0, suggesting that no threshold value is observed here for the entrainment of the sediment particles. On the other hand, the Birling gap regression line suggests that a threshold exists as the regression line intersects the x -axis at a P_1 value of approximately $15W\ m^{-1}$.

Having noted that both sites had equivalent K values, similar sand content (from 0 to 30 %) and similar grain size distributions ($D_{50} = 15\ mm$ at Cayeux and $17\ mm$ at Birling Gap, Appendix 2) and inspired by Van wellen et al. Study (2000; Figure 7-2) the data points from both study sites were plotted to see if the data are matching and to derive a harmonised value for the littoral drift efficiency (Figure 7-11). The derived K value was equal to 0.04 with a $R^2=0.83$. Again, the scatter of the data points on the plot is still distributed on the extremes; however, a few intermediate points attenuate the obvious influence of the extreme values giving a fairly confident and reliable value of K . Here again the regression line suggests that the threshold linked to the entrainment of the beach sediment particles is negligible as it crosses both axes at 0.

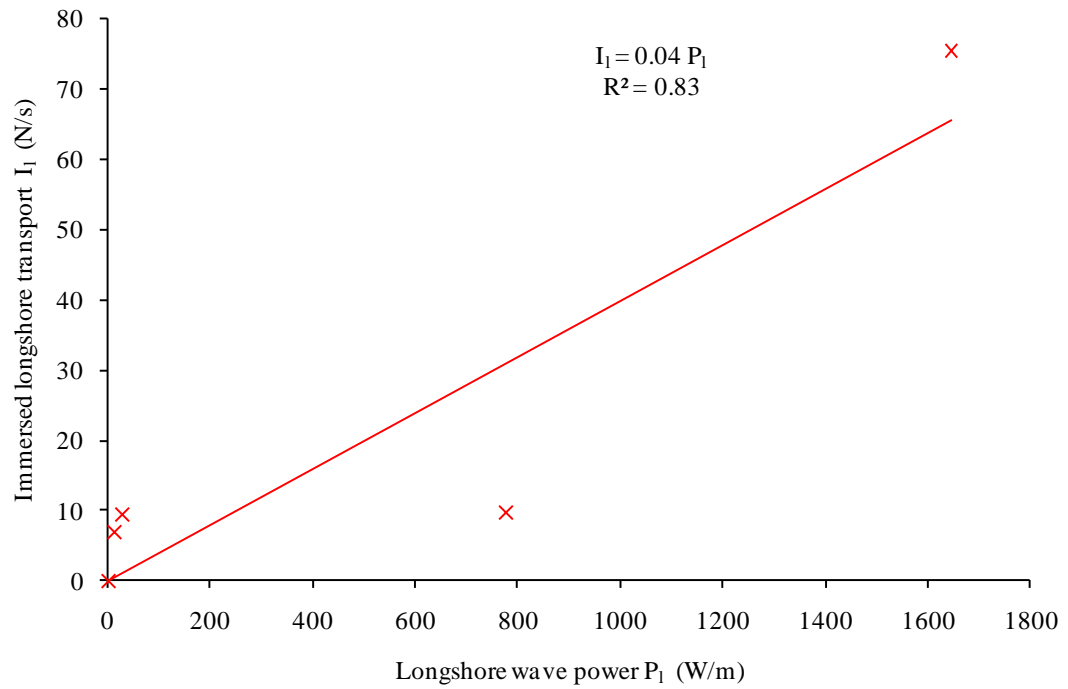
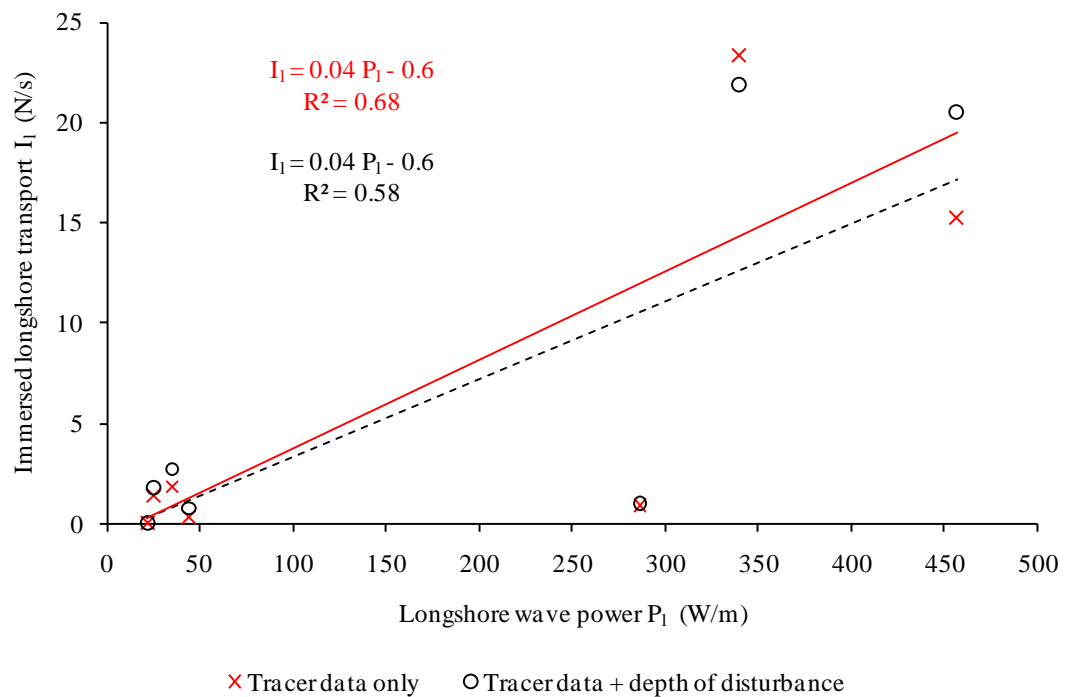


Figure 7-9 Estimation of K at Cayeux-sur-Mer.



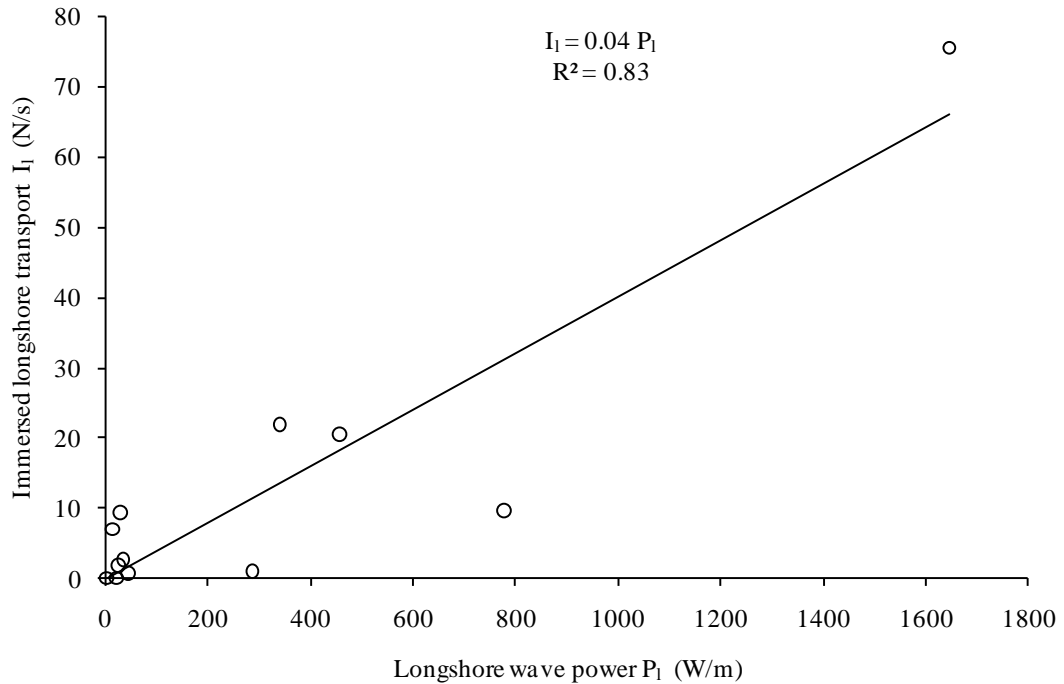


Figure 7-11 Estimation of K using the tracer data measurement points at both sites.

7.4 Discussion

7.4.1 Correlation between longshore wave power and LST rate

Firstly, the DGPS data showed extremely poor correlations at both sites between P_l and Q_l . The performance of the DGPS and the interpolation method on mixed beaches has been discussed earlier in Chapter 6. It is obvious now that the use of DGPS surveys on a short time scale (one tide) is not suitable for the measurement of accurate LST rates. At Cayeux-sur-Mer, which was a semi-closed system, the answer to a better resolution for the determination of the LST rates is to increase the time scale of the observations, allowing larger beach volumes to be removed by the hydrodynamics and therefore minimize the error linked to pebble imbrications and the precise relocation of the beach elevation measurements. However, increasing the time between the surveys would potentially reduce the precision of the K value as it would reduce the precision of the wave conditions which would cover a greater spectrum of wave heights, directions and periods. This compounds the view that the use of DGPS on a mixed beach, even with a centimetre elevation precision from the equipment, is to be taken with care when measuring LST rates. This observation supports Van Wellen et al.'s conclusions (1998)

about the poor performance of GPS techniques to estimate LST rates. At Birling Gap, the situation is slightly different, but the conclusions are the same. The correlation between P_1 and Q_1 are very poor, linked to two reasons. First, as at Cayeux, the error margins associated with such a technique are too great in contrast to the actual beach volume changes and therefore tidal surveys are of no use to measure detailed LST rates. In addition, it is obvious that by not having any controls on either the entry or exit of sediment from the beach system precise quantifications of sediment transport using DGPS surveys is rather difficult. However, it is believed that during the short duration of the survey periods (March, May and December 2006) the entries of sediment to the beach system at Birling Gap were minimal because of the geomorphological context of the area (Chapter 2 Section 2.1).

In contrast, the “strong” correlations between P_1 and Q_1 using tracers ($R^2 \geq 0.82$) indicate the good performance of this technique for measuring LST. The correlation using the depth of disturbance is only slightly greater than that using the depth of the deepest tracers (respectively $R^2 = 0.85$ against $R^2 = 0.82$). However, despite this difference, both techniques give reliable results for LST.

Despite these strong correlations, a number of criticisms about the reliability of the tracing method used in this study can be raised. First, when studying longshore sediment transport using tracer techniques, it is important for the tracers to be representative of the beach sediment in size and also shape to derive accurate LST rates. To obtain a reliable value for the drift efficiency coefficient the tracer should cover a large spectrum of grain size and shape distribution to be representative of mixed beaches (e.g. Nicholls and Wright, 1991). In practice, however, it is very difficult to deploy a wide range of tracers with different grain sizes. For example, tracing sand size particles onto a mixed sediment beach would be extremely difficult given that this particle size tends to percolate towards the deepest layers of the beach via the voids between coarser particles. Coring sediment on such beaches is practically impossible. Similarly, tracing gravel size particles would also be difficult as, in common with sand, gravel size particles are quite often buried under a hard pebbly surface or stuck between the voids of the coarsest classes of sediment. Note that an attempt to trace the gravel size of particles was made at both sites using small gravel size aluminium tracers.

However, many difficulties were encountered to recover such small particles. This was mostly because the paint washed off their surface, making them difficult to relocate, but also because the detection signal was very low which limited the recovery depth.

This study has focused on one specific size of pebbles, 30 to 40mm (b-axis), and so the results obtained are only representative of this fraction of the beach material. This fraction was however dominant in the beach material size distribution of both field sites.

The strong correlations obtained at Cayeux and Birling Gap (Figure 7-4 & 7-7) using the tracer data may seem controversial. On both sites, the lack of data lets the extreme values influence the respective coefficients of the correlation. However, filtering the data has made these values much more reliable with regards to the LST rates on both beaches. One way to clarify this point would be to collect more data on an even broader range of wave energies.

7.4.2 The coefficient of littoral drift (K)

First, at Birling Gap the use of each of the alternatives to measure the LST rate (excluding the method based on GPS surveys) derived equivalent K values (Figure 7-10). Therefore, the differences noted in Chapter 6 of up to 60.7% in the prediction of LST rate, is greatly attenuated when deriving the K value.

The value of K determined by this study is 0.04 (using H_s) which is 10.2 % of that for sand. When comparing this value to those described in the literature, the K value of this study (≈ 0.08 using H_{rms}) is greater than that obtained by Brampton and Motyka (1987), Nicholls and Wright (1991), Chadwick (1989) and Bray et al. (1996) but lower than the one derived by Komar (1988). Therefore, the value for K derived by this study fits well into the range of other published values. However, as Nicholls and Wright (1991) pointed out, on mixed beaches the sediment dynamics are very complex and some longshore energy is lost moving sand. Therefore, the available P_1 tends to be overestimated. As a consequence, K is underestimated here, and it is likely that the actual value of K on mixed beaches would be greater than 0.08 (referring to H_{rms}).

7.5 Conclusion

The decision to limit the amount of data available to those having recovery rates $\geq 60\%$ after one tide clearly reduced the amount of data points available to derive a regression line between P_1 and Q_1 and consequently between P_1 and I_1 . However, it was a necessary step to reduce scatter uncertainty and ensure the reliability of the LST rates measured.

The correlations between P_1 and Q_1 obtained for both sites using the most accurate data possible allowed an assessment of the reliability of the techniques used to measure LST rates. Thus, it could be seen that interpolation of DGPS surveys over single tides are not reliable to derive accurate LST rates whereas the use of tracers is very satisfactory throughout a wide spectrum of wave conditions.

The value of K derived by this study was 0.04 (using H_s) which is 10.2% that of sand. In comparison with other studies, this value is higher than most but still lower than the value given by Komar (1988).

The wide range of wave energy conditions permitted a calibration of the K value that included a few high energy wave conditions, which is relatively rare with data acquired from field experiments. However, the high selectivity of the used data led to a calibration derived from a small amount of data and it is crucial that further studies on the topic collect even more field data to refine the value of K derived by this study.

Chapter 8. Discussion and concluding remarks

8.1 Introduction

This chapter summarizes and discusses the key findings of the thesis in the wider context of research on mixed beaches. First it re-addresses the aim of the work and discusses how this study brings new perspectives to investigations of mixed beach dynamics. Then, it discusses how this study fits into the current stage of the research progress on mixed beaches. Next, it explores the importance of this work to the understanding of sediment transport processes and patterns. Finally, an overview of the principal findings is presented and the limitations of this study and potential future research directions are identified.

8.2 Meeting the overall aim

Aim: *“to contribute to the understanding of the processes of longshore sediment transport in open coast mixed beaches environments and the improvement of existing empirical models by providing reliable data than can be used to calibrate them”.*

In addressing this aim, the thesis has examined the three dimensional characteristics of longshore sediment transport, namely: its width, depth and length. It differs from other studies on gravel beaches in three respects. Firstly, because it focuses on a type of beach, mixed sediment (c.f. Jennings and Shulmeister, 2002), that has been little investigated and whose dynamics are not well understood because of the complexity of the interacting processes in a wide range of sediment classes; secondly, because of the frequency of data acquisition on key parameters necessary to measure LST rates more precisely than in the past; and thirdly because it has developed innovative methods for studying mixed beach dynamics.

This study is one of the first to collect topographic surveys on mixed beaches at a tidal timescale for periods of up to a complete spring-neap-spring tidal cycle. Although Austin and Masselink (2006) have conducted a similar study it was carried out on a pure gravel rather than a mixed beach. The frequency of the surveys facilitated the collection of beach spatial topographic changes at a high enough resolution to permit direct linkages with specific hydrodynamic conditions to be investigated. Responses of the mixed beach topographic profile to hydrodynamic forcing has been investigated in three different coastal environments: the first is a fringing beach where the beach material is restricted to a relatively small area backed by a cliff at Birling Gap, East Sussex, UK; the second is a beach fed by recycled material and the third a beach that does not benefit from any recycling and is not restricted spatially by a cliff or a recharge wall at its back. The latter two study sites are at Cayeux-sur-Mer, Upper Normandy, France.

This study is also one of the first to give precise measurements of the thickness of the active layer and the depth of disturbance along a beach profile under a wide range of wave and tidal conditions. Nicholls and Wright (1991) strongly expressed the necessity to collect data on the thickness of beach sediment that is mobile so that LST rates can be more precisely derived. This study has developed an innovative and precise experimental protocol that can be carried out reasonably quickly during the time that the beach is exposed by the low tide whilst minimising the cost and maximising the number of tracer pebbles deployed.

Finally, the third innovation contributes to sediment tracing on mixed beaches. This study has developed a new type of tracer pebble for use in tracing experiments, devised a new mode of deployment of these pebbles, and also experimented with their short-term recovery. The development of new “low cost” synthetic pebbles permitted the manufacture and deployment of more than 1200 tracers in total over the field experiments conducted during this thesis. This new type of tracer, made of a copper core fitted into epoxy resin, proved to be as reliable as the classic aluminium pebbles in relation to their recovery and their ability to adequately represent the movements of a natural flint pebble of the same size and shape. The originality of these tracing experiments is largely related to the fact that the tracer scatterings used to derive LST rates were those obtained after just one tide so that the scattering of specific pebbles can be related to specific wave and tidal conditions.

8.3 Context and relevance of this study to previous research

LST is the second most popular subject of research on beach dynamics after morphological and sedimentological studies, yet field studies on mixed beaches are relatively scarce in comparison with other types of gravel beach and certainly in comparison with sand beaches. This is partly because of the difficulties of precisely characterising the sediment that ranges from fine sand to cobbles and possibly boulders. A few studies are dedicated to the creation of indices in an effort to adequately represent the sediment mixture of mixed sediment beaches and classify their hydrodynamic behaviour as uni-modal or bi-modal (e.g. Sambroock-Smith et al., 1997; Wilcock et al., 2001). Although Horn and Walton (2007) have shown how useful and reliable such an index is they recommend that the sediment of mixed beaches needs to be characterised more precisely; not only should the sediment size and sorting be measured but also the hydraulic conductivity, the permeability, the porosity and the specific yield. This thesis sampled the beach sediment on a regular basis in order to characterise the beach surface sediment changes over time and space; the results are presented in Appendix II and are referred to where appropriate throughout the thesis.

Beach morphological studies focus on beach profile evolution are another area of research activity. Powell (1990) developed a model to predict the beach profile response on shingle beaches and indicated that this model, together with others, were in urgent need of reliable field data for calibration. He recommended that those data should cover a range of wave and tidal conditions and a variety of beaches. In response to Powell's call, Pontee (1995) and Pontee et al. (2004) collected data on both morphological and sedimentological changes of mixed sand and gravel beaches under managed and unmanaged conditions. However, as Pontee (1995) pointed out, more frequent topographical surveys were necessary to more precisely calibrate morphodynamic models on gravel beaches. Since then, only a few field studies have examined short time-scale gravel beach profile evolution (e.g. Stapleton et al., 1999; Jennings and Shulmeister, 2002; Austin and Masselink, 2006; Ivamy and Kench, 2006). Most observations are from laboratory models (e.g. Pedrozo-Acuña et al., 2006; 2007, 2008; Blanco et al., 2003; Lorang, 2002). This study proposed to fill this gap by providing new information on mixed beach profile elevation changes in three different environments (fringing beach, unmanaged unconfined beach, and recycled beach) on a tidal frequency up to periods of a complete semi-lunar cycle and on a type of beach that is clearly lacking in the scientific literature. The various field measurements taken under a wide range of wave and tidal conditions has permitted a response to Powell's requirements for his model.

Most of the studies investigating LST on gravel beaches agree on the fact that the volumes of transport derived from their tracer experiment measurements generally overestimate the actual sediment transport (Nicholls and Wright, 1991; Van Wellen, 1999; Van Wellen et al., 1998). They have stated that this overestimation is attributable to their way of estimating the depth of disturbance which assumes that the depth of disturbance is uniform and that its thickness corresponds to the deepest, or 95% of the deepest, tracers found during the recovery. Subsequently, Stapleton et al. (1999) investigated the depth of disturbance along the beach profile and found that the deepest thickness of sediment removed corresponded to the location of wave breaking, but there remains a clear requirement to measure and more fully understand the dynamics of such a key component of the LST. This study has investigated the alongshore and across-shore variation of the active layer, providing precise measurements of depth of

disturbance and the change in beach elevation simultaneously. It is recognised for sand beaches that the depth of disturbance is largely dependent on wave conditions, for example wave height, direction and period (Ciavola et al., 1997; Bertin et al., 2008) but the relationship has not been investigated for gravel or mixed beaches. In an attempt to fill this lack of knowledge this study has investigated correlations of wave parameters and grain size characteristics with the depth of disturbance.

In their review of field-databases for longshore sediment transport, Schoonees and Theron (1993) have outlined all the parameters that are essential to provide a reliable measurement of LST, namely: the distribution of the measured transport rate, the wave height, the wave period, the wave incidence angle, the grain size and the beach gradient. As a result, this study has made a point to collect each of these important parameters. In addition, a number of researchers specify that data collected on LST should be collected on the smallest time scales possible in order to reliably link the tracers' transport to specific hydrodynamic conditions (e.g. Nicholls and Webber 1991; Van Wellen, 1999). With the development of new tracers, recent studies such as those of Osborne (2005), Allan et al. (2006) or Bertoni et al. (2010) provide new research perspectives on tracing the pathways of individual sediment particles. This thesis complements such studies by carrying out tracing experiments on a mixed beach in contrast to the mixed sand and gravel beaches and pure gravel beaches investigated by the other studies.

Many studies investigating LST on gravel beaches and based on the energy flux approach have tried to develop empirical formulae based around the constant K (Komar, 1988; Chadwick, 1989; Bray, 1997; Nicholls and Wright, 1991), but so far no real consistent value has been derived that can be generalised to gravel beaches or even more specifically on mixed beaches. Komar (1988) indicated that more studies are needed to reach a K value that would be reliable for gravel beaches. This study's results will contribute to the data banks of K values developed for mixed beaches.

In summary, this thesis has responded to many recommendations from previous studies in order to extend their work and contribute to the scientific understanding of gravel beach dynamics. The specific aims and objectives and resultant findings contribute new

information on a coastal environment that is understudied in comparison to other beach types, namely mixed beaches.

8.4 Overview of main findings of this study

One of the first conclusions concerns the difference observed between the beach profiles at each of the study sites. A fringing gravel beach generally sustains steeper gradients, has a shorter profile, presents lower variability of grain size distribution and is less likely to record long term morphological features such as storm berms or seasonal patterns than an unconfined gravel beach. The presence of recycled/recharged material at the top of the beach profile has been found to influence the beach gradient, allowing the beach to sustain steeper slope angles. The beach surface material in the recycled area is also generally composed of finer sediment than the beach profile in the non-managed area, recycling material being composed of a large matrix of sand. Such characteristics have a significant impact on the beach properties. Indeed, the presence of sand allows the beach to sustain a stronger reflective beach profile in the recycled area but also reduces the hydraulic conductivity of the beach, reinforcing its strong reflective potential.

The short time period between the surveys has allowed a detailed examination of the processes of formation and development of the high water level ridge over time. The greatest changes in elevation have been observed in the sweep zone of the berm in relation to the build up and recession of this feature linked directly to the high water level and the wave height.

The active layer and the mixing depth together with the beach elevation changes, proved to be homogeneous alongshore as long as the hydrodynamic conditions and the beach properties (grain size, slope, orientation, elevation, and beach morphology) remained unchanged. Of the parameters measured, the depth of disturbance was found to be most closely correlated with the wave height and the wave direction, grain size distribution also had an influence, but there was very little correlation with the wave period. Comparison of the relationships linking the depth of disturbance and wave height shows

that at both sites the depth of disturbance, located at the mid-beach - approximately where wave breaking occurs, was 2.5 – 5 times lower at Birling Gap than at Cayeux-sur-Mer. When compared with steep sandy beaches, these depths of disturbance were 26% lower at Cayeux-sur-Mer and between 70 and 85% lower at Birling Gap.

The use of pebble tracers with a b-axis of 3 to 4 cm, which is representative of the dominant grain size in the coarsest fraction of the beach material at both sites, has provided new insights into particle behaviour on mixed beaches. The deployment positions of the tracer pebbles were crucial to their patterns of movement on the beach. Patterns of pebble scattering for the lower, mid-, and upper parts of the beach were linked to existing knowledge of the hydrodynamic conditions, swash flows, groundwater flow, beach slope and grain size. With the rising tide, pebbles from the lower part of the mixed beach move upward supposedly because of an impedance of the ground water flow by the water level, resulting in the uprush becoming dominant.

When the water table and the water level reach the mid-beach, the sediment will be saturated by water, and seaward currents will be strong enough to remobilise the beach material during the high tide. The backwash during the falling tide will drag the surface material down across the beach.

Pebbles located on the upper beach will spend greater time in the swash which moves them the furthest alongshore but also across-shore. Larger pebbles will offer more surface area to the driving hydrodynamics than smaller particles, explaining why they tend to travel further.

Based on the various correlations established by this study between the LST or the active layer and the hydrodynamic parameters or beach characteristics, it can be concluded that the wave height and consequently the swash is the most important parameter driving LST. The wave direction is the second most important parameter followed by the grain size distribution of the beach material. The grain size distribution will be responsible for the beach slope and the beach permeability. However, the beach slope and beach permeability will have a direct influence on the length of the swash reinforcing the fact that these parameters cannot be neglected. Finally, the wave period was the parameter that presented the lowest correlations.

The use of DGPS surveys and digital elevation models proved to be of limited value, at least on a tidal basis, for the accurate measurement of sediment volume transport rates on mixed beaches. In contrast, DGPS surveys regain their precision when the length of time between consecutive surveys is increased to allow greater sediment transport above error measurement. Similarly, the derivation of LST rates using only tracers and based on the assumption of a uniform mobile layer proved to be different from those measured using the depth of disturbance. These differences range from 0 up to 134.2% of the rates derived from the tracers alone.

The good correlations obtained between the longshore wave power (P_l) and the sediment transport rate (Q_l) proved the reliability of the technique of using tracers to derive LST rates whereas those collected on a tidal basis by the DGPS proved to be less satisfactory.

Based on the tracer measurements that experience recovery rates of $\geq 60\%$, a value for K was derived at 0.04 (using H_s , 10.2% of the sand) at each site, but also after merging the data from both sites.

8.5 Limitations of this study and recommendations for future work

This thesis has documented a number of responses and characteristics of mixed beaches. However, in common with most research theses, there are limitations regarding the volume of data collection, the analysis and the validity of the results. Such limitations help to point the way to future research directions and ways in which the work that is reported here can be extended:

1. The morphology and sedimentology of mixed beaches:

It is still necessary to collect more data about the morphological evolution of mixed beaches. Indeed, detailed surveys of the morphodynamic behaviour of such beaches remain understudied on short time scales, e.g. tidal or daily scales, especially during

stormy weather. Understanding more about the short term impact of storminess via pre-, during and post-storm beach profile surveys incorporating both morphology and sedimentology would help to make a significant contribution to coastal defence plans.

It is of primary importance to investigate in more detail the exact relationship between the sandy foreshore and the mixed sediment beach, particularly with respect to the quantities and the directions of sand exchanges between them. It appears that these depend directly on how the wave energy is dissipated but further investigation is needed. This study has highlighted the importance of surveying the maximum extent of the active beach profile of mixed beaches to include the sandy lower foreshore.

This study took the opportunity to examine beach morphodynamic evolution in the different types of coastal environment in which mixed beaches are encountered; however, it is crucial to increase the amount of topographical data collected on mixed beaches across a wide spectrum of wave climate in order to permit further morphodynamic comparisons and continue to improve understanding of their behaviour.

Although this study has collected data on the grain size of the beach surface sediment, time constraints have limited the extent to which these data have been interrogated and there is scope for further analyses. In addition, there has been no test of hydraulic conductivity or permeability or porosity. It is recommended that these parameters are characterised in future studies on mixed beaches as it is clear that their behaviour is strongly influenced by the sediment mixture.

This study has shown how recycled/recharged sediment material placed on the top of the beach can influence the beach gradient. However, it would be very interesting to observe the distribution pathways of this freshly supplied material. Horn and Walton (2007) have begun to examine how the sediment mixture evolves over time after rechargement/recycling. It would be interesting to join both high resolution beach profiles and sediment distribution patterns to work towards identifying the extent to which particular management strategies contribute to beach sustainability.

2. The active layer

This thesis is one of the first studies to have investigated and provide reliable data on the across-shore and alongshore variation of the boundary layer depth of mobile sediment on mixed beaches. It is imperative to collect more data on the active layer and the depth of disturbance over a wide range of wave conditions to gain a clearer understanding of the parameters influencing its depth across or along the beach.

3. The Longshore Sediment Transport

One of the weaknesses of this study is that it relied only on one size of tracer pebbles, which nevertheless was amongst the dominant grain size on both beaches. Further research on mixed beaches will need to investigate the LST for the different grain sizes present in the beach material. This will involve hard labour in terms of recovery depending on the number of tracers deployed. Attempts from this study to trace smaller grain sizes of sediment in the gravel size proved to be too difficult because the particles were too small to be satisfactorily traced within the beach, even using the metal detector. Painting the tracers also proved to be ineffective as the paint wore off after only one tide. The PIT pebbles that Allan et al. (2006) have developed are a potentially promising way to collect sediment transport information for a range of sizes of gravel.

This point leads on to the question of the number of tracers that are necessary to reliably represent the beach material. More statistical tools need to be developed in order to understand the optimum characteristics and number of tracers to be representative of the beach material and therefore give valuable information on the sediment transport. Such tools should take into account the grain size distribution and the shape and size of the particles as it has been shown that those characteristics influence the sediment transport. Such tools will have the advantage of validating the quality of a LST measurement on gravel beaches and permit to satisfactory comparison of results from one study to another (in the same way that Shoonees and Theron (1993) reviewed the field experiments on LST). Overall, it will permit the accurate calibration of predictive formulae and models.

Increasing the frequency of the data collection down to a tidal cycle proved to give reliable data about the LST rates and the sediment movement patterns, however more data are still needed in both cases from other beaches to support these results.

A key question investigated by this thesis concerns the performance of the DGPS surveys and digital elevation models used to derive short term (one tide) LST rates on mixed beaches in the context of low volumes of sediment transport. It is unlikely that adding more elevation data points will increase the precision of the digital elevation models; moreover a compromise is needed between the area covered by the topographical survey and the amount of data points collected. Resolution of this compromise will depend on the aims and objectives of future studies, but the limitations imposed by surface roughness, linked to the coarse grain size of gravel particles, remains.

The most significant achievement of this study has been the collection of a new database for mixed beaches: a large amount of data (grain size distribution in both along and across-shore, tracer pebble experiment, active layer measurements, GPS surveys on a large area of beach) on a tidal basis over a complete neap-spring-neap tidal cycle and large spectrum of wave energies. Interrogation of the resultant database has facilitated new insights into mixed beach dynamics and identified areas for future research. More studies are needed on mixed beaches in order to allow further comparisons of this thesis' field sites with other sites. It is hoped that the new insights that this study provides on the active layer and mixed beach dynamics will help to motivate researchers to add to the existing database so that it can be used to further understanding of the parameters controlling LST.

References

- Allan, J. C., Hart, R., and Tranquili, J. V. (2006). The use of Passive Integrated Transponder (PIT) tags to trace cobble transport in a mixed sand-and-gravel beach on the high-energy Oregon coast, USA. *Marine Geology* **232**, 63-86.
- Andrews, C., and Williams, R. B. G. (2000). Limpet erosion of chalk shore platforms in southeast England. *Earth Surface Processes and Landforms* **25**, 1371-1381.
- Aubrey, D. G. (1989). Measurements errors for electromagnetic current meters. In "Nearshore Sediment Transport." (R. J. Seymour, Ed.), pp. 67-78. Plenum Press, New York.
- Austin, M. J., and Buscombe, D. (2008). Morphological change and sediment dynamics of the beach step on a macrotidal gravel beach. *Marine Geology* **249**, 167-183.
- Austin, M. J., and Masselink, G. (2006). Observations of morphological change and sediment transport on a steep gravel beach. *Marine Geology* **229**, 59-77.
- Bagnold, R. A. (1940). Beach formation by waves: some model-experiments in a wave tank. *Journal of the Institute of Civil Engineers* **5237** 27-53.
- Bagnold, R. A. (1956). The flow of cohesionless grains in fluids. *Philosophical Transactions, Royal Society of London*, 235-297.
- Bagnold, R. A. (1963). Beach and nearshore processes part 1: mechanics of marine sedimentation. In "The sea - ideas and observations on progress in the study of the sea." (Interscience, Ed.), pp. 507-528, New York and London: Interscience Wiley.
- Bailard, J. A. (1984). A simplified model for longshore sediment transport. In "Proceedings of the 19th International Conference on Coastal Engineering." pp. 1454-1470. ASCE, Houston.
- Balouin, Y., Howa, H., and Michel, D. (2001). Swash platform morphology in the ebb-tidal delta of the Barra Nova inlet, South Portugal. *Journal of Coastal Research* **17**, 784-791.
- BAR. (2005). Beach material properties. In "Beaches at Risk." (Department of Geography. Unpublished project report, Ed.), pp. 25 University of Sussex, Falmer (UK).
- BAR. (2008). Geomorphology. In "Final Science report for phase II." (BAR. Unpublished project report, Ed.). Department of Geography, University of Sussex, Falmer (UK).
- Bauer, B. O., and Allen, J. R. (1995). Beach steps: an evolutionary perspective. *Marine Geology* **123**, 143-166.
- Beauchesne, P., and Courtois, G. (1967). Etude du mouvement des galets le long de la côte des Bas-Champs de la Somme. In "Cahiers Océanographiques; XIXeme années." pp. 613-625.
- Bellessort, B. (1990). Expertise du littoral des Bas-Champs (Sogreah, Ed.), pp. 49. DDE de la Somme.
- Bellessort, B., and Migniot, C. (1966). Protection de la côte des Bas-Champs, étude sédimentologique. Ponts et Chaussées, LCHF.
- Benedet, L., Finkl, C. W., Campbell, T., and Klein, A. (2004). Predicting the effect of beach nourishment and cross-shore sediment variation on beach morphodynamic assessment. *Coastal Engineering* **51**, 839-861.
- Bertin, X., Castelle, B., Anfuso, G., and Ferreira, Ó. (2008). Improvement of sand activation depth prediction under conditions of oblique wave breaking. In "Geo-Marine Letters." pp. 65-75. Springer Berlin / Heidelberg.
- Bertoni, D., Sarti, G., Benelli, G., Pozzebon, A., and Raguseo, G. (2010). Radio Frequency Identification (RFID) technology applied to the definition of underwater and subaerial coarse sediment movement. *Sedimentary Geology* **228**, 140-150.
- Bird, E. C. F. (1989). The beaches of Lyme Bay. In "Proc. Dorset Natural History and Archaeological Society." pp. 91-97.
- Bird, E. C. F. (1996). Lateral grading of beach sediments: A commentary. *Journal of Coastal Research* **12**, 774-785.

- Blanco, B., Coates, T. T., and Whitehouse, R. J. S. (2003). Development of Predictive Tools and Design Guidance for Mixed Beaches-Stage 2, pp. 309. HR Wallingford.
- Blott, S. J., and Pye, K. (2004). Morphological and Sedimentological Changes on an Artificially Nourished Beach, Lincolnshire, UK. *Journal of Coastal Research* **20**, 214-233.
- Bluck, B. J. (1967). Sedimentation of Beach Gravels examples from south Wales. *Journal of sedimentary petrology* **37**, 128-156.
- Bluck, B. J. (1999). Clast assembling, bed-forms and structure in gravel beaches. *Transactions of the Royal Society of Edinburgh, Earth Sciences* **89**, 291-323.
- Bodge, K. R., and Kraus, N. C. (1991). Critical examination of longshore transport rate magnitude. In "Proceedings of Coastal Sediments 91." pp. 139-155. ASCE, Seattle.
- Bournerias, M., Pomerol, C. and Turquier, Y. (1992). "Guides naturalists des cotes de France: La Manche, de Dunkerque au Havre". Delachaux et Niestle, 2nd edition.
- Bowen, A. J., and Inman, D. L. (1969). Rip Currents 2. Laboratory and Field Observations. *J. Geophys. Res.* **74**, 5479-5490.
- Bradbury, A. P., and McCabe, M. (2003). Morphodynamic Response of Shingle and Mixed Sand/Shingle Beaches in Large Scale Tests-Preliminary Observations. In "Hydrolab II- Towards a Balanced Methodology in European Hydraulic Research." pp. 9-11, Budapest.
- Bradbury, A. P., and Powell, K. A. (1992). Short term profile response of shingle spits to storm wave action. In "Proceedings of the 23rd International Conference of Coastal Engineering." pp. 2694-2707. ASCE, Venice, Italy.
- Brampton, A. H., and Motyka, J. M. (1987). Recent Examples of Mathematical Models of U.K. Beaches. In "Proceedings Coastal Sediments '87." pp. 515-530. ASCE, New York.
- Bray, M. J. (1996). "Beach budget analysis and shingle transport dynamics in West Dorset." Unpublished PhD thesis, University of London.
- Bray, M. J. (1997). Episodic Shingle Supply and the Modified Development of Chesil Beach, England. *Journal of Coastal Research* **13**, 1035-1049.
- Bray, M. J., Workman, M., Smith, J., and Pope, D. (1996). Field measurements of shingle transport using electronic tracers. In "Proceedings of the 31st MAFF Conference of River and Coastal Engineers." pp. 10.4.1 - 10.4.13, London.
- Briquet, A. (1930). Le littoral du nord de la France, évolution et morphologie (A. Colin, Ed.), pp. 438.
- Buscombe, D. (2008). Estimation of grain-size distributions and associated parameters from digital images of sediment. *Sedimentary Geology* **210**, 1-10.
- Buscombe, D., and Masselink, G. (2006). Concepts in gravel beach dynamics. *Earth-Science Reviews* **79**, 33-52.
- Butt, T., Russell, P., and Turner, I. (2001). The influence of swash infiltration-exfiltration on beach face sediment transport: onshore or offshore? *Coastal Engineering* **42**, 35-52.
- Caldwell, N. E. (1981). Relationship between tracers and background beach material (Wales). *Journal of Sedimentary Petrology* **51**, 1163-1168.
- Caldwell, N. E., and Williams, A. T. (1985). The role of beach profile configuration in the discrimination between differing depositional environments affecting coarse clastic beaches. *Journal Coastal Research* **1**, 129-139.
- Caldwell, N. E., and Williams, A. T. (1986). Spatial and seasonal pebble beach profile characteristics. *Geological Journal* **21**, 127-138.
- Carr, A. P. (1969). Size grading along a pebble beach; chesil beach, England. *Journal of Sedimentary Research* **39**, 297-311.
- Carr, A. P. (1983). Shingle beaches: aspects of their structure and stability. In "Shoreline Prediction." (I. o. C. Engineers, Ed.), pp. 97-104. Thomas Telford Ltd, London.
- Carter, R. W. G. (1988). "Coastal environments an introduction to the physical, ecological and cultural systems of coastlines." Academic Press, London.
- Carter, R. W. G., and Orford, J. D. (1980). Gravel barrier genesis and management. In "Proceedings Coastal Zone 80." (B. L. Edge, Ed.), pp. 1304-1320. ASCE, Hollywood, FL.

- Carter, R. W. G., and Orford, J. D. (1984). Coarse clastic barrier beaches: A discussion of the distinctive dynamic and morphosedimentary characteristics. *Marine Geology* **60**, 377-389.
- Carter, R. W. G., and Orford, J. D. (1993). The morphodynamics of coarse clastic beaches and barriers: a short- and long-term perspective. *Journal of Coastal Research*, 158-179.
- CETMEF. (2009a). <http://candhis.cetmef.developpement-durable.gouv.fr/>.
- CETMEF. (2009b). <http://anemoc.cetmef.developpement-durable.gouv.fr/>.
- Chadwick, A. J. (1989). Field measurements and numerical model verification of coastal shingle transport. In "Advances in Water Modelling and Measurement." (M. H. Palmer, Ed.), pp. 381-401. British Hydromechanics Research Association, Cranfield, UK.
- Chadwick, A. J. (1990). "Nearshore waves and longshore shingle transport." Unpublished PhD thesis, University of Brighton Polytechnic.
- Church, M. A., McLean, D. G., and Wolcott, J. F. (1987). River bed gravels: sampling and analysis. In "Sediment transport in gravel-bed rivers." (C. R. Thorne, J. C. Bathurst, and R. D. Hey, Eds.), pp. 43-79. John Wiley & Sons, Chichester.
- Ciavola, P., and Castiglione, E. (2009). Sediment dynamics of mixed sand and gravel beaches at short time-scales. *Journal of Coastal Research*, 1751-1755.
- Ciavola, P., Ferreira, Ó., Taborda, R., and Alveirinho Dias, J. (1995). Field assessment of longshore transport at Culatra Island (Portugal) using sand tracers. In "Resumos alargados do IV Congresso Nacional de Geologia." (F. SodréBorges, and M. M. Marques, Eds.), pp. 905-909. Mem. Mus. Lab. Mineral. Geol. Univ. Porto.
- Ciavola, P., Taborda, R., Ferreira, Ó., and Dias, J. A. (1997). Field observations of sand-mixing depths on steep beaches. *Marine Geology* **141**, 147-156.
- Clarke, D. J., Eliot, I. G., and Frew, J. R. (1984). Variation in subaerial beach sediment volume on a small sandy beach over a monthly lunar tidal cycle. *Marine Geology* **58**, 319-344.
- Coastal Channel Observatory. (2010). <http://www.channelcoast.org/>.
- Coates, T. T. (1994). Effectiveness of control structures on shingle beaches: physical model studies. HR Wallingford.
- Coates, T. T., Brampton, A. H., and Powell, K. A. (2001). Shingle beach recharge in the context of coastal defence: principles and problems. In "Ecology and geomorphology of coastal shingle." (J. R. Packham, R. E. Randall, R. S. K. Barnes, and A. Neal, Eds.), pp. 394-403, Westbury, Otley.
- Coates, T. T., and Mason, T. (1998). Development of Predictive Tools and Design Guidance for Mixed Beaches. HR Wallingford
- Coco, G., Burnet, B. T., and Werner, B. T. (2004). The role of tides in beach cusp development. *Journal of Geophysical Research*.
- Coco, G., Burnet, B. T., Werner, B. T., and Elgar, S. (2003). Test of a self-organisation model for beach cusp development. *Journal of Geophysical Research*, 21991-22002.
- Coco, G., Huntley, D. A., and O'Hare, T. J. (2001). Regularity and randomness in the formation of beach cusps. *Marine Geology* **178**, 1-9.
- Coco, G., O'Hare, T. J., and Huntley, D. A. (1999). Beach cusps: A comparison of data and theories for their formation. *Journal of Coastal Research* **15**, 741-749.
- Conley, D. C., and Inman, D. L. (1994). Ventilated oscillatory boundary layers. *Journal of Fluid Mechanics* **273**, 261-284.
- Conservatoire du Littoral. (2004). <http://www.conservatoire-du-littoral.fr/front/process/Home.asp>.
- Cooper, J. A. G., Jackson, D. W. T., Navas, F., McKenna, J., and Malvarez, G. (2004). Identifying storm impacts on an embayed, high-energy coastline: examples from western Ireland. *Marine Geology* **210**, 261-280.
- Costa, S. (1997). "Dynamique littorale et risques naturels : L'impact des aménagements, des variations du niveau marin et des modifications climatiques entre la Baie de Seine et la Baie de Somme." Unpublished PhD thesis, Université de Paris I.
- Costa, S., and Delahaye, D. (2002). Beach Erosion of the Rives Manche. In "Pérennité des plages de galets de l'Espace Rives-Manche-BERM." (D. Haute-Normandie, Ed.), pp.

90. Programme Européen de Recherche Interreg II.
- Costa, S., Laignel, B., and Quesnel, F. (1996). Les facteurs de localisation des entonnoirs de dissolution dans les craies de Seine-Maritime (Normandie, France). In "Colloque Formations superficielles et géomorphologie. 19-20 Mars 1996." BRGM, Rouen.
- Costa, S., Levoy, F., Monfort, O., Curoy, J., De Saint Leger, E., and Delahaye, D. (2008). Impact of sand content and cross-shore transport on the morphodynamics of macrotidal gravel beaches (Haute-Normandie, English Channel). *Zeitschrift für Geomorphologie* **52**, 41-62.
- Costa, S., and Regnaud, H. (1992). La vulnérabilité d'une partie du littoral de la Manche face à l'élévation du niveau marin. In "The impacts of recent Sea level and climatic changes en the Coast of Northwest France." (R. W. G. Carter, H. Regnaud, S. C. Jennings, C. Delaney, O. Monnier, S. Costa, and J. McKenna, Eds.), pp. 1-37. CEC Environnement Programme.
- Cowell, P. J., and Thom, B. G. (1994). Morphodynamics of coastal evolution. In "Coastal Evolution: Late Quaternary Shoreline Morphodynamics." (R. W. G. Carter, and C. D. Woodroffe, Eds.), pp. 33-86. Cambridge University Press, Cambridge
- Cressie, N. (1990). The origins of kriging. *Mathematical Geology* **22**, 239-252.
- Crickmore, M. J., Waters, C. B., and Price, W. A. (1972). The measurement of offshore shingle movement. In "Proceedings of the 13th Coastal Engineering Conference." pp. 1006-1023, Vancouver, Canada.
- Curoy, J., Dornbusch, U., Moses, C. A., Robinson, D. A., and Williams, R. B. G. (2007). Cross-Shore and Longshore Transport of Tracer Pebbles on a Macrotidal Mixed Sediment Beach, Somme Estuary, France (N. C. Kraus, and J. D. Rosati, Eds.), pp. 40. ASCE, New Orleans, Louisiana.
- Curoy, J., Moses, C. A., Robinson, D. A., and Williams, R. B. G. (2009). Profile evolution and active layer measurements on a macrotidal composite gravel beach, Somme Estuary, France. *Zeitschrift für Geomorphologie* **53**, 387-409.
- Curtiss, G. M., Osborne, P. D., and Horner-Devine, A. R. (2009). Seasonal patterns of coarse sediment transport on a mixed sand and gravel beach due to vessel wakes, wind waves, and tidal currents. *Marine Geology* **259**, 73-85.
- Dallery, F. (1955). "Les rivages de la Somme, autrefois , aujourd'hui et demain." A. et J. Picard & C., Paris.
- Damgaard, J. S., and Soulsby, R. L. (1996). Longshore bed-load transport. In "Proceedings of the 25th International Conference on Coastal Engineering." pp. 3614-3627. ASCE, Orlando.
- Dawe, I. N. (2006). "Longshore Sediment Transport on a Mixed Sand and Gravel Lakeshore." Unpublished PhD thesis, University of Canterbury.
- De Meijer, R. J., Bosboom, J., Cloin, B., Katopodi, I., Kitou, N., Koomans, R. L., and Manso, F. (2002). Gradation effects in sediment transport. *Coastal Engineering* **47**, 179-210.
- Dean, R. G. (1991). Equilibrium Beach Profiles: Characteristics and Applications. *Journal of Coastal Research* **7**, 53-84.
- Dean, R. G., and Maurmeyer, E. M. (1980). Beach cusps at Point Reyes and Drakes Bay beaches. In "Proc. 17th Int. Conf. Coastal Engineering." pp. 863-884. ASCE, California.
- Dolique, F. (1991). L'évolution du littoral entre Dieppe et Le Hourdel. In "Mémoire de maîtrise de géographie." (U. d. Picardie, Ed.), pp. 143, Amiens.
- Dolique, F. (1998). "Dynamique morphosédimentaire et aménagements induits du littoral Picard au sud de la Baie de Somme." Unpublished PhD thesis, University of Littoral.
- Dolique, F., and Anthony, E. (1999). Influence à moyen terme (10-100 ans) d'un estran sableux macrotidal sur la stabilité d'un cordon de galets : la flèche de Cayeux (Picardie, France). *Géomorphologie: relief, processus, environnement*, 23-38.
- Dornbusch, U., Robinson, D., Moses, C., and Williams, R. B. G. (2006b). Chalk coast erosion and its contribution to the shingle budget in East Sussex. *Zeitschrift für Geomorphologie Supplement Volume*, 215-230.
- Dornbusch, U., Robinson, D., Moses, C., Williams, R. B. G., and Costa, S. (2006a). Retreat of

- Chalk cliffs in the eastern English Channel during the last century. *Journal of Maps*, <http://www.journalofmaps.com>, 71-78.
- Dornbusch, U., Robinson, D. A., Moses, C. A., and Williams, R. B. G. (2008a). Temporal and spatial variations of chalk cliff retreat in East Sussex, 1873 to 2001. *Marine Geology* **249**, 271-282.
- Dornbusch, U., Robinson, D. A., Moses, C. A., and Williams, R. B. G. (2008b). Variation in beach behaviour in relation to groyne spacing and groyne type for mixed sand and gravel beaches, Saltdean, UK. *Zeitschrift für Geomorphologie* **52**, 125-143.
- Dornbusch, U., Williams, R., and Watt, T. (2005). Sedimentary structure of mixed sand and shingle beaches: preservation potential and environmental conditions. In "INQUA-IGCP 495 meeting: Late Quaternary Coastal Changes: Sea Level, Sedimentary Forcing and Anthropogenic Impacts." (C. Baeteman, Ed.). Belgian Geological Survey, Royal Belgian Institute of Natural Sciences, Dunkerque, France 28 June - 2 July 2005.
- Duncan Jr., J. R. (1964). The effects of water table and tide cycle on swash-backwash sediment distribution and beach profile development. *Marine Geology* **2**, 186-197.
- Dunkerley, D. L. (1994). Discussion: Bulk sampling of coarse clastic sediments for particle-size analysis. *Earth Surface Processes and Landforms* **19**, 255-261.
- Elfrink, B., and Baldock, T. (2002). Hydrodynamics and sediment transport in the swash zone: a review and perspectives. *Coastal Engineering* **45**, 149-167.
- Ferreira, Ó., Bairros, M., Pereira, H., Ciavola, P., and Dias, J. A. (1998). Mixing depth levels and distribution on steep fore-shores. *Journal of Coastal Research*, 292-296.
- Ferreira, O., Ciavola, P., Taborda, R., Bairros, M., and Dias, J. A. (2000). Sediment mixing depth determination for steep gentle foreshores. *Journal of Coastal Research* **16**, 830-839.
- Forbes, D. L., and Syvitski, J. P. M. (1995). Paraglacial coasts. In: "Coastal Evolution: Late Quaternary Shoreline Morphodynamics". R. W. G. Carter and C. D. Woodroffe (Editors), Cambridge Univ. Press, Chpt. 10, pp. 373-424.
- Forbes, D. L., Orford, J. D., Carter, R. W. G., Shaw, J., and Jennings, S. C. (1995). Morphodynamic evolution, self-organisation, and instability of coarse-clastic barriers on paraglacial coasts. *Marine Geology* **126**, 63-85.
- Forbes, D. L., Orford, J. D., Taylor, R. B., and Shaw, J. (1997). Interdecadal variation in shoreline recession on the Atlantic Coast of Nova Scotia. In "Proceedings of the Canadian Coastal Conference 1977." pp. 360-374. Canadian Coastal Science and Engineering Association, Canada.
- Fredsoe, J., and Deigaard, R. (1992). "Mechanics of coastal sediment transport." World Sci., River Edge, NJ.
- Gale, S. J., and Hoare, P. G. (1992). Bulk sampling of coarse clastic sediments for particle-size analysis. *Earth Surface Processes and Landforms* **17**, 729-733.
- Gale, S. J., and Hoare, P. G. (1994). Reply: Bulk sampling of coarse clastic sediments for particle-size analysis. *Earth Surface Processes and Landforms* **19**, 263-268.
- Gary, M., McAfee, R. J., and Wolf, C. L. (1974). "Glossary of Geology." American Geological Institute, Falls Church, VA.
- Greenwood, B., and Hale, P. B. (1980). Depth of activity, sediment flux and morphological change in a barred nearshore environment. In "The Coastline of Canada." (S. B. McCann, Ed.), pp. 89-109. Geological Survey of Canada, Halifax, Canada.
- Guza, R. T., and Inman, D. L. (1975). Edge Waves and Beach Cusps. *Journal of Geophysical Research* **80**, 2997-3012.
- H.R. Wallingford. (2010). <http://www.hrwallingford.co.uk/index.aspx>.
- Hascoët, M. (1988). Evolution du littoral Picard, entre le village d'Ault et le port du Hourdel (Somme), étude photogéomorphologique. In "Mer et Littoral, couple à risque.", pp. 465-477. Ministère de l'environnement, Biarritz.
- Hattori, M., and Suzuki, T. (1978). Field experiment on beach gravel transport. In "Proceedings of the 16th international conference on coastal engineering." pp. 1688-1704. ASCE, Hamburg.

- Haugel, A., and Cherubini, P. (1980). Analyse statistiques des surcôtes de pleine mer et des décôtes de basse mer à Dieppe, pp. 35. EDF-DER HE
- Heraud, G. (1880). Rapport sur la reconnaissance de la baie de Somme et de ses abords en 1878. In "Recherches Hydrographiques. Régime côtes.", pp. 77.
- Holland, K. T., and Holman, R. A. (1996). Field observations of beach cusps and swash motions. *Marine Geology* **134**, 77-93.
- Holmes, P., Baldock, T. E., Chan, R. T. C., and Neshaei, M. A. L. (1996). Beach evolution under random waves. In "Proceedings of 25th International Conference on Coastal Engineering." pp. 3006-3018. ASCE, Orlando, Florida.
- Horn, D., and Li, L. (2006). Measurement and Modelling of Gravel Beach Groundwater Response to Wave Run-up: Effects on Beach Profile Changes. *Journal of Coastal Research* **22**, 1241-1249.
- Horn, D. P. (2002). Beach groundwater dynamics. *Geomorphology* **48**, 121-146.
- Horn, D. P. (2006). Measurements and modelling of beach groundwater flow in the swash-zone: a review. *Continental Shelf Research* **26**, 622-652.
- Horn, D. P., and Mason, T. (1994). Swash zone sediment transport modes. *Marine Geology* **120**, 309-325.
- Horn, D. P., and Walton, S. M. (2007). Spatial and temporal variations of sediment size on a mixed sand and gravel beach. *Sedimentary Geology* **202**, 509-528.
- Horrillo-Caraballo, J. M., and Reeve, D. E. (2008). Morphodynamic behaviour of a nearshore sandbank system: The Great Yarmouth Sandbanks, U.K. *Marine Geology* **254**, 91-106.
- Hughes, M. G., and Cowell, P. J. (1987). Adjustment of reflective beaches to waves. *Journal of Coastal Research* **3**, 153-167.
- Hughes, M. G., Masselink, G., and Brander, R. W. (1997). Flow velocity and sediment transport in the swash zone of a steep beach. *Marine Geology*, 91-103.
- Hughes, M. G., Masselink, G., Hanslow, D., and Mitchell, D. (1998). Towards a better understanding of swash-zone sediment transport. In "Proceedings of Coastal Dynamics '97." pp. 804-813. ASCE, Plymouth, U.K.
- Humphreys, B., Coastes, T. T., Watkiss, M. J., and Harrison, D. J. (1996). Beach recharge materials - demand and resources. In "Construction Industry Research and Information Association." pp. 12. CIRIA, London.
- Inman, D. L., and Bagnold, R. A. (1963). Littoral processes, the sea. In "The earth beneath the sea." (M. N. Hill, Ed.), pp. 529-551. Interscience, NY.
- Inman, D. L., Tait, R. J., and Nordstrom, C. E. (1971). Mixing in the surf zone. *Journal of Geophysical Research*, 3493-3514.
- Inman, D. L., Zampol, J. A., White, T. E., Hanes, D. M., Waldorf, B. W., and Kastens, K. A. (1980). Field measurements of sand motion in the surf zone. In "Proceedings of 17th International Coastal Engineering Conference." pp. 1215-1234. ASCE, Australia.
- Inter Ocean systems inc. (2010). <http://www.interoceansystems.com/s4theory.htm>.
- Ivamy, M. C., and Kench, P. S. (2006). Hydrodynamics and morphological adjustment of a mixed sand and gravel beach, Torere, Bay of Plenty, New Zealand. *Marine Geology* **228**, 137-152.
- Jackson, N. L., and Nordstrom, K. F. (1993). Depth of activation of sediment by plunging breakers on a steep sand beach. *Marine Geology* **115**, 143-151.
- Janin, J. M., and Blanchard, X. (1992). Simulation des courants de marée en Manche et proche Atlantique, pp. 73.
- Janin, J. M., and Dumas, F. (1993). Modélisation fine des dérives lagrangiennes en Manche par un code aux éléments finis. In "Journées nationales génie côtier génie civil." pp. 18. EDF-HE, Sète.
- Jennings, R., and Shulmeister, J. (2002). A field based classification scheme for gravel beaches. *Marine Geology* **186**, 211-228.
- Jennings, S., Orford, J. D., Canti, M., Devoy, R. J. N., and Straker, V. (1998). The role of relative sea-level rise and changing sediment supply on Holocene gravel barrier development: the example of Porlock, Somerset, UK. *The Holocene* **8**, 165-181.

- Jolliffe, I. P. (1961). The use of tracers to study beach movements and the measurement of littoral drift by a fluorescent technique. *Revue de Geomorphologie dynamique* **XII**, 81-98.
- Jolliffe, I. P. (1964). An experiment designed to compare the relative rates of movement of beach pebbles. In "Proceedings of the Geologists' Association." pp. 67-86.
- Kallinske, A. A. (1947). Movement of sediment as bed-load in rivers. *Transactions of American Geophysical Union*, 615-620.
- Kamphuis, J. W. (1991). Alongshore Sediment Transport Rate. *Journal of Waterway, Port, Coastal, and Ocean Engineering* **117**, 624-640.
- Kamphuis, J. W. (1992). Basics of coastal sediment transport; Basic shore processes; One dimensional modelling of coastal morphology and 2D and quasi 3D modelling of coastal morphology. In "Proceedings of the Short Course attached to 23rd International Conference on Coastal Engineering." ASCE.
- Kamphuis, J. W., Davies, M. H., Nairn, R. B., and Sayao, O. J. (1986). Calculation of littoral sand transport rate. *Coastal Engineering* **10**, 1-21.
- Kemp, P. H. (1963). A field study of wave action on natural beaches. *Proceedings of the 10th International Association Hydraulic Research* **1**, 131-138.
- Kidson, C., and Carr, A. P. (1959). The Movement of Shingle Over the Sea Bed Close Inshore. *The Geographical Journal* **125**, 380-389.
- King, C. A. M. (1951). Depth of disturbance of sand on sea beaches by waves. *Journal of Sedimentary Petrology* **21**, 131-140.
- King, C. A. M., and Williams, W. W. (1949). The Formation and Movement of Sand Bars by Wave Action. *The Geographical Journal* **113**, 70-85.
- Kirk, R. M. (1969). Beach Erosion and Coastal Development in the Canterbury Bight. *New Zealand Geographer* **25**, 23-35.
- Kirk, R. M. (1992). Artificial beach growth for breakwater protection at the Port of Timaru, east coast, South Island, New Zealand. *Coastal Engineering* **17**, 227-251.
- Kochel, R. C., and Dolan, R. (1986). The Role of Overwash on a Mid-Atlantic Coast Barrier Island. *The Journal of Geology* **94**, 902-906.
- Kokot, R. R., Monti, A. A. J., and Codignotto, J. O. (2005). Morphology and Short-Term Changes of the Caleta Valdés Barrier Spit, Argentina. *Journal of Coastal Research* **21**, 1021-1030.
- Komar, P. D. (1976). "Beach processes and sedimentation." Englewood Cliffs, NJ.
- Komar, P. D. (1983). Rhythmic shoreline features and their origin. In "Mega-Geomorphology." (R. Gardener, and H. Scoging, Eds.), pp. 92-112. Clarendon Press, Oxford University Press, New York.
- Komar, P. D. (1988). Environmental Controls on Littoral Sand Transport. In "Proceedings of 21st Coastal Engineering Conference." pp. 1238-1252. ASCE, Malaga, Spain.
- Komar, P. D. (1998). "Beach processes and Sedimentation." Prentice-Hall, Englewood Cliffs, New Jersey.
- Komar, P. D., and Inman, D. L. (1970). Longshore sand transport on beaches. *Journal of Geophysical Research* **75**, 5914-5927.
- Kraus, N. C. (1985). Field experiments on vertical mixing of sand in the surf zone. *Journal of Sedimentary Petrology* **55**, 3-14.
- Kraus, N. C. (1987). Application of Portable Traps for Obtaining Point Measurements of Sediment Transport Rates in the Surf Zone. *Journal of Coastal Research* **3**, 139-152.
- Kroon, A. (1994). "Sediment transport and morphodynamics of the beach and nearshore zone, near Egmond, The Netherlands." Unpublished PhD thesis, University of Utrecht.
- Laignel, B. (1997). "Les altérites à silex de l'Ouest du Bassin de Paris : caractérisation lithologique, genèse et utilisation potentielle comme granulats". Unpublished PhD thesis, University of Rouen, Edit. BRGM, Orléans, 264, 219 p.
- Lara, J. L., Losada, I.J., Cowen, E.A. (2002). Large-scale turbulence structures over an immobile gravel-bed inside the surf zone. In Smith, J. M. (Ed.), 28th International Conference on Coastal Engineering, ASCE, Sidney, Australia, pp. 624-636.

- Laronne, J., Outhet, D., Carling, P. A., and McCabe, T. (1994). Scour chain employment in gravel bed rivers. *Catena*, 229-306.
- Larson, M., and Sunamura, T. (1993). Laboratory experiment on flow characteristics at a beach step. *Journal of Sedimentary Petrology* **63**, 495-500.
- LCHF. (1965). Baie de Somme, mission d'études en nature, rapport de fin de mission.
- LCHF. (1972). Etude de la production des galets sur le littoral haut-normand, pp. 63. Laboratoire Central d'Hydraulique de France.
- Leatherman, S. P. (1976). Barrier island dynamics: overwash processes and eolian transport. In "Proceedings 15th Coastal Engineering Conference." pp. 1959-1974. ASCE, Honolulu, Hawaii.
- Leatherman, S. P. (1981). Overwash Processes. In "Benchmark Papers in Geology." pp. 376. Hutchinson Ross Publishing Co, Stroudsburg, Pennsylvania.
- Lee, A. J., and Ramster, J. W., (1981). Atlas of the Seas around the British Isles. *Minist. Agric. Fish. Food*, Lowestoft, 140 pp.
- Lee, K.-H., Mizutani, N., Hur, D.-S., and Kamiya, A. (2007b). The effect of groundwater on topographic changes in a gravel beach. *Ocean Engineering* **34**, 605-615.
- Lee, M. W. E., Bray, M. J., Workman, M., Collins, M. B., and Pope, D. (2000). Coastal shingle tracing: a case study using the (electronic tracer system) (ETS). In "Tracers in Geomorphology." (I. L. D. Foster, Ed.), pp. 413-435. John Wiley and Sons.
- Lee, M. W. E., Sear, D. A., Atkinson, P. M., Collins, M. B., and Oakey, R. J. (2007a). Number of tracers required for the measurement of longshore transport distance on a shingle beach. *Marine Geology* **240**, 57-63.
- Levoy, F. (1994). "Evolution et fonctionnement hydrosédimentaire des plages macrotidales-L'exemple de la côte ouest du Cotentin." Unpublished PhD thesis, University of Caen.
- Levoy, F., Anthony, E. J., Barusseau, J. P., Howa, H., and Tessier, B. (1998). Morphodynamique d'une plage macrotidale à barres. *Comptes-Rendus de l'Académie des Sciences*, 811-818.
- Longuet-Higgins, M. S., and Parkin, D. W. (1962). Sea Waves and Beach Cusps. *The Geographical Journal* **128**, 194-201.
- Lorang, M. S. (2002). Predicting the crest height of a gravel beach. *Geomorphology* **48**, 87-101.
- Madsen, O. S. (1989). Tracer theory. In "Nearshore Sediment Transport." (R. J. Seymour, Ed.), pp. 103-114. Plenum Press, New York.
- Mason, T. (1997). "Hydrodynamics and sediment transport on a macro-tidal, mixed (sand and shingle) beach." Unpublished PhD thesis, University of Southampton.
- Mason, T., and Coates, T. T. (2001). Sediment transport processes on mixed beaches: A review for shoreline management. *Journal of Coastal Research* **17**, 645-657.
- Mason, T., Voulgaris, G., Simmonds, D. J., and Collins, M. B. (1997). Hydrodynamics and sediment transport on composite (mixed sand/shingle) and sand beaches: A comparison. In "Coastal Dynamics - Proceedings of the International Conference." pp. 48-57.
- Masselink, G., and Black, K. P. (1995). Magnitude and cross-shore distribution of bed return flow measured on natural beaches. *Coastal Engineering* **25**, pp. 165-190.
- Masselink, G., Hegge, B. J., and Pattiaratchi, C. B. (1997). Beach cusp morphodynamics. *Earth Surface Processes and Landforms* **22**, 1139-1155.
- Masselink, G., and Hughes, M. (1998). Field investigation of sediment transport in the swash zone. *Continental Shelf Research* **18**, 1179-1199.
- Masselink, G., and Hughes, M. G. (2003). "Introduction to Coastal Processes & Geomorphology." Hodder Arnold, London.
- Masselink, G., and Pattiaratchi, C. B. (1998). Morphological evolution of beach cusps and associated swash circulation patterns. *Marine Geology* **146**, 93-113.
- Masselink, G., Russell, P., Coco, G., and Huntley, D. A. (2004). Test of edge wave forcing during formation of rhythmic beach morphology. *Journal of Geophysical Research*, 1-10.
- Masselink, G., and Short, A. D. (1993). Further experiments using radioactive methods to detect the movement of shingle over the sea bed and alongshore. *Journal of Coastal Research*

- 9, 785-800.
- Matsunaga, N., and Honji, H. (1980). The backwash vortex. *Journal of Fluid Mechanics* **99**, 813-815.
- McFarland, S., Whitcombe, L., and Collins, M. (1994). Recent shingle beach renourishment schemes in the UK: some preliminary observations. *Ocean & Coastal Management* **25**, 143-149.
- McKay, P. J., and Terich, T. A. (1992). Gravel Barrier Morphology: Olympic National Park, Washington State, U.S.A. *Journal of Coastal Research* **8**, 813-829.
- Mii, H. (1958). Beach cusps on the Pacific Coast of Japan. In "Science Reports." pp. 77-107. Tohoku University, Sendai.
- Miller, J. R., Orbock Miller, S. M., Torzynski, C. A., and Kochel, R. C. (1989). Beach Cusp Destruction, Formation, and Evolution during and Subsequent to an Extratropical Storm, Duck, North Carolina. *The Journal of Geology* **97**, 749-760.
- Moore, R., Collins, T. and King, A. 2001. The geology and geomorphology at Birling Gap, East Sussex: the scientific case for geo-conservation. *Proceedings of the 36th DEFRA Conference of River and Coastal Engineers*, 02.3.1-02.3.12.
- Morfett, J. (1988). Modelling shingle beach evolution. In "Modelling of Sediment Transport in the Coastal Zone." pp. 148-155. International Association of Hydraulic Engineering and Research, Copenhagen.
- Morfett, J. C. (1989). The development and calibration of an alongshore shingle transport formula. *Journal of Hydraulic Research* **27**, 717 - 730.
- Morton, R. A., Leach, M. P., Paine, J. G., and Cardoza, M. A. (1993). Monitoring Beach Changes Using GPS Surveying Techniques. *Journal of Coastal Research* **9**, 702-720.
- Moses, C. A., and Williams, R. B. G. (2008). Artificial beach recharge: the South East England experience. *Zeitschrift fur Geomorphologie* **52**, 107-124.
- Neal, A., Richards, J., and Pye, K. (2002). Structure and development of shell cheniers in Essex, southeast England, investigated using high-frequency ground-penetrating radar. *Marine Geology* **185**, 435-469.
- Nestoroff, W., and Melieres, F. (1967). L' érosion littorale du pays de Caux. *Bulletin de la Société Géologique de France*, 159-169.
- Nicholls, R. J. (1985). "The stability of the shingle beaches in the eastern half of Christchurch Bay." Unpublished PhD thesis, University of Southampton.
- Nicholls, R. J. (1989). The measurement of the depth of disturbance caused by waves on pebble beaches. *Journal of Sedimentary Petrology* **59**, 630-631.
- Nicholls, R. J., and Webber, N. B. (1987). Coastal erosion in the eastern half of Christchurch Bay. In "Planning and Engineering Geology." (M. G. Culshaw, F. G. Bell, J. C. Cripps, and M. O'Hara, Eds.), pp. 549-554. Geological Society Engineering Geology London.
- Nicholls, R. J., and Wright, P. (1991). Longshore transport of pebbles: experimental estimates of K. In "Proceedings of the Conference on Coastal Sediments '91." pp. 920-933. ASCE, New York.
- Nielsen, P. (1997). Coastal groundwater dynamics. In "Coastal Dynamics '97." (E. B. Thornton, Ed.), pp. 546-555. ASCE, Plymouth, UK.
- Nielsen, P., Robert, S., Møller-Christiansen, B., and Oliva, P. (2001). Infiltration effects on sediment mobility under waves. *Coastal Engineering* **42**, 105-114.
- Nolan, T. J., Kirk, R. M., and Shulmeister, J. (1999). Beach cusp morphology on sand and mixed sand and gravel beaches, South Island, New Zealand. *Marine Geology* **157**, 185-198.
- Nowell, D. (2007). Chalk and landscape of the South Downs, England. *Geology Today* **23**, 147-152.
- Oertel, G. F. (1972). Sediment transport of estuary entrance shoals and the formation of swash platforms. *Journal of Sedimentary Petrology* **42** 858-868.
- Orford, J. D. (1975). Discrimination of particle zonation on a pebble beach. *Sedimentology* **22**, 441-463.
- Orford, J. D. (1977). A proposed mechanism for storm beach sedimentation. *Earth Surface*

- Processes* **2**, 381-400.
- Orford, J. D. (1978). "Methods of identifying and interpreting the dynamics of littoral zone facies using particle facies and form, with special reference to beach gravel sedimentation." Unpublished PhD thesis, University Reading, UK.
- Orford, J. D. (1986). Discussion: Gravel Beach Profile Characterization and Discrimination. *Journal of Coastal Research* **2**, 205-210.
- Orford, J. D., and Carter, R. W. G. (1982). Geomorphological changes on the barrier coasts of South Wexford. *Irish Geography* **15**, 70 - 84.
- Orford, J. D., and Carter, R. W. G. (1995). Examination of mesoscale forcing of a swash-aligned, gravel barrier from Nova Scotia. *Marine Geology* **126**, 201-211.
- Orford, J. D., Carter, R. W. G., and Jennings, S. C. (1996). Control domains and morphological phases in gravel dominated coastal barriers of Nova Scotia. *Journal of Coastal Research* **12**, 589-604.
- Orford, J. D., Carter, R. W. G., Jennings, S. C., and Hinton, A. C. (1995). Processes and timescales by which a coastal gravel-dominated barrier responds geomorphologically to sea-level rise: Story head barrier, Nova Scotia. *Earth Surface Processes and Landforms* **20**, 21-37.
- Orford, J. D., Forbes, D. L., and Jennings, S. C. (2002). Organisational controls, typologies and time scales of paraglacial gravel-dominated coastal systems. *Geomorphology* **48**, 51-85.
- Orford, J. D., Murdy, J. M., and Wintle, A. G. (2003). Prograded Holocene beach ridges with superimposed dunes in north-east Ireland: mechanisms and timescales of fine and coarse beach sediment decoupling and deposition. *Marine Geology* **194**, 47-64.
- Osborne, P. D. (2005). Transport of gravel and cobble on a mixed-sediment inner bank shoreline of a large inlet, Grays Harbor, Washington. *Marine Geology* **224**, 145-156.
- Otvos, E. G. (1965). Sedimentation-erosion cycles of single tidal periods on Long Island Sound beaches. *Journal of Sedimentary Petrology* **35**, 604-609.
- Pedrozo-Acuña, A. (2005). "Concerning swash on steep beaches." Unpublished PhD thesis, University of Plymouth.
- Pedrozo-Acuña, A., Simmonds, D. J., Chadwick, A. J., and Silva, R. (2007). A numerical-empirical approach for evaluating morphodynamic processes on gravel and mixed sand-gravel beaches. *Marine Geology* **241**, 1-18.
- Pedrozo-Acuña, A., Simmonds, D. J., Otta, A. K., and Chadwick, A. J. (2006). On the cross-shore profile change of gravel beaches. *Coastal Engineering* **53**, 335-347.
- Pedrozo-Acuña, A., Simmonds, D. J., and Reeve, D. E. (2008). Wave-impact characteristics of plunging breakers acting on gravel beaches. *Marine Geology* **253**, 26-35.
- Pierowicz, J., and Boswood, P. (1995). Interaction between natural processes on macro tidal beaches. Case study along Capricorn coast, Australia. In "Proceedings of Coastal Dynamics '95." pp. 489-500. ASCE, Gdansk, Poland.
- Pontee, N. I. (1995). "The morphodynamics and sedimentary architecture of mixed sand and gravel beaches." Unpublished PhD thesis, University of Reading.
- Pontee, N. I., Pye, K., and Blott, S. J. (2004). Morphodynamic Behaviour and Sedimentary Variation of Mixed Sand and Gravel Beaches, Suffolk, UK. *Journal of Coastal Research* **20**, 256-276.
- Postford Duvivier (1993). Birling Gap Cliff Stability Report. Report to Wealden District Council.
- Powell, K. A. (1990). Predicting short-term profile response for shingle beaches, pp. 72. HR Wallingford.
- Prêcheur, C. (1960). Le littoral de la Manche : de Saint-Adresse à Ault. In "Etude morphologique." pp. 1-138, Norois.
- Quick, M. C. (1991). Onshore-offshore sediment transport on beaches. *Coastal Engineering* **15**, 313-332.
- Quick, M. C., and Dyksterhuis, P. (1994). Cross-shore transport for beaches of mixed sand and gravel. In "International Symposium: Waves - physical and numerical modelling." pp. 1443-1452. Canadian Society of Civil Engineers, Vancouver.

- Randall, R. E., Sneddon, P., and Doody, P. (1990). "Coastal Shingle in Great Britain: a Preliminary Review." Nature Conservancy Council, Peterborough.
- Regrain, R. (1971). Etude géographique, essai de géomorphologie statique, cinématique et dynamique du littoral Picard. In "C.R.D.P.", pp. 107, Amiens.
- Regrain, R., Vignon, F., and Wattez, J. R. (1979). Un secteur Côtier d'intérêt scientifique particulier: les Bas-Champs de Cayeux (Somme). In "Acte du Colloque N2." pp. 165-179. Publications scientifiques et techniques du CNEXO, Brest.
- Richardson, N. M. (1902). An experiment on the movement of a load of brickbats deposited on the Chesil Beach. In "Proceedings of the Dorset Natural History and Archaeological Society." pp. 123-133.
- Robin, N. (2007). "Morphodynamique des systèmes de fleches sableuses: Etude entre les embouchures tidales de l'Archipel de St Pierre et Miquelon et de la côte ouest du Cotentin (Manche)." Unpublished PhD thesis, Université de Caen.
- Russel, R. J., and McIntire, W. G. (1965). Beach Cusps. *Geological Society of America Bulletin* **76**, 307-320.
- Russell, R. C. H. (1960). The use of fluorescent tracers for the measurement of littoral drift. In "Proceedings of the 7th Conference on Coastal Engineering." The Hague.
- Sager, G., und Sammler, R., (1968). Atlas der Gezeitenströme für die Nordsee und den Kanal und die Irische See, 58 pp. Rostock: Seehydrographischer Dienst der DDR.
- Saini, S., Jackson, N. L., and Nordstrom, K. F. (2009). Depth of activation on a mixed sediment beach. *Coastal Engineering* **56**, 788-791.
- Sallenger Jr., A. H. (1979). Beach-cusp formation. *Marine Geology* **29**, 23-37.
- Sambrook Smith, G. H., Nicholas, A. P., and Ferguson, R. I. (1997). Measuring and defining bimodal sediments: Problems and implications. *Water Resources Research* **33**, 1179-1185.
- Savage, S. B. (1984). The Mechanics of Rapid Granular Flows. In "Advances in Applied Mechanics." (J. W. Hutchinson, and T. Y. Wu, Eds.), pp. 289-366. Elsevier.
- Schoonees, J. S., and Theron, A. K. (1993). Review of the field-data base for longshore sediment transport. *Coastal Engineering* **19**, 1-25.
- Schwartz, R. K. (1975). Nature and Genesis of Some Storm Wash-over Deposits. In "Technical Memorandum 61." U.S. Army Corps of Engineers, Belvoir, Virginia.
- Sear, D. A., Collins, M. B., Carling, P. A., Lee, M. W. E., and Oakey, R. J. (2001). Coarse Sediment Transport Measurement in Rivers and on Coast using Advanced Particle Tracing. In "Review Report for EPSRC ". Univeristy of Southampton.
- Seymour, R. J., and Aubrey, D. G. (1985). Rhythmic beach cusp formation: A conceptual synthesis. *Marine Geology* **65**, 289-304.
- She, K., Horn, D. P., and Canning, P. (2007). Influence of permeability on the performance of shinge and mixed beaches. In "Joint Defra/EA flood and coastal erosion risk management R&D programme." pp. 86. Defra, London.
- Shepard, F. P., and LaFond, E. C. (1940). Sand movements along the Scripps Institution pier. *Am. J. Sci.* **238**, 272-285.
- Sherman, D. J. (1991). Gravel beaches. *National Geographic Research & Exploration* **7**, 442-452.
- Sherman, D. J., Nordstrom, K. F., Jackson, N. L., and Allen, J. R. (1994). Sediment mixing-depths on a low-energy reflective beach. *Journal of Coastal Research* **10**, 297-305.
- Sherman, D. J., Orford, J. D., and Carter, R. W. G. (1993). Development of cusp-related, gravel size and shape facies at Malin Head, Ireland. *Sedimentology* **40**, 1139-1152.
- SHOM. (1997). "La Marée." Service Hydrographique et Océanographique de la Marine, Brest.
- Short, A. D. (1984). Temporal change in beach type resulting from a change in grain size. *Search* **15**, 228-230.
- Short, A. D. (1999). Handbook of beach and shoreface mophodynamics, pp. 376. John Wiley & Sons.
- Shulmeister, J., and Kirk, R. M. (1993). Evolution of a mixed sand and gravel barrier system in North Canterbury, New Zealand, during Holocene sea-level rise and still-stand.

- Sedimentary Geology* **87**, 215-235.
- Shulmeister, J., and Kirk, R. M. (1997). Holocene fluvial-coastal interactions on a mixed sand and sand and gravel beach system, North Canterbury, New Zealand. *Catena* **30**, 337-355.
- Simon, B. (1994). Statistique des niveaux marins extrêmes le long des côtes de France. In "Rapport d'études et de recherches." pp. 78.
- Sneddon, P., and Randall, R. E. (1991). Appendix 3: report on shingle sites in England. In "Shingle Survey of Great Britain." pp. 106. Nature Conservancy Council, London.
- Sogreah. (1990). Expertise du littoral des Bas-Champs, pp. 49. DDE 80.
- Sogreah. (1995a). Etude sédimentologique de la Baie de Somme, pp. 65. Rapport Conseil Général de la Somme.
- Sogreah. (1995b). Littoral des Bas-Champs, pp. 12. DDE80.
- Sogreah. (2009). Réunion à la mairie de Cayeux-sur-Mer. Gestion du cordon de Cayeux Cayeux-sur-Mer.
- Sonu, C. J., and Van Beek, J. L. (1971). Systematic beach changes on the Outer Banks, North Carolina. *Journal Geology*, 416-425.
- Soons, J. M., Shulmeister, J., and Holt, S. (1997). The Holocene evolution of a well nourished gravelly barrier and lagoon complex, Kaitorete "Spit", Canterbury, New Zealand. *Marine Geology* **138**, 69-90.
- South Downs Coastal Group. (1996). South down shoreline, Management plan Selsey to Beachy Head.
- Stapleton, K. R., Mason, T., and Coastes, T. T. (1999). Sub-tidal resolution of beach profiles on a macro-tidal shingle beach. In "Proceedings of the 4th international symposium on coastal engineering and science of coastal sediment." pp. 885-893.
- Stépanian, A. (2002). "Evolution morphodynamique d'une plage macrotidale à barres: Omaha beach (Normandie)." Unpublished PhD thesis, Université de Caen.
- Sunamura, T. (2004). A predictive relationship for the spacing of beach cusps in nature. *Coastal Engineering* **51**, 697-711.
- Sunamura, T., and Kraus, N. C. (1985). Prediction of average mixing depth of sediment in the surf zone. *Marine Geology* **62**, 1-12.
- Takada, I., and Sunamura, T. (1982). Formation and height of berms. *Transactions—Japanese Geomorphological Union* **3**, 145-157.
- Thornton, E. B., and Guza, R. T. (1989). Wind Wave Transformation. In "Nearshore Sediment Transport." (R. J. Seymour, Ed.), pp. 137-172. Plenum Press, New York, NY.
- Ting, F.C.K. (2001), Laboratory study of wave turbulence velocities in a broad-banded irregular wave surf zone. *Coastal Engineering* **43**, 3-4, pp. 183-208.
- Todd Holland, K. (1998). Beach cusp formation and spacings at Duck, USA. *Continental Shelf Research* **18**, 1081-1098.
- Tonk, A., and Masselink, G. (2005). Evaluation of Longshore Transport Equations with OBS Sensors, Streamer Traps, and Fluorescent Tracer. *Journal of Coastal Research* **21**, 915-974.
- Trim, L. K., She, K., and Pope, D. J. (2002). Tidal effects on cross-shore sediment transport on a shingle beach. *Journal of Coastal Research*, 708-715.
- Turner, I. L. (1995). Simulating the influence of groundwater seepage on sediment transported by the sweep of the swash zone across macro-tidal beaches. *Marine Geology* **125**, 153-174.
- US Army Corps of Engineers. (1984). "Shore Protection Manual." Government Printing Office, Washington D.C.
- US Army Corps of Engineers. (2002). Coastal Sediment Processes. In "Coastal Engineering Technical Note ". US Army Corps of Engineers, Washington D.C.
- Van der Meer, J. W. (1988). Rock slopes and gravel beaches under wave attack, pp. 396. Delft Hydraulics Laboratory, Netherlands.
- Van der Meer, J. W. (1990). Static and dynamic stability of loose material. In "Coastal Protection." (Balkema, Ed.), pp. 157-195.

- Van der Meer, J. W., and Pilarczyk, K. W. (1986). Dynamic stability of rock slopes and gravel beaches. In "Proceedings of the 20th Coastal Engineering." pp. 1713-1726. ASCE, Taipei.
- Van Hijum, E., and Pilarczyk, K. W. (1982). Equilibrium profile and longshore transport of coarse material under regular and irregular wave attack, pp. 36. Delft Hydraulics Laboratory, Netherlands.
- Van Wellen, E. (1999). Modelling of swash zone sediment transport on coarse grained beaches. Unpublished PhD thesis, University of Plymouth.
- Van Wellen, E., Chadwick, A. J., Bird, P. A. D., Bray, M. L., M., and Morfett, J. (1997). Coastal sediment transport on shingle beaches. In "Proceedings of the Coastal Dynamics '97." pp. 38-47. ASCE, Plymouth.
- Van Wellen, E., Chadwick, A. J., Lee, M., Baily, B., and Morfett, J. (1998). Evaluation of longshore sediment transport models on coarse grained beaches using field data: a preliminary investigation. In "Proceedings of 26th International Conference on Coastal Engineering." pp. 2640-2653. ASCE, Copenhagen.
- Van Wellen, E., Chadwick, A. J., and Mason, T. (2000). A review and assessment of longshore sediment transport equations for coarse-grained beaches. *Coastal Engineering* **40**, 243-275.
- Vila-Concejo, A., Ferreira, Ó., Ciavola, P., Matias, A., and Dias, J. M. A. (2004). Tracer studies on the updrift margin of a complex inlet system. *Marine Geology* **208**, 43-72.
- Voulgaris, G., and Simmonds, D. (1996). Incident waves. In "Circulation and Sediment Transport Around Banks (CSTAB) Handbook." (B. A. O'Connor, Ed.), pp. 457-467. Department of Civil Engineering, University of Liverpool, Liverpool.
- Voulgaris, G., Workman, M., and Collins, M. B. (1999). Measurement Techniques of Shingle Transport in the Nearshore Zone. *Journal of Coastal Research* **15**, 1030-1039.
- Walker, J. R., Everts, C. H., Schmelig, S., and Demirel, V. (1991). Observations of a tidal inlet on a shingle beach. In "Coastal Sediments '91." pp. 975-989. ACSE, Seattle.
- Wang, P., Kraus, N. C., and Davis, R. A., Jr. (1998). Total Longshore Sediment Transport Rate in the Surf Zone: Field Measurements and Empirical Predictions. *Journal of Coastal Research* **14**, 269-282.
- Watt, T., Dornbusch, U., Moses, C., and Robinson, D. (2006). Measuring cross-shore sediment transport on mixed shingle beaches using GPS survey techniques. In "Proceedings of the Fifth Coastal Dynamics International Conference." ASCE, Barcelona, Spain.
- Watt, T., Robinson, D. A., Moses, C. A., and Dornbusch, U. (2008). Patterns of surface sediment grain size distribution under the influence of varying wave conditions on a mixed sediment beach at Pevensey Bay, southeast England. *Zeitschrift für Geomorphologie* **52**, 63-77.
- Werner, B. T., and Fink, T. M. (1993). Beach cusps as self-organized patterns. *Science* **260**, 968-971.
- Whitcombe, L. J. (1996). Behaviour of an artificially replenished shingle beach at Hayling Island, UK. *Quarterly Journal of Engineering Geology and Hydrogeology* **29**, 265-271.
- White, T. E. (1998). Status of measurement techniques for coastal sediment transport. *Coastal Engineering* **35**, 17-45.
- Wilcock, P. R., Kenworthy, S. T., and Crowe, J. C. (2001). Experimental study of the transport of mixed sand and gravel. *Water Resources Research* **37**, 3349-3358.
- Williams, A. T. (1971). An analysis of some factors involved in the depth of disturbance of beach sand by waves. *Marine Geology* **11**, 145-158.
- Williams, R. B. G. (2005). Beach recharge in Sussex and East Kent: A preliminary inventory and overview. In "Rye Harbour Nature Reserve Management Plan." (B. Yates, Ed.). University of Sussex.
- Wilson, K. C. (1987). Analysis of Bed-Load Motion at High Shear Stress. *Journal of Hydraulic Engineering* **113**, 97-103.
- Wilson, S. F. (1996). Shoreham and Lancing sea defence strategy plan, pp. 3. Southern Region. Final Report to the National Rivers Authority.

-
- Wolman, M. G. (1954). A method of sampling coarse river-bed material. *Transactions-American Geophysical Union* **35**, 951-956.
- Workman, M., Smith, J., Boyce, P., Collins, M. B., and Coates, T. T. (1994). Development of the electronic pebble system. HR Wallingford.
- Wright, L. D., Chappell, J., Thom, B. G., Bradshaw, M. P., and Cowell, P. (1979). Morphodynamics of reflective and dissipative beach and inshore systems: Southeastern Australia. *Marine Geology* **32**, 105-140.
- Wright, L. D., and Thom, B. G. (1977). Coastal depositional landforms *Progress in Physical Geography* **1** 412-459
- Wright, P. (1982). "Aspects of the coastal dynamics of Poole and Christchurch Bays, Dorset." Unpublished PhD thesis, University of Southampton.
- Wright, P., Cross, J. S., and Webber, N. B. (1978). Aluminium pebbles: A new type of tracer for flint and chert pebble beaches. *Marine Geology* **27**, M9-M17.
- Zenkovich, V. P. (1958). Fluorescent Substances as Tracers for Studying the Movement of Sand on the Sea Bed, Experiments Conducted in the U.S.S.R. *Dock and Harbor Authority*, 280-283.

Appendix I Manufacturing of the synthetic tracer pebbles

What are they?



Figure I-1 Synthetic tracer pebble.

These tracers are made of an epoxy resin with a copper inside allowing a recovery with a metal detector. Their size is: a-axis: 60 to 70 mm, b-axis: 40 to 50 mm, c-axis: 40 mm. They are completely smoothed well rounded and have the same weight as a flint pebble of the same size. Each pebble is engraved with an easy identifiable different identity number making each of them unique.

Mould manufacturing-How are they made?

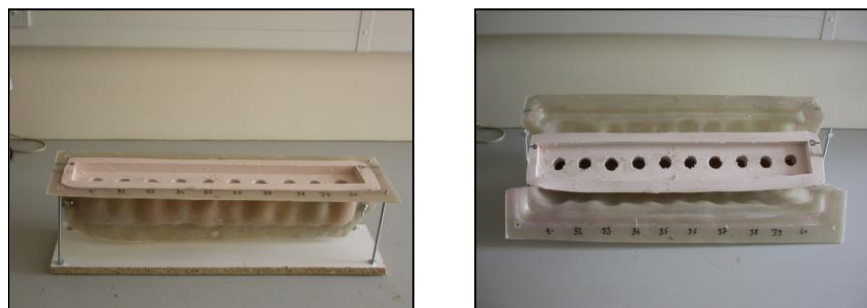


Figure I-2 Moulds

The construction of the ten pebble moulds is a lengthy procedure and has been simplified greatly for the purposes of this manufacturing description. No reference of the plug manufacturing process or tools used is made due to the highly technical nature. Twenty pseudo pebbles are hand formed using identical volumes of fibre reinforced modelling clay. These are then gently dried at 36°C for 72 hours. The pebbles are then very lightly buffed to remove any anomalies then lacquered with a water based gloss varnish. The volume of the finished pseudo-pebble is checked as a small percentage of shrinkage occurs during drying. The ten most uniform pebbles are selected for the mould.

A strip of MDF is cut 540 x 70 x 20 mm. The use of this piece of MDF in the moulding process produces a resin over spill trough in the final silicon mould. Ten 5mm holes are drilled and counter sunk in a line down the centre of the longest axis on the largest surface. Using each of these holes a 25 mm diameter smooth wooden rod approximately

20mm high is screwed. These wooden rod pieces have been rifle barrel drilled with a 5mm internal diameter. A 75 mm long 5 mm screw threaded through the countersunk side of the MDF strip, through the rod, and then screwed into a 4 mm diameter hole which has been drilled into the end of each pebble along its long axis. The joint between the base of the pseudo pebble and the wooden rod is filled with plasticine type filler. Once this is completed ten pebbles perched up on little pedestals are lined up along the MDF. This strip of MDF is then centrally screw mounted on a larger piece of MDF approximately 700 x 200 mm to form the main 'tool'.

A plug, boss and finally a GRP rubber injection casing is then generated from this tool. (See above)

With the injection casing bolted or clamped to the tool. Room temperature vulcanising silicon rubber is injected in to the base of the mould using a pneumatic powered mastic gun and left to set for 24 hours.

The external casing is removed and with the internal tool still in place a two-piece GRP support casing is laid up over the silicon mould. This casing is trimmed drilled for clamping bolts and placed in a framework of threaded rod and MDF.

The whole process takes about three weeks. Material costs for the Tooling required are about £220-£260. The material costs then on for each silicon moulds in cradles are about £110-125 depending on quantity.

Once completed the final epoxy resin pebble volumes are calculated and by knowing the actual densities of flint, resin and copper the required volume (and therefore length of 25mm diameter bar) of copper core can be calculated to give a synthetic resin pebble comparable density to natural flint.

Pebbles manufacturing

➤ Products necessities

-resin and hardener: these products are sold by ADL (Stevens) Resin & Glass. The price depends on the quantity of product ordered. For example, 25 kg of resin plus 12.5 kg of hardener costs 333.16 pounds. This quantity of Epoxy resin allows a production of 450 pebbles.

-copper: The price depends again on the quantity ordered. However, the average price of one copper is around 1.63 pounds.

-Advanced mould release agents: a single spray costs 10 pounds. One spray is used for the production of 450 pebbles.

➤ The Epoxy Resin and the hardener

The resin mixture consists in different ratio of epoxy and hardener. When using epoxy, the hardener ratio must never be altered as under-cure would arise and the manufacturer advices to mix two parts resin to one part hardener by weight. However, experience show that a perfect result is obtained by adding only 45% of hardener. As soon as the mixture (resin and hardener) is homogeneous, the air bubbles are removed from the liquid by using an air vacuum. After the resin has cooled, full cure is attained after 7 days at 25°C or in 1 hour at 100°C.

➤ The copper

The principle aim was to be able to reproduce a perfect fake of a natural flint pebble with an equivalent B-axis. By a simple calculation based on the resin density (1.06 g.cm⁻³), the copper density (8.92 g.cm⁻³), the flint density (2.65 g.cm⁻³) and pebble

volume (73 cm^3 on the average), it has been determined that the copper length inside each pebble should be ranged around 3.3 cm.

➤ Manufacturing of a pebble

The first step consists in pulling a little amount of resin into every mould. After few hours of drying it will constitute a perfect horizontal pedestal for the copper. Moreover, this base allows placing the copper in the middle of the mould and so having the mass centre close to the gravity centre.

Secondly, a bit of copper is introduced in the mould. Pulling a small amount of fresh resin before introducing the piece of copper avoid any air trapped.

Next, the entire mould is filled with resin and after five to six hours of drying, the resin pebbles are extracted. These are also soft enough to be easily well smoothed with a cutter.

Finally, after a week drying at the ambient temperature, the resin is warranted to be full cured and pebbles ready to be deployed.

Before or after every use, a mould release agent has to be used to make moulds life longer and the pebbles extraction easier.



Figure I-1 Synthetic pebble manufacturing.

On the average, making one pebble cost 2.91 pounds (for the production of 3000 pebbles).

This method is the cheapest way allowing tracing pebbles movement in a same way as the aluminium ones or others methods would do. The advantage is also that some abrasion measurements could be collected (providing that as relationship between each abrasion rate can be determined between the resin and the beach material of interest). Large deployments such as a hundred or more are possible for a minimum cost and an efficient data collection. These tracers can also be coloured to fit any particular need. The shape and size can also be adapted, however particular attention needs to be drawn to the density and the distribution of the weight of the fake pebble. This is one of the reasons why only rounded shape pebbles of the same size have been produced. Having identical tracers also simplifies the statistical procedure to derive longshore sediment transport. Finally, by having only one type of tracer, a quick production is possible.

Appendix II Grain size characteristics

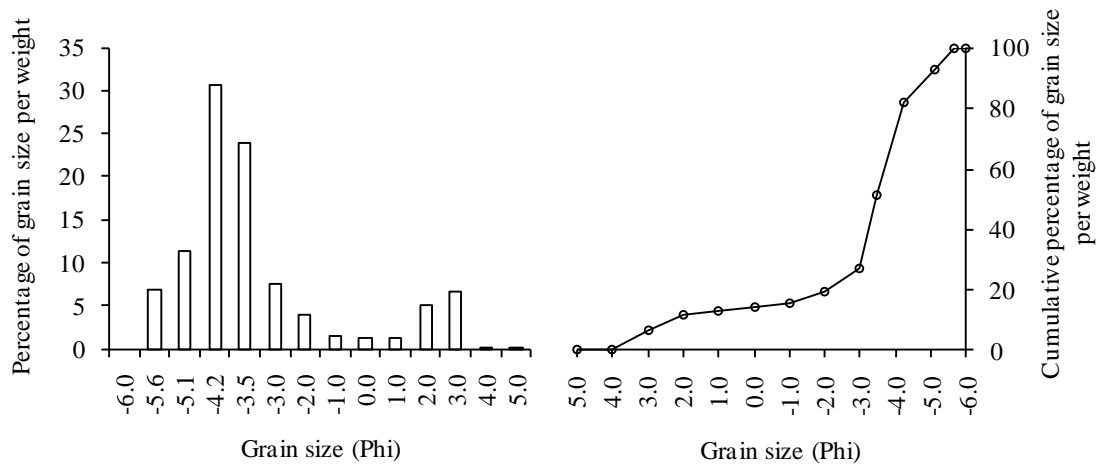
Figure II-1 Grain size characteristics observed at Cayeux-sur-Mer and Birling Gap during the time of the experiments.

Cayeux-sur-Mer

As described in Chapter 3, grain size sampling was conducted on every tide at three locations across-shore (upper, mid- and lower beach). Please note that the samples on October 29th are missing.

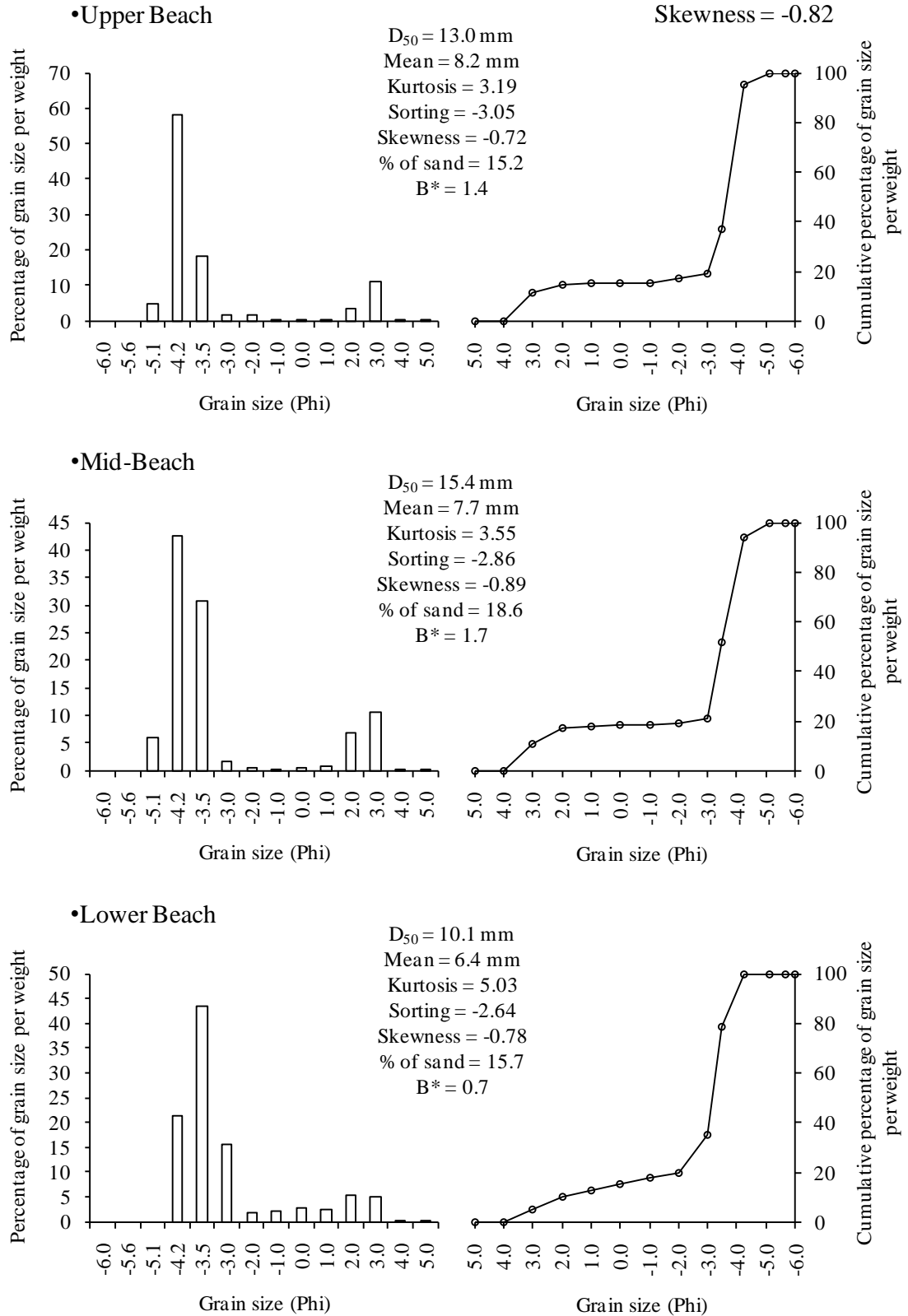
October 28th to November 11th 2005

$D_{50} = 15.4 \text{ mm}$
% of sand = 14.2
Mean = 8.3 mm
Kurtosis = 6.04
Sorting = -3.07
Skewness = -0.72
 $B^* = 1.4$



October 28th pm 2005, (tide 1)

Total Statistics: $D_{50} = 11.0$ mm
 % of sand = 23.7
 Mean = 7.0 mm
 Kurtosis = 4.04
 Sorting = -2.75
 Skewness = -0.82



October 30th am 2005, (tide 3)Total Statistics: $D_{50} = 11.0$ mm

% of sand = 23.7

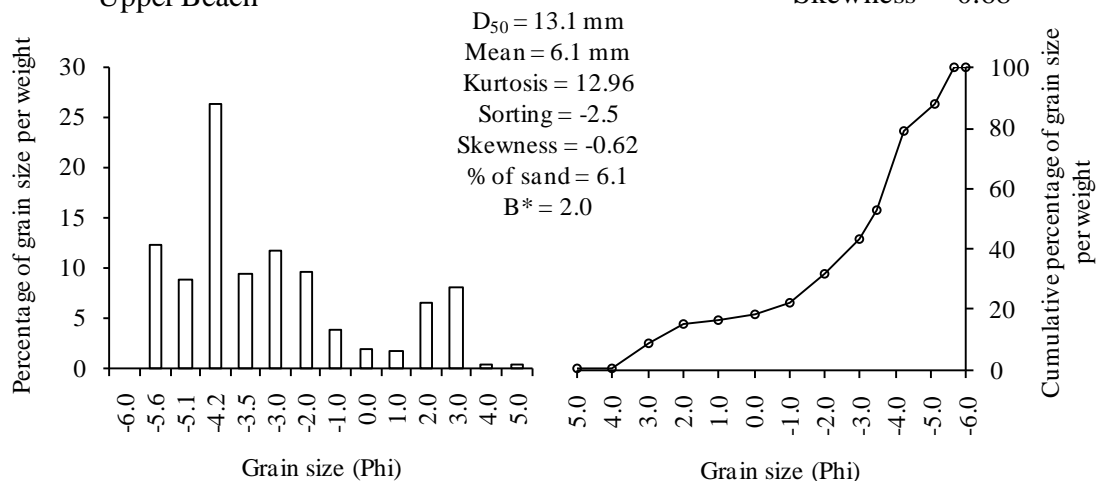
Mean = 4.7 mm

Kurtosis = 14.22

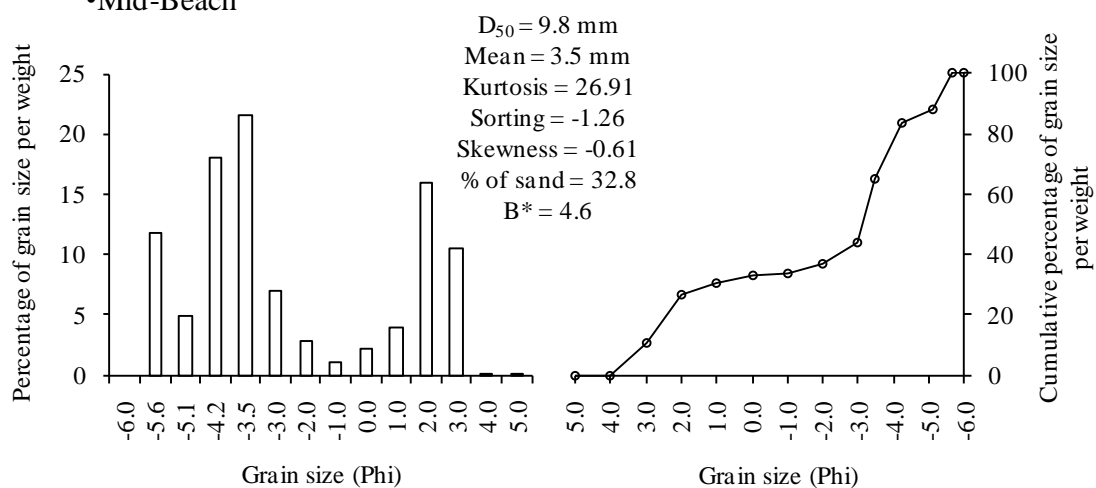
Sorting = -1.82

Skewness = -0.68

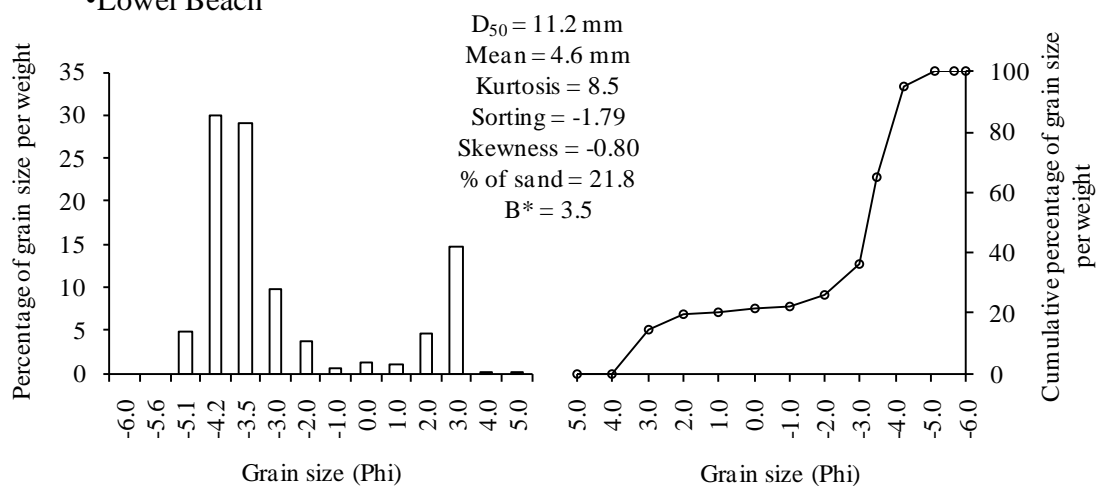
•Upper Beach



•Mid-Beach

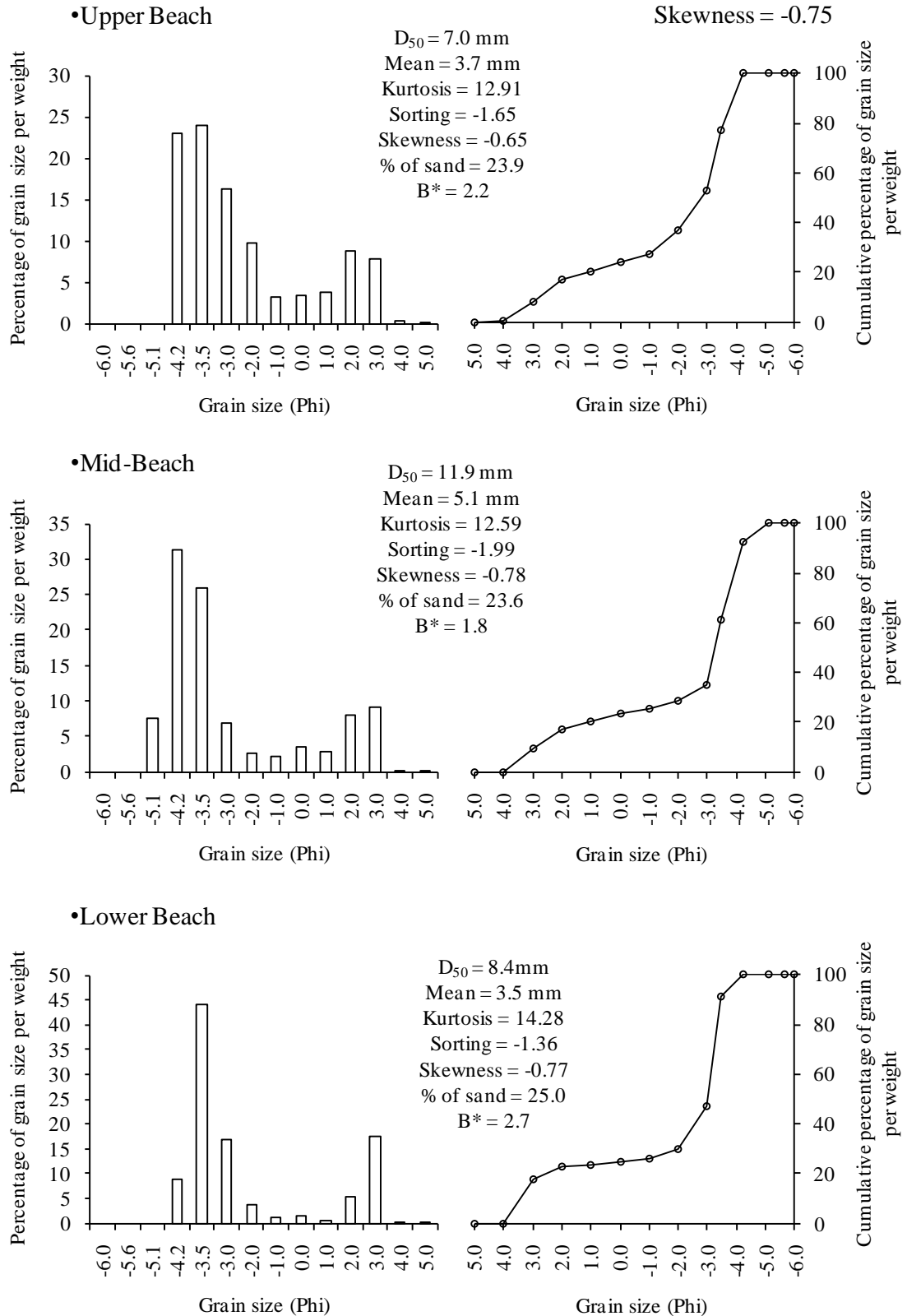


•Lower Beach



October 30th pm 2005, (tide 4)

Total Statistics: $D_{50} = 8.9$ mm
 % of sand = 24.2
 Mean = 3.9 mm
 Kurtosis = 13.74
 Sorting = -1.59
 Skewness = -0.75



October 31st am 2005, (tide 5)Total Statistics: $D_{50} = 8.4$ mm

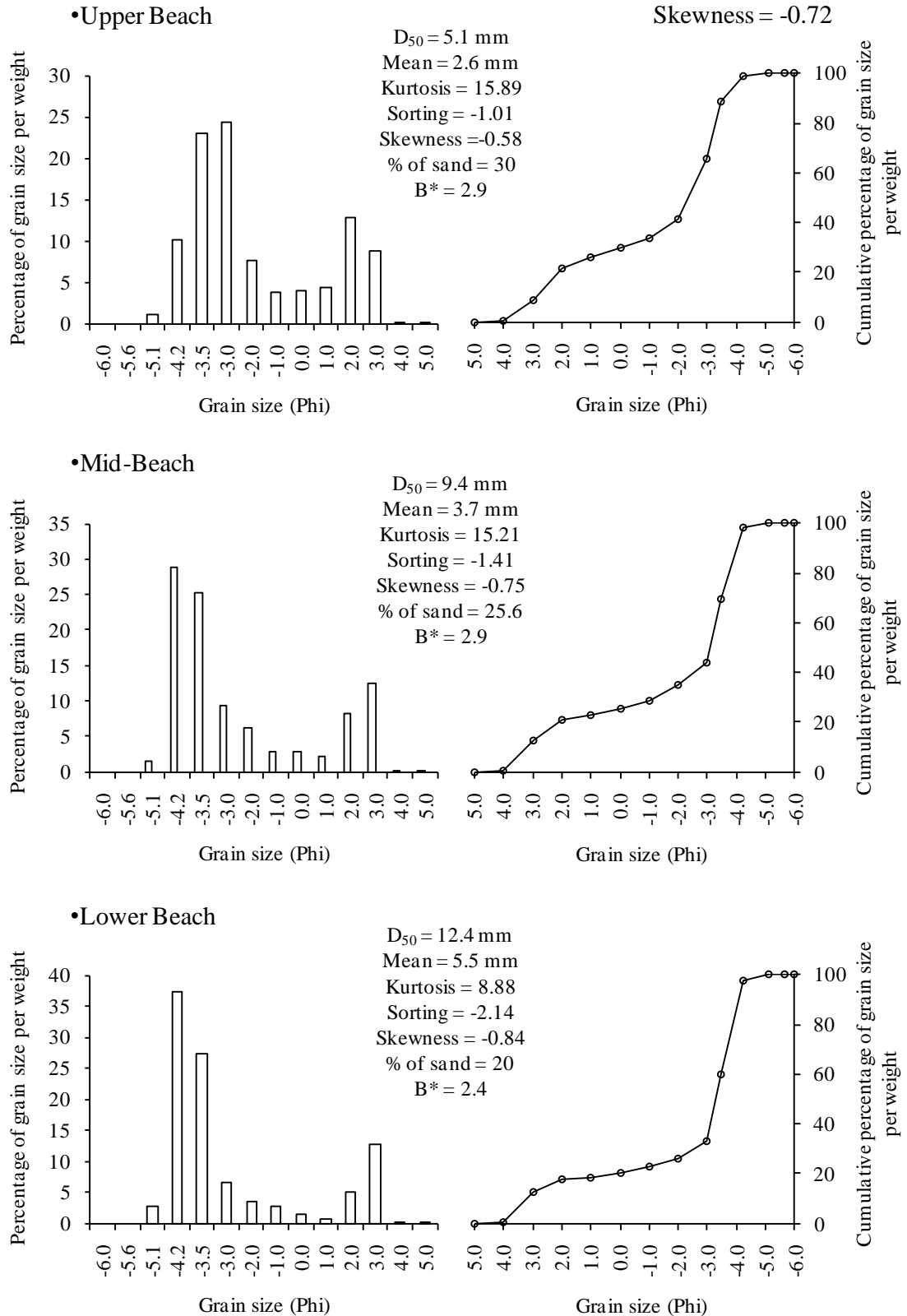
% of sand = 25.2

Mean = 3.7 mm

Kurtosis = 13.99

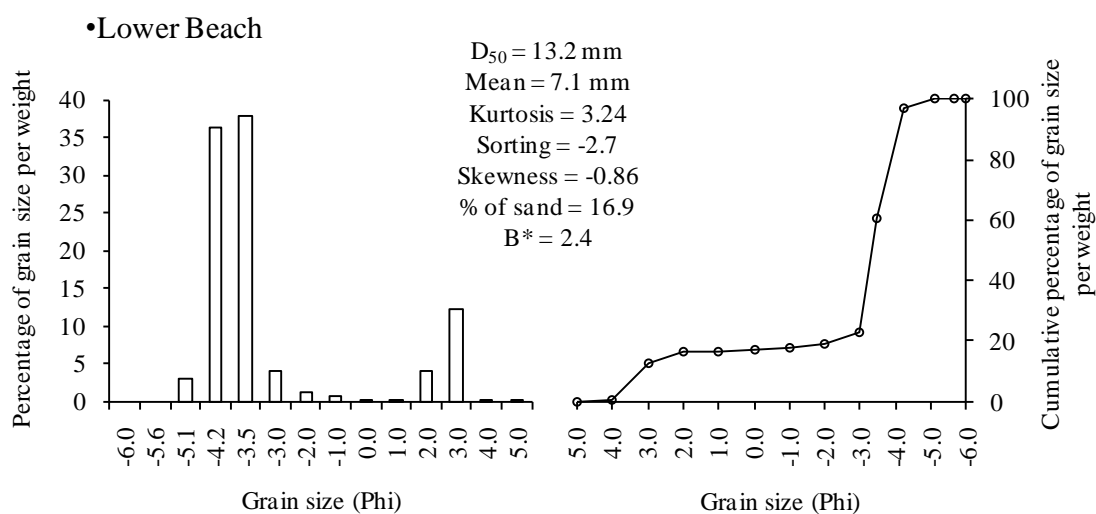
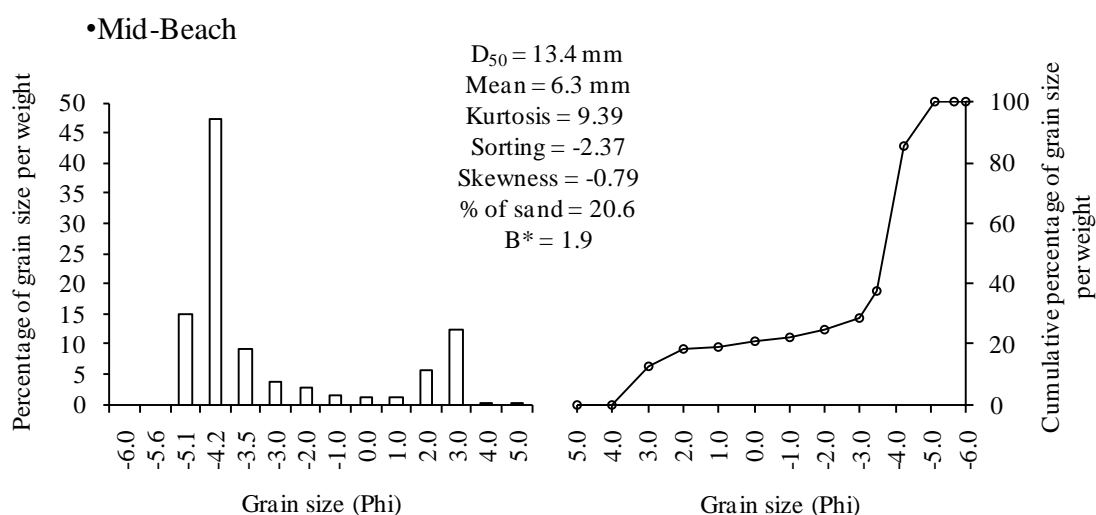
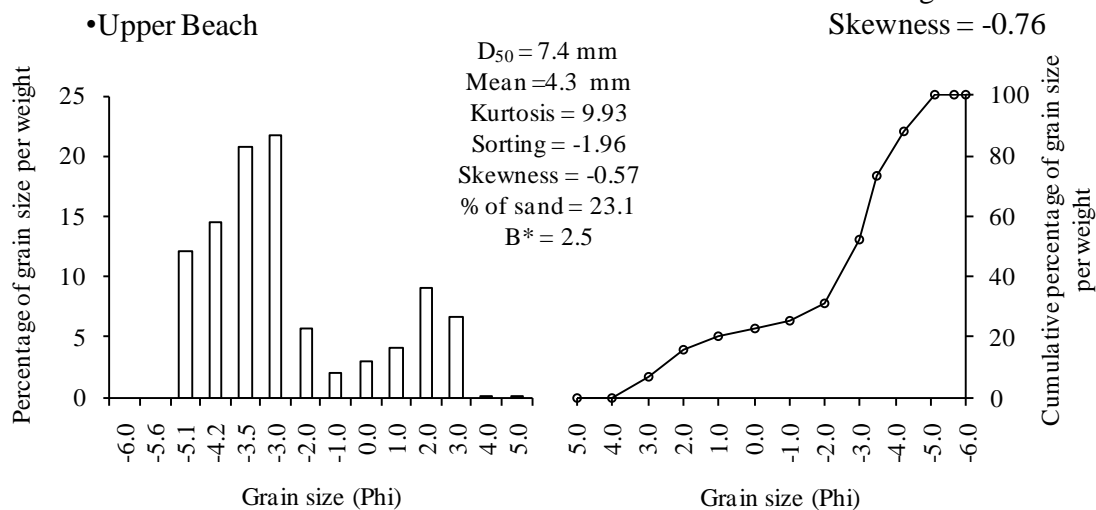
Sorting = -1.49

Skewness = -0.72



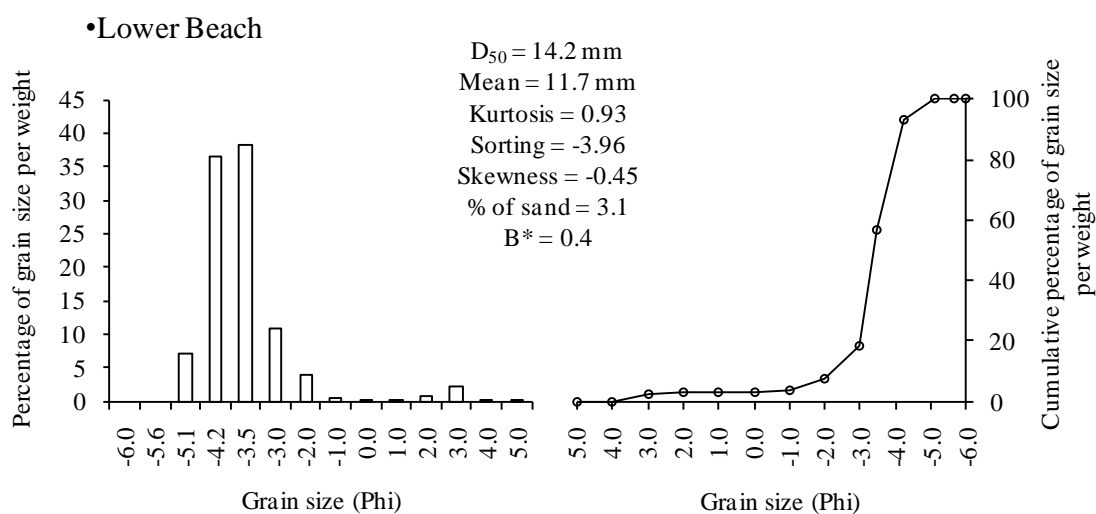
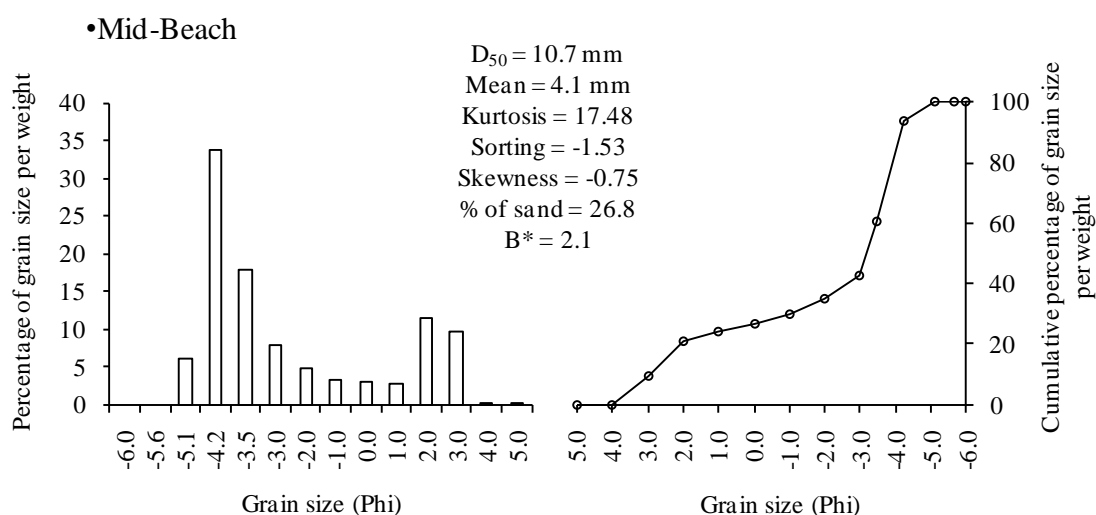
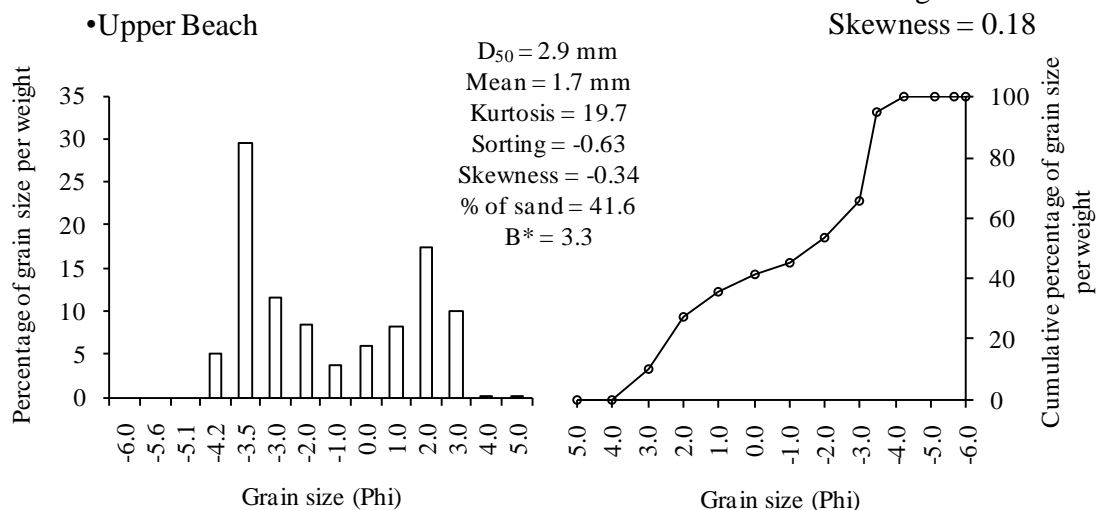
October 31st pm 2005, (tide 6)

Total Statistics: $D_{50} = 11.6$ mm
 % of sand = 20.5
 Mean = 5.5 mm
 Kurtosis = 8.43
 Sorting = -2.16
 Skewness = -0.76



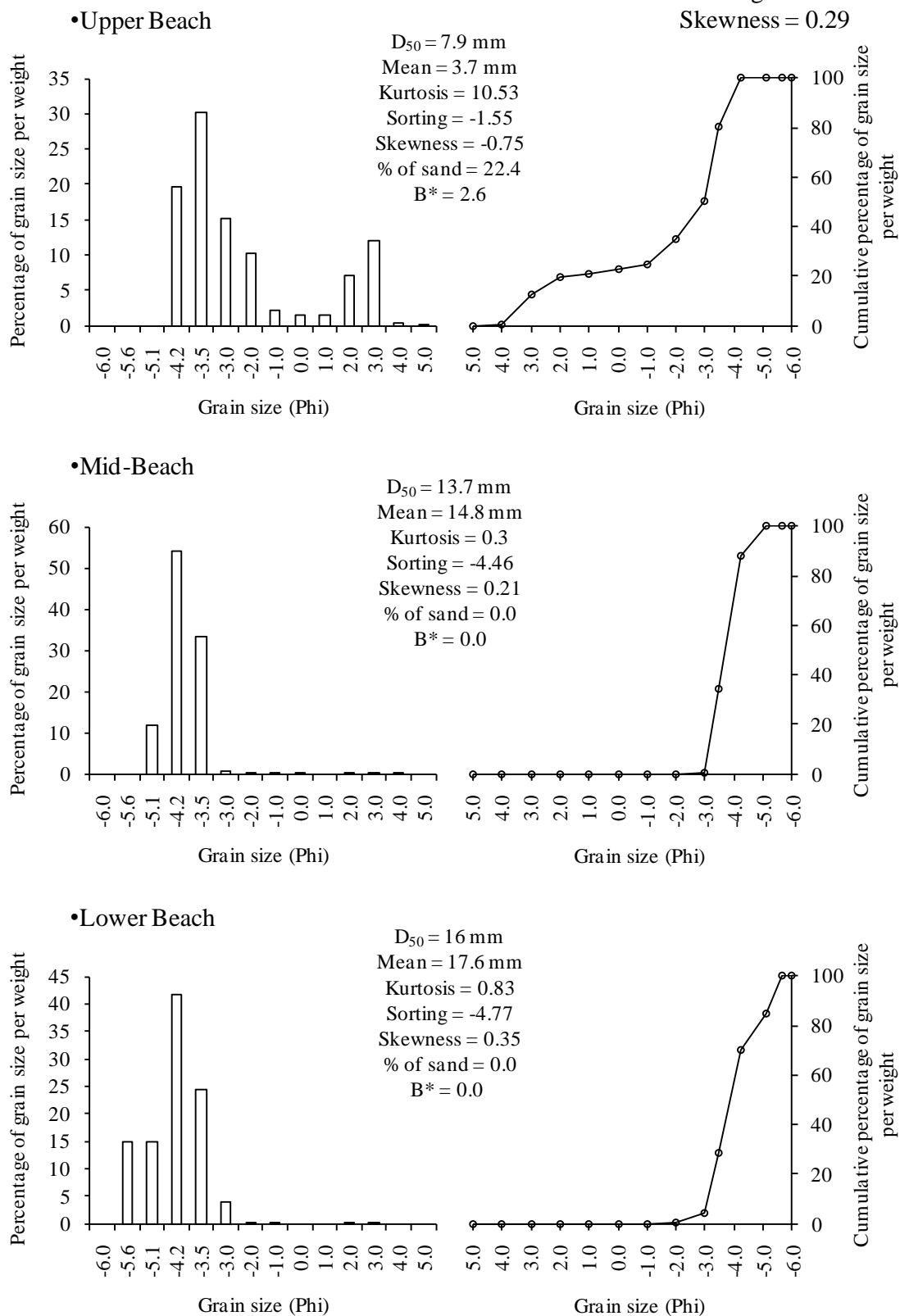
November 1st am 2005, (tide 7)

Total Statistics: $D_{50} = 9.3$ mm
 % of sand = 25.2
 Mean = 4.1 mm
 Kurtosis = 13.46
 Sorting = -1.71
 Skewness = 0.18



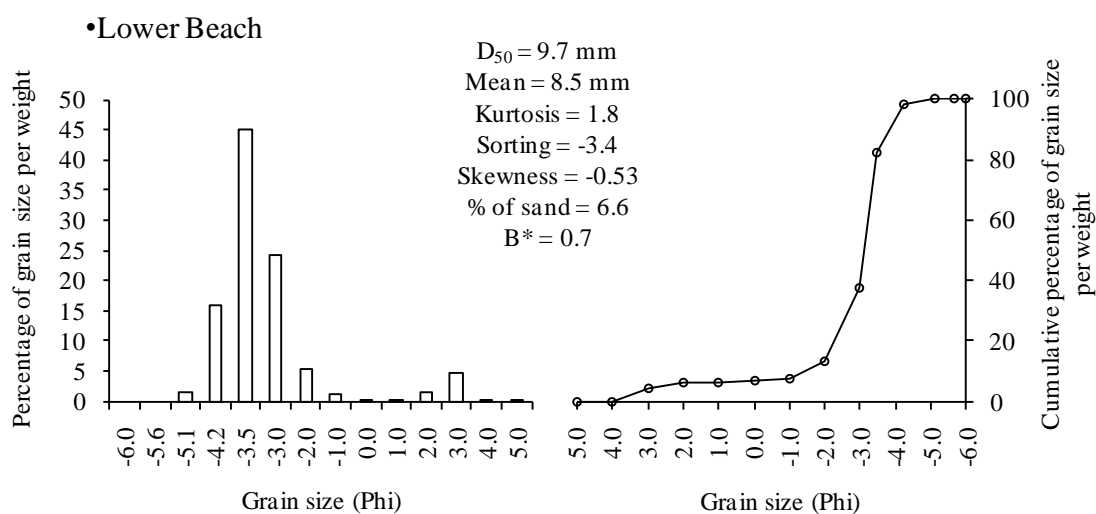
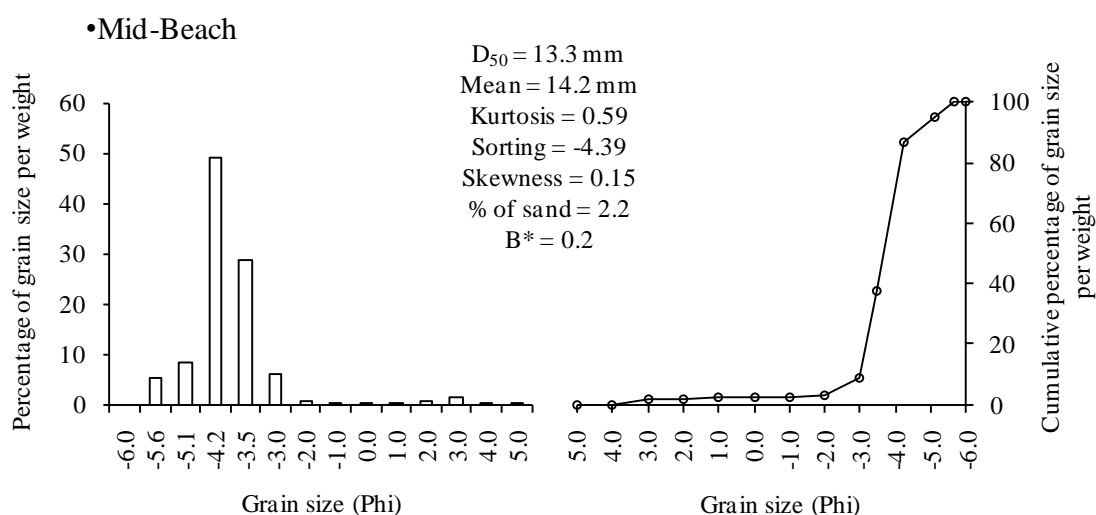
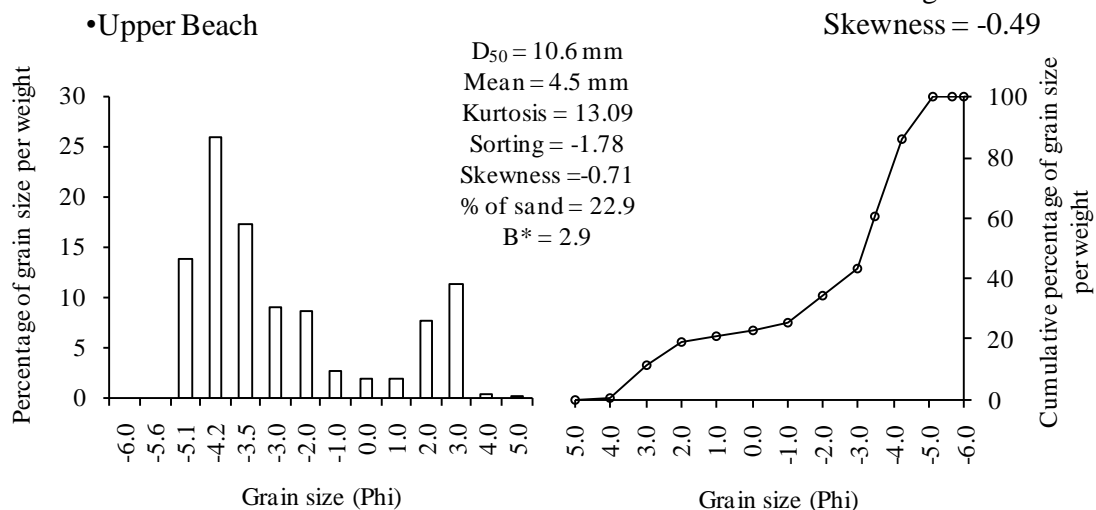
November 1st pm 2005, (tide 8)

Total Statistics: $D_{50} = 12.9$ mm
 % of sand = 4.3
 Mean = 14.3 mm
 Kurtosis = 0.9
 Sorting = -4.33
 Skewness = 0.29



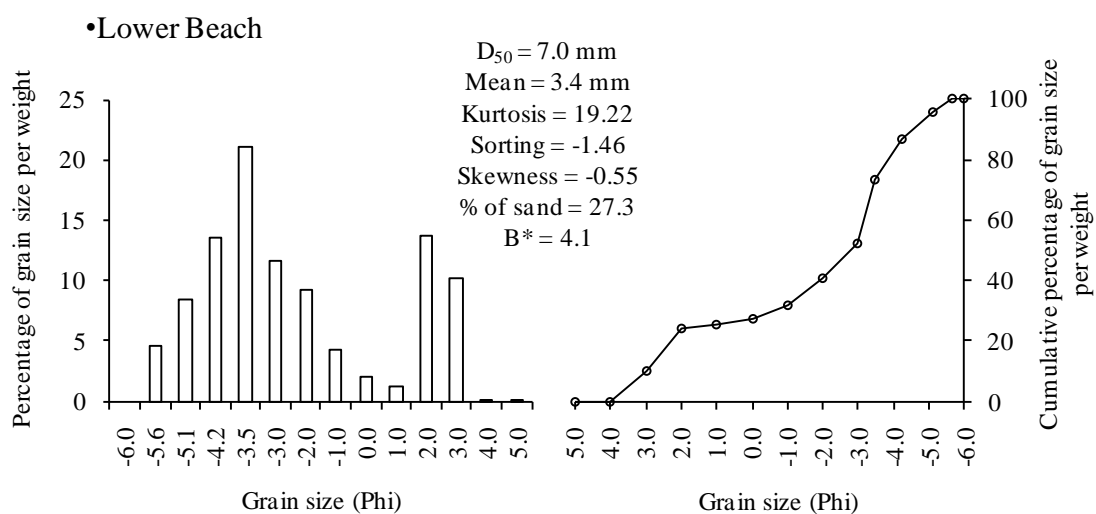
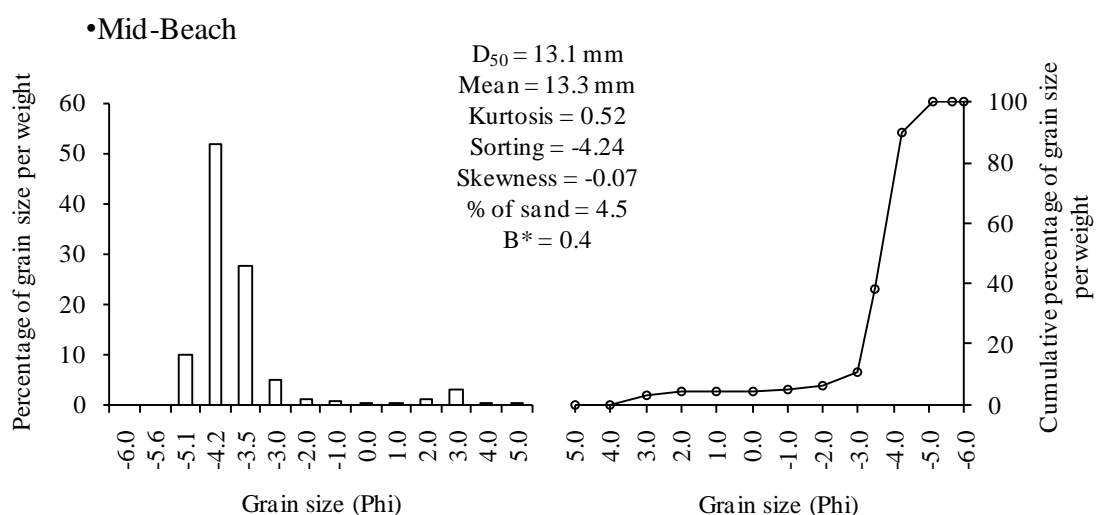
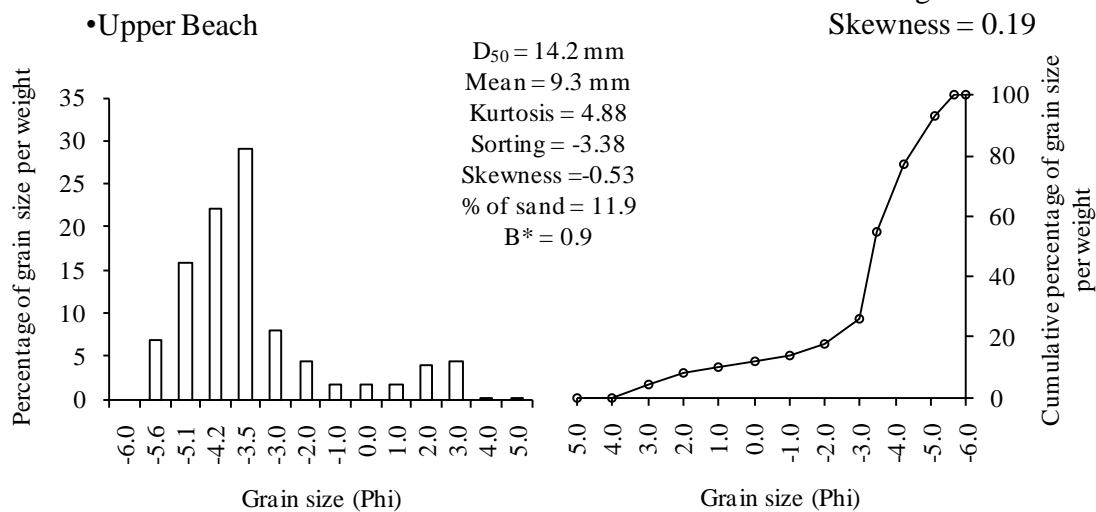
November 2nd am 2005, (tide 9)

Total Statistics: $D_{50} = 13.8$ mm
 % of sand = 6.5
 Mean = 10.9 mm
 Kurtosis = 1.4
 Sorting = -3.8
 Skewness = -0.49



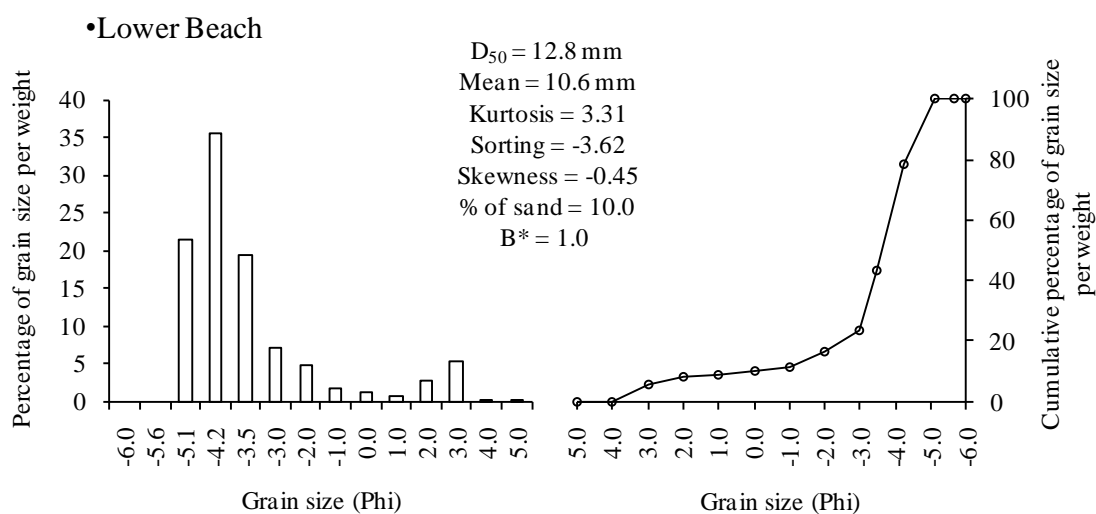
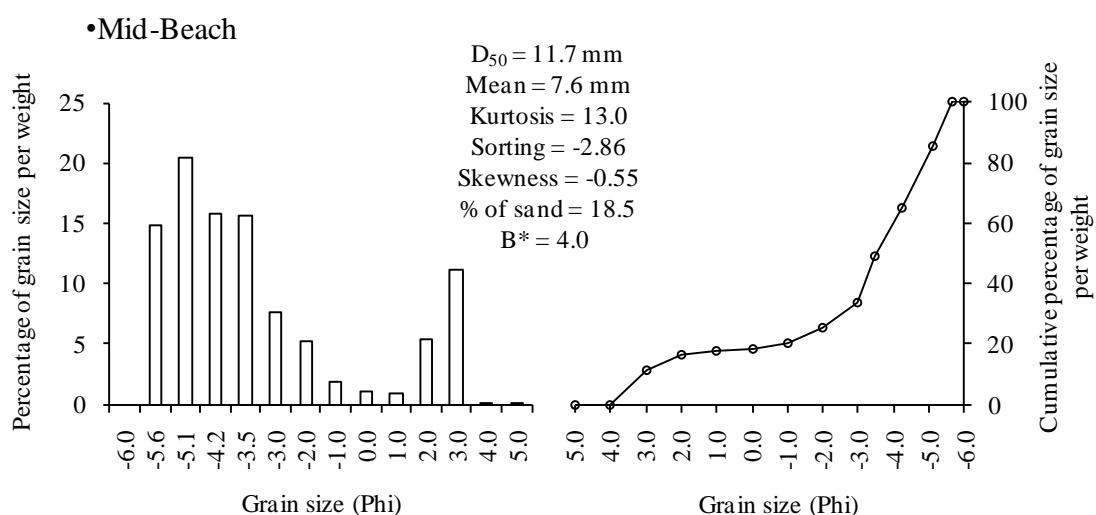
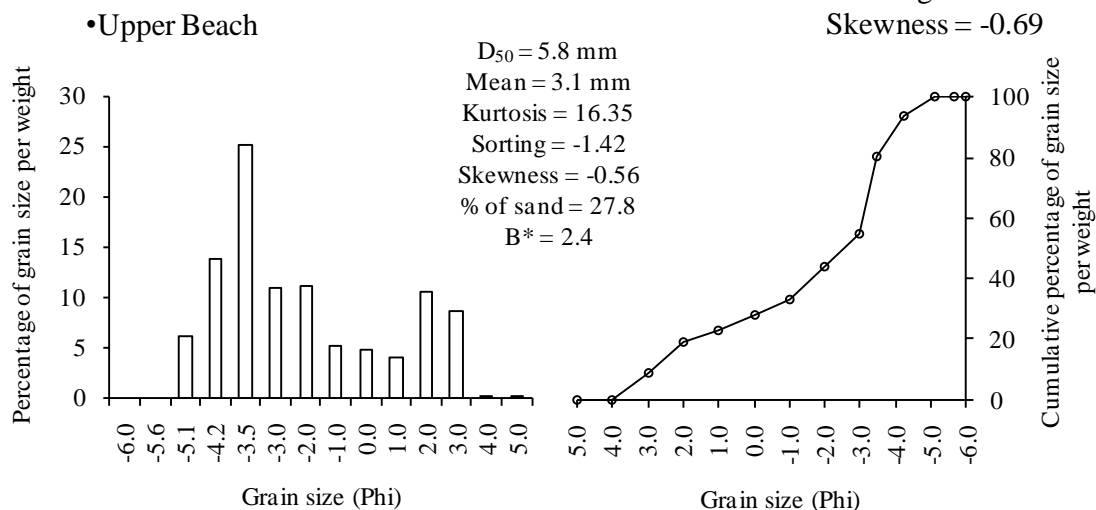
November 2nd pm 2005, (tide 10)

Total Statistics: $D_{50} = 14.1$ mm
 % of sand = 13.7
 Mean = 7.9 mm
 Kurtosis = 5.95
 Sorting = -2.99
 Skewness = 0.19



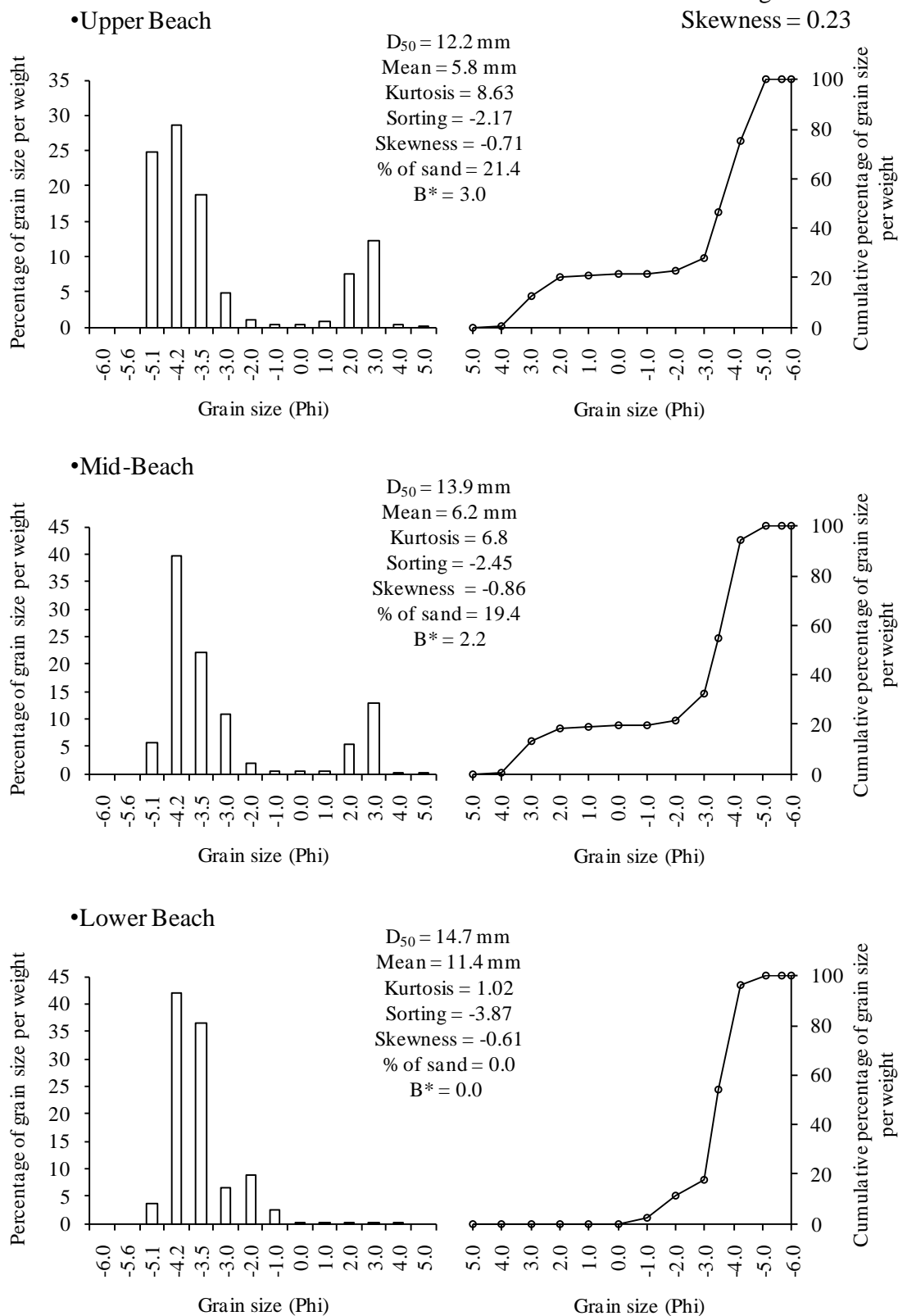
November 3rd am 2005, (tide 11)

Total Statistics: $D_{50} = 12.4$ mm
 % of sand = 18
 Mean = 6.3 mm
 Kurtosis = 10.44
 Sorting = -2.54
 Skewness = -0.69



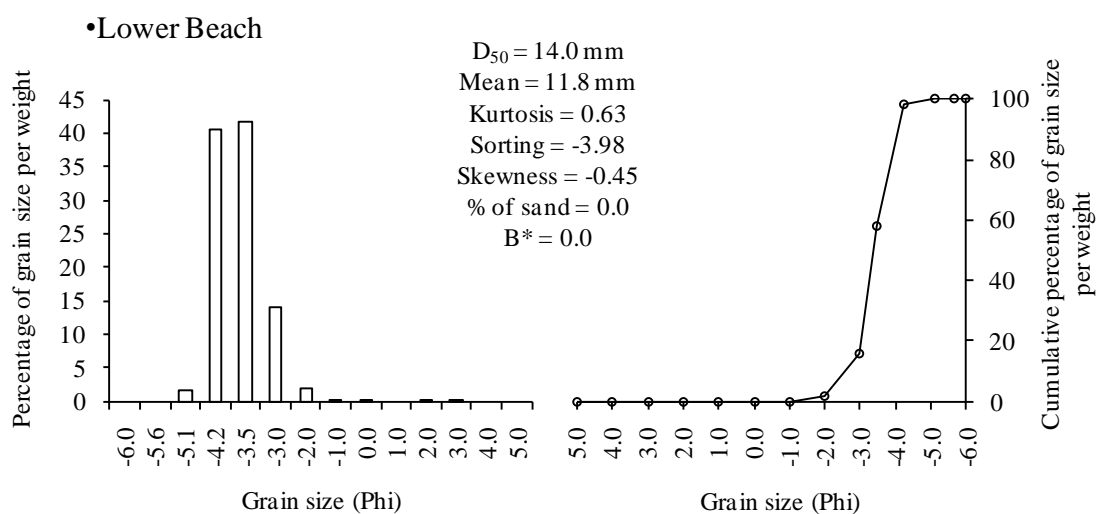
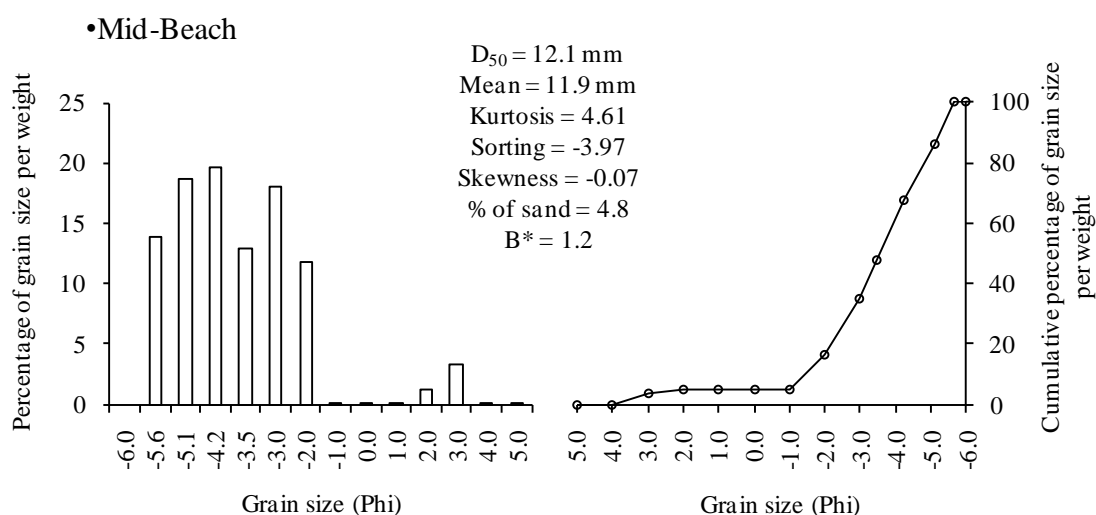
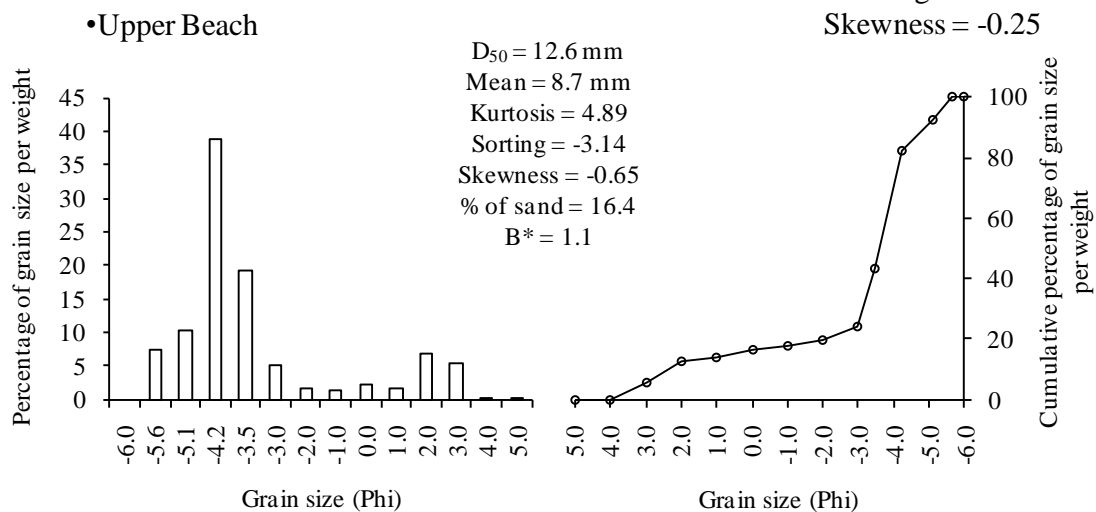
November 3rd pm 2005, (tide 12)

Total Statistics: $D_{50} = 15.1$ mm
 % of sand = 11.1
 Mean = 8.0 mm
 Kurtosis = 3.62
 Sorting = -3.0
 Skewness = 0.23



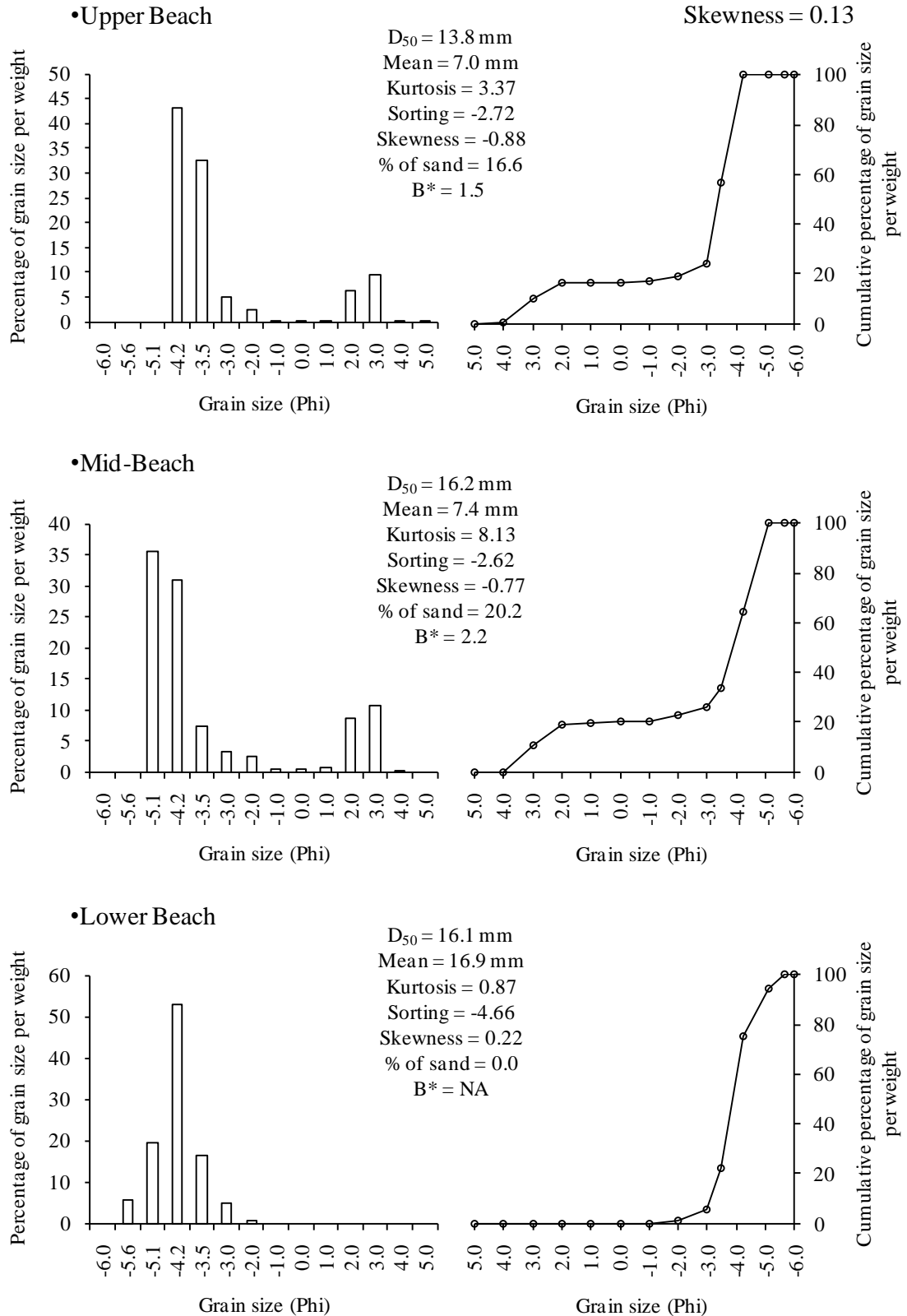
November 4th am 2005, (tide 13)

Total Statistics: $D_{50} = 11.5$ mm
 % of sand = 9
 Mean = 11.1 m
 Kurtosis = 2.53
 Sorting = -3.83
 Skewness = -0.25



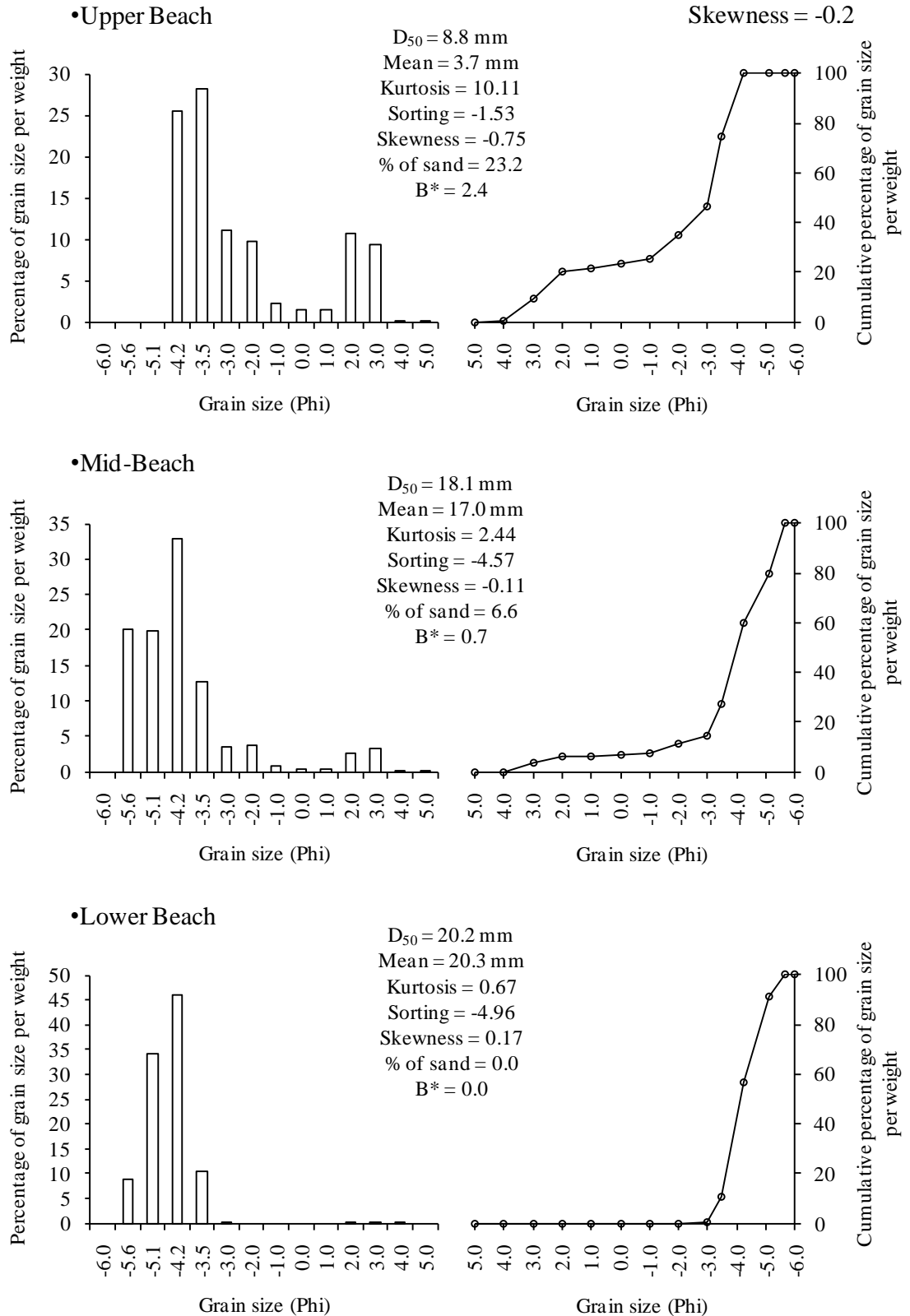
November 4th pm 2005, (tide 14)

Total Statistics: $D_{50} = 14.0$ mm
 % of sand = 10
 Mean = 11.1 mm
 Kurtosis = 2.54
 Sorting = -3.74
 Skewness = 0.13



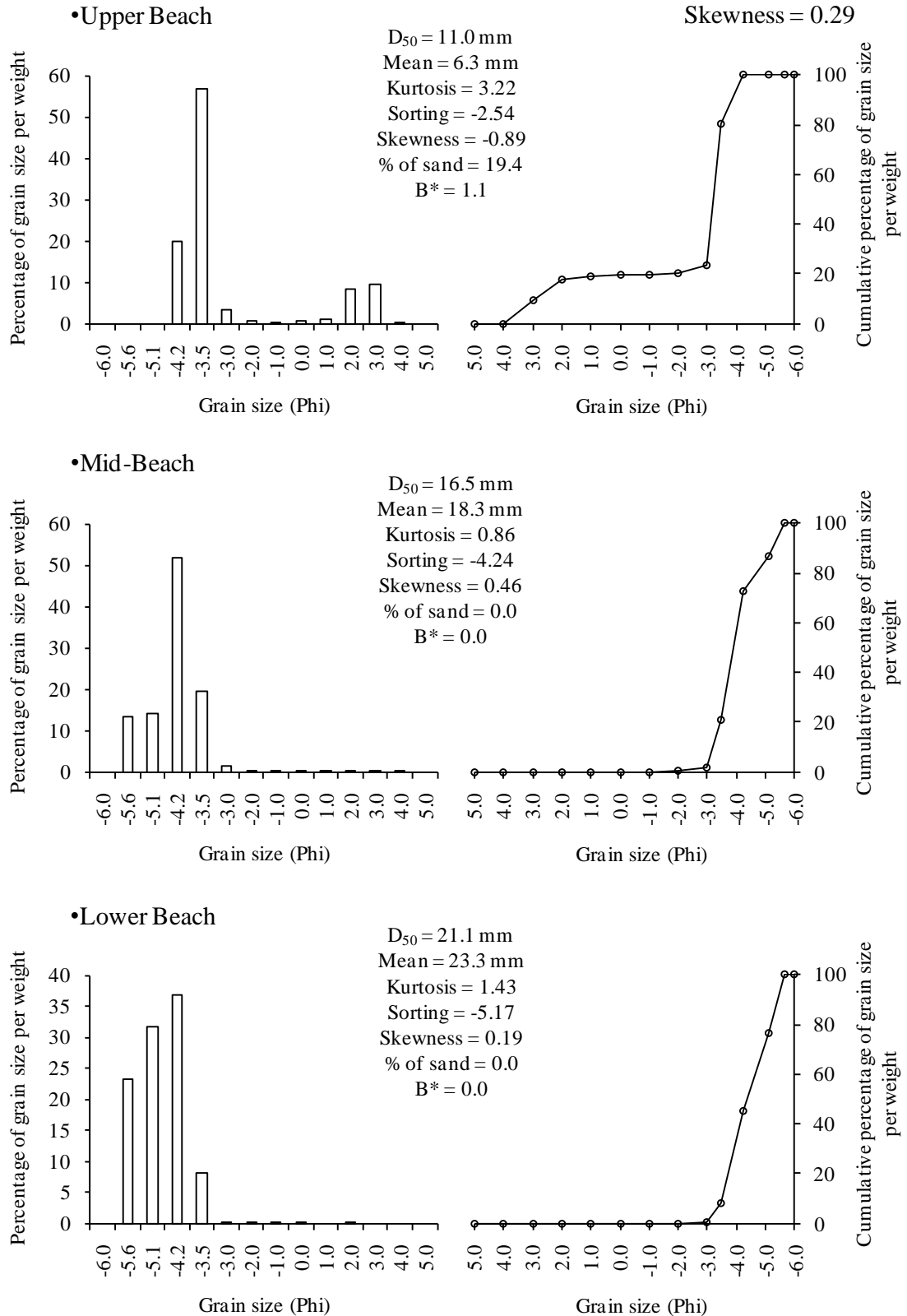
November 5th am 2005, (tide 15)

Total Statistics: $D_{50} = 15.8$ mm
 % of sand = 8.1
 Mean = 14.6 mm
 Kurtosis = 2.3
 Sorting = -4.31
 Skewness = -0.2



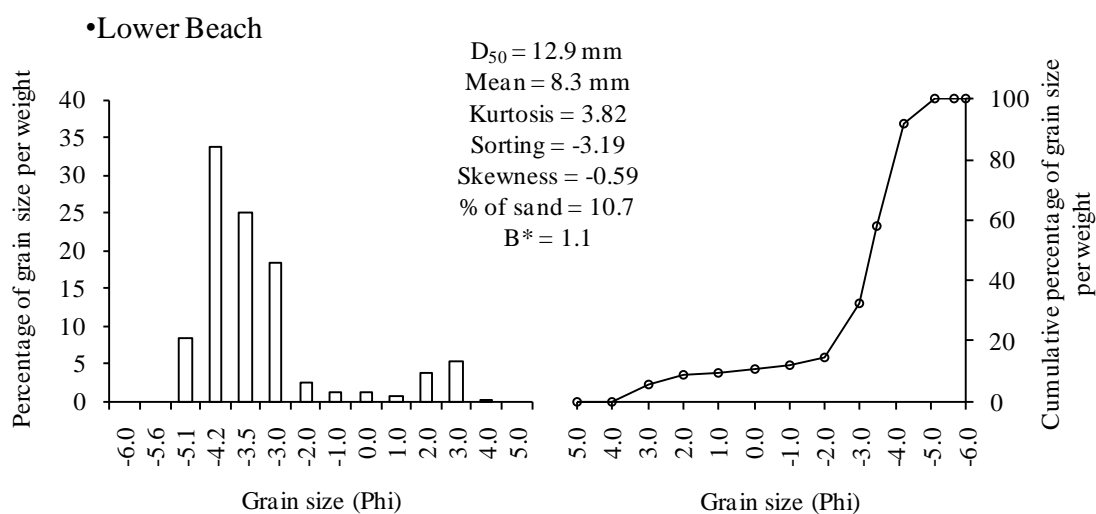
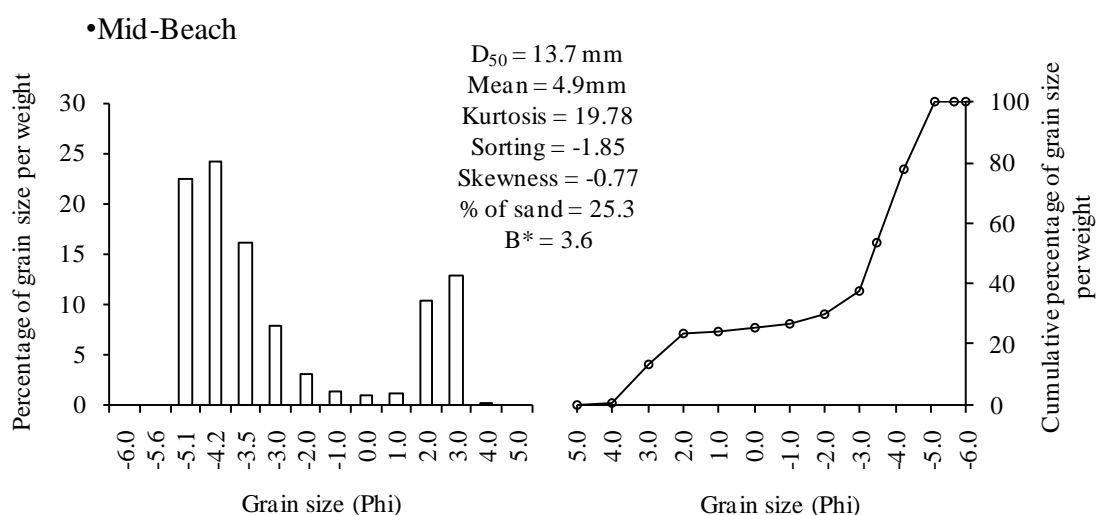
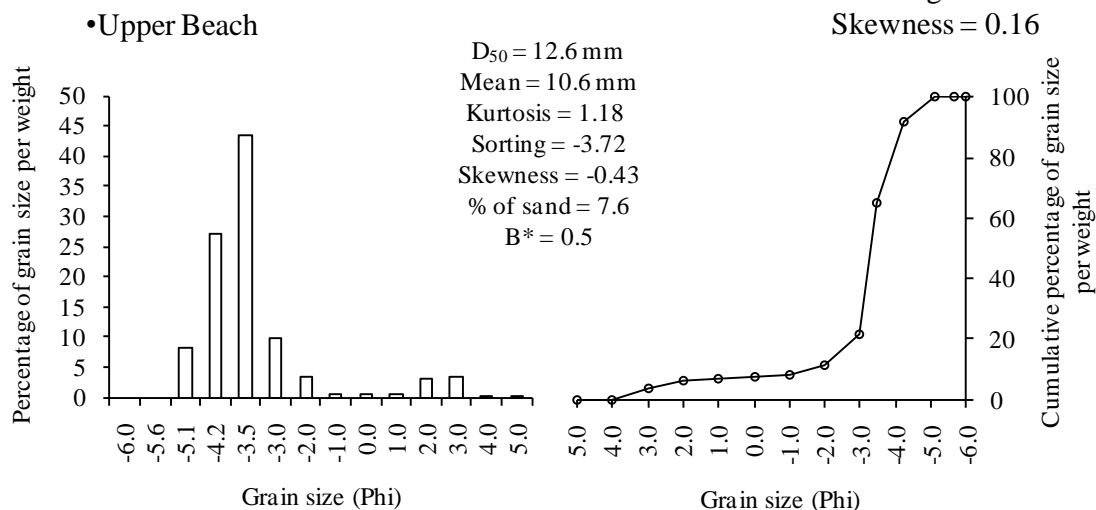
November 5th pm 2005, (tide 16)

Total Statistics: $D_{50} = 17.4$ mm
 % of sand = 3.0
 Mean = 18.8 mm
 Kurtosis = 1.48
 Sorting = -4.85
 Skewness = 0.29



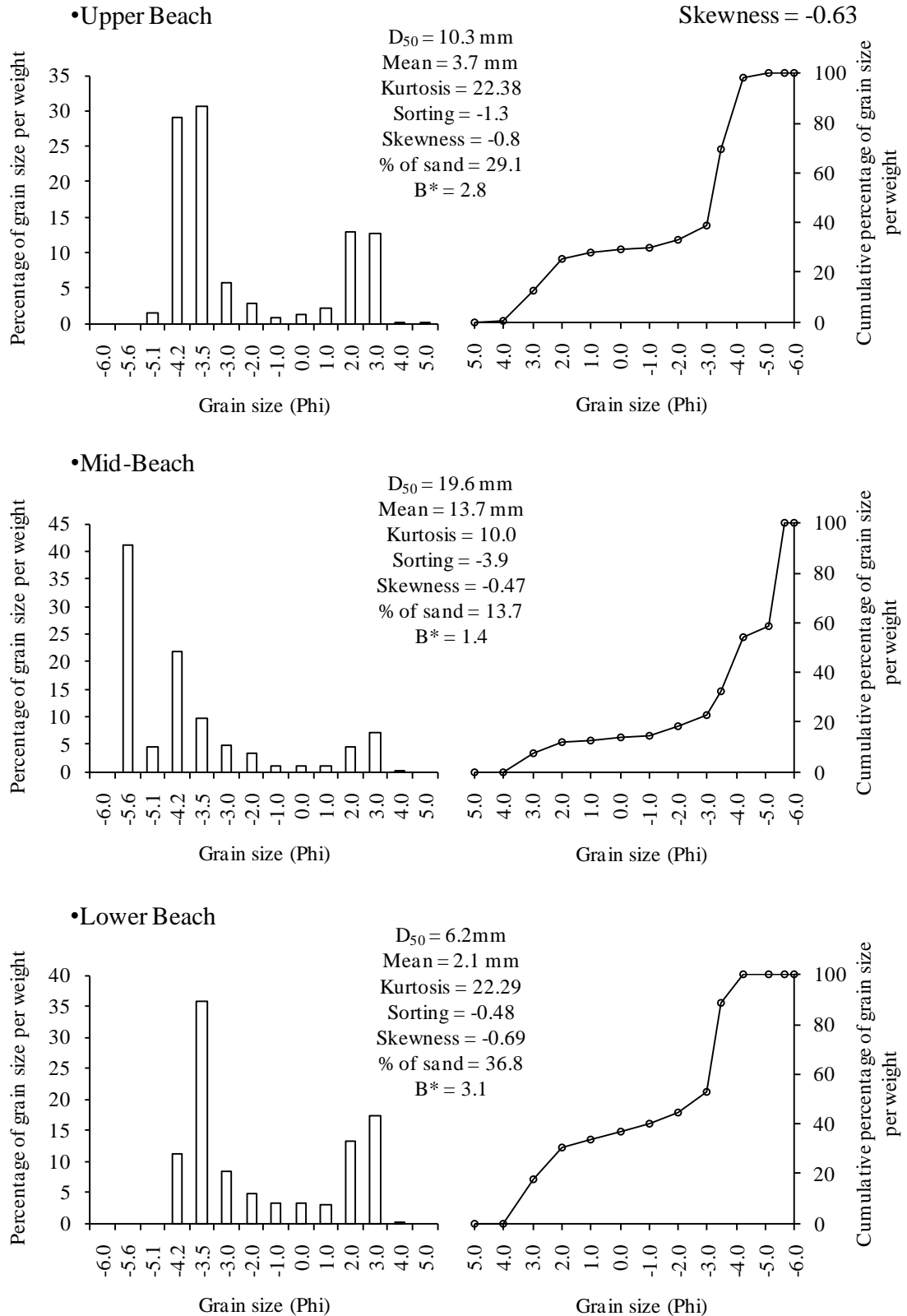
November 6th am 2005, (tide 17)

Total Statistics: $D_{50} = 12.8$ mm
 % of sand = 13.2
 Mean = 7.4 mm
 Kurtosis = 4.95
 Sorting = -2.9
 Skewness = 0.16



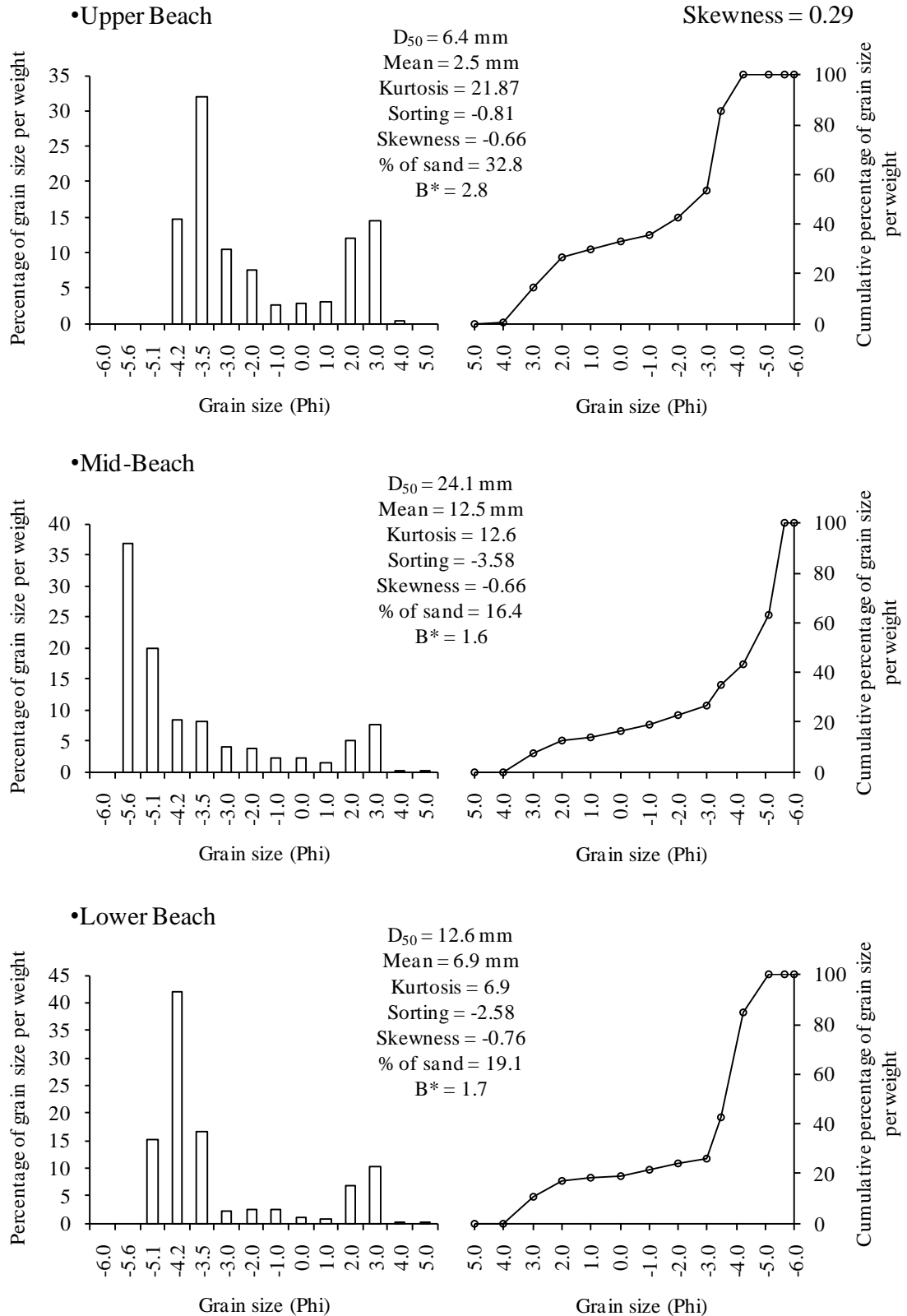
November 6th pm 2005, (tide 18)

Total Statistics: $D_{50} = 14.5$ mm
 % of sand = 19.8
 Mean = 6.9 mm
 Kurtosis = 10.5
 Sorting = -2.66
 Skewness = -0.63



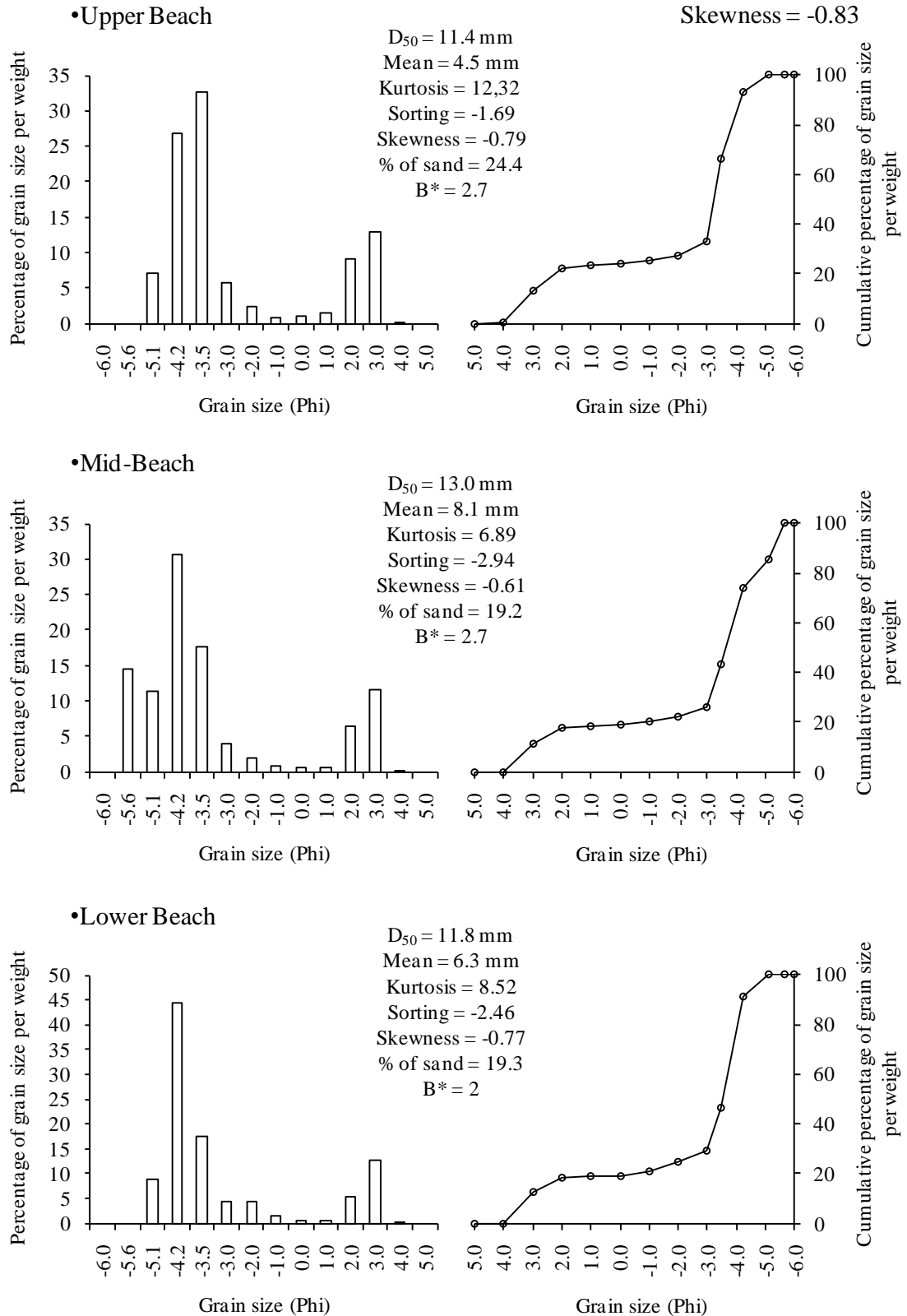
November 7th am 2005, (tide 19)

Total Statistics: $D_{50} = 15.4$ mm
 % of sand = 21.7
 Mean = 6.6 mm
 Kurtosis = 15.1
 Sorting = -2.51
 Skewness = 0.29



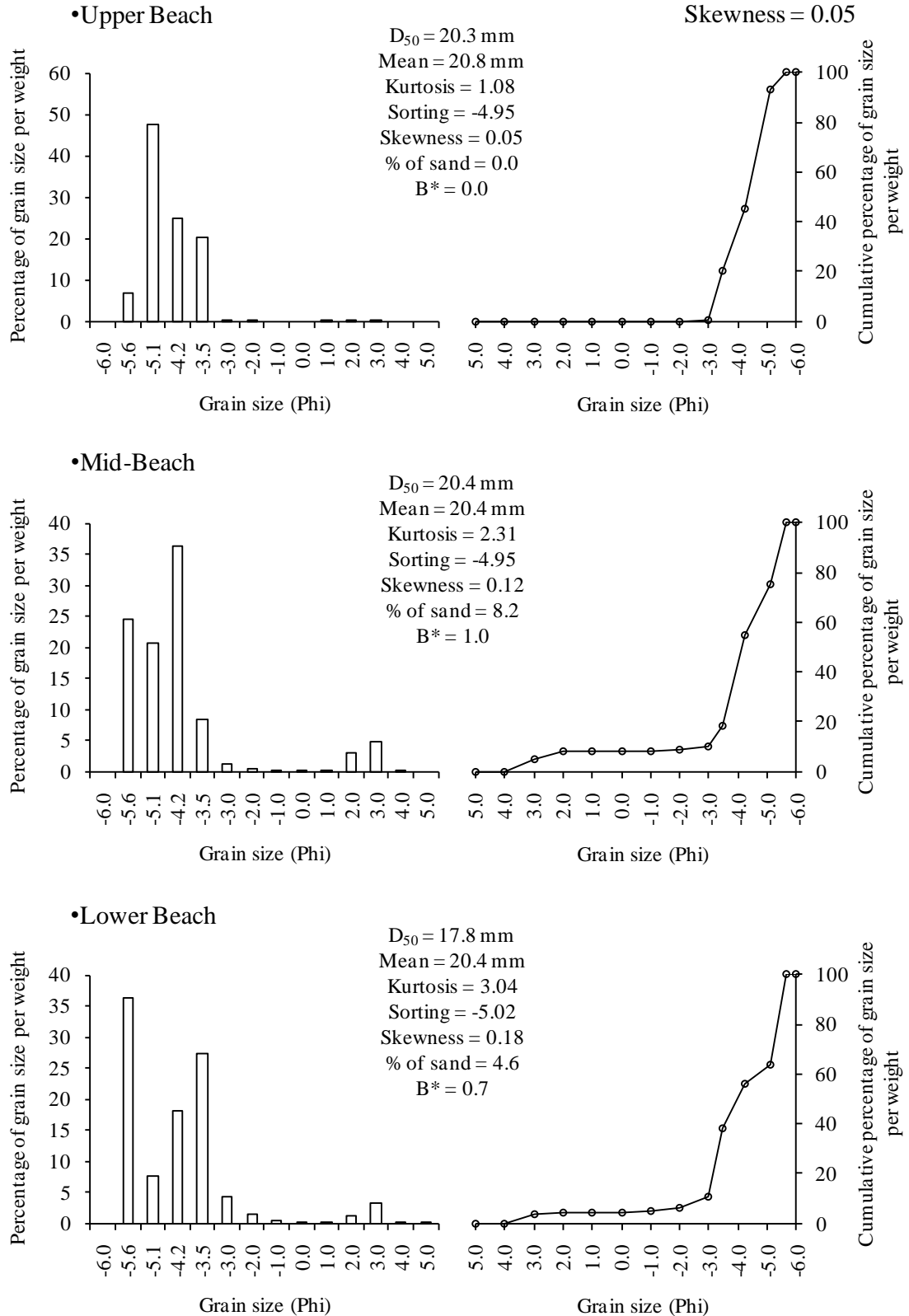
November 7th pm 2005, (tide 20)

Total Statistics: $D_{50} = 15.1$ mm
 % of sand = 20.9
 Mean = 5.7 mm
 Kurtosis = 8.75
 Sorting = -2.17
 Skewness = -0.83



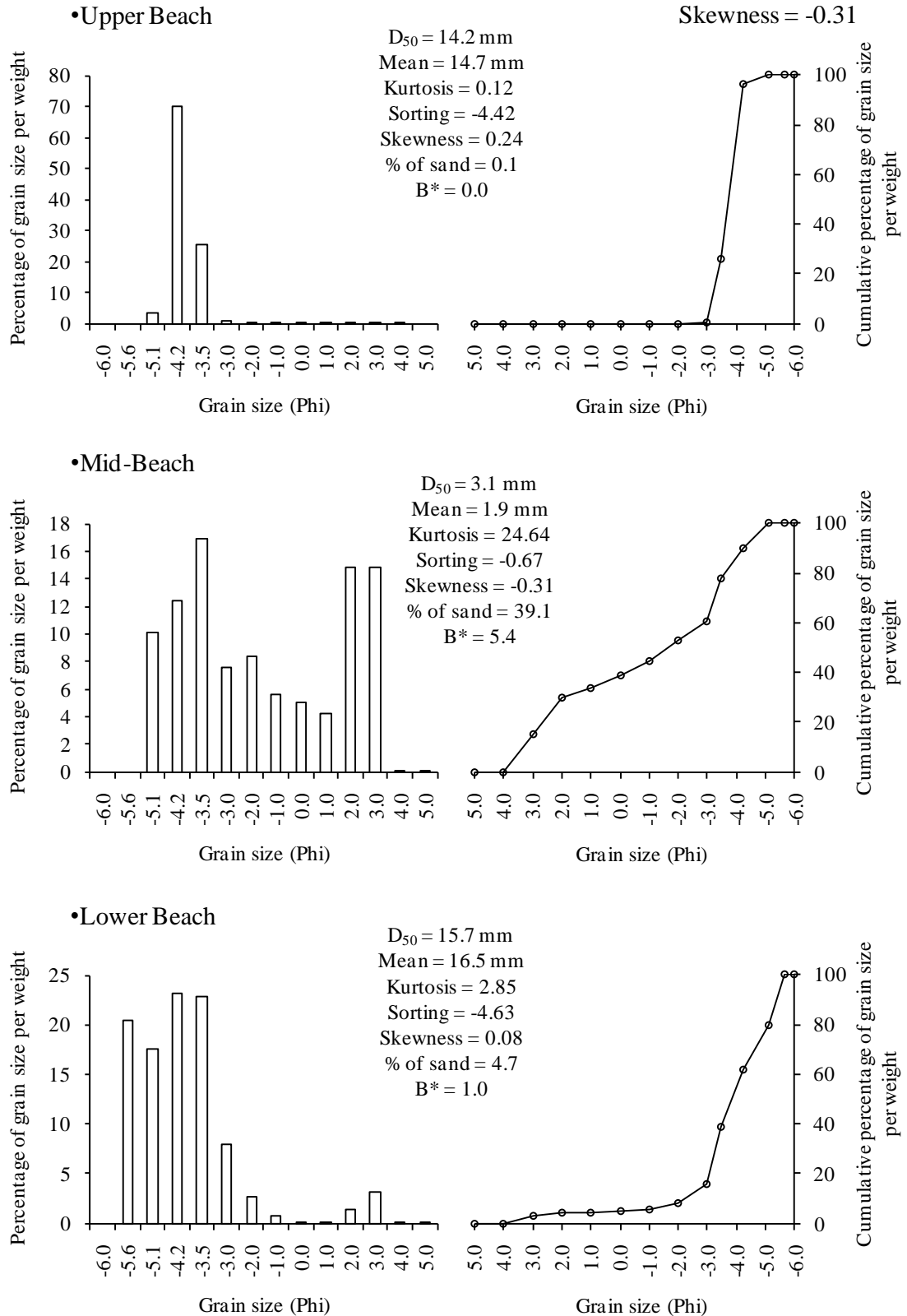
November 8th am 2005, (tide 21)

Total Statistics: $D_{50} = 20.7\text{mm}$
 % of sand = 4.8
 Mean = 20.75
 Kurtosis = 1.77
 Sorting = -4.99
 Skewness = 0.05



November 8th pm 2005, (tide 22)

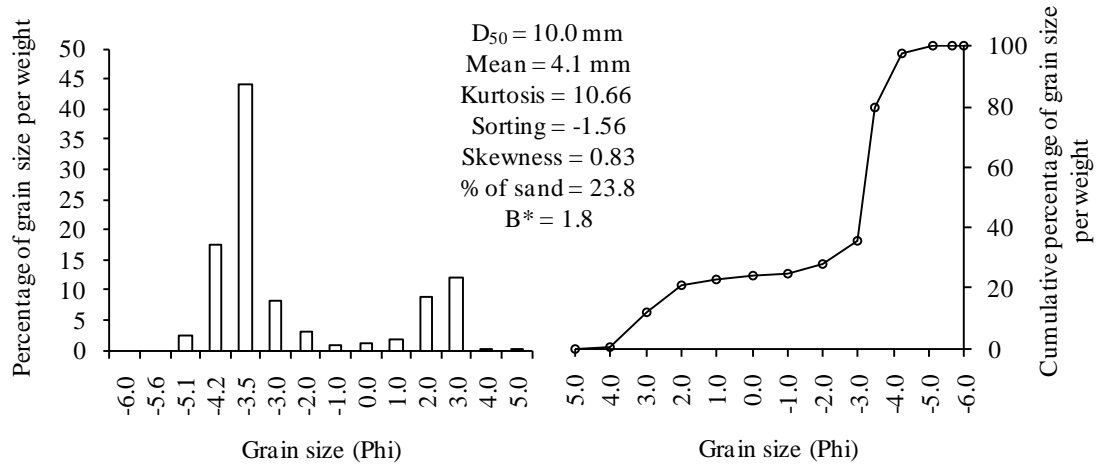
Total Statistics: $D_{50} = 12.7$ mm
 % of sand = 10.9
 Mean = 10.7 mm
 Kurtosis = 4.24
 Sorting = -3.65
 Skewness = -0.31



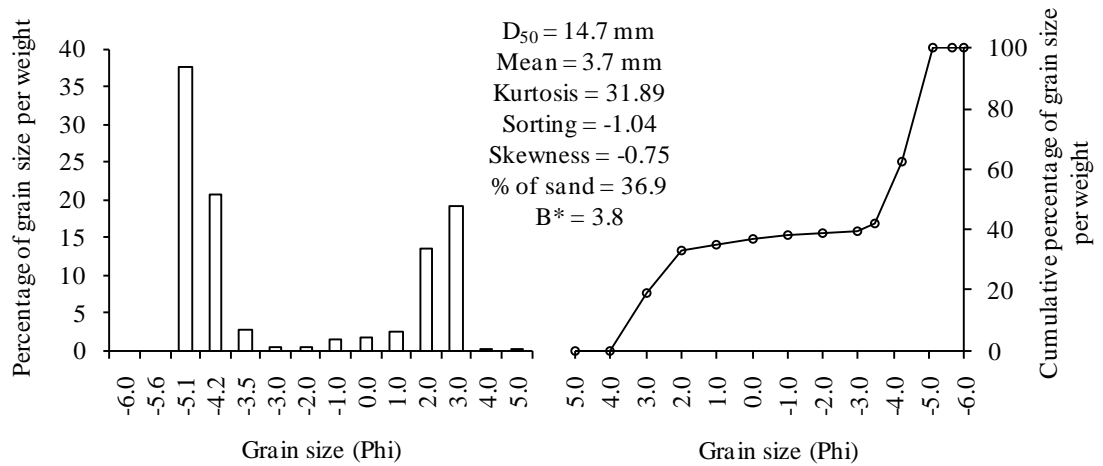
November 9th am 2005, (tide 23)

Total Statistics: $D_{50} = 12.4$ mm
 % of sand = 21.1
 Mean = 5.5 mm
 Kurtosis = 9.4
 Sorting = -2.12
 Skewness = -0.79

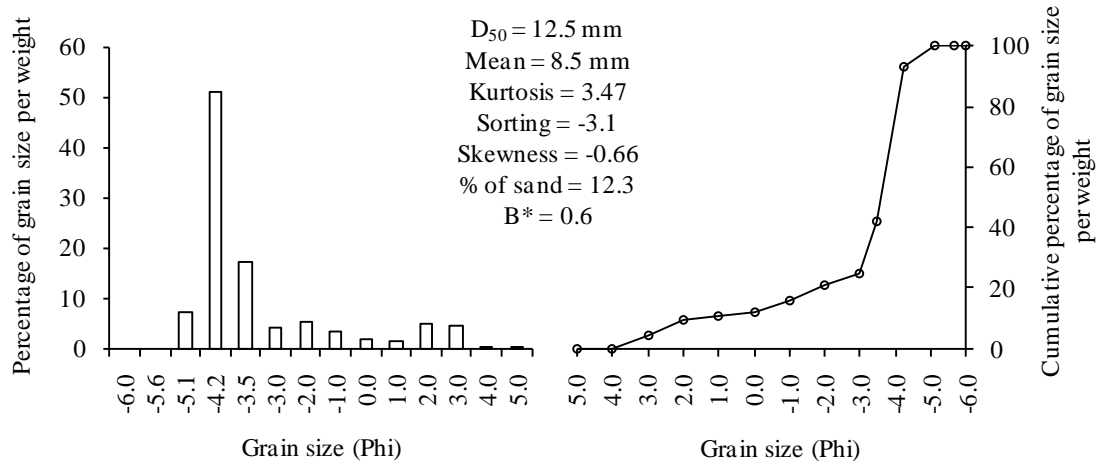
•Upper Beach



•Mid-Beach

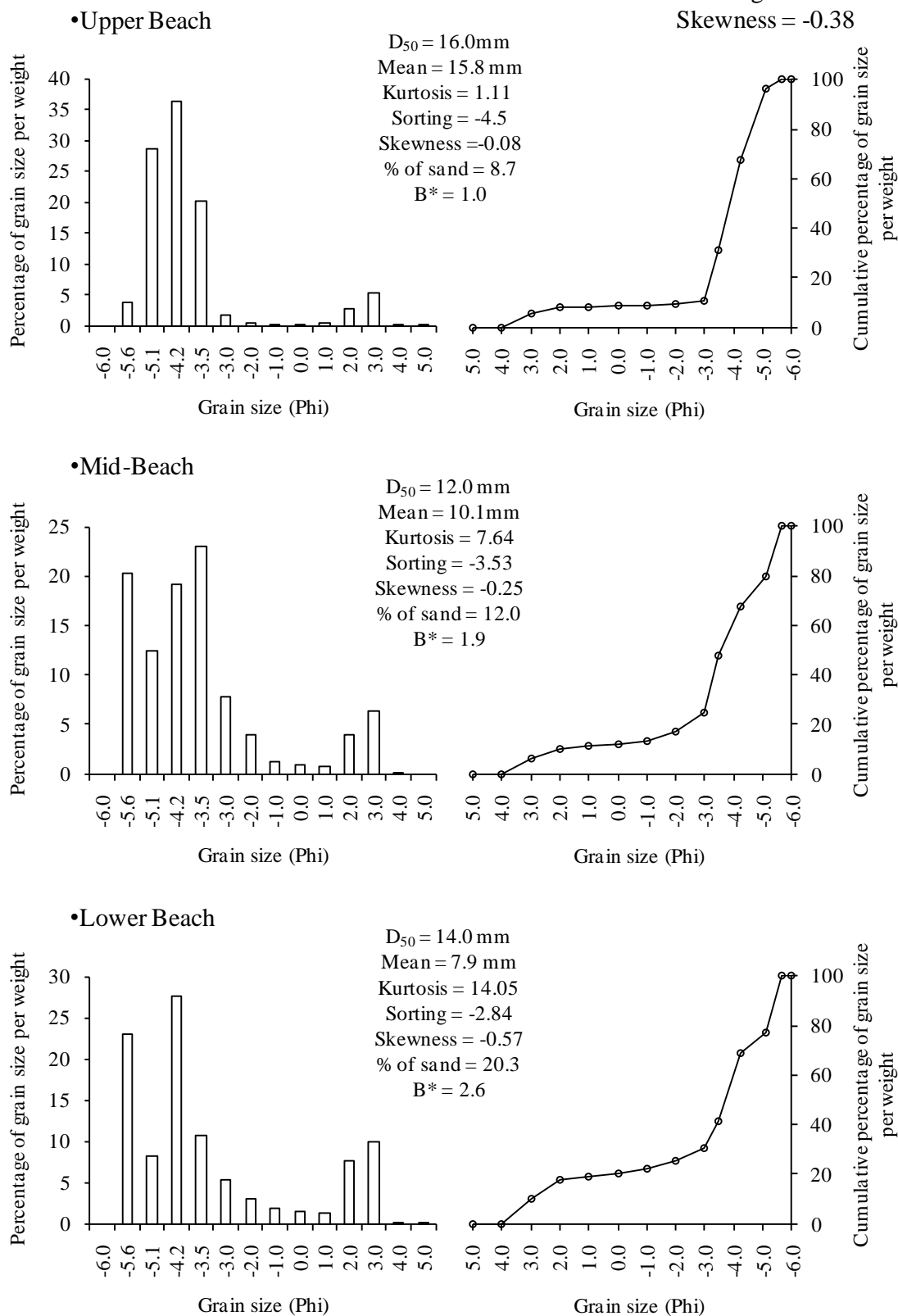


•Lower Beach



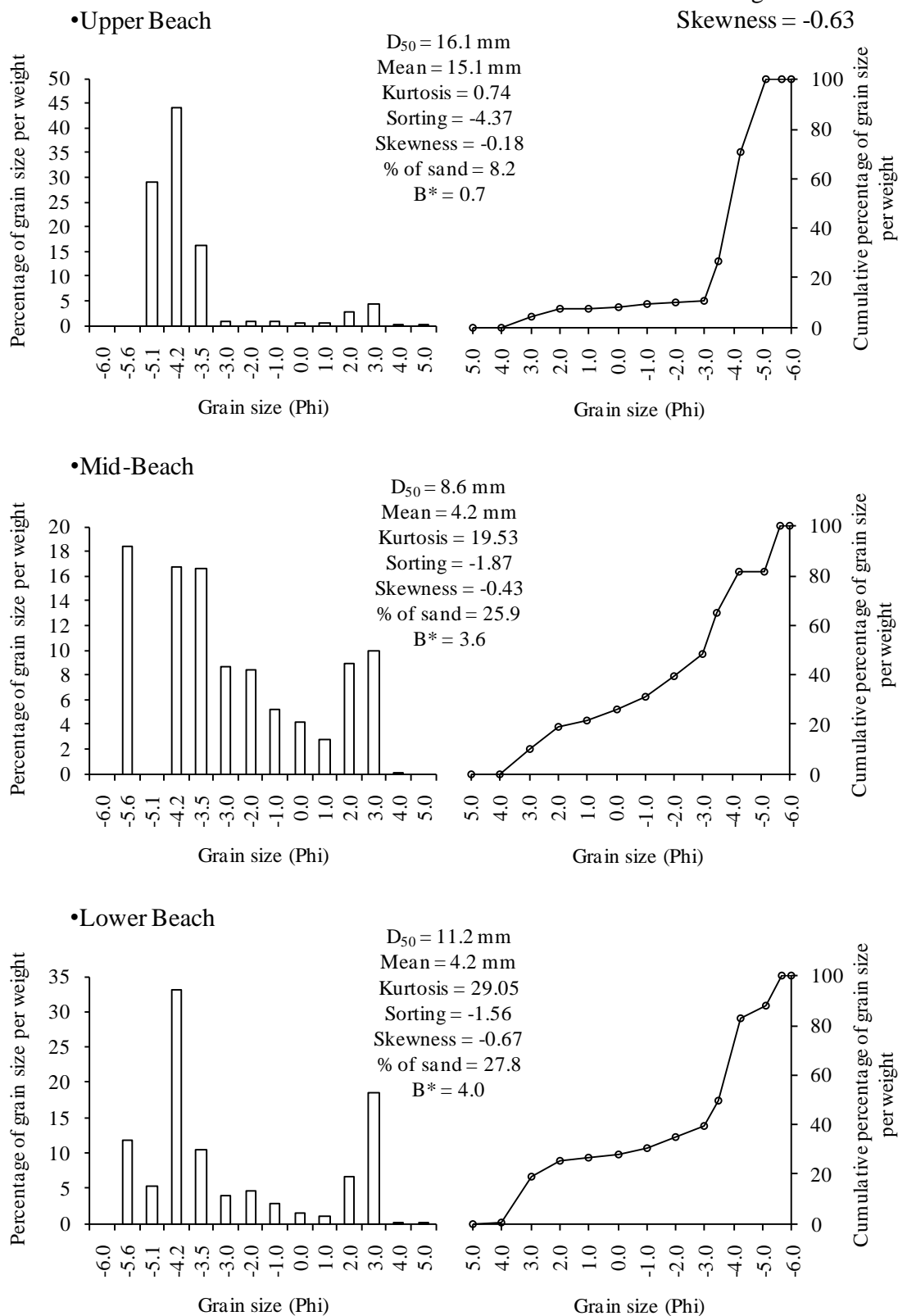
November 10th am 2005, (tide 25)

Total Statistics: $D_{50} = 14.4$ mm
 % of sand = 12.8
 Mean = 10.3 mm
 Kurtosis = 5.89
 Sorting = -3.53
 Skewness = -0.38



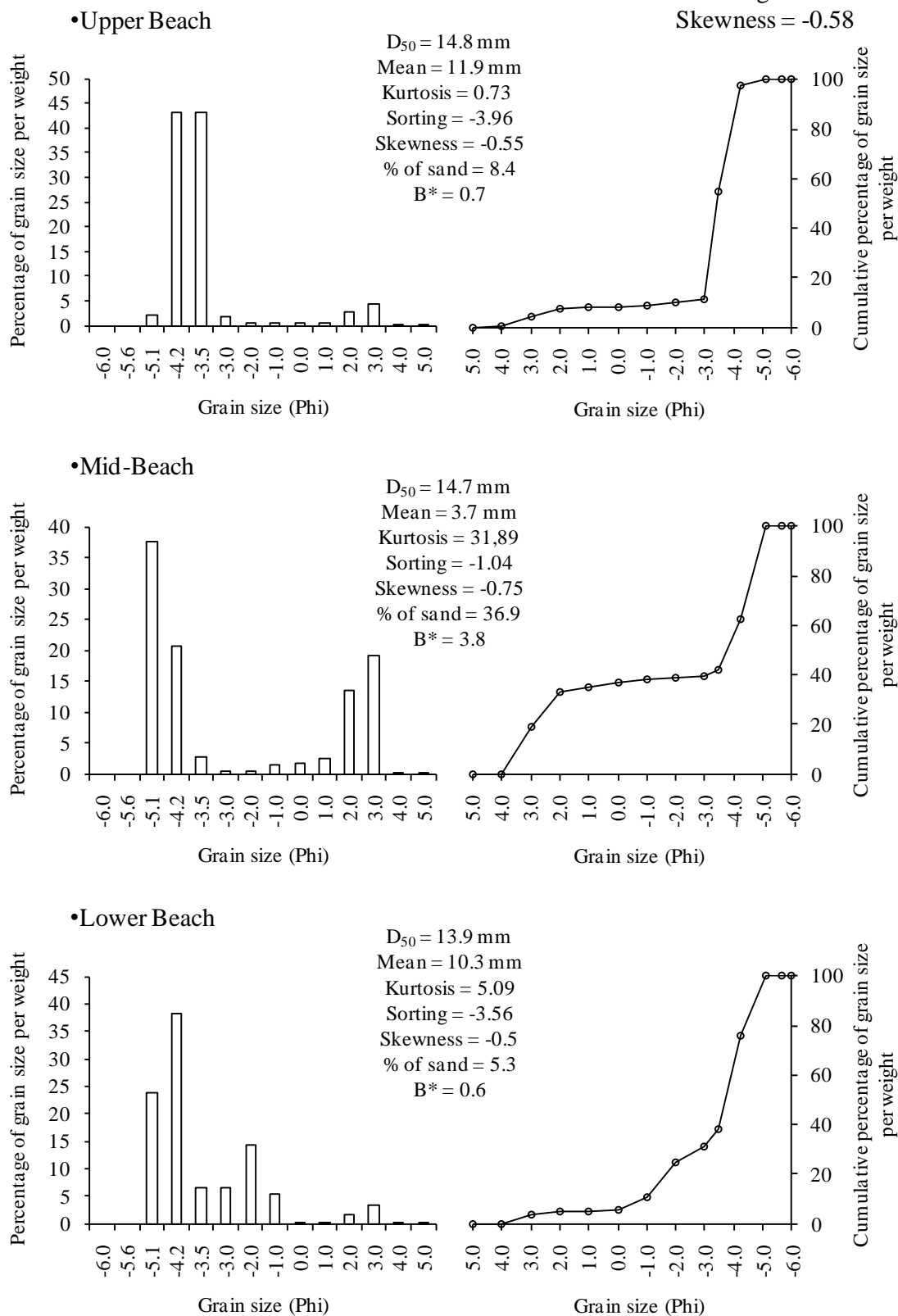
November 10th pm 2005, (tide 26)

Total Statistics: $D_{50} = 13.1$ mm
 % of sand = 16.9
 Mean = 8.0 mm
 Kurtosis = 8.1
 Sorting = -2.92
 Skewness = -0.63



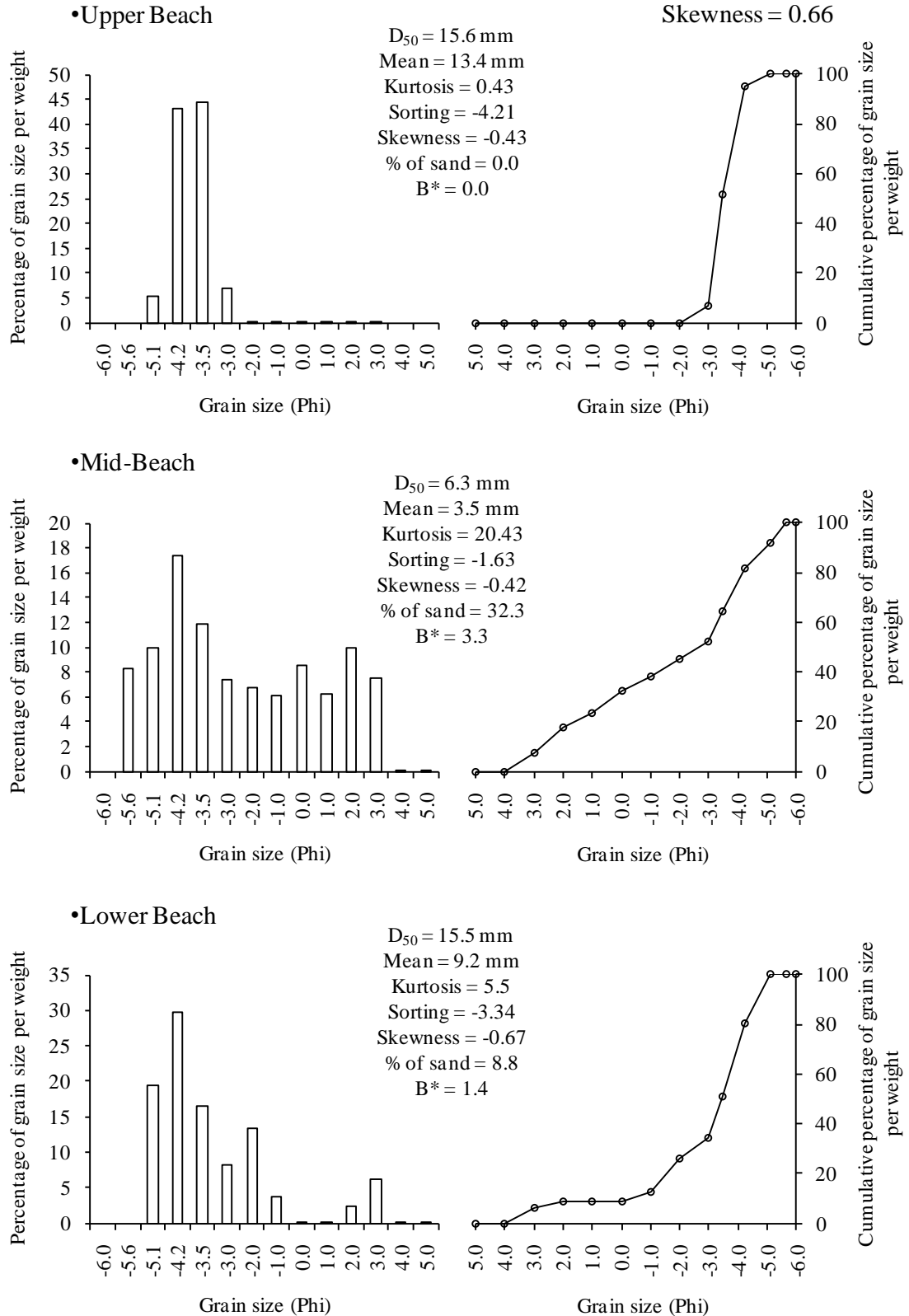
November 11th am 2005, (tide 27)

Total Statistics: $D_{50} = 12.2$ mm
 % of sand = 10.5
 Mean = 9.1 mm
 Kurtosis = 3.59
 Sorting = -3.3
 Skewness = -0.58



November 11th pm 2005, (tide 1)

Total Statistics: $D_{50} = 13.8$ mm
 % of sand = 13.1
 Mean = 7.7 mm
 Kurtosis = 6.84
 Sorting = -2.96
 Skewness = 0.66

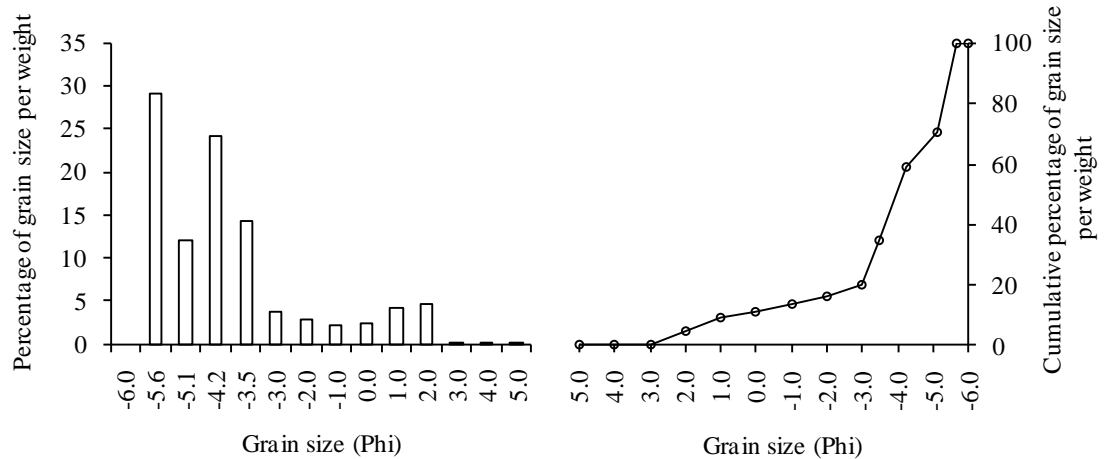


Birling Gap

As mentioned in Chapter 3, Sediment sampling was conducted only when noticeable grain size change on the beach surface was noticeable. As a result, the beach sediment was sampled on two low tides during the survey period in March 2006, and only one low tide during the surveys in May and December 2006.

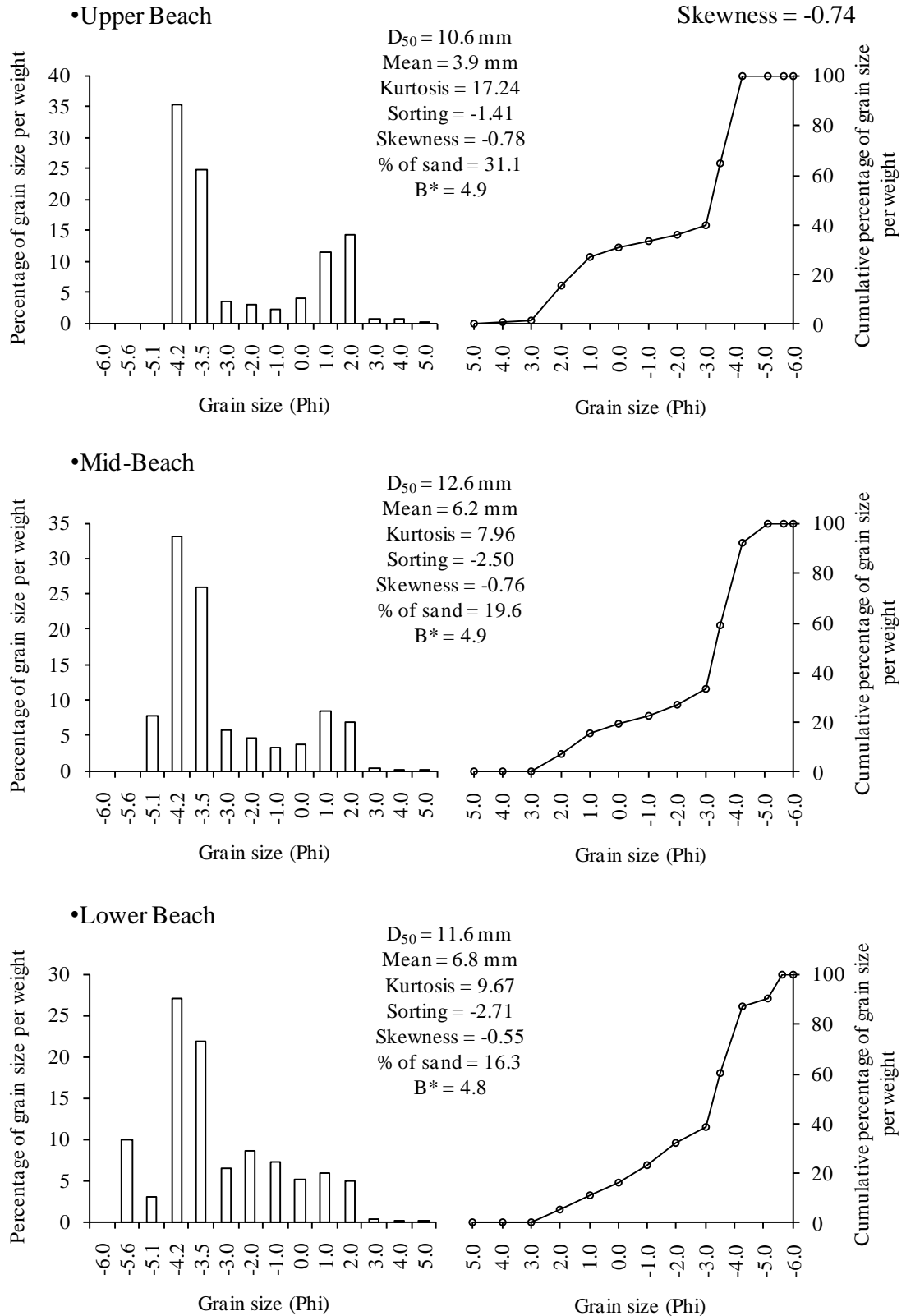
March to December 2006

$D_{50} = 17.4 \text{ mm}$
 % of sand = 11.3
 Mean = 14.4 mm
 Kurtosis = 6.51
 Sorting = -4.23
 Skewness = -0.35
 $B^* = 5.0$



March 20th pm 2006

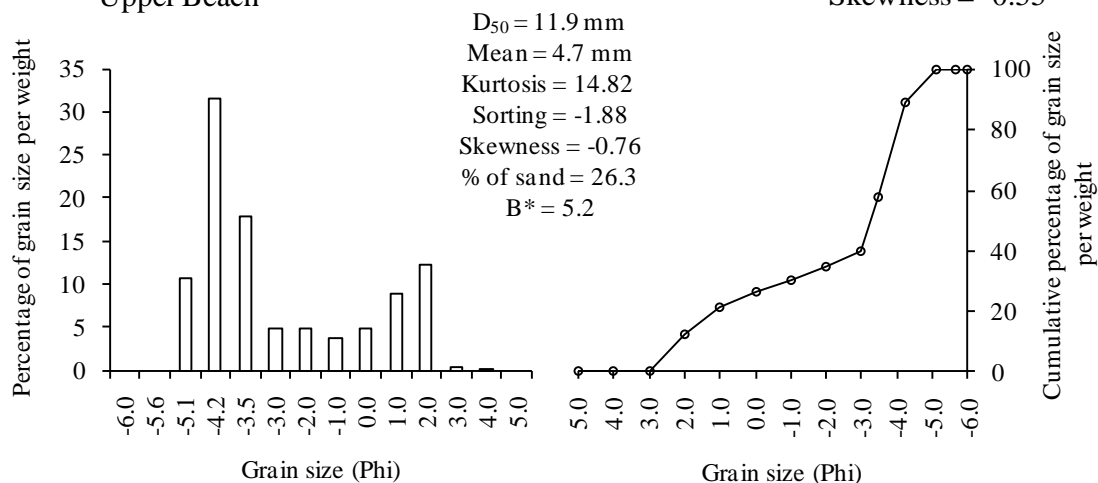
Total Statistics: $D_{50} = 11.5$ mm
 % of sand = 22.5
 Mean = 5.4 mm
 Kurtosis = 11.02
 Sorting = -2.13
 Skewness = -0.74



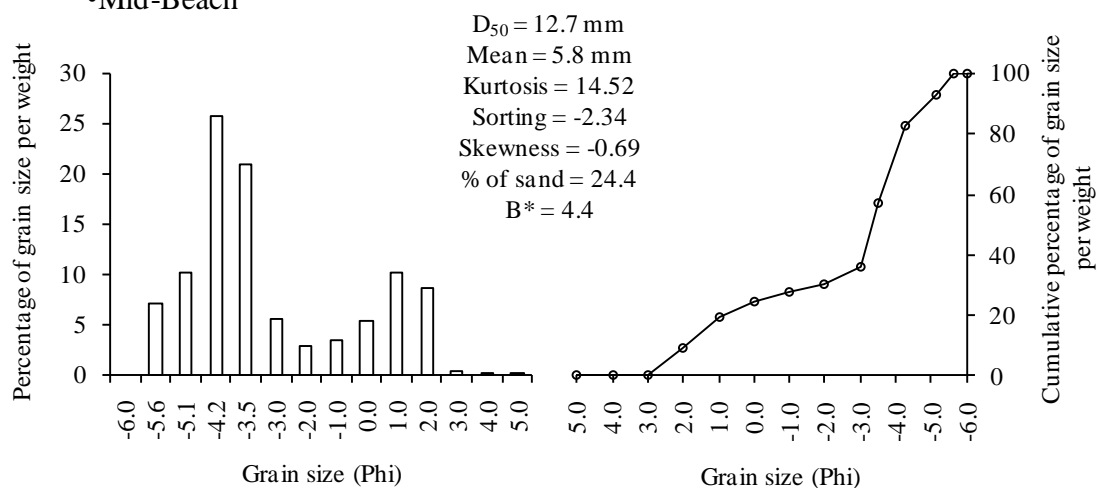
March 22nd pm 2006

Total Statistics: $D_{50} = 14.1$ mm
 % of sand = 22.2
 Mean = 6.7 mm
 Kurtosis = 15.1
 Sorting = -2.61
 Skewness = -0.55

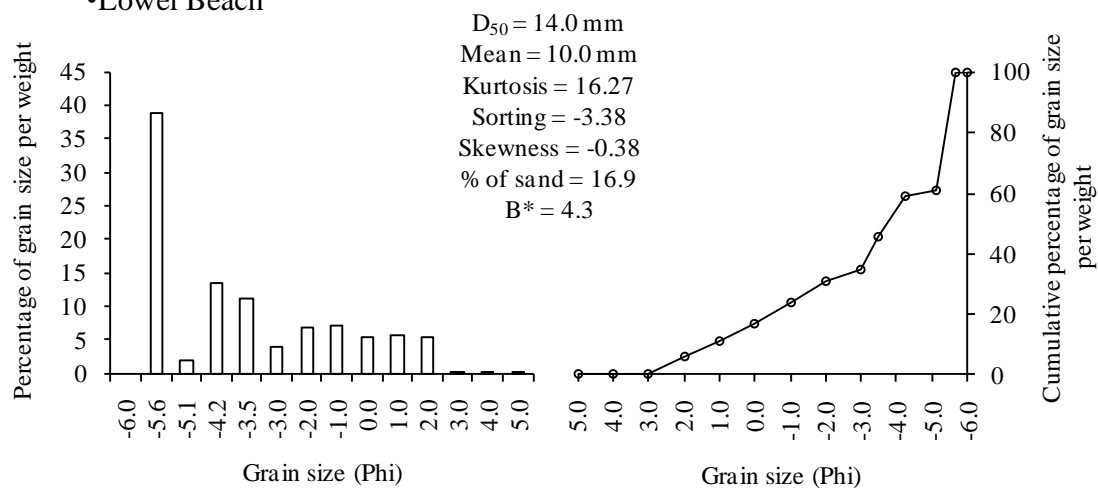
•Upper Beach



•Mid-Beach

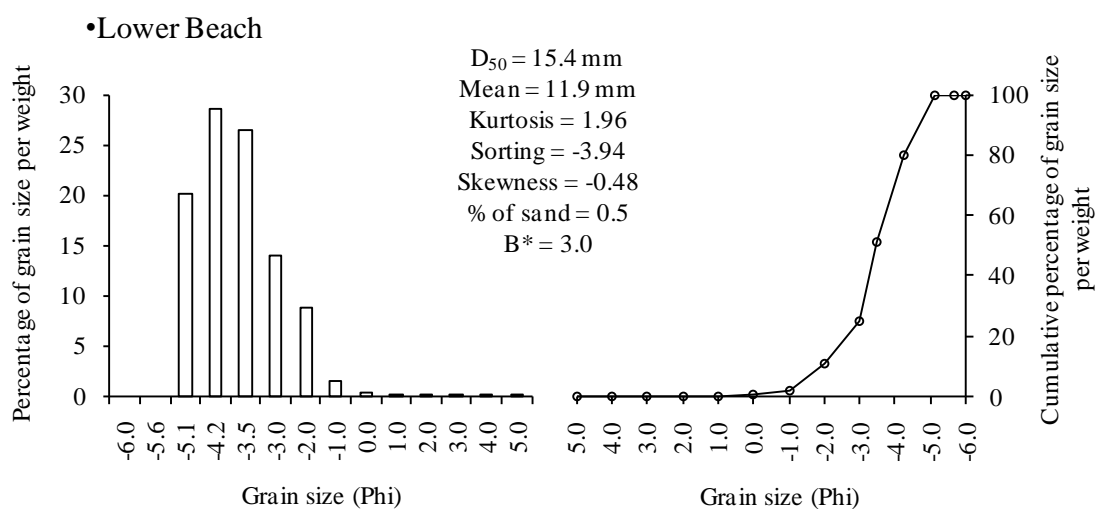
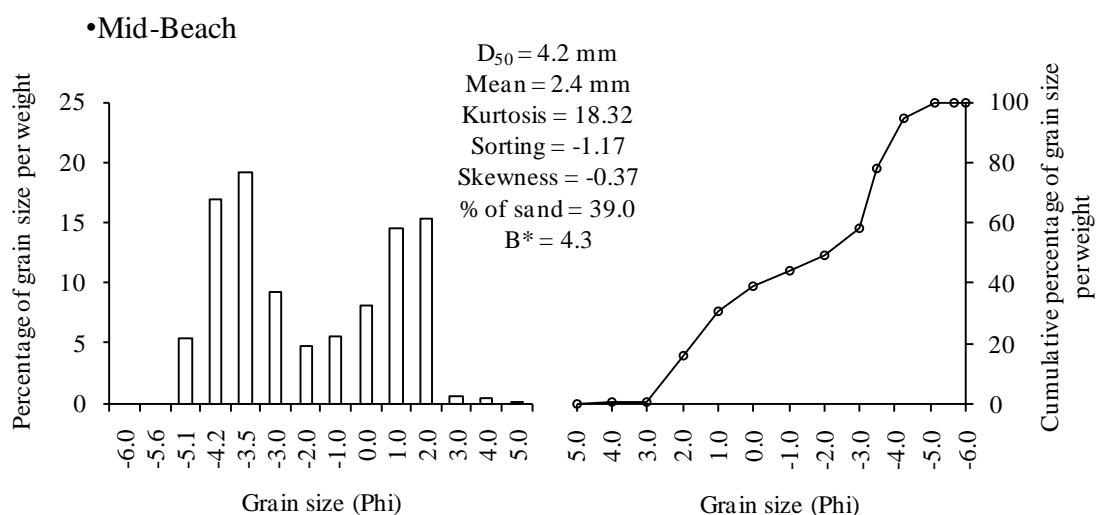
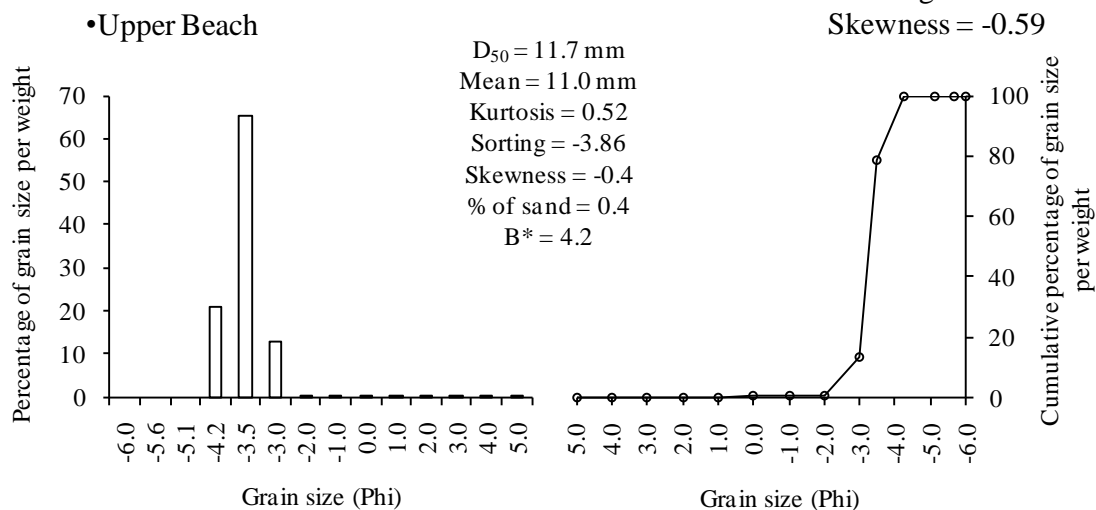


•Lower Beach



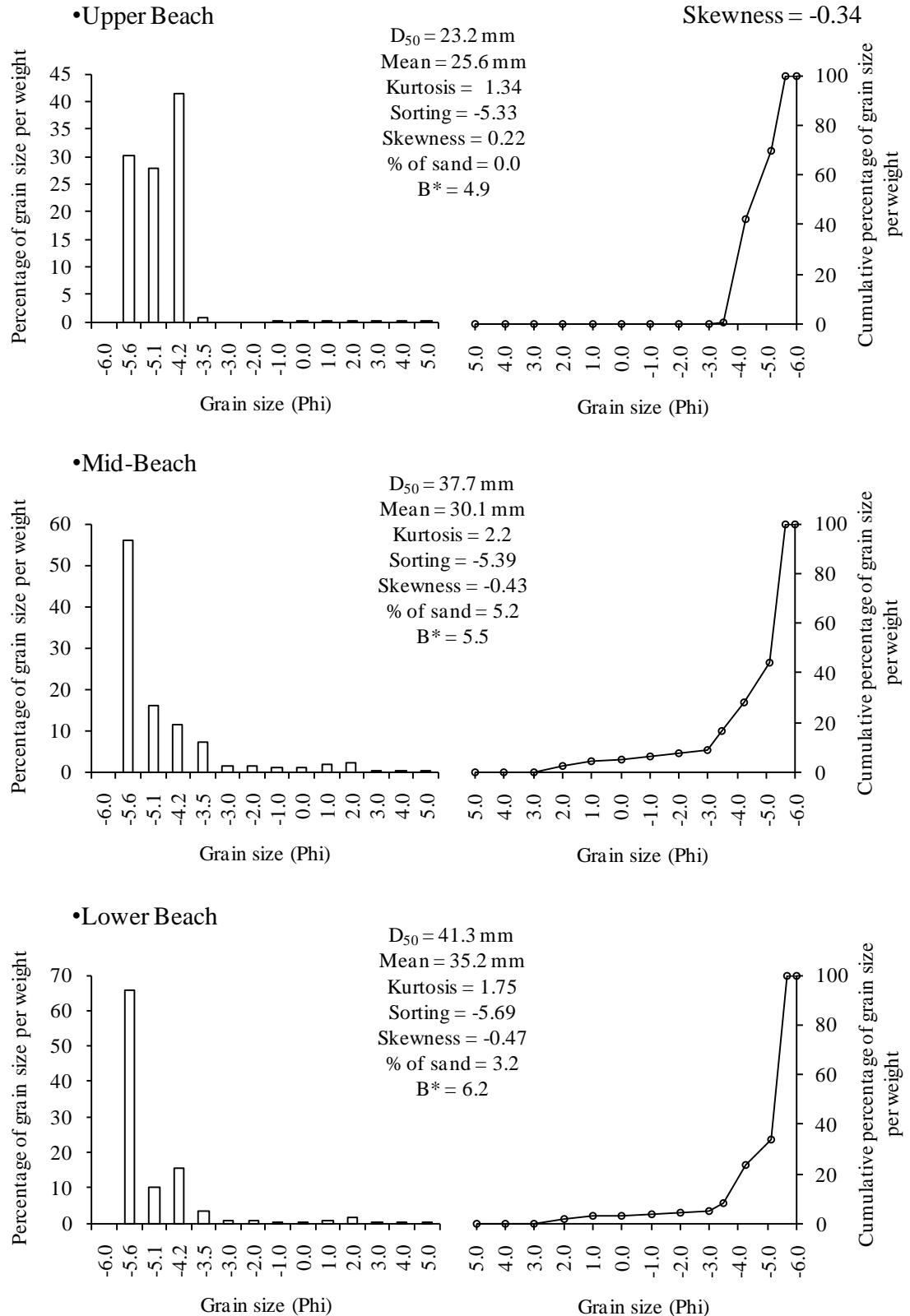
May 2006 (19th am)

Total Statistics: $D_{50} = 11.3$ mm
 % of sand = 12.4
 Mean = 7.68 mm
 Kurtosis = 3.75
 Sorting = -3.01
 Skewness = -0.59



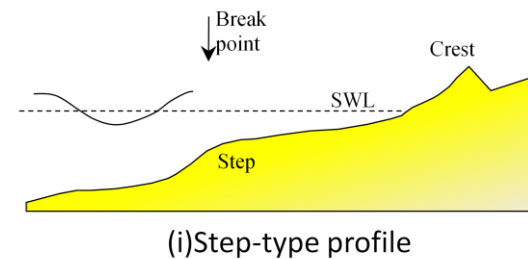
December 2006 (14th pm)

Total Statistics: $D_{50} = 35.5$ mm
 % of sand = 3.0
 Mean = 30.6 mm
 Kurtosis = 1.81
 Sorting = -5.5
 Skewness = -0.34

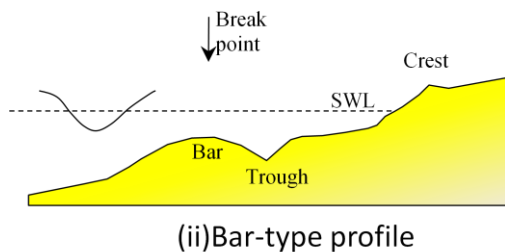


Appendix III Sandy beaches typical profile types

Profile types on sand beaches introduced by Komar (1976):



(i) A step or swell profile formed preferably during the summer in low steepness wave conditions and called “summer profile”. This type of profile presents a step and bars, the beach profile displays a trend to accretion; and,



(ii) A bar or storm profile generally characteristic of the winter wave conditions and called “winter profiles”. The high level energy delivered by the waves induces beach erosion letting the beach profile free of morphological features apart from the highest berm if no washover.

Figure III-1 Idealised sandy beach profile types (Powell, 1990)

Profile types on sandy beaches introduced by Sonu and Van Beek (1971):

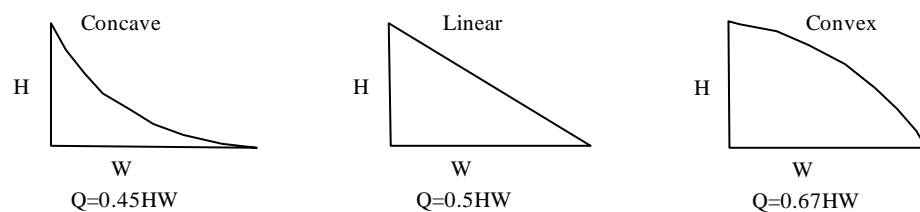


Figure III-2 Basic profile types observed on a sand beach. a) Concave upwards, corresponding to a maximum storage of sediment upward the beach; b) Linear; c) Convex, corresponding to a minimum storage of sediment on the beach (Sonu and Van Beek (1971)).

Appendix IV Active Layer measurements

Cayeux-sur-Mer Winter 2005-Transect 1 (Further South)																
(all data are in cm)	Upper Beach			Upper-middle Beach			Middle Beach			Lower-middle Beach			Lower Beach (Beach step)			H _s max
	Erosion	Accretion	Active layer	Erosion	Accretion	Active layer	Erosion	Accretion	Active layer	Erosion	Accretion	Active layer	Erosion	Accretion	Active layer	
29 dec-05 AM	0	8	8	13	0	13	10	2	10				6	20	20	82
29 dec-05 PM	4	12	12	7	10	10	5	19	19				>39	>29	>39	50
30 dec-05 AM	7	6	7				N/A	N/A	N/A				9	8	9	51
30 dec-05 PM	29	0	29				12	13	13				8	7	8	62
31 dec-05 AM	21	N/A	N/A				10	8	10				9	20	20	69
31 dec-05 PM	12	13	13				18	17	18				20	29	29	136
01 dec-05 AM	>30	>31	>31				>26	>24	>26				0<<36	0<<36	0<<36	89
01 dec-05 PM	N/A	48	N/A				>24	>24	>24				0<<36	0<<19	0<<36	216
02 dec-05 AM	13	13	13				0<<20	19<<39	19<<39				19	4	19	82
02 dec-05 PM	18	14	18				23<<43	0<<12	23<<43				15	18	18	95
03 dec-05 AM	4	18	18				>16	>20	>20				15	11	15	117
03 dec-05 PM	28	0	28				>20	>20	>20				>14	>27	>27	169
04 dec-05 AM	>9	>30	>30				>20	>30	>30				>27	>30	>30	268
04 dec-05 PM	14	6	14				>30	>20	>30				>30	>20	>30	183
05 dec-05 AM	0<<22	34<<56	34<<56				>20	>27	>27				N/A	N/A	N/A	174
05 dec-05 PM	0<<30	34<<64	34<<64				>27	>27	>27				N/A	N/A	N/A	126
06 dec-05 AM	0<<25	9<<53	9<<53				>27	>20	>27				N/A	N/A	N/A	168
06 dec-05 PM	23	6	23				>20	>17	>20				N/A	N/A	N/A	142
07 dec-05 AM	14	12	14				>17	>15	>17				>27	>27	>27	151
07 dec-05 PM	8<<34	0<<26	8<<34				>15	>16	>16				>27	>23	>27	153
08 dec-05 AM	4	9	9				>16	>17	>17				>23	>23	>23	114
08 dec-05 PM	0	17	17				17	10	17				>23	>26	>26	89
09 dec-05 AM	26	3	26				>10	>11	>11				0<<26	1<<27	1<<27	133
10 dec-05 AM	0	0	0				>11	>28	>28	10	18	18	8<<27	0<<19	8<<27	81
10 dec-05 PM	0	0	0				20	2	20	0	5	5	0<<18	0<<4	0<<18	66
11 dec-05 AM	3	7	7				>10	>14	>14	11	15	15	>4	>20	>20	163
11 dec-05 PM	0	0	0				>14	>20	>20	10	19	19	>20	>30	>30	137

Table IV-1 Active layer data measured at Cayeux-sur-Mer in October/November 2005 along transect 1 (Figure 3-11), including the mixing depth (annotated erosion in the table) and the accretion above the top painted pebble found on the column.

Cayeux-sur-Mer Winter 2005-Transect 2																
(all data are in cm)	Upper Beach			Upper-middle Beach			Middle Beach			Lower-middle Beach			Lower Beach (Beach step)			H _s max
	Erosion	Accretion	Active layer	Erosion	Accretion	Active layer	Erosion	Accretion	Active layer	Erosion	Accretion	Active layer	Erosion	Accretion	Active layer	
29 dec-05 AM	0	0	0	>35	N/A	N/A				25	20	25	N/A	>42	N/A	82
29 dec-05 PM	0	0	0	23	13	23				8	16	16	17	17	17	50
30 dec-05 AM	0	0	0	13	10	13				16	17	17	23	7	23	51
30 dec-05 PM	0	18	18	>17	>36	>36				13	24	24	N/A	N/A	N/A	62
31 dec-05 AM	>58	N/A	N/A	7	26	26				24	12	24	14	0	14	69
31 dec-05 PM	10	10	10	>42	>31	>42				N/A	N/A	N/A	>20	>30	>30	136
01 dec-05 AM	10	0	10	>21	>24	>24				N/A	N/A	N/A	>30	>22	>30	89
01 dec-05 PM	N/A	>39	N/A	<14	27<<41	27<<41				>26	>26	>26	>22	>24	>24	216
02 dec-05 AM	10	14	14	18	14	18				>26	>38	>38	20	5	20	82
02 dec-05 PM	14	15	15	0	15	15				20	11	20	>14	>24	>24	95
03 dec-05 AM	28	40	40	37	17	37				25	16	25	>24	>20	>24	117
03 dec-05 PM	30	0	30	17<<26	4<<13	17<<26				>5	>27	>27	>20	>31	>31	169
04 dec-05 AM	>8	>30	>8	<13	36<<49	36<<49				>24	>21	>24	>31	>30	>31	268
04 dec-05 PM	16	3	16	20	11	20				20<<33	30<<42	30<<42	>30	>28	>30	183
05 dec-05 AM	>3	>35	>35	0<<15	12<<27	12<<27				27<<42	15<<29	27<<42	0<<28	0<<28	0<<28	174
05 dec-05 PM	20	33	33	21	15	21				21	20	21	0<<28	0<<12	0<<28	126
06 dec-05 AM	16	20	20	21	15	21				>27	>31	>31	>12	>23	>23	168
06 dec-05 PM	16	14	16	19	0	19				>31	>16	>31	>23	>30	>30	142
07 dec-05 AM	40	38	40	20	13	20				>16	>14	>16	>30	>24	>30	151
07 dec-05 PM	38	8	38	14	15	15				>14	>18	>18	2<<22	0<<20	2<<22	153
08 dec-05 AM	8	5	8	0<<3	10<<28	10<<28				>18	>23	>23	4<<12	0<<8	4<<12	114
08 dec-05 PM	0	0	0	19	0	19				>23	>16	>23	>12	>12	>12	89
09 dec-05 AM	0	18	18	9	11	11				>16	>16	>16	>12	>24	>24	133
10 dec-05 AM	0	0	0	15	16	16				12	15	15	24	13	24	81
10 dec-05 PM	0	0	0	8	4	8				8	12	12	>13	>11	>13	66
11 dec-05 AM	0	0	0	>6	>24	>24				>12	>18	>18	>11	>26	>26	163
11 dec-05 PM	4	13	13	11	5	11				>18	>25	>25	>26	N/A	N/A	137

Table IV-2 Active layer data measured at Cayeux-sur-Mer in October/November 2005 along transect 2 (Figure 3-11), including the mixing depth (annotated erosion in the table) and the accretion above the top painted pebble found on the column.

Cayeux-sur-Mer Winter 2005-Transect 3																
(all data are in cm)	Upper Beach			Upper-middle Beach			Middle Beach			Lower-middle Beach			Lower Beach (Beach step)			H _s max
	Erosion	Accretion	Active layer	Erosion	Accretion	Active layer	Erosion	Accretion	Active layer	Erosion	Accretion	Active layer	Erosion	Accretion	Active layer	
29 dec-05 AM	0	0	0				17	4	17				>34	>27	>34	82
29 dec-05 PM	0	7	7				>21	>35	>35				>15	>36	>36	50
30 dec-05 AM	0	8	8				17	18	18				22	22	22	51
30 dec-05 PM	0	24	24				13	15	15				18	16	18	62
31 dec-05 AM	45	11	45				15	25	25				16	7	16	69
31 dec-05 PM	26	0	26				21	12	21				N/A	N/A	N/A	136
01 dec-05 AM	>5	>25	>25				>40	>24	>40				N/A	>20	N/A	89
01 dec-05 PM	>25	>32	>32				>35	>35	>35				>20	>26	>26	216
02 dec-05 AM	12	8	12				17	30	30				26	22	26	82
02 dec-05 PM	12	20	20				0<<37	1<<38	1<<38				>22	>17	>22	95
03 dec-05 AM	11	27	27				21<<31	0<<10	21<<31				12	25	25	117
03 dec-05 PM	>44	>30	>44				>21	>36	>36				>25	>28	>28	169
04 dec-05 AM	>30	>31	>31				>36	>30	>36				>28	>30	>30	268
04 dec-05 PM	18	5	18				>30	>32	>32				4<<34	4<<34	4<<34	183
05 dec-05 AM	>18	>30	>30				>32	>38	>38				0<<29	0<<29	0<<29	174
05 dec-05 PM	>30	>31	>31				38	20	38				30	15	30	126
06 dec-05 AM	11	23	23				>20	>26	>26				>15	>30	>30	168
06 dec-05 PM	14	18	18				21	17	21				>30	>33	>33	142
07 dec-05 AM	27	15	27				>21	>23	>23				>33	>21	>33	151
07 dec-05 PM	35	2	35				>23	>18	>23				>21	>24	>24	153
08 dec-05 AM	12	15	15				18	19	19				>24	>14	>24	114
08 dec-05 PM	0	7	7				>19	>27	>27				>14	>13	>14	89
09 dec-05 AM	26	12	26	13	13	13	>27	>23	>27				>13	>24	>24	133
10 dec-05 AM	0	0	0	>22	>21	>22	12	2	12				24	12	24	81
10 dec-05 PM	0	0	0	0	13	13	0<<17	3<<20	3<<20				>12	>11	>12	66
11 dec-05 AM	4	4	4	18	13	18	4<<20	0<<16	4<<20				>11	>27	>27	163
11 dec-05 PM	0	13	13	8	25	25	0<<16	7<<23	7<<23				>27	>27	>27	137

Table IV-3 Active layer data measured at Cayeux-sur-Mer in October/November 2005 along transect 3 (Figure 3-11), including the mixing depth (annotated erosion in the table) and the accretion above the top painted pebble found on the column.

Cayeux-sur-Mer Winter 2005-Transect 4 (Further North)																
(all data are in cm)	Upper Beach			Upper-middle Beach			Middle Beach			Lower-middle Beach			Lower Beach (Beach step)			H _s max
	Erosion	Accretion	Active layer	Erosion	Accretion	Active layer	Erosion	Accretion	Active layer	Erosion	Accretion	Active layer	Erosion	Accretion	Active layer	
29 dec-05 AM	0	0	0				14	3	14				15	25	25	82
29 dec-05 PM	4	0	4				>25	>35	>35				>45	>33	>45	50
30 dec-05 AM	0	0	0				13	0	13				19	13	19	51
30 dec-05 PM	0	0	0				16	15	16				>27	>34	>34	62
31 dec-05 AM	0	55	55				15	26	26				14	9	14	69
31 dec-05 PM	45<<55	0<<10	45<<55	6	15	15	>32	>32	>32				13	27	27	136
01 dec-05 AM	19	2	19				>32	>25	>32				>27	>34	>34	89
01 dec-05 PM	>12	>33	>33				>25	>33	>33				42	24	42	216
02 dec-05 AM	5	12	12				21	23	23				24	16	24	82
02 dec-05 PM	19	15	19				19	17	19				18	19	19	95
03 dec-05 AM	4	24	24				28	14	28				22	24	24	117
03 dec-05 PM	37	0	37				>19	>30	>30				0<<38	13<<51	13<<51	169
04 dec-05 AM	>16	>33	>33				>30	>31	>31				>33	>30	>33	268
04 dec-05 PM	20	8	20				28	22	28				0<<30	4<<34	4<<34	183
05 dec-05 AM	17	33	33				>25	>20	>25				7<<34	0<<27	7<<34	174
05 dec-05 PM	8	19	19				>20	>22	>22				15<<27	0<<12	15<<27	126
06 dec-05 AM	15	29	29				>22	>30	>30				31	25	31	168
06 dec-05 PM	16	20	20				22	17	22				>27	>27	>27	142
07 dec-05 AM	33	13	33				11	12	12				>27	>28	>28	151
07 dec-05 PM	29	5	29				18	12	18				>28	>25	>28	153
08 dec-05 AM	10	7	10				0<<19	6<<25	6<<25				25	22	25	114
08 dec-05 PM	3	0	3				13	5	13				>22	>19	>22	89
09 dec-05 AM	>22	>27	>27	>24	>24	>24	0<<7	18<<25	18<<25				>19	>19	>19	133
10 dec-05 AM	0	0	0	>24	>21	>24	9	5	9				>19	>20	>20	81
10 dec-05 PM	0	0	0	0	15	15	11	13	13				4	3	4	66
11 dec-05 AM	0	0	0	>36	>22	>36	10	0	10				>19	>21	>21	163
11 dec-05 PM	4	7	7	>22	>33	>33	>26	>33	>33				>21	>33	>33	137

Table IV-4 Active layer data measured at Cayeux-sur-Mer in October/November 2005 along transect 4 (Figure 3-11), including the mixing depth (annotated erosion in the table) and the accretion above the top painted pebble found on the column.

Birling Gap March 2006-Transect West														
(all data are in cm)	Upper Beach			Upper-middle Beach			Lower-middle Beach			Lower Beach (Beach step)			H _s max	
	Erosion	Accretion	Active layer	Erosion	Accretion	Active layer	Erosion	Accretion	Active layer	Erosion	Accretion	Active layer		
21 mar-06 am	Beach too short to have a measurement at this time and this place.			7	0	7	0	0	0	7	5	7	0.26	
22 mar-06 am				0	6	6	3	3	3	5	3	5	0.27	
22 mar-06 pm				0	4	4	3	5	5	3	2	3	0.18	
23 mar-06 pm				0	0	0	0	6	6	2	0	2	0.22	
24 mar-06 am				0	0	0	11	2	11	0	0	0	0.25	
25 mar-06 am				4	4	4	8	7	8	0	6	6	0.3	
25 mar-06 pm				4	5	5	7	7	7	21	25	25	0.73	

Beach too short to have a measurement at this time and this place.

Table IV-5 Active layer data measured at Birling Gap in March 2006 along the western transect (transect 1 on Figure 3-12), including the mixing depth (annotated erosion in the table) and the accretion above the top painted pebble found on the column.

Birling Gap March 2006-Transect East													
(all data are in cm)	Upper Beach			Upper-middle Beach			Lower-middle Beach			Lower Beach (Beach step)			H _s max
	Erosion	Accretion	Active layer	Erosion	Accretion	Active layer	Erosion	Accretion	Active layer	Erosion	Accretion	Active layer	
21 mar-06 am	0	9	9	5	4	5	2	6	6	2	5	5	0.26
22 mar-06 pm	0	0	0	10	6	10	6	5	6	5	0	5	0.27
22 mar-06 am	0	0	0	6	3	6	5	3	5	0	0	0	0.18
23 mar-06 pm	14	9	14	3	1	3	9	5	9	0	0	0	0.22
24 mar-06 am	0	0	0	5	5	5	5	1	5	5	8	8	0.25
25 mar-06 pm	5	5	5	0	0	0	1	4	4	4	1	4	0.3
25 mar-06 pm	0	0	0	5	7	7	18	17	18	19	35	35	0.73

Table IV-6 Active layer data measured at Birling Gap in March 2006 along the eastern transect (transect 3 on Figure 3-12), including the mixing depth (annotated erosion in the table) and the accretion above the top painted pebble found on the column.

Birling Gap May 2006-Transect East													
(all data are in cm)	Upper Beach			Upper-middle Beach			Lower-middle Beach			Lower Beach (Beach step)			$H_{s \max}$
	Erosion	Accretion	Active layer	Erosion	Accretion	Active layer	Erosion	Accretion	Active layer	Erosion	Accretion	Active layer	
20 may-06 am	9	12	12	44	>32	>32	10	29	29	>23	>29	>29	2.08
20 may-06 pm	15	13	15	15	9	15	29	7	29	>29	>26	>29	2.61
21 may-06 am	5	10	10	>26	>38	>38	11	13	13	>26	>36	>36	1.7
22 may-06 am	10	27	27	13	15	15	16	5	16	>36	>30	>36	1.13
22 may-06 pm	24	12	24	19	9.5	19	12	25.5	25.5	>30	N/A	N/A	2.46

Table IV-7 Active layer data measured at Birling Gap in May 2006 along the eastern transect (transect 3 on Figure 3-12), including the mixing depth (annotated erosion in the table) and the accretion above the top painted pebble found on the column.

Birling Gap May 2006-Transect West													
(all data are in cm)	Upper Beach			Upper-middle Beach			Lower-middle Beach			Lower Beach (Beach step)			$H_{s \max}$
	Erosion	Accretion	Active layer	Erosion	Accretion	Active layer	Erosion	Accretion	Active layer	Erosion	Accretion	Active layer	
20 may-06 am	>28	>29	>29	15	30	30	3	10	10	>27	>28	>28	2.08
20 may-06 pm	12	14	14	23	0	23	27	17	27	9	14	14	2.61
21 may-06 am	8	15	15	>11	>40	>40	7	6	7	28	25	28	1.7
22 may-06 am	<9	N/A	N/A	16	0	16	11	4	11	25	20	25	1.13
22 may-06 pm	N/A	13.5	N/A	17	26	26	4	18	18	>25	N/A	N/A	2.46

Table IV-8 Active layer data measured at Birling Gap in May 2006 along the western transect (transect 1 on Figure 3-12), including the mixing depth (annotated erosion in the table) and the accretion above the top painted pebble found on the column.

Birling Gap December 2006-Transect West													
(all data are in cm)	Upper Beach			Upper-middle Beach			Lower-middle Beach			Lower Beach (Beach step)			H _s max
	Erosion	Accretion	Active layer	Erosion	Accretion	Active layer	Erosion	Accretion	Active layer	Erosion	Accretion	Active layer	
15 dec-06 am	0	4.5	4.5	13.5	23.5	23.5	14	21	21	11	5	11	1.56
16 dec-06 am	0	0	0	18	12	18	18	18	18	9	13.5	13.5	1.64
16 dec-06 pm	0	0	0	>41	>30	>41	18	13.5	18	10	5	10	1.4
17 dec-06 am	0	0	0	0	15	15	21.5	7	21.5	8.5	5	8.5	0.68
17 dec-06 pm	0	0	0	>45	>29	>45	7	12	12	5	3	5	0.79
18 dec-06 am	0	0	0	25	26	26	21	19	21	3	5	5	0.57
18 dec-06 pm	0	0	0	7	0	7	17	16	17	5	0	5	0.39
19 dec-06 am	0	0	0	6	19	19	4.5	10	10	0	0	0	0.47
19 dec-06 pm	0	0	0	0	5	5	13.5	3	13.5	0	0	0	0.26

Table IV-9 Active layer data measured at Birling Gap in December 2006 along the western transect (transect 1 on Figure 3-12), including the mixing depth (annotated erosion in the table) and the accretion above the top painted pebble found on the column.

Birling Gap December 2006-Transect East													
(all data are in cm)	Upper Beach			Upper-middle Beach			Lower-middle Beach			Lower Beach (Beach step)			H _s max
	Erosion	Accretion	Active layer	Erosion	Accretion	Active layer	Erosion	Accretion	Active layer	Erosion	Accretion	Active layer	
15 dec-06 am	0	0	0	18	26	26	18	14.5	18	>31	>29.5	>31	1.56
16 dec-06 am	0	0	0	17.5	11.5	17.5	14.5	24.5	24.5	8.5	12.5	12.5	1.64
16 dec-06 pm	0	0	0	>32	>28	>32	21	7	21	>33.5	>28	>33.5	1.4
17 dec-06 am	8.5	5	8.5	0	3	3	10.5	29	29	9	9.5	9.5	0.68
17 dec-06 pm	0	0	0	0	12	12	24	0	24	20.5	8	20.5	0.79
18 dec-06 am	0	0	0	0	0	0	9	13	13	4.5	7	7	0.57
18 dec-06 pm	0	0	0	9	9	9	17	16	17	7	13	13	0.39
19 dec-06 am	0	0	0	0	0	0	12.5	12	12.5	6	5	6	0.47
19 dec-06 pm	0	0	0	0	0	0	6.5	7	7	5	5	5	0.26

Table IV-10 Active layer data measured at Birling Gap in December 2006 along the eastern transect (transect 3 on Figure 3-12), including the mixing depth (annotated erosion in the table) and the accretion above the top painted pebble found on the column.

Appendix V Pebble tracers' scattering at Cayeux-sur-Mer in December 2004

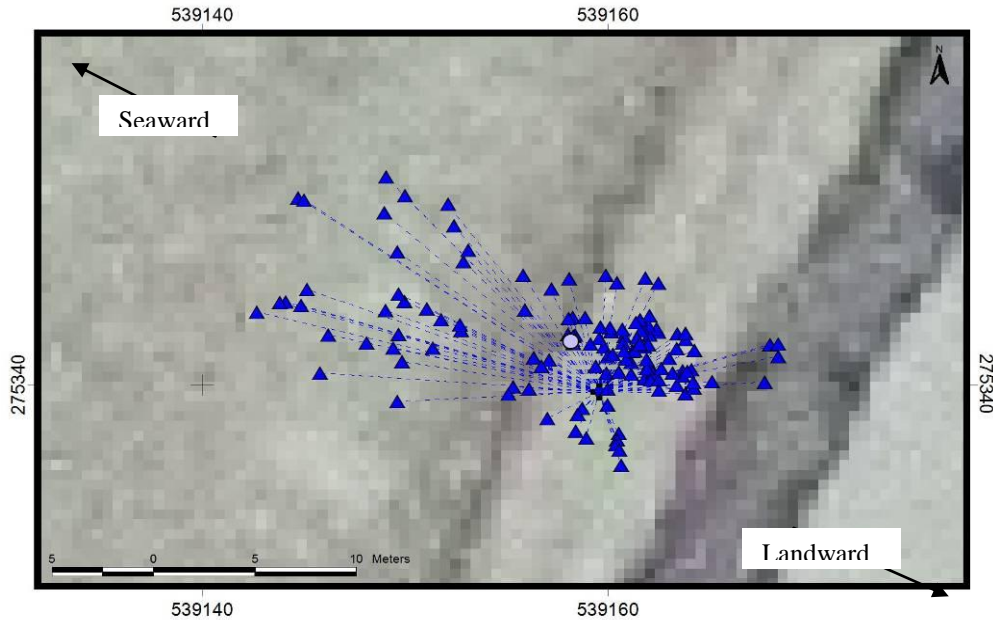


Figure V-1 Tracer pebble dispersion recovered one tide after deployment on the morning of December 14th, 2004. The black cross marks the location of the injection point of the tracer pebbles on the afternoon of December 13th, 2004. Each blue triangle represents a tracer pebble.

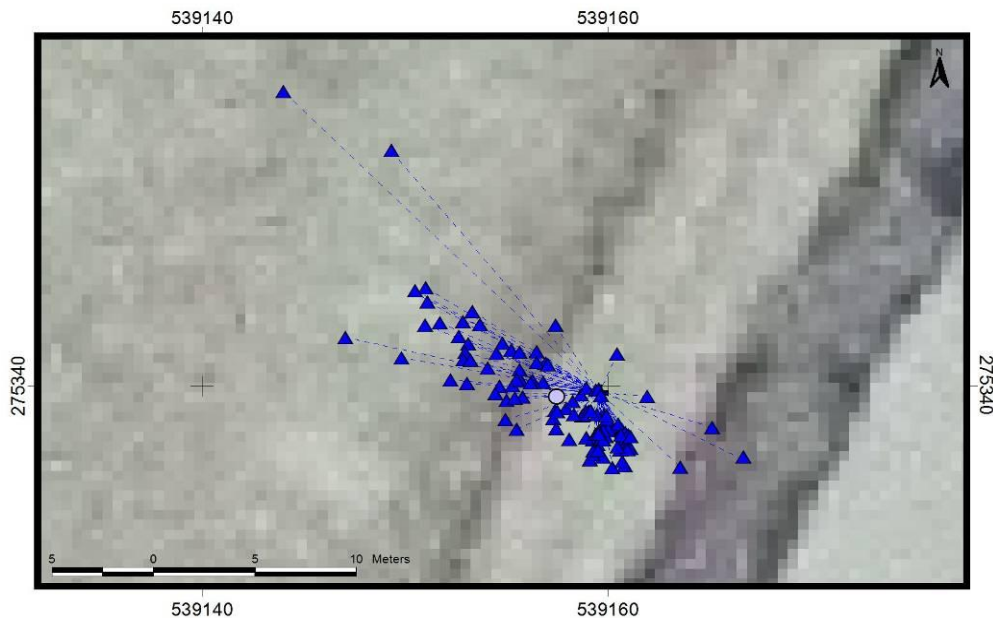


Figure V-2 Tracer pebble dispersion recovered one tide after deployment on the afternoon of December 14th, 2004. The black cross marks the location of the injection point of the tracer pebbles on the morning of December 14th, 2004. Each blue triangle represents a tracer pebble.

Appendix VI Pebble tracers' scattering at Cayeux-sur-Mer in October/November 2005

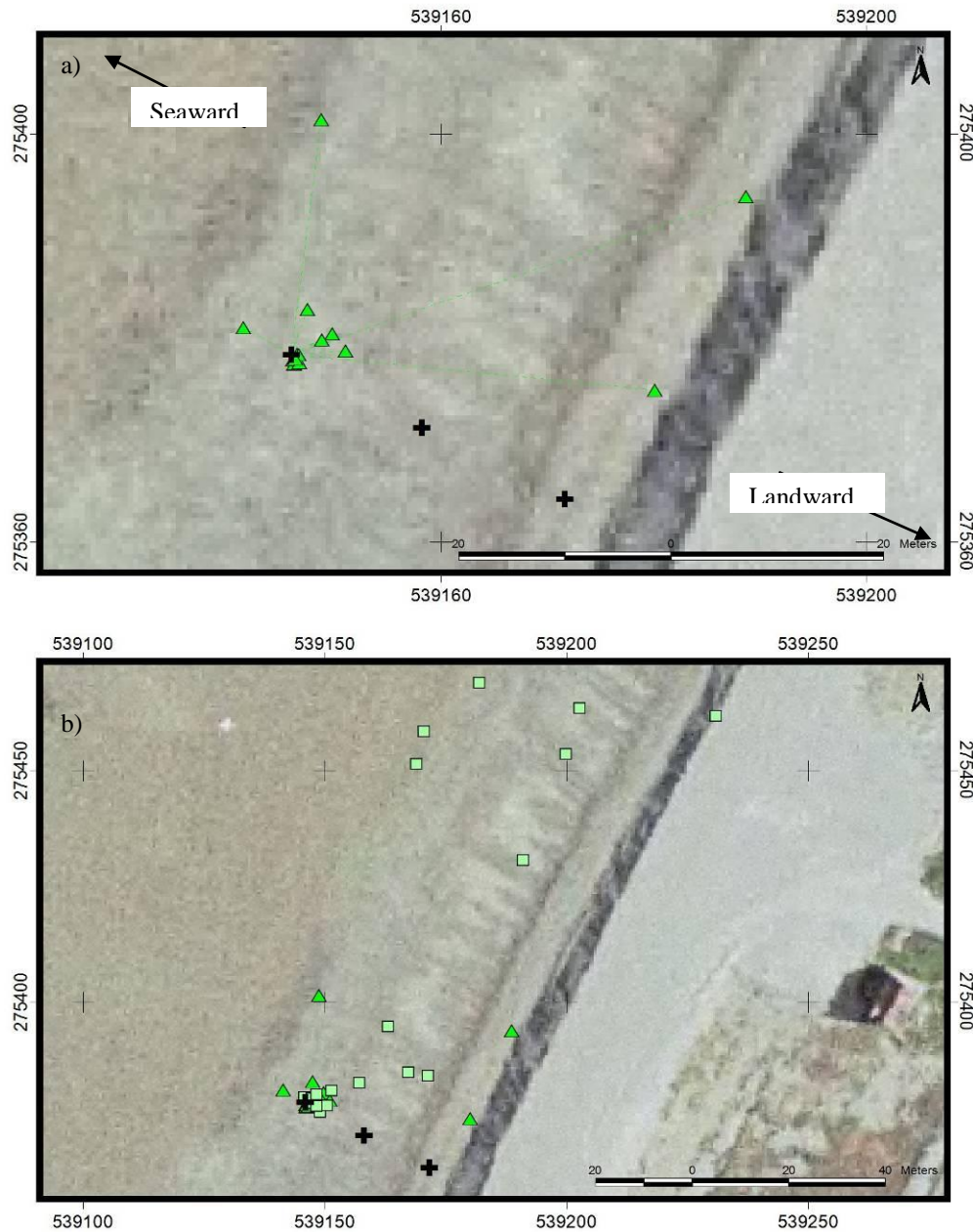


Figure VI-1 Movements of the tracer pebbles deployed on October 29th, 2005.

a) Scattering observed after one tide.

b) Scattering observed over the whole survey period.

The black cross marks the injection point locations. Each triangle represents individual tracer pebbles recovered after one tide while the squares represent individual tracer pebbles recovered after more than one tide. The disks mark the location of the centroids. Pebbles are colour coded: red = upper injection point, blue = middle injection point, green = lower injection point.

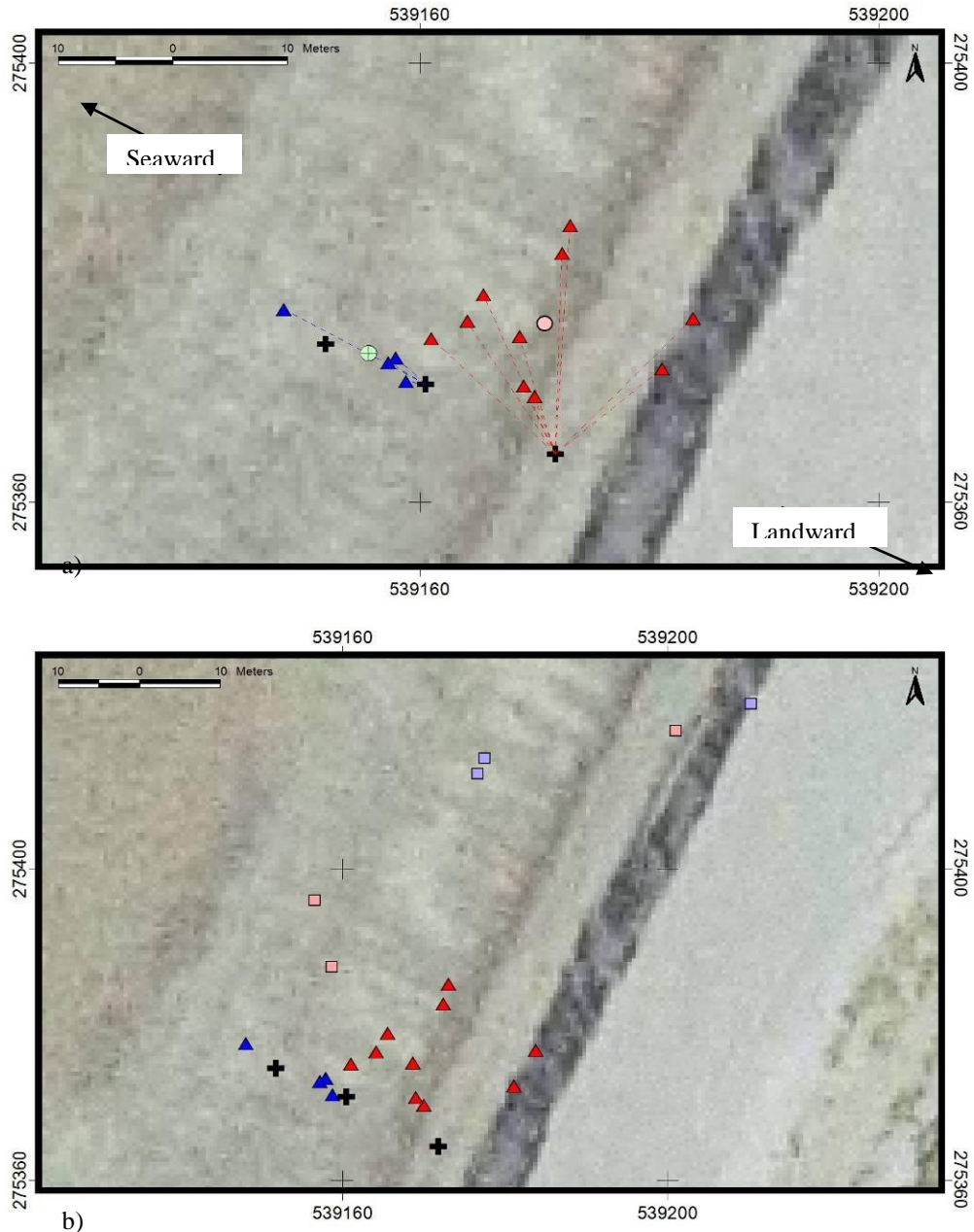


Figure VI-2 Movements of the tracer pebbles deployed on October 30th, 2005.

a) Scattering observed after one tide.

b) Scattering observed over the whole survey period.

The black cross marks the injection point locations. Each triangle represents individual tracer pebbles recovered after one tide while the squares represent individual tracer pebbles recovered after more than one tide. The disks mark the location of the centroids. Pebbles are colour coded: red = upper injection point, blue = middle injection point, green = lower injection point.

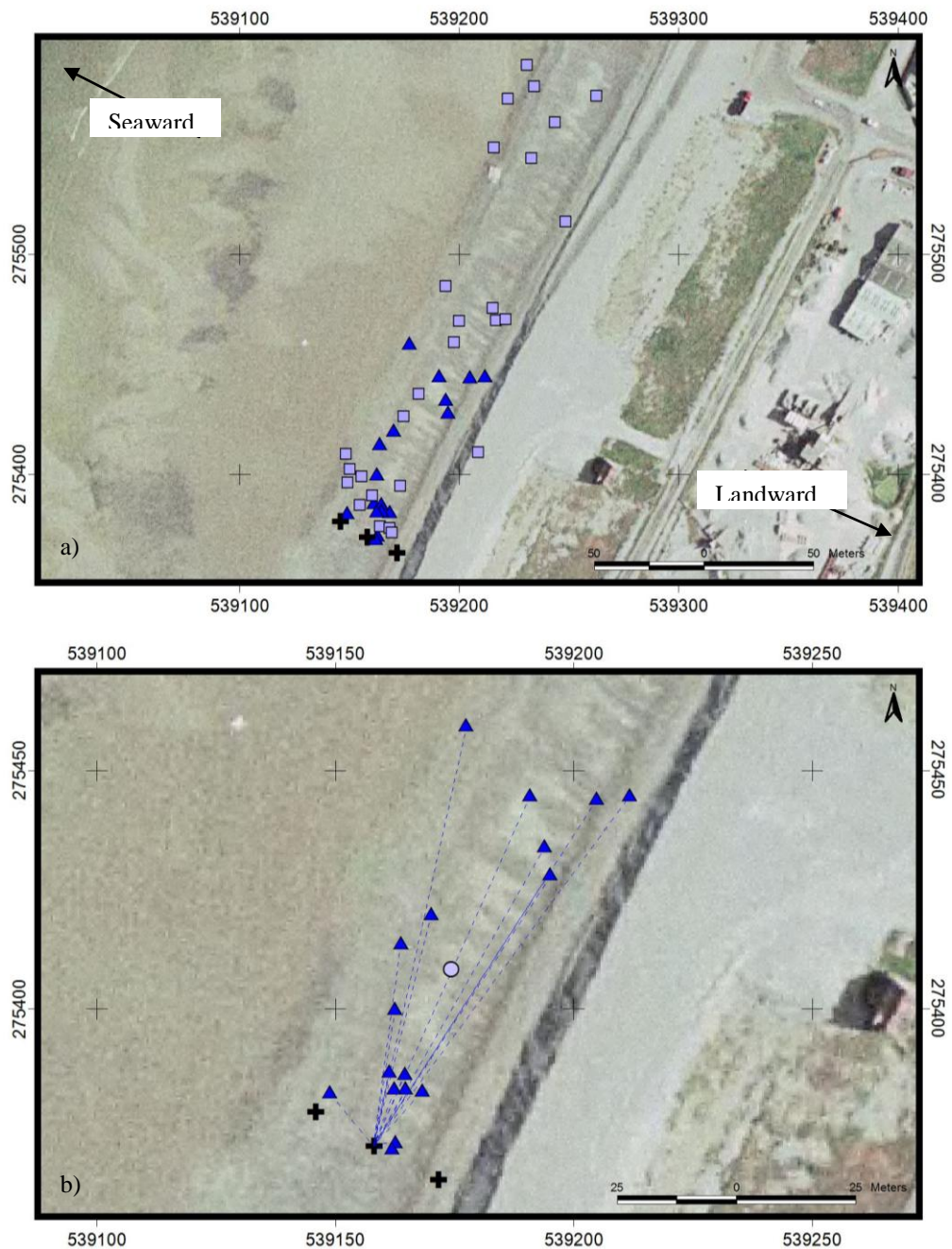


Figure VI-3 Movements of the tracer pebbles deployed on November 1st, 2005.

a) Scattering observed after one tide.

b) Scattering observed over the whole survey period.

The black cross marks the injection point locations. Each triangle represents individual tracer pebbles recovered after one tide while the squares represent individual tracer pebbles recovered after more than one tide. The disks mark the location of the centroids. Pebbles are colour coded: red = upper injection point, blue = middle injection point, green = lower injection point.

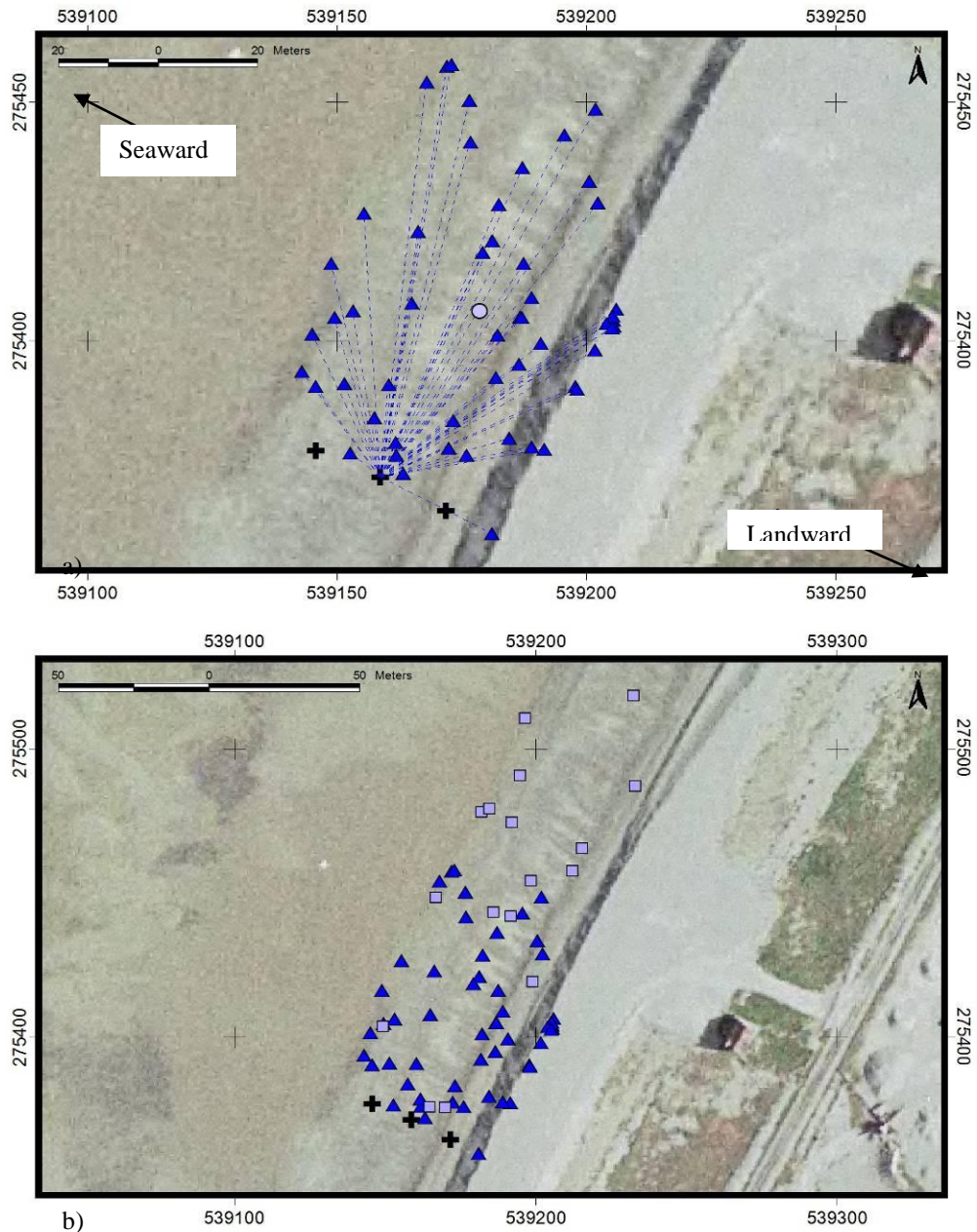


Figure VI-4 Movements of the tracer pebbles deployed on November 2nd, 2005.

a) Scattering observed after one tide.

b) Scattering observed over the whole survey period.

The black cross marks the injection point locations. Each triangle represents individual tracer pebbles recovered after one tide while the squares represent individual tracer pebbles recovered after more than one tide. The disks mark the location of the centroids. Pebbles are colour coded: red = upper injection point, blue = middle injection point, green = lower injection point.

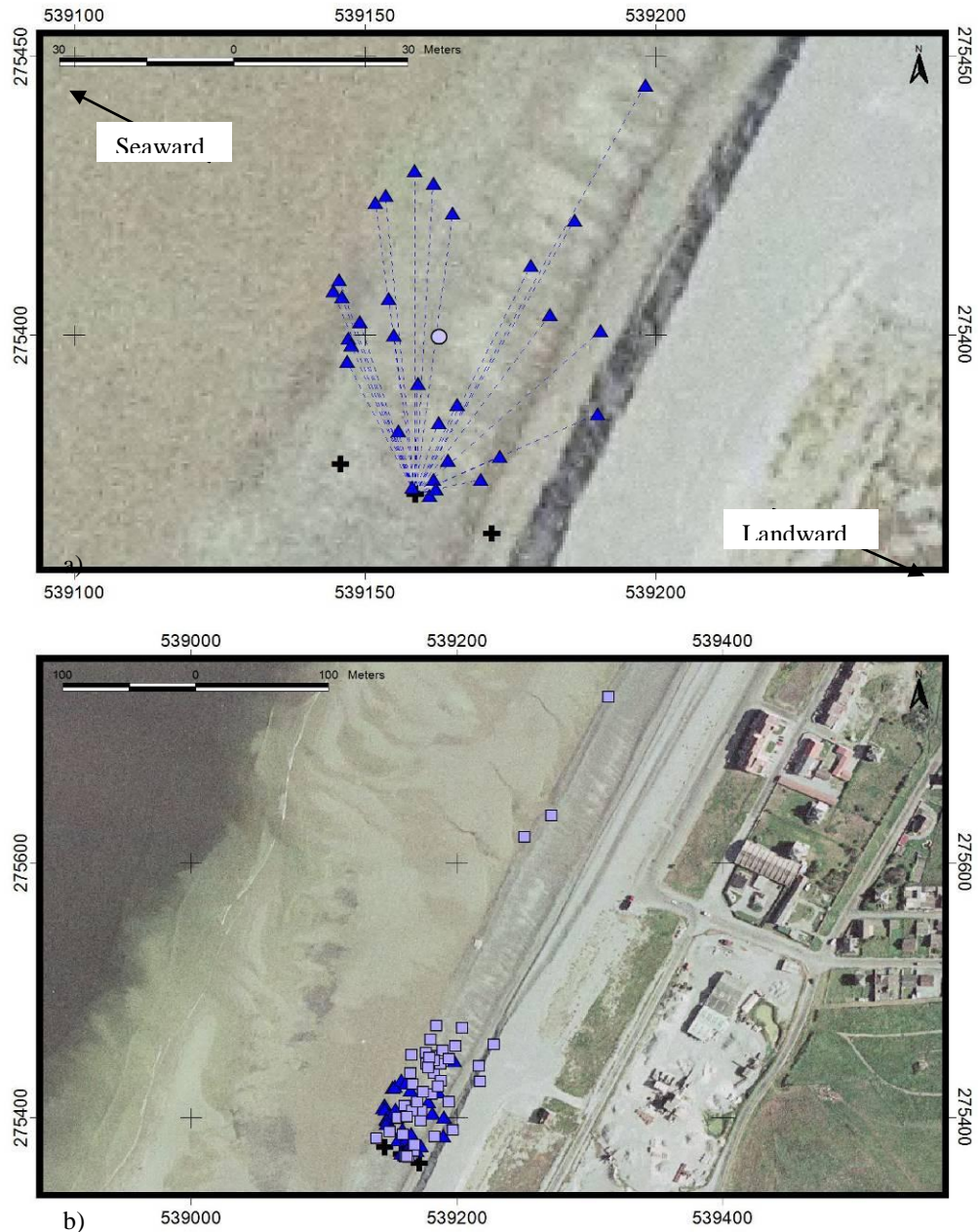


Figure VI-5 Movements of the tracer pebbles deployed on November 4th, 2005.

a) Scattering observed after one tide.

b) Scattering observed over the whole survey period.

The black cross marks the injection point locations. Each triangle represents individual tracer pebbles recovered after one tide while the squares represent individual tracer pebbles recovered after more than one tide. The disks mark the location of the centroids. Pebbles are colour coded: red = upper injection point, blue = middle injection point, green = lower injection point.

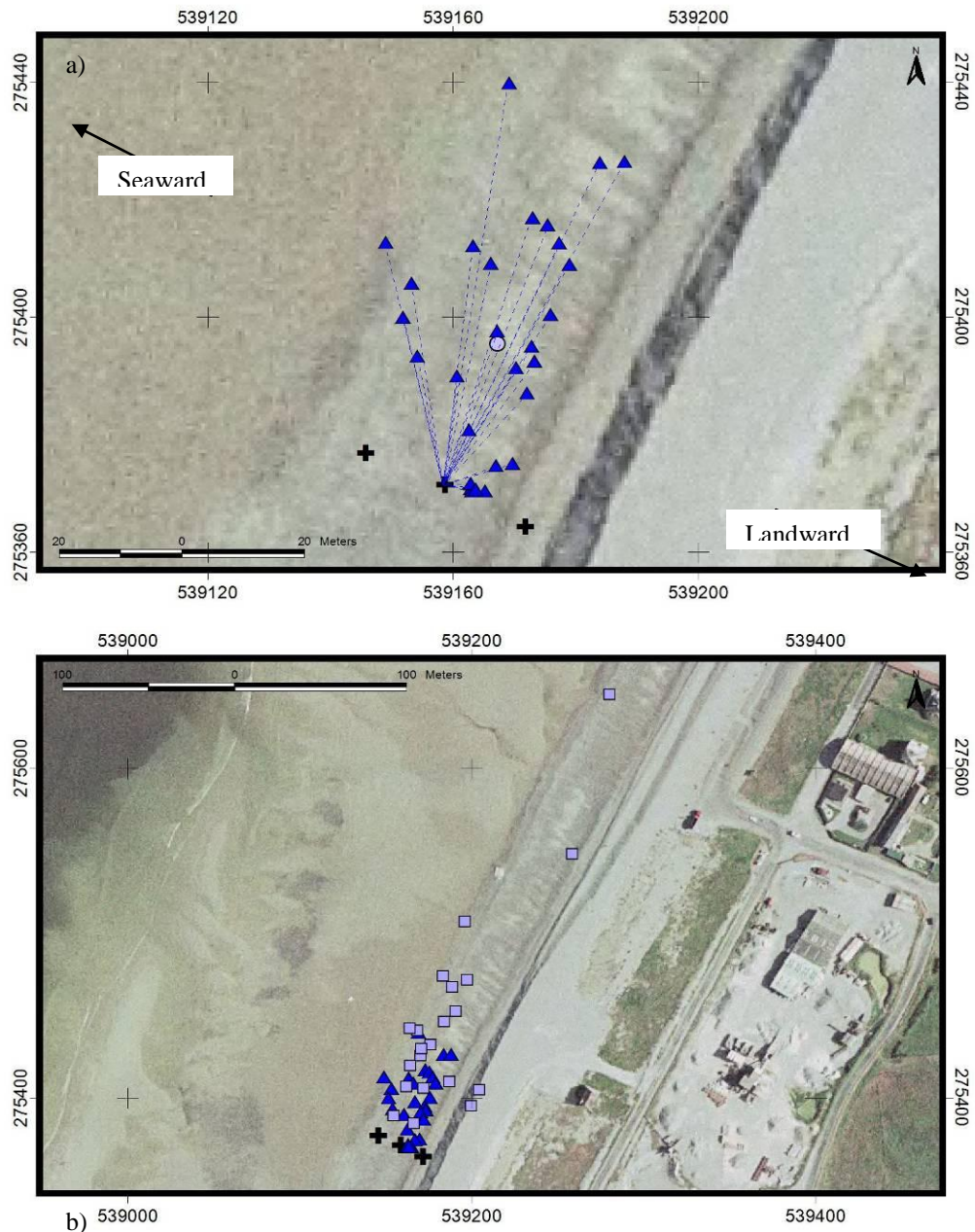


Figure VI-6 Movements of the tracer pebbles deployed on November 5th, 2005.

a) Scattering observed after one tide.

b) Scattering observed over the whole survey period.

The black cross marks the injection point locations. Each triangle represents individual tracer pebbles recovered after one tide while the squares represent individual tracer pebbles recovered after more than one tide. The disks mark the location of the centroids. Pebbles are colour coded: red = upper injection point, blue = middle injection point, green = lower injection point.

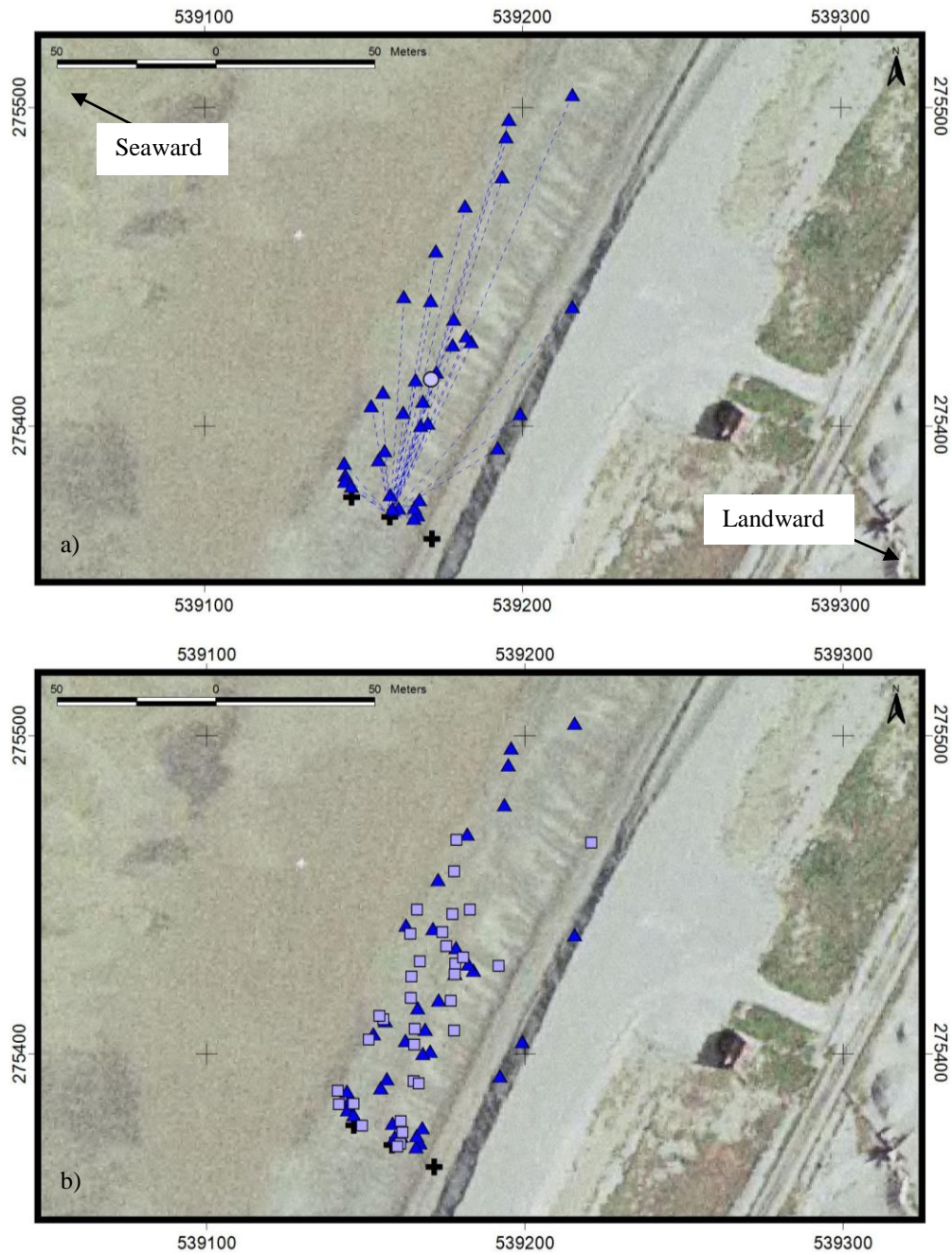


Figure VI-7 Movements of the tracer pebbles deployed on November 6th, 2005.

a) Scattering observed after one tide.

b) Scattering observed over the whole survey period.

The black cross marks the injection point locations. Each triangle represents individual tracer pebbles recovered after one tide while the squares represent individual tracer pebbles recovered after more than one tide. The disks mark the location of the centroids. Pebbles are colour coded: red = upper injection point, blue = middle injection point, green = lower injection point.

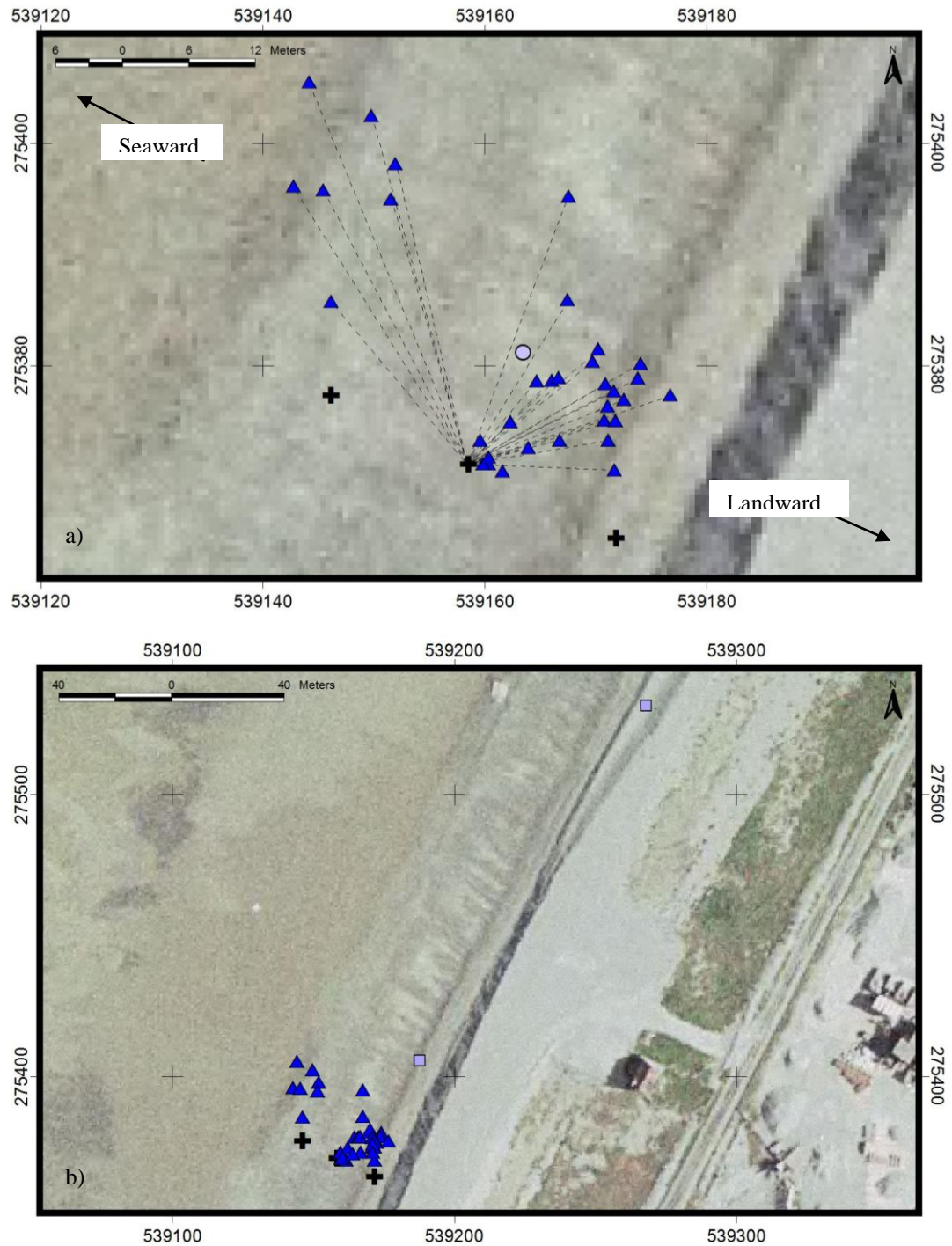


Figure VI-8 Movements of the tracer pebbles deployed on November 9th, 2005.

a) Scattering observed after one tide.

b) Scattering observed over the whole survey period.

The black cross marks the injection point locations. Each triangle represents individual tracer pebbles recovered after one tide while the squares represent individual tracer pebbles recovered after more than one tide. The disks mark the location of the centroids. Pebbles are colour coded: red = upper injection point, blue = middle injection point, green = lower injection point.

Appendix VII Pebble tracers' scattering at Birling Gap in March 2006

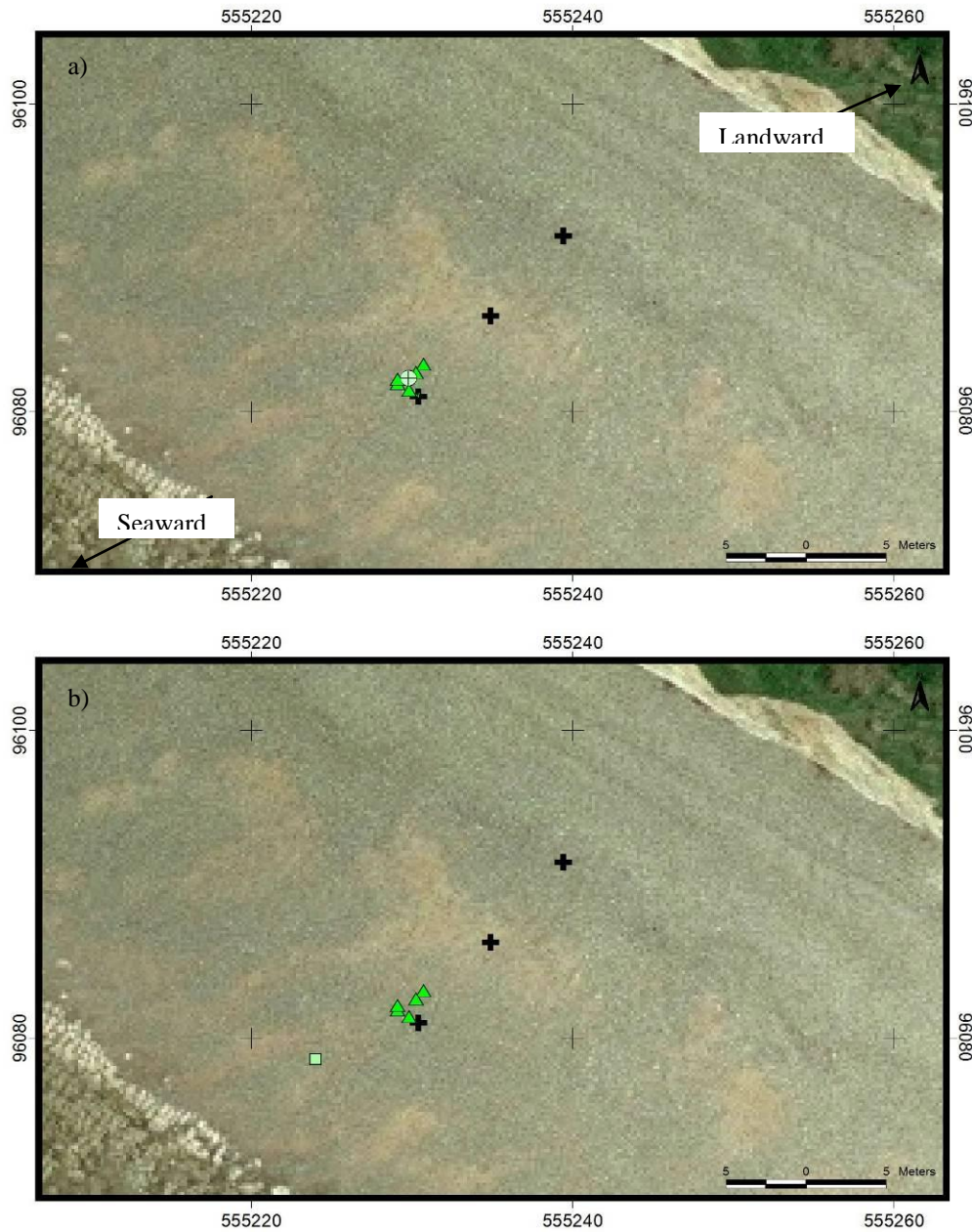


Figure VII-1 Movements of the tracer pebbles deployed on March 20th, 2006.

a) Scattering observed after one tide.

b) Scattering observed over the whole survey period.

The black cross marks the injection point locations. Each triangle represents individual tracer pebbles recovered after one tide while the squares represent individual tracer pebbles recovered after more than one tide. The disks mark the location of the centroids. Pebbles are colour coded: red = upper injection point, blue = middle injection point, green = lower injection point.

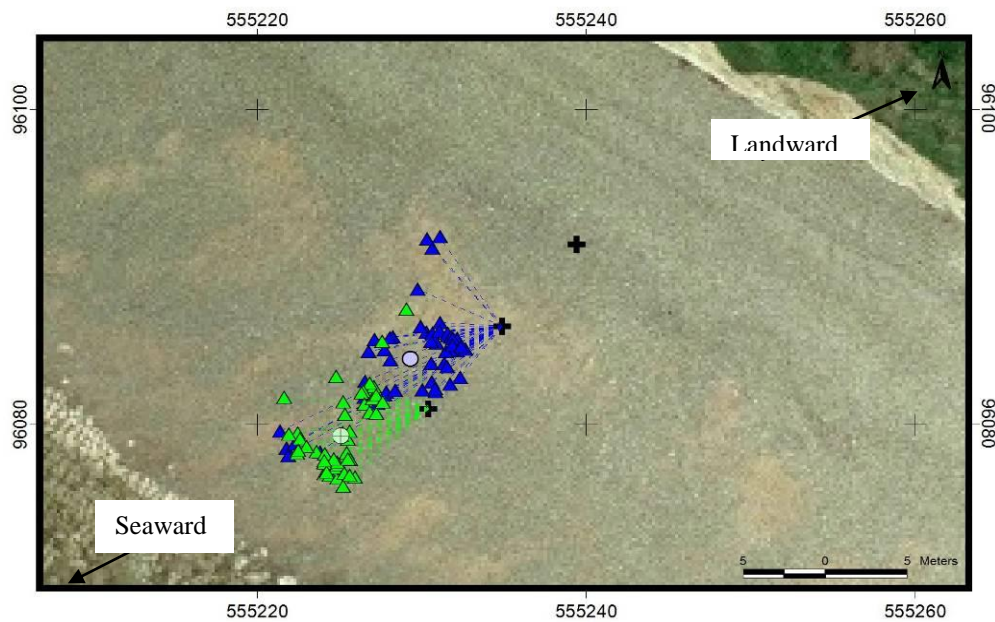


Figure VII-2 Movements of the tracer pebbles deployed on March 23th, 2006. Scattering observed after one tide. (all the tracers were recovered after one tide).

The black cross marks the injection point locations. Each triangle represents individual tracer pebbles recovered after one tide while the squares represent individual tracer pebbles recovered after more than one tide. The disks mark the location of the centroids. Pebbles are colour coded: red = upper injection point, blue = middle injection point, green = lower injection point.